CALTECH Biology Annual Report 2005

Legend for the Front Cover illustration

Structures of HIV-1 virus-like particles, as determined by electron cryotomography. Purified HIV-1 virus-like particles (VLPs) were frozen in a thin layer of buffer and imaged from a series of points-of-view in an electron cryomicroscope. The three-dimensional reconstruction shown was calculated from those images, and many individual VLPs were denoised, segmented, and rendered. The lipid bilayer envelopes are shown in transparent blue, and the capsid shells are colored in either red (for those with the typical cone shape), orange (in a VLP that presented multiple capsids), or yellow (an irregular shape). VLPs are shown in place within the box of density reconstructed. The floor and sides of the box show a projection and various slices through the reconstructed volume, respectively.

Legend for the Back Cover illustration

A three-dimensional reconstruction of the brain of the African elephant, *Loxodonta africana,* based on magnetic resonance images acquired with the 3 T Siemens Trio MRI scanner at the Moore Brain Imaging Center. The top image is a view looking down from above the brain; the bottom image shows the brain from the right side. The images have been segmented into neocortical gray matter, neocortical white matter, cerebellar gray matter, cerebellar white matter, deep cerebellar nuclei, and other structures. The neocortical and cerebellar gray matter are rendered translucent, in order to reveal the structures below. Magnetic resonance images were acquired with the invaluable assistance of Dr. J. Michael Tyszka, and funding for the work was provided by the Gordon and Betty Moore Foundation.
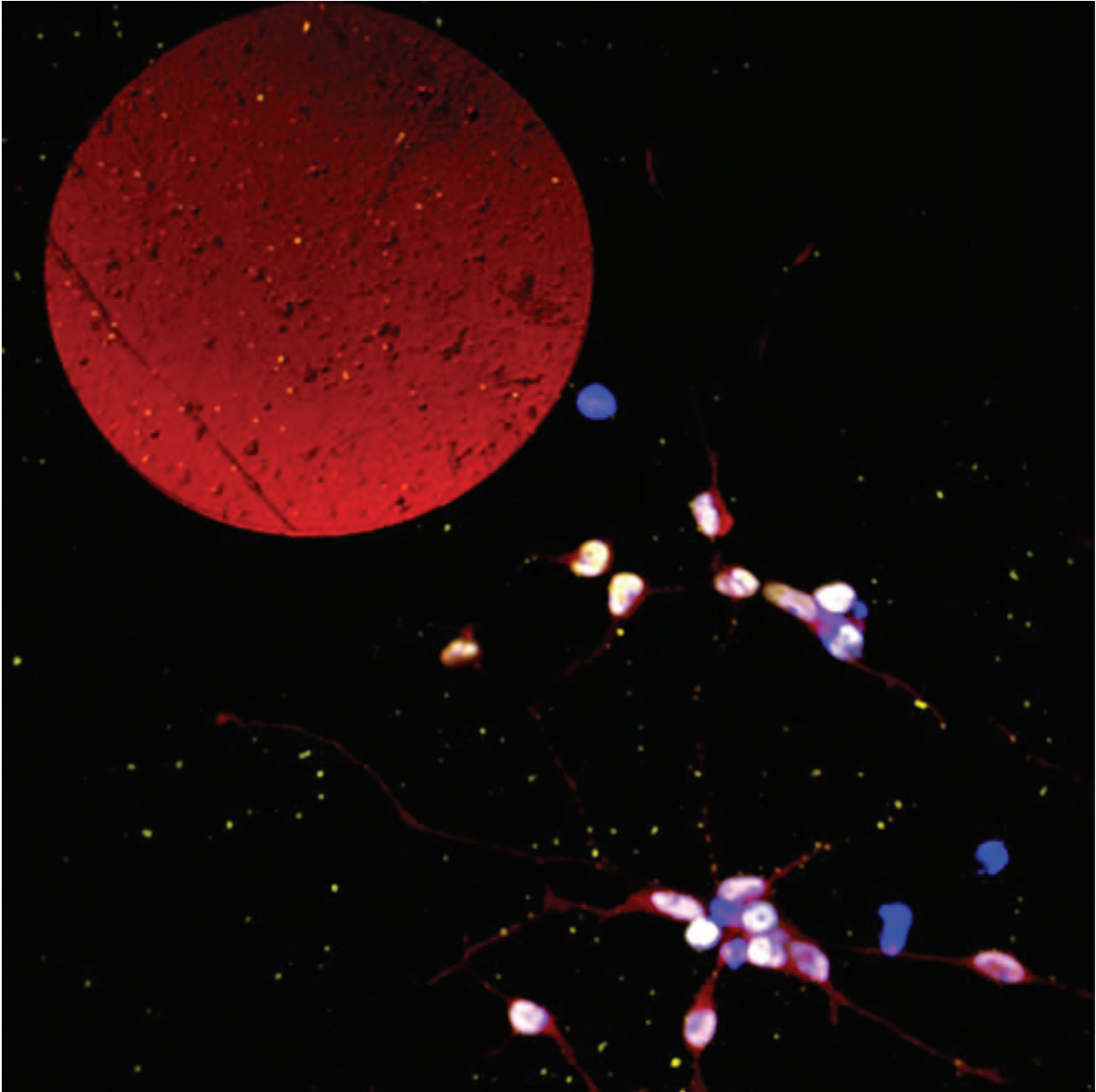
IKKa is a star in the neuronal galaxy. A confocal micrograph demonstrates the nuclear localization of IKKa (pale yellow) expressed from a lentivirus in human neurons differentiated from MESII neuroblasts in the presence of GDNF. IKKa promotes neurite outgrowth, neurotrophin expression, and modulates signaling pathways by neuroprotective molecules. Image provided by Ali Khoshnan from Professor Paul Patterson's lab.

Division of Biology

California Institute of Technology

Pasadena, CA

Annual Report
2004 - 2005

BIOLOGY - 2005

Yolanda Duron, Annual Report Coordinator

Research Reports

Biological research summarized in this report covers the time period from June, 2004, through July, 2005. The annual report is not intended to serve as an official forum, since some portions of the research listed in this report have not yet been published. When referring to an individual abstract(s), special permission must be obtained from the investigator.

References to published papers cited throughout the report are listed at the end of each individual research report.

TABLE OF CONTENTS

INTRODUCTION

MOLECULAR, CELLULAR, AND INTEGRATIVE NEUROSCIENCE

JOHN M. ALLMAN, PH.D.

RICHARD A. ANDERSEN, PH.D.

DAVID J. ANDERSON, PH.D.

HENRY A. LESTER, PH.D.

PAUL H. PATTERSON, PH.D.

iv

STRUCTURAL, MOLECULAR AND CELL BIOLOGY

GRANT J. JENSON, PH.D.

STEPHEN L. MAYO, PH.D.

JAMES H. STRAUSS, PH.D.

DEVELOPMENTAL AND REGULATORY BIOLOGY

BRUCE A. HAY, PH.D.

ELLIOT M. MEYEROWITZ, PH.D.

BARBARA J. WOLD, PH.D.

FACILITIES

INTRODUCTION

100, 75, 50 AND 25 YEARS AGO

100 Years Ago: 1905
From the Throop Polytechnic Institute Catalogue, 1904-1905
"The Natural Science Laboratory is on the second floor… There are tables, lockers, five glass aquaria, two observatory bee-hives, book cases and shelves… Each table is supplied with its own gas burner."

75 Years Ago: 1930
Robert Emerson (1903-1959) was appointed Assistant Professor of Biophysics in 1930. Emerson was a plant physiologist who took his Ph.D. in Otto Warburg's laboratory in Berlin, and at Caltech measured many of the fundamental parameters of photosynthesis. In 1946 he left Caltech to join the faculty of the University of Illinois. He died in an airplane accident at La Guardia airport in 1959.

50 Years Ago: 1955
From the Annual Report:
"During 1954-1955 there were eleven undergraduates in the biology option, twenty-nine graduate students in the Division and seventy-seven postdoctoral research fellows on the staff."
"The Norman W. Church Laboratory for Chemical Biology is nearing completion… and should be ready for occupancy in the fall of 1955."

From Biology News Notes (October 10, 1955, No. 3):
"Those attending the first meeting of the class in biophysics problems found a cryptogram written on the blackboard. They were invited by the instructor, Max Delbrück, to solve it… This was… the cipher: DA TJP XVI IJO XMVXF OCDN XJYZ RDOCDI ORJ CJPMN TJP WZOOZM IJO OVFZ OCDN XJPMNZ.
Delbrück explained later to the curious that there was a purpose to the puzzle-making. Desoxyribonucliec acid (DNA) and protein, he said, are related to each other by a coding mechanism… For the students, cipher-making is a kind of basic training for the obstacle course ahead."

25 Years Ago: 1980
From the Annual Report:
"In celebration of Professor Ray Owen's 65th birthday, a symposium entitled "Frontiers in Immunogenetics" was held at Baxter Hall on June 2-3, 1980… The speakers on the program were all former students or immediate colleagues of Ray Owen… The banquet held in connection with the symposium featured a performance by the Caltech Women's Glee Club, a skit depicting life in Ray's coffee room, and a slide presentation…"
"With the conclusion of Professor Horowitz's term of office as Chairman of the Division, the following appointments took effect this Fall, 1980:

Chairman, Leroy E. Hood
Associate Chairman: Charles J. Brokaw
Executive Officer: A. James Hudspeth
Executive Officer: James H. Strauss"

Professor Angelike Stathopoulos joined the Division of Biology faculty in January of this year. Her primary research interest is patterning of the dorsal-ventral axis in the *Drosophila* embryo. She uses molecular, genetic, and genomic approaches to identify and analyze genes involved in the response to a spatial gradient of the transcription factor DORSAL. Professor Stathopoulos's lab then dissects particular signaling and transcriptional regulatory pathways that control this paradigmatic case of global patterning of an embryo. For example, one such pathway involves the Fibroblast Growth Factors necessary for embryonic heart development.

Professor Stathopoulos received a B.S. in Molecular and Cell Biology from the University of California at Berkeley, and a Ph.D. in Biological Sciences from Stanford University. Before joining Caltech, she pursued postdoctoral research at the University of California at Berkeley.
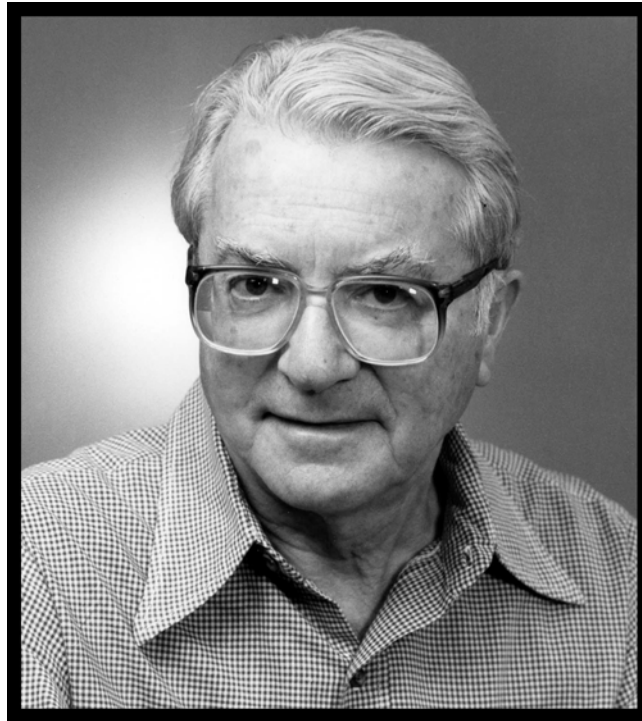
Professor of Biology Norman Horowitz, Emeritus, best known for his work on the "one-gene, one-enzyme" hypothesis and the experiments aboard the Viking Lander to search to search for life on Mars in 1976, died June 1, 2005 at his home in Pasadena. He was 90.

A pioneer of the study of evolution through biochemical synthesis, Horowitz was a professor of biology at the California Institute of Technology for many years. After a distinguished career studying the genetics of the red bread-mold *Neurospora crassa*, he began collaborating with the Jet Propulsion Laboratory in 1965 after becoming interested in the biochemical evolution of life and its possible applications to the search for life on other worlds. He spent five years as chief of JPL's bioscience section.

Horowitz was a member of the scientific teams for both the Mariner and Viking missions to Mars. On the Viking mission, he and two collaborators designed an instrument capable of detecting any biochemical evidence of life on the planet. The results of the experiment were negative at the two Viking sites, but this information in itself was a robust scientific result that continues to inform current efforts in astrobiology to this day.

Horowitz is most renowned in the field of biochemistry for his 1945 thought experiment on biochemical evolution. The paper, published in the *Proceedings of the National Academy of Sciences*, is today considered the origin of the study of evolution at the molecular level. Horowitz also performed a seminal experiment that led to the widespread acceptance of the one-gene, one-enzyme hypothesis that, until the early 1950's, was considered a radical theory of the way that life carries on its chemistry. Horowitz and a colleague used mutations to disprove an alternative interpretation that was gaining credence at the time, thereby indirectly strengthening the one-gene, one-enzyme hypothesis.

A native of Pittsburgh, Horowitz earned his bachelor's degree at the University of Pittsburgh, and then came to Caltech in 1936 for graduate study in the comparatively new division of biology, founded by the famed geneticist Thomas Hunt Morgan. After completing his doctorate in 1939 under embryologist Albert Tyler, Horowitz became a postdoctoral scholar researcher at Stanford University, in the laboratory of George W. Beadle.

When Beadle became chair of the Caltech biology division in 1946, Horowitz returned to his alma mater as a faculty member, and stayed at the Institute for the remainder of his career. He was the biology division chair from 1977 to 1980, and became a professor emeritus in 1982. His contributions to the division also included the endowment of the Horowitz Lecture Series. He was married to Pearl (nee Shykin) Horowitz. Horowitz funded the Pearl S. Horowitz Book Fund at Caltech in her honor.

He was a member of National Academy of Sciences and the American Academy of Arts and Sciences. His honors included a 1998 medal from the Genetics Society of America. He was also the author of a 1986 book entitled: *To Utopia and Back: The Search for Life in the Solar System.*

Honors and Awards - 2005

Anderson　　　　　　　　**Choi**　　　　　　　　**Meyerowitz**

Dr. Gloria B. Choi is the winner of the Ferguson Award for the 2004-2005 academic year. This award goes to the student who is judged by the faculty to have produced the best Ph.D. thesis over the past year. Dr. Choi performed her graduate studies in the laboratory of Professor David Anderson. Her thesis work utilized molecular approaches to bear on a fundamental, and poorly understood, problem in neural circuits and behavior: How do organisms choose between opponent behaviors, when faced with conflicting stimuli in their environment? To address this problem, she studied, at the single-cell level, the amygdalar-hypothalamic pathways that control innate reproductive behaviors, and their anatomical interactions with analogous, pathways that control defensive behaviors, in mice. Using a combination of genetically encoded and conventional axonal tracers, together with double labeling for markers of neuronal activation and neurotransmitter phenotype, she found that a LIM homeodomain protein, Lhx6, delineates the reproductive branch of this pathway. She also revealed the existence of parallel projections from the posterior amygdala, activated by reproductive or defensive olfactory stimuli, respectively, to a point of convergence in the ventromedial hypothalamus. The opposite neurotransmitter phenotypes of these convergent projections suggest a "gate control" mechanisms for inhibiting reproductive behaviors by threatening stimuli. Taken together, her data identify a potential neural substrate for integrating the antagonistic influences of behavioral cues that release opponent reproductive and defensive behaviors, and a transcription factor that may contribute to the development of this substrate.

PROFESSORIAL AWARDS 2005

James G. Boswell Professor of Neuroscience, Richard A. Andersen, was elected a member of the National Academy of Sciences; elected an associate of the Neurosciences Research Program; was a visiting professor at the College de France; was awarded a McKnight Neuroscience Brain Disorders Award; and, his laboratory's research on neural prosthetics was selected as #29 of the top 100 science stories of 2004 by Discover Magazine.

Roger W. Sperry Professor of Biology, David J. Anderson, was awarded the Alexander von Humboldt Research Award for Senior U.S. Scientists.

Caltech President, Professor of Biology, Nobel Laureate, David Baltimore, was the recipient of an Honorary Doctorate Degree from Harvard.

Max Delbrück Professor of Biology, Pamela Bjorkman, received the following honors and awards: National Institutes of Health (NIH) Merit Award; American Society for Histocompatibility and Immunogenetics Rose Payne Distinguished Scientist Award; The University of Kansas Newmark Lecture; New York University School of Medicine Honors Program Lecture; and the Douglass College, Rutgers University Fifth Annual Wyeth/Douglass College Lectureship

Albert Billings Ruddock Professor of Biology, Marianne Bronner-Fraser, was awarded the following honors and awards: Viktor Hamburger Lecturer, Washington University, 2005; BUSAC Award for Excellence in Teaching, 2004-2005; appointed to the Scientific Advisory Board-March of Dimes (2004-present); and Joint Genome Center Sequencing Review Committee (2004-present); and elected to the Board of Directors, Society for Developmental Biology (2005-present). Also selected to be a member of the Council - National Institute for Dental Research in 2005.

Assistant Professor of Biology and Applied Physics, Michael Elowitz, was the recipient of the Searle Scholar Program Award.

Bing Professor of Behavioral Biology, Masakazu Konishi, was awarded the Ralph W. Gerard Prize from the Society for Neuroscience; the Edward M. Scolnick Prize in Neuroscience from the McGovern Institute, MIT; the Lewis S. Rosenstiel Award in Basic Medical Sciences, from Brandeis University; and the Karl Spencer Lashley Award from the American Philosophical Society.

George W. Beadle Professor of Biology and Division Chair, Elliot Meyerowitz, gave a Biology Distinguished Lecture at the National Science Foundation in December, 2004; and Phi Beta Kappa Lectures at Baylor University, Vassar College, Pomona College and Marquette University in January and March, 2005. In September 2005 he was awarded the Ross G. Harrison Prize of the International Society of Developmental Biologists.

Assistant Professor of Computation and Neural Systems, Bren Scholar, Athanassios Siapas, was awarded a McKnight Scholar Award.

Howard and Gwen Laurie Smits Professor of Cell Biology, Alexander Varshavsky, has received the 2005 Stein and Moore Award from the Protein Society. He shares this award with Dr. Avram Hershko (Technion, Israel). In 2005, Varshavsky gave the Distinguished Guest Lecture at the Baylor College of Medicine in Houston, Texas.

The Biology Division hosted the following Kroc Lectures:

April 7, 2004
Margaret Fuller
"Life's a niche: Regulation of stem cell self-renewal and differentiation by a support cell microenvironment"
Departments of Developmental Biology & Genetics
Stanford University School of Medicine

September 22, 2005
Professor James Berger
"Molecular mechanisms for regulating the initiation of DNA replicaion"
Molecular and Cell Biology
UC Berkeley

The Biology Division hosted the following Wiersma Visiting Faculty:

January 19, 2005
Mary Beth Hatten
"New directions in CNS migration"
Laboratory of Developmental Neurobiology
The Rockefeller University

February 23, 2005
Elizabeth Phelps
"The interaction of emotion and cognition: Insights from studies of the human amygdala"
Department of Psychology
New York University

The Biology Division hosted the following Weigle Lecture:

May 31, 2005
Roger Kornberg
"Beyond the structure of RNA polymerase: Understanding eukaryotic gene transcription"
Department of Structural Biology
Stanford University School of Medicine

Photos from the Millard & Muriel Jacobs Genetics & Genomics Laboratory Dedication on Dec 22, 2004

Photos from the Edward Lewis Memorial Weather Station Dedication on April 26, 2005

BIOLOGY DIVISION STAFF

INSTRUCTION AND RESEARCH

ADMINISTRATIVE

INSTRUCTION AND RESEARCH STAFF
DIVISION OF BIOLOGY

Elliot M. Meyerowitz, *Chair*
Pamela J. Bjorkman, *Executive Officer for Biology*
Erin M. Schuman, *Executive Officer for Neurobiology*

PROFESSORS EMERITI

John N. Abelson, Ph.D.
George Beadle Professor of Biology

Seymour Benzer, Ph.D., D.Sc.h.c. Crafoord Laureate
James G. Boswell Professor of Neuroscience (Active)

Charles J. Brokaw, Ph.D., *Biology*

John J. Hopfield, Ph.D.
Roscoe G. Dickinson Professor of Chemistry and Biology

Ray D. Owen, Ph.D., Sc.D.h.c., *Biology*

SENIOR RESEARCH ASSOCIATE EMERITUS

Roy J. Britten, Ph.D.
Distinguished Carnegie Senior Research Associate in Biology

PROFESSORS

John M. Allman, Ph.D.
Frank P. Hixon Professor of Neurobiology

Richard A. Andersen, Ph.D.
James G. Boswell Professor of Neuroscience

David J. Anderson, Ph.D.[1]
Roger W. Sperry Professor of Biology

Giuseppe Attardi, M.D.
Grace C. Steele Professor of Molecular Biology

David Baltimore, Ph.D., D.Sc.h.c., D.Phil.h.c., Nobel
Laureate, *Biology*

Pamela J. Bjorkman, Ph.D.[1]
Max Delbrück Professor of Biology

Marianne Bronner-Fraser, Ph.D.
Albert Billings Ruddock Professor of Biology

Judith L. Campbell, Ph.D.
Chemistry and Biology

Eric H. Davidson, Ph.D.
Norman Chandler Professor of Cell Biology

Raymond J. Deshaies, Ph.D.[1]
Biology

Michael H. Dickinson, Ph.D.
Esther M. and Abe M. Zarem Professor of Bioengineering

William G. Dunphy, Ph.D.
Biology

Scott E. Fraser, Ph.D.
*Anna L. Rosen Professor of Biology and Professor of
Bioengineering and Professor of Applied Physics*

Mary B. Kennedy, Ph.D.
Alan and Lenabelle Davis Professor of Biology

Christof Koch, Ph.D.
*The Lois and Victor Troendle Professor of Cognitive and
Behavioral Biology and Professor of Computation and
Neural Systems*

Masakazu Konishi, Ph.D.
Bing Professor of Behavioral Biology

Gilles Laurent, Ph.D., D.V.M.
Lawrence A. Hanson Jr. Professor of Biology and Computation and Neural Systems

Henry A. Lester, Ph.D.
Bren Professor of Biology

Stephen L. Mayo, Ph.D.[1]
Biology and Chemistry

Elliot M. Meyerowitz, Ph.D.
George W. Beadle Professor of Biology
Chair, Division of Biology

Paul H. Patterson, Ph.D.
Anne P. and Benjamin F. Biaggini Professor of Biological Sciences

Jean-Paul Revel, Ph.D.
Albert Billings Ruddock Professor of Biology
Dean of Students

Ellen V. Rothenberg, Ph.D.
Biology

Erin M. Schuman, Ph.D.[1]
Biology

Shinsuke Shimojo, Ph.D.
Biology

Melvin I. Simon, Ph.D.
Anne P. and Benjamin F. Biaggini Professor of Biological Sciences

Paul W. Sternberg, Ph.D.[1]
Thomas Hunt Morgan Professor of Biology

James H. Strauss, Ph.D.
Ethel Wilson Bowles and Robert Bowles Professor of Biology

Alexander J. Varshavsky, Ph.D.
Howard and Gwen Laurie Smits Professor of Cell Biology

Barbara J. Wold, Ph.D.
Bren Professor of Molecular Biology

Kai Zinn, Ph.D.
Biology

[1]*Joint appointment with Howard Hughes Medical Institute*

ASSOCIATE PROFESSORS

Bruce A. Hay, Ph.D.
Biology

ASSISTANT PROFESSORS

José Alberola-Ila, M.D., Ph.D.
Biology

David C. Chan, M.D., Ph.D.
Biology
Bren Scholar

Michael Elowitz, Ph.D.
Biology and Applied Physics
Bren Scholar

Grant J. Jensen, Ph.D.
Biology

Athanassios G. Siapas, Ph.D.
Computation and Neural Systems
Bren Scholar

Angelike Stathopoulos, Ph.D.
Biology

LECTURERS

Jane E. Mendel, Ph.D.
James R. Pierce, M.D.

DIVISION OF BIOLOGY

SENIOR RESEARCH ASSOCIATES

R. Andrew Cameron, *Ph.D.*
Anne Chomyn, *Ph.D.*
Iain D.C. Fraser, *Ph.D.*
Akiko Kumagai, *Ph.D.*
Jane E. Mendel, *Ph.D.*
Jose Luis Riechmann, *Ph.D.*
Ellen G. Strauss, *Ph.D.*

SENIOR RESEARCH FELLOWS

Maria Elena de Bellard, *Ph.D.*
Laura S. Gammill, *Ph.D.*
Venugopalal Reddy Gonehal, *Ph.D.*
Peter Hájek, *Ph.D.*
Sang-Kyou Han, *Ph.D.*
Byung Joon Hwang, *Ph.D.*
Toshiro Ito, *Ph.D.*
Joanna L. Jankowsky, *Ph.D.*

Yun Kee, *Ph.D.*
Ali Khoshnan, *Ph.D.*
Joon Lee, *Ph.D.*
Helen McBride, *Ph.D.*
David W. McCauley, *Ph.D.*
Jose L. Peña, *M.D.*
Anthony P. West, Jr., *Ph.D.*
Mary An-yuan Yui, *Ph.D.*

FACULTY ASSOCIATE
Alice S. Huang, *Ph.D.*

MOORE DISTINGUISHED SCHOLARS
Elaine L. Bearer, *M.D.*, *Ph.D.*

VISITING ASSOCIATES

Norman Arnheim, *Ph.D.*
Hamid Bolouri, *Ph.D.*
Martin Garcia-Castro, *Ph.D.*
William L. Caton III, *Ph.D.*
Igor Fineman, *M.D.*
Leroy Hood, *M.D., Ph.D., D.Sc.h.c, D.h.c.*
Sorin Istrail, *Ph.D.*
Angelique Y. Louie, *Ph.D.*
Carol Ann Miller, *M.D.*
Eric Mjolsness, *Ph.D.*

Allan L. Reiss, *M.D.*
Kathleen M. Sakamoto, *M.D., Ph.D.*
Stewart Scherer, *Ph.D.*
Johannes Schwarz, *M.D.*
Neil Segil, *Ph.D.*
Ladan Shams, *Ph.D.*
Sandra B. Sharp, *Ph.D.*
Bhavin Sheth, *Ph.D.*
John C. Wood, *M.D., Ph.D.*

MEMBER OF BECKMAN INSTITUTE
Russell E. Jacobs, *Ph.D.*

MEMBERS OF THE PROFESSIONAL STAFF

Eugene Akutagawa, *B.S.*
Janet F. Baer, *D.V.M.*
Gary R. Belford, *Ph.D.*
Lillian E. Bertani, *Ph.D.*
Sangdun Choi, *Ph.D.*
Bruce Cohen, *Ph.D.*
Rochelle A. Diamond, *B.A.*
Mary Dickinson, *Ph.D.*
Gary M. Hathaway, *Ph.D.*
Suzanna J. Horvath, *Ph.D.*

Paola Oliveri, *Ph.D.*
Ker-hwa (Susan) Tung Ou, *M.S.*
Shirley Pease, *B.Sc.*
Piotr Polaczek, *Ph.D.*
Andrew J. Ransick, *Ph.D.*
Hiroaki Shizuya, *M.D.*, *Ph.D.*
Peter Siegel, *Ph.D.*
Julian Michael Tyszka, *Ph.D.*
Zie Zhou, *Ph.D.*

SENIOR POSTDOCTORAL SCHOLARS

Elizabeth Haswell, *Ph.D.*
Tom Taghon, *Ph.D.*
Carol C. Tydell, *D.V.M.*
Frank Wellmer, *Ph.D.*

POSTDOCTORAL SCHOLARS

Vikas Agrawal, *Ph.D.*
Bader Al-Anzi, *Ph.D.*
Gabriela Alexandru, *Ph.D.*

Sylvian Bauer, *Ph.D.*
Ryan L. Baugh, *Ph.D.*
Shlomo Ben-Tabou de-Leon, *Ph.D.*
Smadar Ben-Tabou de-Leon, *Ph.D.*
Marlene Biller, *Ph.D.*
Mark P. Boldin, *Ph.D.*
Ariane Briegel, *Ph.D.*
Christopher Brower, *Ph.D.*
Marina Brozovic, *Ph.D.*

Holly J. Carlisle, *Ph.D.*
David F. Chang, *Ph.D.*
Mark A. Changizi, *Ph.D.*
Ai Chen, *Ph.D.*
Chun-Hong Chen, *Ph.D.*
Hsiuchen Chen, *Ph.D.*
Jae Hyoung Cho, *Ph.D.*
Mee Hyang Choi, *Ph.D.*
Edward G. Coles, *Ph.D.*
Pritsana Chomchan, *Ph.D.*
Markus W. Covert, *Ph.D.*
Karin Crowhurst, *Ph.D.*
He Cui, *Ph.D.*

Pradeep Das, *Ph.D.*
Mindy I. Davis, *Ph.D.*
Benjamin Deneen, *Ph.D.*
Benjamin Deverman, *Ph.D.*
Mohammed Dibas, *Ph.D.*
Daniela Dieterich, *Ph.D.*
Adrienne D. Driver, *Ph.D.*

Wolfgang Einhauser-Treyer, *Ph.D.*
Avigdor Eldar, *Ph.D.*
Maxellende Ezin, *Ph.D.*

Carlos I. Fonck, *Ph.D.*
A. Nicole Fox, *Ph.D.*
Elizabeth-Sharon Fung, *Ph.D.*

Alexander M. Gail, *Ph.D.*
Feng Gao, *Ph.D.*
Emmanuelle Graciet, *Ph.D.*
Bradley E. Greger, *Ph.D.*
Huatao Guo, *Ph.D.*

Agnes Hamburger, *Ph.D.*
Shengli Hao, *Ph.D.*
Wulf Eckhard Haubensak, *Ph.D.*
Wanzhong He, *Ph.D.*
Yongning He, *Ph.D.*
Marcus G.B. Heisler, *Ph.D.*
Veronica F. Hinman, *Ph.D.*
Rong-gui Hu, *Ph.D.*
Taishan Hu, *Ph.D.*
Po-Ssu Huang, *Ph.D.*
Cheol-Sang Hwang, *Ph.D.*
EunJung Hwang, *Ph.D.*
Jong-Ik Hwang, *Ph.D.*

Cristina Valeria Iancu, *Ph.D.*
Takao Inoue, *Ph.D.*

William W. Ja, *Ph.D.*
Mili Jeon, *Ph.D.*
Seong-Yun Jeong, *Ph.D.*

Snehalata Vijaykumar Kadam, *Ph.D.*
Igor Kagan, *Ph.D.*
Jan Piotr Karbowski, *Ph.D.*
Mihoko Kato, *Ph.D.*
Jason A. Kaufman, *Ph.D.*
Soo-Mi Kim, *Ph.D.*
Gary L. Kleiger, *Ph.D.*
David Koos, *Ph.D.*
Alexander Kraemer, *Ph.D.*
Alexander Kraskov, *Ph.D.*

Tracy J. LaGrassa, *Ph.D.*
Tim Lebestky, *Ph.D.*
Vivian Lee, *Ph.D.*
Walter Lerchner, *Ph.D.*
Thomas H.C. Leung, *Ph.D.*
Pingwei Li, *Ph.D.*
Zhuo Li, *Ph.D.*
Michael Liebling, *Ph.D.*
Axel Lindner, *Ph.D.*
J. Russell Lipford, *Ph.D.*
Wange Lu, *Ph.D.*
Evgueniy V. Lubenov, *Ph.D.*
Agnes Lukaszewicz, *Ph.D.*
Peter Y. Lwigale, *Ph.D.*

Natalie Malkova, *Ph.D.*
Edoardo Marcora, *Ph.D.*
Thibault Mayor, *Ph.D.*
Kathryn L. McCabe, *Ph.D.*
Sean Megason, *Ph.D.*
Daniel K. Meulemans, *Ph.D.*
Dane A. Mohl, *Ph.D.*
Jonathan Moore, *Ph.D.*
Fraser John Moss, *Ph.D.*
Yosuke Mukoyama, *Ph.D.*[1]
Israel Muro, *Ph.D.*
Mala Murthy, *Ph.D.*
Sam Musallan, *Ph.D.*

Zoltan Nadasdy, *Ph.D.*
Jongmin Nam, *Ph.D.*
Raad Nashmi, *Ph.D.*
Zachary Nimchuk, *Ph.D.*

Richard A. Olson, *Ph.D.*

Rigo Pantoja, *Ph.D.*
Junghyun Park, *Ph.D.*
Bijan Pesaran, *Ph.D.*
Mathew D. Petroski, *Ph.D.*
Konstantin Pyatkov, *Ph.D.*

Daniel Rizzuto, *Ph.D.*
Benjamin D. Rubin, *Ph.D.*

Melissa Saenz, *Ph.D.*
Alok J. Saldanha, *Ph.D.*
Tatjana Sauka-Spengler, *Ph.D.*
Gary C. Schindelman, *Ph.D.*
Deirdre D. Scripture-Adams, *Ph.D.*
Wei Shen, *Ph.D.*
David R. Sherwood, *Ph.D.*
Nina Tang Sherwood, *Ph.D.*
Kum-Joo Shin, *Ph.D.*
Patrick Sieber, *Ph.D.*
Joel Smith, *Ph.D.*
William Bryan Smith, *Ph.D.*
Elizabeth R. Sprague, *Ph.D.*
David Sprinzak, *Ph.D.*
Jagan Srinivasan, *Ph.D.*[1]
Harald Stögbauer, *Ph.D.*
Gurol M. Suel, *Ph.D.*
Greg Seong-Bae Suh, *Ph.D.*
Michael A. Sutton, *Ph.D.*

Konstantin D. Taganov, *Ph.D.*
Chin-Yin Tai, *Ph.D.*
Andrew R. Tapper, *Ph.D.*
Timothy D. Taylor, *Ph.D.*
Elizabeth B. Torres, *Ph.D.*
Thomas P. Treynor, *Ph.D.*[1]
Le A. Trinh, *Ph.D.*
Qiang Tu, *Ph.D.*
Glenn C. Turner, *Ph.D.*
Phoebe Tzou, *Ph.D.*

Mikko T. Vahasoyrinki, *Ph.D.*
Cheryl Van Buskirk, *Ph.D.*
Luis E. Vasquez, *Ph.D.*
Julien Vermot, *Ph.D.*
Sofia Vrontou, *Ph.D.*

David W. Walker, *Ph.D.*
Haiqing Wang, *Ph.D.*
Horng-Dar Wang, *Ph.D.*
Jinling Wang, *Ph.D.*
Lorraine R. Washburn, *Ph.D.*
Dai Watanabe, *M.D.*, *Ph.D.*
Allyson Whittaker, *Ph.D.*
Elizabeth R. Wright, *Ph.D.*
Reto Wyss, *Ph.D.*

Lili Yang, *Ph.D.*
Zhiru Yang, *Ph.D.*[1]
Hae Yong Yoo, *Ph.D.*
Young Y. Yoon, *Ph.D.*[1]
Zhiheng Yu, *Ph.D.*

Weiwei Zhong, *Ph.D.*
Jianmin Zhou, *Ph.D.*
Lisa Taneyhill-Ziemer, *Ph.D.*
Mark J. Zylka, *Ph.D.*[1]

[1]*Joint appointment with Howard Hughes Medical Institute*

VISITORS

Alejandro Bäcker, *Ph.D.*
Annick Dubois, *Ph.D.*
Pamela l. Eversole-Cire, *Ph.D.*
Idoia Gimferrer, *M.D.*
Ung-Jin Kim, *Ph.D.*
Fumiko Maeda, *Ph.D., M.D.*
Rex A. Moats, *Ph.D.*
Robert J. Peters, *Ph.D.*
Agustin Rodriguez Gonzalez, *Ph.D.*
Orna Rosenthal, *Ph.D.*
Paola Sgobbo, *Sc.D.*
Fredrik Jens Sundstrom, *Ph.D.*

BIOLOGY GRADUATE STUDENTS

Meghan Adams
Oscar Alvizo[2]
Xavier Ambroggio
Meredith Ashby[4]

Magdalena Bak
Susannah Barbee
Mat Barnet[2]
Helen Holly Beale
John Bender
Jordan Benjamin
Rajan Bhattacharyya[1]
Sujata Bhattacharyya
Baris Bingol
Kiowa Bower
Bede Broome
C. Titus Brown
Seth Budick
Charles Bugg[2]

Michael Campos[1]
Ronald M. Carter
Gil Carvalho
Stijn Cassenaer
Cindy Chiu
Eun Jung Choi
Gloria Choi
Gestur B. Christianson[1]
Daniel Cleary
Gregory Cope[2]
Jeffrey Copeland
Robert S. Cox III
Paola Cressy
Laura Croal

Chiraj Dalal[2]
Sagar Damle
Tristan De Buysscher[1]
Scott Detmer
Mary Devlin[2]
Christopher Dionne

Jessica Edwards
Jonathan Erickson[3]

Alexander Farley
Shabnam S. Farivar
Jolene Fernandes
William Ford[1]
Barbara Kraatz-Fortini

Nazli Ghaboosi
Hilary Glidden[1]
Carl S. Gold[1]
Daniel Gold
Sean Gordon[2]
Noah Gourlie[2]
Johannes Graumann
Harry Green
Erik Griffin
Ming Gu[1]

Christopher Hart
Houman Hemmati
Gregory Henderson
Anne Hergarden
Gilberto Hernandez
Christian Hochstim
Alex Holub[1]
Geoffrey Hom[2]
Jean Huang
Jun Ryul Huh

Princess Imoukhuede[3]
Hiroshi Ito
Asha Iyer

Vivek Jayaraman[1]

Jennifer Keeffe[2]
Jane Khudyakov[2]
Jongmin Kim
Joshua Klein[2]
Rajan Kulkarni[2]
Steven Kuntz[2]

Christopher Lacenere
Kyle Lassila[2]
Brian Lee
Jennifer Lee[2]
Pei Yun Lee
Isabella Lesur[2]
Louisa Liberman
Ben Lin
Lilyn Liu
Carolina Livi
Carole Lu
Tinh N. Luong

Angie Mah[2]
Davin Malasarn
Stefan Materna[2]
Ofer Mazor[1]
Andrew Medina-Marino
Daniella Meeker[1]
Anna K. Mitros[1]
Jennifer Montgomery
Farshad Moradi[1]
Dylan Morris[2]
Ali Mortazavi
Eric Mosser
Julien Muffat
Grant H. Mulliken[1]
Gavin Murphy[2]

Anusha Narayan[1]
Patricia Neil[1]
Matthew Nelson[1]
Dirk Neumann[1]
Dylan Nieman[1]

Elizabeth Ottesen

Maria Papadopoulou
Sarah Payne
Yao-Chun Peng
James Pierce
Alexa Price-Whelan

Juan Ramirez-Lugo
Lavanya Reddy[1]
Leila Reddy[1]
Clara Reis[2]
Michael Reiser[1]
Julian Revie[2]
Roger Revilla[2]
Adrian Rice[2]
Ted Ririe
Alice Robie
Jason Rolfe[1]
Ueli Rutishauser[1]

Anna Salazar
Jennifer Sanders
Shu Ping Seah
Premal Shah[2]
Kai Shen[1]
Celia Shiau

Dong Hun Shin
Claudiu Simion
Jasper Simon
Eric Slimko[1]
Stephen E.P. Smith
Amber Southwell

Tracy Teal[1]
Devin Tesar
Naotsugu Tsuchiya[1]

Lawrence Wade
Ward Walkup IV[2]
Dirk Walther[1]
Luigi Warren
Karli Watson
Karen Wawrousek[2]
Jeffrey Wiezorek, M.D.
Casimir Wierzynski[1]
Ashley Wright
Daw-An Wu

Jonathan Young[1]
Suzuko Yorozu
Hui Yu

Mark Zarnegar
Brian Zid
Eric Zollars[2]

[1]*Computational and Neural Systems*
[2]*Division of Biochemistry*
[3]*Bioengineering*
[4]*Chemistry*

BIOLOGY RESEARCH AND LABORATORY STAFF

Stephanie L. Adams
Jennifer M. Alex - *A.A.*
Mary Alvarez
Armando Amaya
Gabriel Amore - *Ph.D.*
Kristen Andersen
Michael Andersen
Igor Antoshechkin - *Ph.D.*
David Arce
Elena Armand - *M.D.*
Cirila Arteaga
Jenny Arvizu
Marie Ary - *Ph.D.*

Carlzen Balagot
Meyer Barembaum - *Ph.D.*
Guillermina Barragan
Carol Bastiani - *Ph.D.*
Ruben Bayon - *B.S.*
Enisa Bekiragik
Gary Belford - *Ph.D.*
Kevin Berney - *A.B.*
Sujata Bhattacharyya - *B.S.*
Brian Blood - *B.S.*
Natasha Bouey
Benoit Boulat - *Ph.D.*
Ana Lidia Bowman
Olga Breceda
Boris Breznen - *Ph.D.*
Lakshmi Bugga - *M.S.*

Cynthia Carlson - *B.A.*
John Carpenter - *B.S.*
Gavin Chan - *Ph.D.*
Juancarlos Chan - *B.S.*
Jung Sook Chang - *B.S.*
Mi Sook Chang - *M.S.*
Ewen Chao
Sherwin Chen - *B.S.*
Wen Chen - *Ph.D.*
Cindy Cheng - *M.S.*
Tsz-Yeung Chiu - *B.S.*
Sangdun Choi - *Ph.D.*
Suk Hen Chow - *M.S.*
Ana Colon - *A.A.*
Sonia Collazo - *M.S.*
Robin Condie - *B.S.*
Stephanie Cornelison - *B.S.*
Christopher Cronin - *B.S., M.E.*

Wei Lien S. Dang
Susan Dao - *B.A.*
John de la Cueva
John Demodena - *B.S.*
Andrey Demyanenko - *Ph.D.*
Tatyana Demyanenko - *Ph.D.*

Elissa Denny - *B.A.*
Purnima Deshpande - *M.S.*
Prabha Dias - *Ph.D.*
Rhonda Digiusto - *B.A.*
Ping Dong - *M.D.*
Leslie Dunipace - *M.A.*
Janet Dyste - *A.A.*

Jean Edens
Lauren Elachi
Pamela Eversole-Cire - *Ph.D.*

Maria Farkas - *B.A.*
Lisa Fields
Stephen Flaherty - *B.S.*
Rosemary Flores
Mary Flowers - *M.A.*
Ian Foe
Michael Fontenette
Paige Fraser

Jessica Gamboa
Martin Garcia-Castro - *Ph.D.*
Arnavaz Garda - *B. Sc.*
Jahlionais (Elisha) Gaston - *B.A.*
Cheryl Gause
Leah Gilera-Rorrer - *B.S.*
Lisa Girard - *Ph.D.*
Michael Goard - *B.A.*
Sidra Golwala - *M.H.S.*
Martha Gomez
Abel Gonzalez
Constanza Gonzalez
Jose Gonzalez
Kenneth Goodrich - *M.S.*
Virginie Goubert
Blanca Granados
Hernan Granados
Rachel Gray - *B.S.*
David Gultekin - *Ph.D.*
Joaquin Gutierrez
Richele Gwirtz - *B.S.*

Julie Hahn - *B.S.*
Atiya Hakeem - *Ph.D.*
Kathleen Hamilton
Sarah Hamilton
Parvin Hartsteen
Heather Hein
Argelia Eve Helguero - *B.S.*
Martha Henderson - *M.S.*
Carlos Hernandez
Christine Hickler
Kristina Hilands
Timothy Hiltner - *M.S.*
Ritchie Ho

Sepehr Hojjati - *B.S.*
Craig Hokanson - *B.S.*
Andrew Hsieh - *B.S.*
Haixia Huang - *Ph.D.*
Qi Huang - *B.S.*
Kathryn Huey-Tubman - *M.S.*
Sanil (David) Hwang

Nahoko Iwata - *M.S.*

Micah Jackson
Cynthia Jones

Tomomi Kano - *B.A.*
Joyce Kato - *B.S.*
Aura Keeter
Bruce Kennedy - M.S.
Eimear Kenny - *B.S., M.Sc.*
Jiseo Ki - *M.S.*
HyunHee Kim - *M.S.*
Brandon King
Ranjana Kishore - *Ph.D.*
Christine Kivork - *B.S.*
Jan Ko
Patrick Koen
Shi-Ying Kou - *M.D.*
David Kremers
Charlotte Krontiris

Santiago Laparra
Nicholas Lawrence - *M.A.*
Patrick Leahy (KLM) - *B.S.*
Kwan F. Lee
Raymond Lee - *Ph.D.*
Jamie Liu - *B.S.*
Lynda Llamas
Liching Lo - *M.S.*
Thomas Lo Jr. - *B.S.*
Anna Maria Lust - *B.A.*
Lloyd Lytle - *B.S.*

Josephine Macenka - *B.S.*
Valeria Mancino - *M.S.*
Gina Mancuso
Andrea Manzo - *B.S.*
Blanca Mariona
Aurora Marquina
Steven Marsh - *B.A.*
Monica Martinez - *B.S.*
Jorge Mata
Jose Mata
David R. Mathog - *Ph.D.*
Sarah May - *B.S.*
Ofer Mazor - *Ph.D.*
Doreen McDowell - *M.S.*
Sheri McKinney - *B.S.*

Rodolfo Mendez - *A.A.*
Edriss Merchant - *B.S.*
Anca Mihalas - *M.S.*
Gabriele Mosconi
Hans-Michael Müller - *Ph.D.*
Gustavo Munoz - *B.A.*
Mary Munoz
Marta Murphy - *B.A.*

Cecilia Nakamura
Inderjit Nangiana - *M.S.*
Paliakaranai Narasimhan - *Ph.D.*
Violana Nesterova - *M.S.*
Lisa Newhouse

Robert Oania
Maria Ochoa
Shannon O'Dell - *A.S.*
Carolyn Ohno - *Ph.D.*
Nick Oldark
Elizabeth Olson - *B.A.*

Dolores Page - *B.A.*
Rashmi Pant - *Ph.D.*
John Papsys - *B.S.*
Ji Young Park - *M.S.*
Neeham Park - *M.S.*
Kelsie Weaver Pejsa - *B.S.*
Sheyla Perez Martinez
Diana Perez
Jason Perillo
Barbara Perry
Andrei Petcherski - *Ph.D.*
Bjoern Phillips
Rosetta Pillow - *A.A.*
Timur Pogodin - *M.D.*
Parlene Puig

John Racs - *B.S.*
Carrie Ann Randle
Anitha Rao - *M.S.*
Vijaya Rao - *M.S.*
Alana Rathbun
Carol Readhead - *Ph.D.*
Jane Rigg - *B.A.*
Maral Robinson - *B.S.*
Carlos Robles
Monica Rodriguez-Torres
Robert Rohrkemper
Maria C. Rosales
Alan Rosenstein - M.S.
Alison Ross - *B.A.*
Donaldo Ruano Campos
Seth Ruffins - *Ph.D.*
Felicia Rusnak - *B.S.*

Nicole Sammons
Lorena Sandoval
Leah Santat - *B.S*
Eric Santiestevan - *A.B.*
Mirna Santos
Nephi Santos - *A.S.*
Viveca Sapin - *B.S.*
Leslie Schenker - *B.S.*
Eric Schwarz - *Ph.D.*
Jun Sheng - *Ph.D.*
Bhavin Sheth - *Ph.D.*
Limin Shi - *M.S., Ph.D.*
Hiroaki Shizuya - *Ph.D.*
Aaron Shoop
Mitzi Shpak - *B.S.*
Peter Siegel - *Ph.D.*
Juan Silva - *B.S.*
John Silverlake - *B.S.*
Geoffrey Smith - *B.S.*
Jeffrey Smith
Kayla Smith - *B.S.*
Peter Snow - *Ph.D.*
Diane Solis - *B.A.*
Raima Solomatina - *M.S.*
Lauren Somma - *B.A.*
Ingrid Soto
Krishnakanth Subramaniam - *M.S.*
Jayne Sutton

Johanna Tan-Cabugao
Deanna Thomas - *B.A.*
Leonard M. Thomas - *Ph.D.*
William Tivol - *Ph.D.*
Diane Trout - *B.S.*
Julian Michael Tyszka - *Ph.D.*

Kimberly Van Auken - *Ph.S.*
Laurent Van Trigt - *M.S.*
Vanessa Vargas
Roberto Vega
Rati Verma - *Ph.D.*

Shawn Wagner - *Ph.D.*
Estelle Wall - *B.S.*
Chi Wang - *M.A.*
Jue Jade Wang - *M.S.*
Qinghua Wang - *B.A.*
Christopher Waters
Brian Williams - *Ph.D.*
Gwen Williams - *A.S., A.G.*
John L. Williams (KML)
Jon B. Williams
Charles Winters Jr.
Sascha Wyss - *M.D.*

Zan-Xian Xia - *Ph.D.*

Vicky Yamamoto - *B.S.*
Lili Yang - *Ph.D.*
Tessa Yao - *M.B.A.*
Hao Ye
Carolina Young - *B.S.*
Rosalind Young - *M.S.*
Changjun Yu - *Ph.D.*
Qui Yuan - *M.S.*
Gina Yun - *B.A.*
Miki Yun - *B.A.*

Joelle Zavzavadjian - *M.S.*
Rosario Zedan
Xiaowei Zhang - *M.S*
Shu Zhen Zhou - *B.S.*
Xiaocui Zhu - *Ph.D.*

ADMINISTRATIVE STAFF
Mike Miranda, Administrator
Tania Davis, Assistant to Chairman
Laura Rodriguez, Assistant to Chairman

ACCOUNTING
Carole Worra

COMPUTER FACILITY
Vincent Ma
Scott Norton
Tom Tubman

GRADUATE STUDENT PROGRAM
Elizabeth M. Ayala

GRANTS
Carol Irwin

INSTRUMENT REPAIR SHOP
Anthony Solyom

LABORATORY ANIMAL CARE ADMINISTRATION
Janet F. Baer, Director
Claire Lindsell, Assistant Veterinarian
Cynthia Tognazzini, Facilities Operations Manager
Peggy Blue

MACHINE SHOP
Leroy Lamb

PERSONNEL
Mary Marsh

RESEARCH FELLOW PROGRAM
Gwenda Murdock

STOCKROOM AND SUPPLIES
William F. Lease, Supervisor
Giao K. Do
Jesse E. Flores
Jose Gonzales
Pat Perrone

WORD PROCESSING FACILITY
Stephanie A. Canada, Supervisor
Yolanda Duron

BECKMAN INSTITUTE
Alice Doyle, Grants
Laurinda Truong, Personnel
Manny de la Torre, Receiving

THE MABEL AND ARNOLD BECKMAN LABORATORIES OF BEHAVIORAL BIOLOGY
Debbie Navarette, Grants
Julie A. Schoen, Grants
Sandra Koceski, Personnel/Accounting
Patricia Mindorff, Special Projects

Michael P. Walsh, Supervisor, Electronics Shop
Tim Heitzman, Electronics Shop

BRAUN LABORATORIES IN MEMORY OF CARL F AND WINIFRED H BRAUN

BROAD CENTER FOR THE BIOLOGICAL SCIENCES
Samantha J. Westcott, Grants
Janie Malone, Personnel
Andreas Feuerabendt, Receiving

WILLIAM G. KERCKHOFF MARINE LABORATORY

Molecular, Cellular and Integrative Neuroscience

John M. Allman, Ph.D.
Richard A. Andersen, Ph.D.
David J. Anderson, Ph.D.
Seymour Benzer, Ph.D., D.Sc.h.c.
Mary B. Kennedy, Ph.D.
Masakazu Konishi, Ph.D.
Gilles Laurent, Ph.D., D.V.M.
Henry A. Lester, Ph.D.
Paul H. Patterson, Ph.D.
Erin M. Schuman, Ph.D.
Shinsuko Shimojo, Ph.D.
Thanassios G. Siapas, Ph.D.
Kai G. Zinn, Ph.D.

Frank P. Hixon Professor of Neurobiology: **John M. Allman**
Postdoctoral Fellow: Jason A. Kaufman
Graduate Student: Karli K. Watson
Research and Laboratory Staff: Virginie Goubert, Atiya Hakeem

Summary: We are mainly concerned with brain evolution as revealed through the comparative study of brain structure and with the neural mechanisms of economic and social decision-making. These two interests come together in our investigation of the Von Economo (spindle) neurons of anterior cingulate and fronto-insular cortex. These neurons are present only in humans and apes and are much more abundant in humans than in apes; they thus represent a recent development in hominoid evolution. The Von Economo cells emerge mainly after birth and are 30% more abundant in the right hemisphere. We think that the Von Economo neurons are part of the circuitry responsible for rapid intuitive choice in complex social situations.

Another facet of our laboratory research is the incorporation of neuroimaging modalities, particularly MRI, into the analysis of comparative brain anatomy. We are investigating the structure of the brain in another highly social mammal, the African elephant, using MRI. And we are currently working with a new variant of MRI, called diffusion tensor imaging, which can be used to characterize the orientation and coherence of white matter tracts in the brain. In order to quantitatively validate this emerging technology, we are comparing measurements of fiber anisotropy from DTI scans with measurements of fiber coherence as measured from histological preparations performed on the same specimens.

1. **Neuroanatomy of the African elephant brain from magnetic resonance images**
   Atiya Y. Hakeem, Patrick R. Hof[1], Chet C. Sherwood[2], Robert C. Switzer III[3], L.E.L. Rasmussen[4], John M. Allman

We acquired magnetic resonance images (MRI) of the brain of an adult African elephant, *Loxodonta africana,* in the axial and parasagittal planes and produced anatomically-labeled images. The elephant has an unusually large and convoluted hippocampus compared to primates and especially to cetaceans. This may be related to the extremely long social and chemical memory of elephants. We quantified the volume of the whole brain and of the neocortical and cerebellar gray and white matter. The white matter to gray matter ratio in the elephant neocortex and cerebellum are in keeping with that expected for a brain of this size. The ratio of neocortical gray matter volume to corpus callosum cross-sectional area is similar in the elephant and human brains, emphasizing the difference between terrestrial mammals and cetaceans, which have a very small corpus callosum relative to the volume of neocortical gray matter.

[1]Department of Neuroscience, Mount Sinai School of Med.
[2]Department of Anthropology and School of Biomedical Sciences, Kent State University
[3]NeuroScience Associates, Knoxville, TN
[4]Oregon Health and Sciences University
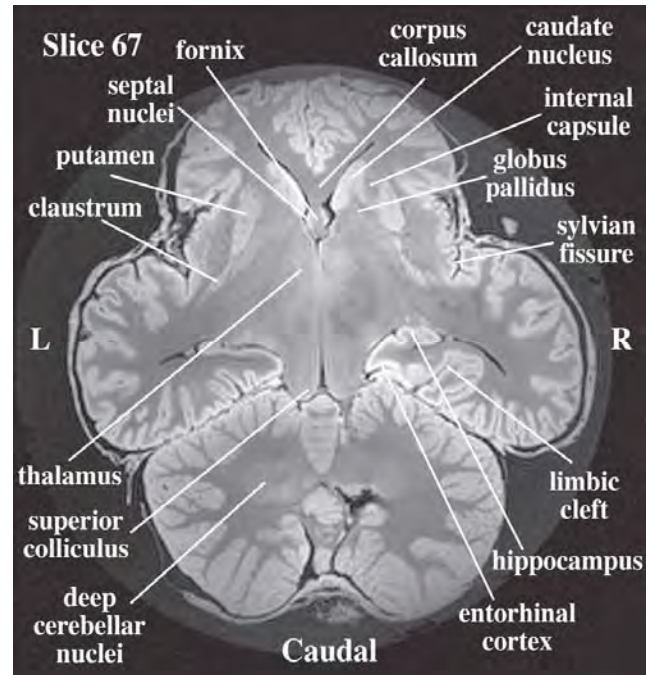
2. **Intuition and autism: A possible role for Von Economo neurons**
   John M. Allman, Karli K. Watson, Nicole A. Tetreault[1], Atiya Y. Hakeem

Von Economo neurons (VENs) are a recently evolved cell type that may be involved in the fast intuitive assessment of complex situations. As such, they could be part of the circuitry supporting human social networks. We propose that the VENs relay an output of fronto-insular and anterior cingulate cortex to the parts of frontal and temporal cortex associated with theory-of-mind, where fast intuitions are melded with slower, deliberative judgments. The VENs emerge mainly after birth and increase in number until age 4 years. We propose that in autism spectrum disorders the VENs fail to develop normally, and that this failure might be partially responsible for the associated social disabilities that result from faulty intuition.

[1]Graduate student, University of California, Los Angeles

3. **The Von Economo neurons develop mainly postnatally in human fronto-insular cortex**
   John Allman, Nicole Tetreault[1], Atiya Hakeem

The Von Economo neurons (VENs, also sometimes called spindle cells) are found only in humans and African apes. The VENs develop late in ontogeny as well as phylogeny. They first appear in very small

numbers in the 35th week of gestation and at full term (38 to 40 weeks postconception) only about 10% of the full complement are present. The number of VENs is increased in a 42 week post-conception neonate and even more in the 7 month old infant, suggesting a fairly rapid increment during infancy. The adult number is attained by 4 years of age. This postnatal increment in VEN population may arise by differentiation from a pre-existing cell type or by migration from a germinal zone in the lateral ventricles. In all of the apes and the 4 year-old and adult human brains, the VENs are about 30% more numerous in right hemisphere fronto-insular cortex (FI). This right hemisphere predominance develops postnatally. The VENs are only about 3% more numerous in the right hemisphere in the 38-40 week neonates; about 19% more in the 42-week neonate; and about 98% more in the 7 month old infant. These data suggest that the VENs in the right FI develop more rapidly than in the left during infancy. The right hemisphere VEN predominance may be related to the right hemispheric specialization for the social emotions. The fact that this 30% right preference is so tightly regulated and consistent across humans and apes (past the infant period) suggests that this ratio is important for normal functioning and that deviations from it could be dysfunctional. The right predominance in the VENs is consistent with the results of Watkins *et al.*, who compared the left and right hemispheres with MRI in a large population of normal subjects and found that the cortical gray matter volume was consistently larger in the right FI.

[1]*Graduate student, University of California, Los Angeles*

Reference

Watkins, K.E., Paus, T., Lerch, J.P., Zijdenbos, A., Collins, D.L., Neelin, P., Taylor, J., Worsley, K.J. and Evans, A.C. (2001) *Cereb. Cortex* **11**(9):868-877.

4.   The role of the frontoinsular cortex in social cognition
Corinna Zygourakis[1], John M. Allman

Several lesion and neuro-imaging studies collectively suggest that FI and adjacent cortex is responsive to "social intention" in the form of angry faces, feelings of guilt, violations of social norms, empathy, and cooperation. We therefore hypothesize that Von Economo neurons play a key role in the detection of social emotions, perhaps by quickly relaying the processing of embarrassment, empathy, guilt, and shame to other brain structures. FI lesions (that destroy the FI Von Economo cells) may hinder a person's ability to detect expressions of these four social emotions.

To test our hypothesis, we develop a protocol based on film clips depicting these emotions. FI lesion and non-brain-damaged control subjects view the film clips and answer questions pertaining to the situational, emotional, and moral content of the stimuli. Statistical analysis indicates that the lesion patients understand the complex social situations depicted in the film clips. In other words, they are not deficient in their ability to detect the non-emotional, objective features of the film clips.

However, the lesion subjects are significantly impaired in their ability to recognize the social emotions. The lesion subjects' scores for embarrassment, empathy, guilt, and shame are significantly lower than those of the control subjects. Moreover, the lesion subjects tend to rate situations as being more reprehensible and morally unacceptable than the non-brain-damaged controls.

Thus, the remarkably abnormal emotional and social behavior of the FI lesion subjects may be explained, at least in part, by their deficiencies in social emotion detection. It appears that the FI is, in fact, part of the neural circuitry that interprets social intention.

[1]*Undergraduate, Caltech*

5.   Measuring reversal learning: Introducing the variable Iowa gambling task
Stephanie Kovalchik[1], John M. Allman

We developed a modification of the Iowa gambling task (IGT) to test whether it is primarily a measure of reversal learning. Named the Variable IGT (VIGT), the design involves a contingency reversal midway through the task. Two versions of the task enabled us to study the effect of a stronger prepotent response on the ability to identify and adapt to contingency reversal. A significant reversal delay was observed among normal young players with a more dominating reward response. Although transitory, this delay is comparable to the characteristic behavioral impairment observed in patients with damage to the ventromedial prefrontal cortex (VM), addicts, psychopaths and individuals with other self-destructive disorders: they persist in a previously rewarding behavior despite long-term heavy costs.

We also conducted the VIGT in a sample of healthy elderly adults. Results from this sample do not support VM-like or risk-aversive theories of aging but are inconclusive regarding the frontal aging hypothesis. Overall, our findings indicate that the VIGT is a sensitive and versatile measure of reversal learning and will serve as a useful instrument in future studies of affective decision making, addiction and other self-destructive behavior.

[1]*Graduate student, University of California, Los Angeles*

6.   Anatomical analysis of an aye-aye brain combining histology, MRI, and DTI
Jason A. Kaufman, Eric T. Ahrens[1], David H. Laidlaw[2], Song Zhang[2], John M. Allman

The aye-aye (*Daubentonia madagascariensis*) is a remarkable primate whose ecological specializations as an extractive forager are unique among the order Primates. We report initial results of a multi-modal analysis of tissue volume and microstructure in the brain of an aye-aye. We scanned the left hemisphere of an aye-aye brain using T2-weighted structural magnetic resonance imaging (MRI) and diffusion-tensor imaging (DTI) prior to histological processing and staining for Nissl substance and myelinated fibers. The objectives of our experiment were to estimate the volume of gross brain regions for comparison with published data on other prosimians, and to validate DTI data on fiber anisotropy with histological measurements of

fiber spread. Measurements of brain structure volumes in our specimen are consistent with those reported in the literature: the aye-aye has a very large brain for its body size, it has a reduced volume of visual structures (V1 and LGN), and an increased volume of the olfactory lobe. This trade-off between visual and olfactory reliance is a reflection of the nocturnal extractive foraging behavior practiced by *Daubentonia*. Additionally, frontal cortex volume is large in the aye-aye, a feature that could also be related to its complex foraging behavior and increased sensorimotor intelligence. Our analysis of white matter fiber structure in the anterior cingulum bundle demonstrates a strong correlation between fiber spread as measured from histological sections and fiber spread as measured from DTI. These results represent the first quantitative comparison of DTI data and fiber-stained histology in the brain.

[1] *Department of Biological Sciences and the Pittsburgh NMR Center for Biomedical Research, Carnegie Mellon University*
[2] *Department of Computer Science, Brown University*

7. 3D visualization and volumetry of two brains with agenesis of the corpus callosum

Jason A. Kaufman, Andréa E. Granstedt[1], Lynn K. Paul[2], John M. Allman

Embryonic dysgenesis of the corpus callosum can produce partial or complete absence of the major body of commissural fibers that unite the cerebral hemispheres. Normal-functioning acallosal patients typically experience varying degrees of sensorimotor and social deficits, but the congenital absence of the corpus callosum is not as functionally debilitating as adult callosotomy. To better understand the gross morphology of acallosal brains, and to investigate possible anatomical compensatory mechanisms, we performed 3D reconstructions and volumetry in two postmortem brains – one with complete agenesis, and one with a partial callosal defect in which the splenium and posterior portion of the corpus callosum were absent. Myelin-stained histological brain sections were digitized and processed for three-dimensional visualization and volume modeling. Analysis of grey and white matter volume and ratio to brain weight suggest a higher ratio of grey to white matter in the acallosal brains compared with published values of normal individuals. The anterior commissure and net white matter volume, adjusted to smaller brain weight, were within normal range, but the ventricles were enlarged. Longitudinal callosal fibers (Probst's bundles) were clearly visible in the complete agenesis brain, but these bundles do not appear large enough to completely account for the mass of the absent corpus callosum. Malformation of the cingulate cortex appears to be a regular feature of callosal dysgenesis, and may contribute to deficits in social functioning in acallosal individuals.

[1] *Graduate Student, Princeton University*
[2] *Division of Humanities and Social Sciences, Caltech*

8. Dendritic architecture of the Von Economo neurons

Karli K. Watson, Tiffanie Jones[1], John M. Allman

Von Economo neurons are bipolar cells located in the frontoinsula (FI) and anterior cingulate cortex (ACC) of humans and great apes. These two regions, and therefore the Von Economo cells themselves, are implicated in rapid, intuitive decision-making, a cognitive skill that is crucial for successful social interaction. We sought to further characterize the anatomy of these unusual cells. The use of Golgi and immunocytochemical techniques enables us to study their dendritic architecture and receptor expression, respectively.

We used the software system Neurolucida to reconstruct Golgi stained pyramidal and Von Economo neurons from post-mortem human tissue, and the resulting three-dimensional models provided us with summary statistics about how the two neuronal populations differ. We found that the elongated and symmetric qualities of the Von Economo neuron soma are also characteristic of the dendritic trees of these cells. They are significantly less complex than their pyramidal counterparts, having fewer branch points and spines. This is particularly evident in the basal dendritic tree: While pyramidal neuron basal dendrites are numerous and branchy, the basal dendrites of the Von Economo cells resemble the sparse trunk characteristic of the apical dendrites in both cell types. This suggests that the Von Economo cells are doing a relatively simple computation. The low density of spines on these cells, together with the high density of dopamine D3 receptors that blanket the cell membrane, may suggest that the majority of the neurochemical transmission reaching these cells is extra-synaptic.

[1] *MURF student, Caltech*

9. Immunohistochemistry of the Von Economo neurons

Karli K. Watson, John M. Allman

Immunohistochemistry of human post-mortem tissue, coupled with fMRI paradigms that activate the Von Economo regions, allow us to make educated guesses as to the function of these cells. For example, the high-affinity dopamine D3 receptor is expressed heavily on the soma and apical dendrites of the Von Economo neurons, which suggests that these neurons have a role in mediating uncertain reward. Additionally, the V1a receptor is strongly expressed in this region, including on the somas of the Von Economo neurons. This is interesting in light of the involvement of this receptor in social bonding and affiliation. We also see strong expression of the 5HT-2b receptor on these cells, an unusual occurrence since this receptor is uncommon in the brain and widely present throughout the gastrointestinal system (Baumgarten and Gothert, 1997). This may link these cells to the phenomenon of "interoception" – the monitoring of one's bodily states. Taken together, these results suggest that these newly evolved cells are part of a circuit mediating the real-time control of behavior in response to quickly changing and ambiguous stimuli.

28

Reference
Baumgarten, H.G. and Gothert M. (1997) Handbook of Experimental Pharmacology: Serotoninergic Neurons and 5-HT receptors in the CNS, Springer-Verlag.

10. Reduction and displacement of Von Economo neurons in agenesis of the corpus callosum

Jason A. Kaufman, Lynn K. Paul[1], John M. Allman

Individuals with congenital absence of the corpus callosum (callosal agenesis) exhibit less severe functional disconnection syndromes than are typical of patients who have had the corpus callosum surgically sectioned as adults. However, individuals with callosal agenesis appear to suffer from psychosocial deficits that are uncommon in callosotomy patients. For example, agenesis patients with normal intelligence have difficulty comprehending humor and affect-laden speech, as well as interpreting emotional cues (Brown and Paul, 2000; Brown *et al.*, 2005; Paul *et al.*, 2004). In order to investigate possible neurohistological malformations that could relate to deficits in emotional processing in these individuals, we analyzed the number and location of Von Economo neurons in the fronto-insular cortex (FI) of postmortem agenesis brains. The Von Economo neurons are a unique morphotype of large, bi-polar projection neuron found in FI, as well as anterior cingulate cortex, and have been implicated in social intuition and emotional cognition.

In three cases of complete agenesis of the corpus callosum, we found the Von Economo neurons to be virtually absent, with only a scattering of cells in FI and ACC. In one case of partial callosal agenesis, the total number of Von Economo neurons in FI was remarkably reduced. The left FI contained approximately 19,200 cells, compared with 47,500 cells in a normal control brain. The right FI contained approximately 24,600 cells, compared with 60,000 in a normal control. Previous work in our lab has demonstrated a consistent right-dominant asymmetry in Von Economo cell number in normal individuals; the right FI typically contains approximately 30% more Von Economo neurons. Despite the reduction in total number of cells in the partial agenesis case, the normal right-dominant asymmetry is retained. However, the Von Economo neurons in FI of the partial agenesis case were displaced medially. Instead of being located in the classic FI gyrus, the cells were abnormally located in the postero-medial orbital frontal cortex (Figure 1). We hypothesize that absence and/or reduction of Von Economo neurons in cases of callosal agenesis may contribute to deficits in social processing in these individuals.

[1]*Division of Humanities and Social Sciences, Caltech*

References
Brown, W.S. and Paul, L.K. (2000) *Cog. Neuropsych.* **5**(2):135-157.
Brown, W.S. and Paul, L.K., Symington, M. and Dietrich, R. (2005) *Neuropsychologia* **43**(6):906-916.
Paul, L.K., Schieffer, B. and Brown, W.S. (2004) *Arch. Clin. Neuropsych.* **19**(2):215.
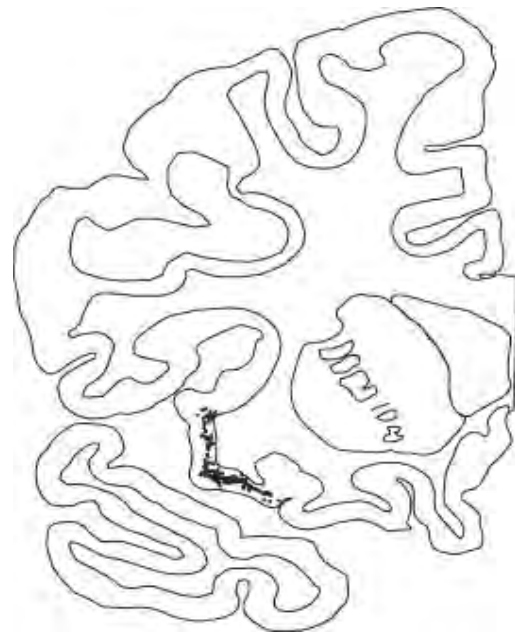
Normal 50 year-old female
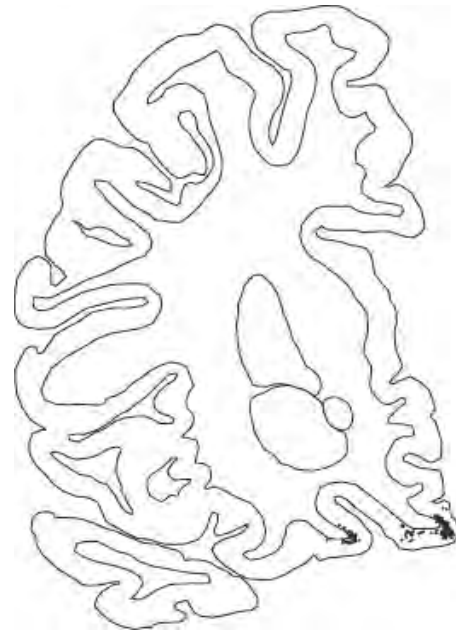
Partial agenesis 71 year-old female

Figure 1. Location of the Von Economo neurons in the fronto-insular cortex of a normal control case, compared with a case of partial agenesis of the corpus callosum. In the partial agenesis case, the Von Economo neurons are abnormally located and reduced in number.

Publications

Allman, J.M., Watson, K.K., Tetreault, N.A. and Hakeem, A.Y. (2005) Intuition and autism: Role of Von Economo neurons. *Trends Cogn. Sci.* **9**(8):367-373.

Bush, E.C. and Allman, J.M. (2004) Three-dimensional structure and evolution of primate primary visual cortex. *Anat. Rec. A* **281**A(1):1088-1094.

Bush, E.C., Simons, E.L. and Allman, J.M. (2004) High-resolution computed tomography study of the cranium of a fossil anthropoid primate, *Parapithecus grangeri*: New insights into the evolutionary history of primate sensory systems. *Anat. Rec. A* **281**A(1):1083-1087.

Hakeem, A.Y., Hof, P.R., Sherwood, C.C., Switazer, R.C., Rasmussen, L.E.L. and Allman, J.M. (2005) The brain of the African elephant (*Loxodonta africana*): Neuroanatomy from magnetic resonance images. *Anat. Rec.* In press.

Kaufman, J.A., Ahrens, E.T., Laidlaw, D.H., Zhang, S. and Allman, J.M. (2005) Anatomical analysis of an aye-aye brain (*Daubentonia madagascariensis*, Primates: Prosimii) combining histology, structural MRI, and diffusion-tensor imaging (DTI). *Anat. Rec.* In press.

Kovalchik, S. and Allman, J. (2005) Impaired reversal learning in normal individuals on a modified Iowa Gambling Task: An emotional decision-making study of healthy young and elderly individuals. Cognition & Emotion. In press.

30

James G. Boswell Professor of Neuroscience: Richard A. Andersen
Visiting Associates: William L. Caton, Igor Fineman, Mel Goodale, Rodrigo Quian-Quiroga
Member of the Professional Staff: Boris Breznen
Research Fellows: Rachel Berquist[1], Marina Brozovic, Chris Buneo, Jorge Cham[1], Jason Connolly, He Cui, Alexander Gail, Bradley Greger, EunJung Hwang, Igor Kagan, Axel Lindner, Sam Musallam, Zoltan Nadasdy, Zoran Nenadic[1], Bijan Pesaran, Dan Rizzuto, Elizabeth Torres
Graduate Students: Rajan Bhattacharyya, Eddie Branchaud[1], Michael Campos, Hilary Glidden, Asha Iyer, Brian Lee, Daniella Meeker, Grant Mulliken, Matthew Nelson, Michael Wolf[1]
Research and Laboratory Staff: Kristen Andersen, Aleksandra Ilicheva, Kelsie Pejsa, Nicole Sammons, Viktor Shcherbatyuk, Tessa Yao
[1]*Mechanical Engineering, Caltech*

Summary: **Neural mechanisms for visual-motor integration, spatial perception and motion perception.**
While the concept of artificial intelligence has received a great deal of attention in the popular press, the actual determination of the neural basis of intelligence and behavior has proven to be a very difficult problem for neuroscientists. Our behaviors are dictated by our intentions, but we have only recently begun to understand how the brain forms intentions to act. The posterior parietal cortex is situated between the sensory and the movement regions of the cerebral cortex and serves as a bridge from sensation to action. We have found that an anatomical map of intentions exists within this area, with one part devoted to planning eye movements and another part to planning arm movements. The action plans in the arm movement area exist in a cognitive form, specifying the goal of the intended movement rather than particular signals to various muscle groups.

One project in the lab is to develop a cognitive-based neural prosthesis for paralyzed patients. This prosthetic system is designed to record the electrical activity of nerve cells in the posterior parietal cortex of paralyzed patients, interpret the patients' intentions from these neural signals using computer algorithms, and convert the "decoded" intentions into electrical control signals to operate external devices such as a robot arm, autonomous vehicle or a computer.

Recent attempts to develop neural prosthetics by other labs have focused on decoding intended hand trajectories from motor cortical neurons. We have concentrated on higher-level signals related to the goals of movements. Using healthy monkeys with implanted arrays of electrodes we recorded neural activity related to the intended goals of the animals and used this signal to position cursors on a computer screen without the animals emitting any behaviors. Their performance in this task improved over a period of weeks. Expected value signals related to fluid preference, or the expected magnitude or probability of reward were also decoded simultaneously with the intended goal. For neural prosthetic applications, the goal signals can be used to operate computers, robots and vehicles, while the expected value signals can be used to continuously monitor a paralyzed patient's preferences and motivation.

Our laboratory also examines the coordinate frames of spatial maps in cortical areas of the parietal cortex coding movement intentions. Recently, we have discovered that plans to reach are coded in the coordinates of the eye. This is particularly interesting finding because it means the reach plan at this stage is still rather primitive, coding the plan in a visual coordinate frame rather than the fine details of torques and forces for making the movement. We have also discovered that when the animal plans a limb movement to a sound, this movement is still coded in the coordinates of the eye. This finding indicates that vision predominates in terms of spatial programming of movements in primates.

Another major effort of our lab is to examine the neural basis of motion perception. One series of experiments is determining how optic flow signals and efference copy signals regarding eye movements are combined in order to perceive the direction of heading during self-motion. These experiments are helping us understand how we navigate as we move through the world. A second line of investigation asks how motion information is used to construct the three-dimensional shape of objects. We asked monkeys to tell us which way they perceived an ambiguous object rotating. We found an area of the brain where the neural activity changed according to what the monkey perceived, even though he was always seeing the same stimulus. In other experiments we have been examining how we rotate mental images of objects in our minds, so-called mental rotation. In the posterior parietal cortex we find that these rotations are made in a retinal coordinate frame, and not an object based coordinate frame, and the mental image of the object rotates through this retinotopic map.

We have successfully performed functional magnetic resonance imaging (fMRI) experiments in awake, behaving monkeys. This development is important since this type of experiment is done routinely in humans and monitors the changes in blood flow during different cognitive and motor tasks. However, a direct correlation of brain activity with blood flow cannot be achieved in humans, but can in monkeys. Thus, the correlation of cellular recording and functional MRI activation in monkeys will provide us with a better understanding of the

many experiments currently being performed in humans. A 4.7 Tesla vertical magnet for monkey imaging has recently been installed in the new imaging center in the Broad building. We will use this magnet, combined with neural recordings, to examine the correlation between neural activity and fMRI signals.

11.   Reaching in depth: Neural activity in posterior parietal cortex reflects distance to target and vergence angle
R. Bhattacharyya, S. Musallam, R.A. Andersen

Neurons in the posterior parietal cortex play a variety of roles in spatial awareness, orienting behavior, and movement planning, such as computing sensorimotor transformations for reaches and eye movements.   To investigate the modulation of neural activity by target distance and vergence angle we obtained extracellular recordings in the intraparietal sulcus of a monkey (*Macaca mulatta*) trained to perform reaches to a remembered location. Eye and hand target stimuli were presented in the dark. They were isolated luminous targets with well-defined edges in order to minimize depth cues other than blur and disparity. Trials were initiated by placing both hands on sensors situated at hip level 15cm in front of the eyes. The animal fixated a target placed in the line of sight and maintained hand positions on sensors for a one second interval after which a cue to a peripheral reach target briefly flashed. After a memory period of 1s the animal was instructed to reach to the remembered target location with his right hand while maintaining his gaze. The four reach targets at 25, 27.5, 30, and 32.5 cm from the monkey's face spanned the animal's full reaching range. Three eye fixation targets at 15, 35, and 105 cm corresponded to 13 degrees, 5.5degrees, and 1.2degrees of vergence angle. Spiking activity from 21 cells revealed significant tuning for reach depth (n=15) and for fixation depth (n=10) in at least one trial epoch (ANOVA, p<0.05), with most cells being modulated in the memory period (n=13 and 7, respectively). Linear regression techniques were used to investigate gain modulation. Planar fits of spiking activity to reach and fixation depth were significant (p<0.05) for 17 cells in at least one trial epoch, with most cells exhibiting planar gain fields in the memory period (n=15).

12.   The role of recurrent connections in the processing of reach movements in the parietal cortex
M. Brozovic, A. Gail, R.A. Andersen

We present a theoretical study on the role of recurrent connections in processing sensorimotor transformations in the posterior parietal cortex.   An experimental study (A. Gail SfN 2005) shows that activity in the monkey parietal reach region (PRR) represents the spatial goal of reach movements rather than the location of the visual cue during an anti-reach task.   A two-dimensional, three-layer neural network (Zipser-Andersen type) with two different kinds of recurrent connections was trained to represent reach goals in its output layer, depending on the location of a visual cue and the behavioral context (reach/anti-reach) fed into its input layer. The network was trained using a backpropagation-

through-time algorithm allowing the network to simulate memory-guided reach planning.

In the first version of the model only the units in the hidden layer were recurrently connected. The units in the hidden layer ('PRR') developed receptive fields with a spatial tuning representing the visual cue that was gain modulated with respect to the task being either a reach or an anti-reach. This means, although the network produced temporal dynamics and the desired output mapping, it could not explain experimental finding of motor-like tuning in PRR.

In a second model version we introduced additional recurrent feedback connections between the output and the hidden layer units.   Again the network learned the proper input-output transformations. But this time the activity of the units in the hidden layer additionally reproduced the experimentally observed dependence of the spatial tuning from the movement goal instead of the visual cue. In conclusion, we suggest that the encoding of movement goals in the parietal cortex depends on top-down projections of motor-related activity from frontal areas during the learning of context-dependent, spatial visuomotor associations.

13.   Time-invariant spatial representations in the posterior parietal cortex
C.A. Buneo, A.P. Batista, M.R. Jarvis, R.A. Andersen

Neurophysiological studies suggest that the transformation of visual signals into arm movement commands involves a simultaneous rather than sequential recruitment of the various reach-related regions of the cortex. However, little is known about how the reference frames used to encode reaches within these areas vary with the time taken to generate a behavioral response. Here we report an analysis of these reference frames in area 5 (N=89) and PRR (N=87) as a function of time within an instructed-delay task.   The reference frame that best accounted for cell activity was identified by quantifying the variability in firing rate when target and/or starting position were held fixed within one reference frame, but varied in other frames. At both the single cell and population levels, data were analyzed during a "cue" epoch (100-400 ms after cue onset), a "memory" (400-800 ms after cue onset), and a "reach" epoch (200 ms before until 200 ms after movement onset). At the population level data were also analyzed using a sliding 200 ms long window centered on consecutive 100 m sec intervals of the task.

At the population level, the reference frames that best described the encoding of reach variables did not evolve dynamically within each area but were fixed as a function of time. At the single cell level, the best fitting reference frame did vary with time for many cells. However, the net result of this coordinate frame "switching" was that close to 50% of the neurons in both areas were encoding in the same preferred reference frame throughout the task; as previously reported this frame was fixed to the eyes in PRR and to both the eye and hand in area 5. The present results suggest that the various stages of the coordinate transformation for reaching do not evolve gradually in time within the cortical visuomotor network;

rather, once target-related information is instantiated in the network, all stages of the transformation coexist simultaneously.

14. Event detection in SEF and spatial representations in LIP during an irrelevant object saccade task

M. Campos, B. Breznen, R.A. Andersen

We have previously reported the representation of object variables in LIP and SEF during the performance of an object-based saccade task, finding that LIP is involved in spatial transformations underlying saccades, while SEF encodes abstract task-specific associations (Breznen *et al.*, 2003, 2004). We now address whether object variables are represented in these areas in a naïve macaque monkey with no exposure to the object-based task. In contrast to other studies (Sereno and Maunsell, 1998), our subject did not perform any tasks in which objects were relevant for task performance. Subjects performed two tasks—a memory-guided saccade task and an irrelevant-object task, in interleaved trials. The irrelevant-object task was identical to the memory task, except that one of three objects, chosen randomly, was presented foveally at a random orientation during the fixation period at the beginning of the trial. We found that most task-related LIP neurons (~70%) and a minority of task-related SEF neurons (~20%) exhibited retinotopic spatial tuning during the memory task. The majority of SEF neurons (~65%) instead responded to different task events (e.g., cue on, fixation point off) with phasic non-spatial increases in firing rate. In the irrelevant-object task we found that both populations of neurons responded to the presentation of the object, but that neither population showed selectivity to the object type. The lack of object-type tuning suggests that the previously reported shape selectivity in LIP (Sereno and Maunsell, 1998) may have resulted from exposure to tasks requiring the discrimination of object shapes for movement planning. Some object-responsive LIP neurons (~30%) were tuned to object orientation, but no SEF cells exhibited orientation tuning. Rather, as in the memory task, SEF neurons indicated that the object presentation and extinction events had occurred without carrying spatial (orientation) information. Thus while LIP tends to represent spatial aspects of the tasks, SEF appears to be more concerned with identifying task events and variables that are not necessarily spatial.

15. Neural activity in the posterior parietal cortex during decision-making for generating visually guided eye and arm movements

H. Cui, H. Scherberger, R.A. Andersen

The posterior parietal cortex (PPC) of the rhesus monkey has been found to encode impending decisions reported by saccadic eye movement or reaching arm movement alone, but it is still unclear if such neural activity merely reflects higher-order sensory integration or early movement planning. To examine the role of PPC in decision-making across effectors, we recorded single-neuron activity from monkey performing an eye or hand target selection task. At the beginning of each trial, the monkey had to fixate and touch a fixation point on a target board. Two green (red) targets were presented inside the

neuronal response field and opposite to the fixation point at the same distance. Immediately after stimulus presentation, the monkey had to select one of the stimuli as a target and touch (fixate) the selected target to receive a juice reward that was independent of the choice. The stimulus onset asynchrony (SOA) between the two stimuli was adjusted by a staircase procedure until both targets were selected equally often. Preliminary results from two monkeys indicated that PPC neurons can be classified into three populations that relate different stages of decision-making. The first class of cells did not show correlation between the firing rate and monkey's behavioral choice, and appeared to encode solely sensory processing. The second class of neurons exhibited significant differences in activity related to target selection for both eye and arm movements, so they may encode a general decision about a spatial goal regardless of the effector. The third class consisted of cells carrying effector-specific activity that were predictive of the monkey's decision only during either saccade or reach trials. As a sensory-motor interface, PPC seems to be involved in different stages of decision-making processes for both eye and arm movements.

16. Touching the void – Posterior parietal cortex encodes movement goals during an anti-reach task

A. Gail, R.A. Andersen

The posterior parietal cortex plays a key role in performing sensorimotor transformations. To determine the relative contributions of visual sensory processing and movement planning for reaches in the neural activity of the medial intraparietal area (MIP) we performed a memory-guided anti-reach experiment in monkey. In an instructed-delay, center-out reach task the monkey had either to reach to a memorized peripheral target position (PRO-reach) or to a diametrically opposed position (ANTI) while keeping central ocular fixation. PRO- and ANTI-trials were pseudo-randomly interleaved and indicated to the monkey from the beginning of the trial by a color cue. We analyzed MIP single unit activity with respect to spatio-temporal response selectivity. The spatial tuning of the recorded neurons mainly depended on the position of the reach goal, not of the instruction stimulus. This was true not only late in the memory period, shortly before the movement initiation, but, more remarkably, immediately after the visual cue presentation at the beginning of the memory period. These findings support the hypothesis that MIP activity represents information about the planned reach movement rather than the memorized cue location or spatial visual attention. Hence, MIP seems capable of integrating spatial sensory information and abstract behavioral rules (PRO/ANTI) to represent the desired movement goal independent of the instruction stimulus (see Brozovic *et al.*, SfN 2005, for accompanying model simulations). The spatial tuning of MIP neurons evolves later in the ANTI- than in the PRO-condition, while the latency of the overall activation is comparable, i.e., the early activity in the ANTI-condition is not tuned. The delay in tuning corresponds well to reaction times being increased by 40-60 ms in the ANTI- as compared to PRO-condition, when the monkey, in a modified version of the task, was allowed to reach immediately once the

peripheral cue was flashed. This could indicate that MIP is involved in computing an inversion vector in case of the anti-reaches.

17. Localizing neuroprosthetic implant targets with fMRI: Premotor, supplementary motor and parietal regions
H.K. Glidden, D.S. Rizzuto, R.A. Andersen

Monkey recordings from premotor and parietal areas, including the parietal reach region (PRR), yield control signals for brain-machine interfaces to move a computer cursor or a robotic arm. Recently, there have been efforts towards transitioning the monkey findings to develop human brain machine interfaces for severely paralyzed patients, but as yet there is little precedent for finding human homologues of these high-level areas that have been functionally-defined in monkeys. Because severely paralyzed patients cannot execute real hand and arm movements, it is crucial to activate these human homologues using imagined movements to localize potential implant regions with fMRI. Utilizing event-related fMRI and a version of the delayed-reach task including both real and imagined pointing movements, we have identified regions involved in preferentially planning real and imagined points and not saccades. Our results in normal subjects reveal that such specialized regions exist in dorsal premotor cortex (PMd), the supplementary motor area (SMA), and medial posterior parietal cortex (PPC), where motor planning (target and effector known) activates these regions more than motor preparation (only effector known) or spatial attention (only target known). Imagined pointing did not elicit activity in primary motor cortex or the cingulate motor area, and point-related activity in these regions was limited to the movement period and not the delay period, reflective of involvement in point-execution and not point planning. Thus, we have identified brain regions specific for planning real and imagined hand vs. eye movements, including PMd, SMA and medial PPC. Combining fMRI with image-guided neurosurgery may allow the extraction of neuroprosthetic control signals from these regions in paralyzed patients.

18. Evidence for gain modulation as a mechanism of sensory-motor adaptation in the posterior parietal cortex
Bradley Greger, Marina Brozovic, Alexander Gail, R.A. Andersen

Neurons in a region of the posterior parietal cortex (PPC), the lateral intra-parietal area (LIP), are known to encode information related to eye movements. We tested LIP's involvement in sensory-motor adaptation by recording the neural activity of LIP neurons in the non-human primate during the performance of a memory-guided saccade task.

Memory guided saccades were adapted using a standard back-stepping paradigm. We tested for significant alterations of receptive fields (RFs) in response to saccadic adaptation and examined RF dynamics throughout the experimental session. Significant alterations of RFs predominately occurred as changes in gain, or changes in gain plus shifts in location. The alterations of RFs could occur during any or all of the three trials periods; stimulus

presentation, memory period, or peri-saccadic period. RF dynamics followed different time courses in different neurons during saccade adaptation, with RFs in some neurons rapidly altered either early or late in adaptation, while RFs in some neurons were altered progressively throughout adaptation.

We also developed a Zipser-Andersen neural network to model how neurons in the PPC alter their RFs when a perturbation mimicking saccade adaptation was introduced to their sensory-motor mapping. The tuning curves of the hidden units showed similar behavior to that observed in LIP neurons. Approximately half of units exhibited gain modulation, while the other half exhibited more complex gain plus shift behavior. The RF dynamics of many hidden units paralleled that observed in LIP neurons.

These results suggest that LIP plays a role in the adaptation of visually guided saccades mediated primarily through gain field modulation. In both the data and model the alteration in RFs paralleled the different aspects of saccadic adaptation, e.g., error feedback or motor output, suggesting different roles in sensory-motor adaptation for different population of LIP neurons.

19. Functional MRI in alert behaving monkeys during goal-directed saccades
Igor Kagan, Asha Iyer, Axel Lindner, R.A. Andersen

We developed experimental techniques to study the neural substrates of goal-directed oculomotor behavior in trained rhesus macaques using a high-field 4.7 T vertical MRI scanner. We recorded BOLD activity, eye movements, reward and timing information while monkeys performed direct and memory saccades to visual cues during GE-EPI scans. Using a saccade vs. fixation block design, we obtained reliable activation maps of cortical and subcortical structures implicated in eye movement control. Next we compared BOLD responses during direct and memory saccades, in order to extract spatial-specific memory and/or planning signals. However, differential activation between memory and direct saccades in the block design was obscured, in part because block activity comprises signals from several task-related components.

We therefore utilized an event-related design to delineate contributions from different epochs within the task sequence - presentation of visual cues, motor planning, spatial memory, saccade execution, as well as reward expectation and acquisition. Many discrete visual, parietal, and frontal areas displayed multiple dependencies on these variables. These findings emphasize the need for cautious interpretation of potentially confounded and overlapping signals in the BOLD time-course. The analysis of "cognitive" (as contrasted to sensory and motor) components is an important prerequisite for future investigation of decision-making. Combined with FMRI-guided neurophysiological recordings in the same monkeys and with human imaging, using identical paradigms, these studies promise to form a comprehensive approach to investigation of various aspects of primate behavior.

20. MSTd represents heading in an eye-centered coordinate frame

B. Lee, B. Pesaran, R.A. Andersen

MSTd neurons are tuned to the focus of expansion of the visual image, but it is not known in which coordinate frame the tuning curves are represented. Visual signals generated by self-motion are initially represented in retinal coordinates in the very early parts of the visual system. Since this information is used to guide movement of the subject through the environment, it likely becomes represented in body or world coordinate frames at later stations in the visual-motor pathway. We performed experiments to determine whether focus tuning curves in MSTd are represented in eye, head, body, or world coordinates. Since MSTd neurons adjust their focus tuning curves during pursuit eye movements to compensate for changes in pursuit and translation speed that distort the visual image, the coordinate frame was determined for three separate conditions: fixed gaze, real pursuit, and simulated pursuit. It is possible that different coordinate frames are used to compensate for tuning curve shifts due to retinal and extraretinal signals. Focus tuning was determined at five eye positions, six degrees apart, along the preferred direction of pursuit. We recorded extracellular responses from 49 MSTd neurons in a rhesus monkey (*Macaca mulatta*). We found that the expansion focus tuning curves were aligned in an eye-centered coordinate frame as opposed to head, body, or world-centered coordinate frames for almost all cells (fixed gaze: 48/49; real pursuit: 46/49; simulated pursuit 43/49; t-test, $p<0.05$). These results indicate that MSTd neurons represent heading in an eye-centered coordinate frame in an early part of the visual-motor pathway that integrates retinal and extraretinal signals.

21. Dynamical state representation in posterior parietal cortex

G.H. Mulliken, S. Musallam, R.A. Andersen

To explore how neurons in posterior parietal cortex (PPC) encode a dynamical sensorimotor state, we recorded simultaneous neural activity from 96 microelectrodes in the medial intraparietal sulcus and area 5 during a continuous visual feedback joystick task. One monkey was trained to move a joystick in 2D to navigate a cursor on a vertical display from a central location to one of eight possible peripheral targets (11 cm away) with central fixation. The monkey was rewarded for guiding the cursor to within 1.5 cm of the target for 150 ms. Space-time receptive fields were constructed for 29 neurons by plotting the instantaneous smoothed firing rate against a set of trajectory parameters (movement angle, speed, fixation-to-target angle) across a range of lag times (-360 to 360 ms). 24/29 neurons were spatiotemporally tuned ($p<0.05$) to the movement angle of the cursor and 15 of these neurons were also spatiotemporally tuned to the speed of the cursor ($p<0.05$). 5/29 neurons were spatially tuned to the fixation-to-target angle ($p<0.05$), persistently encoding target location throughout the trial. We then calculated the optimal lag time for movement and speed-tuned neurons, defined as the lag time (+/-) at which a neuron's tuning curve sharpness (depth/halfwidth) was maximal. The population distribution of optimal lag times was centered at approximately 0 ms, with 70 ms standard deviation. Negative-lag neurons had small lag times (>-100 ms), suggesting the activity does not reflect direct sensory feedback and better reflects estimates of most recent past states. Positive-lag neurons also had small lag times (<100 ms), making it unlikely that they are encoding feedforward motor commands and more likely encoding estimates of upcoming states. This data suggests that PPC serves as a forward model for motor control that predicts movement states at the current moment, in the recent past, and in the near future.

22. Firing rate of V1 neurons predicts perception of ambiguous three-dimensional objects

Zoltan Nadasdy, Melissa Saenz, Bijan Pesaran, Christof Koch, R.A. Andersen

We studied single unit responses of V1 superficial layer neurons in a perceptual discrimination task. A rhesus monkey was trained to hold fixation during presentations of ambiguous and unambiguous (3D) structure-from-motion objects, and was required to report his percept in a two alternative forced choice task. We estimated the probability with which the firing rate of a given V1 neuron allows an ideal observer to predict the monkey's perceptual choice. Neuronal responses to zero-disparity (ambiguous) objects were sorted according to the perceptual choices and the type of object on the preceding trial. The choice probability was determined for each neuron. Based on the sample of 159 neurons, 40% (65) of the cells showed a significant but relatively long latency bias ($p<0.01$) starting 400 ms after the stimulus onset. Analysis of the sequence of trials revealed that perception and neuronal responses during ambiguous trials were affected by the preceding non-ambiguous trials in a time dependent fashion. Neurons recorded during ambiguous trials separated by long 3+/-1s intertrial-intervals (ITIs) revealed a short latency persistent firing rate increase if the preceding trial was congruent with the preferred direction/disparity of the neuron. Thus, the relative firing rate during ambiguous trials was predictive of the monkey's choice. This neuronal bias may reflect a perceptual stabilization following long ITIs. In a second experiment varying the ITI between unambiguous and ambiguous object trials, we found that the percept switched following an ITI<1s, while remained the same following an ITI>1s. These results suggest that a population of V1 neurons contribute to generating a perceptual bias deriving from two sources: a short latency bias induced by the previous exposure and a long latency perceptual bias representing a corroborative feedback from higher visual cortical areas (MT/MST).

23. Dorsal premotor neurons encode the relative position of the hand and the eye

M.J. Nelson, B. Pesaran, R.A. Andersen

When reaching to grasp an object we often move our limb and orient our gaze together. How are these movements controlled and coordinated? Reaching and eye movements are controlled by areas in frontal and parietal cortex that share long-range connections. Neurons in reach-related areas of posterior parietal cortex (PPC) respond to both reaches and saccades and combine

retinotopic and limb position signals suggesting they are involved in hand-eye coordination. In contrast, while eye position can modulate responses in dorsal premotor cortex (PMd) in the frontal lobe, PMd is considered to be downstream from PPC and is thought to respond primarily to reaches in limb, not retinotopic, coordinates. However, responses in PMd to reaches and saccades and their dependence on retinotopic and limb coordinate frames have not been systematically studied. We compared cell responses in PMd in two monkeys using delayed reach and saccade tasks and then studied the coordinate frame of the responses. Reach and saccade activity was examined by instructing either a reach without a saccade or a saccade without a reach from a central location to one of eight targets. 138/205 cells were spatially-tuned to reaches during the delay or movement periods (ANOVA,$p<0.05$). 88/205 cells were spatially-tuned to saccades during the delay or movement periods (ANOVA,$p<0.05$). Next we instructed reaches or saccades to one of four targets while independently varying the starting position of the hand and eye across four locations. Many cells represented both hand and eye position for reaches (57/111) and saccades (49/105; Int. term, 2-way ANOVA,$p<0.05$). These cells encoded the relative position of the hand and eye with most cells preferring the hand ipsilateral to gaze (27/57;23/49) and others on (14/57;9/49) or contralateral (16/57;17/49) to gaze. These data indicate that PMd responds to both reaches and saccades and may coordinate the hand and eye by computing their relative position.

24. Coherence in dorsal premotor cortex and area MIP during free choice and instructed behaviors

B. Pesaran, M.J. Nelson, R.A. Andersen

Dorsal premotor cortex in the frontal lobe and area MIP in posterior parietal cortex form a frontal-parietal (F-P) circuit for reaching but the functional role of connections between them is unclear. To study their role in decision-making, we compared two tasks with freely chosen and instructed reaches. In both tasks three targets were presented and the monkey was rewarded for reaching to one of them following a 1-1.5s delay period. On each trial a different set of three targets was presented from a set of eight potential locations and the reward was assigned to one of the three targets with equal probability. In the choice task, all three targets were circles and the monkeys were allowed to choose reaches to find the reward. In the instructed task, targets were a circle, square and triangle and the monkeys had to reach to them in that order to find the reward. Instructed reaches matched the chosen reaches to make the sensory and motor variables before the first reach the same for both tasks. We simultaneously recorded spike and field activity in both areas of two monkeys and compared the coherency of the signals during each task over time using a 500 ms moving window. The database consisted of 91 spike-field (21 P-F,25 F-P,28 F-F,17 P-P) and 84 field-field (54 F-P,15 F-F,15 P-P) recordings. Population average spike-field and field-field coherency between frontal and parietal cortex was greater during the choice than instructed task from 5-20 Hz for 500 ms after target onset (t-test;$p<0.05$). Spike-field and field-field coherency within either frontal or parietal cortex was

greater during the choice than instructed task from 15-40 Hz after this first 500 ms (t-test;$p<0.05$). These data suggest decision-making involves long-range coherency in frontal-parietal circuits earlier than local coherency within either area. Long-range coherency may reflect cooperative computation between frontal and parietal cortex during decision-making.

25. Decoding planned trajectories in the posterior parietal cortex

E.B. Torres, R. Quian-Quiroga, C.A. Buneo, R.A. Andersen

Recent work suggests that the PPC is involved in the decoding of movement intentions (Andersen Group 2002, 2004), yet it is still unknown whether the PPC is also involved in trajectory formation. Before movement execution, during the planning period, trajectory information was decoded using 34 cells for leftward and 30 cells for rightward targets from the areas 5 and PRR of the Posterior Parietal Cortex (PPC) of one monkey. A new experimental paradigm that required temporal visuomotor adaptation was used. The experiment interleaved a delayed center-out reaching task that was "second nature" to the monkey with a new task that required avoiding a physical obstacle (OB) interposed on the way to visual targets. The new task was simple enough that did not require training, yet complex enough that it elicited highly curved and long paths that called for a change in temporal strategy. Electromagnetic sensors were attached to the arm to measure the behavior concurrently with the neural activity. Learning was monitored across time. The delay activity before movement in the PPC cells was highly different between tasks, so a simple leave-one-out Linear Fisher Discriminant decoding algorithm on the neural data was used to predict not only the target direction of motion across experimental conditions, but also trajectory-related features. The first transition from simple to OB-avoidance reaches enabled prediction of the spatial path, i.e., to distinguish the spatial route in straight vs. curved trajectories. The second transition within the OB block, where the paths had been resolved and conserved from trial one, but the speed profiles continued to change, enabled prediction of speed-related features. From planning activity it was possible to decode broken and slow vs. smooth and fast speed profiles. The data suggest that delay period activity in the PPC reflects both spatial and temporal aspects of reach trajectories for pending movements.

Publications

Andersen, R., Meeker, D., Pesaran, B., Brezen, B., Buneo, C. and Scherberger, H. (2004) Sensorimotor transformations in the posterior parietal cortex. In: *The Cognitive Neurosciences III*, M.S. Gazzaniga (ed.) MIT Press, Cambridge, MA, pp. 463-474.

Andersen, R.A., Budrick, J.W., Musallam, S., Pesaran, B. and Cham, J.G. (2004) Cognitive neural prosthetics. *Trends Cog. Sci.* **8**:(11):486-493.

Andersen, R.A., Burdick, J.W., Musallam, S., Scherberger, H., Pesaran, B., Meeker, D., Corneil, B.D., Fineman, I., Nenadic, Z., Braunchaud, E., Cham, J.G., Greger, B., Tai Y.C. and Mojarradi M.M. Recording advances for neural prosthetics. Proceedings of the 26th Annual International Conference of the IEEE IMBS. San Francisco, CA, USA, September 1-5, 2004, pp. 5352-5355.

Andersen, R.A., Musallam, S. and Pesaran, B. (2004) Selecting the signals for a brain-machine interface. *Curr. Op. Neurobiol.* **14**:1-7.

Andersen, R.A., Musallam, S., Burdick, J.W. and Cham, J.G. (2005) Cognitive based neural prosthetics. Proceedings of the 2005 International Conference Robotics and Automation.

Burdick, J.W. and Andersen, R.A. (2004) By pure thought alone: The development of the first cognitive neural prosthesis. *Engenious*, Caltech.

Campos, M., Breznen, B., Bernheim, K. and Andersen, R.A. (2005) The supplementary motor area encodes reward expectancy in eye movement tasks. *J. Neurophysiol.* **94**:1325-1335.

Cham, J.G., Branchaud, E.A., Nenadic, Z., Andersen, R.A. and Burdick, J.W. (2005) A miniature robot that autonomously optimizes and maintains extracellular neural action potential recordings. Proceedings of the 2005 International Conference Robotics and Automation, Barcelona, Spain.

Cham, J.G., Branchaud, E.A., Nenadic, Z., Greger, B., Andersen, R.A. and Burdick, J.W. (2005) Semi-chronic motorized microdrive and control algorithm for autonomously isolating and maintaining optimal extracellular action potentials. *J. Neurophysiol.* **93**:570-579.

Cohen, Y.E. and Andersen, R.A. (2004) Multimodal spatial representations in the primate parietal lobe. In: *Crossmodal Space and Crossmodal Attention,* J. Driver and C. Spence (eds.), Oxford University Press. pp. 99-122.

Cohen, Y.E. and Andersen, R.A. (2004) Multisensory representations of space in the posterior parietal cortex. In*: Handbook of Multisensory Integration*, G. Calvert, C. Spence, and B. Stein (eds.), MIT Press, Cambridge, MA, pp. 463-479.

Corneil, B.D. and Andersen, R.A. (2004) Dorsal neck muscle vibration induces upward shifts in the endpoints of memory-guided saccades in monkeys. *J. Neurophysiol.* **92**:553-566.

Musallam, S., Corneil, B.D., Greger, B., Scherberger, H. and Andersen, R.A. (2004) Cognitive control signals for neural prosthetics. *Science* **305**(5681):258-262.

Nieman, D.R., Hayashi, R., Andersen, R.A. *et al*. (2005) Gaze direction modulates visual aftereffects in depth and color. *Vis. Res.* **45**(22):2885-2894.

Pang, C., Cham, J.G., Nenadic, Z., Musallam, S., Tai, Y.C., Burdick, W. and Andersen, R.A. A new multi-site probe array with monolithically integrated parylene flexible cable for neural prostheses. The 27th Annual International Conference of the IEEE Engineering in Medicine and Biology Society (EMBS). To be presented in Shanghai, China, September 1-4, 2005.

Quiroga R.Q., Nadasdy Z. and Ben-Shaul Y. (2004) Unsupervised spike detection and sorting with wavelets and superparamagnetic clustering. *Neural Comput.* **16**(8):1661-1687.

Rizzuto, D., Mamelak, A., Sutherling, W., Fineman I. and Andersen, R.A. (2005) Spatial selectivity in human ventrolateral prefrontal cortex. *Nature Neurosci.* **8**(4)415-417.

Scherberger, H., Jarvis, M.R. and Andersen, R.A. (2005) Cortical local field potential encodes movement intentions in the posterior parietal cortex. *Neuron* **46**:347–354.

Roger W. Sperry Professor of Biology: **David J. Anderson**

Research Fellows: David F. Chang, Benjamin Deneen, Xinzhong Dong, Yosuke Mukoyama, Kenji Orimoto, Donghun Shin, Gregory S.B. Suh, Timothy D. Tayler, Sofia Vrontou, Mark John Zylka

Graduate Students: Gloria Choi, Anne C. Hergarden, Christian Hochstim, Suzuko Yorozu

Research and Laboratory Staff: Jung Sook Chang, Ritchie Ho, Liching Lo, Gina Mancuso, Monica Martinez, Gabriele Mosconi, Myra Perez, Laurent Van Trigt

Summary: There are currently three major areas of investigation in this laboratory: the development of neural stem cells; the functional neuroanatomy of emotional behaviors in mice; and the functional neuroanatomy of innate behaviors in *Drosophila*.

Stem cell biology

Stem cells are multipotent, self-renewing progenitor cells. Central nervous system stem cells (CNS-SCs), are believed to generate neurons, astrocytes and oligodendrocytes, the three major cell classes of the CNS. These cells have, however, been characterized primarily *in vitro*. Our recent studies of a population of candidate CNS-SCs in the spinal cord suggest that *in vivo*, the majority of these cells do not self-renew, but rather undergo a unidirectional restriction to a glial fate. Current work is aimed at using a combination of microarray and *in vivo* loss- and gain-of-function genetic manipulations, to identify and functionally characterize genes that control this restriction.

Neural circuitry of behavior

We are developing and applying molecular biological tools to map and manipulate the neural circuitry underlying emotional behaviors, in mice. These studies focus on two distinct but related states: pain and fear. In the former case, we have identified a novel family of G protein-coupled receptors (GPCRs) for neuropeptides, called Mrgs, which are specifically expressed in restricted subsets of primary nociceptive sensory neurons. Using homologous recombination in embryonic stem cells, we have marked the neurons that express different Mrgs with genetically encoded axonal tracers. Remarkably, different Mrg-expressing neurons project to different, and highly specific, peripheral target tissues. We are now engaged in genetic inactivation or killing of these neurons, as well as genetic activation, to understand their function. We are also tracing the higher-order projections of these neurons into the brain, to determine the point at which these novel and distinct sensory circuits converge.

In a separate project, we have developed an experimental system to compare the neural circuits that control behavioral responses to learned versus innately fearful stimuli. We have identified auditory stimuli that can elicit different fear behaviors (flight or freezing) in laboratory mice, depending on the context and/or prior experience of the animals. These stimuli are therefore of the same sensory modality as those typically used for fear conditioning experiments. We have identified genes that are expressed in subpopulations of neurons in the central nucleus of the amygdala, which is thought to be a major output structure that co-ordinates different aspects of learned fear responses. Using the promoters of these genes, we are generating mice in which these neurons can be reversibly silenced, in collaboration with Henry Lester's laboratory. The behavioral consequences of these manipulations for responses to learned and unlearned fearful auditory stimuli can then be compared.

In parallel with these studies in mice, we are engaged in conceptually similar experiments in the fruitfly, *Drosophila melanogaster*. Our goal is to identify simple and robust innate behaviors, and then perform unbiased "anatomical" and genetic screens to map the neuronal circuits and identify the genes that control these behaviors. This dual approach will provide an opportunity to integrate molecular genetic and circuit-level approaches to understanding how genes influence behavior. The "anatomical" screen exploits the availability of "enhancer trap" lines, in which the yeast transactivator protein GAL4 is expressed in specific subsets of neurons, and a conditional (temperature-sensitive) neuronal silencer gene (*shibere^{ts}*) that prevents synaptic transmission. Currently, we have developed assays for an innate avoidance response triggered by an odorant mixture released from traumatized flies, as well as for arousal intensity and hedonic valence, two important axes underlying emotional states in humans.

26.   **Modeling "emotional" behavior in *Drosophila***
    Tim Lebestky

    Emotional behaviors in humans convey a positive or negative response to a stimulus, and this response is manifest in discrete, highly conspicuous ways, such as stereotyped facial expressions and physiological arousal. Although *Drosophila* do not present the richness of human emotions in their behavior, they may share fundamental molecular similarities that could allow us to dissect the way that neural circuits function to provide graded responses in intensity, as measured both qualitatively and quantitatively. To this end, we are developing automated, high-resolution behavioral assays that will allow a

reproducible characterization of behavioral responses to various stimuli for high-throughput genetic screens. One such assay follows the startle effects on locomotion and escape behaviors in response to a series of air-puffs, delivered at regular intervals. We observe a reproducible escalation of locomotor activity and jump-response behaviors as a function of time and puff number. We have performed genetic screens to isolate and characterize insertional mutants and potential neural circuits that mediate startle behavior.

Similar to mammals, *Drosophila* utilize biogenic amines as neurotransmitters for normal neuronal function and behavior. A serotonin transporter, dSERT, with significant functional homology to the mammalian SERT family has been cloned and physiologically characterized *in vitro* (Demchyshyn *et al.*, 1994), however there is no genetic analysis of this, transporter *in vivo*. Given the importance of this molecular family and the successful advancement of *in vivo* RNAi techniques in *Drosophila*, we are currently developing techniques to look at gain-and loss-of-function conditions in a spatially and temporally regulated manner in adult flies. To this end, we have obtained RNAi lines, an insertional mutation in the dSERT locus, and multiple deficiencies that uncover the region. I have also entered into a collaborative project with another postdoctoral fellow, Wulf Haubensak, to engineer new conditional neuronal silencing transgenes. It is our hope that by tightly controlling the gene dosage and induction level of the RNAi or silencing transgenes, we may observe quantifiable phenotypic differences in behaviors that may give insights into how molecular thresholds influence the escalation or decline of distinct internal states in adult animals.

27.   Genes and neural correlates underlying an innate avoidance behavior
Anne Hergarden

The neural control of behavior is not well understood. In order to tackle this problem, we will begin by examining a simple and robust behavior. In other work from this lab, postdoctoral fellow Greg Suh has shown that *Drosophila* adults avoid low concentrations of carbon dioxide. This avoidance behavior is mediated by a single class of olfactory receptor neurons that express the putative gustatory receptor GR21A. This dedication of a few neurons to the perception of a single odorant molecule leads us to the question of whether there is a simple circuit underlying the carbon dioxide avoidance behavior. We are interested in identifying additional neural substrates involved in carbon dioxide avoidance. To this end, we have reversibly silenced subregions of the fly brain by crossing brain-specific Gal4 lines to UAS-Shibire[ts] and tested the progeny for deficits in carbon dioxide avoidance. We then use secondary assays including locomotor and general olfactory assays to ensure the specificity of the behavior and a UAS-reporter line to identify the expression pattern. We are also interested in screening single gene mutant collections in order to identify genes that modulate this avoidance behavior.

28.   A novel endothelial-specific gene, *D1.1*, is a marker of adult neovasculature
Donghun Shin, David J. Anderson

Angiogenesis, the sprouting of new blood vessels from pre-existing vessels, is essential for tumor growth and wound healing in adults, as well as for proper embryonic development.

We characterized a novel endothelial-specific gene, *D1.1*, which encodes a predicted transmembrane protein that is not homologous to any other genes in the mammalian genome. We examined the expression and function of *D1.1* using a *tau-lacZ* knock-in to the endogenous chromosomal locus. We found that *D1.1* is strongly expressed by most or all endothelial cells during embryonic development, and is subsequently, down-regulated in the majority of adult microvessels. *D1.1* is highly upregulated and expressed in most endothelial cells involved in neo-vascularization, including tumor angiogenesis, wound healing and corneal micropocket assays. *D1.1* homozygous null mutant mice appear phenotypically normal. However, a soluble D1.1-Fc fusion protein impairs endothelial cell migration and blood vessel formation in several different acute assays.

These data identify *D1.1* as a novel marker of neovasculature, and suggest it may play a functional role in angiogenesis that is compensated *in vivo* by other, structurally distinct proteins.

29.   Molecular approaches to studying the neuronal circuits of emotions
Walter Lerchner, David J. Anderson

Studies attempting to gain a greater understanding of the neuronal circuits of emotions have mostly relied on electrophysiology or lesion studies. However these methods can only identify regions of the brain involved in a certain emotional behavior but reveal relatively little about the connections of the individual neurons.

To better understand the neuronal circuits that underlie emotional behavior we searched for genes with restricted expression in areas predicted to play important roles in these circuits. Once such a gene is identified, its promoter can be used to drive expression cassettes that label the connections, as well as inducibly silence a molecularly defined subpopulation of neurons.

We identified several genes that show restricted expression in areas of interest. Complicating the issue is that all the genes expressed in a subpopulation of neurons in a region of interest also show expression in other regions of the brain and/or peripheral tissues. Thus, it is necessary to take a combinatorial approach in order to target a molecularly-defined population of neurons in an individual area of the brain.

Two different approaches are being currently tested *in vivo*. In the first approach a knock-in construct is used that requires cre-recombinase to excise a stop cassette in order to bring the silencing cassette under the control of a subpopulation-specific promoter. The silencing cassette is under temporal control by the removal of doxicycline from the drinking water and uses tetanus toxin to block

vesicle release. Cre recombinase can then be provided by expression from a different gene with overlap in the region or interest or by viral injection into a specific region of the brain. Currently knock-in mice are created using ER81 for driving the silencing cassette in regions such as the anterior cingulated cortex, and the basolateral amygdala.

The second approach uses an approach developed by Henry Lester's laboratory. The system involves two subunits of the *C. elegans* glutamate-gated chloride channel (GluCl), which has been modified to only be opened by ivermectin. Both subunits are necessary for a functioning channel. Thus, the individual subunits can be expressed by transgenesis and/or virus injection. Ivermectin can be supplied in the drinking water. We are currently conducting several proof-of-principle tests using injection of a mixture of adeno-associated viruses to express both subunits in several forebrain regions, followed by behavioral experiments and electrophysiology.

30. The amygdala central nucleus in innate vs. conditioned fear
Wulf Haubensak, David J. Anderson

Fear is probably the most conserved emotion, underlying defensive behaviors across species, and, in turn, a basic, medically important, human emotion that can be addressed in experimentally tractable animal model systems. Numerous studies have pointed to a central role of medial temporal lobe structures, particularly the amygdala, in various forms of fear. Typically, these structure-function relationships have been obtained by mapping patterns of neuronal activity accompanying fear-associated behaviors, and functionally validating these correlations by surgical lesions. However, these methods are not suitable to investigate single neuronal circuits with cellular resolution. This is especially important when it comes to assign function to the amygdala subregions, and of the different neuronal populations therein. Among these, neurons expressing the stress promoting neuropeptide CRH in the central amygdala (CeA) are a likely to have a central role in fear processing.

Here, we explore a comprehensive strategy to analyze function and circuitry of these neurons, with higher precision. We use two region specific genes, *PKC-delta* and *vavR*, which are coexpressed exclusively in the CRH neurons of the CeA, in a combinatorial manner, to express, in genetically-modified mice, inducible genetically-encoded neuronal silencers specifically in these neurons. To this end, we generated *PKC-delta* and *vavR* BAC transgenic mice expressing each one of the two subunits of a chloride channel for silencing (Slimko *et al., J. Neurosci.* **22**:7373), such that, in intercrosses of these mice, the functional channel will be reconstituted only in the target cells. This will allow us to silence these cells in a temporally defined manner in behavioral paradigms for conditioned (measuring freezing in tone/foot-shock conditioned mice), and innate fear (measuring ultrasound induced freezing in foot-shock sensitized mice (Mongeau *et al., J. Neurosci.* **23**:3855). Similarly, we will direct the

expression of genetically-encoded *trans*-synaptic tracers (wheat germ agglutinin) and the c-terminal fragment of tetanus toxin) selectively to these cells to identify projections to and from these neurons.

31. Distinct nociceptive circuits revealed by axonal tracers targeted to *Mrgprd*
Mark J. Zylka, Liching Lo, David J. Anderson

We recently identified a large family of G protein-coupled receptors, called *Mas-Related Genes* (*Mrgprs*). Several of these genes are expressed in subsets of small-diameter nociceptive (pain-sensing) neurons. To determine what role these genes and sensory circuits play in pain signaling, we generated several *Mrgprd* knock-out mouse lines where the coding region of *Mrgprd* was replaced with EGFP-F (farnesylated EGFP) or hPLAP (human placental alkaline phosphatase) axonal markers and the doxycycline-inducible transcription factor rtTA-M2. By studying axonal projections in these animals, we found that *Mrgprd*+ neurons terminate exclusively in the epidermis as free-nerve endings. *Mrgprd*+ neurons do not innervate any other known targets of nociceptive neurons such as hair follicles, blood vessels, or visceral organs. *Mrgprd*+ fibers comprise 70% of the free-nerve endings in the epidermis, with CGRP+ fibers representing the remaining 30%. Centrally, *Mrgprd*+ and CGRP+ fibers terminate in adjacent but non-overlapping lamina in the spinal cord. These neuroanatomical studies indicate that cutaneous nociceptive stimuli are conveyed by two molecularly distinct and parallel pain circuits. Currently, we are using the knocked-in copy of rtTA, in combination with TRE-driven transgenes, to inducibly silence and/or ablate the circuitry defined by *Mrgprd* expression. These selective molecular and cellular manipulations will permit us to uncover the functional and behavioral significance for parallel cutaneous pain circuitry in mammals.

Reference
Zylka, M.J., Rice, F.L. and Anderson, D.J. (2005) *Neuron* **45**:17-25.

32. LIM homeodomain transcription factors delineate the amygdalar-hypothalamic pathway involved in innate reproductive and defensive behaviors
Gloria B. Choi, David J. Anderson

We bring molecular approaches to bear on a fundamental, and poorly understood, problem in neural circuits and behavior: How do organisms choose between opponent behaviors, when faced with conflicting stimuli in their environment? To address this problem, we have begun to trace, at the single-cell level, the neural pathways that control innate reproductive behaviors, and their anatomical interactions with analogous pathways that control defensive behaviors, in mice.

Numerous functional studies demonstrated that different nuclei in two brain regions, the amygdala and hypothalamus, are involved in the expression of either reproductive or defensive behaviors. More interestingly,

the projections from the medial amygdala to the various hypothalamic nuclei are topographically organized in such a way that the circuitry critical for the expression reproductive behaviors largely remains segregated from the one controlling the behavioral output of defense.

By doing an expression screening and microarray analysis, we showed that a LIM homeodomain transcription factor, Lhx6, is expressed in the MEApd (medial amygdala posterior dorsal), a reproductive nucleus of the medial amygdala. Using a combination of genetically-encoded and conventional axonal tracers, together with double labeling for markers of neuronal activation and neurotransmitter phenotype, we found that Lhx6 delineates the reproductive branch of the amygdalar-hypothalamic pathway. Moreover, we have traced parallel projections from the MEApv (medial amygdala posterior ventral), activated by defensive stimuli, to a point of convergence in the VMHdm (ventromedial hypothalamic nucleus). The opposite neurotransmitter phenotypes of these convergent projections suggest a "gate control" mechanisms for inhibiting reproductive behaviors by threatening stimuli. The data, therefore, identify a potential neural substrate for integrating the influences of conflicting behavioral cues, and a transcription factor family that may contribute to the development of this substrate.

We are in the process of making conditional knock-out's of Lhx6 in order to study whether Lhx6 expression is necessary and/or sufficient for setting up the specific and topographically organized amygdalar-hypothalamic circuit. Moreover, we are trying to test whether an animal is no longer able to gate reproductive behaviors by threatening stimuli in the absence of functional amygdalar-hypothalamic connections.

References

Choi, G.C., Dong, H.W., Murphy, A.J., Valenzuela, D.M., Yancopoulos, G.D., Swanson, L.W. and Anderson, D.J. (2005) *Neuron* **46**(4):647-660.

Zhou, Q., Choi, G. and Anderson, D.J. (2001) *Neuron* **31**(5):791-807.

33. *In vivo* transplantation studies of Olig2+ neuroepithelial progenitors of motoneurons and oligodendrocytes

Yosuke Mukoyama

A fundamental question in neuronal development is what controls the transition from neurogenesis to gliogenesis. We focus on the pMN domain of the ventricular zone in the developing spinal cord, to which expression of the bHLH transcription factor *Olig2* is restricted. This domain gives rise first to motoneurons (MNs) at embryonic day 9.5 (E9.5) and then to oligodendrocytes (oligos) at E13.5. It remains unclear whether neurons and glia are actually generated from Olig2+ self-renewing CNS stem cells *in vivo*. If so, the multipotency of these Olig2+ progenitors should be maintained during the MN→oligo transition. On the other hand, if the transition to gliogenesis involves cell-intrinsic

restrictions, then it would argue that Olig2+ progenitors are not self-renewing stem cells. To address this question, we have compared the neurogenic and gliogenic capacities of Olig2+ pMN progenitors at different stages, using direct *in vivo* transplantation. FACS-isolated Olig2+ pMN progenitors from dissociated mouse spinal cord were transplanted into host chick embryo spinal cord, at a stage permissive for neurogenesis. E9.5 Olig2+ pMN progenitors differentiate to MNs in the E2 ventral chick spinal cord following transplantation. In contrast, E13.5 Olig2+ pMN progenitors do not differentiate to MNs, but rather to glial cells, primarily oligos, in the E2 ventral chick spinal cord. These data suggest that Olig2+ progenitors undergo cell-intrinsic restrictions in their developmental potentials during the MN→oligo transition. This in turn implies that MNs and oligos may be generated by a mechanism not involving self-renewal.

34. Olig gene targets in CNS glial cell fate determination

Christian Hochstim, David J. Anderson

We are interested in the process of cell fate specification in embryonic CNS progenitor cells. Our specific focus is on the specification of the two major subtypes of glial cells: oligodendrocytes and astrocytes. In the spinal cord, these glial cells are generated from ventricular zone progenitors after neurogenesis is completed. The bHLH transcription factor Olig2 is essential for oligodendrocyte generation in the spinal cord. Furthermore, lineage tracing in the Olig1,2 -/- homozygous mutant spinal cord using an Olig2-GFP knockin allele reveals that GFP+ cells generate astrocytes, a fate transformation in the absence of Olig expression. In an attempt to identify Olig target genes involved in this fate specification, we have performed a screen where GFP+ oligodendrocyte (+/-) and astrocyte (-/-) precursors were FACS isolated and their mRNA expression profiles were compared using Affymetrix mouse cDNA microarrays. The paired homeodomain transcription factor pax6 was identified as being upregulated in the Olig -/- population, and expression data confirmed pax6 co-expression with GFP in Olig-/- but not Olig+/- spinal cord in both progenitors (E13.0) and migrating glial cells in the white matter (E18.5). Furthermore pax6 was found to label a subset of GFAP+ astrocytes in the ventral-lateral white matter of the spinal cord at E18.5. At this stage pax6 also marks a subdomain of NF1+ astrocytic precursors in the middle portion of the ventricular zone, as well as a subpopulation of migrating NF1+ precursors throughout the gray and white matter. Interestingly, pax6 expression in the astroglial lineage is entirely mutually exclusive with olig2 expression in oligodendrocyte precursors, which like our microarray data suggests an antagonistic relationship between these transcription factors. We are currently focusing on gain of function and loss-of-function experiments to determine the relationship between pax6 and olig2 and whether pax6 has any pro-astrocytic or anti-oligodendrocytic role in the context of its observed expression in the spinal cord at late embryonic stages.

35. Rapid, systematic identification of genomic regulatory elements controlling region- and neuron-subtype-specific gene expression in mammalian brain

David F. Chang, David J. Anderson

A major research opportunity in the post-genomic era is to understand how genes influence behavior. The difficulty in studying this topic is that genes do not directly dictate behavioral phenotype; rather, neural circuits control behavior. Identification of enhancer elements controlling brain region- and neuron-subtype-specific gene expression facilitates genetic approaches to mark, map, manipulate the activity of specific neuronal circuits and determine the effects of these manipulations on specific behavior.

At present, comparative analysis of genomic sequences from multiple organisms using bioinformatics tools such as VISTA and Mussa programs have permitted the identification of conserved non-coding regions across species. Since the functional assays to validate the activity of such putative brain region-specific enhancers are difficult to recapitulate in neuronal cell lines, this leaves transgenesis as the only current viable assay system. However, functional analysis in transgenic mice is laborious, time consuming, expensive and confounded by position effects due to the site of chromosomal integration.

Our project aims to develop a rapid, systematic brain expression assay to identify transcriptional regulatory elements for brain region and neuron subtype-specific gene expression. We have set up an electroporation system to transfer plasmid DNA reporter constructs to short-term, brain-slice cultures. So far, we have optimized various parameters, including age of the animal used, DNA concentration, number of pulses, pulse amplitude and frequency, the size and thickness of the slice and the length of the culture period. Further, we have manufactured an electroporation apparatus to achieve uniform and consistent transfection that may be adaptable for high-throughput studies in the future. Our current aim focuses on the study of putative enhancer elements. If the slice culture approach is successful, we will achieve proof-of-principle by demonstrating that the regulatory elements identified drive expression specifically in the appropriate regions of the mouse brain *in vivo*.

36. Specific olfactory circuits in *Drosophila* direct an innate avoidance behavior

Greg S. Suh, Allan Wong[*], Anne Hergarden, Richard Axel[*], Seymour Benzer[**], David J. Anderson

We have developed a novel behavioral paradigm for an innate avoidance response in *Drosophila*. This paradigm involves avoidance of a substance emitted by flies subjected to stress, called *Drosophila* Stressed Odorant (dSO). Responder flies were given a choice in a T-maze between a fresh tube and a conditioned tube in which a set of emitter flies was previously traumatized. Most responders choose the fresh tube; performance Index typically falls between 95 and 80 under optimal conditions. Gas chromatography mass spectrometry and respirometer

analyses indicated that CO_2 is a component of dSO. And flies exhibit avoidance response to CO_2 in a dosage-dependent manner. We next sought to functionally map olfactory circuits mediating avoidance response to CO_2. Flies in which a genetically-encoded, calcium-responsive indicator (GCaMP) was expressed throughout the antenna lobe revealed that a single pair of the ventral-most glomeruli, known as V, are activated by CO_2. Moreover, functional inactivation of the GR21A+ sensory neurons which project to the V glomerulus, using UAS- *Shibire[ts]*, was sufficient to abolish avoidance response to CO_2. In addition, the fact that these CO_2-blind flies carrying GR21A-Gal4 & UAS- *Shibire[ts]* nevertheless exhibited an avoidance response to dSO, argues that CO_2 is only one component of dSO.

To identify the groups of ORNs activated by NCO (**N**on-**C**O_2 component of dSO), imaging experiments were performed in collaboration with Allan Wong and Richard Axel at Columbia. They expressed GCaMP using Elav-Gal4, a driver expressed throughout the nervous system, and monitored the patterns of glomerular activation in response to air from tubes in which flies were traumatized. Consistent with our predication, another single pair of glomeruli, known as Dm1, are activated by traumatized fly air while the Dm1 glomeruli are not activated by undisturbed fly air, which does not have repelling activity toward naïve flies. These data suggested that the Dm1 glomeruli are specific for the unidentified NCO substance emitted by traumatized flies.

[*]*Columbia University, School of Medicine*
[**]*Professor, Division of Biology, Caltech*

Reference

Suh, G.S., Wong, A.M., Hergarden, A.C., Wang, J.W., Simon, A.F., Benzer, S., Axel, R. and Anderson, D.J. (2004) *Nature* **431**(7010):854-859.

37. Molecular specification of motor neuron progenitor cell fate

Agnes Lukaszewicz

The pMN domain of the spinal cord, characterized by Olig1/2 expression, is a specific progenitor domain of the central nervous system, which generate motor neurons (MNs) and oligodendrocytes (OLs). So as to understand the molecular control of the neuron-to-glia switch in this domain, a systematic characterization of changes in gene expression has been carried. Genes coding for cell cycle regulators, the Cyclin Ds, have been isolated. Interestingly, mouse spinal cord precursors specifically expressed either CyclinD1 or CyclinD2, but not both. In addition, whereas CyclinD2 remains expressed after the transition to gliogenesis, CyclinD1-expression disappears. Considering that CyclinD1 has been shown to modify the activity of transcription factors, these data raise the possibility that it may be involved in the temporal control of the neuron-to-glia switch. In order to examine to what extent Cyclin Ds contribute to regulate the developmental capacities of Olig2-expressing precursors, we have modified the

endogenous pattern of expression of Cyclin Ds, using electroporation of chick spinal cord. The impact of CyclinD1 misexpression on neurogenesis has been monitored by quantifying the percentage of precursors committed to the neurogenic pathway (i.e., expressing ngn2). As opposed to CyclinD3, CyclinD1 misexpression at E2 increases the percentage of neurogenic precursors at E7 (by 36%). On the other hand, the impact of CyclinD1 misexpression on gliogenesis can be monitored by quantifying the number of migrating cells expressing glial makers, that is to say that are committed to the gliogenic pathway. At E6, CyclinD1 misexpression reduces the number of migratory cells expressing Sox9 (by 32%), Olig2 (by 34%) and Nkx2.2 (by 17%) whereas CyclinD3 greatly increase these numbers, as a secondary effect on the cell cycle.

Once the specificity of this effect is confirmed, using loss-of-function experiments, the next step would be to investigate in more detail the molecular mechanism(s) by which CyclinD1 regulates the onset of oligodendrogliogenesis. The molecular and functional interactions between CylinD1 and Sox9 (a master gene for gliogenesis) will be deciphered.

38. Neural circuitry of nociception in the skin and viscera

Sophia Vrontou

The brain detects noxious stimulation of the skin, viscera and other internal structures via different subsets of primary nociceptive sensory neurons. These subsets possibly engage distinct circuitry all the way up to the brain, explaining the ability to distinguish the bodily sites at which noxious stimuli are detected. Our objective is to get new molecular markers for such subsets and especially for visceral nociceptors that project to the gut and other internal organs and that form the sensory basis of interoception, the brain's perception of the body's internal states. The ultimate goal is to use them, in conjunction with already identified markers for nociceptors innervating other targets, to trace their sensory maps, so as to illuminate whether these circuits are distinct labelled lines. This analysis might help deciphering the logic of brain decoding in the understudied visceral pain.

In order to do that we will dissect the circuitry, by gene targeting, of MrgB4/B5 members of the GPCR family of Mrgs, which is believed to be involved in nociception. Since the MrgD member is specifically expressed in cutaneous afferents, it is implied that the other Mrgs might be characteristic for nociceptor subsets innervating different organs, including viscera.

Furthermore since the purinergic receptor, P2X3, is expressed by both cutaneous and viscera nociceptive sensory neurons and MrgD neurons appear to innervate exclusively cutaneous targets, it follows that P2X3+ and MrgD- neurons are likely to contain visceral afferents. Thereby by creating appropriate targeted mutations in P2X3 and exploiting the already made in MrgD locus, we will be able to trace and compare the circuitry of the P2X3+ and MrgD- sensory neurons with that of P2X3+ and MrgD+.

Additionally, in order to isolate new visceral nociceptor markers, we will conduct a screen that will be based on the separation by FACS and the comparison of the gene expression profile of cells from cutaneous nociceptors (marked by MrgD) and nociceptor afferents enriched by other markers for visceral targets (like c-RET, known to be expressed in P2X3 neurons).

Selected References

Fear/amygdala

Han, C.J., O'Tuathaigh, C.M., van Trigt, L., Quinn, J.J., Fanselow, M.S., Mongeau, R., Koch, C. and Anderson, D.J. (2003) *Proc. Natl. Acad. Sci. USA* **100**:13087-13092.

Mongeau, R., Miller, G. A., Chiang, E., and Anderson, D. J. (2003) *J. Neuroscience* **23**:3855-68.

Zirlinger, M. and Anderson, D.J. (2003) *Genes Brain Behav.* **2**:282-294.

Neural development/stem cells

Gabay, L., Lowell, S., Rubin, L.L. and Anderson, D.J. (2003) *Neuron* **40**:485-499.

Kim, J., Lo, L., Dormand, E. and Anderson, D.J. (2003) *Neuron* **38**:17-31.

Zhou, Q. and Anderson, D.J. (2002) *Cell* **109**:61-73.

Pain/Nociception

Dong, X., Han, S., Zylka, M.J., Simon, M.I. and Anderson, D. J. (2001) *Cell* **106**:619-32.

Publications

Choi, G.C., Dong, H.W., Murphy, A.J., Valenzuela, D.M., Yancopoulos, G.D., Swanson, L.W. and Anderson, D.J. (2005) Lhx6 delineates a pathway mediating innate reproductive behaviors from the amygdala to the hypothalamus. *Neuron* **46**(4):647-660.

Lo, L.C., Dormand, E. and Anderson D.J. (2005) Late-emigrating neural crest cells in the roof plate are restricted to a sensory fate by GDF7. *Proc. Natl. Acad. Sci.* **102**(20):7192-7197,

Mukouyama, Y., Gerber, H.P., Ferrara, N., Gu, C. and Anderson, D.J. (2005) Peripheral nerve-derived VEGF promotes arterial differentiation via neuropilin-1-mediated positive-feedback. *Development* **132**(5):941-952. Epub.

Suh, G.S., Wong, A.M., Hergarden, A.C., Wang, J.W., Simon, A.F., Benzer, S., Axel, R. and Anderson, D.J. (2004) A single population of olfactory sensory neurons mediates an innate avoidance behavior in *Drosophila*. *Nature* **431**(7010):854-859.

Zylka, M.J., Rice, F.L. and Anderson, D.J. (2005) Topographically distinct epidermal nociceptive circuits revealed by axonal tracers targeted to *Mrgprd*. *Neuron* **45**:17-25.

James G. Boswell Professor of Neuroscience, Emeritus (Active): Seymour Benzer
Visiting Associate: Carol A. Miller
Postdoctoral Fellows: Bader Al-Anzi, Shlomo Ben-Tabou de Leon, Ted Brummel, William Ja, Pankaj Kapahi, David W. Walker
Graduate Students: Gil Carvalho, Julien Muffat, Brian Zid
Research and Laboratory Staff: Stephanie Cornelison, Nick Lawrence, Viveca Sapin, John Silverlake, Rosalind Young

Summary: Our group uses *Drosophila* as a model system in which to identify and characterize genes involved in behavior, aging, and neurodegeneration. The high degree of homology between the fly and human genomes forms the basis of a strategy for understanding the corresponding human genes. Three behavioral paradigms are currently under investigation. One is a model of nociception that bears much resemblance to human pain, with mutants such as *painless* representing an entry into a molecular genetic analysis of this phenomenon. The second is an alarm response, in which flies subjected to vibration emit an odor that induces avoidance by other flies, which is being studied in collaboration with Professor David Anderson's group. The third is a genetic analysis of appetite and obesity.

To study the genetics of aging, we use a single-gene approach to screen for mutants with enhanced longevity, and analyze the functions of the genes involved. For instance, the mutant, *methuselah*, extends the average lifespan of *Drosophila* by some 30%, and also provides increased resistance to different stresses.

The methuselah protein is related to G protein-coupled receptors of the secretin receptor family, and has a unique N-terminal ectodomains. In collaboration with Professor Bjorkman's group, the crystal structure of the ectodomains was solved at 2.3 Å resolution. The structure represents one of only a few available three-dimensional structures of GPCRs. It reveals a folding topology likely to be conserved in Mth-related proteins, and contains a potential ligand-binding site in the form of a shallow interdomain groove with a solvent-exposed tryptophan, the only tryptophan residue in the ectodomains. Antagonists that reduce the effective activity of the receptor would be expected to mimic the defect in *methuselah*, thus possibly extending lifespan. In collaboration with Professor Richard Roberts' group, a library of peptides was generated, from which a subset was selected that show very high binding affinity to Mth protein. In collaboration with Dr. Anthony West, of the Bjorkman group, we have produced monoclonal antibodies to the protein, and expression of mth in cultured cells shows localization of the protein at the cell membrane. We are using such cultures, along with the small peptides as putative ligands, to test for G-protein activation in a suitable reporter system.

Exposure of flies to 100% oxygen causes early death, and we have found that an early-induced event is local disruption of mitochondrial structure in the form of internal "swirls." These also accumulate in normal aging, and their formation can be suppressed by mutations in the *methuselah* gene. Other mutants, such as *hyperswirl*, are unusually sensitive to oxygen, and display large numbers of swirls. Analysis of such mutants may provide clues to primary mechanisms of oxidation damage.

Dietary caloric restriction extends lifespan in various organisms, and we are investigating that phenomenon in *Drosophila*, as well as the role of steroid hormones and bacterial flora. We have developed biomarkers to monitor the progress of aging during lifetime, and have shown that lifespan can be extended by simple feeding of a drug which alters the balance of induction and repression of different sets of genes.

39.   Response of *Drosophila* to wasabi is mediated by *painless*, the fly homolog of mammalian TRPA1/ANKTM1
Bader Al-Anzi, William D. Tracey Jr.*, Seymour Benzer

A number of compounds produced by plants elicit a spicy or pungent sensation in mammals. In several cases, this has been found to occur through activation of ion channels in the transient receptor potential TRP family *(1-6)*. However, whether plant compounds deter non-mammalian species through activation of TRP channels is not known. We report that isothiocyanate, the pungent ingredient of wasabi, is a repellent to the herbivorous insect, *Drosophila melanogaster*, and that the *painless* gene, previously discovered to be required for larval nociception, is required for this avoidance behavior. A *painless* reporter gene is expressed in the bristle neurons of the labellum, tarsus, and wing anterior margin, but not in olfactory receptor neurons, suggesting a gustatory role. However, *painless* mutants are not taste blind; they show normal aversive gustatory behavior with salt and quinine, and attractive responses to sugars and capsaicin. The *painless* gene is an evolutionary homologue of the mammalian "wasabi receptor" TRPA1/ANKTM1, which is also thought to be involved in nociception. Our results suggest that the stinging sensation of isothiocyanate is caused by activation of an evolutionarily conserved molecular pathway that is also used for nociception.
*Present address: Duke University, Durham, NC

40. **Specific olfactory circuits in *Drosophila* direct an innate avoidance behavior to a stress odor (USO)**

Greg S. Suh, Allan Wong[1], Anne Hergarden, Richard Axel[1], Seymour Benzer, David J. Anderson

Gas Chromatograph/ Mass Spectrometry and Respirometer analyses indicate that CO_2 is a component of dSO, and flies exhibit avoidance response to CO_2 in a dosage dependent manner. Flies in which a genetically encoded, calcium-responsive indicator (GCaMP) was expressed throughout the antenna lobe reveal that a single pair of the ventral most glomeruli, known as V, is activated by CO_2. Moreover, functional inactivation of the GR21A+ sensory neurons, which project to the V glomerulus, using UAS- *Shibire*[ts], was sufficient to abolish the avoidance response to CO_2. However, the fact that these CO_2-blind flies carrying GR21A-Gal4 & UAS-*Shibire*[ts] still exhibit avoidance to dSO argues that CO_2 is not the only active component of dSO.

To identify the groups of ORNs activated by NCO (**N**on-**C**O2 component of d**SO**), we expressed GCaMP using Elav-Gal4 expressed throughout the nervous system and monitored the patterns of glomerular activation in response to air from tubes in which flies were traumatized. Consistent with the predication, another single pair of glomeruli, known as Dm1, is activated by traumatized fly air, while the Dm1 glomeruli are not activated by undisturbed fly air, which does not have repelling activity toward naïve flies. These suggested that the Dm1 glomeruli are specific for the unidentified substance emitted by traumatized flies.

[1]*Present address: Columbia University School of Medicine*

41. **A mitochondrial electron transport defect leads to oxygen sensitivity and premature aging in *Drosophila***

David W. Walker, Dan Knoepfle, Julien Muffat, Seymour Benzer

Oxidative stress has been widely implicated as a major cause of aging and age-related diseases. The mitochondrial electron transport chain is the principal source of reactive oxygen species (ROS) within cells. Despite the overwhelming evidence supporting a causal relationship between ROS and degenerative diseases, little is known about the genetic elements that regulate ROS formation within the mitochondrion. As the formation of ROS is a function of ambient oxygen concentration, exposure to hyperoxia (100% O_2) offers an attractive model for physiological studies of oxidative stress. To identify genes that protect the mitochondrion against toxic oxygen radicals, we performed a genetic screen for mutations that cause increased sensitivity to hyperoxia and isolated a mutant with a defect in subunit *b* of succinate dehydrogenase (SDH; mitochondrial complex II). Strikingly, under hyperoxia, the mean lifespan of *sdhB -/-* flies is reduced by 91%. Under normoxic conditions, the mutant also displays relatively early onset mortality and

behavioral decay. We observe morphological abnormalities in muscle mitochondria in the *sdhB -/-* flies, particularly under conditions of oxygen stress, and the ability of complex II to catalyze electron transport is compromised. We propose that the *sdhB* gene product is critical in the prevention of ROS formation within the mitochondrion. This may be responsible for the observed sensitivity to elevated oxygen concentration and decreased life span in mutant flies. We are currently testing this hypothesis by measuring hydrogen peroxide production fluorometrically, using its dependence on substrates, inhibitors, and added superoxide dismutase, to determine sites of ROS production in normal and *sdhB* mutant mitochondria.

42. **Exposure to hyperoxia leads to selective loss of dopaminergic neurons in the fly brain**

David W. Walker, Seymour Benzer

Parkinson's disease (PD) is a movement disorder characterized by the selective degeneration of nigrostriatal dopaminergic neurons. Both familial and sporadic cases present tremor, rigidity, slowness of movement, and postural instability. An increasing body of evidence supports the idea that mitochondrial dysfunction and reactive oxygen species (ROS) are a common underlying mechanism in the pathogenesis of a number of neurodegenerative disorders, including PD. As the formation of ROS is a function of ambient oxygen concentration, exposure to hyperoxia (100% O_2) offers an attractive model for physiological studies of oxidative stress.

We studied the neurodegenerative and behavioral effects of a sub-lethal exposure to hyperoxia in *Drosophila*. After six days, the treated flies presented characteristic locomotor impairments. Using a combination of antibodies and GAL4 enhancer traps, we discovered a dramatic and selective loss of dopaminergic neurons in the dorsomedial clusters. In contrast, the glial and cholinergic systems appear remarkably resistant to the toxic affects of hyperoxia. Therefore, acute exposure to hyperoxia recapitulates key aspects of PD in *Drosophila* and provides a new *in vivo* model for studying the mechanisms of dopaminergic neurodegeneration.

43. **Modeling the role of Apolipoprotein D in normal and pathological aging in *Drosophila***

Julien A. Muffat, David W. Walker, Derek Tam, Seymour Benzer

Human Apolipoprotein D (ApoD) is upregulated in cases of neuronal injury, including Alzheimer's disease. The protein appears to be secreted by astrocytes or other reactive glial cells, and is recruited to sites of neuronal injury and amyloid deposition. As ApoD and its homologs are small, hydrophilic molecules capable of carrying hydrophobic ligands (such as cholesterol and arachidonic acid), they may play a role in neuronal maintenance and survival by carrying trophic factors or essential building blocks of cell membranes. The closest *Drosophila*

homolog is *Glial Lazarillo* (*Glaz*), which shares 40% of its protein sequence with ApoD.

We have shown that a 10-fold overexpression of *Glaz*, using the UAS/GAL4 bipartite system, results in 30% longer lifespan for *Drosophila* under normal conditions. This overexpression also enhances stress resistance, as assessed under conditions of starvation, dessication, hear shock, or hyperoxia. Flies overexpressing *Glaz* appear to eat more, and the lipid dye Nile Red points to a change in the distribution and availability of lipid stores. To test whether the *Glaz* provides a protective function in the nervous system, the effect of overexpression will be tested on neurodegenerative disease models in *Drosophila*.

44. Neurophysiological analysis of aging in *Drosophila*
Shlomo Ben-Tabou de-Leon, Seymour Benzer

The discovery of single-gene mutations and transgenes that affect longevity in *Drosophila* and other model organisms has implicated stress-resistance mechanisms, cellular-signaling pathways and dietary restriction as mechanistic mechanisms that regulate lifespan. However, relatively little is known about the effects of age on cellular neurophysiology in the fly. We are studying age-related changes in neurophysiological function of adult *Drosophila*: photoreceptor and muscle cells. As oxidative stress is considered one of the major causes of cell function deterioration during aging, we compare the results with wild-type flies with those exposed to hyperoxia.

Electroretinogram recordings from flies maintained under nontoxic conditions show an age-related decrease in the amplitude of the photoreceptor response, with an almost complete loss of response in very old flies. Intracellular recordings from single dorsal longitudinal indirect flight muscle fibers in the thorax show that there is a decrease in the spontaneous activity of these muscle cells with age. This is manifested by both a decrease a frequency of action potential bursts and a decreased number of action potentials within each burst. Under hypoxic conditions, these changes are accelerated. These studies are being extended to genetically altered lifespans.

45. Extension of *Drosophila* lifespan using peptide antagonists of Methuselah
William W. Ja, Anthony P. West, Jr., Silvia L. Delker, Pamela J. Bjorkman, Seymour Benzer, Richard W. Roberts

Down-regulation of the G protein-coupled receptor, *methuselah* (*mth*), or of its endogenous ligand, Stunted, extends *Drosophila melanogaster* lifespan. Modulators of Mth signaling would thus be expected to affect longevity and provide insight into Mth function and lifespan regulation. We performed *in vitro* selection, using mRNA display of a random peptide library, to isolate ligands targeting the extracellular domain (ectodomains) of Mth. The selected peptides share a conserved sequence – the RWR motif (consensus = [R/P]xxWxxR). Synthetic

RWR motif peptides exhibit high affinity for the Mth ectodomains, recognize cells expressing the full-length receptor, and antagonize Meth signaling in cell-based assays. Structural studies indicate that the peptides bind at an interface between the Mth ectodomains and extracellular loops, suggesting that extracellular/transmembrane domain coupling plays a role in receptor activation. Flies that constitutively express a Mth antagonist peptide exhibit a robust extension of lifespan. These findings provide a possible model system for the design of lifespan-extending drugs.

46. Compensatory ingestion upon dietary restriction in *Drosophila melanogaster*
Gil B. Carvalho, Pankaj Kapahi, Seymour Benzer

Dietary restriction extends the lifespan of numerous, evolutionarily diverse species. In *D. melanogaster*, a prominent model for research on the interaction between nutrition and longevity, dietary restriction is typically based on medium dilution, with possible compensatory ingestion commonly being neglected. Possible problems with this approach are revealed by using a method for direct monitoring of *D. melanogaster* feeding behavior. This demonstrates that dietary restriction elicits robust compensatory changes in food consumption. As a result, the effect of medium dilution is overestimated and, in certain cases, even fully compensated for. Our results strongly indicate that feeding behavior and nutritional composition act concertedly to determine fly lifespan. Feeding behavior thus emerges as a central element in *D. melanogaster* aging.

47. A high-carbohydrate diet promotes longevity in *Drosophila melanogaster*
Pankaj Kapahi[1], Gil B. Carvalho, Horng-Dar Wang[2], Paul Karayan[3], Seymour Benzer

We demonstrated that lifespan in *Drosophila* is favored by high carbohydrate and low yeast extract levels, suggesting the importance of both nutritional quality and quantity. We showed that *Drosophila* feeding rate is strongly affected by medium composition. When administered during development, a diet containing high carbohydrate and low yeast extract maximized adult lipid stores and starvation resistance. These findings recapitulate the "Atkins effect," in which a protein-rich, carbohydrate-poor diet is claimed to help lose fat in humans. However, the long-term consequences of such a dietary regime are largely unknown. In *Drosophila* at least, they include impaired resistance to starvation and shortened lifespan.

[1] *Present address: Buck Institute for Age Research, Novato, CA 94945*
[2] *Present address: Institute of Biotechnology, 101, Section 2, National Tsing-Hua University, Kuang-Fu Road, Hsingchu 30043, Taiwan, R.O.C.*
[3] *Present address: Duke University, Durham, NC 27710*

46

48. Allocrine modulation of appetite by the sex peptide of *Drosophila*

Gil B. Carvalho, Pankaj Kapahi*, David J. Anderson, Seymour Benzer

In numerous insect species, mating elicits a dramatic remodeling of female behavior. In *Drosophila*, this post mating response (PMR) is controlled by a family of small peptides produced in the male reproductive tract and transferred via the seminal fluid. We show that copulation induces a marked increase in female appetite, and that this change requires a single male seminal factor, the Sex Peptide (SP). Constitutive expression of SP in virgin females mimics the effect of mating on feeding behavior, demonstrating that SP is the main agent controlling the behavioral switch. SP thus represents a molecular link between energy acquisition and reproductive investment. Our observations identify altered feeding behavior as a novel component of the *Drosophila* PMR

*Present address: Buck Institute for Age Research, Novato, CA 4945

49. A genetic screen to isolate fly mutants with an obese phenotype

Bader F. Al-Anzi, Seymour Benzer

Although efforts to identify mutations that predispose humans to obesity have had relatively little success, remarkably progress has been made in identifying five monogenic mouse models of obesity (*obese, diabetes, fat, tubby*, and *yellow*). However, it is doubtful that the list of all genes responsible for regulating body weight is complete. Although large forward genetic screens may identify the missing genes, such screens are difficult to perform in mice. Therefore, obesity research would benefit greatly from the use of a more economical and genetically accessible model organism, such as *Drosophila*. Our research goals are: screening for *Drosophila* gene mutations that cause excess fat accumulation; determination of the underlying defects that cause the obese mutant phenotype; screening for mutations that cause excessive feeding; and identification and cloning of the responsible genes.

In various wild *Drosophila* lines, there is a strong correlation between fat content and starvation resistance (Zwaan *et al.*, 1991). One therefore can select for obese mutants based on their ability to resist starvation. Potentially obese flies survive, while others die, making it possible to screen thousands of mutagenized flies in a relatively short time.

We have begun by screening the X-chromosome via an attached-X screen for recessive mutations in the F1 generation, a method that greatly reduces the time spent in mutant line establishment and crossing. 34,000 mutagenized X-chromosomes have been screened so far, yielding a collection of starvation-resistant lines..

Two mutants, *fatso* and *Butterball*, have been the foci of special interest. Both male and female *fatso* and *Butterball* adults show a clear increase in neutral lipid content... increased starvation both by ether extraction and histological staining with the neutral lipid-specific dye Nile Red. We hypothesize five potential sources of obesity: a) overeating; b) excess of fat cells; c) metabolism shifted toward *de novo* fatty acid synthesis; d) reduced activity, either because of a lower metabolic rate or a defect in neuromuscular activity; e) defect in fat store utilization. We are currently using behavioral and biochemical assays to determine the class to which each obesity mutant belongs. In *fatso*, there is an increase in food intake. This mutant also shows reduced activity levels, but not a correspondingly reduced metabolic rate, suggesting that the obesity phenotype may be due to both overeating and reduction of physical activity. *Butterball*, unlike *fatso*, has elevated CO_2 emission with no increase in activity, which might indicate a metabolic abnormality.

50. Analysis of mechanisms involved in dietary restriction

Brian M. Zid, Pankaj Kapahi, Tony Au Lu, Seymour Benzer

Dietary restriction is the most robust method of lifespan extension, across multiple species, yet the molecular mechanism is poorly understood. We have found that downregulation of the nutrient-sensing TOR pathway can extend lifespan, with differential effects upon dietary restriction. Downstream mediators of the TOR pathway are the eIF4E-binding protein (4EBP) and, consequently, the translation initiation factor eIF4E. It is also known that 4EBP is upregulated upon DR. We have investigated whether modulating either 4EBP or eIF4E have any effects on the DR response in *Drosophila*. Flies under DR show many phenotypes, including lifespan extension, increased stress resistance, decreased fertility and a shift in metabolism towards lipid storage with ubiquitous overexpression of eIF4E, the metabolic shift towards lipid storage seen under DR is suppressed. We have also found that neither 4E-BP loss of function nor eIF4E overexpression show lifespan extension upon DR. However, these flies can still respond to some aspects of DR, as their fecundity shows the normal shift. Currently, the metabolic state of the fly is being investigated by metabolomics. It has been found in other systems that some mRNAs are very sensitive to the levels of eIF4E. We plan on investigating what happens to the translation states of these mRNAs under DR.

Publications

Carvalho, G.B., Kapahi, P. and Benzer, S. (2005) Compensatory ingestion upon dietary restriction in *Drosophila melanogaster*. *Nature Meth.* 2. In press.

DeVeale, B., Brummel, T. and Seroude, L. (2004) Immunity and aging: The enemy within? *Aging Cell* **3**(4):195-208.

Suh, G.S.B., Wong, A.M., Hergarden, A.C., Wang, J.W., Simon, A.F., Benzer, S., Axel, R. and Anderson, D.J. (2004) A single population of olfactory sensory neurons mediates an innate avoidance behavior in *Drosophila. Nature* **431**:854-859

Zheng, J., Edelman, S.W., Tharmarajah, G., Walker, D.W., Pletcher, S.D. and Seroude, L. (2005) Differential patterns of apoptosis in response to aging in *Drosophila*. *Proc. Natl. Acad. Sci. USA* **102**:12083-12088.

48

Allen and Lenabelle Davis Professor of Biology: Mary B. Kennedy
Associate Researcher: Leslie T. Schenker
Assistant Researcher: Alan Rosenstein
Senior Postdoctoral Scholars: Pat Manzerra
Postdoctoral Scholars: Holly Carlisle, Mee-Hyang Choi, Eugenia Khorosheya, Edoardo Marcora, Luis Vazquez, Lori Washburn
Graduate Students: Holly Beale, William Ford[1], Tinh Luong, Andrew Medina-Marino, Stefan Mihalas[2], Ward Walkup IV (BMB)[3]
Undergraduate Student: Qinzi Ji
Research and Laboratory Staff: Cheryl Gause
[1]*CNS, Caltech*
[2]*Physics, Caltech*
[3]*BMB, Caltech*

Summary: The Kennedy lab studies molecular mechanisms of synaptic regulation in the central nervous system. Memories are stored in the brain through long-lasting changes in the strength of synapses between neurons. These changes are triggered when the synapses are used to perceive an object or event being remembered. Regulation of synaptic strength is important for minute by minute information processing and may also underlie mood changes.

Certain neurotransmitters, including glutamate and acetylcholine that activate ligand-gated ion channels, can also initiate long-lasting biochemical changes that change synaptic strength. We are interested in the structure and functional organization of protein signaling complexes within a structure called the postsynaptic density (PSD) and their roles in synaptic plasticity. Over the last ten years, most of the major proteins located in the PSD have been identified. In addition, sequencing and assembly of the human and mouse genomes are nearly finished, providing us with a complete "parts list" for many signaling complexes. This is an exciting time, because we can turn our attention to the task of understanding how proteins are organized at the synapse and how they function together as a signaling machine.

One important synaptic signaling complex assembles around the cytosolic tail of the NMDA-type glutamate receptor. This receptor initiates changes in synaptic strength when it is activated by electrical activity. The complex around the NMDA receptor includes many of the proteins that we originally found in the postsynaptic density. Activation of the NMDA receptor leads to influx of calcium and activation of a large enzyme called Ca^{2+}/calmodulin-dependent protein kinase II (CaM kinase II). It is well known that disruption of the CaMKII gene leads to derangement of synaptic regulation. CaMKII can phosphorylate the AMPA-type glutamate receptor and also a PSD protein termed synGAP but the physiological function of synGAP is unknown. We used homologous recombination in embryonic stem cells to create mutant mice in which the synGAP protein is deleted, and have used the mutant mice to establish some of the influences of synGAP on brain development and function.

The complex signaling machinery at the synapse integrates a variety of signaling influences and determines the "set-point" of synaptic strength at individual synapses. In conjunction with biochemical and cell biological experiments, we are beginning to use computer simulations and measurements of rapid kinetics to study the interactions and dynamics of signaling pathways in the tiny postsynaptic compartment. We are collaborating with scientists at the Salk Institute to build computer simulations of the interactions of Ca^{2+} with signaling proteins in postsynaptic spines in the hippocampus. We are using the program MCell to implement stochastic simulation methods that model the position and behavior of immobilized signaling molecules that are regulated by Ca^{2+} within the spine. Our proximal goal is to generate testable predictions about the conditions that activate different biochemical pathways leading to different kinds of plastic changes in excitatory spines and dendrites. Predictions arising from the simulations will be tested experimentally by measuring the time course and spatial distribution of activation of CaMKII and other synaptic molecules under a variety of physiological conditions. Our ultimate goal is to create simulations that will illuminate our understanding of biochemical information coding at distinct types of synapses in the brain. This effort will lay the groundwork for understanding the behavior of highly interconnected signaling pathways at the synapse.

References

Kennedy, M.B. (2000) *Science* **290**:750-754.
Kennedy, M.B., Beale, H.C., Carlisle, H.J. and Washburn, L.R. (2005) *Nat. Rev. Neurosci.* **6**:423-434.

51.   Quantitative model of interactions of Ca^{2+} calmodulin and CaMKII in spines
Stefan Mihalas

Calmodulin (CaM) is an abundant neuronal enzyme that mediates many second messenger actions of Ca^{2+}, some of which lead to synaptic plasticity. CaM binds to and activates Ca^{2+}/calmodulin-dependent protein kinase II (CaMKII) and this event is required for long-term potentiation (LTP) of synaptic currents. CaM also binds to calcineurin, activation of which is required for long-term depression (LTD) of synaptic currents. A quantitative model is needed to understand how these interactions are controlled in the spine because differences in the interactions of CaM with these target proteins can produce opposite effects. Comparison of such a model to experimental data can help to identify crucial variables that determine the output of different Ca^{2+} signals.

We have first built a simple deterministic model of Ca^{2+} dynamics in spines. This model describes the formation of time-dependent Ca^{2+} microdomains. While most experimental measurements of Ca^{2+} binding to CaM are made in Ca^{2+} concentrations that are constant over time; in fact, the Ca^{2+} concentration in spines varies rapidly. We added to the model of Ca^{2+} dynamics equations that describe activation of CaM in rapidly varying Ca^{2+} concentrations. CaM binds most of its effectors in a Ca^{2+}-dependent manner. Consequently, upon binding to its effectors, the affinity of CaM for Ca^{2+} increases. Therefore, we have also added to the model equations that describe the interactions of CaM with its binding partners in time varying Ca^{2+} concentrations. Our goal now is to measure or derive appropriate parameters for the model, using available experimental data and techniques. So far, we have measured or deduced several parameters from data, and we have calculated other parameters with the use of an automatic parameter search algorithm that deduces appropriate parameters to fit experimental data. The parameters for the model are not yet fully determined; however, we have learned which remaining parameters will be most important for us to measure.

52.   A possible role of Huntingtin in activation of transcription by synaptic activity
Edoardo Marcora

Synaptic activity can induce the expression of proteins that are critical for neuronal survival. Recently, synaptic stimulation has been shown to regulate neuronal gene expression by activating transcription factors such as NF-κB that are initially located right at the synapse. The activated transcription factor is then retrogradely transported from the synapse to the nucleus, where it promotes the transcription of neuroprotective target genes. Our long-term goal is to investigate whether and how dysregulation of dendritic transport can contribute to neurodegeneration.

Huntington's disease (HD) is an inherited neurodegenerative disorder caused by the expansion of a polyglutamine (polyQ) stretch in a protein named Huntingtin (Htt), which appears to have several functions. Loss of a neuroprotective function of Htt has been implicated in the molecular pathogenesis of HD. Interestingly, Htt interacts with NF-κB, a transcription factor that promotes the expression of several neuroprotective genes such as BDNF. Downregulation of BDNF expression has been strongly implicated in the etiology of HD. Htt has also recently been shown to stimulate neuronal retrograde transport via its interaction with the dynein motor protein complex. Remarkably, the polyQ expansion results in loss of this function of Htt. Since wild-type Htt is present in synapses, interacts with active NF-κB, and participates in neuronal retrograde transport, we are investigating the hypothesis that wild-type Htt participates in the retrograde transport of active NF-κB from the synapse to the nucleus following synaptic stimulation. Moreover, we are testing the hypothesis that the polyQ expansion, by interfering with the synaptic localization of Htt and with its ability to stimulate neuronal intracellular transport, impairs the movement of active NF-κB from the synapse to the nucleus. Such an impairment could blunt the induction of neuroprotective NF-κB target genes in response to synaptic activity. It is important to better understand the neuroprotective function of wild-type Htt, and whether and how loss of this function may contribute to the etiology of HD. Strategies aimed at restoring or mimicking the normal function of Htt may be a viable approach to the development of therapies capable of attenuating the progression of HD.

53.   A Rac-dependent signaling pathway that controls actin polymerization is upregulated in synGAP-deficient neurons
Holly J. Carlisle

SynGAP is a synaptic Ras GTPase activating protein (GAP) that is abundant in the postsynaptic density where it is part of a complex of proteins that includes the NMDA receptor and CaMKII. CaMKII has been shown to phosphorylate synGAP, increasing its GAP activity and thus suppressing active GTP-bound Ras. Previous work from this lab has shown that cultured hippocampal neurons from homozygous synGAP KO embryos develop abnormally large spines. Since the morphology of spines is determined by the underlying actin cytoskeleton, we investigated whether upregulation of Ras activity might influence Rac-dependent signaling known to regulate actin polymerization. Homozygous synGAP KO mice die a few days after birth, therefore we have studied synGAP^{+/-} KO (het) KO mice. Consistent with synGAP's known function, we found that GTP-bound Ras was elevated from 12% of total Ras in wild-type (wt) mouse forebrain homogenates to 22% in het homogenates ($p<.05$). We also detected an increase (~10%, $p<.05$) in the level of Rac-GTP in het vs. wt homogenates. In the PSD fraction we found that phosphorylation of the ubiquitous Rac effector, p21-activated kinase (PAK), was dramatically increased in het compared to wt PSDs (326% of wt, $p<.05$). PAK is known to activate LIM kinase that phosphorylates cofilin, inhibiting its ability to bind and sever F-actin. As predicted, we also detected an increase in phosphorylation of cofilin in het synaptosomal fractions (175% of wt, $p<.05$). An increase in cofilin phosphorylation would be consistent with an increase in the formation of filamentous actin and larger spine heads. These data indicate that synGAP has a large influence on the level of active Ras (Ras-GTP) in spines and this Ras-GTP may drive activation of Rac and its downstream signaling pathways that control actin dynamics.

54. Differential regulation of dephosphorylation of synGAP

Lorraine Washburn, Pat Manzerra

Four serine residues are the major sites of phosphorylation by Ca^{2+}/calmodulin-dependent protein kinase II (CaMKII) that stimulate the ras GTPase (GAP) activity of synGAP, a synaptic GAP protein. We have shown that phosphorylation of two of these sites, serines 764/5 and 1123, is increased in cultured cortical neurons after 30 seconds of exposure to NMDA, a specific agonist of NMDA-type excitatory glutamate receptors[1]. The level of phosphorylation was measured by immunoblotting neuronal extracts with phospho-site-specific antibodies specific for each site. Interestingly, phosphorylation of synGAP at site 1123 is biphasic, falling below baseline by 5 min after stimulation. Thus, we sought to determine how the dephosphorylation of synGAP is regulated and what phosphatases act on site 1123 and also on site 764/5.

Two possible phosphatases that could act on synGAP are protein phosphatase 1 (PP1) and calcineurin. They can be specifically inhibited by the drugs okadaic acid and cyclosporin A, respectively. We treated cultured cortical neurons (DIV14) with these inhibitors and then stimulated with NMDA to determine the effect on phosphorylation at sites 764/5 and 1123. Pretreatment with okadaic acid before a 5 min treatment with NMDA did not significantly affect the level of phospho-synGAP after the treatment at either site 764/5 or 1123. Similarly, pretreatment with cyclosporin A before a 5 min treatment with NMDA did not significantly affect the level of phospho-synGAP at site 764/5. However, the same treatment with cyclosporin A significantly increased the level of phospho-synGAP at site 1123. This suggests that calcineurin is the principal phosphatase responsible for the slow dephosphorylation of synGAP at site 1123, and that there is a difference in the regulation of dephosphorylation of synGAP at the two phosphorylation sites. It is an intriguing possibility that synGAP could differently regulate GTPase pathways depending on which of its sites are phosphorylated.

Reference

[1]Oh, J.S., Manzerra, P. and Kennedy, M.B. (2004) *J. Biol. Chem.* **279**:17980-17988.

55. Protein-protein interactions in the postsynaptic density (PSD): A focus on the NMDA receptor and densin, docking sites for CaMKII

Tinh Luong

Calcium influx through N-methyl-D-aspartate (NMDA) receptors and subsequent activation of Ca^{2+}/Calmodulin-dependent kinase (CaMKII) in the PSD is a critical step in transducing membrane activity to different signaling cascades that control a broad range of cellular processes. We are investigating by structural and biochemical methods two-binding partners of CaMKII that can localize it to the PSD: the NMDA receptor and Densin, a putative cell adhesion molecule that is also enriched in the PSD. An investigation of these binding interactions should help us to improve our understanding of how different complexes can come together under particular conditions that create specificity and avoid inappropriate cross-talk

The NMDA receptor is composed of two NR1 subunits with at least two NR2 subunits. In the cortex and hippocampus, NR2A and NR2B are the available subunits to bind to NR1, and have long intracellular tails that act as anchors for signaling complexes. The catalytic domain of CaMKII, which contains an ATP binding site and a substrate-binding site, is sufficient to bind the NMDA cytosolic tail. In collaboration with Pamela Bjorkman's lab, we hope to obtain a high-resolution crystal structure of NR2A and NR2B alone or in complex with CaMKII to study the interaction interface in detail. These studies may provide insight into the molecular basis for observed differences in function between NR2A and NR2B containing NMDA receptors. We will also attempt to identify residues in the interaction interface of the complex by amide deuterium/hydrogen exchange techniques and other biophysical methods.

We are also pursuing structural and biochemical studies of the association of CaMKII with the intracellular tail of densin. Densin is putative transmembrane protein that contains an N-terminal leucine rich repeat (LRR) and a C-terminal intracellular domain that includes a PDZ domain. The intracellular portion of densin forms a ternary complex with CaMKII and alpha-actinin, suggesting that it may organize CaMKII into a protein complex other than the NMDA receptor complex and thus alter signal transduction dynamics. We aim to solve the crystal structure of the intracellular domain of Densin in complex with CaMKII.

56. Stochastic model of CaMKII activation in spines

William Ford, Stefan Mihalas

Most excitatory synapses in the central nervous system have specialized postsynaptic structures called spines extending from their dendrites. Spines have been shown to have a high diffusional barrier that isolates them from the rest of the dendrite. The membrane of the spine that is directly apposed to the presynaptic terminal has another specialized structure associated with it called the postsynaptic density (PSD). We are studying the functions of Ca^{2+}/ calmodulin-dependent protein kinase II (CaMKII) that is an abundant protein in the PSD and has been shown to play a crucial role in control of plastic changes that occur at synapses during formation of memories. In particular, CaMKII plays a role in a form of plasticity called long-term potentiation (LTP). The extent of potentiation after patterned synaptic activity depends on the timing of Ca^{2+} influx into the spine triggered by receptors and channels. We are studying how CaMKII competes with other target that Ca^{2+} might bind to in the spine.

We are using a modeling program called MCell to help us understand activation of CaMKII by Ca^{2+} during

patterned synaptic activity. MCell is a probabilistic reaction-diffusion modeling application that allows one to model stochastic reactions within arbitrarily complex physical spaces (e.g., a spine). Using MCell we plan to construct a detailed model of activation of CaMKII, taking into account its position with respect to sources of Ca^{2+} influx into the spine. We have expanded an existing simple model of a glutamatergic spine [Franks *et al.* (2002) *BioEssays* to add the kinetics of interaction of Ca^{2+} with calmodulin. We are now constructing a kinetic model of CaMKII, based upon experimental work by V. Lucic, M. Choi and S. Mihalas, which will be suitable for addition to the spine model.

57.   The role of the intracellular domain of the NMDA-type glutamate receptor

Leslie Schenker, Rolf Sprengel*, Peter Seeburg*, Mary Kennedy

The NMDA-type glutamate receptor in the central nervous system is composed of two NR1 subunits of approximately 110 kDal and two NR2 subunits of approximately 160 to 180 kDal. The larger size of the NR2 subunits reflects the presence of carboxyl terminal tails of about 300 amino acids that extend into the cytosol. The cytosolic tails of the NR2 subunits associate with intracellular signaling machinery that regulates the strength of synaptic transmission. The principal NR2 subunits in the hippocampus and cerebral cortex are NR2A and NR2B. Mutant mice lacking the intracellular C-terminal tails of the NR2A (NR2ADeltaC) and NR2B (NR2BDeltaC) subunits were created in the Seeburg lab to study the role of these domains in receptor function *in vivo* (1). NR2BDeltaC mice die shortly after birth, whereas NR2ADeltaC mice are viable, but show defects in regulation of synaptic transmission. We have bred mice that produce embryos lacking the tails of both NR2A and NR2B subunits. We can culture dissociated neurons from the brains of these embryos. Consistent with work from other labs, we find that the carboxyl terminus of at least one NR2 subunit is needed to target the receptor to the spine and to avoid degradation by proteolytic enzymes. However, when a receptor oligomer contains at least one NR2 subunit with an intact C-terminal, the NMDA receptor can be clustered along dendrites and colocalize with PSD-95, a post-synaptic density scaffolding protein. The NR2B carboxyl terminal appears to be more effective than that of NR2A in preventing degradation of the subunits and in localizing the receptor in dendritic clusters in our cultures. In immature cultures targeting of some of the PSD-95 to clusters along the dendrite is dependent on the C-terminal of the NR2B subunit. In mature cultures the localization of PSD-95 to spines is not obviously dependent on NMDA receptor subunit levels.

*Max Planck Institute for Medical Research, Heidelberg, Germany

Reference

(1) Sprengel, R. *et al.* (1998) *Cell* **92**:279-289.

Publications

Carlisle, H.J. and Kennedy, M.B. (2005) Spine architecture and synaptic plasticity. *Trends Neurosci.* **28**:182-187.

Kennedy, M.B., Beale, H.C., Carlisle, H.J. and Washburn, L.R. (2005) Integration of biochemical signaling in spines. *Nat. Rev. Neurosci.* **6**:423-434.

Knuesel, I., Elliot, A., Chen, H.-J., Mansuy, I.M. and Kennedy, M.B. (2005) A role for synGAP in regulation of neuronal apoptosis. *Eur. J. Neurosci.* **21**:611-621.

Lucic, V., Greif, G.J. and Kennedy, M.B. Detailed state model of CaMKII activation and autophosphorylation. Submitted for publication.

Shifman, J.M., Choi, M.H., Mihalas, S., Mayo, S.L. and Kennedy, M.B. Activation of Ca^{2+}/calmodulin-dependent protein kinase II by computationally designed mutant calmodulins. Submitted for publication.

Vazquez, L.E., Chen, H.-J., Sokolova, I. and Kennedy, M.B. (2004) SynGAP regulates spine formation. *J. Neurosci.* **24**:8796-8805.

52

Bing Professor of Behavioral Biology: Masakazu Konishi
Member of the Professional Staff: Eugene Akutagawa
Senior Research Fellow: Jose Luis Peña
Postdoctoral Scholars: Yuichiro Hayashi, Sharad Shanbhag, Dai Watanabe
Research and Laboratory Staff: Maria Lucia Perez
Graduate Student: Bjorn Christianson

Summary: Our group has become small after the departure of six members during the last two years. Kazuo and Yasuko Funabiki returned to Kyoto University and Yuichiro Hayashi joined Kazuo as an assistant. Teresa Nick is now an assistant professor at the University of Minnesota and Anthony Leonardo is a postdoctoral fellow in the laboratory of Markus Meister at Harvard. Anthony has received a Helen Hay Whitney Fellowship and also a Young Investigator Award from the International Society for Neuroethology. Ben Arthur is a postdoctoral fellow in the laboratory of Ron Hoy at Cornell University.

Our research projects on song birds and owls continue. Postdoctoral fellow Dai Watanabe, an expert in both molecular biology and neurobiology, and Gene Akutagawa work on the mechanisms of central auditory gating. Gene's expertise in histology has revealed new connections between the song control system and other parts of the brain. These connections may explain the relationships between sleep and neuronal responses to the bird's own song. In zebra finches, neurons within the song control system respond to the bird's own song only when the bird is asleep or under anesthesia.

We have four people working on the owl's auditory system. Space-specific neurons in the owl's midbrain respond selectively to sound coming from a particular direction, because they are tuned to specific combinations of interaural time and level differences, which define the owl's auditory space. We previously showed that the space-specific neuron multiplies postsynaptic potentials from the time and level processing pathways. Jose Luis Peña now finds that the rule of multiplication applies even when the input from the time pathway is greatly reduced. Bjorn Christianson and Jose are working on another mathematical process that the owl's brain performs. Lucia and Jose are finding basic physiological differences between the auditory pathway that goes to a terminal in the midbrain and the one that goes to the thalamus in the owl. She finds few neurons that satisfy the definition of space-specific responses in the thalamus. Sharad Shanbhag has been assembling and testing a new electrode-drive system for recording from the behaving owl.

58.   Nucleus uvaeformis controls auditory responsiveness of HVC in the zebra finch song system

Yuichiro Hayashi

Songbirds learn their vocalizations in their early stage of life. Neurons of the vocal motor pathway of songbirds convey neural signals for song production and respond to auditory stimuli only when the bird is silent, asleep or under anesthesia. This behavioral state-dependent modulation or gating has been observed in nucleus HVC and its efferent target RA. We have recently shown that auditory response of NIf, a major source of auditory input to HVC, is also modulated by behavioral state. This result indicates that NIf relays the behavioral state-dependent change of auditory responses of other nuclei in the vocal motor pathway. One candidate controlling this modulation (gating) is thalamic nucleus uvaeformis (Uva) which projects to both NIf and HVC. To understand how this gating of auditory responses occurs, we tested whether stimulation of Uva affects HVC activity or not. Electrical stimulation of Uva in the anesthetized bird completely inhibited both ongoing and auditory activity in HVC. Interestingly, the inhibition caused by single brief (100 ms) stimulation of Uva lasted ~1 min, and then the spontaneous and auditory activity of HVC gradually recovered. The result supports the idea that Uva controls the gating of auditory activity in the vocal motor pathway.

59.   Running cross-correlation in the owl's nucleus laminaris

Gestur Bjorn Christianson, José Luis Peña

The response of nucleus laminaris neurons of barn owls is tuned to interaural time difference (ITD). These and similar neurons in mammals are thought to perform a running (local) cross-correlation between neural signals encoding binaural auditory stimuli. However, the theoretical significance of the local nature of this computation has never been fully examined. We derived an analytic expression of the running cross-correlation of arbitrary stimuli in terms of the Fourier series, and tested the predictions of this theory.

Laminaris neurons respond in a phase ambiguous manner, where ITDs separated by integer multiples of the period of the stimulating frequency elicit similar responses. When a broadband noise stimulus is used, the response is similarly ambiguous for ITDs close to the characteristic delay (CD) of the neuron. However, as the difference between the ITD and the CD increases, the rate of response gradually declines and the frequency of oscillation of the ITD curve drifts. The existence, time-scale, and magnitude of this effect are consistent with the predictions of the running cross-correlation model, which attribute it entirely to the effective frequency tuning of the neuron. The relationship between the ITD tuning and the effective frequency tuning of the neurons was studied using both iso-intensity frequency stimulation and reverse correlation techniques. Frequency tuning properties could

be derived entirely by the ITD curves of the neurons, and vice versa.

60.   Frequency convergence in the auditory thalamus of the owl

María Lucía Pérez, José Luis Peña

The owl's forebrain and optic tectum contain "space-specific neurons" which are selective for the direction of sound propagation. Their spatial receptive fields result from the sensitivity to combinations of interaural time (ITD) and intensity differences across frequency. The neural pathways that lead to the thalamic and tectal representation of auditory space are separate, before receptive fields tuned to a unique and restricted area of space are synthesized. The first nuclei of these pathways are the nucleus ovoidalis (OV) and the external nucleus of the inferior colliculus (ICx), respectively. Both receive projections from the lateral shell of the inferior colliculus (ICls) but are not interconnected. Whereas the map of auditory space of ICx has been extensively studied, little is known about how auditory spatial cues are combined in single neurons of the thalamic pathway.

We examined how OV neurons responded to ITDs in different frequency bands. Of the neurons tuned to ITD (n = 194), those broadly tuned to frequency (n = 94) responded preferentially to only one value of ITD, when the stimulus was broadband. However, their selectivity to ITD as measured with tones varied for different frequencies, in contrast to space-specific neurons of the tectal pathway. Although the owl's brain can encode time at high frequencies, some OV neurons showed ITD sensitivity restricted to the low frequency bands. We used tracers to identify the ICls neurons that project to the forebrain and tectal pathways. Dextran-amine tracers were injected in OV and ICx. Brain sections were examined with a confocal microscope. No double-labeled cells were found in ICls.

Our electrophysiological findings suggest that the integration of frequency and ITD by space-specific neurons is different in the two pathways. The anatomical tracing indicates that ICx and OV receive projections from different midbrain neurons.

61.   Robustness of multiplicative processes in auditory spatial tuning

José Luis Peña, Masakazu Konishi

The space-neurons of the owl's external nucleus of the inferior colliculus are selective for the direction of sound sources. They are tuned to particular pairs of interaural time (ITD) and level (ILD) differences, which define the horizontal and vertical coordinates of auditory space, respectively. Mathematical analyses show that the amplitude of postsynaptic potentials in these neurons is a product of two components that vary with either ITD or ILD. The study of how this computation works for different input levels requires an independent control of the input. Since the owl's auditory system uses a process similar to cross-correlation for detection of ITD, addition of random noise to correlated signals reduces the output of the ITD processing pathway. By varying the degree of binaural correlation we could accurately and reversibly change the amplitude of the ITD component of postsynaptic potentials in the space-specific neurons. Multiplication worked for the entire range of postsynaptic potentials created by manipulation of ITD.

62.   Miniature microdrive for chronic recording in barn owls

Sharad Shanbhag

The barn owl is an ideal model system for studying the behavioral and neural mechanisms of auditory localization. Over the past 30 years, much work has been done to characterize this behavior as well as understand the neural mechanisms of auditory localization. However, most studies have been performed on owls that are either restrained or anesthetized. In order to better understand the neurophysiology of auditory localization during behavior, we have developed a miniature motorized microdrive system to enable recording of neurons from awake, behaving owls. The assembled microdrive is 10 mm in diameter and 22 mm high. Each of three miniature DC brushless motors (Micro Position Systems, Biel-Bienne, Switzerland) is coupled to a threaded drive shaft using miniature gears with a 1:1 ratio. Rotation of the drive shafts causes linear motion of the electrodes carried by shuttles threaded onto the drive shafts. A modified Sutter MP-285 motor controller (Sutter Instruments, Novato, CA) is used to drive the motors and allows positioning of the electrode in 5 µm steps. Maximum travel distance for each electrode is 14 mm which allows recording from deeper midbrain and brainstem auditory structures of the owl. The assembled drive with motors, electrodes and connectors weighs 10 g, well within the carrying capability of the owl. Electrodes may be replaced by removing the top cap and driving the shuttles up and out of the drive, eliminating the need to remove the microdrive from the animal if the drive is chronically implanted in the owl. In addition to our use in owls, the drive is also suitable for use in larger rodents and other vertebrate species.

Special thanks to Susumu Kitamura and the J. Morita Company for fabricating the drive and drive components.

Publications

Arthur, J.B. (2004) Sensitivity to spectral interaural intensity difference cues in space-specific neurons of the barn owl. *J. Comp. Physiol.* A **190**:91-104.

Konishi, M. (2004) The role of auditory feedback in birdsong. *Ann. NY Acad. Sci.* **1016**:463-476.

Pena, J.L. and Konishi, M. (2004) Robustness of multiplicative processes in auditory spatial tuning. *J. Neurosci.* **24**:8907-8910.

54

Lawrence A. Hanson Jr. Professor of Biology and Computation and Neural Systems: Gilles J. Laurent
Postdoctoral Scholars: Mala Murthy, Benjamin Rubin, Glenn Turner, Mikko Vähäsöyrinki
Graduate Students: Bede M. Broome, Stijn Cassenaer, Cindy N. Chiu, Sarah (Shabnam) Farivar, Vivek Jayaraman, Ron Jortner[1], Ofer Mazor, Anusha Narayan[2], Maria Papadopoulou, Kai Shen, Jonathan Young
Moore Distinguished Scholar: Markus Meister (Harvard University, MCB Department)
Visitor: Ralf Wessel[3]

[1]*Joint with the Interdisciplinary Center for Neural Computation, Hebrew University, Jerusalem, Israel*
[2]*Joint with Professor Paul Sternberg, Division of Biology, Caltech – see his annual report*
[3]*Washington University, Physics Department*

Summary: We are interested in information coding in the brain and in the design principles of circuits involved in processing sensory information. We are particularly interested in understanding the role of time, synchronization and oscillations in information coding and in relating the biophysical properties of neurons and synapses to the function of the networks in which they are embedded. We therefore study the cellular, synaptic and network aspects of neural processing. We focused our research this year on the olfactory system of insects (antennal lobes and mushroom bodies, circuits analogous to the vertebrate olfactory bulbs and anterior/posterior piriform cortices), using locusts, *Drosophila* and honeybees as primary model systems. Our work combines experimental (behavioral, electro physiological and two-photon imaging) and modeling techniques and aims at understanding functional aspects of brain circuits design and the rules of information coding used by the nervous system, and identity-specific responses with varying degrees of concentration invariance. In locust, the tuning of KCs to identity and concentration and the patterning of their responses are consistent with piecewise decoding of their PN inputs over oscillation-cycle length epochs. We also studied the connectivity between antennal lobes and mushroom bodies, and found that the nature of the connectivity between projection neurons and Kenyon cells

is consistent with the general notion that mushroom body representations are sparse, synthetic and specific.

63. Dense connectivity for sparse representation in an olfactory network

Ron A. Jortner, S. Sarah Farivar, Gilles Laurent

Sparse neural codes, where each stimulus activates only a small subset of the neurons, have been described in many systems and phyla. One example is the olfactory system of the locust, *Schistocerca americana*. Each of the 800 projection neurons (PNs) in the first relay of this system responds to many odors with rich, complex spike trains. In contrast, each of the 50,000 Kenyon cells (KCs) in the mushroom body, the second relay, fires very rarely and responds to odors with exquisite selectivity. To understand how this transformation is achieved, we studied the connectivity between PNs and KCs using electrophysiological tools. By simultaneously recording from both populations using a combination of extracellular and intracellular techniques, and applying cross-correlation analysis to this data, we were able to detect and quantify the synaptic connections between them.

Surprisingly, we found that each Kenyon cell receives input on average from 50% of the PNs. Simple combinatorial considerations reveal that this design is optimal for generating specificity: If there are n PNs in total (n=800 in our case) and each Kenyon cell samples m PNs, the number of possible ways for wiring any given KC is given by the binomial coefficient [n,m]. If m=n/2, as we find, the number of possible PN-KC connection patterns is maximized, and is around 10^{240}, a gigantic number (for comparison, less than 10^{20} seconds passed since the big bang). As only 50,000 connection patterns are realized out of 10^{240} possible ones, and if they are randomly drawn, as anatomical evidence supports, the 50,000 connection patterns will on average be maximally different from each other. Hence each of the KCs samples maximally different sets of PNs. The rare spiking can be achieved by setting a high enough firing threshold so as to ensure the KC responds to an arbitrarily small subset of stimuli, while the probability of "accidental" threshold crossing is minute. Sparseness is, counter-intuitively, explained by massive connectivity.

64. Odor representations in the *Drosophila* mushroom body

Glenn C. Turner

The mushroom body (MB) of the insect brain is essential for olfactory learning and memory. We are using electrophysiological techniques to study odor representations in the MB of *Drosophila*, an insect with established olfactory conditioning paradigms and genetic variants with specific learning and memory defects. Our goal is to determine how odors are represented in a brain area involved in learning. We have used whole cell patch clamp recordings to characterize the odor response properties of the Kenyon cells (KCs), the principal neurons of the MB. All recorded KCs were spiking neurons and fired sodium action potentials in response to current

injection. In the absence of odor stimulation KCs showed significant ongoing synaptic activity. Baseline firing rates, however, were extremely low. Odor presentation increased subthreshold synaptic activity, but the overall probability of a spiking response to a given odor was only ~5%. Thus KCs are highly odor selective compared to their inputs, the antennal lobe (AL) projection neurons, which have a 50% probability of response (1). A similar transformation from dense representations in the AL to sparse representations in the MB was first observed in locust (2). A sparse format minimizes overlap between the representations of similar stimuli and could contribute to the accuracy of memory formation and recall. We are currently examining the mechanisms responsible for this transformation. Although periodic phase-lagged excitatory-inhibitory synaptic inputs to KCs are essential for sparse representations in locust, we do not find strong evidence for such oscillations in *Drosophila*. We are examining the contribution of other mechanisms including: i) fast synaptic kinetics; ii) spike threshold; iii) phasic, non-oscillatory inhibition.

References
(1) Wilson, R. *et al.* (2004) *Science* **303**:366-370.
(2) Perez-Orive, J. *et al.* (2002) *Science* **297**:359-365.

65.   Ensemble processing of random odor patterns in the locust antennal lobe
Bede Broome, Markus Meister

Odors evoke complex sequences of activity in antennal lobe projection neurons (PNs), the insect analogs of mammalian mitral/tufted cells. These PN activity patterns evolve over hundreds of milliseconds, are consistent from trial to trial, and contain information about odor identity and concentration. In natural settings, olfactory systems are often confronted with the task of identifying odor blends or multiple odorants that are received in short temporal succession.

To address these questions, we have presented locusts with multiple presentations of identical, rapidly varying, randomly patterned, naturalistic stimuli that contain multiple odors while recording extracellular multi-single-unit activity from ensembles of up to 25 PNs and the local field potential elicited by PNs in a downstream processing center, the mushroom body. In addition, we adapted an "electronic nose" sensor and monitored the temporal structure of the odor plumes that crossed the animals' antennae to facilitate stimulus reconstruction. Our linear reconstruction method used a filter in which each action potential contributed additively to a final estimate of the original stimulus. Our non-linear reconstruction employed multiple discriminant analysis to analyze the time varying activity patterns generated simultaneously across a large group of PNs (n=97). Using these methods we were able to generate a faithful reconstruction of the stimulus time course and discriminate the odors contained within single- and multi-odor stimuli. Furthermore, we are currently investigating how varying the number and identity of the selected PNs in both

reconstruction techniques affects stimulus reconstruction. We are investigating whether reconstructions based on cells with, for example, the strongest responses during the stimulus period correlate better with the stimulus than those that include more cells with other —possibly more informative—characteristics. Finally, we are examining the influence of the dynamics and intermittency of a stimulus on the nature of the spatio-temporal codes so far examined mainly for long and well-isolated odor stimuli.

References
1.   Perez-Orive, J. and Mazor, O. *et al.* (2002) *Science* **297**(5580).
2.   Stopfer, M., Jayaraman, V. and Laurent, G. (2003) *Neuron* **39**(6).
3.   Warland, D., Reinagel, P. and Meister, M. (1997) *J. Neurophysiol.* **78**(2336-2350).

66.   Two-photon imaging and electrophysiology in the *Drosophila* brain
Vivek Jayaraman

We are trying to understand the neurophysiological basis of a recently developed system of imaging with genetically expressed calcium sensors in the *Drosophila* brain. The expression of the sensor, a calcium-sensitive fluorescent protein named G-CaMP[1], can be restricted to genetically-defined populations of neurons, which are then imaged using a laser scanning two-photon microscope. Recent experiments using this sensor have reported narrow odor tuning of cells in the antennal lobe[2] and mushroom body[3]. However, it is unclear what electrophysiological signal the imaging signal being measured corresponds to. The narrow odor tuning seen in these imaging experiments could, for example, be a result of the relatively high threshold of activation of G-CaMP[4,5].

In our experiments, we are simultaneously imaging G-CaMP expressing PNs in an intact, *in vivo* fly preparation and recording their physiology using intracellular and loose-patch techniques. We want to establish the correlation between physiology and G-CaMP signal. We are also interested in the potential changes in the G-CaMP fly's behavior and G-CaMP-expressing neuron's activity that might be produced by the presence of a sensor that likely affects calcium buffering in the cell. To investigate this issue, we are doing behavioral and electrophysiological experiments comparing wild-type flies to G-CaMP-expressing flies. If flies expressing G-CaMP do not show any abnormalities in behavior or in neuronal physiology, and once we have a clear understanding of the electrophysiological underpinnings of the G-CaMP signal, we plan to use the sensor (and possibly others, such as AM dyes, which we are also exploring) to understand odor-evoked responses of populations of neurons in the early areas of the fly olfactory system.

56

References
1. Nakai, J. *et al.* (2001) *Nature Biotechnol.* **19**:137-141.
2. Wang, J.W. *et al.* (2003) *Cell* **112**:271-282.
3. Wang, Y. *et al.* (2004) *J. Neurosci.* **24**:6507-6514.
4. Pologruto, T. *et al.* (2004) *J. Neurosci.* **24**:9572-9579.
5. Reiff, D.F. *et al.* (2005) *J. Neurosci.* **25**:4766-4778.

67. Role of inhibition of the giant GABAergic neuron in the mushroom body

Maria Papadopoulou, Glenn Turner

The giant GABAergic neuron (GGN) is a non-spiking neuron that arborizes extensively in the mushroom body (MB) to contact the dendrites of Kenyon cells (KCs) (Leitch and Laurent, 1996), neurons required for learning and memory (Heisenberg, 2000). We are interested in characterizing the functional role of GGN in the olfactory circuit because its pattern of connectivity makes it an attractive candidate for modulating KC responses with potential implications for learning and memory. Physiological recordings of KCs in locust have shown these cells to represent odors sparsely despite receiving continuous, dense and slowly evolving excitatory input from antennal lobe projection neurons (Perez-Orive *et al.*, 2002). Inhibition appears to be important for the sparseness and brevity of the KC response, because it contributes to odor-induced oscillations of the KC membrane potential that create a narrow window of KC temporal integration of excitatory input (Perez-Orive *et al.*, 2002). While part of the source of inhibition has been identified, we are interested in elucidating the role of the odor-evoked GGN inhibition in the sparseness and synchrony of KC responses. This work could have implications for learning and memory since sparseness in the KCs has been suggested as a mechanism to facilitate storing and handling of memories (Perez-Orive *et al.*, 2002).

References
1. Heisenberg, M. (2000) *Nat. Rev. Neurosci.* **4**:266-275.
2. Perez-Orive, J., Mazor, O., Turner, G.C., Cassenaer, S., Wilson, R. and Laurent, G. (2002) *Science* **297**:359-365.
(3) Leitch, B. and Laurent, G. (1996) *J. Comp. Neurol.* **372**:487-514.

68. Olfactory learning in zebrafish larvae

Jonathan Young

The zebrafish larva provides a vertebrate model system for studying olfaction that offers the advantages of complete transparency, complex behavior, and established genetics. Work has already previously been done in this lab to characterize the responses of mitral cells in the adult zebrafish olfactory bulb. We will use the larval form of the zebrafish to study olfactory learning. Using a combination of behavioral, electrophysiological, and calcium imaging techniques, we will investigate the capabilities of the larval olfactory system to learn, and observe how these changes are encoded in the activity of the olfactory bulb and later brain areas. We will aversively condition fish to odors while simultaneously either imaging calcium activity in the olfactory bulb using two photon microscopy or doing electrophysiological recording from mitral cells. We hope to be able to observe changes in the activity of the mitral cell population of the olfactory bulb during olfactory learning, and gain an understanding of the circuit mechanisms underlying this process.

69. Processing of multisensory information in honeybee mushroom bodies

Mikko Vähäsöyrinki

The success of an individual depends upon accurately determining and executing the appropriate behavior based on sensory information gathered from the surroundings. How does the nervous system extract biologically germane information from a complex multisensory environment to generate adaptive behaviors? To address this question we are studying the neuronal representation of olfactory and visual information in honeybee mushroom bodies (MBs). The function of MBs with respect to behavior has been studied extensively in honeybee[1] and *Drosophila*[2]. Resulting findings suggest that MBs play a central role in tasks such as olfactory discrimination learning and context generalization in visual and spatial learning. However, it is unclear how these tasks are performed by the underlying neuronal networks.

Honeybees display impressive perceptual and cognitive capabilities that can be studied in the laboratory by appetitive training. In this procedure, bees are conditioned to form an association between sensory stimuli and a sucrose reward. The learning process is robust and fast, which enables us to study the corresponding changes at both a single neuron and population level using electrophysiological methods. Although these recordings have proven to be extremely challenging, preliminary experiments suggest them to be feasible and possibly provide crucial information about the system that is unavailable by indirect methods[3].

The honeybee MBs consists of ca. 340000 densely packed Kenyon cells (KCs) that receive second-order olfactory and higher-order visual input, with different modalities innervating spatially distinct areas[4]. We plan to record from a population of KCs in olfactory and visual areas while presenting honeybees with odor or/and visual stimuli. The experiments are aimed to investigate the possibility that KCs integrate the two sensory modalities, a function that has been suggested by several authors. We also want to repeat these experiments during appetitive learning to study the role of KCs in memory formation. We hope to gain insights into how memory traces are encoded by a population of neurons and to find out whether this code differs within and across sensory modalities.

57

References

1. Menzel, R. and Giurfa, M. (2001) *Trends Cogn. Sci.* **5**:62-71.
2. Heisenberg, M. (2003) *Nat. Rev. Neurosci.* **4**:266-275.
3. Szyzka, P. *et al.* (2005*) J. Neurophysiol.* Epub, doi:10.1152/jn.00397.2005.
4. Mobbs, P.G. (1982) *Phil. Trans. Roy. Soc. Lond. B* **298**:309-354.

70. Functional stereotypy within the mushroom body
Mala Murthy

Can neurons in a plastic brain area, such as the *Drosophila* mushroom body (MB), be functionally identifiable across animals? Identifiable neurons are easily distinguished on the basis of several criteria: morphology, lineage, molecular identity and physiology. Kenyon cells (KCs) of the MB belong to a large population (>2,000 in *Drosophila*) of similar neurons: morphological and molecular subtypes have been described, but identifiable individuals have not. Yet, the neurons from which they receive olfactory input, the projection neurons (PNs), are unambiguously identifiable, by virtue of their restricted projections to individual antennal lobe glomeruli, expression of molecular markers, and odor response profiles. In the *Drosophila* MB, there is conflicting evidence regarding anatomical and functional stereotypy. The extent to which KCs are deterministically stereotyped affects how experience and learning may modify odor representations within the MB. By focusing on a small, genetically labeled KC subset, we are examining the possibility that plasticity operates on a more or less constant matrix of connections between PNs and KCs.

The mushroom body is derived from four neuroblasts; each generates ~500 neurons, which can be subdivided into three KC classes based on adult axonal projection patterns. We have screened through a small collection of GAL4 lines for ones with restricted expression within the MB. GAL4 line *NP7175* is expressed in a subset of KCs that project to the core of the a/b lobes. We have performed *in vivo* whole-cell patch clamp recordings of these GFP-labeled KCs in response to a panel of odors at two concentrations. We are also employing two-photon calcium imaging of this KC subset using the reporter *GCaMP*. With these methods, we are examining whether KC odor response profiles within a neuroblast clonal unit are correlated across animals (do they respond to the same or different odors?) and whether odor tuning is correlated across clonal units.

71. Population coding of odor mixtures of increasing complexity by principal neurons of the antennal lobe
Kai Shen

Odor perception is largely synthetic. Most natural odors are complex blends (e.g., flower fragrances) whose components cannot be easily segmented. It is therefore likely that neural representations of odor mixtures involve nonlinear interactions, such that the representation of a mixture is not a simple combination of the representation of its components. We examined the encoding and decoding of odor mixtures and their components by neurons in the antennal lobe and the mushroom body, the first and second relays of the locust olfactory system. We recorded the single-unit activity of ensembles of projection neurons (PNs), the principal cells of the antennal lobe, and Kenyon cells (KCs), the intrinsic cells of the mushroom body, as well as the local field potential (LFP) within the mushroom body, while presenting mixtures of monomolecular odors. First, we examined the evolution of PN ensemble response patterns as we systematically varied the ratio of concentrations of two components within a binary mixture. Applying principal component analysis for dimensionality reduction of the PN population response, we observed that responses to different mixtures formed distinct clusters and varied in a nonlinear manner with odor ratio. We applied locally linear embedding to visualize the time-varying dynamics of the PN ensemble as a function of the ratio of odor components.

Second, we estimated the ensemble PN response vectors to odor mixtures by adding the response vectors corresponding to the mixture components. We then examined the degree of deviation between these estimated response vectors and the experimentally observed response vectors as the number of odorants within the mixture increased from 2 to 3, 4, 5, 6, 7, 8. Finally, we examine the degree to which these representations mirror the responses of the targets of the PNs in the mushroom body, the KCs.

72. Decoding the sparse representations of the locust mushroom body
Stijn Cassenaer

The insect mushroom body (MB) is used as a model system to address several questions of general neurobiological interest such as sensory discrimination, multi-modal integration, the control of complex behavioral repertoires, as well as learning and memory (1). Among these, the role of the MB in olfaction and memory has received considerable attention. A number of studies have addressed how olfactory information reaches the MB and how it is transformed along the way (2, 3). A particularly dramatic transformation occurs between the antennal lobe (AL) and the MB. Whereas odor representations in the AL are densely distributed and dynamic, only one synapse further downstream, odor representations are sparse, comprised of brief activation of a small fraction of the MB intrinsic neurons (Kenyon cells, KCs). This sparse representation should be advantageous for learning and memory, as it reduces the number of synapses that need to be modified and the number of comparisons necessary for pattern matching (4). There are several lines of evidence that implicate the synaptic contacts between KCs and their downstream targets in memory storage and recall (5).

In order to address the question of how the sparse representations carried by KCs are decoded and further transformed before leaving the MB, we are investigating

the cells that take KC activity as their input, the MB extrinsic cells. There appear to be several distinct cell types within this population that differ most obviously with respect to the neuropils they invade (6, 7). We are characterizing these neurons in terms of their physiological and morphological properties by means of intracellular and tetrode recordings. We are investigating how odors are represented by this population, how efficacious the KC-extrinsic cell synapses are, how they can be modified, and how the extrinsic cells integrate their KC inputs.

References

(1) Strausfeld, N., Hansen, L., Yongsheng, L., Gomez, R.S. and Ito, K. (1998) *Learning & Memory* **5**:11-37.
(2) Wilson, R.I., Turner, G.T. and Laurent, G. (2004) *Science* **303**:366-370.
(3) Perez-Orive, J., Mazor, O., Turner, G.T., Cassenaer, S., Wilson, R.I. and Laurent, G. (2002) *Science* **297**:359-365.
(4) Laurent, G. (2002) *Nature Rev. Neurosci*. **3**:884-895.
(5) Heisenberg, M. (2003) *Nature Rev. Neurosci*. **4**:266-275.
(6) MacLeod, K, Backer, A. and Laurent, G. (1998) *Nature* **395**:693-698.
(7) Farivar, S. (2005) Ph.D. thesis, Caltech

73.   Imaging population activity in the honeybee brain during olfactory learning
Cindy N. Chiu

Honeybees are capable of an impressive repertoire of complex learning behaviors such as contextual learning, categorization and discrimination. Since the areas of the honeybee brain that are crucial to learning contain only thousands to tens of thousands of cells, honeybees offer the unique opportunity to study complex cognitive processes at a mechanistic level. Though honeybees are notoriously difficult electrophysiology subjects, imaging studies have had some modest and increasing success in monitoring the neural activity of honeybees. Currently, we attempt to develop an experimental protocol to load hundreds of neurons en masse with functional fluorescent indicators (such as dextran conjugated or acetoxymethyl (AM) ester derivative calcium indicators) in a live insect preparation. Using this method, we hope to record the activity of populations of single neurons at or near single spike resolution in the honeybee brain during the course of olfactory learning.

Publications

Bazhenovz, M., Stopfer, M., Sejnowski, T.J. and Laurent, G. (2005) Fast odor learning improves reliability of odor responses in the locust antennal lobe. *Neuron* **46**:483-492.
Friedrich, R.W., Habermann, C.J. and Laurent, G. (2004) Multiplexing using synchrony in the zebrafish olfactory bulb. *Nature Neurosci.* **7**(8):862-871.

Jortner, R., Farivar, S. and Laurent, G. Dense connectivity for sparse representation in an olfactory network. Submitted.
Laurent, G. Olfactory microcircuits, dynamics of the output of the olfactory system. In: *Microcircuits: The Interface between Neurons and Global Brain Function*, Sten Grillner and Randolf Menzel, Eds., Springer Verlag. In press.
Laurent, G. Shall we even understand the dly's brain? In: *23 Problems in Neuroscience*, Leo Van Hemmen and Terrence Sejnowski, Eds. In press.
Laurent, G. and Borst, A. Short stories from invertebrate dendrites: Linking biophysics to computation. In: *Dendrites*, G. Stuart, N. Spruston, M. Häusser, Eds. Oxford University Press, 2nd edition. In press.
Mazor, O. and Laurent, G. Transient dynamics vs. fixed points in odor representations by locust antennal lobe projection neurons. Submitted

Bren Professor of Biology: Henry A. Lester
George Grant Hoag Professor of Chemistry: Dennis Dougherty[1]
Members of the Professional Staff: Bruce N. Cohen
Associate Biologist: Purnima Deshpande
Postdoctoral Scholars: Daniel Clayton, Mohammed Dibas, Carlos Fonck, Joanna Jankowsky, Herwig Just, Fraser Moss, Raad Nashmi, Rigo Pantoja, Nivalda Rodrigues-Pinguet, Andrew Tapper, Jinling Wang
Graduate Students: Kiowa San Bower[1], Amanda Cashin[1], Amy Lynn Eastwood[1], Ariele Patrice Hanek[1], Princess Imoukhuede[2], Lori Waihang Lee[1], Kathryn McMenimen[1], Tingwei Mu[1], E. James Petersson[1], Erik Ali Rodriguez[1], Eric Slimko[2], Michael Torrice[1], Jinti Wang, Xinan (Joanne) Xiu[1]
Research and Laboratory Staff: Pamela Fong, Kathleen Hamilton, Qi (Stephanie) Huang, Sarah May, Sheri McKinney
Undergraduate Laboratory Assistants: Charlotte Guo, Robin Hunter
Surf Student: Simona Tescu
Visiting Associate: Johannes Schwarz[3]
[1]*Division of Chemistry and Chemical Engineering, California Institute of Technology*
[2]*Division of Engineering and Applied Science, California Institute of Technology*
[3]*Department of Neurology, University of Leipzig, Germany*

Summary: We continue our work on biophysical, neuroscience, and medical aspects of ion channels, receptors, and transporters. We have analyzed several strains of knock-in mice generated in our laboratory for the nicotinic α4 receptor. The nicotinic receptor work is enhanced by a promising new strain, Leu9'Ala, which has generated interesting insights into nicotine addiction. We find that activation of α4-containing receptors by nicotine is sufficient for tolerance, sensitization, and reward behavior. Strains that contain GFP tags on their nicotinic receptors are now being analyzed, and they show good function. We are employing it to understand the cell biology of nicotinic receptors during nicotine addiction.

The α4 nicotinic receptor, or its partner the β2 subunit are mutated in a rare series of human epilepsies. We studied the nAChR epilepsy mutations in oocyte expression systems and, in collaboration with other labs, are constructing knock-in mouse strains that also have these mutations. Another α4 knock-in strain, the Leu9'Ser, presents a model system for studying neurodegenerative disease.

Our work on selective silencing of mammalian neurons has generated a promising set of techniques and reagents based on ligand-activated chloride channels. In collaboration with the David Anderson laboratory, we are now developing "proof of concept" transgenic mouse strains.

We continue our joint work with the Dougherty group, in Caltech's Chemistry Division, on aspects of ion channel structure function. We have brought novel techniques to these studies, including mass spectrometry and fluorescence. We also concentrate on unnatural amino-acid mutagenesis. We have now found that a cation-π interaction helps agonists bind to several cys-loop receptors—for acetylcholine, serotonin, and GABA. Proline is the only naturally occurring cyclic amino acid; and unnatural mutagenesis must be used to introduce proline derivatives. We have now found a compelling relationship between the energy of *cis-trans* isomerization at a particular proline and the energy of channel gating, suggesting that this isomerization actually governs the gating of the channel.

With the Dougherty group and with Neurion Pharmaceuticals in Pasadena, we have started to analyze the binding of blocking drugs to the hERG potassium channel, also using unnatural amino acid mutagenesis. The channel is important because it underlies many instances of drug-induced long-QT syndrome. We are working hard to incorporate unnatural amino acids into the hERG channel when expressed in mammalian cells, where the pharmacology of blockade is much more similar to that in heart muscle.

Our work continues on quantitative aspects of transporter function, primarily measured with fluorescence and with knock-in mice. We are using fluorescence to analyze the mobility of GABA transporters. As an interesting side benefit of the GABA transporter knock-in mouse, we have generated and analyzed a knockout mouse for the same molecule.

Our group's home page has additional up-to-date information, images, and notices of positions. It's at http://www.cco.caltech.edu/~lester.

74. **The carboxyl terminus of the *M. tuberculosis* mechanosensitive channel of large conductance (MscL) modulates channel gating**

Daniel J. Clayton, Joshua A. Maurer[*], Donald E. Elmore[*], Henry A. Lester, Dennis A. Dougherty[*]

Intracellular domains are a common regulatory and modulatory motif among eukaryotic ion channels. The mechanosensitive channel of large conductance from *Mycobacterium tuberculosis* (Tb-MscL) provides an opportunity to study such a domain, because the crystal structure is known; and we show that the carboxyl terminal domain is such a regulatory or modulatory domain. A combination of structural stability, measured by circular dichroism thermal denaturation, and channel function, measured by patch clamp measurements, was used to characterize multiple single point mutations in the Tb-MscL carboxyl terminal regions. As seen previously for other regions of the channel, this work clearly highlights differences between the two channel homologues, as the carboxyl terminal region of Tb-MscL is quite sensitive to mutation while the same domain plays no functional role in Ec-MscL. Single-channel measurements, using a newly developed rapid purification scheme on some of these mutants confirm a gain-of-function, because *bona fide* channel openings are observed at membrane pressures below the breaking level. The present results indicate the carboxyl terminal should be incorporated in a comprehensive model of channel gating.

[*]*Division of Chemistry and Chemical Engineering, Caltech*

75. **Microscopic kinetic aspects of ACh activation for modified cation-π interactions**

Bruce N. Cohen, Michael M. Torrice[1]

We are studying single-channel records for nicotinic ACh receptors bearing unnatural amino acid mutations. Initial records were obtained from cell-attached patches on *Xenopus* oocytes exposed to 300 μM and 1000 μM acetylcholine (ACh), showing isolated clusters of wild-type (WT) and mutant (αTrp149 mutated to 5-F-Trp) channel openings. We have successfully recorded single channels from > 80% of the mutant patches, in the both cell-attached configuration (at pipette potentials of -100 and +100 mV) and in the outside-out configuration (at -100 mV). This excellent success rate opens up various possibilities: (a) including holding at positive potentials to eliminate channel block; (b) applying several [agonist] to a single patch; and (c) recording single-channel currents from less robustly expressing mutants. Dr. Anthony Auerbach, our consultant, has been analyzing the traces with the QUB software. The fluorinated unnatural amino acid 5-F-Trp increases the cluster duration and closed time within the cluster. Apparently fluorination decreases β, the rate constant for channel opening, by at least several fold. These observations agree with the hypothesis that decreasing the cation-π interaction slows the rate of conformational change that opens the channel.

[1]*Division of Chemistry & Chemical Engineering, Caltech*

76. **Fluorescence studies of the muscle nicotinic receptors**

Mohammed Dibas, David Dahan, Princess Imoukhuede, Simona Tescu[1]

We use fluorescence to study conformational transitions at the muscle nAChR. Previously, we tethered a sulforhodamine fluorophore by reacting an MTS derivative (MTSR) with a Cys side chain introduced at the β19' position in the M2 region of the nAChR expressed in *Xenopus* oocytes. The previous data detected a time-resolved signal that distinguishes desensitization from simple long-duration closing of the channel. Cys-loop receptors have five (pseudo) symmetrical subunits, but at most Cys-loop receptors, the dose–response relationship for agonist activation has a Hill coefficient approaching 2, indicating that the open state of the channel is much more likely to be associated with two bound agonist molecules than with only one. We wish to test the hypothesis that during activation, the upper M2 helix of all five subunits re-orients with respect to neighboring helices. The new data show that the hypothesis can be tested, because good fluorescence signals (ΔF) can be obtained from the MTSR-labeled M2-Cys19' position of any nAChR subunit during activation. Yet each subunit has a characteristic amplitude and sign of ΔF. Interestingly, the ΔF for either the γ, or its paralog the ε subunit, is negative, as opposed to the pattern for all the other subunits [the oocytes were injected with αβ(γ19'Cys)δ or αβ(ε19'Cys)δ, respectively]. We have begun analyzing the consequences of mutations in helices neighboring M2, in order to localize the fluorescent probe in the resting and active state. The data (1) suggest that the fluorescent probe is indeed contacting the M3 helix in the resting state, and (2) explain the fluorescence *decrease* for (γ, ε) vs. the *increase* for all other subunits.

[1]*Undergraduate, Caltech*

77. **Exploring the external TEA block of the voltage gated potassium channel *Shaker* with unnatural amino acids**

Christopher A. Ahern[1], Amy Eastwood[2], Richard Horn[1], Dennis Dougherty[2]

In electrically excitable cell types, such as nerve and muscle, voltage gated potassium channels are responsible for returning the cell membrane to hyperpolarized potentials after an action potential. Additionally, some potassium channels are externally blocked by the monovalent cation tetraethylammonium (TEA). A high affinity blockade by extracellular TEA requires the presence of an aromatic residue, either Tyr or Phe, at position 449 (in *Shaker*) that sits at the external entrance of the permeation pathway. This observation may have physiological relevance as the same residue is mechanistically involved in a type of channel inactivation that occurs during prolonged depolarized potentials. With this in mind, we investigated whether a cation-π interaction contributes to the binding of TEA by Tyr449. This was accomplished using the *in vivo* nonsense suppression method to incorporate a series of increasingly

fluorinated phenylalanine amino acids at position 449. *Xenopus* oocytes expressing functionally suppressed *Shaker* potassium channels were voltage clamped and exposed to a range of extracellular TEA concentrations. Consistent with a cation-π interaction, fluorination serially increased the K_i for TEA block from (in mM) 0.38 for wild-type channels to 0.79, 18.2 and 55.7 for 4F-Phe, $3,5F_2$-Phe and $3,4,5F_3$-Phe-containing channels, respectively. These results suggest a strong cation-π component to the TEA block, similar to previously studied cation-π systems such as the binding of acetylcholine to the nAChR receptor and of serotonin to the 5HT3 receptor. However, a recent crystal structure of a potassium channel in the presence of an external TEA analog orients the Tyr residues in a manner inconsistent with a cation-π interaction. Furthermore, a number of theoretical and modeling studies have cast doubt on the role of cation-π interactions in external TEA block. To clarify these discrepancies, we intend to investigate TEA block further with *Shaker* channels containing additional unnatural amino acids at site 449.

[1]*Institute of Hyperexcitability, Thomas Jefferson Medical College, Philadelphia PA, 19147*
[2]*Division of Chemistry and Chemical Engineering, Caltech*

78.   Investigating cation-π interactions in the local anesthetic block of voltage gated sodium channels

Christopher A. Ahern[1], Amy Eastwood[2], Richard Horn[1], Henry Lester, Dennis Dougherty[2]

Voltage gated sodium channels control the upstroke of the cardiac action potential and are therefore, important for cardiac electrical excitability. Class I antiarryhthmic drugs block sodium conduction in this family of ion channels and are commonly used to treat numerous life threatening conditions, including ventricular fibrillation. We investigated the possibility of a cation-π interaction between the class I antiarrhythmic cationic drug lidocaine with the voltage gated sodium channel $rNa_V1.4$. To this end, a series of phenylalanine derivatives deactivated in the cation-π interaction by the addition of fluorine substituents were inserted at aromatic amino acid sites that line the internal pore of the channel, using the *in vivo* nonsense suppression methodology. These sites were previously shown to be important for channel block by lidocaine. The effect of 200 μM lidocaine was investigated using two-electrode voltage clamp recordings from *Xenopus* oocytes expressing sodium channels carrying these unnatural amino acid derivatives. The nature of the channel block was investigated for steady state tonic conditions and with a use-dependent protocol employing repetitive 20-ms depolarizations from -100 mV to 0 mV over a range from 2 to 20 Hz. For one site in particular, Phe1579, the lidocaine block was highly sensitive to fluorination. The use-dependent block was successively alleviated by addition of multiple fluorine substituents. Furthermore, suppression at this site with the unnatural amino acid cyclohexylalanine, a side chain sterically similar to phenylalanine but lacking aromatic character, abolished use-dependent block by lidocaine at frequencies as high as 20 Hz. WT channels are roughly 90% blocked under similar conditions. Two other aromatic sites that line the pore, Tyr1574 and Tyr1587, showed no effect or mild relief of block, respectively, upon incorporation of the same series of unnatural amino acids. Our results suggest a cation-π contribution to lidocaine block of voltage gated sodium channels.

[1]*Institute of Hyperexcitability, Thomas Jefferson Medical College, Philadelphia PA, 19147*
[2]*Division of Chemistry and Chemical Engineering, Caltech*

79.   Novel seizure phenotype and sleep disruptions in knock-in mice with hypersensitive α4* nicotinic receptors

Carlos Fonck, Bruce N. Cohen, Paul Whiteaker[1], Raad Nashmi, Daniel A. Wagenaar[2], Nivalda Rodrigues-Pinguet, Purnima Deshpande, Steven Kwoh, Jose Munoz, Sheri McKinney, Cesar Labarca, Allan C. Collins[1], Michael J. Marks[1]

A leucine to alanine substitution (L9'A) was introduced in the M2 region of the mouse α4 neuronal nicotinic acetylcholine receptor (nAChR) subunit. Expressed in *Xenopus* oocytes, α4(L9'A)β2 nAChRs were ≥ 30-fold more sensitive to both ACh and nicotine. We generated knock-in mice with the L9'A mutation and studied their cellular responses, seizure phenotype, and sleep-wake cycle. Seizure studies on α4-mutated animals are relevant to epilepsy research because all known mutations linked to autosomal dominant nocturnal frontal lobe epilepsy (ADNFLE) occur in the M2 region of α4 or β2 subunits. Thalamic cultures and synaptosomes from L9'A mice were hypersensitive to nicotine-induced ion flux. L9'A mice were ~15-fold more sensitive to seizures elicited by nicotine injection than their WT littermates. Seizures in L9'A mice differed qualitatively from those in WT: L9'A seizures started earlier, were prevented by nicotine pretreatment, lacked EEG spike-wave discharges and consisted of fast repetitive movements. Nicotine-induced seizures in L9'A mice were partial whereas WT seizures were generalized. When L9'A homozygous mice received a 10 mg/kg nicotine injection, there was temporal and phenomenological separation of mutant and WT-like seizures: an initial seizure, ~20 s after injection was clonic and showed no EEG changes. A second seizure began 3-4 min after injection, was tonic-clonic and had EEG spike-wave activity. No spontaneous seizures were detected in L9'A mice during chronic video-EEG recordings, but their sleep-wake cycle was altered. Our findings show that hypersensitive α4* nicotinic receptors in mice mediate changes in the sleep-wake cycle and nicotine-induced seizures resembling ADNFLE.

[1]*Institute of Behavioral Genetics, University of Colorado, Boulder, CO 80309*
[2]*Division of Physics, Mathematics, and Astronomy, California Institute of Technology, Pasadena, CA 91125*

62

80. Functional characterization of the L9'A mutation in the α4-nicotinic receptor: Implications for ADNFL epilepsy

Carlos Fonck, Nivalda Rodrigues-Pinguet, Bruce N. Cohen

We are interested in characterizing the L9'A mutation because similar mutations in the pore-lining region of the α4-containing nicotinic receptor are associated with Autosomal Dominant Nocturnal Frontal Lobe Epilepsy (ADNFLE). We previously studied mice expressing the L9'A mutation and found that nicotine-induced seizures in these mice have pharmacological, electroencephalographic and behavioral similarities with seizures experienced by ADNFLE patients. By expressing nicotinic receptors with ADNFLE mutations in *Xenopus* oocytes, several authors have examined changes in channel function and proposed potential mechanisms responsible for ADNFLE, including increased agonist sensitivity, reduced Ca^{2+} permeability, enhanced desensitization and decreased Ca^{2+} potentiation. We tested several of these hypotheses by expressing nicotinic receptors with the L9'A mutation in oocytes. The L9'A mutation dramatically increased agonist sensitivity compared to WT receptors, as evidenced by a 30-fold leftward shift in the EC_{50} for nicotine and acetylcholine (ACh). We studied receptor desensitization by exposing oocytes to a sustained dose of nicotine, while measuring peak responses to brief ACh pulses. WT and L9'A IC_{50}s for steady-state desensitization were 22 ± 5 nM and 8.2 ± 0.5 nM respectively. Thus, the L9'A mutation reduced the IC_{50} for steady-state nicotine desensitization only ~three-fold, compared to a 30-fold reduction in the EC_{50} for nicotine activation of the receptor. We also estimated the permeability of WT and L9'A mutant receptors to Na^+ and Ca^{2+} relative to K^+ (P_{Na}/P_K, P_{Ca}/P_k), by measuring shifts in the reversal potential of the ACh response after extracellular ion substitutions. The L9'A mutation did not affect P_{Na}/P_K or P_{Ca}/P_k. In summary, the L9'A mutation is more sensitive to nicotine activation and desensitization than WT, but it does not alter ion selectivity for physiologically relevant cations. We speculate that increased sensitivity to agonist could result in the activation of specific brain circuits, which may underlie pathological responses such as those found in ADNFLE.

81. Nicotinic receptors containing the α4 subunit modulate respiratory patterns in the preBötzinger complex

Xuesi M. Shao[*], Wenbin Tan[*], Carlos Fonck, Henry A. Lester, Jack L. Feldman[*]

Smoking has been associated with disorders of respiratory control such as sudden infant death syndrome (SIDS) and sleep apnea. SIDS is known to correlate with maternal smoking and is the second-leading cause of infant death between one month and one year of age. Nicotine, a major component of cigarette smoke, acts on nicotinic acetylcholine receptors (nAChRs) in the brain, affecting a variety of brain functions including control of breathing. To explore the molecular composition of nAChRs that control breathing and their contribution to the pathogenesis of SIDS, we used a knock-in mouse strain with a hydrophilic mutation (L9'A) in the M2 pore-lining region of the α4 subunit. This mutation renders α4-containing receptors hypersensitive to nicotinic agonists. We recorded respiratory-related rhythms from the hypoglossal nerve (XIIn) and whole-cell patch-clamped preBötC inspiratory neurons in a slice preparation obtained from newborn mice. Bath-applied nicotine induced significantly larger responses in preBötC inspiratory neurons and XIIn respiratory-related rhythmic activity in homozygous L9'A mice than those induced in WT mice. These responses included tonic nerve activity, an increase in frequency and duration of inspiratory bursts of the XIIn motor output, and at the cellular level, a tonic inward current, an increase in membrane noise and a decrease in the phasic inspiratory drive current in voltage-clamped preBötC inspiratory neurons. These responses were completely blocked by the nAChR antagonist dihydro-β-erythroidine. Our data indicate that nAChRs in the preBötC of L9'A mutant mice are hypersensitive to nicotine and thus, suggest that the nAChRs mediating nicotinic modulation of respiratory pattern contain α4 subunits. Identifying the molecular composition of the nAChRs in the preBötC that mediate respiratory modulation may provide a pharmacological target for the prevention, diagnosis and treatment of tobacco-related pathological conditions in central control of breathing such as SIDS.

[*]Department of Physiological Science, University of California, Los Angeles, CA 90095

82. Neurochemical studies of the L9'A substitution in the α4 nicotinic receptor subunit

Michael J. Marks[*], Nancy M. Meinerz[*], Todd del Vecchio[*], Carlos Fonck, Purnima Deshpande, Henry A. Lester, Allan C. Collins[*]

Nicotinic acetylcholine receptors (nAChR), in which a Leu in the second transmembrane domain of the α4 subunit is substituted with Ala (L9'A), show a gain-of-function. Mice engineered to express the L9'A mutation are more sensitive to several effects of nicotine than are wild-type mice (WT). The effects of the L9'A mutation on nAChR function were evaluated by agonist-stimulated Rb^+ efflux from synaptosomes prepared from cortex and thalamus of WT, homozygotic L9'A (Hom) and heterozygotic (Het) mice. The concentration effect curves for ACh-stimulated Rb^+ efflux in both brain regions of WT were biphasic with apparent EC_{50}s of 2 and 200 μM. Rb^+ efflux for Het was also biphasic, but EC_{50}s (0.7 and 25 μM) and maximal responses were lower than WT. EC_{50} (0.15 μM) and responses were further reduced in Hom, and efflux curves appeared monophasic. Concentration-effect curves for nicotine-stimulated Rb^+ efflux were not obviously biphasic, but did have low Hill coefficients; and genotype-dependent decreases in EC_{50} (WT = 5 μM, Het =1.5 μM, Hom = 0.15 μM) resembled those for ACh. Het and Hom mice also displayed decreased total Rb^+ efflux. In measurements on nAChR binding sites, there was a

gene dose-dependent decrease in cytisine-sensitive epibatidine binding: binding in Hom was ~ 50% that of WT. In contrast, neither cytisine-resistant nor A85380-resistant epibatidine binding was affected by the mutation. These results suggest lower expression of $\alpha 4(L9'A)\beta 2$ nAChR, leading to lower overall maximal function of these receptors. However, the significant increase in affinity for both ACh and nicotine dominates at lower concentrations: L9'A receptors are activated by much lower concentrations of either endogenous or exogenous agonists. This explains, in part, the increased sensitivity of these mice to nicotine.

*Institute of Behavioral Genetics, University of Colorado, Boulder, CO 80309

83. Visualizing the trafficking of the GABA transporter, mGAT1 using TIR-FM

Princess I. Imoukhuede

This project aims to understand the trafficking of mGAT1 in neuro-2A cells transiently transfected with the mGAT1-eYFP8 and in the cerebellum of homozygous mice expressing GAT1-GFP. In collaboration with Dr. Robert Chow of the University of Southern California, we use Total Internal Reflection Fluorescence Microscopy (TIR-FM) to observe the movement of mGAT1-containing vesicles onto the plasma membrane and to quantify the number of mGAT1 molecules on each vesicle. mGAT1-eYFP8 vesicle fusion is induced with a translocation cocktail containing an inactivator of PKC, an inhibitor of tyrosine phosphatases, and a suppressor of endocytosis. We find that local application of the translocation cocktail to N2a cells transiently transfected with mGAT1-YFP8 induces an immediate increase in fluorescence. Another technique we apply to observe vesicle fusion is Fluorescence Recovery after Photobleach (FRAP). Combining TIR-FM with FRAP increases our ability to sensitively detect the arrival of mGAT1-YFP8-containing vesicles on or near the membrane. Finally, [Chiu *et al.* (2002) *J. Neurosci.* **22**:10251] showed that GAT1 molecules can be counted on axons and boutons by creating fluorescent beads that calibrate bouton fluorescence. We will apply this pioneering procedure to count the numbers of GAT1-eYFP8 molecules within vesicles using TIR-FM. To this end we will create histidine-tagged eYFP molecules bound to Ni-NTA moieties on transparent beads.

84. Persistent amyloidosis following suppression of Aβ production in a transgenic model of Alzheimer's disease

Joanna L. Jankowsky, Hilda H. Slunt[1], Victoria Gonzales[2], Alena V. Savonenko[2], Jason Wen[3], Nancy A. Jenkins[4], Neal G. Copeland[4], Linda H. Younkin[5], Steven G. Younkin[5], David R. Borchelt[6]

Considerable effort has focused on development of secretase inhibitors for the treatment of Alzheimer's disease (AD) that will diminish production of amyloid-β (Aβ) peptide from the amyloid precursor protein (APP). These therapies predict that reducing Ab levels in the brain, even after the onset of clinical symptoms and the development of associated pathology, will halt the progression of disease and allow the repair of damaged tissue. However, no long-term studies using animal models to test the outcome of such treatment have yet been published, so little is known about what effects, positive or negative, will result from therapies designed to chronically lower Aβ production in the brain. In the present study, we have generated a transgenic mouse model that genetically mimics the arrest of Aβ production expected from treatment with secretase inhibitors. These mice over-express mutant APP (swe/ind) from a vector that can be regulated by doxycycline (dox). Under normal conditions, high-level expression of APPswe/ind quickly induces fulminant amyloid pathology. We show that dox administration inhibits transgenic APP expression by >95% and reduces Aβ production to levels found in non-transgenic mice. Suppression of transgenic Aβ synthesis in this model abruptly halts the progression of amyloid pathology. However, β formation and clearance amyloid deposits appear to be in disequilibrium as the plaques require far longer to disperse than to assemble. Mice in which APP synthesis was suppressed for as long as 6 months after the formation of Aβ deposits retain a considerable amyloid load, with little sign of active clearance. This study demonstrates that amyloid lesions in transgenic mice are highly stable structures *in vivo* that are not rapidly cleared in the absence of immune system activation. Our findings suggest that arresting Aβ production in AD patients should halt the progression of pathology, but that early treatment may be imperative as amyloid deposits, once formed, will require additional intervention to resolve.

[1,2,3]*Departments of Pathology, Neuroscience, Cellular and Molecular Medicine Program, The Johns Hopkins University School of Medicine, 558 Ross Research Building, 720 Rutland Ave., Baltimore, MD 21205*
[4]*Mouse Cancer Genetics Program, NCI-Frederick Cancer Research and Development Center, Frederick, MD 21702*
[5]*Mayo Clinic Jacksonville, 4500 San Pablo Road, Jacksonville FL 32224*
[6]*Department of Neuroscience, McKnight Brain Institute, University of Florida, 100 Newell Drive, PO Box 100244, Gainesville, FL 32610*

85. Selective silencing of mammalian neurons using glutamate-gated chloride channels

Herwig Just, Eric Slimko

The neuroscience underlying diseases (neurological, psychiatric and drug abuse) can be understood best if the function of the various types of neurons in the central nervous system is known. Conventionally, function of neurons is investigated by inactivating them with pharmacological and lesion approaches. To overcome the disadvantages of these methods, we seek to continue developing a strategy to selectively silence neurons by using glutamate-gated

chloride channels (GluCl). Invertebrate GluCl channels are introduced into mammalian neurons; their activation by the drug Ivermectin (IVM) inhibits subsequent firing of action potentials ("silencing").

GluCl channels are a heterooligomer of α- and β-subunits. We have modified these subunits for our purposes: (i) They have been codon optimized for expression in mammalian cells; (ii) tagged with the cyan or yellow fluorescent proteins to allow for direct visualization; and (iii) glutamate sensitivity has been reduced greatly by mutating Tyr182 to Phe in the β-subunit (without affecting response to IVM). Our lab has generated a transgenic mouse line expressing the engineered GluCl-subunits in Purkinje cells under the control of the L7 promoter. We will record electrophysiological activity from Purkinje cells in cerebellar brain slices to monitor neuronal silencing in response to IVM treatment.

In an alternative approach, we are using the Cre-Lox-system: A transgenic mouse line is being generated that will express the β-subunit in all tissues. We will confirm GluCl β-subunit expression by immunofluorescence microscopy. These animals will then be crossed with mice that express the enzyme Cre-recombinase in specific types of neurons. Cre-recombinase removes a stop-codon in the coding sequence of the α-subunit. This will result in tissue-specific α-subunit expression and reconstitution of functional channels. Our first cross will be with mice selectively expressing Cre-recombinase in dopaminergic neurons. Upon IVM treatment, we expect the animals to exhibit a Parkinson-like phenotype in behavioral studies. Measurement of the electrophysiological activity from isolated neurons and brain slices will determine if the behavior is a result of selective neuronal silencing.

86. *Cis-trans* isomerization at a proline opens the pore of a neurotransmitter–gated ion channel
Sarah C.R. Lummis*, Darren L. Beene**, Lori W. Lee**, R. William Broadhurst*, Dennis A. Dougherty**

5-HT$_3$ receptors are members of the Cys-loop receptor superfamily. Neurotransmitter binding in these proteins triggers the opening (gating) of an ion channel, by means of an as yet uncharacterized conformational change. Here we show that a specific proline (Pro 8*), located at the apex of the loop between the 2nd and 3rd transmembrane helices (M2-M3), can link binding to gating through a *cis-trans* isomerization of the protein backbone. Using unnatural amino acid mutagenesis, a series of proline analogues with varying preference for the *cis* conformer was incorporated at the 8* position. Proline analogues that strongly favor the *trans* conformer produced non-functional channels. Among the functional mutants there was a strong correlation between the intrinsic *cis-trans* energy gap of the proline analogue and the activation of the channel, suggesting that *cis-trans* isomerization of this single proline provides the switch that

interconverts the open and closed states of the channel. Consistent with this proposal, NMR studies on an M2-M3 loop peptide reveal two distinct, structured forms. Our results thus confirm the structure of the M2-M3 loop and the critical role of Pro 8* in the 5-HT$_3$ receptor. In addition, they suggest a molecular rearrangement at Pro 8* is the structural mechanism that opens the receptor pore.

*Department of Biochemistry, University of Cambridge, Tennis Court Road, Cambridge, CB2 1GA, United Kingdom
**Division of Chemistry and Chemical Engineering, Caltech

87. A cation-π binding interaction with a tyrosine in the binding site of the GABAc receptor
Sarah C.R. Lummis[1], Darren L Beene[2], Neil J Harrison[1], Dennis A Dougherty[2]

GABAc (ρ) receptors are members of the Cys-loop superfamily of neurotransmitter receptors, which includes nicotinic acetylcholine (nACh), 5-HT3 and glycine receptors. As in other members of this family, the agonist-binding site of GABAc receptors is rich in aromatic amino acids, but while other receptors bind agonist through a cation-π interaction to a tryptophan, the GABAc binding site has tyrosine at the aligning positions. Incorporating a series of tyrosine derivatives at position 198 using unnatural amino acid mutagenesis reveals a clear correlation between the cation-π binding ability of the side chain and EC$_{50}$ for receptor activation, thus demonstrating for the first time, a cation-π interaction between a tyrosine side chain and a neurotransmitter. Comparisons among four homologous receptors show variations in cation-π binding energies that reflect the nature of the cationic center of the agonist.

[1]Department of Biochemistry, University of Cambridge, UK
[2]Division of Chemistry and Chemical Engineering, Caltech

88. Studies of the N-methyl-D-aspartate receptor Mg^{2+} block using unnatural amino acids
Kathryn A. McMenimen*, Ernest J. Petersson*, Dennis A. Dougherty*

The N-methyl-D-aspartate (NMDA) receptor is a ligand-gated, ionotropic glutamate receptor central to mediating excitatory synaptic transmission involved in learning and memory processes. The NMDA receptor is a member of the ionotropic glutamate receptor (iGluR) family of glutamate-gated ligand-gated ion channels (LGICs), a family that also encompasses the kainate and AMPA receptors. Upon activation, these receptors allow the influx of intracellular Ca^{2+}, Na$^+$, and K$^+$. The binding of glutamate and glycine to independent binding sites is required to activate the NMDA receptor. Mg^{2+} blocks the receptor at resting membrane potentials therefore, Ca^{2+} flow through the channel only occurs after the binding of agonists and the voltage-dependent release of Mg^{2+} from the pore. Previous studies suggest there is a cation-π interaction between a tryptophan (NR2B W607) in the

pore of the NMDA receptor and the Mg^{2+} ion during blockade of the receptor. Studies on the Mg^{2+} binding site of the NMDA receptor focus on this conserved tryptophan.

The use of unnatural amino acids to study the Mg^{2+} blockade of the NMDA receptor will provide chemical-scale studies of this binding site deep within the pore of the receptor. Prior work in this group has shown that acetylcholine, a cationic agonist, binds to the nicotinic acetylcholine receptor through a cation-π interaction with a conserved tryptophan in the binding site. These experiments were performed using a series of fluorinated Trp amino acids. Present experiments explore the importance of the cation-π interaction during the Mg^{2+} blockade by incorporating the fluorinated Trp amino acids at a conserved site, NMDA NR2B W607. Further studies will utilize unnatural amino acids to study the chemical-scale interactions between several conserved Asn residues and Mg^{2+} during blockade of the receptor.

Division of Chemistry and Chemical Engineering, California Institute of Technology

89. hERG block in acquired long-QT syndrome probed with unnatural amino acids
Fraser J. Moss

The human ether-a-go-go-related gene (hERG1, KCNH2) encodes a K^+ channel α-subunit expressed primarily in the ventricles, producing the voltage-dependent K^+ current termed IKr. A large variety of therapeutic drugs block hERG, prolonging the cardiac action potential QT interval. This is defined as acquired long-QT (LQT) syndrome that in turn may lead to ventricular arrhythmia, torsades de pointes, and possibly to fatal ventricular fibrillation. Acquired LQT syndrome arising from hERG block has become the number one safety issue in the development of pharmaceuticals. Drugs under development must show no hERG blockade if they are to move forward. We propose to elucidate the subtle yet critically important nature of the binding interactions that determine how and why many non-cardiovascular clinical drugs bind to hERG to cause acquired LQT syndrome. We will combine the exquisite sensitivity of patch-clamp electrophysiology and the versatility of nonsense unnatural amino acid (UAA) suppression to investigate this problem. Most importantly, all experiments will be done in mammalian cell lines because a major limitation of the standard *Xenopus* oocyte model is that test substances accumulate in the oocyte yolk, causing significant variability and error in potency estimates. Our laboratory has pioneered the application of UAA suppression to study all the major non-covalent interactions that govern ligand-receptor binding in proteins, as well as related interactions between moieties on the protein. We have now expanded these technologies for application in mammalian expression systems. hERG residues to be investigated include Thr623, Ser624, Tyr652 and Phe656. We will replace these naturally occurring residues with UAA's with side chains that highlight cation-π interactions, hydrophobic interactions, and hydrogen bonds. We expect the initial experiments to generate further hypotheses about additional positions. The drugs to be studied will be from a wide variety of structural classes and include; terfenadine, dofetilide, cisapride, astemizole, MK-499, quinidine, vesnarinone, chloroquine. We expect to make a series of conclusions about the nature of contact points for the unique interaction between each drug and the channel.

90. Fluorescent mGAT1 constructs for correct trafficking and dimerization
Fraser J. Moss, Princess I. Imoukhuede, Joanna L. Jankowsky

We seek knock-in mice carrying fusions between mGAT1 and yellow and cyan fluorescent protein (YFP, CFP) to understand the density, intracellular processing, PDZ interactions, trafficking, and possible dimerization of the GABA transporter mGAT1 *in vivo*. Synaptosomes from previously described mGAT1-green fluorescent protein (GFP) knock-in mice [Chiu *et al.* (2002) *J. Neurosci.* **22**:10251] displayed only 33% of wt surface functional GAT1, probably because the GFP molecule masks a PDZ-type II interacting motif, AYI. The new strains will preserve or substitute this motif so that mGAT-1-XFP (X= C or Y) exhibits wt-like surface distribution and GABA uptake, as well as high fluorescent resonance energy transfer (FRET) efficiencies. We constructed several C-terminal mGAT1-XFP fusions. XFP with an additional 3, 8, 20 or, 45 residues from the hGAT1 C-terminus was fused with the mGAT C-terminus (mGAT1-XFP3, -XFP8, -XFP20, -XFP45). mGAT1-XFP* had an alternative PDZ-type II interacting region (YKV) at the C-terminus. mGAT1-XFPCT fused the XFP moiety into the junction between the penultimate and final exon of mGAT1. We measured [^{3}H]-GABA uptake in N2A cells, in assays optimized for linearity. The data: mGAT1-XFP8 most closely resembled wt. Co-expression of mGAT1-CFP8 and mGAT1-YFP8 gave a FRET efficiency of 10%, a reasonable value for side by side 12 TM domain transporters. mGAT1-XFP3 and mGAT1-XFP* gave enhanced uptake compared to wt. Thus, a PDZ-type II binding domain at the C-terminus restores at least wt uptake levels, but its sequence and/or upstream residues influence interactions with PDZ-proteins. mGAT-1XFP45 and mGAT1-XFPCT had poor uptake; thus, two copies of the 17 AA immediately after TM12, or bisecting this region with XFP, interferes with transporter export to the membrane. Interestingly, FRET efficiency for the poorly trafficked mGAT1-XFPCT's was 50%. We conclude that mGAT1-XFP8 is the most suitable construct to build a fluorescent mGAT1 mouse; but other constructs reveal signals that regulate normal mGAT1 trafficking.

66

91. The hydrogen-bonding pattern of serotonin in the MOD-1 receptor

Tingwei Mu[*], Dennis A. Dougherty[*]

Previous modeling studies suggested that serotonin could form three hydrogen bonds in the binding pocket of MOD-1. We aimed to prove this hydrogen-bonding pattern experimentally. In order to confirm the hydrogen bond between a ligand and a specific residue in a receptor, we need to show: first, the specific residue forms a hydrogen bond; second, the ligand is the actual hydrogen bond partner of this specific residue. To prove the first point that a specific residue forms a hydrogen bond, we can change the structure of this residue to perturb its hydrogen bonding ability and monitor the resulting functional change. Conventional mutations can be used as a starting point for this purpose. With the unnatural amino acid mutagenesis methodology, one can finely tune the hydrogen bonding ability of this residue, thus confirming this point with more confidence. To prove the second point that the ligand is the actual hydrogen bond partner of this specific residue, we need to modify the hydrogen bonding ability of the ligand. Functional studies can then be performed to provide compelling evidence on the hydrogen bond between the ligand and the specific residue. If forward pharmacology is used to describe the structural modification of the ligand, and reverse pharmacology to the residue, this strategy can then be termed as the forward and reverse pharmacology method.

The forward and reverse pharmacology method was applied to test the hydrogen-bonding pattern of serotonin in MOD-1. The hydrogen bond between the indolic amine group of serotonin and Gln 228 was confirmed. Furthermore, the EC_{50} values measured in the experiment were in good agreement with the hydrogen bond binding energies calculated from *ab initio* quantum mechanics. Our results provide good support for the existence of two hydrogen bonds between serotonin and Asn 223 and the main chain carbonyl group of Tyr 180. Therefore, we obtained a high-resolution image of the orientation of serotonin in the binding pocket. This advances the study of the Cys-loop superfamily of ligand-gated ion channels and drug design for this family.

[*]*Division of Chemistry and Chemical Engineering, California Institute of Technology*

92. FRET studies of cross-inhibition between P2X and nicotinic channels

Raad Nashmi, James Fisher[*], David N. Bowser[*], Baljit S. Khakh[*]

ATP-gated P2X channels and ACh-gated nicotinic channels exhibit functional interactions when expressed either in heterologous coexpression systems or at endogenous levels in neurons: co-activation of both channel types results in responses that are smaller than the predicted sum of the individual components. This lack of summation is termed cross-inhibition [Khakh *et al.* (2000) *J. Neurosci.* 25:6911-6920]. We have now extended previous work on cross-inhibition to P2X2 and α4β2 nicotinic channels, and used electrophysiology,

fluorescence resonance energy transfer (FRET) and total internal refection fluorescence (TIRF) microscopy between CFP and YFP-tagged channels to probe mechanisms. Co-activation resulted in currents that deviated from the predicted current by 39±4%, and this and other electrophysiological properties were consistent with occlusion of the nicotinic component. TIRF and FRET microscopy of fluorescently-labeled P2X2 and α4β2 nicotinic channels demonstrated close spatial arrangement of the channels in human embryonic kidney cells and in hippocampal neuron membranes. We measured FRET efficiency (*e*) of 28±8% for P2X2 channels labelled on their C termini with CFP and YFP, and 25±3% for α4β2 channels labelled with CFP (β2) and YFP (α4) within the M3-M4 intracellular loop (Nashmi *et al.*, 2003). We measured strong FRET between CFP or YFP labelled P2X2 and α4β2 channels when the cognate acceptor or donor fluorophore was on the β2 subunit (*e* = 26±3 and 23±6%), but weak or no FRET between P2X2 and α4β2 channels when the acceptor (*e*=10%) or donor (*e*=0%) fluorophores were on the α4 subunit. The data suggest that P2X2 and α4β2 channels may form a dimer, with the channels approximately 80 Å apart. The measurements also show that P2X2 subunits interact specifically and robustly with the β2 subunits in α4β2 channels. The data provide direct evidence for the close spatial apposition of full-length P2X2 and α4β2 channels within 100 nm of the plasma membrane of living cells.

[*]*MRC Laboratory of Molecular Biology, Cambridge, CB2 2QH*

93. Fluorescently-tagged α4 nicotinic receptor knock-in mice

Raad Nashmi, Purnima Deshpande, Cesar Labarca, Sheri L. McKinney, Michael J. Marks[*], Sharon Grady[*], Paul Whiteaker[*], Qi Huang, Tristan McClure-Begley[*], Allan C. Collins

α4b2 nicotinic acetylcholine receptors (nAChRs) constitute the most abundant high affinity nicotinic receptors in the brain. Their physiological contributions to neurotransmission signaling and behavior are not completely understood. A precise mapping of the subcellular and neuroanatomical localizations of α4 nAChR subunits will help delineate the physiological role of α4 and its role in nicotine addiction. Using the homologous recombination technique, we have genetically engineered knock-in mice that express α4 nAChR subunits fused to yellow fluorescent protein (α4YFP) inserted in the M3-M4 cytoplasmic loop of α4. Confocal microscopic imaging and spectral unmixing was performed in order to separate specific YFP fluorescence from autofluorescence background. α4YFP fluorescence intensities were measured in various brain regions of wild-type, heterozygous and homozygous mice. The summed α4YFP fluorescence intensities from various brain regions of the heterozygous mice were 45% of homozygous. The strongest α4YFP fluorescence was detected in neurons

from the medial habenula. α4YFP could be traced from axonal fibers in the faciculus retroflexus emanating from the medial habenula and terminating in the interpeduncular nucleus. Strong α4YFP expression was found throughout the entire thalamus, in the thalamocortical and corticothalamic fibers in the internal capsule and also in fibers coursing between dopaminergic fibers of the caudate putamen. "Hot spots" of α4YFP expression overlapped with tyrosine hydroxylase positive dopaminergic fibers in the caudate putamen. α4YFP showed robust expression in the cell bodies and dendrites of dopaminergic neurons in the substantia nigra pars compacta (SNC) and in the ventral tegmental area (VTA). 98% and 85% of the dopaminergic neurons in the SNC and VTA, respectively, contained α4YFP while the remainder had nondetectable levels of α4. These α4YFP mice will allow us a unique opportunity to examine α4 nAChR expression and to delineate the role of α4 in neurotransmission in the CNS.

*Institute for Behavioral Genetics, University of Colorado, Boulder 80309

94.   Incorporating a fluorescent unnatural amino acid into the nicotinic receptor

Rigo Pantoja

Fluorescent markers on proteins are a valuable tool for insights on structure, dynamics and intermolecular interactions. One method involves cysteine mutagenesis: a cysteine inserted in the site of interest can react with the thiol group of a fluorophore. Nevertheless, a limitation is that extra steps must be taken in order to shield or eliminate endogenous cysteine residues. Another alternative is to fuse the gene for a fluorescent protein (such as GFP) to the desired protein at the site of interest. Nevertheless, the bulky size – roughly 2.4 nm x 4.2 nm – of GFP analogs places a serious limitation on the sites where they may be introduced. In addition, mutations by the methods described lead, in many cases, to failure of protein expression, either because of improper folding or because a crucial residue is substituted. Fluorescent unnatural amino acids represent an attractive alternative for labeling ion channel proteins with minimal structural and amino acid sequence perturbations. Therefore, the nonsense suppression methodology was used to incorporate a fluorescent unnatural amino acid into the extracellular domain of the nicotinic acetylcholine receptor (nAChR). An α subunit with a Aps70TAG mutation was used to incorporate the Lys(NBD) fluorescent unnatural amino acid. The α70 is in the main immunogenic region of the nAChR. Previous unnatural amino acid mutagenesis studies carried out in conjunction with biotin-streptavidin binding were used to demonstrate that αAsp70 is a surface-exposed residue. This mutationally tolerant site was selected for incorporating the Lys(NBD) unnatural amino acid, which is larger than natural amino acids. The nAChR proteins were expressed in *Xenopus* oocytes. The presence of surface-expressed nAChRs was confirmed by measuring macroscopic currents with a two-electrode voltage-clamp two days after injection. The nAChR dose-

response relationships were used to confirm phenotype characteristics. The EC50 for the α70TAGLys(NBD) β9'Ser was 0.70 ± 0.20 μM (n = 4). Potential applications include higher resolution inter- and intra-molecular fluorescence resonance energy transfer (FRET) experiments that can be used to elucidate nAChR conformational states.

95.   Mutations linked to autosomal dominant nocturnal frontal lobe epilepsy affect allosteric Ca²⁺ activation of the α4β2 nicotinic acetylcholine receptor

Nivalda O. Rodrigues-Pinguet, Thierry J. Pinguet[1], Antonio Figl[2], Bruce N. Cohen

Extracellular Ca^{2+} robustly potentiates the acetylcholine response of α4β2 nicotinic receptors. Rat orthologs of five mutations linked to autosomal dominant nocturnal frontal lobe epilepsy (ADNFLE)-α4(S252F), α4(S256L), α4(+L264), β2(V262L), and β2(V262M)-reduced 2 mM Ca^{2+} potentiation of the α4β2 1 mM acetylcholine response by 55-74%. To determine whether altered allosteric Ca^{2+} activation or enhanced Ca^{2+} block caused this reduction, we co-expressed the rat ADNFLE mutations with an α4 N-terminal mutation-α4(E180Q)-that abolished α4β2 allosteric Ca^{2+} activation. In each case, Ca^{2+} inhibition of the double mutants was less than that expected from a Ca^{2+} blocking mechanism. In fact, the effects of Ca^{2+} on the ADNFLE mutations near the intracellular end of the M2 region-α4(S252F) and α4(S256L) were consistent with a straightforward allosteric mechanism. In contrast, the effects of Ca^{2+} on the ADNFLE mutations near the extracellular end of the M2 region-α4(+L264)β2, β2(V262L), and β2(V262M)-were consistent with a mixed mechanism involving both altered allosteric activation and enhanced block. However, the effects of 2 mM Ca^{2+} on the α4β2, α4(+L264)β2, and α4β2(V262L) single-channel conductances, the effects of membrane potential on the β2(V262L)-mediated reduction in Ca^{2+} potentiation, and the effects of eliminating the negative charges in the extracellular ring on this reduction failed to provide any direct evidence of mutant-enhanced Ca^{2+} block. Moreover, analyses of the α4β2, α4(S256L), and α4(+L264) Ca^{2+} concentration-potentiation relations suggested that the ADNFLE mutations reduce Ca^{2+} potentiation of the α4β2 acetylcholine response by altering allosteric activation rather than by enhancing block.

[1]Luxtera, Inc., Carlsbad, CA
[2]Molecular Devices Corp., Union City, CA

96. Enhanced expression of hypersensitive α4* nAChR in adult mice increases the loss of midbrain dopaminergic neurons

*Johannes Schwarz[*1], Sigrid C. Schwarz[1], Oliver Dorigo[2], Alexandra Stützer[1], Florian Wegner[1], Cesar Labarca, Purnima Deshpande, Jose S. Gil[2], Arnold J. Berk[2]*

We describe an inducible genetic model for degeneration of midbrain dopaminergic neurons in adults. In previous studies, knock-in mice expressing hypersensitive M2 domain Leu9'Ser (L9'S) α4 nicotinic receptors (nAChR) at near-normal levels displayed dominant neonatal lethality and dopaminergic deficits in embryonic midbrain, because the hypersensitive nAChR is excitotoxic. However, heterozygous L9'S mice that retain the neomycin resistance cassette (neo) in a neighboring intron express low levels of the mutant allele (~25% of normal levels), and these neo-intact mice are therefore, viable and fertile. The neo cassette is flanked by loxP sites. In adult animals, we locally injected helper-dependent adenovirus (HDA) expressing *cre* recombinase. Local excision of the neo cassette, via *cre*-mediated recombination, was verified by genomic analysis. In L9'S HDA-*cre* injected animals, locomotion was reduced both under baseline conditions and after amphetamine application. There was no effect in L9'S HDA-control treated animals or in wild-type (WT) littermates injected with either virus. Immunocytochemical analyses revealed marked losses (> 70 %) of dopaminergic neurons in L9'S HDA-*cre* injected mice compared to controls. At 20 - 33 days post injection in control animals, the coexpressed marker gene, YFP, was expressed in many neurons and few glial cells near the injection, emphasizing the neurotrophic utility of the HDA. Thus, HDA mediated gene transfer into adult midbrain induced sufficient functional expression of *cre* in dopaminergic neurons to allow for postnatal deletion of neo. This produced increased L9'S mutant nAChR expression, which in turn led to nicotinic cholinergic excitotoxicity in dopaminergic neurons.

[1]*Department of Neurology, University of Leipzig, Liebigstr. 22a, 04103 Leipzig, Germany*

[2]*Molecular Biology Institute and Department of Microbiology, Immunology and Molecular Genetics, University of California, Los Angeles, CA 90095, USA*

97. Selective neuronal silencing in zebrafish retinal ganglion cells

Eric Slimko, Ethan Scott[*], Herwig Baier[*]

Using the retinal ganglion cell promoter ath5, we have generated transgenic zebrafish that express two engineered subunits of a *C. elegans* chloride channel, optGluClα-ECFP and optGluClβ-Y182F-EYFP. In previous *in vitro* work, we have shown that neurons expressing both of these genes will be electrically silenced only when exposed to low concentrations (5 nM) of the anthelmintic drug Ivermectin (IVM). We started with five transgenic fish lines, and first screened them for expression with immunohistochemistry. We found that the channel was expressed robustly in the periphery of the retina in one line, less so in a second, and hardly at all in the remaining three. The expression pattern matched native ath5 expression. We then screened all five lines for deficits in three different visual behaviors: 1) visual background adaptation (VBA), where 5-day old fish larvae are expected to adapt to the color of their local background; 2) the optokinetic response (OKR), where larvae are immobilized, presented with a moving visual stimulus, and eye tracking speed, saccade rate, and saccade amplitude are measured; and 3) the optomotor response (OMR), where larvae are placed in a clear channel with a moving background and their distance swum in a set time is measured. Transgenic larvae not exposed to IVM performed statistically equivalent to wild type; and low concentrations (up to 10 nM tested) of IVM do not affect the performance of wild-type larvae under any of these assays. However, in 10 nM of IVM, transgenic fish larvae completely fail at the VBA behavior and have a severe deficit in performance in the OKR. The OMR is left completely unaffected. Both lines with positive immunohistochemistry data show these effects, although one line has stronger behavioral defects than the other. This data would seem to suggest that the periphery of the retina is critical for VBA and the OKR, but is not necessary the OMR. Further experiments are in progress.

[*]*Department of Physiology and Programs in Neuroscience, Genetics, Developmental Biology, and Human Genetics, University of California at San Francisco, San Francisco, CA*

98. Mecamylamine precipated withdrawal syndrome in hypersensitive α4 nicotinic acetylcholine receptor knock-in mice

Andrew R. Tapper, Sheri McKinney, Purnima Deshpande

Nicotine withdrawal is a multi-symptom response to nicotine cessation after chronic nicotine exposure that affects and, in many cases, prevents millions of people from quitting smoking. Little is known about the molecular mechanism underlying withdrawal. Identification of the nAChR subtypes involved in the initiation, and onset of withdrawal should provide insights into the pathophysiology of addiction and will also help identify potential smoking cessation targets. In rodents, injection of the nicotinic antagonists, mecamylamine, during chronic nicotine infusion conditions a place aversion that is thought to represent the negative affect associated with withdrawal. To identify the role of α4* nicotinic acetylcholine receptors in withdrawal we injected mice expressing hypersensitive α4* nAChRs (the Leu9'Ala line) with mecamylamine. Previous work indicates that α4* nAChRs in Leu9'Ala midbrain cultures are activated by as little as 10 nM agonist, a concentration within the range of basal acetylcholine levels in the CNS. Remarkably, doses of mecamylamine that have no effect in drug naïve wild-type animals condition a place aversion in Leu9'Ala homozygotes. In addition, mecamylamine produces hypolocomotion in mutant animals, an additional

withdrawal symptom. Mecamylamine-precipitated hypolocomotion is centrally mediated because the nicotinic antagonist, hexamethonium, which does not readily pass the blood-brain barrier, has little effect on mutant animals. Recent evidence indicates that opioid receptor blockade can precipitate withdrawal in nicotine-dependent rodents. Leu9'Ala mice challenged with the opioid antagonist, naloxone, display hypolocomotion at doses that have no effect on wild-type animals providing further evidence for a nicotine-independent withdrawal syndrome in the Leu9'Ala line. Together, these data indicate that Leu9'Ala mice may be dependent on basal CSF acetylcholine levels, and, that persistent activation of α4* nAChRs may be sufficient for initiation of the negative affective aspects of withdrawal.

99. **Microarray analysis of VTA in Leu9'Ala and WT mice after nicotine exposure identifies genes involved in nicotine dependence**
Andrew R. Tapper, Sheri McKinney, Purnima Deshpande

Increasing evidence indicates that the first step towards nicotine dependence is nicotine activation of ventral tegmental area (VTA) α4β2* neuronal nicotinic acetylcholine receptors (nAChR). However, little is known about the cascade of events that occurs between initial nicotine exposure and addiction. It is likely that hundreds of additional gene products downstream of receptor activation play a role in establishing a nicotine-dependent state. To identify these genes we are using microarray chips to analyze changes in wild-type and Leu9'ala VTA gene expression during either acute or chronic nicotine exposure. Leu9'ala mice harbor hypersensitive α4* nAChRs that can be selectively activated with small doses of nicotine that have little effect on wild-type animals. Single daily injections of sub-threshold doses of nicotine produces behaviors associated with dependence including tolerance, sensitization, and reward. Thus, Leu9'Ala mice can be used to identify specific changes in gene expression that are induced only by activation of α4* nAChRs. Preliminary data indicates that selective activation of α4* nAChR once daily for 9 consecutive days significantly down-regulates 97 gene transcripts while up-regulating 101 transcripts in Leu9'Ala VTA. These results will be compared with gene expression changes in VTA of nicotine treated wild-type animals. If genes identified in Leu9'Ala mice are important for nicotine dependence, then they should also be modulated in wild-type animals treated with fifty-fold higher nicotine doses. After microarray analysis, RT-PCR will be used to verify nicotine-modulated transcripts. Together these experiments should identify genes involved in nicotine dependence.

100. **α4 nicotinic acetylcholine receptors mediate disinhibition of dopaminergic neuron**
Jinling Wang

Using knock-in mice expressing hypersensitive L9'A α4 acetylcholine receptors (nAChR), our lab demonstrated that nicotine activation of α4 subtype is sufficient for reward, tolerance and sensitization. We propose here to investigate the underlying synaptic mechanism of this α4-mediated nicotinic addiction. Enhancement of dopaminergic neuron activity in ventral tegmental area (VTA) and subsequent dopamine release in nucleus accumbens (NAcc) are key predictors of reward behavior in drug abuse. Output of VTA dopaminergic neuron is determined by the coordination of excitatory and inhibitory synaptic inputs from various brain regions including medial prefrontal cortex and midbrain cholinergic centers. Different subtypes of nAChRs are thought to modulate these two types of inputs. Activation of α7 nAChR was shown to induce short- and long-term enhancement of excitatory glutamatergic synaptic transmission. Evidence also implies that β2-containing nAChR interacts with GABAergic transmission. We thus, hypothesize that selective activation of α4 nAChR results in disinhibition of dopaminergic neurons by suppressing inhibitory GABAergic transmission. We will perform whole-cell patch clamp experiments in the VTA region of hypersensitive L9'A mice slice preparation. We expect to see decreased spontaneous IPSC frequencies, as well as increased action potential firing rate of dopaminergic neurons in the presence of a low concentration of nicotine. We will include specific α4 nAChR blocker dihydro-β-erytroidine(DHβE) to verify subtype specificity. We will monitor spontaneous EPSCs and expect no change in their frequencies. Furthermore, we will investigate the functional role of α4 nAChR in VTA GABAergic neurons. We will establish time-course of activation and desensitization of DHβE-sensitive nicotinic currents in these neurons. We will then make correlation to the time-course of changes in synaptic transmission. Finally, we will attempt to examine α4-mediated long-term depression of synaptic strength at inhibitory synapses at dopaminergic neurons. With these experiments, we aim to establish the role of α4 nAChR as a modulator of inhibitory synaptic input to dopaminergic neurons.

101. **A unified view of the role of electrostatic interactions in modulating the gating of Cys-loop receptors**
Xinan Xiu, Ariele P. Hanek, Jinti Wang*, Dennis A. Dougherty**

In the Cys-loop superfamily of ligand gated ion channels (LGICs), a global conformational change, initiated by agonist binding, results in channel opening and the passage of ions across the cell membrane. The detailed mechanism of channel gating is a subject that has lent itself to both structural and electrophysiological studies. Here, we define a gating interface that incorporates elements from the ligand binding domain and

transmembrane domain previously reported as integral to proper channel gating. An overall analysis of charged residues within the gating interface across the entire superfamily, shows a conserved charging pattern, though no specific interacting ion pairs are conserved. We utilize a combination of conventional mutagenesis and the high precision methodology of unnatural amino acid incorporation to extensively study the gating interface of the mouse muscle nicotinic acetylcholine receptor (nAChR). We find that charge reversal, charge neutralization, and charge introduction at the gating interface are often well tolerated. Furthermore, based on our data and a reexamination of previously reported data on GABA$_A$ and glycine receptors, we conclude that the overall charging pattern of the gating interface, and not any specific pairwise electrostatic interactions, controls the gating process in the Cys-loop superfamily.

Division of Chemistry and Chemical Engineering, Caltech

Publications

Cashin, A.L., Petersson, E.J., Lester, H.A. and Dougherty, D.A. (2005) Using physical chemistry to differentiate nicotinic from cholinergic agonists at the nicotinic acetylcholine receptor. *J. Am. Chem. Soc.* **127**:350-356.

Chiu, C., Brickley, S., Jensen, K., Southwell, A., Mckinney, S., Cull-Candy, S., Mody, I. and Lester, H. (2005) GABA transporter (GAT1) deficiency causes tremor, ataxia, nervousness, and increased GABAinduced tonic conductance in cerebellum. *J. Neurosci.* **25**:3224-3245.

Fonck, C., Cohen, B.N., Nashmi, R., Whiteaker, P., Wagenaar, D., Rodrigues-Pinguet, N., Deshpande, P., Kwoh, S., Munoz, J., Labarca, C., Collins, A., Marks, M., and Lester, H. (2005) Novel seizure phenotype and sleep disruptions in knock-in mice with hypersensitive α4 nicotinic receptors. Submitted.

Jankowsky, J., Slunt, H.H., Gonzales, V., Savonenko, A.V., Wen, J., Jenkins, N.A., Copeland, N.G., Younkin, L.H., Lester, H.A., Younkin S.G. and Borckelt, D.R. (2005) Persistent amyloidosis following suppression of Aβ production in a transgenic model of Alzheimer's disease. *PLoS Medicine*. In press.

Khakh, B.S., Fisher, J.A., Nashmi, R., Bowser, D.N. and Lester, H.A. (2005) An angstrom-scale interaction between plasma membrane ATP-gated P2X2 and α4β2 nicotinic channels measured with FRET and TIRF microscopy. *J. Neurosci.* **25**:6911-6920.

Kovoor, A., Seyffarth, P., Ebert, J., Barghshoon, S., Chen, C.-K., Schwarz, S., Axelrod, J.D., Cheyette, B.N.R., Simon, M.I., Lester, H.A. and Schwarz, J. (2005) D$_2$ dopamine receptors colocalize regulator of G-protein signaling 9-2 (RGS9-2) via the RGS9 DEP domain, and RGS9 knock-out mice develop dyskinesias associated with dopamine pathways. *J. Neurosci.* **25**:2157-2165.

Lummis, S.C., Beene, D.L., Harrison, N.L., Lester, H.A. and Dougherty, D.A. (2005) A cation-π binding interaction with a tyrosine in the binding site of the GABA$_C$ receptor. *Chem. Biol.* In press.

Lummis, S.C.R., Beene, D.L., Lee, L.W., Lester, H.A., Broadhurst, R.W. and Dougherty, D.A. (2005) *Cis-trans* isomerisation at a proline opens the pore of a neurotransmitter–gated ion channel. *Nature*. In press.

Rodrigues-Pinguet, N.O., Pinguet, T.J., Figl, A., Lester, H.A. and Cohen, B.N. (2005) Mutations linked to autosomal dominant nocturnal frontal lobe epilepsy affect allosteric Ca^{2+} activation of the alpha 4 beta 2 nicotinic acetylcholine receptor. *Mol. Pharmacol.* **68**:487-501.

Schwarz, J., Schwarz, S., Dorigo, O., Stützer, A., Wegner, F., Labarca, C., Deshpande, P., Gil, J., Berk, A. and Lester, H.A. (2005) Enhanced expression of hypersensitive α4* nAChR in adult mice increases the loss of midbrain dopaminergic neurons. Submitted.

Shapovalov, G. and Lester, H. (2004) Gating transitions in bacterial ion channels measured at 3 μs resolution. *J. Gen. Physiol.* **124**:1118-1124.

Tapper, A., McKinney, S., Nashmi, R., Schwarz, J., Deshpande, P., Labarca, C., Whiteaker, P., Collins, A. and Lester, H. (2004) Nicotine action on α4* receptors: Sufficient for reward, tolerance and sensitization. *Science* **306**:1029-1032.

Tapper, A.R., Nashmi, R. and Lester, H. (2005) Neuronal nicotinic acetylcholine receptors and nicotine dependence. In: *The Cell Biology of Addiction*, J.D. Pollock, (Ed.) Cold Spring Harbor, NY 11724, Cold Spring Harbor Laboratory Press.

Xiu, X.X., Hanek, A.P.H., Wang, J., Lester, H. and Dougherty, D.A. (2005) A unified view of the role of electrostatic interactions in modulating the gating of Cys-loop receptors. Submitted.

Anne P. and Benjamin F. Biaggini Professor of Biological Sciences: Paul Patterson
Senior Research Fellow: Ali Khoshnan
Research Fellows: Sylvian Bauer, Benjamin Deverman, Natalia Malkova
Graduate Students: Walter Bugg, Jennifer Montgomery, Stephen Smith, Amber Southwell
Research and Laboratory Staff: Jan Ko, Viviana Gradinaru[1], Kathleen Hamilton, Jennifer Li[1], Doreen McDowell, Limin Shi, Andrea Vasconcellos[1], Erin Watkin
[1]*Undergraduate student, Caltech*

Summary: Much of the research in this laboratory involves the study of interactions between the nervous and immune systems. Using knockout (KO) mice and over-expression *in vivo* with viral vectors, we are exploring the role of the neuropoietic cytokine leukemia inhibitor factor (LIF) in Alzheimer's disease and inflammation. This cytokine is further being used to manipulate neural stem cell proliferation and fate in the brain. Also in the context of neuroimmune interactions, we are investigating a mouse model of mental illness based on the known risk factor of maternal influenza infection. Huntington's disease (HD) is another focus, where we are investigating potential therapies using intracellular expression of antibodies, and manipulating NFkB activity. An additional project involves the study of the endothelin B receptor and melanoma tumor progression.

Cytokines are diffusible, intercellular messengers that were originally studied in the immune system. Our group contributed to the discovery of a new family that we have termed the neuropoietic cytokines, because of their action in both the nervous and hematopoietic/immune systems. We have demonstrated that one of these cytokines, LIF, can coordinate the neuronal, glial and immune reactions to injury. Using both delivery of LIF *in vivo* and examination of the consequences of knocking out the LIF gene in mice, we find that this cytokine has a powerful regulatory effect on the inflammatory cascade. Moreover, LIF can regulate neurogenesis and gliogenesis. We find that LIF is a critical regulator of astrocyte and microglial activation following stroke, seizure or trauma, and that this cytokine also regulates inflammatory cell infiltration, neuronal and oligodendrocyte death, gene expression, as well as the production of new neurons from stem cells following injury. These results highlight LIF as an important therapeutic target. We are also examining the role of LIF in a transgenic mouse model of Alzheimer's disease, where its administration can alter the level of senile plaques.

Cytokine involvement in a new model for mental illness is also being investigated. This mouse model is based on findings that maternal respiratory infection can increase the likelihood of schizophrenia or autism in the offspring. We are using behavioral, neuropathological, molecular and brain imaging methods to investigate the effects of maternal influenza infection on fetal brain development and how this leads to altered behavior in adult offspring.

We are utilizing intracellular antibody expression to block the toxicity of mutant huntingtin (Htt), the protein that causes HD. We have produced single chain antibodies (scFvs) that bind to various domains of Htt, and these can either exacerbate or alleviate Htt toxicity in cultured cells, acute brain slices, and in a *Drosophila* HD model. Work has begun on viral vectors for delivering scFvs in a mouse model of HD. We have also implicated the NFkB signaling pathway in the pathogenesis of HD, and identified several steps in this signaling cascade as potential therapeutic targets.

102. Antibodies as potential therapeutics for Huntington's disease
Amber L. Southwell, Jan Ko, Ali Khoshnan, Paul Patterson

Huntington's disease (HD) is a progressive neurodegenerative disorder characterized by chorea, cognitive alterations and selective degeneration of striatal neurons. The autosomal dominant mutation responsible for HD is an expansion of a CAG repeat coding for polyglutamine in exon 1 of the Htt protein. Our group has generated single chain monoclonal antibodies that bind Htt and can be expressed intracellularly (intrabodies). Intrabodies directed against expanded polyglutamine increase mutant Htt-induced aggregation and cell toxicity in culture. In contrast, MW7, an intrabody directed at a pair of polyproline stretches in Htt, decreases mutant Htt-induced aggregation and cell death. This effect has been demonstrated in cell culture, acute brain slices (with P. Reinhart and D. Lo at Duke), and in a *Drosophila* model of HD (with G. Jackson at UCLA). The high MW7:mutant Htt ratio required for effectiveness (4:1) prompted the isolation and characterization of other anti-Htt, anti-polyproline intrabodies. Thus far, two human anti-polyP (HAPP) intrabodies isolated from a synthetic (non-immunized) single chain library exhibit beneficial effects on mutant Htt-induced aggregation. We are also characterizing a single domain intrabody recognizing the first seventeen amino acids of Htt (VL12.3). This intrabody also reduces mutant Htt-induced aggregation. The therapeutic potential of these intrabodies will next be tested in a mouse model of HD using viral-mediated gene therapy. Insights acquired through such experiments may contribute to the generation of therapeutics for HD.

103.   Production of anti-polyQ antibodies that distinguish various forms of amyloid proteins

Jan Ko, Merav Geva[1], Brian O'Nuallain[1], Lezlee Dice[1], Susan Ou, Ron Wetzel, Paul Patterson

With the aim of developing new reagents for the study of mutant Htt structure and function, we produced of a new set of mAbs generated against normal and expanded repeat polyQ peptides that were prepared so as to have different structures. Seven mAbs were selected for detailed study. While one mAb (PGA11) strongly prefers binding to mutant Htt over other proteins with an amyloid structure, PGA1 and 8 strongly prefer the amyloid protein Aβ over Htt on ELISAs, and do not bind Htt on Western blots. Thus, some of the polyQ antigen used for the immunization must have taken on a structure specific to Aβ. Since PGA1 and 8 do not stain plaques in mouse Alzheimer brains, we hypothesize that this unique structure precedes the formation of Aβ aggregates into plaques *in vivo*. In addition, on Western blots, PGA4, 12, 13 and 14 bind to oligomers formed by Htt, but not to the large Htt aggregates on the top of the gel. This is in contrast to PGA11, which binds aggregates but not oligomers. A very striking aspect of these findings is that the Western data only apply to Htt exon1 that lacks the polyP domain. That is, PGA4, 11, 12, 13 and 14 only bind to Htt lacking polyP. This is consistent with prior observations of an incompatibility between exposure of the polyQ and polyP epitopes. *In vivo*, anti-polyQ mAbs bind cytoplasmic Htt but not when it is in nuclear inclusions, while anti-polyP mAbs bind nuclear inclusions but not cytoplasmic Htt. In contrast, our MW8 mAb, which binds the C-terminus of Htt exon1, binds oligomers and aggregated Htt, as well as nuclear inclusions *in vivo*. This binding is seen only for Htt that contains polyP.

[1]*University of Tennessee*

104.   Interaction of mutant huntingtin with the NF-κB pathway

Ali Khoshnan, Erin Watkin, Jan Ko

Transcriptional dysregulation by mutant Htt protein has been implicated in the pathogenesis of HD and we found that mutant Htt activates the NF-κB pathway. Mutant Htt physically associates with IKKγ, a regulatory component of the IκB kinase complex (IKK). In cultured cells, this interaction results in the activation of IKK, leading to the phosphorylation and degradation of the inhibitory protein IκBα. These findings have *in vivo* relevance, as striatal extracts from HD transgenic mice have higher levels of IKK than extracts from control mice, and activated NF-κB is found in the nucleus of striatal and cortical neurons in HD mice. Binding to IKKγ is mediated by the expanded polyglutamine stretch in mutant Htt, and is augmented by the proline-rich motifs of Htt. Expression of IKKγ promotes mutant Htt aggregation and nuclear localization. Conversely, an N-terminally truncated form of IKKγ, which interferes with IKK activity, blocks Htt-induced NF-κB activation and reduces the toxicity of mutant Htt in cell culture and in an acute brain slice model

of HD. Toxicity is also inhibited by expression of a mutant F-box deleted E-3 ubiquitin ligase, ΔF-βTRCP, which specifically blocks degradation of IκB inhibitory proteins. Thus, aberrant interaction of mutant Htt with IKKγ, and subsequent NF-κB activation, may be important for HD pathology. On the other hand, IKKγ can influence Htt actions through non-NF-κB pathways. Expression of IKKγ promotes the toxicity of full-length mutant Htt, implicating IKKγ as a modifier of mutant Htt toxicity. In neurons, IKKγ is predominantly located in the nucleus. Microarray analysis shows that expression of IKKγ from a recombinant lentivirus influences expression of many genes implicated in neuronal survival and differentiation. Studies are in progress to examine specific genes affected by IKKγ that may regulate the toxicity of mutant Htt and neurodegeneration.

105.   The role of IκB-kinase complex in neuronal development and function

Ali Khoshnan, Jan Ko

The role of the IκB-kinase complex (IKK) in neuronal development, survival and degeneration is not understood. In non-neuronal cells, IKK regulates the activity of the transcription factor NF-κB. The core components of the IKK complex include two serine-threonine kinases IKKα (IKK1) and IKKβ (IKK2), and a regulatory non-catalytic module, IKKγ (NEMO). IKKα and IKKγ also have NF-κB-independent functions. We showed that binding of mutant Htt to IKKγ leads to aberrant IKK activity and enhances mutant Htt neurotoxicity (Khoshnan *et al.*, 2004). On the other hand, mice deleted for both IKKα and IKKβ die at E12 and display enhanced apoptosis in the neuroepithelium, indicating normal and regulated activity of the IKK complex is essential for development and function of neurons. We are specifically interested in the function of IKKα, as it has been implicated in chromatin modification in epithelial cells. We find that IKKα promotes neurite outgrowth in differentiating rat cortical stem cells and it is found in the growing tips of neurites. Growth cone cues such as netrin activate IKK. IKKα is activated in response to neuroprotective molecules such as IGF and estrogen, suggesting a role in neuronal survival. IKKα is translocated to the nucleus upon IGF treatment, where it colocalizes with CREB binding protein. We are studying the mechanism of IKKα regulation of neurite outgrowth, as well as the signaling pathways influenced by the nuclear function of IKKα in neurons and neuroblasts.

106. **Maternal influenza infection alters fetal brain development**

Limin Shi, Paul Patterson

Epidemiological studies have shown that maternal infection can increase the risk for mental illness in the offspring. In a mouse model of maternal respiratory infection with influenza virus, the adult offspring display striking behavioral, pharmacological and histological abnormalities. Using RT-PCR assays for four viral genes, we find no evidence of viral infection of the fetal brain. This supports our earlier evidence that it is the mother's immune response to infection, rather than viral infection of the fetus, that is key to altering fetal brain development. Pathology studies have shown a number of abnormalities in prefrontal cortex, hippocampus and cerebellum of patients with autism and schizophrenia. Using immunohistochemistry and *in situ* hybridization, we are characterizing various changes in the brains of the offspring of infected mothers, at several development stages.

107. **The maternal inflammatory response and its effects on fetal development and behavior of the adult offspring**

Benjamin E. Deverman, Wendy Xu[1], Paul Patterson

Significant epidemiological evidence suggests that there is an increased incidence of schizophrenia and autism in the offspring of women exposed to infection during pregnancy. In a mouse model based on these findings, the adult offspring of mothers exposed to influenza during pregnancy exhibit several behavioral and neuropathological abnormalities that are consistent with those observed in schizophrenia and autism. Moreover, at least one of these abnormalities is also seen in the adult offspring of mothers injected with poly(I:C), a dsRNA that elicits an inflammatory response similar to that induced by influenza infection.

The inflammatory response to viral infection and poly(I:C) administration is mediated by numerous cytokines, many of which could have profound effects on fetal brain development. Therefore, in an effort to determine which cytokines may be responsible for the observed behavioral and neuropathological abnormalities, we are measuring cytokine induction during the inflammatory response to poly(I:C) in both maternal and fetal tissues. As expected, we have found that the levels of numerous cytokines are strongly induced in the maternal serum during the response to poly(I:C). In addition, we observe a significant increase in IL-6, a pro-inflammatory cytokine, and KC, a chemoattractant for neutrophils, in the local fetal environment (i.e., the placenta and decidua) during the response to poly(I:C). In contrast, we have not detected significantly increased levels of any cytokines examined thus far in the fetus following poly(I:C) administration.

To complement and extend these findings, we are looking for evidence of downstream cytokine signaling pathway activation during the response to poly(I:C) both in the fetus and in the fetal environment as a means to localize the effects of the maternal inflammatory response. Because of our finding that IL-6 and KC are elevated in the fetal environment during the response to poly(I:C), we have begun by focusing on their downstream effectors. IL-6 signaling induces the phosphorylation and activation of the Stat3 transcription factor. In fact, Stat3 is activated in the uterus but not in the fetus, which fits with our finding that maternal IL-6 does not appear to cross into the fetus. Since KC is a chemoattractant for neutrophils, we examined neutrophil infiltration following poly(I:C) administration, and our preliminary evidence suggests that there is indeed an increase in neutrophil infiltration into the placenta, specifically within the trophoblast giant cell layer, cells known to synthesize KC under certain conditions. We do not yet know what effect, if any, the observed activation of these pathways has on fetal development.

[1]*Caltech undergraduate student*

108. **Interactions between the immune system and the developing brain**

Stephen Smith, Paul Patterson

Human studies demonstrate an increased risk for both schizophrenia and autism in children born to mothers who experienced a viral infection during pregnancy. We are exploring a mouse model in which administration of influenza virus during pregnancy induces behavioral abnormalities in the adult offspring. As no virus is found in the fetal brain, and immune stimulation by LPS or poly(I:C) is sufficient to cause behavioral abnormalities in the offspring, we hypothesize that the maternal immune response to infection alters fetal brain development and results in abnormal adult behavior. We are attempting to mimic the effects of maternal infection with administration of individual cytokines to determine which components of the immune response alter fetal development. We are also testing the effects of maternal injection of anti-cytokine antibodies along with poly(I:C) in pregnant mice, and identifying vulnerable cells expressing cytokine receptors in the fetus. Another project involves the study of inflammatory cells in the fetuses of infected or poly(I:C)-injected mothers.

109. **The effect of prenatal influenza infection on neurobehavioral development of mouse offspring**

Natalia Malkova, Paul Patterson

On the basis of epidemiological evidence indicating that maternal infection leads to an increased risk of schizophrenia and autism in the offspring, a mouse model has been developed in which the pregnant mother receives a respiratory infection of human influenza virus at mid-gestation. At birth, the offspring display no signs of encephalopathy or direct viral infection. They do, however, display neuropathology at birth and in adulthood, including reduction in neocortical and hippocampal thickness, pyramidal cell atrophy and reduced levels of reelin. Neurobehavioral development of pups born to

influenza-infected mothers is studied using their ability to emit ultrasound vocalizations. Repeated vocalizations are observed in most mammalian species, including humans, when infants are separated from their familiar surroundings and social companions. This early vocalization response is considered to be strongly conserved in evolution as an affective and communicative display, most likely because of its survival value in eliciting maternal search and retrieval responses, nursing and caretaking. Preliminary data show that C57BL/6J pups born to influenza-infected or poly(I:C)-treated mothers have lower rates of ultrasound calling compared to controls. Studies are in progress to test pups using other behavioral assays, such as potentiation of pup calling after a brief period of interaction with the mother, and responses to familiar vs. unfamiliar bedding.

110.   Imaging hallucinations in mice
Natalia Malkova, Paul Patterson

Hallucinations result from normal activation of the visual or auditory system in the absence of appropriate sensory input. Moreover, such activity is enhanced by drugs that are known to induce hallucinations in normal people and exacerbate this symptom in schizophrenic subjects. Activation of 5-HT$_{2A}$ receptors (5-HT2AR) is thought to underlie the psychomimetic properties of hallucinogenic chemicals in humans. Recently, it was shown that 5-HT$_{2A}$ receptor agonists such as 2,5-dimethoxy-4-iodoamphetamine (DOI) and lysergic acid diethylamide (LSD) stimulate head twitches in mice, which are not seen in 5-HT2AR null mutant mice. Histochemistry of the brain revealed DOI and LSD up-regulation of the immediate early genes *erg-1, erg-2* and *period-1*, as well. Our aim is to extend these observations of hallucinogen-specific induction of *erg-1, erg-2* and *period-1* by mapping their distribution in the brain, in order to determine if the pattern of activation resembles that seen in schizophrenic brain during hallucinations.

111.   The effect of endothelin receptor antagonists on cancer cells
Jennifer Montgomery, Paul Patterson

We are investigating the effect of two distinct endothelin receptor B (ETRB) antagonists on the proliferation of melanoma and glioma cells. Previous work in this laboratory indicated that the ETRB antagonist BQ788 decreases melanoma cell proliferation *in vitro* and *in vivo*. We find that this is also true for the antagonist A-192621 *in vitro*. Moreover, both ETRB antagonists decrease proliferation in some glioma cell lines. Current experiments are exploring the effects of siRNA knockdown of ETRB or the active form of endothelin-1. We are also using FACS analysis to assess the effect of ETRB antagonists on the cell cycle.

112.   Effects of LIF on adult neural stem cells in normal and APP23 mice
Sylvian Bauer, Andrea Vasconcellos[1]

In the adult brain, newly generated neurons are incorporated into the olfactory bulb (OB) and the subgranular zone of the hippocampus. This neurogenesis can be modulated *in vivo* by exogenous growth factors, which can promote neuronal replacement after injury. We have previously shown that the cytokine leukemia inhibitory factor (LIF) is necessary *in vivo* for the lesion-induced proliferation of neuronal progenitors that regenerate olfactory sensory neurons in the adult mouse. We are now asking if LIF regulates neurogenesis in the normal adult brain and in the context of a chronic neurodegenerative condition by using APP23 mice, a model of Alzheimer's disease. C57Bl/6J and APP23 mice received a single, intracerebroventricular injection of recombinant adenovirus (AdV) expressing either LIF or LacZ. Bromodeoxyuridine (BrdU) was then injected i.p. daily for seven days, and the animals were perfused two weeks after the first BrdU injection. Compared to control and LacZ-AdV brains, LIF-AdV treatment strongly represses neurogenesis in the SVZ-OB system by reducing cell proliferation and neuronal differentiation in the SVZ. In contrast, cell proliferation is increased in the cortex and periventricular areas, where more newly generated astrocytes are detected. In addition, a strong induction of inflammation is seen in LIF-AdV brains, suggesting that the majority of proliferating cells in the parenchyma are microglia. Effects on neurogenesis in the hippocampus are currently under investigation. Examination of APP23 brains shows that LIF-AdV significantly lowers amyloid plaque levels in a time-dependent manner.
[1]*Caltech undergraduate*

Publications

Armstrong, B.D., Hu, Z., Abad, C., Yamamoto, M., Rodriguez, W.I., Cheng, J., Tam, J., Gomariz, R.P., Patterson, P.H. and Waschek, J.A. (2004) Lymphocyte regulation of neuropeptide gene expression following neuronal injury. *J. Neurosci. Res.* **74**:240-247.

Berry, M.F., Pirolli, T.J., Jayasankar, V., Moriine, K.J., Moise, M.A., Fisher, O., Gardner, T.J., Patterson, P.H and Woo, Y.J. (2004) Targeted overexpression of leukemia inhibitory factor to preserve myocardium in a rat model of postinfarction heart failure. *J. Thoracic Cardiovasc. Surg.* **128**:866-875.

Kerr, B.J. and Patterson, P.H. (2004) Potent pro-inflammatory actions of leukemia inhibitory factor (LIF) in the spinal cord of the adult mouse. *Exper. Neurol.* **188**:391-407.

Kerr, B.K. and Patterson, P.H. (2005) Leukemia inhibitory factor (LIF) promotes oligodendrocyte survival after spinal cord injury. *Glia* **51**:73-79.

Khoshnan, A., Ko, J., Watkin, E.E., Paige, L.A., Reinhart, P.H. and Patterson, P.H. (2004) Activation of the Iκ-B kinase complex and NF-κB contributes to mutant huntingtin neurotoxicity. *J. Neurosci.* **24**:7999-8008.

Khoshnan, A., Ou, S., Ko, J. and Patterson, P.H. (2004) Antibodies against huntingtin: Production and screening of monoclonal and single chain recombinant forms. In: *Methods in Molecular Biology* **277**:87-191.

Trinucleotide Repeat Protocols, M. Kohwi, Ed., Human Press, Totowa, NJ.

Lahav, R., Suva, M.-L., Rimoldi, D., Patterson, P.H. and Stamenkovic, I. (2004) Endothelin B inhibition triggers apoptosis and enhances angiogenesis in melanomas. *Cancer Res*. **64**:8945-8953.

Patterson, P.H. (2004) Maternal infection causes altered behavior in the offspring. In: *Neuropsychiatric Disorders and Infection*, S.H. Fatemi, Ed., Taylor and Francis, London, pp. 83-90.

Shi, L., Tu, N. and Patterson, P.H. (2005) Maternal influenza infection is likely to alter fetal brain development indirectly: The virus is not detected in the fetus. *Intl. J. Develop. Neurosci*. **23**:299-305.

Watanabe, Y., Hashimoto, S., Kakita, A., Takahashi, H., Ko, J., Mizuno, M., Someya, T., Patterson, P.H. and Nawa, H. (2004) Neonatal impact of leukemia inhibitory factor on neurobehavioral development in rats. *Neurosci. Res*. **48**:345-353.

Professor of Biology: Erin M. Schuman
Visiting Associate: Adam Mamelak[1]
Postdoctoral Fellows: Daniela Dieterich, Changan Jiang, Gentry Patrick, Michael Sutton, Chin-Yin Tai, Young Yoon
Graduate Students: Baris Bingol, Cindy Chiu, Paola Cressy, Noah Gourlie, Hiroshi Ito, Jennifer Lee, Eric Mosser, Shreesh Mysore, Ueli Rutishauser, W. Bryan Smith, Hwan-Ching Tai
Technical Staff: Lin Chen, Holli Weld
Administrative Staff: Ana Maria Lust, Alana Rathbun
Undergraduate Students: Christian Kempf[2]
[1]*Huntington Memorial Hospital, City of Hope*
[2]*Undergraduate student, University of Heidelberg, Germany*

Summary: Synapses, the points of contact and communication between neurons, can vary in their size, strength and number. The ability of synapses to change throughout the lifetime of the animal contributes to the ability to learn and remember. We are interested in how synapses are modified at the cellular and molecular level. We are also interested in how neuronal circuits change when synapses change their properties. We conduct all of our studies in the hippocampus, a structure known to be important for memory in both humans and animals. We use molecular biology, electrophysiology and imaging to address the questions detailed below.

A major focus of the lab concerns the cell biological mechanisms that govern modifications at individual synaptic sites. In particular, we are interested in the idea that dendritic protein synthesis and degradation may contribute to synaptic plasticity. We are also interested in mRNA and protein trafficking during synaptic plasticity.

We are also examining the role of the cadherins family of cell adhesion molecules in synaptic plasticity. Several labs have shown that cadherins are localized to synapses in the hippocampus. Earlier, we demonstrated that function-blocking cadherin antibodies or peptides can prevent long-term potentiation, without interfering with basal synaptic transmission. We hypothesize that cadherin bonds may be sensitive to local fluxes in extracellular calcium imposed by action potential activity. We are now examining the molecular mechanisms by which cadherins influence synaptic strength and the involvement of cadherins in the formation and maintenance of synapses,

using fluorescence resonance energy transfer and endocytosis assays.

A relatively new endeavor in the lab involves the recording of single neuron activities in the medial temporal lobe of human epilepsy patients. In these studies we are able to correlate single neuron responses with behavioral experience and performance. These studies should elucidate some fundamental mechanisms of brain coding and representation.

113.   A novel approach for the identification of locally synthesized proteins in neuronal dendrites
Daniela C. Dieterich*, A. James Link[1], David A. Tirrell[2], Johannes Graumann[3], Erin M. Schuman

Alterations in protein synthesis and degradation enable cells, including neurons, to adapt to changing external conditions. In neurons, there is increasing evidence that local dendritic protein synthesis is used to allow individual synapses to respond dynamically to the environmental changes that accompany the establishment, maintenance and plasticity of synaptic connections. The identification of the activity-modulated dendritic proteome promises to offer a more thorough understanding of synaptic plasticity at the molecular level. To isolate and identify dendritically synthesized proteins, we are developing a new protein tagging strategy in combination with mass spectrometry. The protein tagging is based on an azide-alkyne ligation using the azide-group bearing the non-canonical amino acid azidohomoalanine (AHA) that serves as a surrogate for methionine. Proteins bearing AHA can subsequently be tagged with an alkyne-bearing affinity tag. After tryptic digestion of affinity-purified proteins, mass spectral analysis is achieved by utilizing MudPIT (Multidimensional Protein Identification Technology) followed by bioinformatical analysis. Initial experiments show that AHA can be incorporated into newly synthesized proteins of HEK293 cells and cultured hippocampal neurons. In control experiments where AHA was replaced with methionine, no biotinylated proteins were recovered following avidin-chromatography. In a first series of tandem mass spectrometry analysis of avidin-purified proteins from AHA-treated whole cell lysates of HEK293, more than 200 proteins, including an overexpressed control protein, were identified. To identify the dendritic proteome, newly synthesized proteins from either rat brain synaptoneurosomes or isolated dendrites of hippocampal cultures are analyzed. Synaptoneurosomes are a biochemical fraction enriched with translation-active synaptic terminals, but devoid of somata and nuclei. Isolated dendrites will be obtained from a special culture system using polycarbonate nets to separate dendrites from cell bodies.

114. Regulation of spine morphological dynamics by N-cadherin

Shreesh P. Mysore, Chin Yin Tai

Morphological dynamics of dendritic spines (or "spine motility") has been the focus of considerable research recently. However, the regulation of motility by cell adhesion molecules has remained largely unstudied. We are investigating the role of N-cadherin, a key cell adhesion molecule, in this regulation using time-lapse confocal imaging in cultured hippocampal neurons. We find that the disruption of surface N-cadherin function produces novel effects on spine size and number. We also find that β-catenin, which serves to link cadherins to the actin cytoskeleton, may be implicated in this effect. We are currently exploring the downstream effects of cadherin disruption on synaptic transmission. Additionally, we are cloning a pH sensitive GFP tagged N-cadherin construct into a Sindbis virus vector in order to visualize the fate of surface cadherin and the dynamics involved, following a disruption of function.

115. NMDA receptor-dependent regulation of N-cadherin internalization at the synapse

Chin-Yin Tai, Cindy Chiu, Shreesh P. Mysore

N-cadherin, one of the major cell adhesion molecules at excitatory synapses, regulates synaptic structure and plasticity. The amount of N-cadherin present at synapses regulates the strength of the adhesive force across the synaptic junction. Very little is known, however, about the turnover of N-cadherin at the synapse and the mechanism that underlies its exo- and endocytosis. To address this issue, we have initiated a series of biochemical and imaging experiments. We have studied the kinetics of N-cadherin internalization and recycling by surface biotinylation assays and have investigated the spatial distribution of surface cadherins using an antibody live-labeling approach. We find that NMDAR-dependent activity affects the internalization of N-cadherin, but not its recycling. In addition, we have observed this regulation occurs at synapses using an antibody live-labeling approach. It has been suggested that the cytoplasmic tail of N-cadherin protein contains several potential endocytosis signals, some of which overlap with the -catenin binding site, suggesting a role for of β-catenin in regulating cadherin's internalization. In view this, we are currently investigating the involvement of β-catenin in this activity-dependent regulation of N-cadherin endocytosis.

116. Miniature synaptic transmission stabilizes excitatory synaptic function

Michael A. Sutton, Paola Cressy, Christian Kempf

Chronic blockade of action potential (AP)-evoked neurotransmission (e.g., with tetrodotoxin, TTX) induces a compensatory scaling of quantal amplitude at glutamatergic synapses (Turrigiano *et al.*, 1998). Here, we show that the miniature synaptic transmission that persists during AP blockade profoundly shapes the time-course of this homeostatic scaling. Similar to extended periods of TTX treatment alone (~24 hrs), blockade of NMDA receptors (NMDARs) in the presence of TTX scales the amplitude of AMPA receptor miniature excitatory postsynaptic currents (mEPSCs), but does not change their frequency. However, the scaling induced by NMDAR mini blockade is over an order of magnitude faster than with action potential blockade alone, suggesting that the stabilizing influence of these local miniature events initially outweighs the dramatic loss of overall synaptic drive that accompanies AP blockade. The precocious scaling induced by NMDAR mini blockade requires *de novo* protein synthesis and is associated with the insertion of AMPA-type glutamate receptors with a unique subunit composition at active (i.e., non-silent) synapses. These results indicate that an alternative mode of NMDAR signaling during miniature synaptic transmission acts to stabilize excitatory synaptic function.

117. NDMA receptor-mediated spontaneous synaptic currents in hippocampal neurons

W. Bryan Smith, Ueli Rutishauser

NMDA receptors are critically involved in synaptic plasticity, serving as "molecular coincidence detectors" due to partial blockade of the channel pore by Mg^{2+} ions at resting membrane potentials. In the traditional view, the NMDA receptor does not pass *any* current during basal synaptic transmission unless the postsynaptic cell is depolarized coincident with presynaptic neurotransmitter release. A number of recent findings have begun to challenge this idea, however, implicating NMDA receptors in biochemical and electrophysiological phenomena even when evoked activity in the cells is blocked with tetrodotoxin (e.g., WB Smith *et al.*, *Neuron*, 2005; MA Sutton *et al.*, *Science*, 2004). We are directly testing the activity of NMDA receptors under basal (non-stimulated) conditions using a combination of modeling and experimental work. If NMDA receptors are active in the absence of frank depolarization, then miniature excitatory postsynaptic currents (mEPSCs, or minis) should be detected.

118. Delivery of molecular cargo into neurons using the penetratin peptide

Hwan-Ching Tai

We are interested in utilizing the penetratin peptide to develop new tools to study synaptic function in cultured neurons. Penetratin is a short peptide sequence found in the homeodomain of *Drosophila Antennapedia* protein. Penetratin is capable of crossing the cytoplasmic membrane by both active and passive mechanisms. Its penetration causes only minimal membrane disruption and toxicity to the cell, and appears to function in many of the mammalian cell lines tested to date, including neurons. Penetratin's ability to enter the cell is generally retained when it is covalently linked to other molecules, including peptides, nucleic acids and other small compounds. Thus, penetratin can be utilized to deliver a wide variety of cargos into cultured mammalian cells, although there are size restrictions with respect to each type of cargo. When

the covalent linkage is a disulfide bond, the cargo can be automatically released intracellularly due to the reducing environment inside the cell.

Our laboratory studies synaptic function in hippocampal neuronal cultures from postnatal rats, which are generally difficult to transfect. We are interested in using penetratin to deliver nucleic acids into cultured neurons. The first type of nucleic acid cargo of interest is a small-interfering RNA which is capable of down-regulating the expression of homologous genes. We believe penetratin-based RNA interference may be a better alternative to existing viral strategies. Another potential application of penetratin is the delivery of membrane impermeable compounds. Currently, we are trying to deliver fluorophores that highlight different molecular components or cellular compartments in neurons. Our laboratory routinely utilizes laser-scanning confocal microscopy combined with molecular fluorescence to monitor real-time changes in dendrites. We wish to expand the repertoire of fluorescent reporter systems with the delivery capability afforded by penetratin.

119. Investigating a role for EJC proteins in RNA transport and local translation in neurons
Young J. Yoon

There is a growing body of evidence suggesting that RNA transport and local translation in dendrites of hippocampal neurons are important for synaptic plasticity and memory formation. In addition, recent studies have shown that components of the exon-junction complex (EJC) are necessary for trafficking RNA in *Drosophila* oocytes. As such, investigation of EJC proteins may reveal a potential role in dendritic RNA transport and translation in rat neurons.

EJC proteins bind to 20-24 nucleotides upstream of exon-exon junctions and have been shown to play a role in nuclear export, nonsense-mediated decay (NMD), and enhancing translation. Previously, it had been shown that Y14 remains bound to spliced RNA until the initial translation event, where it is removed by the ribosome. If mature mRNAs are transported to dendrites along with Y14 and Mago, the study of EJC components may provide clues to how RNA transport and translation are coupled or modulated in dendrites via EJC components. Our preliminary results suggest that Y14 and Mago are indeed present in dendrites, and further work will be necessary to address what specific functions the EJC proteins play in dendrites.

120. Regulation of spine morphological dynamics by miniature synaptic events
Shreesh P. Mysore, Michael A. Sutton

The role of miniature synaptic events in synaptic function is only recently being uncovered. Work in the lab has shed light on their effects on protein synthesis regulation. Other work in the literature shows that long-term blockade of minis (for seven days) produces a loss in spine density. We wish to determine the effects of acute mini blockade on spine density and dynamics. Further, we wish to know if the previously reported loss in spine density following prolonged mini blockade sets in monotonically, or is first preceded by a transient phase of high spine density, and a flurry of dynamics. Towards these ends, we are performing time-lapse imaging experiments for up to 24 hours after mini blockade. We have also performed immunostaining experiments on similar time scales. Results so far lend support to the hypothesis of a transient increase in spine density, presumably followed by the eventual decline. Insight into these issues will help us better understand synaptic stability and structural plasticity in neural circuits.

121. Dynamic regulation of the proteasome localization in hippocampal neurons
Baris Bingol

The molecular composition of synapses constantly changes in order to regulate the strength of the synaptic transmission between individual presynaptic terminals and postsynaptic dendrites. These changes in molecular composition are mediated by modification of existing proteins or the addition and removal of proteins by synthesis and degradation. The vast majority of proteins in a cell are degraded through attachment of a polyubiquitin chain to the target protein. This chain is recognized by a protein complex called the proteasome, which also carries the enzymatic activities that degrade the target protein. The initial attachment of polyubiquitin chain to the target protein by an enzymatic cascade and delivery of the polyubiquitinated proteins to the proteasome are all highly regulated events. In this study, we focus on the dynamics of the components of ubiquitin-proteasome system in hippocampal neurons in culture and slices. In particular, we examine how the proteasome changes its localization in response to neural activity.

122. Visualization of cadherin-cadherin association in living cells
Eric Mosser, Chin-Yin Tai

Classic cadherins, in particular N- and E-cadherins, are expressed and localized at synaptic sites of the adult rat hippocampus and involved in LTP. Cadherins exhibit Ca^{2+}-dependent adhesion: The removal of Ca^{2+} from the extracellular solution results in a loss of adhesion. Thus, it is possible that changes in extracellular Ca^{2+} associated with synaptic activity may alter cadherin-cadherin interactions. We are attempting to visualize cadherin-cadherin associations at cell-cell junctions with the eventual goal of monitoring hippocampal synapses during synaptic activity. This will enable us to determine if synaptic activity and plasticity affect cadherin dynamics and synaptic structures. To visualize cadherins in living cells, we have utilized a transposon-mediated random GFP insertion technique to create E-cadherin constructs with ECFP or EYFP variants inserted on a flexible linker at various sites on the extracellular domain in mouse L cells. ECFP can act as a fluorescence resonance energy transfer (FRET) donor for EYFP and FRET will be used to visualize the *'trans'* homophilic interactions between

cadherins on adjacent cells in co-cultures, or the 'cis' interactions between cadherins on cells expressing both FRET donor and acceptor cadherin constructs. We have demonstrated FRET between ECFP- and EYFP-labeled cadherins in HEK 293 and COS-7 cells transiently expressing both donor and acceptor constructs (which represents *cis* cadherin-cadherin interactions) as well as FRET at the cell-cell junctions of cells singly transfected with either ECFP- or EYFP-labeled cadherins and then co-cultured (representing *trans* cadherin-cadherin interactions). Removal of extracellular Ca^{2+} by chelation results in a significant decrease in FRET signal, indicating that our cadherin FRET pairs can act as reporters for cadherin-cadherin interactions across cell junctions. Viral vectors are being prepared for expression of these constructs in neurons. Cadherin containing one GFP variant will be expressed in presynaptic neurons, while cadherin containing the other GFP variant will be expressed in postsynaptic neurons. FRET will then be used to detect these exogenous cadherins and their homophilic interactions between pre- and postsynaptic cells in differing conditions. In particular, we will examine the effects of synaptic activity and varying extracellular calcium concentrations on cadherin-cadherin dynamics. Surprisingly little is known about the cadherin homophilic interaction; hopefully, this approach will not only allow us to learn something about cadherin's role in the synapse, but also shed some light on the basic nature of this interaction.

123. Information integration in CA1 pyramidal neurons
Hiroshi Ito

A number of studies indicate that the hippocampus is required to form certain types of memory. The development of large-scale recording techniques from behaving animals has clarified the characteristic patterns of neural activities in the hippocampus during several learning tasks. Among the subregions of the hippocampus, area CA1 is considered as a final relay station of the hippocampal formation and thus is expected to play a significant role in hippocampal function. The CA1 region receives two distinct inputs; one from area CA3 (Schaffer-collateral pathway) and the other from the entorhinal cortex (temporoammonic pathway). Considering large differences in *in vivo* neural activities between area CA3 and the entorhinal cortex, information integration among the two pathways is likely crucial for hippocampal function. We previously showed that the temporoammonic (TA) pathway modulates synaptic inputs from area CA3 and influences the spike probability in CA1 pyramidal neurons. To further elucidate the integration mechanism in dendrites, we are examining the effects of several stimulation patterns to the two pathways. Since the TA pathway projects onto distal parts of dendrites, we will take an advantage of dendritic patch clamp recording technique to separate impacts of the two pathways and analyze its computation. To emulate an *in vivo* learning state, we will pharmacologically induce oscillatory

activities in slices and investigate its role in dendritic integration. As previously shown, we have confirmed that carbachol (50 µM) can reliably induce theta-range (4-12 Hz) of oscillations in hippocampal slices. Considering the suggestive importance of neural oscillations in hippocampal function, we expect that phase-locked inputs relative to oscillatory activities may differentially modulate dendritic computation.

124. Single-unit neural correlates of novelty detection in the human hippocampus
Ueli Rutishauser, Adam N. Mamelak

The medial temporal lobe (MTL) is crucial for the acquisition of long-term declarative memories. A converging set of experimental and theoretical evidence indicates that that the detection of new stimuli (novelty) is a prerequisite for many types of learning. To investigate novelty detection on the single cell level we recorded *in vivo* from single microwire depth electrodes implanted in epilepsy surgery patients. We found single neurons in the human hippocampus and amygdala which can discriminate novel vs. familiar stimuli. These neurons reliably change their firing patterns in response to either novel or familiar "natural" visual stimuli. Moreover, we observe that individual neurons can rapidly change their firing to stimuli as a result of single trial learning (a.k.a."one-shot learning"). This plasticity does not depend on successful recall of the stimulus - successful recognition is sufficient. We further developed a decoding framework to investigate whether observing the responses of single neurons is sufficient to predict whether the subject is currently viewing a novel or familiar stimulus. We find that the response of single neurons allows an ideal observer to decode, with high accuracy and on a single-trial basis, whether the subject is viewing a novel or familiar stimulus.

Publications

Bhattcharya, J., Edwards, J., Mamelak, A.N. and Schuman, E.M. (2005) Long-range temporal correlations in the spontaneous spiking of neurons in the hippocampal-amygdala complex of humans. *Neurosci.* **131**:547-555.

Bingol, B. and Schuman, E.M. (2004) A proteasome-sensitive connection between PSD-95 and GluR1 endocytosis. *J. Neuropharmacol.* **47**:755-763.

Bingol, B. and Schuman, E.M. (2005) Proteasomal degradation and synapses. *Curr. Op. Neurobiol*. In press.

Goard, M., Aakalu, G., Fedoryak, O.D., Quinonez, C., St. Julien, J., Poteet, S.J., Schuman, E.M. and Dore, T.M. (2005) Light-mediated inhibition of protein synthesis. *Chemistry and Biolog*y **12**. In press.

Patrick, G.N. and Schuman, E.M. (2005) Trafficking of AMPAR in the mammalian CNS is regulated by ubiquitination. Submitted.

Remondes, M. and Schuman, E.M. (2004) Role for a cortical input to hippocampal area CA1 in the consolidation of a long-term memory. *Nature* **431**:699-703.

Rutishauser, U., Mamelak, A.N. and Schuman, E.M. (2005) Online detection and sorting of extracellularly recorded action potentials. Submitted.

Rutishauser, U., Mamelak, A.N. and Schuman, E.M. (2005) Single neurons in the human hippocampus-amygdala complex learn stimulus novelty and familiarity on a single-trial basis. Submitted.

Schuman, E.M. and Chan, D. (2004) Fueling synapses. *Cell* **119**:738-740.

Smith, W.B., Starck, S.R., Roberts, R.W. and Schuman, E.M. (2005) Dopaminergic stimulation of local protein synthesis enhances surface expression of GluR1 and synaptic transmission in hippocampal neurons. *Neuron* **45**:765-779.

Sutton, M.A. and Schuman, E.M. (2005) Local translational control in dendrites and its role in long-term synaptic plasticity. *J. Neurobiol.* **64**:116-131.

Sutton, M.A, Aakalu, G.N., Wall, N. and Schuman, E.M. (2004) Miniature synaptic events regulate local protein synthesis in the dendrites of hippocampal neurons. *Science* **304**:1979-1983.

Professor of Biology: Shinsuke Shimojo
Visiting Associates: Bhavin Sheth[1], Masataka Watanabe
Visitors: Fuiko Maeda[2], Orna Rosenthal[2], Stephan Schleim[3], Simone Wehling[4]
Postdoctoral Scholars: **Mark Changizi, Hackjin Kim, Junghyn Park, Claudiu Simion, Harald Stoegbauer**
Graduate Students: Signe Bray, Farshad Moradi, Patricia Neil, Dylan Nieman, Daw-An Wu
Undergraduate Students: Chika Arakawa, Michael Chang, Ewen Chao, Alice Lin, Hao Ye, Qiong Zhang
Research and Laboratory Staff: Andrew Hsieh
[1]*University of Houston*
[2]*UCLA Medical School, Los Angeles, CA*
[3]*Johannes Gutenberg University Mainz*
[4]*Austrian Academy of Sciences*

S u m m a r y: We continue to examine the dynamic/adaptive nature of human visual perception – including its crossmodal, representational, sensory-motor, developmental, emotional, and neurophysiological aspects. The biggest landmark progress in the last year was that ERATO (Exploratory Research for Advanced Technology) Shimojo "Implicit Brain Functions" project (supported by JST, Japan Science and Technology Corporation) was kick-started between our psychophysics laboratory at Caltech and the Japan site located at NTT Communication Science Laboratories, Atsugi, Kanagawa, Japan.

Using a variety of methods including eye tracking, EEG, fMRI and MEG, we examine how exactly peripheral sensory stimuli, neural activity in the sensory cortex, and the mental experience of perception are related to each other. As for objectives of the new ERATO project, we aim to understand implicit, as opposed to explicit or conscious, cognitive functions and underlying neural mechanisms. To be more specific, we are interested in the implicit behavioral and neural processes, as well as their interactions preceding emotional decision making such as preference.

(1) We continue our work applying TMS (Transcranial Magnetic Stimulation) to the visual cortex of alert normal subjects, to reveal neural mechanisms underlying conscious visual perceptual experience. In the latest study, we have demonstrated that after one has seen a flashed visual object, administration of dual-pulse TMS to the occipital cortex causes portions of the object to be seen again. We surmise that neurons that were previously activated by visual stimuli are more excitable by TMS, possibly due to residual neural activity. This paradigm has turned out to provide a unique opportunity to assess how exactly the visual cortical activity brings about the content of our perceptual experience, particularly in a feature-bound fashion. In yet another study using TMS, we have provided the first evidence for causal relationship between neural activity of PPC (the posterior parietal cortex) and the coordinate transformation that is necessary to maintain visual constancy across saccadic eye movements.

(2) We continue our effort to understand auditory-visual integration in both adults and in infants. In adult ERP study, we found a surprisingly early (<150 ms from the onset of A-V stimuli) evidence of non-linear interaction between these two sensory modalities that is consistent with behavioral reaction-time data. In infants, we provided a systematic full-set data, for the first time in the field, of how auditory, visual, and auditory-visual processing develop in the first year of life. Against commonsensical notion, we found a surprisingly rich and complicated pattern of interaction between the modalities in the early period of human life. In short, there seems to be the first indication of A-V interaction at the age of 8 months. Finally, we found a tactile-visual version of the "double flash" illusion, in which a single visual flash appeared to be doubled when accompanied with two tactile taps.

(3) Applying adaptation/aftereffect paradigm and fMRI, we investigate how consciously visible/invisible adaptor contributes to aftereffect. In the special case of face adaptation, unlike lower-level perceptual adaptations such as tilt or contrast adaptation, we found that only visible duration of adaptor face contributes to face-identity aftereffect later. On a related issue, when the eye re-fixates elsewhere after adaptation, there was a gaze-dependent modulation of color and depth aftereffects. The effect of face adaptation seems to be spatially un-tuned, that is, remains everywhere regardless of the location on the retina or the space.

(4) Following our earlier work indicating that dynamic gaze shift (and perhaps orienting response in general) is a somatic precursor of conscious preference judgment, we extended the analyses in a new "peep-hole" paradigm, in which the observer's view was limited to the fovea and contingent upon gaze. We found a qualitatively similar gaze cascade effect towards the choice, but extended in time scale. We interpreted it as a further support of our dynamical view of orienting mechanism as intrinsically involved in emotional decision making.

(5) As a part of the ERATO project, we examined ERP data while the observer was engaged in a preferential decision task. We found that there is strong coherence of neuronal activity bilaterally localized in the lateral-medial frontal lobe (but specifically localized on the right side if activity in a control task was subtracted) and limited in the lower gamma range of frequency.

(6) We meta-analyzed neocortex size and area-area connectivity across various species. We found that the number of areas scales lawfully with regard to the volume of gray matter, and that total number of area-area connections scales as the square of the number of areas. These scaling results constrain theories on neocortical organization.

(7) We examined how natural written languages (i.e., characters) are constrained by visual perception constraints. Pooling data across more than 100 writing systems over human history, we found some commonalities in terms of number of strokes (approximately three independent of the number of characters) and redundancy (50% independent of writing system size). These may be considered a fingerprint of the visuo-motor system under selective pressure.

125. Gaze direction modulates visual aftereffects in depth and color
Dylan R. Nieman, Ryusuke Hayashi, Richard A. Andersen, Shinsuke Shimojo

Prior physiological studies indicate that gaze direction modulates the gain of neural responses to visual stimuli. Here, we test gaze modulation in the perceptual domain using color and depth aftereffects. After confirming retinotopy of the effects, we employed a balanced alternating adaptation paradigm (adaptation alternates between opponent stimuli) to demonstrate that opposite color and depth aftereffects can co-develop at the same retinal location for different gaze directions. The results provide strong evidence for: (a) gaze modulation of aftereffects; (b) generality of gaze modulation across-two visual attributes; and (c) perceptual correlates of the modulation of neural activity by gaze direction.

Reference

Nieman, D.R., Hayashi, R., Andersen, R.A. and Shimojo, S. (2005) *Vis. Res.* **45**(22):2885-2894.

126. Parcellation and area-area connectivity as a function of neocortex size
Mark A. Changizi, Shinsuke Shimojo

Via the accumulation of data from across the neuroanatomy literature, we estimate the manner in which (i) the number of neocortical areas varies with neocortex size, and (ii) the number of area-area connections varies with neocortex size. Concerning parcellation, we find that the number of areas scales approximately as the 1/3 power of gray matter volume, or, equivalently, as the square root of the total number of neocortical neurons. A consequence of this is that the average number of neurons per area also scales approximately as the square root of the total number of areas. Concerning area-area connectivity, we find evidence that the total number of area-area connections scales as the square of the number of areas. These scaling results help constrain theories about the principles underlying neocortical organization.

Reference

Changizi, M.A. and Shimojo, S. (2005) *Brain Behav. Evol.* **66**(2):88-98.

127. Character complexity and redundancy in writing systems over human history
Mark A. Changizi, Shinsuke Shimojo

A writing system is a visual notation system wherein a repertoire of marks, or strokes, is used to build a repertoire of characters. Are there any commonalities across writing systems concerning the rules governing how strokes combine into characters, commonalities that might help us identify selection pressures on the development of written language? In an effort to answer this question we examined how strokes combine to make characters in more than 100 writing systems over human history, ranging from about 10 to 200 characters, and including numerals, abjads, abugidas, alphabets and syllabaries from five major taxa—Ancient Near-Eastern, European, Middle Eastern, South Asian, Southeast Asian. We discovered underlying similarities in two fundamental respects. (1) The number of strokes per characters is approximately three, independent of the number of characters in the writing system; numeral systems are the exception, having on average only two strokes per character. (2) Characters are approximately 50% redundant, independent of writing system size; intuitively, this means that a character's identity can be determined even when half its strokes are removed. Because writing systems are under selective pressure to have characters that are easy for the visual system to recognize and for the motor system to write, these fundamental commonalities may be a fingerprint of mechanisms underlying the visuo-motor system.

Reference

Changizi, M.A. and Shimojo, S. (2005) *Proc. Roy. Soc. B-Biol. Sci.* **272**(1560):267-275.

128. Four correlates of complex behavioral networks: Differentiation, behavior, connectivity, and compartmentalization
Mark Changizi, Darren He

Some of the most complex networks are those that (i) have been engineered under selective pressure (either economic or evolutionary), and (ii) are capable of eliciting network-level behaviors. Some examples are nervous systems, ant colonies, electronic circuits and computer software. Here we provide evidence that many such *selected*, *behavioral* networks are similar in at least four respects. (1) *Differentiation*: Nodes of different types are used in a combinatorial fashion to build network *structures* through local connections, and networks accommodate more structure types via increasing the number of node types in the network (i.e., increasing differentiation), not via increasing the length of structures. (2) *Behavior*: Structures are themselves combined globally to implement *behaviors*, and networks accommodate a greater behavioral repertoire via increasing the number of lower-level behavior types (including structures), not via increasing the length of behaviors. (3) *Connectivity*: In order for structures in behavioral networks to combine with other structures within a fixed behavior length, the network must maintain an invariant network diameter, and this is accomplished via increasing network connectivity in larger networks. (4) *Parcellation*: Finally, for reasons of

economical wiring, behavioral networks become increasingly parcellated. Special attention is given to nervous systems and computer software, but data from a variety of other behavioral selected networks are also provided, including ant colonies, electronic circuits, web sites and businesses. A general framework is introduced illuminating why behavioral selected networks share these four correlates. Because the four above features appear to apply to computer software, as well as to biological networks, computer software provides a useful framework for comprehending the large-scale function and organization of biological networks.

Reference
Changizi, M. and He, D. (2005) *Complexity* **10**:13-40.

129.   Face adaptation depends on seeing the face
Farshad Moradi
Retinal input that is suppressed from visual awareness can nevertheless produce measurable aftereffects, revealing neural processes that do not directly result in a conscious percept. We here report that the face identity-specific aftereffect requires a visible face; it is effectively cancelled by binocular suppression or by inattentional blindness of the inducing face. Conversely, the same suppression does not interfere with the orientation-specific aftereffect. Thus, the competition between incompatible or interfering visual inputs to reach awareness is resolved before those aspects of information that are exploited in face identification are processed. We also found that the face aftereffect remained intact when the visual distracters in the inattention experiment were replaced with auditory distracters. Thus, cross-modal or cognitive interference that does not affect the visibility of the face does not interfere with the face aftereffect. We conclude that adaptation to face identity depends on seeing the face.

Reference
Moradi, F., Koch, C. and Shimojo, S. (2005) *Neuron* **45**(1):169-175.

130.   Perceptual-binding and persistent surface segregation
Farshad Moradi
Visual input is segregated in the brain into subsystems that process different attributes such as motion and color. At the same time, visual information is perceptually segregated into objects and surfaces. Here we demonstrate that perceptual segregation of visual entities based on a transparency cue precedes and affects perceptual binding of attributes. Adding an irrelevant transparency cue paradoxically improved the pairing of color and motion for rapidly alternating surfaces. Subsequent experiments show: (1) attributes are registered over the temporal window defined by the perceptual persistence of segregation, resulting in

asynchrony in binding, and (2) attention is necessary for correct registration of attributes in the presence of ambiguity.

Reference
Moradi, F. and Shimojo, S. (2004) *Vision Res.* **44**(25):2885-2899.

131.   Perceptual alternation induced by visual transients
Ryota Kanai, Farshad Moradi*
When our visual system is confronted with ambiguous stimuli, the perceptual interpretation spontaneously alternates between the competing incompatible interpretations. The timing of such perceptual alternations is highly stochastic and the underlying neural mechanisms are poorly understood. Here, we show that perceptual alternations can be triggered by a transient stimulus presented nearby. The induction was tested for four types of bistable stimuli: structure-from-motion; binocular rivalry; Necker cube; and ambiguous apparent motion. While underlying mechanisms may vary among them, a transient flash induced time-locked perceptual alternations in all cases. The effect showed a dependency on the adaptation to the dominant percept prior to the presentation of a flash. These perceptual alternations show many similarities to perceptual disappearances induced by transient stimuli [Kanai and Kamitani (2003); Moradi and Shimojo, 2004)]. A mechanism linking these two transient-induced phenomena is suggested based on modulation of the energy landscape of the neural network with changes in the activation function of its units by the transient input and by adaptation.
Universiteit Utrecht, Helmholtz Research Institute, Utrecht, The Netherlands

Publication
Kanai, R., Moradi, F., Shimojo, S. and Verstraten, F.A.J. Perceptual alternation induced by visual transients. *Perception.* In press.

132.   Adaptation to invisible gratings in Troxler filling-in
Farshad Moradi, Shinsuke Shimojo
Under strict fixation, a stationary or slowly changing peripheral stimulus gradually disappears from awareness (Troxler, 1804). This phenomenon is often attributed to early sensory adaptation at the level of retinal ganglion cells or LGN. Yet, evidence from binocular rivalry, motion-induced blindness, and induced disappearance indicates a cortical origin for disappearance. Here, we examined whether Troxler fading occurs before processing orientation information in V1. Six participants viewed two low-contrast peripheral (11.5 deg eccentricity) Gabor patterns for 15 s. Gratings drifted slowly (0.1 Hz) to reduce receptor adaptation. Observers monitored the visibility of one of the gratings by holding a key while it disappeared. On the average, the grating was invisible for 2.2 s. The second grating served as a control and was erased from the screen whenever the first grating was reported as invisible. After adaptation, a test Gabor pattern (with either same or orthogonal orientation) appeared at one of the two locations, and observers were asked to report its location and alignment.

Orientation-selective adaptation was stronger when the adapting stimulus was physically present than when it was erased (48% vs. 64% correct detection for same orientation, p<0.01). Subjects had little difficulty detecting an orthogonal grating in both conditions (89% vs. 90%, n.s.). Notably, the aftereffect was stronger in trials that observer reported fading during adaptation (42% vs. 56% for the same orientation, 94% vs. 82% for orthogonal). Thus, fading from awareness did not result in reduction of orientation-selective aftereffect compared to the control. We conclude that consistent with other disappearance phenomena, Troxler fading occurs at least in part after the site of orientation-selective processing. Results may be accounted for by attentional modulation of the visibility of peripheral targets.

Vision Sciences Society Annual Meeting, Sarasota, FL May 2005

133. Adaptation to face identity and emotional expression without attention

Farshad Moradi, Christof Koch, Shinsuke Shimojo

Retinal inputs that are not attended result in buildup of various well-known aftereffects such as motion, orientation, or color. In a previous study, we showed that the identity-specific face aftereffect following 4 s of adaptation is effectively cancelled by withdrawing attention from the adapting stimulus. Here, we examined whether (1) some gradual buildup of face-identity aftereffect is preserved without attention, (2) adaptation to emotional expressions is modulated by selective attention, and (3) attentional manipulation has any effect on conscious face identification. In Experiment 1, an "anti-face" image was displayed for 10 s, while a stream of digits (3Hz) was displayed at fovea. Observers (n=9) were instructed to either attend to the distracting digits and report occurrences of letters, or ignore them. A test image followed and was identified by pressing a key. The identity strength of the test face varied between 0 (average) and 0.4. The antiface and digits were presented for 1 s between trials (readaptation). The same adapting antiface was presented during each run. When the distracting stimuli were ignored, there was significant shift in the identification curve as a function of identity strength (p<0.01). This shift disappeared completely when subjects monitored the digits. In Experiment 2, happy and angry expressions were tested on five observers. The paradigm was similar to Experiment 1. Although when the distracters were attended, adaptation to emotion was reduced (p<0.05), some aftereffect still remained (p<0.05). In Experiment 3, observers concurrently performed both digit/letter and face identification tasks. To our surprise, the shift in the identification curve due to inattention was negligible. We conclude that the implicit processing of face identity and emotion underlying the corresponding aftereffects require different levels of selective attention. In contrast, explicit face identification seems to be robust in the near absence of attention.

Vision Sciences Society Annual Meeting, Sarasota, FL May 2005

134. Perception of solid color: Rapid filling-in depends on surface attribution

Daw-An Wu, Ryota Kanai, Shinsuke Shimojo*

When we see a solidly colored shape, the early visual cortex is not responding very much to the interior of the shape. Instead, activity corresponds almost entirely to the edges of the shape. We continue to investigate how this early map of edges is "filled-in" to give rise to our visual experience of solidly colored surfaces. Previously, we studied a slow process of color filling-in known as Troxler fading, finding that color could jump across widely separated regions of space if those regions appeared to be parts of a common surface. Here, we investigate rapid color filling-in, which is the process whereby solid color surfaces are interpreted in everyday life.

We adapt a method from Paradiso and Nakayama (1991). If a thin luminance contour and a larger solid disk are dichoptically flashed to opposite eyes, a dark hole is seen in the disk. The contour masks the disk's interior by blocking brightness information which normally "fills-in" from disk's edge.

Extending on this paradigm, we find that the disk's color will fill-in through the contour mask if the mask is perceived to be part of a separate surface. A solid red disk (target) and thin green contour (mask) are flashed simultaneously to opposite eyes. The mask is either square or #-shaped (the same square with arms extending outside the target). Observers found the # to mask much more weakly than the square. Some observers reported that the # configuration often failed to mask the center at all, while the square configuration was consistently a strong mask. Adding to a mask usually increases its effectiveness, but it had the opposite effect here because it created cues that the mask was a separate, occluding object.

This generalizes our previous findings to the rapid processing of everyday vision. Perceived color is based on edge information that is attributed to the same surface. Edges from separate surfaces tend to be ignored, even if they lie in retinotopically intervening space.

Vision Sciences Society 2005 conference abstract. http://www.journalofvision.org

Universiteit Utrecht, Helmholtz Research Institute, Utrecht, The Netherlands

135. Neural correlates of preference choices

Hackjin Kim*, Michael Chang, Claudiu Simion, Shinsuke Shimojo

Despite their ubiquity and social importance, how we make preference decisions and how they are distinguished from other types of decision making still remain largely unknown. We recently suggested that preference related decision-making is qualitatively different from other types of decision making, by demonstrating unique eye tracking patterns while judging two faces based on their attractiveness, compared to when judging the same faces based on other criteria such as roundness. In the present study, we investigate how preference decision-making can be neurally distinguished from other relatively more objective decision-making by using functional MRI. There are four different condition blocks, which consist of judging two different kinds of visual stimuli based on different criteria: faces on attractiveness; faces on roundness; abstract visual patterns on preference; and abstract visual patterns on complexity. Each block contains ten decision trials, in each of which subjects are asked to inspect two stimuli by using their right hands to toggle between two visual stimuli, which are alternatively presented at the center of the screen, and to make decisions by using their left hands. The order of blocks is counterbalanced across subjects. We expect a slowly increasing likelihood of inspecting the to-be-chosen stimuli approaching the time of decision regardless of the types of stimuli, consistent with our previously reported data. Regions of interest for fMRI data analysis include the orbitofrontal cortex and some subcortical structures such as the striatum and/or the amygdala, which have been reportedly involved in affective information processing and are expected to show increased activities during preference judgments, compared to objective judgments.

*Department of Humanities and Social Sciences, Caltech

136. Orienting contributes to preference even in the absence of visual stimuli

Claudiu Simion

We previously demonstrated the active contribution of orienting to preference decision-making (Shimojo *et al*., 2003) in the "gaze cascade effect," a continually increasing likelihood that subjects' gaze was directed to the stimulus eventually chosen. The effect was robust across a wide range of stimuli and conditions (VSS 04); thus, we suspected that whenever a preference decision needs to be made the gaze cascade accompanies it. We here show an extreme case where gaze cascade effect was observed even when the stimuli were no longer visually present. Unlike our previous studies, the observation duration was controlled and randomized by the experimenter while subjects were trying to decide the preferred one. In roughly half of the trials the presentation time was long enough for a decision, mimicking our previous

experiments. However, in the other half, a decision had to be made after the stimuli were taken off the screen. Testing whether visual input is required for the cascade effect was one the motivations of this study. We used eye tracking and our gaze likelihood analysis (VSS 02).

First, as expected, we show the gaze cascade effect before decision in the trials in which observers had enough time to choose the preferred stimulus. Moreover, the bias slowly decreases in the next second after decision, when the stimuli were still presented on the screen, confirming that the cascade is linked to the decision process and not to observers' already-made preference. Second and intriguingly, in the trials where a decision came after the stimuli were removed from the screen, the cascade was still present. Thus, gaze is participating in the decision process even when the decision is made purely in memory. Observers made fixations in the approximate regions previously occupied by faces, and their gaze pattern was still correlated with their decision. Thus, our claim that gaze cascade is intrinsically involved in the decision-making process is extended beyond perceptual domain.

137. Machine vision system to induct binocular wide-angle foveated information into both the human and computers

Sota Shimizu, Hao Jiang, Shinsuke Shimojo, Joel W. Burdick

This paper introduces a machine vision system, which is suitable for cooperative works between the human and computer. This system provides images inputted from a stereo camera head not only to the processor but also to the user's sight as binocular wide-angle foveated (WAF) information; thus, it is applicable for Virtual Reality (VR) systems such as tele-existence or training experts. The stereo camera head plays a role to get required input images foveated by special wide-angle optics under camera view direction control and 3D head mount display (HMD) displays fused 3D images to the user. Moreover, an analog video signal processing device much inspired from a structure of the human visual system realizes a unique way to provide WAF information to plural processors and the user. Therefore, this developed vision system is also much expected to be applicable for the human brain and vision research, because the design concept is to mimic the human visual system. Further, an algorithm to generate features using Discrete Fourier Transform (DFT) for binocular fixation in order to provide well-fused 3D images to 3D HMD is proposed. This paper examines influences of applying this algorithm to space variant images such as WAF images, based on experimental results.

Sota Shimizu, Hao Jiang and Shinsuke Shimojo and Joel W. Burdick, Proceedings of the 2005 IEEE International Conference on Robotics and Automation Barcelona, Spain, pp.806-811, 19th April, 2005

138. Binocular fixation on wide-angle foveated vision system

Sota Shimizu, Hao Jiang, Shinsuke Shimojo, Joel W. Burdick

This paper introduces a fovea vision system with the 120 degrees-wide view field, which is suitable for cooperative works between the human and computer. This system provides images inputted from a stereo camera head not only to the processor but also to the user's sight as human-like binocular wide-angle foveated (WAF) information; thus, it is applicable for Virtual Reality systems such as tele-existence or training experts. The stereo camera head plays a role to get required images foveated by special wide-angle optics with controlling camera view directions and 3D head mount display (HMD) displays fused 3D images to the user. This developed vision system is much expected to be applicable for the human brain and vision research, because the design concept is to mimic the human visual system. A method to generate shift-, rotation-, scale-invariant feature based on contour using Discrete Fourier Transform, is proposed for binocular fixation of this system in order to provide well-fused 3D images to 3D HMD. This paper examines about the influences to the feature generated from space-variant WAF images, based on experimental results.

Sota Shimizu, Hao Jiang and Shinsuke Shimojo and Joel W. Burdick, Proceedings of the 2005 IEEE/ASME International Conference on Advanced Intelligent Mechatronics Monterey, California, USA, pp.366-372 (MC4-03), 25th, July 2005, published.

139. Perceptual basis of synesthetic metaphor: Capture of visual motion by changing pitch

F. Maeda, Ryota Kanai, S. Shimojo*

We often associate moving objects and changing pitch; for example, most people associate falling stones with descending and launching rockets with ascending pitch, even when these do not happen in the real-world. The mechanism of this association is unknown. The association may occur at a semantic level; indeed, expressions such as *descending/ascending* and *high/low* are used to describe both pitch and visual motion/space. Alternatively, it could occur prior to semantic processing, via cross-modal interaction at a perceptual level. Here we show a novel cross-modal illusion that supports the latter. The direction of motion of counter-phase gratings was perceived *in accord with* the direction of pitch change. Control data indicate that this cannot be explained by eye movement, response bias, cueing or semantic influences, nor occurs at the lowest sensory level. Our findings indicate that some synesthetic metaphors may have their neural bases at a perceptual level.

*Universiteit Utrecht, Helmholtz Research Institute, Utrecht, The Netherlands

Reference
Maeda, F., Kanai, R. and Shimojo, S. (2004) *Curr Biol.* **14**(23):R990-R991.

Publications
Bhattacharya, J., Watanabe, K. and Shimojo, S. (2004) Nonlinear dynamics of evoked neuromagnetic responses signifies potential defensive mechanisms against photosensitivity. *Int. J. Bifurcation & Chaos* **14**(8):2701-2720.

Changizi, M.A. and He, D. (2005) Four correlates of complex behavioral networks: Differentiation, behavior, connectivity, and compartmentalization. *Complexity* **10**:13-40.

Changizi, M.A. and Shimojo, S. (2005) Parcellation and area-area connectivity as a function of neocortex size. *Brain Behav. Evol.* **66**(2):88-98.

Changizi, M.A. and Shimojo, S. (2005) Character complexity and redundancy in writing systems over human history. *Proc. Roy. Soc. B-Biological Sci.* **272**(1560):267-275.

Fujisaki, W., Shimojo, S., Kashino, M., Nishida, S. (2004) Recalibration of audiovisual simultaneity. *Nature Neurosci.* **7**:773-778.

Hayashi, R., Maeda, T., Shimojo, S. and Tachi, S. (2004) An integrative model of binocular vision: A stereo model utilizing interocularly unpaired points produces both depth and binocular rivalry. *Vision Res.* **44**(20):2367-2380.

Kanai R., Sheth, B.R. and Shimojo, S. (2004) Stopping the motion and sleuthing the flash-lag effect: Spatial uncertainty is the key to positional mislocalization. *Vision Res.* **44**:2605-2619.

Kanai, R., Moradi, F., Shimojo, S. and Verstraten, F.A.J. Perceptual alternation induced by visual transients. *Perception.* In press.

Maeda, F., Kanai, R., Shimojo, S. (2004) Changing pitch induced visual motion illusion. *Curr. Biol.* **14**(23):R990-R991.

Maeda, F., Wu, D.-W., Gabrieli, J.D.E. and Shimojo, S. (2005) A new transcranial magnetic stimulation (TMS). Tool for cognitive neuroscience. *J. Cogn. Neurosci.* A175 Suppl. S APR.

Moradi, F. and Shimojo, S. (2004) Perceptual-binding and persistent pre-attentive surface segregation. *Vision Res.* **44**(25):2885-2899.

Moradi, F. and Shimojo, S. (2004) Suppressive effect of sustained low-contrast adaptation followed by transient high-contrast on peripheral target detection. *Vision Res.* **44**:449-460.

Moradi, F. and Shimojo, S. (2005) Adaptation to invisible grating in Troxler filling-in. *Vision Sciences Society* (Abstract), 267.

Moradi, F., Koch, C. and Shimojo, S. (2005) Face adaptation depends on seeing the face. *Neuron* **45**(1):169-175.

Moradi, F., Koch, C. and Shimojo, S. (2005) Face adaptation is reduced by binocular suppression. *J. Cogn. Neurosci.* B145, Suppl.

Nieman, D.R., Hayashi, R., Andersen, R.A. and Shimojo, S. (2005) Gaze direction modulates visual aftereffects in depth and color. *Vis. Res.* **45**(22):2885-2894.

Nijhawan, R., Watanabe, K., Khurana, B., *et al.* (2004) Compensation of neural delays in visual-motor behaviour: No evidence for shorter afferent delays for visual motion. *Visual Cogn.* **11**:275-298.

Sheth, B.R. and Shimojo, S. (2004) Extrinsic cues suppress the encoding of intrinsic cues. *J. Cogn. Neurosci.* **16**:339-350.

Sheth, B.R. and Shimojo, S. (2004) Sound aided recovery from and persistence against filling-in. *Vision Res.* **44**:1907-1917.

Shimojo, S., Moradi, F. and Koch, C. (2005) Differential adaptation to face identity and emotional expression in the near absence of attention. *Vision Sciences Society* (Abstract).

Simion, C. and Shimojo, S. (2005) Orienting contributes to preference even in the absence of visual stimuli. *Vision Sciences Society* (Abstract), 123.

Violentyev, A., Shams, L. and Shimojo, S. (2005) Touch-induced visual illusion. *Vision Sciences Society* (Abstract), 207.

Watanabe, K., Sayres, R., Shimojo, S., Imada, T. and Nihei, K. (2004) Effect of sodium valproate on neuromagnetic responses to chromatic flicker: Implication to photosensitivity. *Neurol. Clin. Neurophysiol.* **61**:1-7.

Watanabe, M. and Shimojo, S. (2005) Dynamic, not static, MAE follows the illusory perception. *Vision Sciences Society* (Abstract), 256.

Wehling, S., Shimojo, S. and Bhattachara, J. (2005) Alteration of visual perception by direct influence from auditory cortex to visual cortex. *Association for Study of Consciousness, 9th Annual Conference* (June 25-27, Caltech, Pasadena, CA).

Wu, D.A., Kanai, R., Shimojo, S. (2004) Steady-state misbinding of colour and motion. *Nature* **429**:262-262.

Wu, D-A. and Shimojo, S. (2005) Ability of contours to block rapid color filling-in is dependent on global configuration. *Vision Sciences Society* (Abstract), 198.

Assistant Professor of Computation and Neural Systems: **Thanos G. Siapas**
Postdoctoral Scholar: Evgueniy Lubenov
Graduate Students: Ming Gu, Jason Rolfe, Casimir Wierzynski

Summary: The central focus of our research is the study of learning and memory formation in freely behaving animals at the level of networks of neurons. Previous research has shown that the hippocampus is critical for the formation of long-term declarative memories, and that this hippocampal involvement is time-limited. The current predominant conjecture is that memories are gradually established across distributed neocortical networks through the interactions between cortical and hippocampal circuits.

However, the direct experimental investigation of these interactions has been difficult since, until recently, simultaneous chronic recordings from large numbers of well-isolated single neurons were not technically feasible. These experiments became possible with the advent of the technique of chronic multi-area tetrode recordings in freely behaving rodents. Using this technique we monitor the simultaneous activity of large numbers of cortical and hippocampal cells during the acquisition and performance of memory tasks, as well as during the sleep periods preceding and following experience.

Our research efforts focus on analyzing the structure of cortico-hippocampal interactions in the different brain states and on characterizing how this structure is modulated by behavior, how it evolves throughout the learning process, and what it reflects about the intrinsic organization of memory processing at the level of networks of neurons. Our experimental work is complemented by theoretical studies of network models and the development of tools for the analysis of multi-neuronal data.

140. Dynamics of phase locking across cortico-hippocampal networks

Evgueniy Lubenov, Thanos Siapas

During awake behavior hippocampal activity is marked by the presence of pronounced 4-10 Hz LFP oscillations known as theta oscillations [1]. We demonstrated that a significant proportion (about 40%) of the cells in the medial prefrontal cortex of the rat fire preferentially during particular phases of the hippocampal theta rhythm [2]. Furthermore, we showed that prefrontal neurons phase lock best to theta oscillations delayed by approximately 50 ms and confirmed this hippocampo-prefrontal directionality and timing at the level of correlations between single cells. Finally, phase locking of prefrontal cells is predicted by the presence of significant correlations with hippocampal cells at positive delays up to 150 ms. This indicates that direct hippocampal input is likely to have a considerable contribution to the observed prefrontal phase locking. We are currently characterizing how these phase-locking properties evolve over time and how they are modulated by behavior.

References
[1] Vanderwolf, C.H. (1969) *Electroencephalogr. Clin. Neurophys.* **26**:407–418.
[2] Siapas, A.G., Lubenov, E.V. and Wilson, M.A. (2005) *Neuron* **46**:141-151.

141. Interactions between prefrontal and hippocampal circuits in associative learning

Casimir Wierzynski, Thanos Siapas

Eyeblink conditioning is a form of associative learning that has been shown to engage the hippocampus across a wide range of species and parameters [1]. Moreover, in its trace form, where the conditioned and unconditioned stimuli do not overlap in time, eyeblink conditioning has been shown to require an intact hippocampus for successful acquisition [2]. This hippocampal dependence falls off with time, implying that the long-term locus of the CS-US association is extra-hippocampal. Furthermore, lesions to the medial prefrontal cortex in rats have been shown to disrupt the long-term recall of the eyeblink response, but not its acquisition [3]. Using simultaneous chronic recordings from the hippocampus and medial prefrontal cortex, we are interested in characterizing the relationships between the activity patterns in these brain areas during the acquisition of the CS-US association, with the eventual goal of understanding how this association is represented across the prefrontal-hippocampal networks.

References
[1] Christian, K.M. and Thompson, R.F. (2003) *Learning & Memory* **10**:427-455.
[2] Weiss, C., Bouwmeestev, H., Power, J.M. and Disterhoft, J.F. (1999) *Behav. Brain Res.* **99**:123–132.
[3] Takehara, K., Kawahare, S. and Kirino, Y. (2003) *J. Neurosci.* **23**(30):9897-9905.

142. Contribution of hippocampal subregions to information processing and memory formation

Ming Gu, Thanos Siapas

The hippocampus consists of several subfields with different intrinsic architecture and electrophysiological properties. The characteristic organization of each region has inspired many models of the computational roles of each subfield in memory formation. However, experimental support for the different models has been limited [1]. Using simultaneous recordings from the different hippocampal subfields (dentate gyrus, CA3, CA1, subiculum), we are interested in characterizing how activity patterns get transformed

across the different subfields during the acquisition and performance of spatial and associative learning tasks.

Reference
[1] Gozowski, J.F., Knierim, J.J. and Moser, E.I. (2004) *Neuron* **44**:581-584.

143.   Dopaminergic modulation of hippocampal activity

Jason Rolfe, Thanos Siapas

Many lines of evidence suggest that the ventral tegmental area (VTA) interacts with the hippocampus to modulate the entry of information into long-term memory [1]. The VTA-hippocampal loop has been hypothesized to be important for the detection of novelty and signaling of the behavioral relevance of stimuli in the environment. However, the organization of VTA-hippocampal interactions remains unknown, as simultaneous recordings from these areas have not been reported in the literature. Leveraging our experience with chronic multi-area tetrode recordings, we are examining the simultaneous response of multiple dopaminergic cells in the VTA and pyramidal cells in hippocampus during exposure to novel stimuli as well as during the acquisition of instrumental conditioning paradigms.

Reference
[1] Lisman, J.E. and Grace, A.A. (2005) *Neuron* **46**:703-713.

Publication

90

Professor of Biology: Kai Zinn
Postdoctoral Scholars: A. Nicole Fox, Mili Jeon, Mitsuhiko Kurusu, Anuradha Ratnaparkhi, Nina Tang Sherwood
Graduate Students: Anna Salazar, Ashley Palani Wright
Staff: Elena Armand, Lakshmi Bugga, Kaushiki Menon, Violana Nesterova

Summary: Our overall focus is on the molecular mechanisms of axon guidance and synaptogenesis in *Drosophila*. Our approach combines genetics, molecular biology, biochemistry, and cell biology. We are especially interested in cell-surface and signal-transduction proteins that function in growth cones, presynaptic terminals, and their postsynaptic partners. We are also studying the molecular mechanisms involved in control of local translation at synapses.

Signal transduction via receptor tyrosine phosphatases. Receptor-linked protein tyrosine phosphatases (RPTPs) are selectively expressed on CNS axons and growth cones in the *Drosophila* embryo, and they regulate motor and CNS axon guidance during embryonic and larval development. RPTPs are likely to directly couple cell recognition *via* their extracellular domains to control of tyrosine phosphorylation *via* their cytoplasmic enzymatic domains. The extracellular regions of the fly RPTPs all contain immunoglobulin-like (Ig) and/or fibronectin type III (FN3) domains, which are usually involved in recognition of cell-surface or extracellular matrix ligands. Their cytoplasmic regions contain either one or two PTP enzymatic domains. The fly genome encodes six RPTPs. We have studied the phenotypes associated with mutations in all six genes (see Jeon abstract). Our current focus is on defining the other components of the signaling pathways in which the RPTPs function. In particular, we are trying to identify RPTP substrates (the targets for their cytoplasmic domains) and the cell-surface ligands recognized by their extracellular domains.

Searching for RPTP substrates. It is difficult to identify PTP substrates using their enzymatic activity as a guide, because PTPs usually do not display strong specificity *in vitro*. We have devised an approach to this problem in which we conducted yeast two-hybrid screens with 'substrate-trap' versions of DPTP52F, DPTP10D, DPTP69D, and DPTP99A. We introduced a constitutively activated chicken Src tyrosine kinase into the yeast together with the PTP 'bait' constructs, in the hope that it would phosphorylate relevant substrate fusion proteins made from cDNA library plasmids. We have identified several classes of clones whose interactions with the substrate-trap RPTPs are dependent on coexpression of the tyrosine kinase, suggesting that they may be substrates. We are currently analyzing these further to determine which ones are likely to be of interest for the future (see Bugga abstract).

Screening for RPTP ligands. We have devised a new strategy for identifying ligands for 'orphan receptors' and applied it to the search for RPTP ligands. This strategy is based on the observation that fusion proteins in which the extracellular domains of RPTPs are joined to human placental alkaline phosphatase (AP) can be used to stain live *Drosophila* embryos. Each of four fusion proteins (LAR-AP, DPTP69D-AP, DPTP10D-AP, DPTP99A-AP) binds in a specific manner to the embryonic CNS. Most of the observed staining is on CNS axons. We are now screening a 'deficiency (Df) kit' of ~300 fly lines, each of which lacks a specific region of the genome, by staining homozygous Df embryos from each line with each of the fusion proteins. This method should identify the genomic regions encoding each of the RPTP ligands.

We have already identified a putative LAR ligand through this deficiency screen. This is the heparan sulfate proteoglycan (HSPG) Syndecan. LAR interacts with the glycosaminoglycan chains of Syndecan with nanomolar affinity. Genetic interaction studies using *Sdc* and *Lar* LOF mutations demonstrate that Sdc contributes to LAR's function in motor axon guidance. We also show that overexpression of Sdc on muscles generates the same phenotype as overexpression of LAR in neurons, and that genetic removal of LAR suppresses the phenotype produced by ectopic Sdc. These results demonstrate that Sdc can interact with LAR in *trans*, and suggest that Sdc is a positive regulator of LAR signaling. These results are described in a recent paper (Fox and Zinn, 2005) and also in the Fox abstract.

Targeting of motor axons to specific muscle fibers. The 32 motor neurons in each hemisegment of a *Drosophila* embryo innervate 30 muscle fibers, and each motor axon extends along a stereotyped route and always targets the same fiber. We are employing a gain-of-function (GOF) approach to identify genes involved in the targeting of motor axons to specific muscles.

Despite advances in characterizing molecules such as the RPTPs that regulate motor axon pathfinding, we still understand little about how specific muscle fibers are recognized as targets for synapse formation by these axons. Many mutations affect pathfinding decisions, leading to aberrant wiring of the neuromuscular system, but no single LOF mutations are known that block recognition of a specific muscle target. These results are most easily explained by invoking genetic redundancy in target labeling. If each muscle fiber were defined by a combination of several cell surface labels, removing one of

the labels might not have a major effect on targeting of axons to that fiber. This would explain why targeting molecules have not been identified in conventional LOF genetic screens.

Studies of GOF phenotypes are consistent with the redundancy hypothesis. For example, the homophilic cell adhesion molecule Fasciclin III (Fas III) is expressed on only two muscle fibers, 6 and 7, and on the growth cone of the RP3 neuron that innervates these two fibers. Fas III appears to be a functional target label, because when it is ectopically expressed on other muscle fibers near 6 and 7, the RP3 neuron makes abnormal synapses on these Fas III-expressing fibers. However, Chiba and his colleagues have shown that when Fas III is removed by a LOF mutation, there is no effect on targeting of RP3 to 6 and 7. These results imply that Fas III can be used for muscle targeting, but that targeting of 6 and 7 can still proceed in its absence, presumably because these fibers are also labeled by other surface molecules that can be detected by the RP3 growth cone when Fas III is not present. Similar observations have been made for another cell adhesion molecule, Capricious, by Nose and colleagues.

These findings suggest that cell-surface proteins that label specific targets in the motor axon system might be identifiable by a GOF genetic screen in which candidate labels are ectopically expressed on all muscle fibers. If these proteins are functional labels, their misexpression might produce alterations in target recognition, as observed in the Fas III experiments described above. By identifying all the genes encoded in the *Drosophila* genome that can confer pan-muscle overexpression phenotypes in which pathfinding or synaptogenesis on specific muscle targets are perturbed, we will acquire the tools to understand the mechanisms involved in target recognition in this system. This type of screen should allow us to overcome the redundancy problem. For example, suppose one could identify three different cell-surface proteins that are normally expressed on a specific muscle fiber, but whose misexpression on other, neighboring muscle fibers produces targeting errors. One might then predict that removing all three of these proteins by making a triple LOF mutant (through conventional or RNAi techniques) would now prevent targeting of this muscle fiber. Through these kinds of experiments, we could begin to understand the combinatorial code for muscle targeting. Insights into the motor axon targeting code would be likely to facilitate an understanding of targeting in other neuronal systems, since candidate target labels are usually expressed by a variety of neuronal and non-neuronal cell types.

Control of local synaptic translation at the NMJ. Motor growth cones reach their muscle targets during late embryogenesis and then gradually mature into presynaptic terminals. These synapses continue to expand and change as the larva grows, because their strengths must be matched to the sizes of the muscle fibers they drive. The pattern of Type I neuromuscular junction (NMJ) synapses in the third instar larva is simple and highly stereotyped,

with boutons restricted to specific locations on each muscle fiber. The fly NMJ is a useful genetic model system for excitatory synapses in the vertebrate CNS, because it uses glutamate as its neurotransmitter, is organized into boutons, and exhibits synaptic plasticity during development.

A few years ago, we executed a GOF screen of live larvae to find genes involved in synaptogenesis in this system [Kraut *et al.* (2001) *Curr. Biol.* **11**:417-430]. We then initiated further study of a number of genes identified in the screen that encode RNA-binding proteins potentially involved in regulation of synaptic translation. *pumilio* (*pum*) encodes an RNA-binding protein that shuts down translation of *hunchback* and other mRNAs during early embryonic development through binding to specific sequences in their 3' untranslated regions. We found that Pum protein is expressed in a small subset of CNS neurons, and *pum* LOF mutations alter motor axon guidance in the embryo. Pum protein is also localized to NMJs in third instar larvae, and is primarily postsynaptic. *pum* LOF larvae have NMJs that do not grow in a normal manner. Postsynaptic Pum regulates expression of a translation initiation factor, eIF-4E, which is localized to postsynaptic aggregates. eIF-4E is limiting for translation in many systems. Schuster and his colleagues have provided evidence that eIF-4E and poly-A binding protein regulate local postsynaptic translation in at the fly NMJ. Pumilio appears to be an essential component of this translational regulation mechanism. In *pum* mutant larvae, we observe a dramatic increase levels in the number and size of postsynaptic eIF-4E aggregates, but there is no effect on eIF-4E within the rest of the muscle cytoplasm. Pum protein binds tightly and specifically to the 3'UTR of *eIF-4E* mRNA, suggesting that it is a direct target. There is also a large increase in the amount of the GluRIIa glutamate receptor at the NMJ; GluRIIa may be an indirect target whose translation is increased as a consequence of the elevation in postsynaptic eIF-4E (Menon *et al.*, 2004; see also Menon abstract). We have since initiated study of the NMJ functions of *nanos*, a gene involved in regulation of translation by Pumilio, and of *cup*, a gene encoding a protein that regulates eIF-4E activity and is essential for localized translation in the early embryo.

144.   Searching for RPTP substrates
Lakshmi Bugga
To isolate RPTPs in a complex with their target substrates, we are using yeast two-hybrid system. We are looking for proteins that interact with *Drosophila* neuronal RPTPs-10D, 69D, 99A and 52F. To attempt to achieve stable binding of the RPTPs to a tyrosine phosphorylated substrate, we have used 'substrate-trap' mutants of the RPTPs, which can bind to substrates but do not catalyze dephosphorylation, instead remaining bound to substrate in a stable complex. We constructed plasmids encoding GAL4 DBD/RPTP bait proteins and introduced them into yeast together with fly cDNA libraries encoding GAL4AD-cDNA fusion proteins [from Steve Elledge (Baylor)]. We also introduced a plasmid containing a constitutively active

form of chicken c-Src, driven by a constitutive yeast promoter. Positive interactions are detected by selecting on plates lacking the auxotrophic marker and screening for reporter expression.

Our screen with all four DPTPs resulted in several positive clones - about 15 genes that interact with either of the four DPTPs. We identified seven genes that interact specifically with a given DPTP, four of these genes as potential substrates based on Src dependence. Of the seven genes, four are known genes-Tartan (a cell adhesion molecule expressed in embryonic CNS and PNS), Cysteine string protein (a chaperone protein expressed in larval neuromuscular junction and adult brain), Xmas-1 (a RNA Binding protein that is involved in spermatogenesis, oogenesis and embryogenesis) and BEST:LD07122(a DNA binding protein). Of the three unknown genes, one is rich in proline residues and also has proline motifs which are known to bind to SH3 domains. RNA *in situ* with this gene showed expression in the embryonic CNS.

We are currently testing these interactions *in vitro* by transient transfection experiments with *Drosophila* cell line-S2 cells and finding out the expression of the rest of the unknown genes by RNA in situ, and looking for double mutant phenotypes with DPTP and tartan mutant flies. Our biochemical experiments with full-length tartan showed association with substrate-trap 52f, and this association decreased/disappeared with the wild-type 52F, showing that tartan is a substrate for 52f. We are trying to map the area of the tartan gene that specifically interacts with 52F.

145. Syndecan is a candidate ligand for the *Drosophila* RPTP Dlar
Nicki Fox

The structural similarity of receptor protein tyrosine phosphatases (RPTPs) to receptor tyrosine kinases (RTKs) has led to the hypothesis that ligands might also modulate receptor protein tyrosine phosphatase (RPTP) activity, as they do with RTKs. To date, most RPTPs are "orphan receptors," as their physiologically relevant ligands are unknown. The identification of ligands for RPTPs is crucial for better understanding of the exact mechanisms by which RPTP signaling affects the growth cone.

We have identified a candidate ligand, Syndecan (Sdc), for one *Drosophila* RPTP, Dlar. Dlar is known to affect axon guidance decisions in the embryonic neuromuscular system as well as the visual system. Dlar is necessary for normal development, as flies null for Dlar do not survive to adulthood. While it is well established that Dlar is an important player in development, proteins that interact upstream of Dlar have not been identified.

Sdc is a heparan sulfate proteoglycan (HSPG) that consists of an extracellular core protein to which heparin sulfate side chains are attached. HSPGs have been implicated in axon guidance in other systems.

Dlar and Sdc genetically interact, as lowering Sdc levels results in an enhancement of the characteristic Dlar intersegmental nerve b (ISNb) bypass phenotype. Sdc appears to act as a ligand, rather than a co-receptor, for

Dlar, which is expressed in axons. Overexpression of Sdc in the muscles, but not the neurons, causes an axon guidance phenotype. This phenotype is suppressed by removing Dlar function. One sees the same axon guidance phenotype (in the segmental nerve A [SNa]) when overexpression Dlar in the neurons, suggesting that Sdc may in fact act to activate Dlar.

Dlar and Sdc also interact biochemically, and we have been able to map the region in Dlar responsible for this interaction. There is a canonical heparan sulfate binding site (BBXBB, where B is R or K and X is any amino acid) in the first immunoglobulin domain in Dlar and another basic motif, both of which are necessary for Dlar binding to the heparan sulfate moieties of Sdc.

We have performed immunohistochemistry in developing embryos, demonstrating that Sdc is expressed in the muscle tissues through which Dlar-expressing axons would be pathfinding during development. Thus, Sdc does seem to be present at the correct time and place to be a ligand for Dlar during axonal development.

We are presently continuing our screen for additional ligands for Dlar and ligands for the other RPTPs.

146. Characterization of receptor protein tyrosine phosphatase RPTP4E
Mili Jeon, Alice Schmid*

Previous genetic analysis carried out in the lab revealed that RPTPs interact with each other in distinct ways to regulate axon guidance during embryonic development. Among the RPTPs, the role of *Ptp4E* is the only one that has not yet been investigated. We decided to start our studies by investigating the different genetic interactions that *Ptp4E* might have with other RPTPs. At the sequence level, *Ptp4E* is most similar to *Ptp10D*. Because many RPTPs have overlapping functions in axon guidance, we started our investigation of *Ptp4E* function in the nervous system by looking at *Ptp4E Ptp10D* double mutant embryos. Either of these mutants alone are fully viable and do not show any detectable CNS or motor axon guidance defects. However, animals that are doubly mutant for *Ptp4E* and *Ptp10D* die during the embryonic-to-larval transition stage. These embryos, when labeled with antibodies against Fas II, show a disorganized CNS, where the longitudinal axons appear wavy with breaks and show invasion of one axon bundle to its neighboring tracks. To better characterize the guidance phenotypes, we are collaborating with Alice Schmid to label single neuroblasts with DiI, and visualize by confocal microscopy, the axon tracks of the progenitor neurons. This will allow us to characterize guidance errors at much higher resolution and will help us understand the breaks and disorganization we see in the Fas II stained CNS.

In addition to genetic interaction studies, we are raising monoclonal antibodies against PTP4E. In contrast to other RPTPs that are exclusively expressed in the nervous system, *in situ* hybridization experiments by others showed that *Ptp4E* mRNA is expressed in the nervous system as well as in the developing gut. The

expression studies of *Ptp4E* will help us understand additional roles that *Ptp4E* may have during development. Finally, we also have PTP4E-AP fusion protein expressed from insect cells (Caltech Protein Expression Facility) that will allow us to detect expression of PTP4E ligands using the techniques developed in the lab.

Eccles Institute of Human Genetics, University of Utah

147. Translational control mechanisms at the larval neuromuscular junction
Kaushiki P. Menon

Pumilio is a translational repressor that localizes postsynaptically at larval neuromuscular junctions (NMJs). It is required both pre- and post-synaptically in the nervous system. In neurons, it is required for synaptic growth. Postsynaptically, it represses accumulation of the cap-binding protein, Eukaryotic Initiation Factor eIF4E at the NMJ. eIF4E accumulation has been shown to control both morphological and functional properties of the larval NMJ. Pumilio binds specifically to the 3'untranslated region of eIF4E mRNA and thereby presumably controlling eIF4E accumulation and indirectly controlling translation of glutamate receptor, GluRIIA mRNA at the NMJ.

To identify other components of the control mechanism operating at the NMJ, we have taken advantage of the fact that Pumilio's function in the early embryo has been thoroughly examined. It interacts with Nanos, a Zn-finger binding protein, to form a repression complex that prevents translation of the target *hunchback* mRNA. Recently, several reports have shown that Cup, a germline protein, interacts with eIF4E protein and represses its function in the developing embryo.

We have found that both Nanos and Cup proteins show similar localization patterns as Pumilio at the larval NMJ. We are currently investigating their functions in translational control by analyzing synaptic bouton structure and electrophysiological properties of loss-of-function alleles.

148. Protein aggregation and synaptic function
Anna Salazar

Protein aggregation has been implicated in numerous human diseases, including prion-based encephalopathies. Prions are capable of catalyzing their own propagation in a process whereby the protein serves as a seed or template in which the WT protein becomes folded into the abnormal structure and aggregates. This process has been observed in various organisms, including yeast, in which a system has been developed to better understand prion-like behavior. In yeast, the [psi+] phenotype is caused by the aggregation of Sup35p, a translational termination factor, causing it to become inactivated. Because the aggregation of other proteins enhances the aggregation of Sup35p, this system can be used as an assay for proteins that display prion-like behavior. In response to a talk by Kandel, which implicated the existence of prion-like proteins at synapses, the *C. elegans* and *Drosophila* databases were analyzed to

search for RNA binding proteins with Q/N rich domains. One of the genes obtained in this search, *pumilio*, encodes a protein that was obtained through an axon guidance screen at the larval neuromuscular junction by Kaushiki Menon in the lab (Menon abstract). Two Q/N rich domains of this protein, the full-length protein, the *C. elegans* homolog, and numerous controls were cloned into several different yeast expression vectors in order to probe their ability to exhibit prion-like behavior in well-established yeast assays. Transgenic fly lines that contain the UAS Gal4 binding site and one Q/N-rich domain of *pumilio* have been created in order to drive overexpression of the aggregating domain of *pumilio* in a tissue- and time-specific manner in the fly. These flies are being analyzed with one goal being to determine whether this construct can recapitulate known *pumilio* loss-of-function phenotypes in the early embryo and at the larval neuromuscular junction.

149. What is the role of *Drosophila beached* in motor nervous system development?
Ashley Wright, Rachel Kraut*

We identified *Drosophila beached (bchs*; known in Flybase as *blue cheese)* in an overexpression screen for axon guidance and synaptogenesis defects. Overexpression of Beached in motor neurons causes bulges to form at synaptic branchpoints, and the morphology of synaptic boutons is altered. Kim Finley and her colleagues at the Salk Institute have shown that mutations in this gene cause progressive neurodegeneration in adult flies and lead to shortened lifespan. Paul Garrity and his colleagues at MIT have also generated *bchs* mutations. We have employed both sets of mutant alleles in our experiments, and the phenotypes we observe are consistent between alleles.

Our experiments on *bchs* loss-of-function mutants have focused on development of the larval neuromuscular system. By larval stages we observe thickening of certain nerve bundles and synaptic abnormalities. We have also been able to identify a subset of motor neurons that die during larval development in these mutants.

beached encodes a protein of about 3500 amino acids which contains a BEACH domain, FYVE domain, and WD40 repeats. Other members of this family of proteins have been shown to have roles in endolysosomal trafficking. We are working to determine the subcellular localization of Beached protein by co-localization with known markers of the endolysosomal pathway and we will look in the mutant larvae at these same markers to determine if any compartment in this pathway is altered in size or morphology. We are overexpressing cell death inhibitors in this subset of motor neurons in order to determine if the motor neurons are dying through apoptosis. We are also investigating which signaling pathways are implicated in the death of these neurons, including trophic support pathways, and whether ubiquitination plays any role in the death of these neurons.

Institute of Bioengineering & Nanotechnology, Singapore

94

Publications

Fox, A.N. and Zinn, K. (2005) The transmembrane heparan sulfate proteoglycan Syndecan is an *in vivo* ligand for the DLAR receptor tyrosine phosphatase. *Curr. Biol.* **15**:1701-1711.

Kraut, R. and Zinn, K. (2004) Roundabout 2 regulates migration of sensory neurons by signaling in *trans*. *Curr. Biol.* **14**:319-329.

Menon, K., Sanyal, S. Habara, Y., Sanchez, R., Wharton, R.P., Ramaswami, M. and Zinn, K. (2004) The translational repressor Pumilio regulates presynaptic morphology and controls postsynaptic accumulation of translation factor eIF-4E. *Neuron* **44**:663-676.

Sherwood, N.T., Sun, Q., Xue, M., Zhang, B. and Zinn, K. (2004) *Drosophila* spastin regulates synaptic microtubule networks and is required for normal motor function. *PLOS Biology* **2**:2094-2111.

Zinn, K. (2004) Dendritic tiling: New insights from genetics. *Neuron* **44**:211-213.

Structural, Molecular and Cell Biology

Giuseppe Attardi, Ph.D.
David Baltimore, Ph.D.
Pamela J. Bjorkman, Ph.D.
Charles J. Brokaw, Ph.D.
Judith L. Campbell, Ph.D.
David C. Chan, Ph.D.
Raymond J. Deshaies, Ph.D.
William G. Dunphy, Ph.D.
Grant J. Jensen, Ph.D.
Stephen L. Mayo, Ph.D.
James H. Strauss, Ph.D.
Alexander Varshavsky, Ph.D.

Summary: In the past year there has been good progress in some of the projects being pursued in our laboratory, as well as initiation of novel directions of our research program. Thus, an interesting development has been the observation that some of the mutations that we had previously demonstrated to accumulate with age, in subjects of Caucasian populations, in the mitochondrial DNA (mtDNA) main control region, and, in particular, at critical control sites for mtDNA replication, are associated with higher cell respiratory capacity. This is true for the T414G transversion, within the promoter for the RNA primer of heavy strand synthesis in skin fibroblasts, and for the C150T transition, adjacent to an origin for heavy strand synthesis in fibroblasts and leukocytes. These results strongly suggest the positive value for the organism of the above-mentioned aging-related mutations.

There has been progress also in our understanding of the phenotypic effects of the C150T mutation. The transfer into mtDNA-less cells, derived from 143B.TK⁻ osteosarcoma cells, of mtDNA from fibroblasts carrying the C150T mutation has permitted the construction of transformants exhibiting either 100% or 0% of the mutation in a very similar nuclear background. A detailed comparison of the two phenotypes has revealed that 100% C150T mutation-carrying cells exhibit higher and more coupled endogenous respiration and an increase in cytochrome *c* oxidase activity, and produce less reactive oxygen species than wild-type cells at that position.

In another area, considerable progress is also being made in the analysis of the role of mitofusins in mitochondrial organization in human cells. Recent findings have indicated that Mfn1 and Mfn2 have non-overlapping functions. However, analysis of several human cell lines and human tissues has so far failed to reveal any clear correlation between the levels of Mnf1 and Mnf2 and mitochondrial morphology. In our current work, strong evidence has been obtained for the occurrence in HeLa cells of two electrophoretically distinguishable forms of Mfn2, a slower migrating transient one and a faster migrating, steady state form.

150. **Termination factor mTERF-mediated DNA loop between termination and initiation sites drives human mitochondrial rRNA synthesis**

Jaehyoung Cho†, Miguel Martin†, Anthony J. Cesare[1], Jack D. Griffith[1]

According to evidence that we obtained about 25 years ago (1), transcription of the HeLa cell mtDNA heavy (H)-strand starts from two initiation sites within the main control region. One site (H1) is situated 16 bp upstream of the tRNA[Phe] gene, and produces a transcript that terminates at the 3'-end of the 16S rRNA gene, and is destined to be processed, yielding the two rRNAs, the tRNA[Phe] and the tRNA[Val]. The second site (H2) is near the 5'-end of the 12S rRNA gene and produces a polycistronic molecule, which corresponds to almost the entire H-strand, and is processed to yield the mRNAs and most of the tRNAs encoded in the H-strand. Subsequently we showed that termination of transcription at the boundary between the 3'-end of the 16S rRNA gene and the tRNA[Leu(UUR)] genes is mediated by a termination factor, mTERF (2, 3). This factor is a 342 residue DNA-binding protein that carries three leucine zippers, of which one is bipartite, and two widely spaced basic domains. This factor was previously shown to bind to a 28-base pair region within the tRNA[Leu(UUR)] gene, at a position immediately adjacent to the 16S rRNA gene.

The rate of synthesis of rRNA is 15 to 60-fold higher relative to mRNA (1). A striking observation in the analysis of mTERF was that, in an *in vitro* transcription system, mTERF stimulates transcription of mitochondrial rDNA, starting from its natural starting site (H1) (2, 4). However, the fact that this stimulation by mTERF was not observed when template DNAs containing a non-natural starting site were used, even with a natural termination site (5, 6) suggested that mTERF interaction with both the natural termination and H1 initiation sites may be essential for this specific stimulation effect.

To understand the mechanism controlling human mitochondrial rDNA transcription by mTERF, we tested many biochemical aspects of mTERF in this process under *in vitro* and *in vivo* conditions. In the present work, we found that addition of mTERF to a HeLa cell mitochondrial lysate-based reaction mixture containing an artificial rDNA template did specifically stimulate rDNA transcription. This stimulation required that mTERF be *simultaneously* bound to the rDNA transcription termination and initiation sites in the *same* molecule, thus forming a loop. Most significantly, a double binding of mTERF to the rDNA molecule, with resulting loop formation, was also shown *in vivo* by a chromatin immunoprecipitation assay and a chromosome conformation capturing assay. The most plausible interpretation of these results is that human mitochondrial rRNA synthesis is mediated by rDNA looping. An electron microscopic analysis has indeed revealed a DNA-loop structure in the same DNA template utilized for the *in vitro* transcription experiments driven by mTERF.

These results strongly suggest that, to satisfy the need for high rate of rDNA transcription, human mitochondrial rRNA synthesis involves mTERF-mediated rDNA looping, that promotes recycling of the transcription machinery.

[1]University of North Carolina, Chapel Hill, NC
†These authors contributed equally

References
(1) Montoya, J., Gaines, G.L. and Attardi, G. (1983) *Cell* **42**:151-159.
(2) Kruse, B., Narasimhan, N. and Attardi, G. (1989) *Cell* **58**:391-397.
(3) Fernández-Silva, P., Martinez-Azorin, F., Micol, V. and Attardi, G. (1997) *EMBO J.* **16**:1066-1079.
(4) Asin-Cayuela, J., Helm, M. and Attardi, G. (2004) *J. Biol. Chem.* **279**:15670-15677.
(5) Hess, J.F., Parisi, M.A., Bennett, J.L. and Clayton, D.A. (1991) *Nature* **16**:351, 2326-2329.
(6) Prieto-Martin, A., Montoya, J. and Martínez-Azorín, F. (2004) *J. Biochem.* **136**:825-830.

151. Investigation of proteins interacting with sites of the human mtDNA main control region specifically targeted by an aging-dependent accumulation of mutations

Jaehyoung Cho

Mitochondria have their own genome and cooperate with the nuclear genome in regulating respiration, energy metabolism, and, more surprisingly, aging and longevity (1, 2). Recent papers reported that the mitochondrial metabolic enzymes binds to mtDNA and have direct function for mtDNA biogenesis (3, 4). The D-loop region of human mitochondrial DNA (mtDNA) harbors very crucial control sequences, such as replication origins and a transcription promoter, and this control region undergoes some mutations which occur in aging-dependent manner (1, 2). To investigate the molecular basis of the aging-dependent mutagenesis and its selection, we planned to identify possible protein-DNA interactions in this region. During the replication process, an early intermediate mtDNA form is a long, triple helix-containing D-loop. The stability of the single-stranded portion of the D-loop may have an important role in the regulation of mtDNA copy number. Thus, we have searched for possible protein-DNA interactions in both the single-stranded DNAs (heavy and light strands) of this region. In the case of the DLP4 subregion, which harbors major replication origins and CSB1, only the light strand showed binding activity to several proteins in DNA mobility shift assays. We purified the proteins by ssDNA affinity chromatography, and found that these have molecular weights of 70, 55, 37, 28 and 15 kDa. Among them, the 37 kDa protein shows specific binding to a previously known origin of heavy-strand replication (OH2). This OH2 region is the site of a very interesting aging-dependent mutation (C150T). Previous work in this laboratory showed that, in leukocytes from subjects of an Italian population, the homoplasmic C150T transition occurs in approximately 17% of 52 subjects 99-106 years old, but, in contrast, in only 3.4% of 117 younger individuals. Interestingly, the 37 kDa protein preferably interacts with the mutant sequence rather than with the wild-type sequence. Since 5'-end analysis of nascent heavy strands consistently revealed a new replication origin at position 149, substituting for that at 151, only in C150T mutation-carrying samples of fibroblasts or immortalized lymphocytes (1, 2), the 37 kDa protein may have an important role for the selection of a remodeled replication origin. Recently, we characterized the molecular nature of this protein by LC/MS/MS (liquid chromatography and tandem mass spectrometry). The result showed that this protein is a member of the group of critical enzymes for the TCA cycle. We confirmed that the commercially available purified enzyme can also bind specifically to the OH2 region *in vitro*, and that the antibody against this protein can make a super-shifted band in a DNA mobility shift assay. Very interestingly, this interaction was inhibited by NADH in a dose-dependent manner. We also verified the specificity of this protein-OH2 interaction by DNase I footprinting analysis and chromatin immunoprecipitation. We are now testing the effect on mtDNA biogenesis of the overexpression of this protein in HeLa cells and C150T mutant cells. Our data suggest the possibility that two important factors in aging, i.e., energy metabolism and mtDNA function, regulate the aging process during the lifespan.

References
(1) Michikawa, Y., Mazzucchelli, F., Bresolin, N., Scarlato, G. and Attardi, G. (1999) *Science* **286**:774-779.
(2) Zhang, J., Asin-Cayuela, J., Fish, J., Michikawa, Y., Bonafe, M., Olivieri, F., Passarino, G., De Benedictis, G., Franceschi, C. and Attardi, G. (2003) *Proc. Natl. Acad. Sci. USA* **100**:1116-1121.
(3) Hall, D.A., Zhu, H., Zhu, X., Royce, T., Gerstein, M. and Snyder, M. (2004) *Science* **306**:482-484.
(4) Chen, X.J., Wang, X., Kaufman, B.A. and Butow, RA. (2005) *Science* **307**:714-717.

152. Large-scale detection and quantification of aging-dependent human mitochondrial DNA polymorphisms by two-color single base extension genotyping (2C-SBEG)

Jaehyoung Cho

It has been recently shown that the loss of integrity of human mitochondrial DNA (mtDNA) is closely related to the aging process, as well as to human metabolic disorders. In the past few years, we have reported the occurrence of an aging-dependent large accumulation of point mutations in the mtDNA main control region of the majority of individuals above a certain age. To understand the role of these point mutations in human aging, genotyping of a large number of samples is essential. The presently available methods, such as DGGE (denaturing gradient gel electrophoresis) and differential primer extension technique, require

several time-consuming steps, including polyacrylamide gel electrophoresis, and are not applicable for large-scale analysis. Recently, another efficient method using quantitative PCR has been developed for a large-scale genotyping, but this method is too expensive. Therefore, we planned to develop an efficient way to analyze polymorphisms of human mtDNA on a large scale.

In the differential primer extension technique, a radio-labeled primer targeted to a specific locus is extended by Vent polymerase, and the extension products are differentially terminated by incorporation of a dideoxynucleotide at the 3' end. The extended primers carrying wild-type or mutated mtDNA sequence have different length and can be analyzed by polyacrylamide-urea gel electrophoresis. Usually, the whole procedure requires an entire week, and the quantification of the polymorphism is not possible in some cases. We have modified the original procedure by using different fluorescent dye-labeled ddNTP mixtures. In this new method, a single base is incorporated at the 3' end of a cold primer by using two different fluorescent dye-labeled ddNTPs (for example, green Cy3-ddCTP and red Cy5-ddTTP). The extended primers are blotted on a Zeta-probe nylon membrane using a 96-well dot blotting system, and the membrane is washed twice with washing buffer to remove un-incorporated fluorescent ddNTPs. The genotype of the each sample is analyzed by the color difference detected by the Molecular Imager FX pro plus system (Biorad). This system is very sensitive and can detect 0.2 fmol of Cy3 or Cy5 end-labeled DNA using laser light. The quantification of polymorphism is quite efficient and easy. The quantity and ratio of wild type and mutant genomes can be calculated from the color difference using standard mixtures containing various known amounts of wild-type and mutant DNA. The whole procedure of this new technique just needs a single day even for a large-scale analysis, and is still economic. We named this new technique as two-color single base extension genotyping (2C-SBEG).

153.   Analysis of a possible association between the aging-dependent T414G mutation in human mtDNA and improvement in respiratory capacity
Paola Sgobbo

Previous work performed in our laboratory had shown an aging-related accumulation of a T414G transversion at a critical control site for mtDNA replication in skin fibroblasts. This mutation is one of those that accumulate in an aging-dependent manner occurring, in fact, in about half the individuals above 65 years of age (1). Since this mutation is localized in the D-loop region of human mitochondrial DNA (mtDNA), which plays an important role in the replication of mtDNA, we investigated the role that the mutation played, and the reason for its presence in older individuals, and tried to associate a particular phenotype with it.

In particular, we studied some biochemical aspects of transformant cells in which the nuclear background is that of mtDNA-less 143B ρ^o cells, while the mtDNA is that of mutation-carrying fibroblasts.

In order to carry out experiments showing possible effects of the T414G mutation, we analyzed transformant cell lines carrying mitochondria that contain mtDNA either 100% mutant or 100% wild type at position 414. In our preliminary experiments, the non-mutant cell lines seemed to have an higher doubling time as compared to mutants. The measurements of rate of respiration, either endogenous or substrate-driven, showed higher values in mutant cells than in control cells. These results seemed to indicate a segregation of normal function of the mitochondrial respiratory complexes with the mutation. We tested also for a possible increase in mtDNA content but Southern blot assays did not reveal any significant changes in the relative amount of mtDNA.

Further investigations will be directed at analyzing other pairs of transformant cell lines derived from different fibroblast donors, in order to identify a general phenotype associated with the T414G mutation that could clarify the functional effect of this transversion.

Reference
(1) Michikawa, Y. *et al.* (1999) *Science* **286**:774-779.

154.   Effects of the C150T mutation in the main mtDNA control region in human transformant cells
Ai Chen

Recently, our laboratory has found a strikingly higher frequency of a C150T mutation in mitochondrial DNA (mtDNA) from centenarians and twins, and also that the mutation causes a remodeling of the mtDNA 151 replication origin in leukocytes (1). To further understand the mechanism of the C150T mutation located in the mitochondrial D-loop region, we have investigated the transformants obtained by transferring fibroblast DNA carrying the C150T mutation into human mtDNA-less cells (ρ^0 cells). In particular, we chose for analysis six non-mutant and six 100% C150T mutation-carrying transmitochondrial subclones, which came from different original fibroblast donor cells. A biochemical characterization of these non-mutant or mutant transformants was carried out by measuring in intact cells their doubling times and their rates of total O_2 consumption or DNP- or ascorbate/N,N,N,N-tetramethyl-p-phenylenediamine (TMPD)-driven respiration. Compared to the average levels measured in non-mutant transformants analyzed, a lower doubling time, and a higher total O_2 consumption rate, DNP/endogenous-respiration ratio, and TMPD-driven respiration rate, which usually reflects the activity of complex IV, were observed in 100% C150T mutation-carrying transformants. In addition, when we checked the ROS level in both non-mutant and 100% C150T transformants by using CM-H_2DCFDA as a fluorescence probe, a significantly lower ROS level was observed in 100% C150T mutant transformants. It is known that inhibition of complex IV activity by KCN can greatly enhance ROS production.

According to the above mentioned results, we propose the hypothesis that the increased complex IV activity resulting from the C150T mutation may lead to 100% C150T mutant cells having higher and more coupled endogenous respiration and producing less ROS than non-mutant cells. Thus, the C150T mutation may be associated with a resistance to the aging-related complex IV activity decline and may increase longevity.

155. Hypersensitivity of the outer mitochondrial membrane to digitonin in the early stages of apoptosis
*Cindy Cheng, Anne Chomyn**

143B osteosarcoma cells treated with the apoptosis inducer staurosporine, undergo marked changes in the outer mitochondrial membrane early in the cell death program, long before cytochrome *c* is released from the mitochondria in the living cell [Duan *et al*. (2003) *J. Biol. Chem.* **278**:1346-1353].

One of these changes is an increase in the sensitivity of the outer mitochondrial membrane to the detergent digitonin. This increased sensitivity is manifested by a loss of cytochrome *c in vitro* from the mitochondria of digitonin-permeabilized cells. At the concentration of digitonin used in these experiments, control cells, i.e., those not undergoing apoptosis, retain an intact outer mitochondrial membrane and do not lose cytochrome *c*.

We are testing 143B cells that have been transfected with an expression clone encoding phospholipid glutathione hydroperoxide peroxidase (PHGPx). These cell lines were created by Katia Altomare (see Annual Report 2004, #182) to determine whether peroxidized lipids were the basis of the hypersensitivity to digitonin. We will determine by Western blotting the level of overexpression of PHGPx. We will determine also the effect of selenium on its overexpression level, and whether PHGPx overexpression delays or prevents apoptosis in our cell lines.
In collaboration with Hirotaka Imai and Yasuhito Nakagawa, Kitasato University, Japan

Reference
Duan, S., Hajek, P., Lin, C., Shin, S.K., Attardi, G. and Chomyn, A. (2003) *J. Biol. Chem.* **278**:1346-1353.

156. Characterization of mitofusin 2: Implications for mitochondrial organization
Petr Hájek

Mitochondria differ in size, shape and organization. They are dynamic structures; their morphology is maintained by an equilibrium between fusion and fission. In man, mitochondrial fusion is mediated by mitofusins Mfn1 and Mfn2 and by Opa1. Mfn1 and Mfn2 are integral mitochondrial outer membrane proteins with both the large N-terminal portion, containing a GTPase domain, and the C-terminal portion projecting into the cytosol. Both the N-terminal and C-terminal cytosolic portions contain coiled-coil domains.

Previously, polyclonal antibodies against a His-tagged recombinant protein, coding for a large portion of the N-terminal cytosolic segment of Mfn2, and against Mfn1, have been produced in rabbits. We analyzed the Mfn1 and Mfn2 protein levels by Western blotting of whole cell lysates from various human cell lines. In these, Mfn1 and Mfn2 varied greatly in amount. Although these cells exhibited striking differences in mitochondrial morphology, from a long-filament/network pattern in HeLa CCL2 cells to mostly punctate mitochondria in 143B cells, with an intermediate morphology in HeLa S3 (suspension culture), HepG2 and A549 cells, surprisingly, no clear correlation between the levels of Mfn2 or Mfn1 and mitochondrial morphology was observed. Mfn2 levels varied greatly also in human tissues, with high levels in heart, kidney and testis, an intermediate level in placenta, and low levels in brain, skeletal muscle, and liver.

Recent findings indicate that Mfn1 and Mfn2 have non-overlapping functions. We turned our attention to Mfn2 and its possible signaling/regulatory function in mitochondrial fusion. Purified antibodies against Mfn2 identified on Western blots a single band of Mfn2. $[^{35}S]$ methionine pulse labeling of HeLa CCL2 and HeLa S3 cells followed by immunoprecipitation under denaturing conditions using purified anti-Mfn2 antibodies revealed two bands of different electrophoretic mobilities, one corresponding to the steady-state form of Mfn2, the other characterized by a slower electrophoretic mobility. The intensities of these bands were increased when HeLa CCL2 cells were transiently transfected with human Mfn2 cDNA. In addition, the majority of Mfn2 synthesized *in vitro* from the human cDNA corresponds in electrophoretic mobility to the slower-migrating Mfn2 band. Taken together, these data indicate a presence of two protein forms of Mfn2, the slower-migrating transient form and the faster-migrating steady state form. The slower migrating form may be either less stable or is modified to the faster-migrating, steady state form. Our going investigations are aimed at the characterization of the two Mfn2 forms.

To further understand Mfn2 function, we searched for possible mitofusins-interacting proteins, using *in vivo* formaldehyde crosslinking of HeLa cells followed by immunoprecipitation under denaturing conditions with purified anti-Mfn2 antibody. This approach helped us to detect a 42 kDa protein, specifically co-immunoprecipitated with Mfn2 only from crosslinked cellular or mitochondrial lysates. Our current research is focused on the identification and characterization of the 42 kDa protein.

Publications

Altomare, K., Cheng, C., Imai, H., Nakagawa, Y. and Chomyn, A. Peroxidized lipids cause hypersensitivity to digitonin of outer mitochondrial membrane of 132B human osteosarcoma cells induced to apoptosis with staurosporine. In preparation.

Chen, Ai, Cho, J. and Attardi, G. Study of the C150T mutation in mitochondrial DNA of human transmitochondrial transformants reveals a positive effect. In preparation.

Cho, J. Large-scale detection and quantification of aging-dependent human mitochondrial DNA polymorphisms by two-color single base extension genotyping (2C-SBEG). In preparation.

Martin, M., Cho, J., Cesare, A.J., Griffith, J.D. and Attardi, G. (2005) Termination factor mTERF-mediated DNA loop between termination and initiation sites drives human mitochondrial rRNA synthesis. *Cell.* In press.

Sgobbo, P. and Attardi, G. Detection of a possible association between the aging-related T414G mutation in human mtDNA and improvement in respiratory capacity. In preparation.

Zhang, J., Iwata, N., Raule, N., Cho, J., Burk, R., Barzilai, N. and Attardi, G. Aging-related accumulation in Ashkenazi Jews of specific leukocyte mtDNA mutation adjacent to secondary replication origin. Submitted.

102

Professor of Biology: David Baltimore
Postdoctoral Scholars: Mark Boldin, Markus Covert, Huatao Guo, Shengli Hao, Konstantin Taganov, Jeff Wiezorek, Lili Yang
Senior Research Fellows: Mollie Meffert, Wange Lu
Graduate Students: Thomas Leung
Research Staff: Elissa Denny, Jahlionais Gaston, Anca Mihalas, Eric Santiestevan, Vicky Yamamoto

Summary: My laboratory has two on-going major programs, one on transcriptional control by NF-κB and the other on engineering the immune system. We are also just finishing up study of Ryk, a co-receptor for Wnt, which will be continued by a present post-doc in his new laboratory.

The NF-κB program has numerous facets, all of which relate to how this powerful and widely used cellular system of gene control is itself controlled, both negatively and positively. One aspect is the A20 protein, the gene for which is activated by TNFα treatment of cells through the mediation of NF-κB. This provides negative feedback control but the mechanism has been obscure. We have learned that A20 interacts with the ubiquitin system and we hope to understand this interaction. Another aspect of the program is study of B94, a positive NF-κB-induced regulatory protein that is active on certain but not all NF-κB regulated genes. Here we are finding that the regulation is at a different level but we are not yet sure just how it works. We are also examining the kinetics of NF-κB induction using different inducers and studying different genes. Recently we have extended this to cytologic study of the movement of NF-κB in and out of the nucleus. Finally, because NF-κB is a dimer, drawing its subunits from a pool of five different monomers, it has numerous incarnations. To understand the role of each dimer, it would be optimal to be able to control dimer formation. To do this, we are engineering the subunits so that only particular pairs will form.

In the Engineering Immunity program, we are taking various approaches to modifying the immune system of mice, using retroviral vectors to incorporate genes into T and B lymphocytes by infecting stem cells. The aim is to stimulate immunity against cancer and infectious diseases, initially HIV. We have been quite successful with cancer, making mice immune to an experimental tumor. We are now concentrating most of our attention on HIV under funding provided by the Grand Challenge program of the Gates Foundation. This is growing to be the biggest single program in the laboratory.

157. **Analysis of function of TNF primary response gene B94**
Konstantin Taganov, David Baltimore

Inflammation is a complex, highly regulated defense reaction orchestrated by an organism in response to an invading pathogen or injury. Pro-inflammatory cytokine, called tumor necrosis factor (TNF), has been found to play a pivotal role in nearly all aspects of this reaction. TNF-induced triggering of cell surface receptors results in activation of multiple signaling cascades that ultimately alter the expression of many genes, among them is B94. Our preliminary results lead us to believe that B94 can potentiate the TNF effects; however, the mechanism of B94 action and its target(s) in the TNF signaling pathways are currently unknown. We would like to extend our knowledge using a number of experimental approaches that are aimed to define the molecular mechanism of B94s function and pinpoint its place in the TNF-signaling cascade. The fact that TNF can activate multiple regulatory pathways that stimulate different and possibly even opposing programs raises important questions about the relative contribution and possible coordination. Additional studies of the TNF signaling are likely to reveal further layers of complexity that are involved in the regulation of the pathway. Dissecting the complex pathway of TNF signaling network can identify key pathway molecules and contribute to the rational target selection for therapeutic interventions.

158. **Designer immunity to treat cancer and HIV**
Lili Yang, Sascha Wyss-Stoeckle, David Baltimore

We have developed a method to genetically program mouse hematopoietic stem cells (HSCs) to develop into functional CD8 or CD4 T cells of defined specificity *in vivo*. For this purpose, a bicistronic retroviral bicistronic retroviral vector was engineered that efficiently delivers genes for both α and β chains of T cell receptor (TCR) to HSCs. When modified cell populations were used to reconstruct the hematopoietic lineages of recipient mice, significant percentages of antigen-specific CD8 or CD4 T cells were observed. These cells expressed normal surface markers and responded to peptide antigen stimulation by proliferation and cytokine production. Moreover, they could mature into memory cells after peptide stimulation. Using TCRs specific for a model tumor antigen, the recipient mice were able to partially resist a challenge with tumor cells carrying the antigen. Combining cells modified with CD8- and CD4-specific TCRs, and boosting with dendritic cells pulsed with cognate peptides, complete suppression of tumor could be achieved and even tumors that had become established would regress and be eliminated after dendritic cell/peptide immunization. This methodology of "Designer Immunity" could be developed for controlling the growth of human tumors and for attacking established pathogens. This work

has been published at *PNAS*. Our next step is to extend the work to human tumors and HIV.

Another focus of our research is to develop a method for targeted gene delivery *in vivo*. As a hallmark of gene therapy, targeted gene delivery *in vivo* can greatly facilitate the application of gene therapy, including our "Designer Immunity" strategy. To this end, we have developed a gene delivery system to transfer genes to chosen cell types. In particular, we have generated lentiviruses that can specifically infect mouse HSCs expressing c-kit. We have proved this system to be highly specific and efficient *in vitro*, by targeted infection of mouse HSCs in culture. Furthermore, we have performed *in vivo* HSC targeting by injecting lentiviruses encoding GFP reporter gene into mouse. Our preliminary results are very promising, indicating that GFP gene has been integrated into HSCs. At the next step, we will continue to optimise the gene delivery system, and explore the potential of this system to execute our "Designer Immunity" strategy for treating cancer and HIV. Other applications of this system include the *in vivo* correction of blood cell genetic deficiencies, holding potential for treating diseases such as SCID and the X-linked autoimmunity.

Publication

Yang L. and Baltimore D. (2005) *Proc. Natl. Acad. Sci. USA* **102**(12):4518-4523.

159.   Molecular mechanisms of modulation of TNF receptor signaling by A20 and B94 proteins
Mark Boldin, David Baltimore

Members of the tumor necrosis factor (TNF)/nerve growth factor (NGF) receptor superfamily play a crucial role in activation, proliferation, survival and death of cells in the immune system. The prototype death receptor of the family is the type I TNF receptor (TNFR1). The biological functions triggered by the TNFR1 are characterized by a remarkable duality – infliction of tissue damage and cell death goes hand in hand with activation of tissue repair and expansion. The physiological reason for this duality lies in the ability of this receptor to trigger two kinds of intracellular signaling programs: Aa proteolytic cell death cascade and a number of kinase cascades leading to activation of gene expression, some of which may protect cells against cytotoxicity. TNF activates hundreds of genes at the transcriptional level of which a significant portion encodes intracellular modulators of the TNF receptor signaling or regulators of crosstalk between the TNF receptors and other signaling systems. Molecular mechanisms of action of two such regulatory molecules, called A20 and B94, are at the focus of our research.

While much knowledge has been accumulated in the past about activation of the core TNF signaling pathways, very little is known about their regulation and termination. A20 is a TNF-inducible gene that works in a negative feedback loop fashion and inhibits the TNFR1 signaling. We are currently trying to understand the molecular mechanism of A20 action and its target(s) in the

TNF signaling pathways using a combination of proteomics and molecular biology approaches. We have recently discovered that the C-terminal part of the A20 molecule can bind ubiquitin and A20 overexpression has a negative effect on the ubiquitination of some of the key signaling molecules in the TNF-induced NF-κB pathway.

B94 is an intracellular protein, which, like A20, is induced by TNF and other proinflammatory stimuli. Our preliminary findings indicate that B94 can act as a positive modulator in the NF-κB activation pathway. We plan to use B94 RNAi knockdown cell lines and B94 gene knockout mice to clearly establish the physiological role of this gene. We are also addressing the question of the molecular mechanism of action of B94 utilizing a combination of yeast two-hybrid and proteomics techniques.

160.   Dynamics of LPS and taxol-stimulated activation of NF-κB
Markus Covert, David Baltimore

This was a productive year for my research. As stated last year, I had three specific aims: (1) to quantitatively describe the time response to Lipopolysaccharide and/or Taxol in terms of IKK activity, NF-κB nuclear concentration and IκBα gene expression in wild type, as well as key knockout/knockdown MEF cell lines; (2) to develop a detailed computational model incorporating the data from Aim (1) to simulate the dynamics and interactions of the MyD88-dependent and independent signaling pathways, and (3) to determine whether the difference in pathway dynamics could in part explain differential gene expression between TNFα and LPS or Taxol-stimulated cells. In fact, these aims have now been essentially completed with respect to LPS.

Together with others in the Baltimore lab, I found that the activation dynamics of the transcription factor NF-κB exhibit damped oscillatory behavior when cells are stimulated by tumor necrosis factor a (**TNFa)** but stable behavior when stimulated by lipopolysaccharide (LPS). LPS binding to Toll-Like Receptor-4 (TLR-4) causes activation of NF-κB that requires two downstream pathways, each of which when isolated exhibits damped oscillatory behavior. Computational modeling of the two TLR-4-dependent signaling pathways suggests that one pathway requires a time-delay to establish early anti-phase activation of NF-κB by the two pathways. The MyD88-independent pathway required IRF-3-dependent expression of TNFα to activate NF-κB, and the time required for TNFα synthesis established the delay. This work was recently accepted by *Science*.

References

Covert, M.W.,[*] Leung, T.H.,[*] Gaston, J.E. and D. Baltimore, D. (2005) *Science*. In press, ([*]denotes equal authorship).

Covert, M.W., *Computational Systems Biology*, Elsevier. To be published, October, 2005.

161. Regulation of inflammation by NF-κB network system
Shengli Hao, David Baltimore

Inflammatory response is a double-edged sword. Whereas it is important for the host to clear out the pathogenic insults and to repair injuries, unregulated or prolonged inflammatory response leads to tissue damage which underlies the symptoms of a great number of diseases including AIDS, autoimmune diseases such as type I diabetes, multiple sclerosis (MS), cancer, and vascular diseases. Therefore, the effective prevention and treatment of these diseases depends on a deep understanding of how inflammatory response is controlled in the body. NF-κB is a key regulator for inflammatory response. It functions as a homodimer or heterodimer of five members: RelA, RelB, c-Rel, p50 and p52. It is the dimer, but not each NF-κB member, that determines the specificity of gene regulation. In addition, the NF-κB dimers have different functions in regulation of various aspects of inflammatory response, and thus may contribute differently to the pathogenesis of the inflammation-associated diseases. Therefore, exploration of the specific property and function of each dimer is crucial to understand this disease and ultimately to discover effective treatment. However, this approach faces a huge obstacle because altering one NF-κB protein member affects all the dimers containing this member. To overcome this problem, we will use a novel approach by performing site-directed mutagenesis of the NF-κB protein (using p50 as an example) on its dimerization domain and selecting the mutant (designated as p50*) that can only form a homodimer with itself (p50*/p50*) but not with any wild-type of NF-κB members. Since the dimerization domain is a separate domain from other protein domains, the mutant p50* dimer maintains its biological functions like the wild type. While RelA/p50 mainly mediates the initiation of inflammatory response, less is known about how inflammation is terminated and how NF-κB dimers regulate cell tolerance. Using this mutant p50*, we will analyze the specific role of the p50 homodimer in termination of inflammatory response and in cell tolerance without interference with the endogenous NF-κB dimers. This methodology can also be applied to the generation of other mutant NF-κB dimers and analyze their specific roles in regulating various aspects of these processes. This study will greatly enhance our understanding of how inflammation is controlled in various physiological contexts and eventually provide the basis for design effective therapy for all those inflammation-associated diseases.

162. Ryk as a functional receptor for Wnt
Wange Lu, David Baltimore

Cell-cell communications play essential roles in regulating cell fate determination, cell proliferation and differentiation. The receptor tyrosine kinases are a big family of proteins involved in cell signaling. The receptor related to tyrosine kinase (Ryk) is a unique member of receptor tyrosine kinases since it contains a cryptic protein tyrosine domain. The *Drosophila* homologue of Ryk is required for learning, memory and axon guidance. However, the ligand and downstream component of this orphan receptor has been unknown.

We have found Wnt associates with Ryk at the extracellular WIF domain. Ryk is required for the canonical Tcf pathway activation induced by Wnt. We have also generated transgenic mice expressing Ryk siRNA to knock down the expression of endogenous Ryk. We have found that Ryk is required for axon guidance *in vivo*. Explant outgrowth assay *in vitro* suggested that Ryk is required for Wnt3a-mediated neurite outgrowth. Based on these results, we concluded that Ryk is a functional receptor for Wnt proteins.

Ryk knockout mice have smaller brains. Using markers for neural precursor cells, we have found that the number of neural progenitor cells was significantly reduced. This result was further confirmed *in vitro* using monolayer cell culture assays. This defect is due to aberration in neural stem cell proliferation. We are now working on identifying the genes regulated by the Ryk pathway and required for neural stem cell proliferation.

Publications

Baltimore, D. (2004) Editorial, Science and the Bush administration. *Science* **305**:1873.

Covert, M.W. Integrated regulatory and metabolic models. In: *Computational Systems Biology*, Elsevier. To be published, October, 2005.

Covert, M.W.,* Leung, T.H.,* Gaston, J.E. and Baltimore, D. (2005) Achieving stability of LPS-induced NF-κB activation. *Science* **309**:1854-1857 (*denotes equal authorship).

Leung, T.H., Hoffmann, A. and Baltimore, D. (2004) One nucleotide in a κB site can determine cofactor specificity for NF-κB dimers. *Cell* **118**:453-464.

Lu, W. and Yamamoto, V. (2004) Mammalian Ryk is a Wnt coreceptor required for stimulation of neurite outgrowth. *Cell* **119**:97-108.

Meffert, M. and Baltimore, D. (2005) Physiological functions for brain NF-κB. *TRENDS in Neurosci.* **28**:37-42.

Yang L. and Baltimore D. (2005) Long term *in vivo* provision of antigen-specific T cell immunity by programming hematopoietic stem cells. *Proc. Natl. Acad. Sci. USA* **102**(12):4518-4523.

Max Delbrück Professor of Biology: Pamela J. Bjorkman

Research Fellows: Mindy Davis, Agi Hamburger, Wanzhong He, Yongning He, Pingwei Li, Rich Olson, Elizabeth Sprague, Anthony P. West, Jr., Zhiru (Jenny) Yang

Graduate Students: Alex Farley, Joshua Klein, Adrian Rice, Devin Tesar, Fan Yang

Visiting Graduate Student: Anna Gail*

Undergraduate Students: Evelyn Cheung, Ruby Feng, Damien Soghoian, Christine Tung

High School Students: Kevin McKenzie, Julia Nesterova

Research and Laboratory Staff: Beth Huey-Tubman, Lynda Llamas, Suman Machinani, Marta Murphy, Leonard Thomas, Anya Wyman

Technical University of Munich, Germany

Summary: My laboratory is interested in protein-protein interactions, particularly those mediating immune recognition. We use X-ray crystallography and biochemistry to study purified proteins (Figure 1), and are beginning to include confocal and electron microscopy to examine protein complexes in cells. Some of our work focuses upon homologs and mimics of class I MHC proteins. These proteins have similar three-dimensional structures, but different functions including immune functions (IgG transport by the neonatal Fc receptor, FcRn, and evasion of the immune response by viral MHC mimics), and non-immune functions (regulation of iron or lipid metabolism by HFE and ZAG, and serving a chaperone function for pheromone receptors in the case of the M10 proteins). We are also comparing the structures and functions of host and viral Fc receptors with FcRn.

Transfer of maternal IgG molecules to the fetus or infant is a mechanism by which mammalian neonates acquire humoral immunity to antigens encountered by the mother. The protein responsible for the transfer of IgG is the MHC class I-related receptor FcRn. MHC class I molecules have no reported function as immunoglobulin receptors; instead they bind and present short peptides to T cells as part of immune surveillance to detect intracellular pathogens. We solved the crystal structures of rat FcRn both alone and complexed with Fc. We are now interested in using information obtained from our crystallographic and biochemical studies to address how FcRn-IgG complexes are transported across polarized epithelial cells. We are using a combination of confocal and electron microscopy to study the itineraries of FcRn-containing endosomes in transfected epithelial cells and in the proximal small intestine of neonatal rats. We are also doing structure/function studies of other Fc receptors that are not MHC homologs: gE/gI, a viral Fc receptor for IgG; FcaRI, a host receptor for IgA; and the polymeric immunoglobulin receptor (pIgR), a receptor that transports dimeric IgA and polymeric IgM into secretions.

HFE is a recently discovered class I MHC homolog that is involved in the regulation of iron metabolism, an unexpected function for an MHC-related protein. The gene encoding HFE is mutated in patients with the iron overload disease hereditary hemochromatosis. HFE has been linked to iron metabolism with the demonstration that it binds to transferrin receptor, the receptor by which cells acquire iron-loaded transferrin. We solved crystal structures of HFE alone and HFE bound to transferrin receptor. The interaction of HFE with transferrin receptor is a fascinating system to study because we can use crystal structures to answer biochemical, functional, and evolutionary questions that address how binding of HFE interferes with transferrin binding, if conformational changes in the receptor are involved in the binding of either transferrin or HFE, which part of the MHC-like HFE structure binds transferrin receptor, and how the HFE interaction with the receptor compares with interactions of ligands with MHC and MHC-like (e.g., FcRn) proteins. We are expanding our studies to include cell biological investigations of HFE and transferrin receptor intracellular trafficking in transfected cell lines using confocal microscopy and other imaging techniques.

We are also interested in other MHC homologs, including proteins encoded by viruses. Both human and murine cytomegalovirus (HCMV, MCMV) express relatives of MHC class I heavy chains, probably as part of the viral defense mechanism against the mammalian immune system. Our biochemical studies show that the HCMV homolog associates with endogenous peptides resembling those that bind to class I MHC molecules. Our current efforts focuses upon defining the structure and function of these homologs in order to understand why viruses make them and how they interfere with the host immune system.

Recent studies from other laboratories have revealed expression of an interesting family of class Ib MHC proteins (M10s) that interact with putative pheromone receptors in the rodent vomeronasal organ. This interaction may play a direct role in the detection of pheromonal cues that initiate reproductive and territorial behaviors. We have solved the crystal structure of M10.5, an M10 family member. The structure shows that M10.5 folds into a similar structure as a *bona fide* class I MHC molecule. Unexpectedly, however, the M10.5 counterpart of the MHC peptide-binding groove is open and unoccupied, revealing the first structure of an empty class I MHC molecule. Our biochemical data suggest that M10.5 associates with some sort of groove occupant, most likely non-peptidic. The challenge now is to discover the

physiological ligand(s) of M10 proteins and understand how they associate with pheromone receptors to influence mating behaviors.

Our structural work on class I MHC homologs has elucidated new and unexpected recognition properties of the MHC fold. For FcRn and HFE, the structural and biochemical studies have revealed a similar fold and some common properties, including the assumption that both receptors "lie down" parallel to the membrane when binding ligand, and a sharp pH-dependent affinity transition near neutral pH. In the case of FcRn, we have elucidated the structural basis of its pH-dependent interaction with IgG and will now focus upon cell biological studies of intracellular trafficking, for which the pH-dependent interaction is critical. The pH dependence of the HFE-TfR interaction suggested to us that intracellular trafficking studies of HFE would be interesting, so much of our future efforts on both the FcRn and HFE systems will center around probing their function in a cellular context using imaging techniques. Our functional studies of M10 proteins are just beginning, since we don't understand the nature of the interaction between an M10 protein and a pheromone receptor and how that relates to binding to an as yet unidentified groove occupant. We are at an even earlier stage in our studies of the viral MHC homologs, in which our primary goal will be to solve crystal structures of a viral homolog alone and complexed with its cellular receptor.

HFE

HFE/TfR complex

Hemolin

PSMA

FcRn

FcRn/heterodimer-Fc Complex

Neuroglian Fn-III repeats

ZAG

FcRn dimer

Fc

FcRn dimer

FcRn/Fc ribbon

Invasin

Ferritin

FcαRI

FcαRI/Fcα Complex

Methuselah

pIgR domain 1

LIR-1

LIR-1/HLA-A2

mannose receptor cysteine-rich domain

M10.5
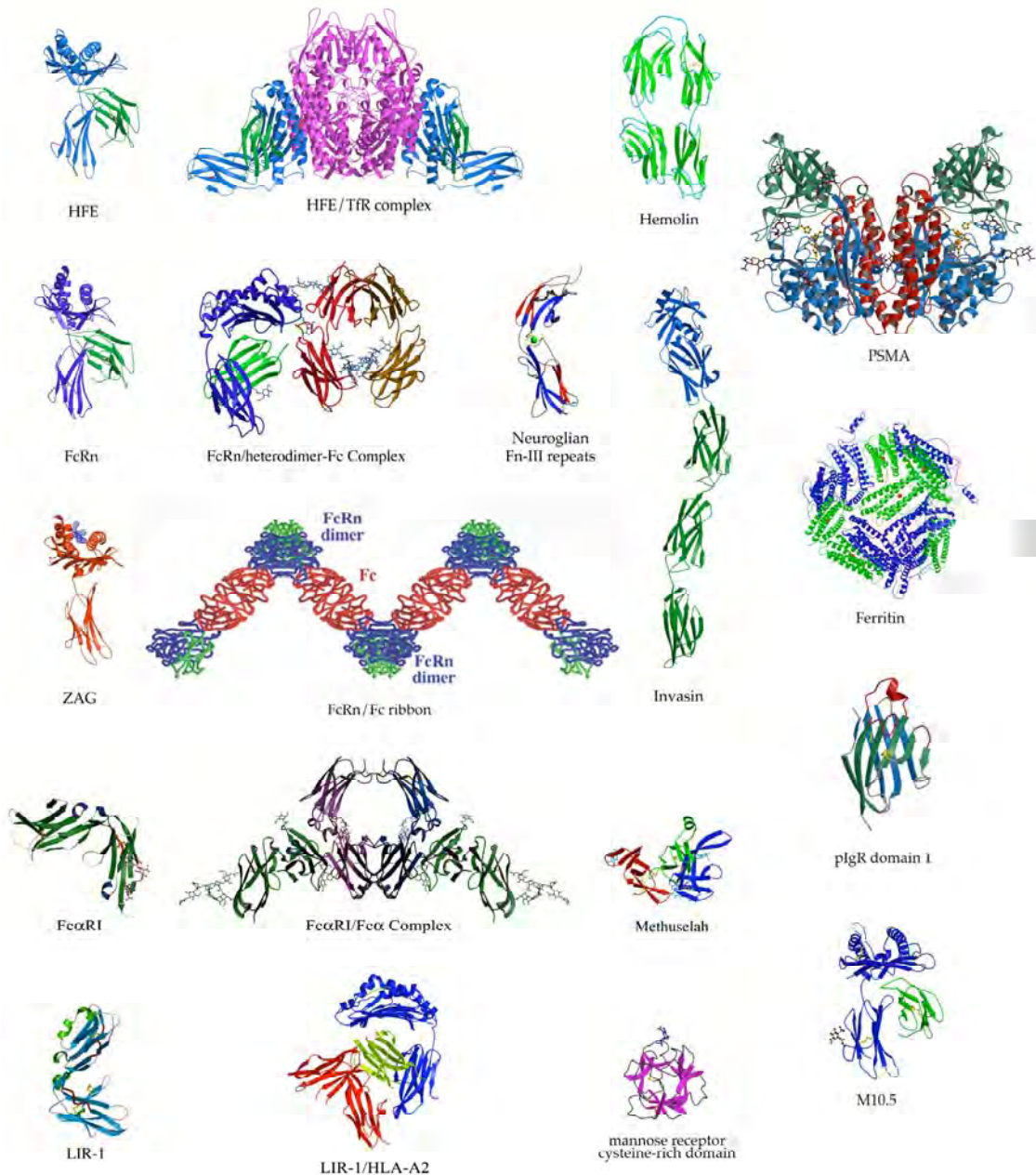
163. Characterization of FcRn-mediated transport pathways via confocal microscopy
Devin B. Tesar, Noreen Tiangco

Movement of specific protein molecules across epithelial cell barriers by their cognate receptors is achieved via a multivesicular transport pathway known as transcytosis. Discrete steps in the procession of a receptor-bound ligand through the transcytotic network are characterized by association with distinct subpopulations of endosomal compartments. These subpopulations of endosomes can be identified by confocal microscopy using fluorescent markers (such as transferrin) or antibodies against such markers (such as anti-Rab antibodies). We are currently working to decipher the transcytotic itinerary of FcRn, with or without its IgG ligand, by colocalizing FcRn and IgG with different endosomal markers. To achieve this, FcRn can be visualized by expressing a C-terminal GFP-fused form of FcRn, or by staining with an anti-FcRn monoclonal antibody that is directly conjugated to Alexa488. Rat IgG or Fc fragment can be directly labeled with fluorescent dyes (such as RITC or Cy3), and antibodies against specific endosomal markers can be viewed using secondary antibodies conjugated to a far-red dye (such as Cy5). This allows for three-color confocal analysis to determine the intracellular localization of FcRn, it ligand, and marker proteins for particular compartments at different stages within the transport process. These data can then be compared to the transport pathways of more well characterized receptors such as the polymeric Ig receptor (pIgR) to evaluate which steps might be unique to, or particularly important during FcRn-mediated transport of IgG. Future work will focus on developing techniques for following trafficking events in live cells over the course of several minutes in real time.

164. Assay for ligand-induced dimerization of FcRn
Devin B. Tesar, Ruby Feng

The 6.0 Å crystal structure of FcRn complexed with wild-type Fc demonstrates the formation of an oligomeric array of FcRn dimers bridged by Fc ligands. This "oligomeric ribbon" may have functional implications in living cells. First, transport vesicles containing the oligomeric ribbon would have their opposing membrane faces brought into close (~200 Å) proximity of one another. In addition, ribbon formation would induce an ordered linear arrangement of FcRn cytoplasmic tails. The cytosolic trafficking machinery may use one or both of these features as a means of distinguishing between vesicles that contain FcRn-IgG complexes and those that contain FcRn alone or unbound IgG. Oligomeric ribbon formation would require the simultaneous occurrence of two phenomena; 1.) FcRn dimerization, and 2.) bridging of FcRn molecules on opposing membrane faces by Fc ligands. To determine if FcRn forms a non-covalent dimer at the cell surface, either constitutively or in response to binding to its IgG ligand, we are using a bimolecular fluorescence complementation (BiFC)-based assay. BiFC is a phenomenon whereby two recombinantly-expressed non-fluorescent truncations of yellow or cyan fluorescent protein can combine to generate a mature and active fluorophore when brought into close proximity. BiFC constructs in which the full-length rat FcRn is recombinantly fused either to YN (the N-terminal fragment of YFP consisting of residues 1-172 of the mature fluorophore) or YC (the C-terminal fragment consisting of residues 172-238) on the C-terminal end of the cytoplasmic tail domain have been generated and will be co-transfected into Madin-Darby canine kidney (MDCK) cells. The presence of a fluorescent signal will suggest that the fragments are being brought into close and stable proximity to one another as a result of FcRn dimerization. Constructs in which HFE, another MHC class I-related molecule that does not dimerize or interact with FcRn, is fused to YN and YC will serve as negative controls.

165. Three-dimensional EM studies of IgG transport and cell adhesion
Yongning He, Noreen Tiangco, Devin Tesar, Grant Jensen

FcRn is a cell surface receptor responsible for passive acquisition of humoral immunity in the vertebrate newborn. It also regulates the IgG half-life in serum and IgG transport in different tissues. The physiological roles of FcRn rely on its pH-dependent binding interaction with IgG and its transport activity after ligand binding. Serum proteins are normally taken up by vascular endothelial cells and degraded by lysosomes through a default degradation pathway, which shortens their half-lives in the blood. As the IgG protection receptor, FcRn binds IgG in acidic endosomes and escorts it back to the cell surface so IgG re-enters the bloodstream, thereby increasing its serum half-life. In our studies, FcRn molecules have been incorporated onto the surface of liposomes as a mimic FcRn transcytotic vesicles. CryoEM tomography is applied to bulid a three-dimensional model of the structure of FcRn-Fc complexes attached to a membrane. Gold-labeled Fc fragments have been used as ligands to locate the bridging structure formed between FcRn-containing liposomes. The visualization of gold particles between aggregated liposomes illustrates the potential for forming a higher order structure between adjacent FcRn-containing membranes inside intracellular vesicles. In parallel with the FcRn studies, a similar liposome-based three-dimensional tomography study of the cell adhesion molecule L1 has been initiated. The homophilic adhesion activity of L1 is involved in neural and tumor cell migration and plays an important role in tumor invasion. L1-incorporated liposomes aggregate, and we are working on improving the resolution of 3D tomograms to in order to visualize the structure of the adhesive interface. L1 mutants that include protease cleavage sites between the adhesion domains have been generated to investigate different models of the adhesion mechanism.

108

166. Preparation of gold-labeled ligands for electron microscopy studies of FcRn

Suman Machinani, Anna Gail*

Receptor-mediated transcytosis of IgG in polarized cells expressing the neonatal Fc receptor (FcRn) is crucial for the passive delivery of IgGs from mother to young. X-ray analysis has provided a wealth of structural knowledge of the FcRn-IgG interaction. Neither confocal microscopy nor X-ray analysis alone is capable of investigating the arrangement of FcRn-IgG complexes *in vivo*. Electron tomography is capable of bridging the resolution gap between light microscopy and X-ray crystallography by providing 3D images at an xyz resolution from 3-8 nm. The combination of electron tomography with labeled ligands to facilitate identification of FcRn-containing vesicles remains a major goal. In this context, gold cluster-labeled IgG was prepared to ascertain co-localization with FcRn expressed in Madin Darby canine kidney cells. MDCK cells transfected with FcRn were grown for four days on filter supports. Polarized MDCK cells grown on filter supports then served as model system for exploring IgG uptake. The functional fidelity of gold-labeled antibodies was confirmed by confocal microscopy using fluorophore conjugated secondary antibodies. Co-localization of FcRn and gold-labeled Fc was observed, a feature previously observed with uptake of unlabeled Fc. Further, gold-cluster labeled BSA was prepared to serve as a fluid-phase marker, thus allowing both gold-labeled antibodies and BSA to be used in subsequent electron tomography studies.

*Visiting graduate student from the Technical University of Munich

167. Electron tomography of selective IgG transport across the epithelial barrier in suckling rat small intestine and FcRn-expressing MDCK cells

Wanzhong He, Suman Machinani, Devin B. Tesar, Grant Jensen

Before its own immune system is fully developed, the suckling rat is dependent upon the neonatal Fc receptor (FcRn) to transport maternal IgG from ingested milk into its bloodstream. FcRn also functions to protect IgG from lysosomal degradation. In both its transport and protection roles, FcRn binds to IgG at acidic pH (6.0) inside endosomes and releases IgG at the pH (7.4) of blood. Early conventional electron microscopy studies using immunoglobulin tracers provided direct evidence that the proximal small intestine of neonatal rat selectively transports antibody into the circulation [1]. However, the large dimension of the tracers (ferritin, colloidal gold particles), which may bind to multiple antibodies and/or have a strong surface ionic charge, may not reveal the true pathway taken by IgG bound to FcRn when it crosses intestinal epithelial cells. In order to trace the transport pathway during dynamic endocytic processes and to examine configurations of FcRn-IgG complexes within different types of intracellular vesicles in an *in vitro* model system (FcRn-expressing MDCK cells; see abstract 163 by Tesar *et al.*) and in the intact neonatal rat small intestine, we need a technique that permits us to capture the full physiological state of the dynamic vesicles with high

resolution. We are using 1.4 nm nanogold clusters which are small chemically-defined particles covalently attached to the hinge region of rat Fc, as a more a reliable tracer to explore functional endocytic processes. To capture and trace the nanogold-Fc conjugates inside intact cells at high resolution (3-6 nm), we are combining techniques such as high pressure freezing, freeze-substitution, frozen-hydrated thin sectioning, and electron tomography. These techniques will enable us to derive a 3D map of transport vesicles within FcRn-expressing MDCK cells and intact small intestinal epithelial cells, which is sufficient for measuring the distance between adjacent membranes, identify and trace FcRn-IgG complexes within vesicles, define transport pathways and analyze the dynamical events in the process of transcytosis.

Reference
1. Rodewald, R. (1973) *J. Cell Biol.* **58**:189-211.

168. Structural studies of the interaction between FcRn and albumin

Anya Wyman, Anthony P. West Jr., Julia Nesterova, Chaity Chaudhury*, Clark L. Anderson*

FcRn, an MHC class I homolog, binds and transfers maternal IgG antibodies to fetal or newborn mammals[1]. Recent studies have shown that FcRn binds albumin, the most common protein in blood plasma, at acidic pH and suggest that FcRn might play a similar role in protecting IgG and albumin from serum protein degradation. According to this mechanism, albumin enters the cell by fluid-phase endocytosis, binds to FcRn in acidic vesicles, and is recycled back to the cell surface where it dissociates from FcRn at the basic pH of the blood[2]. In order to elucidate the interaction between albumin and FcRn, we have attempted to co-crystallize human and rat versions of the complex using commercial sources of serum albumin and soluble, recombinant FcRn expressed in mammalian cells. Albumin consists of three repeating domains, but only domain III is believed to bind FcRn. We therefore, expressed domain III of human serum albumin in baculovirus-infected insect cells. We were able to show by surface plasmon resonance (SPR) that domain III binds to FcRn with a micromolar affinity at pH 5.5. We plan to purify domain III on a larger scale for crystallization trials with FcRn.

*Ohio State University

References
1. West, A.P., Jr. and P.J. Bjorkman. (2000) *Biochemistry* **39**:9698-9708.
2. Chaudhury, C., Mehnaz, S., Robinson, J.M., Hayton, W.L., Pearl, D.K., Roopenian, D.C. and Anderson, C.L. (2003) *J. Exp. Med.* **197**:315-322.

169. **Structural studies of a herpes simplex virus immunoglobulin G receptor**
Elizabeth R. Sprague

The herpes simplex virus type 1 (HSV-1) immunoglobulin G (IgG) receptor is a heterodimer composed of the gE and gI proteins that is found on the surface of the HSV virion or HSV-infected cells. The gE/gI heterodimer binds the Fc portion of IgG, and this interaction has been implicated in several mechanisms of immune evasion, including inhibition of virus neutralization, interference with complement- and cell-mediated lysis pathways, and antibody-bipolar bridging. The gE protein has also been implicated in the cell-to-cell transmission of HSV. In order to facilitate understanding how the gE/gI heterodimer binds the Fc portion of IgG and how this recognition event affects the ability of the host immune system to eradicate the virus, we have undertaken biochemical and crystallographic studies of the gE protein, gE/gI heterodimer, and the gE/gI-Fc complex. We previously showed that the gE/gI-Fc complex is composed of two gE-gI heterodimers per Fc homodimer and the binding is pH-dependent with K_D values of ~340 nM and ~930 nM for the first and second binding events, respectively, at the slightly basic pH of the cell surface (pH 7.4), but undetectable binding at pH 6.0. By combining these biochemical data with crystallographic data on the Fc-binding domain of gE and the gE/gI-Fc complex, we are constructing a model for Fc recognition by gE. The gE/gI-Fc binding model suggests a mechanism for the sharp pH dependence of the complex and allows a comparison of Fc binding with other Fc-binding proteins, such as FcRn.

170. **Intracellular trafficking of herpes simplex virus receptor-antiviral immunoglobulin G bipolar bridging complex**
Alex Farley

Herpes simplex virus (HSV) is a model member of the alphaherpesvirus family, which also includes varicella-zoster virus (ZVZ) and pseudorabies virus (PrV). Alphaherpesviruses are characterized by a relatively short replicative cycle in epithelial tissues and egression to and latent infection of the sensory neurons. HSV encodes two type 1 membrane-bound glycoproteins which together function as a receptor for the Fc portion of IgG. The heterodimer is composed of glycoprotein E (gE) and glycoprotein (gI) and it is found on the surface of virions and infected cells. The Fc receptor function of gE-gI is thought to provide a mechanism for immune evasion by blocking the effector function of host Fc recognition proteins in both the adaptive and innate immune systems. The gE-gI heterodimer is thought to bind to antigen-bound IgG in a process called bipolar bridging in which the antigen-binding fragments (Fabs) bind to an antigen, and gE-gI binds to the Fc. This process could provide a mechanism for HSV-1 to evade antibody-mediated immune responses via Fc receptors. The binding affinity of gE-gI for Fc is pH dependent, whereby gE-gI binds IgG with high affinity at the slightly basic pH of the cell surface (~7.4) and releases IgG at acidic pH (≤6.4). The sharply pH-dependent binding suggests that IgG that is endocytosed by gE-gI dissociates from gE-gI at the low

pH of endosomal compartments, where it could be degraded, while gE-gI is recycled back to the cell surface. Our hypothesis is that Fc binding to gE-gI results in endocytosis of the antibody/antigen complex and its consequent degradation possibly in the lysosome. We have shown that the gE-gI heterodimer can internalize the Fc domain of IgG. Future work will include experiments to address the intracellular trafficking patterns of gE-gI and the fates of gE-gI/IgG and gE-gI/IgG/antigen complexes.

171. **Structural studies of the human cytomegalovirus immunoglobulin G receptors**
Elizabeth R. Sprague, Alex Farley, Evelyn Cheung[1], Harmut Hengel[2]

We have expanded our work on viral Fc receptors to include the recently cloned Fc receptors from HCMV, which is a member of the betaherpesvirus family. HCMV encodes two glycoproteins, gp34 and gp68, that bind the Fc region of IgG; however, unlike gE-gI, the HCMV Fc receptors are composed of a single polypeptide whose sequence is unrelated to either gE or gI. We have expressed the ectodomain of gp68 in baculovirus-infected insect cells and purified milligrams of the protein. Using an analytical gel filtration assay to investigate binding of one of these receptors to Fc, we have shown that the recombinantly-expressed ectodomain of gp68 binds to the Fc portion of human IgG1 with a stoichiometry of two gp68 molecules per one Fc homodimer. Furthermore, we localized the gp68 binding site to the C_H2-C_H3 hinge region of Fc, which is where gE-gI binds, using Fc molecules where residues in this region were mutated in either one or both of the Fc subunits, analogous to our studies of the gE-gI/Fc interaction. In a surface plasmon resonance-based binding assay, the affinity of gp68 for Fc was measured as ~ 300 nM, and preliminary data suggest that unlike gE-gI/Fc, the gp68/Fc complex is unaffected by small changes in pH near neutral, indicating a possible divergent function between betaherpesvirus and alphaherpesvirus Fc receptors. We are undertaking crystallization of gp68 alone and bound to Fc. For gp34, we do not see expression of the gp34 ectodomain in baculovirus-infected insect cells, whereas we do see expression in CHO cells. The gp34 from CHO cell supernatants binds IgG; however, because it appears to be oligomerized, it is not ideal for further characterization at this time.

[1] *Caltech undergraduate student*
[2] *University of Düsseldorf, Germany*

172. **Structural studies of IgA-binding proteins**
Agnes E. Hamburger, Evelyn Cheung*

The human polymeric immunoglobulin receptor, pIgR, is a type I transmembrane protein expressed on the basolateral surface of secretory epithelial cells. pIgR plays a key role in mucosal immunity and, together with bound immunoglobulins (Igs), provides a first line of specific defense against pathogens and their toxins. pIgR binds dimeric IgA (dIgA) and pentameric IgM (pIgM) produced by local plasma cells and transports them to the apical surface of the cell where the complexes are deposited into mucosal secretions. The Fc portion of dIgA interacts non-covalently with the N-terminal domain (D1) of pIgR,

followed by a covalent interaction with D5. To gain insight into the molecular details of the initial interaction, we solved the 1.9 Å resolution crystal structure of D1 of pIgR. The structure reveals a folding topology similar to variable Ig domains with differences in the complementarity determining regions (CDRs). CDR1, the primary determinant in dimeric IgA binding, contains a single helical turn. CDR2, the main determinant in binding to pIgM, is very short and contains a potentially critical glutamic acid involved in pIgM binding. CDR3 points away from the other CDRs, preventing dimerization of D1 analogous to the variable heavy and light chains in antibodies. Surface plasmon resonance studies showed that D1, regardless of its glycosylation state, binds dIgA with an equilibrium dissociation constant of 300 nM in the absence of other pIgR domains, but does not bind to monomeric IgA1-Fcα. To further characterize the interaction between intact pIgR and dIgA, we have initiated structural studies of the other extracellular domains of pIgR, both alone and in complex with the Fc portion of dIgA. Additionally, we have undertaken structural studies of pIgR in complex with the choline-binding protein A, CbpA, a protein found on the surface of *Streptococcus pneumoniae*, a pathogen that uses pIgR as a receptor to invade the human mucosal epithelium. Finally, we are also beginning biochemical and structural studies of other streptococcal proteins that bind to the Fc portion of IgA and interfere with the normal function of the antibody.

Caltech undergraduate student

173. Structural and functional studies of MHC class I homologs in HCMV

Zhiru (Jenny) Yang, Yan Qi

HCMV affects 70-90% of all human populations and can be life threatening to immunocompromised individuals, such as cancer, transplant, and AIDS patients. HCMV achieves its lifelong infection in host cells by adopting multiple mechanisms to evade the immune system, including down-regulation of host class I MHC molecules. HCMV encodes two MHC class I homologs, UL18 and UL142, which may be components of a strategy to avoid immune detection of class I-MHC negative cells. UL18 is heavily glycosylated (13 potential N-linked glycosylation sites) and able to bind host-derived β2-microglobulin (the class I MHC light chain) and endogenous peptides. The host cell receptor for UL18 is LIR-1, which is most abundant in B cells, monocytes, macrophages, and dendritic cells. The UL18/LIR-1 interaction is likely to contribute to the latency and persistence of HCMV as well as the viral evasion of host NK cell surveillance. In addition to UL18, LIR-1 also binds a broad range of host MHC class I molecules, but with an affinity that is over 1000-fold reduced compared to its affinity for UL18[1]. The structures of LIR-1 and a LIR-1/HLA-A2 complex have been solved in our lab[2,3]. We are now working on the co-crystallization and structure determination of UL18 bound to LIR-1. We are also generating deglycosylated mutants of UL18 for our crystallization trials. These studies will be extended to include a newly identified HCMV class I MHC homolog, UL142, which is present in clinical HCMV strains such as

Toledo[4]. UL142 shares about 20% amino acid sequence identity with MHC class I molecules. It could play a role in the virulence of the wild-type HCMV. Immunological, biochemical and structural studies are underway to characterize this protein. Altogether, our work on UL18 and UL142 will expand our basic understanding of the MHC class I homologs and the virus-host interaction.

References
1. Chapman, T.L., Heikema, A.P. and Bjorkman, P.J. (1999) *Immunity* **11:**603-613.
2. Chapman, T.L., Heikema, A.P., West, A.P. Jr. and Bjorkman, P.J. (2000) *Immunity* **13:**727-736.
3. Willcox, B.E., Thomas, L.M. and Bjorkman, P.J. (2003) *Nature Immunol*. In press.
4. Davison, A.J. (2003) *et al.*, *J. Gen. Virol.* **84:**17-28.

174. Structure of a pheromone receptor-associated MHC molecule with an open and empty groove

Rich Olson, Kathryn E. Huey-Tubman, Catherine Dulac[*]

Neurons in the murine vomeronasal organ (VNO) express a family of class Ib major histocompatibility complex (MHC) proteins (M10s) that interact with the V2R class of VNO receptors. This interaction may play a direct role in the detection of pheromonal cues that initiate reproductive and territorial behaviors. The crystal structure of M10.5, an M10 family member, is similar to that of classical MHC molecules. However, the M10.5 counterpart of the MHC peptide-binding groove is open and unoccupied, revealing the first structure of an empty class I MHC molecule. Similar to empty MHC molecules, but unlike peptide-filled MHC proteins and non-peptide–binding MHC homologs, M10.5 is thermally unstable, suggesting that its groove is normally occupied. However, M10.5 does not bind endogenous peptides when expressed in mammalian cells or when offered a mixture of class I–binding peptides. The F pocket side of the M10.5 groove is open, suggesting that ligands larger than 8–10-mer class I–binding peptides could fit by extending out of the groove. Moreover, variable residues point up from the groove helices, rather than toward the groove as in classical MHC structures. These data suggest that M10s are unlikely to provide specific recognition of class I MHC–binding peptides, but are consistent with binding to other ligands, including proteins such as the V2Rs.

[*]*Department of Molecular and Cellular Biology, Howard Hughes Medical Institute, Harvard University, Cambridge, Massachusetts*

175. Improved neutralizing antibodies against HIV

Anthony P. West, Jr., Joshua Klein, Lili Yang, David Baltimore

We have begun an effort to develop an improved set of antibody reagents that neutralize HIV. This is a component of an "Engineering Immunity" project we are undertaking together with David Baltimore's laboratory, which has the overall goal of developing a new approach to treating HIV/AIDS. Although the vast majority of natural anti-HIV antibodies are highly strain-specific, a small number of broadly neutralizing anti-HIV antibodies

have been identified. In the Engineering Immunity approach to treat HIV, which builds upon previous work from the Baltimore laboratory, the immune system does not produce antibodies in response to an injected antigen. Instead, the antibody repertoire in humans is altered to direct production of specified antibodies with desired properties; for example, neutralizing antibodies or designed antibodies or antibody-like proteins engineered to bind more tightly to a pathogen or to recruit immune effector cells. The goal of our part of the Engineering Immunity project is to design, produce, and evaluate a series of optimized antibody or antibody-like anti-HIV proteins for further testing in a mouse model system.

176. Studies in the design and characterization of HIV neutralizing molecules
Joshua S. Klein, Anthony P. West, Jr.

HIV is an enveloped retrovirus that is estimated to currently infect approximately 40 million people worldwide. Life-extending drug regimens are credited for the precipitous drop in HIV-related mortality for developed countries, but their high cost and the requirement for life-long treatment has blocked distribution in underdeveloped countries where 90% of all HIV+ people reside, leaving the development of a prophylactic vaccine a widely accepted goal for stopping the spread of this disease. Unfortunately, researchers have been unable to design an immunogen capable of eliciting resistance to HIV infection because the viral spike positioned on the outer surface of the virus, which is necessary for fusion with target cells, has evolved uncommonly effective properties and mechanisms for evading the natural host antibody immune response. In collaboration with the laboratory of David Baltimore, we seek to develop a therapeutic vaccine capable of clearing an established infection using hematopoetic stem cells transduced with a lentiviral vector encoding pre-characterized anti-HIV molecules. Because this approach does not rely on the ability of the host immune system to develop neutralizing antibodies, it is not limited to the naturally occurring antibody architecture but can employ alternative formats such as bispecific antibodies and comparatively small monovalent molecules with accelerated pharmokinetic properties. Valuable human monoclonal antibodies against the gp120 and gp41 envelope glycoproteins of HIV have been isolated and characterized and are being used as starting points for the development of more effective anti-HIV molecules using techniques such as phage display and computational protein design to enhance their viral recognition properties and expand their abilities to recognize and neutralize different HIV variants. Distinct classes of neutralizing molecules differing in specificity and binding stoichiometry will be used establish design principles for HIV neutralization based on the results of surface plasmon resonance, analytical ultracentrifugation, and *in vitro* neutralization studies.

177. Cloning, expression, affinities, and structure of antibody fragments specific for poly-glutamine
Pingwei Li, Kathryn E. Huey-Tubman, Anthony P. West, Jr.

The pathogenic mechanism in Huntington's and related neurological diseases is proposed to involve a conformational transition in expanded poly-glutamine (poly-Gln) tracts (>36 Gln). Models for poly-Gln toxicity include the formation of aggregates that recruit and sequester essential cellular proteins, or functional alterations, such as improper interactions with other proteins. Based on structural studies of fusion proteins of huntingtin exon 1 (HD1) with normal and extended poly-Gln tracts, and binding studies of these proteins with the Fab fragment of an anti-poly-Gln monoclonal antibody, a linear lattice model was proposed for the solution structure of poly-Gln tracts in HD1 (1). The model suggests that the poly-Gln tracts of HD1 adopt a random coil structure in solution, without a global conformational change when the number of glutamines exceeds the pathological threshold. The model predicts that long stretches of poly-Gln residues, such as those in mutant huntingtin, are accessible for binding with multiple copies of a ligand, and that avidity effects result in stronger binding of a multivalent ligand than a monomeric ligand to a long stretch of poly-Gln. This model provides a structural framework for the development of potential therapeutic reagents specific for mutant huntingtin. To test this model, we cloned the genes of the variable domains of MW1, an anti-poly-Gln antibody produced by the Patterson laboratory (2), determined the 2.1Å crystal structure of the Fv fragment of MW1, generated monovalent and multivalent antibody fragments, and compared their binding affinities for fusion proteins of HD1 that contain 16 to 46 glutamines (HD1-16Q; HD1-46Q). Consistent with predictions of the linear lattice model, we find that multivalent MW1 fragments bind to HD1-46Q with a higher apparent affinity than to HD1-16Q.

References
(1) Bennett, M.J., Huey-Tubman, K.E., Herr, A.B., West, A.P., Jr., Ross, S.A. and Bjorkman, P.J. (2002) *Proc. Natl. Acad. Sci. USA* **99**:11634-11639.
(2) Ko, J., Ou, S. and Patterson, P.H. (2001) *Brain Res. Bull.* **56**:319-329.

178. A hydrophobic patch on transferrin receptor regulates the iron-release properties of receptor-bound transferrin
Anthony M. Giannetti[1], Peter J. Halbrooks[2], Anne B. Mason[2], Todd M. Vogt, Caroline A. Enns[3]

The transferrin receptor (TfR), a dimeric membrane glycoprotein, is responsible for iron uptake in most mammalian cells. TfR binds iron-loaded transferrin (Fe-Tf) and transports it to acidic endosomes where iron is released in a TfR-facilitated process. Consistent with our hypothesis that TfR binding stimulates iron release from Fe-Tf at acidic pH by stabilizing the apo-Tf conformation, a TfR mutant (W641A/F760A-TfR) that binds Fe-Tf, but

not apo-Tf, cannot stimulate iron release from Fe-Tf, and less iron is released from Fe-Tf inside cells expressing W641A/F760A-TfR than cells expressing wtTfR. EPR spectroscopy shows that binding at acidic pH to wtTfR, but not W641A/F760A-TfR, changes the Tf iron-binding site $\geq$30 Å from the TfR W641/F760 patch. Mutation of Tf histidine residues predicted to interact with the W641/F760 patch eliminates TfR-dependent acceleration of iron release. Identification of TfR and Tf residues critical for TfR-facilitated iron release, yet distant from a Tf iron, demonstrates that TfR transmits long-range conformational changes and stabilizes the conformation of apo-Tf to accelerate iron release from Fe-Tf.

[1]Department of Biophysics and Crystallography, Roche Palo Alto, LLC3431 Hillview Ave, R6E-3, Palo Alto, CA 94304

[2]Department of Biochemistry, University of Vermont, College of Medicine, Burlington, VT 05401

[3]Department of Cell and Developmental Biology, Oregon Health Sciences University, Portland, OR 97239-3098

179. A core histidine cluster controls the pH dependent conformational change in transferrin receptor

Joshua S. Klein, Anthony M. Giannetti*

Transferrin receptor (TfR) is a 180 kD dimeric type II transmembrane glycoprotein that transports the primary iron carrier, transferrin, between the endosome and the extracellular environment by clathrin-mediated endocytosis. Previous biochemical evidence suggests that TfR exists in two distinct pH-dependent conformations: one which allows it to maintain high affinity for both iron-loaded transferrin and the haemochromatosis protein, HFE, in the slightly basic extracellular environment and another conformation that only allows it to maintain high affinity for iron-free transferrin in the acidic environment of the endosome. High-resolution crystal structures of the soluble ectodomain of both ligand-free TfR and TfR bound to HFE have been solved previously under basic conditions, but the acidic conformation of TfR with or without its ligands has resisted analysis by high resolution X-ray crystallography. Nevertheless, comparison of the ligand-free and HFE-bound crystal structure under basic conditions demonstrates conformational flexibility in a cluster of four histidines at the core of the dimeric TfR interface, and it has been hypothesized that they may help mediate the pH-dependent conformational change of TfR, which occurs near the pKa of the N-epsilon nitrogen of histidine's imidazole ring. Through analysis by surface plasmon resonance (Biacore) of individual mutations of these histidines to alanine across a range of acidic and basic pH values, we have confirmed a significant decrease in the sensitivity of TfR to changes in pH as measured by changes in its affinity for iron-free transferrin and HFE along with concurrent decreases in the number of protons exchanged, confirming the long range effect of the histidine core, which sits approximately 20 Å away from the ligand binding surfaces.

*Department of Biophysics and Crystallography, Roche Palo Alto, LLC3431 Hillview Ave, R6E-3, Palo Alto, CA 94304

180. Structural studies of TfR/Tf complexes

Fan Yang, Anne B. Mason[1]

Transferrin receptor 1 (TfR) is responsible for the primary iron uptake pathway in most mammalian cells. Cell surface TfR binds to circulating iron-loaded transferrin (Fe-Tf) and transports it to acidic recycling endosomes where the acidic pH causes iron to dissociate from transferrin (Tf) in a TfR-assisted process. The iron-free form of Tf (apo-Tf) remains bound to TfR and is recycled back to the cell surface, where the complex dissociates upon exposure to the slightly basic pH of the blood. Crystallographic studies have revealed the structures of TfR and of several Tf family members. The crystal structure of the soluble ectodomain of TfR has been reported alone (Lawrence et al., 1999) and in complex with HFE (Bennett et al., 2000), the protein mutated in patients with the iron-overload disorder hereditary hemochromatosis. Although mutagenesis studies done previously in our lab reveal some hints of the binding sites (Giannetti et al., 2003), understanding the mechanism of TfR-facilitated iron release from Tf requires structural information about how TfR binds to both Fe-Tf and apo-Tf. However, the only current structure of a TfR/Tf complex is an ~7.5 Å resolution structure of an Fe2-Tf:TfR complex derived by cryoelectron microscopy (Cheng et al., 2004). Using various forms of wild-type and mutant iron-loaded and iron-free Tf, we are setting up crystallization trials of Fe-Tf/TfR and apo-Tf/TfR complexes with the goal of deriving high resolution structures that can be used to compare the binding of Fe-Tf and apo-Tf to TfR.

[1]Department of Biochemistry, University of Vermont, Burlington, VT 05405

References
1. Lawrence, C.M., Ray, S., Babyonyshev, M., Galluser, R., Borhani, D.W. and Harrison, S.C. (1999) *Science* **286**:779-782.
2. Bennett, M.J., Lebrón, J.A. and Bjorkman, P.J. (2000) *Nature* **403**:46-53.
3. Giannetti. A.M., Snow, P.M., Zak, O. and Bjorkman, P.J. (2003) Public Library of Science, Biology **1**:341-350.
4. Cheng, Y., Zak, O., Aisen, P., Harrison, S.C. and Walz, T. (2004) *Cell* **116**:565-576.

181. Structural and biophysical studies of transferrin receptor 2

Mindy I. Davis, Valerie J. Karplus, Caroline A. Enns*

Transferrin receptor 2 (TfR2) is a type II membrane glycoprotein that is expressed predominantly on the surface of hepatocytes. While the exact role of TfR2 in iron homeostasis is unknown, mutations in TfR2 lead to the disease hereditary hemochromatosis, a disease of iron overload. The extracellular domain of human TfR2 has 45% amino acid identity to transferrin receptor 1 (TfR1) whose function as a receptor for iron-loaded transferrin is well understood. Previous surface plasmon resonance (SPR) experiments showed that TfR1 binds both iron-loaded Tf (Fe-Tf) and the hemochromatosis protein (HFE) at the pH of the cell surface (pH = 7.4). The complex is

endocytosed into acidic endosomes, where iron is released from Tf and stored in the cytoplasm in the iron storage protein ferritin. Iron-free Tf or apo-Tf stays bound to TfR1 and recycles back to the cell surface, where it is released at the slightly basic pH of the blood. Like TfR1, TfR2 binds Fe-Tf at pH 7.4, but unlike TfR1, TfR2 does not bind HFE at basic pH. We would like to do SPR experiments to determine whether apo-Tf binds to TfR2. Our primary focus has been on obtaining a form of TfR2 that is amenable to further biophysical studies. TfR2 is unstable unless it is bound to transferrin, complicating our SPR experiments with apo-Tf at acidic pH and our crystallization trials. Our efforts have been directed at co-expression of TfR2 and Fe-Tf. This complex is more stable and can be purified and used for crystallization studies.

*Oregon Health Sciences University

182. Biochemical and structural studies of ferroportin

Adrian E. Rice, Damien Z. Soghoian, Douglas C. Rees

All known organisms, save two bacteria, require iron for survival. Despite its importance, iron in overabundance is toxic. In order to maintain a balance of iron levels, organisms have developed a highly specialized network of molecules designed to monitor and maintain iron homeostasis. When the fidelity of these networks is compromised, diseases such as iron deficiency and iron overload result. Mammals lack any regulated mode of iron excretion and therefore, must have highly regulated mechanisms for controlling the acquisition of iron from the diet. The primary site of iron absorption is the duodenum of the small intestine. This process can be categorized by two phases: 1) iron uptake across the brush border into the cytoplasm of duodenal enterocytes; and 2) iron export across the basolateral membrane of these cells into the blood. Iron from the diet is reduced from Fe^{3+} to Fe^{2+} by the membrane-bound iron reductase Dcytb and is transported across the apical brush border by an integral membrane protein called divalent metal transporter 1 (DMT1; also known as DCT1 and NRAMP2). Iron is then transported across the cell to the basolateral side where it is exported by the basolateral integral membrane iron transporter ferroportin (Fpn; also known as IREG1 and MTP1). Fpn is the only identified iron exporter in vertebrates and is an integral membrane protein containing 9-12 predicted alpha-helical transmembrane segments. Point mutations in Fpn lead to an autosomal dominant iron overload disease called ferroportin disease. Our project aims to characterize Fpn from both a structural and biochemical standpoint. Current plans in our laboratory aim at obtaining purified recombinant Fpn for these studies.

183. Structural studies of prostate-specific membrane antigen

Mindy I. Davis, Melanie J. Bennett, Leonard Thomas

Prostate-specific membrane antigen (PSMA) is highly expressed in prostate cancer cells and non-prostatic solid tumor neovasculature and is a target for anti-cancer imaging and therapeutic agents. PSMA acts as a glutamate carboxypeptidase (GCPII) on small molecule substrates, including folate, the anti-cancer drug methotrexate, and the neuropeptide a-NAAG. We have determined the 3.5 Å crystal structure of the PSMA ectodomain, which reveals a homodimer with structural similarity to transferrin receptor (TfR1), a receptor for iron-loaded transferrin that lacks protease activity. Unlike TfR1, the protease domain of PSMA contains a binuclear zinc site, catalytic residues and a proposed substrate-binding arginine patch. Elucidation of the PSMA structure combined with docking studies and a proposed catalytic mechanism provides insight into the recognition of inhibitors and the natural substrate a-NAAG. The PSMA structure will facilitate development of chemotherapeutics, cancer-imaging agents, and agents for treatment of neurological disorders.

184. Characterization of hemojuvelin and its interaction with neogenin

Anthony P. West, Jr., Anya E. Wyman, An-Sheng Zhang*, Caroline A. Enns*

A number of genes important for regulating iron homeostasis have been identified by studying families with hereditary iron overload diseases. Mutations in two proteins, hemojuvelin (HJV) and hepcidin, have been found to cause juvenile hemochromatosis, a severe form of iron overload. Hepcidin, a small peptide synthesized by the liver, is released into the serum and controls the rate of intestinal iron absorption. HJV is a GPI-linked protein expressed on the surface of muscle and liver cells, and strongly affects hepcidin transcription. To understand the molecular basis of HJV action, we have begun to biophysically characterize HJV. A soluble form of HJV was expressed in baculovirus-infected insect cells. The purified protein appears as three bands on SDS-PAGE, at approximately 46, 30, and 16 kD, indicating partial proteolysis. A similar cleavage has been noted in related repulsive guidance molecules, and we found that the Gly-Asp-|-Pro-His cleavage sequence is identical to that of human MUC2 mucin, a protein noted to undergo autocatalytic proteolysis under acidic conditions. Incubation of purified HJV under acidic conditions appeared to increase the fraction of cleaved protein. To obtain a more homogeneous form of HJV for crystallography, we identified a mutant (D172A) that does not undergo cleavage. Experiments in Caroline Enns' lab at OHSU have demonstrated that HJV co-immunoprecipitates with neogenin, a cell surface molecule involved in axonal guidance. We have expressed a soluble form of neogenin and have begun to characterize its interaction with HJV.

*Department of Cell and Developmental Biology, Oregon Health & Science University

114

Publications

Davis, M.I., Bennett, M.J., Thomas, L.M. and Bjorkman, P.J. (2005) Crystal structure of prostate-specific membrane antigen, a tumor marker and glutamate carboxypeptidase. *Proc. Natl. Acad. Sci. USA* **102**:5981-5986.

Delker, S.L., West, A.P., Jr., McDermott, L., Kennedy, M.W. and Bjorkman, P.J. (2004) Crystallographic studies of ligand binding by Zn-α2-glycoprotein. *J. Struct. Biol.* **148**:205-213.

Giannetti, A.M. and Bjorkman, P.J. (2004) HFE and transferrin directly compete for transferrin receptor in solution and at the cell surface. *J. Biol. Chem.* **279**:25866-25875.

Giannetti, A.M., Halbrooks, P.J., Mason, A.B., Vogt, T.M., Enns, C.A. and Bjorkman, P.J. (2005) The molecular mechanism for receptor-stimulated iron release from the plasma iron transport protein transferrin. *Structure.* In press.

Giannetti, A.M., Snow, P.M., Zak, O. and Bjorkman, P.J. (2003) Mechanism for multiple ligand recognition by the human transferrin receptor. *Public Library of Science (PloS)* **1**:341-350.

Halbrooks, P.J., Giannetti, A.M., Klein, J.S., Bjorkman, P.J., Larouche, J.R., Smith, V.C., MacGillivray, R.T.A., Everse, S.J. and Mason, A.B. (2005) Composition of pH-sensitive triad in C-lobe of human serum transferrin, ovotransferrin and lactoferrin provides insight into functional differences in iron release. Submitted for publication.

Hamburger, A.E., West, A.P., Jr. and Bjorkman, P.J. (2004) Crystal structure of a polymeric immunoglobulin-binding fragment of the human polymeric immunoglobulin receptor. *Structure* **12**:1925-1935.

Hamburger, A.E., West, A.P., Jr., Hamburger Z.A., Hamburger, P. and Bjorkman, P.J. (2005) Crystal structure of a secreted insect ferritin reveals a symmetrical arrangement of heavy and light chains. *J. Mol. Biol.* **349**:558-569.

Herr, A.B., Ballister, E.R. and Bjorkman, P.J. (2003) Insights into IgA-mediated immune responses from the crystal structures of human FcαRI and its complex with IgA1-Fc. *Nature* **423**:614-620.

Herr, A.H., White, C.L., Milburn, C., Wu, C. and Bjorkman, P.J. (2003) Bivalent binding of IgA1 to FcαRI suggests a mechanism for cytokine activation of IgA phagocytosis. *J. Mol. Biol.* **327**:645-657.

Kacskovics, I., Kis, Z., Mayer, B., West, A.P., Jr., Tiangco, N.E., Tilahun, M., Cervenak, L., Bjorkman, P.J., Goldsby, R.A., Szenci, O. and Hammarström, L. (2005) FcRn mediates elongated serum half-life of human IgG in the cattle. Submitted for publication.

Luo, R., Mann, B., Lewis, W.S., Rowe, A., Heath, R. Stewart, M.L., Hamburger, A.E., Sivakolundu, S., Lacy, E.R., Bjorkman, P.J., Tuomanen, E. and Kriwacki, R.W. (2005) Solution structure of choline binding protein A, the major adhesin of *Streptococcus pneumoniae*. *EMBO J* **24**:34-43.

McDermott, L., Freel, J.A., West, A.P., Jr., Bjorkman, P.J. and Kennedy, M.W. (2005) Zn-α2-glycoprotein, an MHC class I-regulated glycoprotein associated with regulation of adipose tissues and cancer cachexia: Modification or abrogation of ligand binding by site-directed mutagenesis. Submitted for publication.

Olson, R., Huey-Tubman, K.E., Dulac, C. and Bjorkman, P.J. (2005) Structure of a pheromone receptor-associated MHC molecule with an open and empty groove. *Public Library of Science (PloS)*: *Biology*. In press.

Sprague, E.R., Martin, W.L. and Bjorkman, P.J. (2004) pH dependence and stoichiometry of binding to the Fc region of IgG by the herpes simplex virus Fc receptor gE-gI. *J. Biol. Chem.* **279**:14184-14193.

Vogt, T.M., Blackwell, A.D., Giannetti, A.M., West, A.P., Jr., Bjorkman, P.J. and Enns, C.A. (2003) Heterotypic interactions between TfR2 and TfR. *Blood* **101**:2008-2014.

West, A.P., Jr., Herr, A.B. and Bjorkman, P.J. (2004) The chicken yolk sac IgY receptor, a functional equivalent of the mammalian MHC-related Fc receptor, is a phospholipase A2 receptor homolog. *Immunity* **20**:601-610.

Willcox, B.E., Thomas, L.E. and Bjorkman, P.J. (2003) Crystal structure of HLA-A2 bound to LIR-1, a host and viral MHC receptor. *Nature Immunol.* **4**:913-919.

Zhang, A.-S., West, A.P., Jr., Wyman, A.E., Bjorkman, P.J. and Enns, C.A. (2005) Interaction of HJV with neogenin results in iron accumulation in HEK293 cells. Submitted for publication.

Professor of Biology, Emeritus: **Charles J. Brokaw**

Summary: Motor enzymes — dyneins, kinesins, and myosins — convert energy from ATP dephosphorylation into most of the movements performed by eukaryotic cells. We think that myosin and kinesin are reasonably well understood, although new experimental results from time to time surprise us. On the other hand, we have very little knowledge or understanding of the functioning of the axonemal dyneins that power the movements of flagella and cilia; these molecular complexes are a major challenge for the future. My current work uses computer simulation methods to explore ideas about motor enzyme function in situations ranging from experimental studies on individual motors to an intact flagellum containing tens of thousands of dyneins. Some of the simulation programs, as Macintosh applications, are available at www.cco.caltech.edu/~brokawc/software.html

185. Circling motions and symmetry breaking in a model for nodal cilia
Charles J. Brokaw

A computer model of flagella in which oscillation results from regulation of active sliding force by sliding velocity can simulate the movements of very short flagella and cilia. This model includes nine outer doublets, arranged on the surface of a cylinder, and calculates the active sliding force between each doublet from a simple mathematical formulation used previously. Of particular interest are the movements of the short nodal cilia of the mammalian embryo, which determine the development of the asymmetry of the internal organs. These cilia must generate a counterclockwise (viewed from base to tip) circling motion. A three-dimensional computer model can generate this circling motion. Without the introduction of a symmetry breaking mechanism, the computer models start randomly in either direction, and maintain either clockwise or counterclockwise circling. Symmetry can be broken by at least two mechanisms: 1) control of active sliding force on one outer doublet by sliding velocity can be influenced by the sliding velocity experienced on an adjacent outer doublet; or 2) a constant twist of the axoneme caused by an off-axis component of dynein force. The circling direction established within the first beat cycle remains stable even if the symmetry-breaking mechanism is removed or reversed. The second mechanism appears reasonable, because rotation of microtubules has been observed in motility assays with inner arm dyneins from *Tetrahymena* or *Chlamydomonas.* However, the simulations indicate that it has too weak an effect to explain the consistent counterclockwise circling of nodal cilia.

Models in which sliding force is generated from stochastic kinetics of each individual dynein behave very erratically when the total number of dyneins is small, as it must be in very short cilia. These models may not be adequate for evaluation of symmetry-breaking mechanisms. However, new observations on nodal cilia indicate that they are not as short as originally reported (2-3 µm). They are now reported to be about 5 µm in length, so that they will have twice as many dynein motors as originally estimated. Our modeling work needs to be repeated with this new information.

186. Mechanochemical coupling in flagella: Interpretation by computer simulations
Charles J. Brokaw

Measurements of the amount of ATP used by sea urchin sperm flagella during movement, at a range of ATP concentrations and viscosities, were made many years ago. These results indicated a fairly tight coupling between movement and ATP usage. If the amount of ATP used is divided by the number of dynein motors in the flagella, a turnover of about two ATP per beat cycle is obtained. During movement, the amplitude of back and forth sliding between adjacent microtubular doublets averages about 100 nm. This indicates that each dynein motor uses one ATP for about 50 nm of movement. However, microtubule motors such as kinesin, cytoplasmic dynein, and sometimes axonemal dynein can move processively, using one ATP every 8 nm. What restrains the ATP usage in a sea urchin sperm flagellum?

Computer simulations with models that include the kinetics of each individual dynein confirm that adjustment of the kinetic parameters of a conventional model for motor enzyme function, based on the original ideas of Andrew Huxley, cannot easily reproduce these results. Dynein activity in a moving flagellum appears to be regulated in ways that are still totally unknown.

Publications

Brokaw, C.J. (2005) Computer simulation of flagellar movement IX. Oscillation and symmetry breaking in a model for short flagella and nodal cilia. *Cell Motil. Cytoskel.* **60**(1):35-47.

Brokaw, C.J. (2005) Symmetry breaking in a model for nodal cilia. *American Institute of Physics Conference Proceedings* **755**:107-116.

116

Professor of Chemistry and Biology: Judith L. Campbell

Member of the Professional Staff: Elizabeth Bertani, Martin Budd, Piotr Polaczek
Postdoctoral Scholars: Hui-Qiang Lou, Taro Masuda Sasa
Graduate Students: Barbara Fortini, Isabelle Lesur, Clara Reis
Laboratory Staff: Santiago Laparra

Summary: A hallmark of cancer cells, in addition to uncontrolled proliferation, is genomic instability, which appears in the form of chromosome loss or gain, gross chromosomal rearrangements, deletions, or amplifications. The mechanisms that suppress such instability are of the utmost interest in understanding the pathogenesis of cancer. Our lab studies the components of the DNA replication apparatus that promote genomic stability, primarily using yeast genetics, biochemistry, and functional genomics.

Several years ago, Rajiv Dua in the laboratory discovered that DNA polymerase ε, one of four essential DNA polymerases in yeast, had not one, but two essential functions. Deletion of the polymerase domain left the cells viable because another polymerase activity could substitute. Conversely, deletion of the remaining, non-catalytic half of the protein was lethal. Shaune Edwards in the laboratory carried out a two-hybrid screen for proteins that interact with the enigmatic C-terminal region of pol ε in order to discover its function. She found that pol ε interacts with Trf5, a protein involved in establishing cohesion of sister chromatids during passage of the replication fork. She has gone on to develop evidence that the essential function of the C terminus of pol ε is to aid in establishing efficient sister chromatid cohesion during S phase. Another postdoctoral fellow in the laboratory, Caroline Li has characterized the Trf5 protein. She has shown that it encodes a previously unknown poly A polymerase and that it stimulates the activity of pol ε dramatically. Future studies are aimed at defining the mechanism by which these two proteins regulate interaction of the replisome with the cohesin complex, the glue that holds the chromosomes together, and how failure of cohesion leads to genomic instability.

At least seven human diseases characterized by cancer predisposition and/or premature aging are correlated with defects in genes encoding DNA helicases. The yeast genome contains 134 open reading frames with helicase motifs, only eight of which have been characterized. Martin Budd in our laboratory identified the first eukaryotic helicase essential for DNA replication, Dna2. He showed by interaction studies that it was a component of the machine that is required for accurate processing of Okazaki fragments during lagging strand DNA replication. Enzymatic studies to elucidate the sequential action of the DNA polymerase, helicase, and nuclease required for this processing form an ongoing mechanistic biochemistry project in the laboratory.

Stimulated by various reports in the literature implicating Dna2 in telomere biogenesis and structure, Wonchae Choe made the interesting observation that the bulk of Dna2 is localized to telomeres and that this localization is dynamic. During G1 and G2 phases of the cell cycle, Dna2 is at telomeres. During S phase Dna2 is present on the replicating chromatin. Current studies are aimed at defining the genes that regulate the localization, including phosphorylation by the yeast ATR ortholog, Mec1. In addition to defects in replication, *dna2* mutants are also very sensitive to agents that induce double strand breaks (DSBs). Osamu Imamura has shown that Dna2 is mobilized from telomeres in response to the induction of double strand breaks. He is carrying out experiments to test the model that Dna2 delocalization from telomeres is part of the signaling system that induces the DNA damage and S phase checkpoints, as has also been suggested for yKU, a protein involved in non-homologous end joining and in stabilizing telomeres.

One model of cellular aging suggests that accumulation of DNA damage leads to replicative senescence. Most endogenous damage occurs during S phase and leads to replication fork stress. At least three human diseases of premature aging or cancer predisposition, Werner, Bloom, and Rothmund-Thompson, are caused by defects in helicases similar to Dna2. Martin Budd and Laura Hoopes found that *dna2* mutants have a significantly reduced life span. Microarray analysis by Isabelle Lesur shows that the *dna2* mutants age by the same pathway as wild-type cells; they just age faster. Interestingly, the human Bloom and Werner genes suppress the replication defect of *dna2* mutants. Yeast transcriptome analysis shows that old *dna2* mutants have a gene expression pattern strikingly similar to cells senescing due to telomerase defects. Future work will take advantage of the yeast system to further delineate the role of BLM and WRN proteins in mammalian cells. The work of Tao Wei in the lab suggests that instability of repetitive DNA, such as the ribosomal locus and telomeric DNA, is a major cause of genomic instability in the aging *dna2* mutants.

187.   Biochemical analysis of human DNA2 protein
    Taro Masuda Sasa

    DNA2 is an essential gene conserved from yeast to human. Budding yeast Dna2p (ScDna2p) is a nuclease/helicase, and required for assisting FEN1 nuclease in processing a subset of Okazaki fragments that have long, single-stranded 5' flaps. Additionally, *DNA2* performs an essential function in the maintenance of telomeres. In *S. cerevisiae*, *dna2* mutants have defects in the maintenance of telomeres and in *de novo* telomere synthesis, and ScDna2p shows dynamic localization to telomeres at G1 and G2 phases. *S. pombe* Dna2p also localizes to telomeres and functions

there, suggesting that telomeric function of Dna2p is conserved. However, little is known about the function of *DNA2* in higher eukaryotes, although previous reports have shown that human and *Xenopus DNA2* genes can complement a budding yeast dna2 mutant, and that *Xenopus* Dna2p is essential for the DNA replication in egg extracts.

To understand the function of *DNA2* in higher eukaryotes, we characterized the biochemical activity of human Dna2p (hDna2p). Recombinant hDna2p was expressed in insect cells and affinity purified. The hDna2p showed nuclease activity against single-stranded 5' flaps and 3' flaps. It also showed single-stranded DNA dependent ATPase activity. Moreover, a nuclease negative mutant of hDna2p partially unwound fork substrate in the presence of ATP, suggesting that it is a DNA helicase. The ATPase activity is considerably lower than that of the ScDna2p, consistent with its weak helicase activity. These results show that both of nuclease and helicase activities of Dna2p are conserved in eukaryotes, suggesting that these activities are part of the essential function of Dna2p. The activity of hDna2p is stimulated by hRPA, but hBLM (gift of Ian Hickson) does not stimulate hDna2p. Western blotting by anti-hDna2p antibody detected endogenous hDna2p in Hela nuclear extracts, indicating that hDna2p localizes to nuclei in Hela cells.

188. Expression of the *fts*Z genes in *Magnetospirillum magnetotacticum*
Kendra Turk[1], Elizabeth Bertani

The product of the *fts*Z gene of *E. coli*, a bacterial analog of tubulin, plays a structural role in bacterial cell division. In most bacteria studied so far, the gene is present in single copy and is located on the chromosome in a cluster of genes having similar function. Four sequences with a tubulin signature can be seen in the draft genome sequence of the magnetotactic organism, *Magnetospirillum magnetotacticum*. One of these is located together with other genes of similar function, as in the case with *E. coli*, but the others are scattered at different sites in the chromosome. The presence of multiple copies of *fts*Z is not necessary simply for magnetotaxis or because of the spirillum shape, since only one copy is seen in the draft sequences of the magnetotactic organism MC-1 or the similarly shaped *Rhodospirillum*. Are all four *fts*Z paralogs expressed in the bacteria?

The predicted molecular weights of the ftsZ proteins are sufficiently different that we can hope to distinguish some of them on Western blots. In addition, a probe for the blots was made possible by a generous gift of *E. coli* anti-ftsZ antibody from Harold Erickson (Duke University). Cultures of three of the ftsZ paralogs of *Magnetospirillum* that had been cloned into *E. coli* were induced to produce ftsZ proteins. Only one produced enough ftsZ protein to test, but it gave a good signal with the *E. coli* antibody. Total proteins, prepared from *Magnetospirillum* and

separated on polyacrylamide gels, also gave a signal with the antibody and will be analyzed further to determine how many of the ftsZ paralogs are expressed.
[1]Division of Geological and Planetary Sciences, Caltech

189. Dna2 helicase/nuclease is a substrate of Mec1
Barbara Fortini

The Dna2 protein is a yeast helicase/nuclease that is involved in Okazaki fragment processing, repair of x-ray and MMS-induced DNA damage, rDNA stability, and the telomere position effect. We have shown previously that Dna2 exhibits an unusual subcellular distribution for a replication protein. The bulk of Dna2 is localized to telomeres in G1, leaves telomeres in S phase to be found at internal chromosomal sites, and returns to telomeres in G2. In addition, upon treatment with DNA damaging agents, Dna2 is released from telomeres. We have now shown that damage-induced release from telomeres depends on the Mec1 checkpoint kinase. Further, we utilized an *in vitro* kinase assay to demonstrate that Dna2 is an efficient substrate of purified Mec1 kinase. Mec1 is member of the PI-3-kinase-related kinase (PIKK) family whose members preferentially phosphorylate SQ or TQ motifs upon DNA damage. To ascertain whether Dna2 is an *in vivo* substrate of Mec1, we have used site-directed mutagenesis to alter the putative Mec1 phosphorylation sites in Dna2 to alanine residues and are analyzing the phenotypes of the resulting mutants. To date, two of these mutants show increased DNA damage sensitivity, suggesting Mec1 phosphorylation may play a role in regulating the *in vivo* activity of Dna2.

190. Interaction between *S. cerevisiae* DNA polymerase epsilon and Trf4/Trf5
Clara C. Reis, Caroline Li, Judith L. Campbell

The essential DNA polymerase epsilon (pol ε) is required for DNA replication, repair, and the S/M checkpoint. The N-terminal catalytic function can be deleted and cells retain viability, suggesting that there is a second essential function encoded in the C terminus (1,2).

We aim to explore further the interaction between the essential but non-catalytic C terminal domain of pol ε with Trf5 shown via a two-hybrid screen (4). Trf5, and its redundant homologue, encoded by TRF4, was originally designated as DNA polymerase sigma (pol σ) and proposed to be involved in replicating sites of cohesion (3). Trf4 is also implicated in RNA stability (5).

Myc-Trf5 can be immunoprecipitated specifically with HA-Pol2 in yeast cells verifying physical interaction. In asynchronous cells, Trf4 is expressed at levels approximately equivalent to the pol ε subunit Dpb2 and in about 4-fold excess over Trf5. We also observe similar fluctuations in the levels of the three proteins throughout the cell cycle, with a peak in S-phase, consistent with a role in DNA replication.

Overexpression of *RNR1* partially suppresses the *ts* phenotypes of *trf5Δpol2-12* and *trf4-tstrf5Δ* and the *cs* phenotype *trf4Δpol2-12*, suggesting that the interaction may be part of the checkpoint-signaling pathway and/or of dNTP level regulation during S phase. The *trf4-tstrf5Δ*, however, is

118

proficient in Rad53 phosphorylation when exposed to MMS at the restrictive temperature.

A *trf4-tstrf5Δ* strain exhibits, at the restrictive temperature, a significant delay in completion of S phase and presents, following release from alpha-factor arrest, an accumulation of cells with a 2C DNA content.

Recombinant yeast Trf4 and Trf5, but not Trf4 or Trf5 mutants with changes in the putative active site, show polyadenylation activity.

References
1. Dua, R. *et al.* (1999) *J. Biol. Chem.* **274**:22283-22288.
2. Kesti, T. *et al.* (1999) *Mol. Cell* **3**:679-685.
3. Wang, Z. *et al.* (2000) *Science* **289**:774-779.
4. Edwards, S. *et al.* (2003) *Mol. Cell. Biol.* **23**:2733-2748.
5. Kadaba, S. *et al.* (2004) *Genes & Dev.* **18**(11):1227-1240.

191. Physical interaction between *Saccharomyces cerevisiae* DNA Pol ε and Mrc1

Huiqiang Lou, Clara Reis, Judith L. Campbell

Pol ε is one of the three essential nuclear DNA polymerases (Pol α,δ,ε) in eukaryotic cells. Previous study has shown that the essential region of Pol ε lies between the two zinc fingers at the extreme Pol2 C terminus. But its function still remains enigmatic. The interaction between Mrc1 and Pol2 was firstly identified in a global two-hybrid screen for all gene products in yeast that interact specifically with the Pol2 C terminus. Because Mrc1 participates in DNA replication as part of the replication fork, the cell cycle checkpoint as a key mediator, and sister chromatid cohesion, this interaction may help to understand the essential function of Pol ε.

In yeast two-hybrid assay, both Mrc1 and the non-phosphorylatable *mrc1AQ* mutant interact with Pol2 C terminus. It suggests that this interaction is independent of phosphorylation. We characterized the interactions functionally using yeast genetic techniques - synthetic lethality and suppression. The *mrc1Δ* and *pol2-11* double mutant strain is lethal, while the *mrc1AQ* and *pol2-11* double mutant stain is viable. The *mrc1AQ* mutant is defective in the checkpoint, but not in DNA replication. Furthermore, the latter double mutant strain shows almost the same sensitivity to growth temperature and drugs (HU, MMS) as a pol2-11 mutant strain. Furthermore, the *mrc1AQ/pol2-11/rad9Δ* triple mutant strain is lethal. These results indicate that the interaction between Mrc1 and Pol2 both as replication proteins is essential for cell viability. In response to DNA replication stress, Mrc1 and Pol2 may probably be involved in the same checkpoint pathway, that is, they are epistatic in the checkpoint pathway, while Rad9 belongs to another parallel pathway.

Strains transformed with the multicopy plasmid containing the mrc1 gene can grow at temperatures higher than those transformed with the empty vector. Overexpression of MRC1 can also suppress HU sensitivity of the *pol2-11* cells. This suggests that overproduction of Mrc1 can help mutant *pol2-11* protein folding, which in turn means that they truly interact physically *in vivo*. Physical interaction between Mrc1 and Pol2 is further confirmed by the coimmunoprecipitation assay. Physiological relevance of this interaction is under investigation.

192. Synthetic lethal and synthetic suppressive interaction with DNA2 mutants

Martin Budd, Judith L. Campbell, Amy Tong*, Charles Boone*

To elucidate the network of that maintains high fidelity genome replication, we have introduced two dna2 mutant alleles into each of 4700 viable yeast deletion mutants and determined the fitness of the double mutants. Dna2 was used because its precise role in replication remains highly controversial, especially it's proposed role in Okazaki fragment processing and the nature of its *in vivo* substrates.

All previously defined interactions as well as approximate 50 new interacting genes are identified. Analysis of previously derived synthetic lethality profiles of each of 45 of the Dna2-interacting genes defines network consisting of 322 genes and 826 interactions whose topology provides clues as to how replication proteins coordinate repair and replication to protect genome integrity. Furthermore, the interacting genes reveal most of the Dna2-requiring pathways in the cell. These and additional studies provide a significant advance in defining the range of *in vivo* substrates for Dna2.

This approach used here arrives at a whole that is more than the the of the parts. Because of the multi-functional nature of virtually all proteins at the replication fork, identification of the interaction of Dna2 with just one gene in a pathway does not define the function of Dna2. This study achieves completeness by identification of a single gene in a pathway with follow up experiments to identify the remaining genes in the pathway.

*Department of Medical Genetics and Microbiology, University of Toronto, ON, Canada

Publications
Budd, M.E., Tong, A.H.Y., Polaczek, P., Peng, X., Boone, C. and Campbell, J.L. (2005) A network of multi-tasking proteins at the DNA replication fork preserves genome stability. *PloS Genet.* Pre-pub on line.

Campbell, J.L. (2004) DNA Polymerase II Bacterial. In: *Encyclopedia of Biological Chemistry*, W.J. Lennarz and M.D. Lane, (Eds), 1st ed. Elsevier, Amsterdam, Boston.

Kao, H.I., Campbell, J.L. and Bambara, R.A. (2004) Dna2p helicase/nuclease is a tracking protein, like FEN1, for flap cleavage during Okazaki fragment maturation. *J. Biol. Chem.* **279**:50840-50849.

Kao, H.I., Veeraraghavan, J., Polaczek, P., Campbell, J.L. and Bambara, R.A. (2004) On the roles of *Saccharomyces cerevisiae* Dna2p and FEN1 in Okazaki fragment processing. *J. Biol. Chem.* **279**:15014-15024.

Assistant Professor of Biology: David C. Chan
Postdoctoral Scholars: Hsiuchen Chen, Takumi Koshiba, Sungmin Park-Lee, Zhiyin Song, Yan Zhang
Graduate Students: Scott Detmer, Erik E. Griffin, Tara Suntoke
Research and Laboratory Staff: Lloyd Lytle, Priscilla Tee

Summary: The primary focus of our lab is to understand the role of mitochondrial dynamics in normal cellular function and human disease. Mitochondria are remarkably dynamic organelles that undergo continual cycles of fusion and fission. The equilibrium of these two opposing processes determines the overall morphology of mitochondria in cells and has important consequences for mitochondrial function.

Our research falls into several broad areas:
(1) What are the cellular and physiological functions of mitochondrial fusion and fission?
(2) What is the molecular mechanism of mitochondrial membrane fusion and fission?
(3) What role do mitochondrial dynamics play in human diseases?

To address these issues, we use a wide range of approaches, including genetics, biochemistry, cell biology, and structural biology.

Cellular and physiological functions of mitochondrial fusion and fission
A typical mammalian cell can have hundreds of mitochondria. However, each mitochondrion is not autonomous, because fusion and fission events mix mitochondrial membranes and contents. As a result, such events have major implications for the function of the mitochondrial population. We are interested in understanding the cellular role of mitochondrial dynamics, and how changes in mitochondrial dynamics can affect the function of vertebrate tissues.

Much of our work focuses on proteins called mitofusins (Mfn1 and Mfn2), which are transmembrane GTPases embedded in the outer membrane of mitochondria. These proteins are essential for fusion of mitochondria. To understand the role of mitochondrial fusion in vertebrates, we have constructed mice deficient in either Mfn1 or Mfn2. We find that mice deficient in either Mfn1 or Mfn2 die in mid-gestation. Mfn2 mutant embryos have a specific and severe disruption of a layer of the placenta called the trophoblast giant cell layer. These findings indicate that mitochondrial fusion is essential for embryonic development. We have also generated conditional alleles of Mfn1 and Mfn2 and are currently using these mouse lines to examine the role of mitochondrial fusion in adult tissues (Hsiuchen Chen). These studies are relevant to our understanding of several human diseases.

Embryonic fibroblasts lacking Mfn1 or Mfn2 display fragmented mitochondria, a phenotype due to a severe reduction in mitochondrial fusion. Cells lacking both Mfn1 and Mfn2 have completely fragmented mitochondria and show no detectable mitochondrial fusion activity. Our analysis indicates that mitochondrial fusion is important not only for maintenance of mitochondrial morphology, but also for cell growth, mitochondrial membrane potential, and respiration (Hsiuchen Chen). We are also using RNA interference to disrupt the function of other proteins involved in mitochondrial fusion and fission.

Molecular mechanism of membrane fusion and fission
The best understood membrane fusion proteins are viral envelope proteins and SNARE complexes. Viral envelope proteins, such as gp41 of HIV, reside on the lipid surface of viruses and mediate fusion between the viral and cellular membranes during virus entry (Tara Suntoke). SNARE complexes mediate a wide range of membrane fusion events between cellular membranes. In both cases, cellular and crystallographic studies have shown that the formation of helical bundles plays a critical role in bringing the merging membrane together. We would like to understand mitochondrial fusion at a similar level of resolution and to determine whether there are common features to these diverse forms of membrane fusion.

Mitofusins are the only conserved mitochondrial outer membrane proteins involved in fusion. Therefore, it is likely that they directly mediate membrane fusion. Consistent with this idea, mitofusins are required on adjacent mitochondria to mediate fusion. In addition, mitofusins form homotypic and heterotypic complexes that are capable of tethering mitochondria (Takumi Koshiba, Scott Detmer, Hsiuchen Chen). We are trying to determine how tethered mitochondria, mediated by mitofusins, proceeds to full fusion. It should be noted that mitochondrial fusion is likely to be more complicated than most other intracellular membrane fusion events, because four lipid bilayers must be coordinately fused. We have also set up a yeast system to study the mechanism of fusion by the mitofusin ortholog, Fzo1 (Erik Griffin).

We have used proteomic approaches in yeast cells to identify novel proteins involved in mitochondrial fission (Erik Griffin). Such approaches have also identified promising candidates for additional players in mitochondrial fusion. The structures of proteins involved in mitochondrial fusion and fission are being solved by X-ray crystallography to gain an understanding of molecular mechanism (Yan Zhang).

Mitochondrial dynamics in human disease

Two inherited human diseases are caused by defects in mitochondrial dynamics. Charcot-Marie-Tooth (CMT) disease is a neurological disorder that affects the peripheral nerves. Patients with CMT experience progressive weakness of the distal limbs and some loss of sensation. A specific type of CMT, termed CMT2A, is caused by mutations in Mfn2 and result from degeneration of axons in peripheral nerves. We are currently analyzing the functional consequences of such disease alleles, and using transgenic and targeted mutagenesis approaches to develop mouse models (Scott Detmer).

The most common inherited form of optic neuropathy (autosomal dominant optic atrophy) is caused by mutations in OPA1. This mitochondrial protein is localized to the intermembrane space and is essential for mitochondrial fusion.

Finally, an understanding of mitochondrial dynamics will be essential for understanding a large collection of diseases termed mitochondrial encephalomyopathies. Many mitochondrial encephalomyopathies result from mutations in mitochondrial DNA (mtDNA). In mtDNA diseases, tissues maintain their mitochondrial function until pathogenic mtDNA levels exceed a critical threshold. Experiments with cell hybrids indicate that mitochondrial fusion, by enabling cooperation between mitochondria, can protect respiration even when >50% of mtDNAs are mutant. To understand the pathogenesis of mtDNA diseases, it is critical to explore how mitochondria can be functionally distinct and yet cooperate as a population within a cell. We anticipate that our studies with mice lacking mitochondrial fusion will help to shed light on this group of often devastating diseases (Hsiuchen Chen).

192. Disruption of fusion results in mitochondrial heterogeneity and dysfunction
Hsiuchen Chen

Mitochondria undergo continual cycles of fusion and fission, and the balance of these opposing processes regulates mitochondrial morphology. Paradoxically, cells invest many resources to maintain tubular mitochondrial morphology, when reducing both fusion and fission simultaneously achieves the same end. This observation suggests a requirement for mitochondrial fusion, beyond maintenance of organelle morphology. Here, we show that cells with targeted null mutations in *Mfn1* or *Mfn2* retained low levels of mitochondrial fusion and escaped major cellular dysfunction. Analysis of these mutant cells showed that both homotypic and heterotypic interactions of Mfns are capable of fusion. In contrast, cells lacking both Mfn1 and Mfn2 completely lacked mitochondrial fusion and showed severe cellular defects, including poor cell growth, widespread heterogeneity of mitochondrial membrane potential, and decreased cellular respiration (in collaboration with Anne Chomyn). Disruption of *OPA1* by RNAi also blocked all mitochondrial fusion and resulted in similar cellular defects. These defects in Mfn-null or OPA1-RNAi mammalian cells were corrected upon restoration of mitochondrial fusion, unlike the irreversible defects found in *fzo* yeast. In contrast, fragmentation of mitochondria, without severe loss of fusion, did not result in such cellular defects. Our results showed that key cellular functions decline as mitochondrial fusion is progressively abrogated.

193. The role of mitochondrial fusion in neurons and skeletal muscle
Hsiuchen Chen

Mitochondrial fusion is developmentally and physiologically significant. In humans, mutations in *Mfn2* give rise to Charcot-Marie-Tooth disease (an inherited peripheral neuropathy), and mutations in *OPA1* lead to dominant optic atrophy (an inherited optic neuropathy). Mice lacking either of the mitofusins die as embryos. To examine effects of fusion deficiencies later in life, we have created conditional knockout mice of *Mfn1* and *Mfn2*. By mating these mice with *cre* excision lines, we have uncovered an important role of Mfn2 in cerebellar function. Analysis of these mice will likely lead to a better understanding of the role of mitochondrial dynamics in neuronal function. In addition, we have found a critical role of Mfn1 and Mfn2 in skeletal muscle function. Such mice may be a good model for understanding mitochondrial myopathies.

194. Cellular analysis of Mfn2 mutations in Charcot-Marie-Tooth Disease 2A (CMT2A)
Scott Detmer, Zhiyin Song

Charcot-Marie-Tooth (CMT) disease is a peripheral neuropathy of motor and sensory neurons affecting roughly 1 in 2,500 individuals. Recently, multiple missense mutations in Mitofusin 2 were discovered to cause subtype 2A, which is characterized by loss of peripheral neurons leading to progressive muscle weakness and sensory loss in the feet and hands. In this disease, the longest neurons in the body are selectively affected. The roles of Mfn2 and mitochondrial dynamics in this process are unknown. Because such long neurons require active processes to mobilize mitochondria from the cell body to the metabolically active nerve terminal, we hypothesize that the Mfn2 mutations disrupt mitochondrial dynamics in the nerve terminal.

We are investigating the pathogenesis of CMT2A by studying the Mfn2 alleles with cell culture, biochemistry, and mouse models. When expressed in fibroblasts, the majority of Mfn2 CMT2A alleles cause dramatic reorganization of the mitochondria in the cell. This suggests that the alleles are dominant, in agreement with their inheritance pattern. In mitochondrial fusion assays, we find that some of the mutant alleles are fusion-incompetent. We anticipate that the mitochondrial reorganization phenotype and loss of function are relevant to disease progression. In addition to this structure-function analysis, we find that some of the Mfn2 mutant alleles are defective in an inter-domain interaction by a co-immunoprecipitation assay. We are correlating the

defect in domain interactions with the cellular phenotypes to gain insight into the mechanism of Mfn2 action.

195. Mouse models of peripheral neuropathy in CMT2A disease
Scott Detmer

We are establishing both transgenic and knock-in mouse models of CMT2A. We have generated multiple transgenic lines of mice expressing mutant Mfn2 under a motor neuron-specific promoter and have confirmed localized transgene expression. Interestingly, one of these lines exhibits a striking phenotype: affected mice are unable to dorsi-flex their hindpaws and subsequently display a gait defect characterized by dragging of the hindlimbs during walking. Over time, this leads to deformities in the hindlimbs. This phenotype is remarkably similar to the symptoms of CMT2A patients. Such patients have distal limb weakness, which is manifested by an inability to dorsi-flex the foot, leading to "foot-drop" during walking. Eventually this leads to foot deformities such as hammertoe caused by muscle imbalance.

In a second approach, we have generated conditional knock-in alleles of two of the Mfn2 mutant alleles. Transmission of the knock-in alleles has been confirmed. Both transgenic and knock-in mice will be characterized at the level of the cell and organism. We will examine motor control, fitness, neuronal histology, and neuronal mitochondrial morphology. We anticipate these to be valuable models for the study of CMT disease progression and for the physiological role of mitochondrial morphology and dynamics. In addition, these model disease models will be excellent systems to explore therapeutic options, particularly using stem cell approaches.

196. Structural basis of mitochondrial tethering by mitofusin complexes
Takumi Koshiba, Scott Detmer, Hsiuchen Chen

Vesicle fusion involves vesicle tethering, docking, and membrane merger. We show that mitofusin, an integral mitochondrial membrane protein, is required on adjacent mitochondria to mediate fusion, indicating that mitofusin complexes act in trans. A heptad repeat region (HR2) mediates mitofusin oligomerization by assembling a dimeric, anti-parallel coiled coil. The transmembrane segments are located at opposite ends of the 95 Å coiled coil, providing a mechanism for organelle tethering. Consistent with this proposal, truncated mitofusin, in an HR2-dependent manner, causes mitochondria to become apposed with a uniform gap. Our results suggest that HR2 functions as a mitochondrial tether prior to fusion.

197. Inter- and intramolecular Fzo1p interactions
Erik Griffin

To understand the mechanism of Fzo1p action, it is necessary to identify its critical domains. Our structure/function analysis has defined several critical regions in Fzo1p required for mitochondrial fusion. Additionally, allelic complementation between null point mutants has allowed us to determine which regions are required on a single molecule, and which can be separated onto distinct molecules. We have recently established a novel mitochondrial fusion assay that will allow us to test for allelic complementation between Fzo1p molecules located on opposing mitochondria.

To understand the inter- and intramolecular interactions between Fzo1p molecules, we are testing the effect of mutations and truncations in co-immunoprecipitation assays. Interestingly, non-overlapping N- and C-terminal fragments of Fzo1p interact with each other and restore mitochondrial fusion. This interaction may define a critical step in Fzo1p function because it is sensitive to several point mutations. These approaches should allow us to define the role each region of Fzo1p plays in mitochondrial fusion and to generate a model for its role in mitochondrial fusion.

198. Identification of a new component of the mitochondrial fission machinery
Erik Griffin

The mitochondrial division machinery regulates mitochondrial dynamics and consists of Fis1p, Mdv1p, and Dnm1p. Mitochondrial division relies on the recruitment of the dynamin-related protein Dnm1p to mitochondria. Dnm1p recruitment depends on the mitochondrial outer membrane protein Fis1p. Mdv1p interacts with Fis1p and Dnm1p, but is thought to act at a late step during fission because Mdv1p is dispensable for Dnm1p localization. These observations have led to two important features of the mitochondrial fission model. First, Fis1p acts to assemble and distribute Dnm1p on mitochondria in an Mdv1p-independent step. Second, Mdv1p acts *downstream* of Dnm1p localization to stimulate membrane scission.

In collaboration with Johannes Graumann in Ray Deshaies' laboratory, we sought to identify new components in the fission pathway. By applying affinity purification and mass spectrometry to Fis1p, we have identified Caf4p as a novel component of the mitochondrial fission machinery. Caf4p interacts with each component of the fission apparatus: with Fis1p and Mdv1p through its N-terminal half and with Dnm1p through its C-terminal WD40 domain. We have demonstrated that *mdv1Δ* yeast contain residual mitochondrial fission due to the redundant activity of Caf4p. Moreover, recruitment of Dnm1p to mitochondria is disrupted in *mdv1Δ caf4Δ* yeast, demonstrating that Mdv1p and Caf4p are molecular adaptors that recruit Dnm1p to mitochondrial fission sites. Based on these data, we have proposed a revised model for mitochondrial fission in which Fis1p recruits Dnm1p to mitochondrial

122

fission complexes through Mdv1p or Caf4p, which act as molecular adaptors.

199. X-ray crystallography of the fusion and fission apparatus of mitochondria
Yan Zhang

During mitochondrial division, the mitochondrial outer membrane protein Fis1 binds to Mdv1 and Caf4, which act as molecular adaptors to recruit the dynamin-related protein Dnm1 to mitochondria. Once recruited to mitochondria, Dnm1 is thought to undergo confromational changes resulting in construction of mitochondrial tubules that leads to fission.

To elucidate the mechanism of Dnm1 recruitment to mitochondria, we are using X-ray crystallography to solve the atomic structure of the Fis1/Mdv1 complex. We have expressed and purified the Fis1/Mdv1 complex and will be begin crystallization trials.

200. The fusion activity of HIV-1 gp41 depends on interhelical interactions
Tara Suntoke

Infection by human immunodeficiency virus type I (HIV-1) requires the fusogenic activity of gp41, the transmembrane subunit of the viral envelope protein. Crystallographic studies have revealed that fusion-active gp41 is a "trimer-of-hairpins," in which three central N-terminal helices form a trimeric-coiled coil surrounded by three antiparallel C-terminal helices. This structure is stabilized primarily by hydrophobic, interhelical interactions, and several critical contacts are made between residues that form a deep cavity in the N-terminal trimer and the C-helix residues that pack into this cavity. In addition, the trimer-of-hairpins structure has an extensive network of hydrogen bonds within a conserved glutamine-rich layer of poorly understood function. Formation of the trimer-of-hairpins structure is thought to directly force the viral and target membranes together, resulting in membrane fusion and viral entry. We test this hypothesis by constructing four series of gp41 mutants with disrupted interactions between the N- and C-helices. Notably, in the three series containing mutations within the cavity, gp41 activity correlates well with the stability of the N-C interhelical interaction. In contrast, a fourth series of mutants involving the glutamine layer residue Gln-653 show fusion defects even though the stability of the hairpin is close to wild type. These results provide evidence that gp41 hairpin stability is critical for mediating fusion and suggest a novel role for the glutamine layer in gp41 function.

Publications

Chen, H. and Chan, D.C. (2005) Emerging functions of mammalian mitochondrial fusion and fission. *Hum. Mol. Genet*. In press.

Chen, H., Chomyn, A. and Chan, D.C. (2005) Disruption of fusion results in mitochondrial heterogeneity and dysfunction. *J. Biol. Chem.* **280**:26185-26192.

Griffin, E.E., Graumann, J. and Chan, D.C. (2005) The WD40 protein Caf4p is a component of the mitochondrial fission machinery and recruits Dnm1p to mitochondria. *J. Cell Biol*. **170**:237-248.

Koshiba, T., Detmer, S.A., Kaiser, J.T., Chen, H., McCaffery, J.M. and Chan, D.C. (2004) Structural basis of mitochondrial tethering by mitofusin complexes. *Science* **305**:858-862.

Schuman, E. and Chan, D.C. (2004) Fueling synapses. *Cell* **119**:738-740.

Suntoke, T.R. and Chan, D.C. (2005) The fusion activity of HIV-1 gp41 depends on interhelical interactions. *J. Biol. Chem.* **280**:19852-19857.

Associate Professor of Biology: Raymond J. Deshaies
Research Specialist I: Rati Verma
Research Fellows: Gabriela Alexandru, Gary Kleiger, Rusty Lipford, Thibault Mayor, Dane Mohl, Matthew Petroski
Visiting Fellow: Agustin Rodriguez
Graduate Students: Gregory Cope, Nazli Ghaboosi, Johannes Graumann, Angie Mah
Research and Laboratory Staff: Robert Oania, Daphne Shimoda, Geoff Smith

Summary: The Deshaies lab works on two basic biological processes: control of cell division, and regulation of cell function by attachment of ubiquitin or ubiquitin-like proteins to target polypeptides. We are particularly interested in how attachment of ubiquitin to proteins enables their degradation, and how this degradation is harnessed to regulate cell division.

Defective control of cell division can result in disease, as when unrestrained cell proliferation leads to cancer. Defects of the ubiquitin system can also lead to cancer, as well as neurodegenerative diseases. An understanding of how the cell division machinery and the ubiquitin system operate will thus provide insight into basic cellular processes essential to the life of eukaryotic cells, and may suggest cures for diseases that affect millions of people.

We are using biochemical, molecular, and genetic approaches in baker's yeast and mammalian cells to investigate cell proliferation and the ubiquitin system. Our long-term goal is to understand how these processes work and how they are controlled. Baker's yeast is an excellent organism for basic cell biological studies because it is easy to work with, and many studies have confirmed that yeast and animal cells use essentially identical proteins to regulate basic cellular processes.

Below, I summarize in more detail the four major areas of investigation in the lab, and provide thumbnail descriptions of all current projects.

SCF ubiquitin ligases: Mechanism, regulation, and physiology

Cellular proteins are marked for degradation by attachment of the polypeptide ubiquitin. Ubiquitin is attached to substrates by a cascade comprising ubiquitin-activating (E1), ubiquitin-conjugating (E2), and ubiquitin ligase (E3) enzymes. Ubiquitination occurs when an E3 enzyme binds to both substrate and E2 ubiquitin conjugating enzyme, bringing them into proximity so that ubiquitin is transferred from the E2 to substrate. Specificity and regulation of ubiquitination are typically imparted by E3s, which are the most diverse components of the system. Once ubiquitin is attached to a substrate, the reaction can either terminate (in which case the ubiquitin serves as a regulatory signal to modulate protein function or localization) or continue, leading to the assembly of a multiubiquitin chain. A chain of four ubiquitins suffices to specify destruction of the substrate by the proteasome.

Mechanism of action of SCF ligases: In 1999, we and others reported that RING domains underlie ubiquitin ligase activity (Seol *et al*., 1999). This discovery revealed the largest class of ubiquitin ligases, with up to 385 members. The progenitor of the RING-based ubiquitin ligases, SCF (which we co-discovered in 1997) (Feldman *et al.,* 1997), defines a subfamily of multisubunit cullin–RING ligases that may number as many as 300-350 members, due to combinatorial mixing of subunits. Thus, there may be as many as 700 distinct RING ligase complexes, which would make it the largest known family of enzymes in human cells (Petroski and Deshaies, 2005). As befits such a large family, the cullin–RING ligases have been implicated in a dazzling array of cellular and organismal processes, ranging from circadian rhythms to sulfur assimilation. However, despite the biological import of these enzymes, the mechanism of how they work remains unknown.

Over the past few years, we have made substantial progress towards understanding how SCF enzymes work. Our key innovation was to develop a reconstituted system in which a physiological substrate (budding yeast Cdk inhibitor Sic1 assembled into cyclin–Cdk complexes) is ubiquitinated by SCF and degraded by the proteasome – work that was carried out by Renny Feldman, Craig Correll, and Rati Verma (Feldman *et al.,* 1997; Verma *et al*., 2001). This remains the only system that enables the ubiquitination *and* degradation of a physiological substrate to be studied with defined components. Matt Petroski then constructed Sic1 substrates bearing single ubiquitin acceptor lysines, and used these substrates to characterize the impact of ubiquitin chain position on substrate recognition and degradation by the proteasome (Petroski and Deshaies, 2003).

We believe that the system that we have developed is the best available for studying biochemical mechanisms of ubiquitination, because our substrate is multiubiquitinated and degraded at rates that approach those that must occur *in vivo*, and the nature of the reaction products is defined due to the substrate having only a single lysine acceptor. We now have a terrific opportunity to exploit our *in vitro* systems to address basic questions that are of great importance to understanding the mechanisms that underlie the operation of the ubiquitin-proteasome system (UPS). For example, how does the RING subunit of SCF activate ubiquitin transfer from ubiquitin-conjugating enzyme Cdc34 to substrate? What is the basis for the linkage specificity of Cdc34? How is processive ubiquitination of Sic1 achieved, and how does it relate to the dynamics of substrate and Cdc34 association

with SCF? How does ubiquitin transfer occur across an ~50 Å gap that is thought to exist between the substrate and E2 enzyme bound to SCF? None of these questions are resolved for any RING E3, and thus illuminating the answers will establish paradigms that inform our understanding of how hundreds of ubiquitin ligases work. The insights that emerge from this effort may also provide clues to the development of drugs that modulate the activity of RING-based ligases.

Regulation of SCF ubiquitin ligases: It was originally thought that SCF ubiquitin ligases are constitutively active, and substrate turnover is regulated by phosphorylation of the substrate. Subsequently, it was shown that the Cul1 subunit of SCF is modified covalently by the ubiquitin-like protein Nedd8, thus raising the possibility that SCF might be regulated post-translationally. In 2001, two students from the lab, Svetlana Lyapina and Greg Cope, reported that a poorly understood protein complex known as COP9 signalosome (CSN) binds SCF in animal cells, and promotes the cleavage of Nedd8 from Cul1 via a tightly-associated Nedd8 isopeptidase activity (Lyapina *et al.,* 2001). This was the first biochemical function ascribed to CSN, and opened the door to the study of SCF regulation by reversible cycles of 'neddylation.' Subsequently, Greg Cope discovered that the Csn5 subunit harbors a motif that we named 'JAMM' (for JAb1/Mpn domain metalloenzyme) (Cope *et al.,* 2002). We predicted that JAMM comprises a novel metalloprotease active site. Later, Xavier Ambroggio, who was a joint student with Doug Rees in the Division of Chemistry, substantiated this prediction by employing X-ray crystallography to show that the conserved residues of the JAMM motif coordinate a zinc ion in an active site-like cleft of the protein AF2198 from *Archaeglobulus fulgidis* (Ambroggio *et al.*, 2004). We continue to investigate the regulation of SCF by CSN. We hope to understand how CSN itself is controlled, and what role CSN plays in sustaining active SCF complexes and sculpting the repertoire of SCF complexes in a cell.

Mechanism of action and regulation of the 26S proteasome

Once substrates are ubiquitinated by E3s, they are degraded by the 26S proteasome. The 26S proteasome is a large protein machine that comprises two major subcomplexes: the 20S 'core' proteasome and the 19S regulatory 'cap.' The 20S core forms a cylindrical structure that houses the protease active sites of the proteasome. Each end of the 20S cylinder is decorated by a 19S cap. The 19S cap can be further subdivided into the 'lid' and the 'base.' The base contains six ATPases that are thought to form a ring that abuts the end of the 20S cylinder. The lid, in turn, sits upon the base. The base is thought to control access of substrates into the 20S proteolytic chamber, whereas the lid confers ubiquitin-dependence. The 26S proteasome degrades proteins that are linked to a chain of at least four ubiquitins. The tetraubiquitin chain mediates binding of the attached substrate to the proteasome, after which it is disengaged from bound partners, unfolded,

deubiquitinated, and translocated into the proteolytic chamber of the proteasome where the denuded substrate is degraded.

A fully reconstituted system to study Sic1 Degradation: Pre-2000, all *in vitro* studies of protein degradation by the UPS relied either on crude systems such as *Xenopus* or reticulocyte extracts, or non-natural substrates. No assay was available to harness the power of yeast molecular genetics to enable dissection of the mechanism-of-action of the proteasome. We thus developed a system wherein ubiquitinated Sic1 generated *in vitro* with recombinant SCF^{Cdc4} is degraded by affinity-purified yeast proteasomes (Verma *et al.,* 2001). Remarkably, purified proteasomes can extract ubiquitinated Sic1 from complexes with S phase cyclin-Cdk, degrade the Sic1 and release active S phase cyclin-Cdk protein kinase. This result emphasized that the proteasome has the intrinsic ability to disassemble protein complexes to selectively degrade ubiquitinated substrates, and set the stage for our subsequent studies on substrate targeting and deubiquitination.

Role of deubiquitination in the degradation of Sic1: In the course of characterizing the degradation of ubiquitinated Sic1, we noticed that when the 20S protease inhibitor epoxomicin was present, ubiquitinated Sic1 was converted to a completely deubiquitinated species (Verma *et al.*, 2002). Fortuitously, at about the same time as this we observed that the CSN – which is related to the lid subcomplex of the proteasome 19S cap – cleaves the ubiquitin-like protein Nedd8 from the Cul1 subunit of SCF. Spurred by this confluence of observations, we demonstrated that the Rpn11 subunit of the proteasome lid contains a putative metalloprotease active site analogous to that of Csn5, and this motif is essential for the deubiquitination of Sic1 *in vitro* and the degradation of multiple UPS substrates *in vivo*.

Multiubiquitin chain receptors target substrate to the proteasome: Although it has long been clear that a multiubiquitin chain targets an appended substrate to the proteasome for degradation, the mechanism of targeting has remained controversial. Genetic studies in yeast have suggested a potential role for multiubiquitin chain-binding proteins, including Rad23, Dsk2, Ddi1, and Rpn10. In contrast, biochemical studies in mammalian systems have emphasized a role for the proteasome ATPase Rpt5 as a multiubiquitin chain receptor, and have suggested that proteins such as Rad23 prevent premature metabolism of substrate-linked ubiquitin chains. We reasoned that our reconstituted system would enable us to address this fundamental question from a functional, mechanistic perspective. We first demonstrated using mutant proteasomes and add-back experiments that Rad23 and Rpn10 play a direct role in targeting ubiquitinated Sic1 to the proteasome for degradation (Verma *et al.*, 2004). We then went on to show that the multiubiquitin chain receptor activities of Rad23 and Rpn10 play a redundant role in sustaining turnover of Sic1 *in vivo*. Surprisingly, individual deletion of these and other receptor proteins led to the accumulation of different UPS substrates, suggesting

that the receptors define a layer of specificity that resides downstream of the E3s and upstream of the proteasome. This hypothesis opens up a host of interesting questions about how specificity is achieved in the targeting step, and what its biological purpose is. We plan to address these key questions over the next several years using a combination of biochemical, molecular genetic, and proteomic approaches.

In a parallel effort, we demonstrated that the substrate-targeting step can be blocked by a small molecule that emerged from a chemical genetic screen conducted in the lab of our collaborator, Dr. Randy King. We demonstrated that this compound, which we named 'ubistatin A', binds to the ubiquitin chain in the same intersubunit cleft that is normally bound by the multiubiquitin chain receptors (Verma *et al*., 2004). We believe that ubistatins will be useful tools for studies on the UPS.

Role of Cdc48 in targeting and degradation of ubiquitinated proteins: Recently, we have become intrigued by a poorly understood protein, Cdc48, that, like the ubiquitin chain receptors, operates downstream of ubiquitin ligases to promote degradation of ubiquitinated proteins by the proteasome. The role of Cdc48 in protein turnover was originally thought to be confined to pulling malfolded secretory proteins through the endoplasmic reticulum membrane so that they can be degraded by the proteasome. However, several lines of evidence hint at a far broader role. Interestingly, there may be as many as six distinct Cdc48 complexes in budding yeast, and unpublished data from my lab points to the existence of ~15 distinct Cdc48 complexes in human cells (see abstract by G. Alexandru). Why all of this complexity? It is difficult to even begin to answer this question, because we know so little about Cdc48's function apart from its role in translocation across the ER membrane. Whatever Cdc48 is doing, it appears to be a fundamental component of the UPS, and thus understanding how it works is important. We plan to attack this problem by first identifying substrates whose degradation depends on particular Cdc48 complexes by employing the mass spec-based proteomics technology discussed below (see abstract by J. Graumann). We will then reconstitute the degradation of these substrates using defined components. The objective will be to develop a reconstituted system in which turnover of the substrate is dependent upon Cdc48. We will then use this system to establish the mechanism-of-action of Cdc48. Armed with this information, we will be in a position to initiate investigations on how ubiquitin receptors and Cdc48 complexes collaborate to enable degradation of ubiquitinated substrates. Given the diversity of receptors that guide ubiquitinated proteins to the proteasome and the diversity of Cdc48 complexes that appear to act in concert with these receptors, there is clearly much about the targeting and degradation of ubiquitinated proteins that we do not understand, and thus this topic may be fertile ground for making unexpected discoveries.

Proteomics
The Yates laboratory at Scripps has developed a method dubbed, "multidimensional protein identification technology" (MudPIT). In this method, a complex mixture of proteins is digested with protease and the resulting peptides are fractionated by two-dimensional chromatography on a column that is in-line with the electrospray interface of a mass spectrometer. Johannes Graumann and Thibault Mayor have been applying MudPIT to the study of ubiquitination in yeast. As an example of this approach, we have used subtractive comparisons of samples from wild-type and mutant cells to identify the ubiquitinated polypeptides that accumulate when the Rpn10 multiubiquitin chain receptor is absent (see abstract by T. Mayor). During the next few years, we plan to more fully integrate multidimensional mass spectrometry into ongoing projects in the lab. I believe that this technology will allow us to ask questions that we have never been able to ask before, and will also provide us with a new perspective. Our initial focus will be to marry our approach with quantification methods to systematically identify proteins that are targets of the various multiubiquitin chain receptors encoded in the yeast genome. By identifying the set of substrates whose abundance is altered when a particular ubiquitin pathway component is mutated or blocked by the action of a drug, we can gain insight into enzyme-substrate relationships, which in turn may yield insights into the mechanisms that underlie specificity. Moreover, knowledge of the substrates affected can provide clues to the phenotypes that may occur upon inactivation of a particular component. Finally, the ability to quantify substrate accumulation may enable us to see subtle defects, such as those that occur when one member of a redundant pair of enzymes is mutated.

Functions of the RENT complex in cell cycle control and nucleolar biogenesis
Several years ago, a graduate student, Wenying Shou, discovered the RENT complex, and proposed that the mitotic exit network (MEN) specifies the exit from mitosis in budding yeast by promoting disassembly of RENT (Shou *et al*., 1999). RENT is comprised of the nucleolar anchor protein Net1, the cell cycle regulatory protein phosphatase Cdc14 and the chromatin silencing protein Sir2. Cdc14 is required for the exit from mitosis, which it promotes by dephosphorylating (and thereby activating) proteins that mediate the inactivation of cyclin/CDK activity at the end of mitosis. Throughout the cell cycle, Cdc14 is confined to the nucleolus through its interaction with Net1. At the end of mitosis, the successful completion of anaphase activates the MEN signaling pathway, which disengages Cdc14 from Net1. The emancipated Cdc14 goes on to inactivate cyclin/CDK and thereby trigger the exit from mitosis. This hypothesis for how the exit from mitosis is controlled in budding yeast was dubbed 'RENT control' by Shou, *et al*. Over the past few years, it has become apparent that RENT is disassembled by a two-step mechanism. In early

126

anaphase, Cdc14 is released from Net1 through the actions of the Cdc14 early anaphase release (FEAR) network, whereas in late anaphase the MEN serves to sustain Cdc14 release such that its substrates are dephosphorylated and the cell exits mitosis. Over the past year, a graduate student, Ramzi Azzam, reported that phosphorylation of Net1 by cyclin B-Cdk complexes is a key step that underlies the release of Cdc14 from the nucleolus during early anaphase (Azzam *et al*., 2004). Our current goal is to understand how the terminal signaling component of the MEN, the protein kinase Dbf2, mobilizes the sustained release of Cdc14 from the nucleolus, thereby triggering exit from mitosis.

The following Deshaies Lab publications were cited in the preceding overview:

Ambroggio, X.I., Rees, D.C. and Deshaies, R.J. (2004) JAMM: A metalloprotease-like zinc site in the proteasome and signalosome. *PLoS Biol.* **2**(1):E2.

Azzam, R., Chen, S.L., Shou, W., Mah, A.S., Alexandru, G., Nasmyth, K., Annan, R.S., Carr, S.A. and Deshaies, R.J. (2004) Phosphorylation by cyclin B-Cdk underlies release of mitotic exit activator Cdc14 from the nucleolus. *Science* **305**(5683):516-519.

Cope, G.A., Suh, G.S., Aravind, L., Schwarz, S.E., Zipursky, S.L., Koonin E.V. and Deshaies, R.J. (2002) Role of predicted metalloprotease motif of Jab1/Csn5 in cleavage of Nedd8 from Cul1. *Science* **298**(5593):608-611.

Feldman, R., Correll, C., Kaplan K. and Deshaies, R.J. (1997) A complex of Cdc4p, Skp1p, and Cdc53p/cullin catalyzes ubiquitination of the phosphorylated CDK inhibitor Sic1p. *Cell* **91**:221-230.

Lyapina, S., Cope, G., Shevchenko, A., Serino, G., Tsuge, T., Zhou, C., Wolf, D.A., Wei, N. and Deshaies, R.J. (2001) Promotion of NEDD-CUL1 conjugate cleavage by COP9 signalosome. *Science* **292**(5520):1382-1385.

Petroski, M. and Deshaies, R.J. (2005) Mechanism and regulation of cullin-RING ubiquitin ligases. *Nat. Rev. Mol. Cell Biol.* **6**:9-20.

Petroski, M.D. and Deshaies, R.J. (2003) Context of multiubiquitin chain attachment influences the rate of Sic1 degradation. *Mol. Cell* **11**(6):1435-1444.

Seol, J., Feldman, R., Zachariae, W., Shevchenko, A., Correll, C., Lyapina, S., Chi, Y., Galova, M., Claypool, J., Sandmeyer, S., Shevchenko, A., Nasmyth, K. and Deshaies, R.J. (1999) Cdc53/cullin and the essential Hrt1 RING-H2 subunit of SCF define a ubiquitin ligase module that activates the E2 enzyme Cdc34. *Genes Dev.* **13**:1614-1626.

Shou, W., Seol, J.-H., Shevchenko, A., Baskerville, C., Moazed, D., Shevchenko, A., Charbonneau, H. and Deshaies, R.J. (1999) The exit from mitosis is triggered by Tem1-dependent release of Cdc14 protein phosphatase from nucleolar RENT complex. *Cell* **97**:233-244.

Verma, R., Aravind, L., Oania, R., McDonald, W.H., Yates, J.R., Koonin, E.V. and Deshaies, R.J. (2002) Role of Rpn11 metalloprotease in deubiquitination and degradation by the 26S proteasome. *Science* **298**(5593):611-615.

Verma, R., McDonald, H., Yates 3rd, J.R. and Deshaies, R.J. (2001) Selective degradation of ubiquitinated Sic1 by purified 26S proteasome yields active S phase cyclin-Cdk. *Mol. Cell* **8**(2):439-448.

Verma, R., Oania, R., Graumann, J. and Deshaies, R.J. (2004) Multiubiquitin chain receptors define a layer of substrate selectivity in the ubiquitin-proteasome system. *Cell* **118**(1):99-110.

Verma, R., Peters, N., D'Onofrio, M., Tochtrop, G., Sakamoto, K., Varadan, R., Zhang, M., Coffino, P., Fushman, D., Deshaies, R.J. and King, R. (2004) Ubistatins inhibit proteasome-dependent degradation by binding the ubiquitin chain. *Science* **306:**117-120.

201. p97 regulation via interaction with a variety of p47-related co-factors

Gabriela M. Alexandru

The 97 kDa valosin-containing protein (p97 or VCP) is a type II AAA (ATPase associated with a variety of activities) ATPase, highly conserved from archaebacteria to mammals. p97 plays a role in seemingly unrelated cellular activities, such as membrane fusion, endoplasmic reticulum-associated degradation (ERAD) and cell cycle regulation. All of these functions involve recognition of ubiquitinated protein-substrates and, at least in some cases, their subsequent degradation by the proteasome. In its active form, p97 forms homohexameric barrel structures in which the N-termini are free to bind specific co-factors. Thus, p97 in complex with p47 is thought to regulate membrane fusion, while p97/Npl4/Ufd1 complexes are mainly required for ERAD. In an attempt to further understand the molecular basis of p97's diverse functions we have analyzed p97 immunoprecipitates from human tissue culture cells by MuDPIT mass spectrometry, searching for new p97 co-factors. This analysis revealed a whole group of previously unidentified p97 binding partners, all sharing a domain structure similar at least in part to p47. Two of them have been linked to the human diseases, atopic dermatitis and alveolar soft part sarcoma. However, the biological function for most of these proteins is largely unknown. Comparative MuDPIT analysis of immunoprecipitates from human cells overexpressing each of the newly identified co-factors will give us further insight into the specific p97 function they might regulate.

202. Nedd8 protein modification, the COP9 signalosome and SCF
Gregory Cope

The COP9 signalosome (CSN) is a multi-subunit complex conserved from human to fission yeast *S. pombe*. This complex has been attributed to play a role in multiple processes, including photomorphogenesis in plants and cell cycle control in *S. pombe*. We have recently identified the CSN to be associated with multiple cullin proteins (termed Cul1-5) in mammalian and yeast cells (Lyapina *et al.* [2001] *Science* **292**:1382-1385). Cullins are members of a class of E3 ubiquitin ligases that target specific substrates for ubiquitin dependent proteolysis. One mode of regulation of Cullins is through the covalent modification with the ubiquitin-like protein Nedd8. This modification increases Cul1 ubiquitin ligase activity toward substrates *in vitro* and is essential in the fission yeast *S. pombe*. Interestingly, we have found that CSN can promote the cleavage of the ubiquitin-like molecule Nedd8 from *S. pombe* Cul1 *in vitro* and *in vivo*. Moreover, this activity requires a putative metallo-enzyme motif in Jab1/Csn5, which we term JAMM (Jab1 associated metallo motif). Through genetic and biochemical analysis, we have found that JAMM is essential for Cul1 deneddylation and acts positively on Cul1 activity *in vivo* [(Cope *et al.* [2002] *Science* **298**:608-611)].

In an effort to more thoroughly understand the role of deneddylation of Cullins in mammalian cells, we have utilized siRNA techniques to deplete Csn5 from cultured human cells. We have established a human cell line from which we can inducibly deplete Csn5. Marked changes in SCF activity and composition are found within these cells, suggesting an essential role for deneddylation in maintaining SCF integrity *in vivo*. We are currently attempting to characterize the mechanisms by which both neddylation and denddylation exert their influence on SCF *in vivo* and *in vitro*.

203. Role of ubiquitination in targeting protein substrates to the 26S proteasome
Nazli Ghaboosi

The ubiquitin-dependent degradation pathway begins with the activation of ubiquitin by the E1 ubiquitin-activating enzyme. The ubiquitin moiety is transferred to one of several E2 ubiquitin-conjugating enzymes and is subsequently attached to the substrate with the aid of an E3 ubiquitin ligase. The multi-ubiquitinated substrate is then targeted for destruction by the 26S proteasome through a poorly understood mechanism. While the list of known E2s, E3s, and substrates is steadily growing, there is only one E1 gene in all somatic eukaryotic cell types. At the apex of this intricate network, E1 offers a unique perspective from which to address the many unanswered questions regarding the physiological roles of ubiquitin conjugation.

We created a temperature-sensitive mutant of the essential yeast E1 gene, UBA1, using random PCR mutagenesis. The resulting mutant strain, uba1-204, allows us to conditionally disrupt the entire downstream ubiquitination pathway. At the restrictive temperature, mutant cells exhibit rapid loss of all detectable ubiquitin-protein conjugates as well as stabilization of diverse ubiquitin pathway substrates. These cells also have the hallmarks of other ubiquitin pathway mutants, such as cell cycle arrest and sensitivity to cellular stress.

Using this novel yeast mutant, we are examining the effect that ubiquitin activation has on substrate recognition and interaction of substrate receptors with the proteasome. Recent work in the lab showed that multiubiquitin chain binding proteins (MCBPs) such as Rad23, Dsk2, and Rpn10 function as receptors to selectively recruit substrates to the proteasome (Verma *et al.*, 2004a). While the ubiquitin activation and conjugation defects in uba1-204 do not affect proteasome assembly or activity, we have shown that they do influence how the proteasome interacts with some MCBPs and substrates. Using traditional biochemical methods in addition to quantitative mass spectrometry of affinity-purified proteasomes, we are investigating the role ubiquitination plays in protein substrate targeting to the 26S proteasome for degradation.

204. Using MudPIT to characterize components of the proteasome pathway in yeast
Johannes Graumann

Multidimensional protein identification technology (MudPIT) is a method developed by the laboratory of John Yates at Scripps to analyze complex protein mixtures. In MudPIT, a sample is digested with protease and the resulting peptides are separated on a multidimensional capillary column that is in-line with the electorspray interface of an ion trap mass spectrometer [(Link *et al.* [1999] *Nat. Biotechnol.* **17**:676-682)]. We recently demonstrated that this technology is sufficiently mature to be imported into a cell biology lab and applied to the proteomic characterization of multiple components of a cellular reaction pathway, i.e., pathway proteomics [(Graumann *et al.*, 2004)].

Recent work in the lab [(Verma *et al.*, 2004a)] has revealed a novel layer of substrate specificity in the ubiquitin-proteasome system. Ubiquitinated proteins bind specific receptor proteins, which help guide the substrate to the proteosome for proteolysis. By performing MudPIT analysis of immunoprecipitated proteasomes from wild type cells and mutants lacking specific substrate receptor proteins, we hope to shed light on the mechanism by which different substrates are sorted to different receptors.

205. Determining the function of the six ATPases in the 19S subunit of the proteosome
Gary Kleiger

Ubiquitin-dependent proteolysis of proteins by the proteosome is highly regulated. The 19S particle, a large protein complex containing at least 20 distinct protein subunits, regulates degradation of ubiquitinated proteins in yeast. The 19S contains six ATPases that are all essential for viability in yeast. After more than a decade since their discovery, the relevance of the ATPase

activity of each of these proteins towards proteosome function is largely undetermined. The goal of this research project is to find a molecule that binds to the ATP binding pocket of these proteins and acts as an inhibitor of ATPase activity. This will be achieved by using ATP analogues that have been modified with various alkyl groups. Only those ATP binding proteins that have been mutated to enlarge the ATP binding pockets will accept the ATP analogues. All other ATP binding proteins in the cell should be unaffected, as the ATP analogue would be too big to be accommodated in the ATP binding site. This will allow the targeting of a specific ATPase in the 19S for inhibition in both *in vivo* and *in vitro* proteosome degradation assays. Identification of an ATP analogue and corresponding ATP binding site mutation that accepts the analogue may be useful to other researchers for studying the function of the more than 100 ATPases in yeast cells.

206.   The roles of ubiquitin-mediated proteolysis in transcription

Rusty Lipford

The ubiquitin-proteasome system (UPS) plays numerous diverse roles in the regulation of transcription. We are studying the impact of the UPS on the function of yeast transcriptional activators, like Gcn4 and Gal4, which are targeted for ubiquitination and degradation. Previous studies of Gcn4 established that this activator of amino acid biosynthesis genes is a target for SCF-mediated ubiquitination and proteolysis. In addition these studies illuminated a role in Gcn4 ubiquitination for the cyclin-dependent kinase, Srb10, a component of the Mediator complex of the RNA polymerase II holoenzyme. These findings suggest that the transcription machinery and, therefore, the transcription process are coupled to turnover of the activator. To characterize further this coupling we have determined that Srb10-dependent phosphorylation and subsequent ubiquitination and proteolysis of Gcn4 require promoter association and transcriptional activation function. In addition multiple transcription initiation mutants disrupt phosphorylation and turnover of Gcn4.

On the other side of the coupling between transcription and turnover, we have now demonstrated that inhibition of the UPS at any step (e.g., ubiquitin expression, E2 function, E3 function, or proteasome function) reduces the transcriptional activity of Gcn4 and Gal4. In fact compromised UPS function appears to prevent the association of RNA polymerase II with target genes despite the accumulation of excess activator at their promoters. In addition the transcriptional activity of stable versions of Gcn4 that lack CDK phosphorylation is largely insensitive to UPS impairment. These findings suggest that CDK-phosphorylation of Gcn4 creates a requirement for subsequent turnover to promote normal levels of transcriptional activation. We call this mode of activator regulation, where turnover is required to fully stimulate a reaction, "activation by destruction." Such a mode appears to be a common regulatory motif involved in numerous normal and disease-related cellular processes. We are now attempting to further characterize "activation by

destruction" through the reconstitution, *in vitro*, of UPS-stimulated Gcn4-dependent transcription.

207.   Control of mitotic exit in *S. cerevisiae*

Angie Mah, Ramzi Azzam

Exit from mitosis is triggered by the loss of cyclin-dependent kinase (Cdk) activity by degradation of mitotic cyclins and accumulation of Cdk inhibitors. Cdc14 plays a critical role as it dephosphorylates, and thereby activates, the inhibitors of mitotic Cdk. Cdc14 is held in an inactive state in the nucleolus by Net1. Its release is modulated by two groups of proteins, the FEAR (Cdc **F**ourteen **E**arly **A**naphase **R**elease) network and **M**itotic **E**xit **N**etwork (MEN). The FEAR network consists of Cdc5, Spo12, Esp1 and Slk19, which control release of Cdc14 from the nucleolus during early anaphase. This release is transient, and though not essential for mitotic exit, is required for timely exit. Recent data from our group has shown that Net1 phosphorylation by Clb/Cdk is required for FEAR [(Azzam *et al.*, 2004)]. We are currently investigating how the FEAR network regulator Fob1 contributes to Net1 phosphorylation by CDK.

Unlike the FEAR network, the MEN is essential for mitotic exit. This regulatory group consists of Tem1, Lte1, Cdc15, Dbf2/20, Mob1 and Cdc5. MEN is required for the sustained release of Cdc14 during late anaphase. We previously demonstrated that Cdc15 directly phosphorylates and thereby activates Dbf2, another protein kinase, but only when Dbf2 is bound to Mob1 [(Mah *et al.* [2001] *Proc. Natl. Acad. Sci.* **13**:7325-7330)].

The substrate for the Dbf2-Mob1 kinase complex remains elusive. In collaboration with Michael Yaffe's group, we have determined the optimal phosphorylation motif for Dbf2. By defining a consensus phosphorylation sequence, we hope to identify a Dbf2 substrate(s) that ultimately links the MEN pathway to its effector, Cdc14. To narrow the list of candidate substrates that contains this sequence, we have collaborated with Michael Snyder's group. Their lab has produced protein chips imprinted with the yeast proteome. By using these chips, proteins that are phosphorylated by the Dbf2-Mob1 kinase complex were detected. Combining these results with mass spectrometry data of Cdc14-interacting proteins, we hope to determine the downstream target(s) of the Dbf2-Mob1 kinase complex that mediates the effects of Dbf2 on the Cdc14-Net1 protein complex.

208. Profiling the ubiquitin proteome by quantitative mass spectrometry

Thibault Mayor

In the human genome there is an estimated 400-600 genes that encode ubiquitin ligases (enzymes that catalyze the conjugation of ubiquitin or ubiquitin chain to a substrate, also named E3-liagases) and 50-80 genes that encode de-ubiquitylating enzymes (responsible for the reverse reaction). This puts ubiquitylation on par with phosphorylation as the most common reversible posttranslational modifications in eukaryotic cells.

A key challenge is to identify the proteins that are the substrates for this large collection of enzymes. To begin to address this daunting challenge, we have established a new approach to analyze proteins that are ubiquitylated by quantitative mass spectrometry. Proteins conjugated to ubiquitin in yeast cells are enriched using a two-step affinity-based biochemical purification. The mixture of purified proteins is digested by trypsin and then analyzed by a multi-dimensional liquid chromatography-tandem mass spectrometry system (LC/LC-MS/MS) that is capable of identifying 150 to 200 proteins in one experiment [(Mayor *et al.*, 2005)]. Quantification is achieved after labeling each of the two separated cell populations with a stable isotope (^{14}N or ^{15}N). The mass spec is capable of distinguishing identical peptides that differ only by the added mass from the ^{15}N labeling and then compare their relative abundance. For instance, we have compared cells treated with a proteasome inhibitory drug with untreated cells to determine which proteins are targeted to the proteasome. Ubiquitylated proteins accumulate in cells treated with the drug because the proteasome is rendered inactive. This increase can be determined by measuring the ^{14}N/^{15}N ratio of the purified proteins. Most recently, we have shown that this method can be adapted to identify substrates/targets for different ubiquitin pathways. This can be achieved by comparing, for instance, wild-type cells with cells that lack a particular E3-ligase or de-ubiquitylating enzyme and identifying which ubiquitylated proteins are affected.

209. Regulation of *Saccharomyces cerevisiae* Cdc14

Dane Mohl

Faithful inheritance of the genome requires tight control over chromosome segregation and cytokinesis. In budding yeast, two regulatory networks coordinate the activation of protein phosphatase Cdc14 with progression through anaphase in order to ensure accurate partitioning of the chromosomes.

Cdc14 is bound to Net1 and sequestered to the nucleolus in an inactive state during the majority of the cell cycle. In early anaphase, Cdc14 is briefly released from Net1 through the activity of the FEAR (Cdc fourteen early anaphase release) network. This transient release is believed to play a role in stabilizing the elongating microtubule spindle and recruiting to the nucleolus factors that are necessary for rDNA segregation. During late anaphase, the mitotic exit network (MEN) coordinates sustained release of Cdc14 with the completion of DNA

segregation by monitoring the movement of a single spindle pole body into the daughter compartment of the predivisional cell. Sustained release of Cdc14 ultimately triggers the destruction of B type cyclins (Clb) and accumulation of Sic1, a Clb/Cdk inhibitor. These two events conspire to eliminate mitotic cyclin-Cdk activity, leading to exit from mitosis.

The focus of my work is to understand how the MEN brings about release of Cdc14 from the nucleolus. Our results suggest that both the FEAR network and MEN oppose the sequestration of Cdc14 by activating cell cycle kinases that phosphorylate members of the RENT complex and disrupt binding of Cdc14 to Net1.

210. Mechanisms of multiubiquitin chain synthesis by Cdc34

Matthew D. Petroski

A lysine 48-linked ubiquitin chain is fundamental to recognition of ubiquitinated proteins by the proteasome. However, the mechanisms underlying polymerization of this targeting signal on a substrate are unknown. Our efforts to molecularly dissect and understand this process have focused on the ubiquitination of the cyclin-dependent kinase inhibitor Sic1 by the evolutionarily conserved cullin-RING ubiquitin ligase SCFCdc4 and its ubiquitin-conjugating enzyme Cdc34. We have determined that Sic1 ubiquitination can be molecularly separated into two distinct steps: attachment of the first ubiquitin, which is rate-limiting, followed by rapid ubiquitin chain elongation. Mutation of an acidic loop conserved among Cdc34 and Ubc7 orthologs has no effect on attachment of the first ubiquitin onto Sic1, but alters the processivity and linkage specificity of ubiquitin chain synthesis. We propose that the acidic loop favorably positions lysine 48 of substrate-linked ubiquitin to attack SCF-bound Cdc34~ubiquitin thioester, and thereby enables processive synthesis of K48-linked ubiquitin chains by SCF^Cdc34.

211. Targeting cancer-promoting proteins for ubiquitination and degradation

Agustin Rodriguez

We developed a new approach to cancer therapy that exploits the unique characteristics of the ubiquitin-dependent proteolytic system of eukaryotic cells. The goal of our project has been to identify a cell-permeable molecule that binds to the substrate-docking site of a ubiquitin ligase. By covalently linking this molecule to compounds that bind the target, we developed a novel class of drugs, ProTacs (Proteolysis Targeting Chimeric Pharmaceuticals) that trigger the destruction of proteins in cells for which there exists a small, cell-permeable ligand. As "proof of principle," we designed a ProTac that contains a peptide that binds with high affinity to the substrate-docking domain of the ubiquitin ligase SCF^β-TRCP. We then chemically linked the peptide to the fungal metabolite ovalicin, which binds covalently and specifically to the cellular enzyme methionine aminopeptidase-2 (MetAP-2). We demonstrated that the resulting peptide-ovalicin ProTac chimera tethers MetAP-2

130

to SCF$^{\beta\text{-TRCP}}$, and targets MetAP-2 for ubiquitination and degradation [(Sakamoto *et al*. [2001] *Proc. Natl. Acad. Sci. USA* **98**:8554-8559)]. To determine whether ProTacs could recruit different substrates to the SCF$^{\beta\text{-TRCP}}$ ubiquitin ligase for ubiquitination through non-covalent interactions, we generated ProTacs containing the Iκ Bα phosphopeptide linked to estradiol and testosterone. Both the estrogen receptor (ER) and androgen receptor (AR) have been shown to enhance growth of breast and prostate cancer, respectively. We demonstrated that ProTacs can also promote the ubiquitination and degradation of ER and AR *in vitro* and *in vivo* (Sakamoto *et al*. [2003] *Mol. Cell. Proteomics* **2**:1350-1358). Making a cell-permeable ProTac is been the next step in this project to induce the specific degradation of a target in whole living cells. This new ProTaC contains the HIF-1 peptide linked to testosterone that targets the AR to the VHL ubiquitin ligase. HIF-1 peptide, as a degron, is not dependent on phosphorylation to bind VHL and is therefore cell permeable. Treatment of cells with the HIF-1-DHT ProTac resulted in AR degradation by the proteasome [(Schneekloth *et al*. 2004)]. We are now focusing on developing ProTacs into an effective drug for the treatment of cancer.

212. Determining the requirements for proteolysis by purified 26S proteasomes

Rati Verma, Robert Oania

Labile substrates of the 26S proteasome are earmarked for proteolysis by the covalent attachment of a multiubiquitin chain on acceptor lysines. Ubiquitinated proteins are then recruited to the 26S proteasome, where they are destroyed. We have recently shown that the multiubiquitin chain binding proteins (MCBPs) Rad23 and Rpn10 function as receptors to recruit substrates to the proteasome [(Verma *et al*., 2004a)]. Under physiological conditions, the receptors display selectivity in substrate targeting, even though all substrates presumably contain the same universal targeting signal-a tetraubiquitin chain. We are currently investigating the molecular basis of this selectivity. In addition, we are also investigating novel putative receptor pathways, namely those involving Cdc48.

Publications

Ambroggio, X.I., Rees, D.C. Deshaies, R.J. (2004) JAMM: A metalloprotease-like zinc site in the proteasome and signalosome. *PLoS Biol*. **2**:0113-0119.

Azzam, R., Chen, S.L., Shou, W., Mah, A.S., Alexandru, G., Nasmyth, K., Annan, R.S., Carr, S.A. and Deshaies, R.J. (2004) Phosphorylation by cyclin B-Cdk underlies release of mitotic exit. *Science* **305**:516-519.

Graumann, J., Dunipace, L.A., Seol, J.H., McDonald, W.H., Yates, J.R. III, Wold, B.J. and Deshaies, R.J. (2003) Applicability of TAP-MudPIT to pathway proteomics in yeast. *Mol. Cell. Proteomics* **3**:266-237.

Lipford, J.R., Smith, G.T., Chi, Y. and Deshaies, R.J. (2005) A putative role for activator turnover in gene expression. *Nature*. In press.

Mayor, T., Lipford, J.R., Graumann, J., Smith G.T. and Deshaies, R.J. (2005) Analysis of poly-ubiquitin conjugates reveals that the Rpn10 substrate receptor contributes to the turnover of multiple proteasome targets. *Mol. Cell. Proteomics* **4**:741-751.

Petroski, M.D. and Deshaies, R. J. (2005) Function and regulation of cullin-RING ubiquitin ligases. *Nat. Rev. Mol. Cell. Biol.* **6**:9-20.

Schneekloth, J.S. Jr., Fonseca, F.N., Koldobskiy, M., Mandal, A., Deshaies, R., Sakamoto, K. and Crews, C.M. (2004) Chemical genetic control of protein levels: selective *in vivo* targeted degradation. *J. Am. Chem. Soc.* **126**:3748-3754.

Verma, R., Oania, R., Graumann, J. and Deshaies, R.J. (2004a) Multiubiquitin chain receptors define a layer of substrate selectivity in the ubiquitin-proteasome system. *Cell* **118**:99-110.

Verma, R., Peter, N.R., Tochtrop, G.P., Sakamoto, K.M., D'Onofrio, M., Varadan, R., Fushman, D., Deshaies, R.J. and King, R.W. (2004b) Inhibition of proteasome-dependent degradation by a small molecule that binds the ubiquitin chain. *Science* **306**:117-120.

Wertz, I.E., O'Rourke, K.M., Zhang, Z., Dornan, D., Arnott, D., Deshaies, R.J. and Dixit, V.M. (2004) Human De-etiolated-1 regulates cJun by assembling a CUL 4A ubiquitin ligase. *Science* **303**:1371-1374.

Professor of Biology: **William G. Dunphy**
Senior Research Associate: Akiko Kumagai
Senior Research Fellow: Joon Lee
Research Fellows: Seong-Yun Jeong, Soo-Mi Kim, Zheng Meng, Hae Yong Yoo
Graduate Students: Daniel Gold, Juan Ramirez-Lugo, Karen Wawrousek
Research and Laboratory Staff: Esther Bae, Timur Pogodin

Summary: In eukaryotic cells, the cyclin-dependent kinases (Cdks) control the progression of the cell cycle by regulating the accurate replication of the genome during S-phase and the faithful segregation of the chromosomes at mitosis (M-phase). The entry into these phases of the cell cycle is controlled by Cdks called S-phase promoting factor (SPF) and M-phase promoting factor (MPF). The action of these Cdks must be controlled both temporally and spatially in a very stringent manner. This strict regulation is imparted by a number of checkpoint mechanisms. For example, cells containing unreplicated DNA cannot enter mitosis due to the mobilization of the replication checkpoint. The Dunphy laboratory is engaged in the elucidation of the molecular mechanisms underlying the regulation of SPF and MPF during the cell cycle. Most of these experiments are conducted with *Xenopus* egg extracts, a system in which the entire cell cycle can be reconstituted *in vitro*.

The first member of the cyclin-dependent protein kinase family described is M-phase promoting factor (MPF), which contains the Cdc2 protein kinase and a regulatory subunit known as cyclin B. Since the identification of the molecular components of MPF, there has been rapid and extensive progress in unraveling the biochemistry of mitotic initiation. It is now well established that MPF acts by phosphorylating a myriad of structural and regulatory proteins that are involved directly in mitotic processes such as nuclear membrane disintegration, chromosome condensation, and mitotic spindle assembly. An ongoing challenge to the cell cycle field is the elucidation of how these phosphorylation reactions regulate the structural and functional properties of the various targets of MPF.

We have been most interested in how the cyclin-dependent protein kinases are regulated during the cell cycle. The principal focus of our laboratory has been on the regulatory mechanisms that govern the activation of MPF at the G2/M transition. Some immediate and long-term issues that we are tackling include:

1. What controls the timing of MPF activation so that it occurs at a defined interval following the completion of DNA replication?

2. How do various checkpoint or feedback controls influence the Cdc2/cyclin B complex?

3. What are the molecular differences between the simple biphasic cell cycle found in early embryonic cells and the more complex cell cycles that arise later in development?

More recently, we have been able to study at the molecular level some of the key events leading to the initiation of DNA replication at the G1/S transition. These events involve a cooperative interaction between the Origin Recognition Complex (ORC), the Cdc6 protein, and members of the Mcm family. These studies may ultimately help us understand how S-phase and M-phase are integrated with one another.

In principle, the regulation of cyclin-dependent kinases such as MPF could occur at any of several levels, including synthesis of the cyclin protein, association between the Cdc2 and cyclin proteins, or posttranslational modification of the Cdc2/cyclin complex. The posttranslational regulation of the Cdc2/cyclin complex is particularly important, even in early embryonic cells which manifest the simplest cell cycle programs. In recent years, many of the elaborate details of this Cdc2 modification process have been defined. For example, the binding of cyclin results in three phosphorylations of Cdc2: one at threonine 161 that is required for Cdc2 activity, and two dominantly inhibitory phosphorylations at threonine 14 and tyrosine 15. A variety of genetic and biochemical experiments have established that the inhibitory tyrosine phosphorylation of Cdc2 is an especially important mechanism of cell cycle regulation. As described in greater detail below, there is now strong evidence that the decision to enter mitosis involves considerably more than the tyrosine dephosphorylation of Cdc2. However, a thorough understanding of the kinase/phosphatase network that controls the phosphotyrosine content of Cdc2 will provide a firm foundation for understanding other facets of mitotic regulation.

Our laboratory has made substantial contributions to understanding the molecular mechanisms controlling the activation of the Cdc2 protein. For our studies, we utilize cell-free extracts from *Xenopus* eggs. Due to pioneering work in a number of the laboratories, it is now possible to re-create essentially all of the events of the cell cycle in these extracts. Consequently, it is feasible to study the molecular mechanisms of Cdc2 regulation in intricate detail with this experimental system. To facilitate these studies, we make extensive use of recombinant DNA technology to overproduce cell cycle proteins in either bacteria or baculovirus-infected insect cells. Moreover, in conjunction with our biochemical studies, we are taking advantage of the fission yeast system to exploit genetic approaches to identify novel *Xenopus* regulators of the cell cycle.

213.   Repeated phosphopeptide motifs in Claspin mediate the regulated binding of Chk1
Akiko Kumagai, William G. Dunphy

In vertebrates, the checkpoint-regulatory kinase Chk1 mediates cell cycle arrest in response to DNA replication blocks and UV-damaged DNA. The activation of Chk1 depends on both the upstream regulatory kinase ATR and Claspin. Claspin is a large acidic protein that

becomes phosphorylated and binds to Chk1 in the presence of checkpoint-inducing DNA templates in *Xenopus* egg extracts. Through deletion analysis, we have identified a 57 amino acid region of Claspin that is both necessary and sufficient for binding to *Xenopus* Chk1. This Chk1-binding domain (CKBD) contains two highly conserved repeats of approximately ten amino acids. A serine residue in each repeat (Ser-864 and Ser-895) undergoes phosphorylation during a checkpoint response. A mutant of Claspin containing non-phosphorylatable amino acids at positions 864 and 895 cannot bind to Chk1 and is unable to mediate its activation. These experiments indicate that two phosphopeptide motifs in Claspin are essential for checkpoint signaling.

214. Claspin, a Chk1-regulatory protein, monitors DNA replication on chromatin independently of RPA, ATR, and Rad17
Joon Lee, Akiko Kumagai, William G. Dunphy

Claspin is required for the ATR-dependent activation of Chk1 in *Xenopus* egg extracts containing incompletely replicated DNA. We show here that Claspin associates with chromatin in a regulated manner during S-phase. Binding of Claspin to chromatin depends on the pre-replication complex (pre-RC) and Cdc45 but not on replication protein A (RPA). These dependencies suggest that binding of Claspin occurs around the time of initial DNA unwinding at replication origins. By contrast, both ATR and Rad17 require RPA for association with DNA. Claspin, ATR, and Rad17 all bind to chromatin independently. These findings suggest that Claspin plays a role in monitoring DNA replication during S-phase. Claspin, ATR, and Rad17 may collaborate in checkpoint regulation by detecting different aspects of a DNA replication fork.

215. *Xenopus* Drf1, a regulator of Cdc7, accumulates on chromatin in a checkpoint-regulated manner during an S-phase arrest
Stephanie K. Yanow, Daniel A. Gold, Hae Yong Yoo, William G. Dunphy

We have cloned a *Xenopus* Dbf4-related factor named Drf1 and characterized this protein by using *Xenopus* egg extracts. Drf1 forms an active complex with the kinase Cdc7. However, most of the Cdc7 in egg extracts is not associated with Drf1, which raises the possibility that some or all of the remaining Cdc7 is bound to another Dbf4-related protein. Immunodepletion of Drf1 does not prevent DNA replication in egg extracts. Consistent with this observation, Cdc45 can still associate with chromatin in Drf1-depleted extracts, albeit at significantly reduced levels. Nonetheless, Drf1 displays highly regulated binding to replicating chromatin. Treatment of egg extracts with aphidicolin results in a substantial accumulation of Drf1 on chromatin. This accumulation is blocked by addition of caffeine and by immunodepletion of either ATR or Claspin. These observations suggest that the increased binding of Drf1 to aphidicolin-treated chromatin is an active process that is mediated by a caffeine-sensitive checkpoint pathway containing ATR and Claspin. Abrogation of this pathway also leads to a large increase in the binding of Cdc45 to

chromatin. This increase is substantially reduced in the absence of Drf1, which suggests that regulation of Drf1 might be involved in the suppression of Cdc45 loading during replication arrest. We also provide evidence that elimination of this checkpoint causes resumed initiation of DNA replication in both *Xenopus* tissue culture cells and egg extracts. Taken together, these observations argue that Drf1 is regulated by an intra-S phase checkpoint mechanism that downregulates the loading of Cdc45 onto chromatin containing DNA replication blocks.

216. Phosphorylated Claspin interacts with a phosphate-binding site in the kinase domain of Chk1 during ATR-mediated activation
Seong-Yun Jeong, Akiko Kumagai, Joon Lee, William G. Dunphy

Claspin is essential for the ATR-dependent activation of Chk1 in *Xenopus* egg extracts containing incompletely replicated or UV-damaged DNA. The activated form of Claspin contains two repeated phosphopeptide motifs that mediate its binding to Chk1. We show that these phosphopeptide motifs bind to Chk1 by means of its N-terminal kinase domain. The binding site on Chk1 involves a positively charged cluster of amino acids that contains lysine 54, arginine 129, threonine 153, and arginine 162. Mutagenesis of these residues strongly compromises the ability of Chk1 to interact with Claspin. These amino acids lie within regions of Chk1 that are involved in various aspects of its catalytic function. The predicted position on Chk1 of the phosphate group from Claspin corresponds to the location of activation-loop phosphorylation in various kinases. In addition, we have obtained evidence that the C-terminal regulatory domain of Chk1, which does not form a stable complex with Chk1 under our assay conditions, nonetheless has some role in Claspin-dependent activation. Overall, these results indicate that Claspin docks with a phosphate-binding site in the catalytic domain of Chk1 during activation by ATR. Phosphorylated Claspin may mimic an activating phosphorylation of Chk1 during this process.

217. Adaptation of a DNA replication checkpoint response depends upon inactivation of Claspin by the Polo-like kinase
Hae Yong Yoo, Akiko Kumagai, Anna Shevchenko, Andrej Shevchenko, William G. Dunphy

The checkpoint mediator protein Claspin is essential for the ATR-dependent activation of Chk1 in *Xenopus* egg extracts containing aphidicolin-induced DNA replication blocks. We show that during this checkpoint response Claspin becomes phosphorylated on threonine-906 (T906), which creates a docking site for Plx1, the *Xenopus* Polo-like kinase. This interaction promotes the phosphorylation of Claspin on a nearby serine (S934) by Plx1. After a prolonged interphase arrest, aphidicolin-treated egg extracts typically undergo adaptation and enter into mitosis despite the presence of incompletely replicated DNA. In this process, Claspin dissociates from chromatin and Chk1 undergoes inactivation. By contrast, aphidicolin-treated extracts containing mutants of Claspin with alanine substitutions at positions 906 or 934 (T906A

or S934A) are unable to undergo adaptation. Under such adaptation-defective conditions, Claspin accumulates on chromatin at high levels and Chk1 does not decrease in activity. These results indicate that the Plx1-dependent inactivation of Claspin results in termination of a DNA replication checkpoint response.

218. **Absence of BLM leads to accumulation of chromosomal DNA breaks during both unperturbed and disrupted S-phases**
Wenhui Li, Soo-Mi Kim, Joon Lee, William G. Dunphy

Bloom's syndrome (BS), a disorder associated with genomic instability and cancer predisposition, results from defects in the BLM protein. In BS cells, chromosomal abnormalities such as sister chromatid exchanges occur at highly elevated rates. Using *Xenopus* egg extracts, we have studied *Xenopus* BLM (Xblm) during both unperturbed and disrupted DNA replication cycles. Xblm binds to replicating chromatin and becomes highly phosphorylated in the presence of DNA replication blocks. This phosphorylation depends upon *Xenopus* ATR (Xatr) and Rad17 (Xrad17), but not Claspin. Xblm and *Xenopus* topoisomerase IIIα (Xtop3α) interact in a regulated manner and associate with replicating chromatin interdependently. Immunodepletion of Xblm from egg extracts results in accumulation of chromosomal DNA breaks during both normal and perturbed DNA replication cycles. Disruption of the interaction between Xblm and Xtop3α has similar effects. The occurrence of DNA damage in the absence of Xblm, even without any exogenous insult to the DNA, may help to explain the genesis of chromosomal defects in BS cells.

219. **Mcm2 is a direct substrate of ATM and ATR during DNA damage and DNA replication checkpoint responses**
Hae Yong Yoo, Anna Shevchenko, Andrej Shevchenko, William G. Dunphy

In vertebrates, ATM and ATR are critical regulators of checkpoint responses to damaged and incompletely replicated DNA. These checkpoint responses involve the activation of signaling pathways that inhibit the replication of chromosomes with DNA lesions. In this report, we describe isolation of a cDNA encoding a full-length version of *Xenopus* ATM. Using antibodies against the regulatory domain of ATM, we have identified the essential replication protein Mcm2 as an ATM-binding protein in *Xenopus* egg extracts. *Xenopus* Mcm2 undergoes phosphorylation on serine 92 (S92) in response to the presence of double-stranded DNA breaks or DNA replication blocks in egg extracts. This phosphorylation involves both ATM and ATR, but the relative contribution of each kinase depends upon the checkpoint-inducing DNA signal. Furthermore, both ATM and ATR phosphorylate Mcm2 directly on S92 in cell-free kinase assays. Immunodepletion of both ATM and ATR from egg extracts abrogates the checkpoint response that blocks chromosomal DNA replication in egg extracts containing double-stranded DNA breaks. These experiments indicate that ATM and ATR phosphorylate the functionally critical replication protein Mcm2 during checkpoint responses that prevent the replication of abnormal chromosomes.

220. **Claspin and the activated form of ATR-ATRIP collaborate in the activation of Chk1**
Akiko Kumagai, Soo-Mi Kim, William G. Dunphy

Claspin is necessary for the ATR-dependent activation of Chk1 in *Xenopus* egg extracts containing incompletely replicated DNA. ATR possesses a regulatory partner called ATRIP. We have studied the respective roles of ATR-ATRIP and Claspin in the activation of Chk1. ATR-ATRIP binds well to various DNA templates in *Xenopus* egg extracts. ATR-ATRIP bound to a single-stranded DNA template is weakly active. By contrast, the ATR-ATRIP complex on a DNA template containing both single-stranded and double-stranded regions displays a large increase in kinase activity. This observation suggests that ATR-ATRIP normally undergoes activation upon association with specific nucleic acid structures at DNA replication forks. Without Claspin, activated ATR-ATRIP phosphorylates Chk1 weakly in a cell-free reaction. Addition of Claspin to this reaction strongly stimulates the phosphorylation of Chk1 by ATR-ATRIP. Claspin also induces significant autophosphorylation of Chk1 in the absence of ATR-ATRIP. Taken together, these results indicate that the checkpoint-dependent phosphorylation of Chk1 is a multi-step process involving activation of the ATR-ATRIP complex at replication forks and presentation of Chk1 to this complex by Claspin.

221. **Roles of replication fork interacting and Chk1-activating domains from Claspin in a DNA replication checkpoint response**
Joon Lee, Daniel A. Gold, Anna Shevchenko, Andrej Shevchenko, William G. Dunphy

Claspin is essential for the ATR-dependent activation of Chk1 in *Xenopus* egg extracts containing incompletely replicated DNA. Claspin associates with replication forks upon origin unwinding. We show that Claspin contains a replication fork-interacting domain (RFID, residues 265-605) that associates with Cdc45, DNA polymerase epsilon, RPA, and two RFC complexes on chromatin. The RFID contains two basic patches (BP1 and BP2) at amino acids 265-331 and 470-600, respectively. Deletion of either BP1 or BP2 compromises optimal binding of Claspin to chromatin. Absence of BP1 has no effect on the ability of Claspin to mediate activation of Chk1. By contrast, removal of BP2 causes a large reduction in the Chk1-activating potency of Claspin. We also find that Claspin contains a small Chk1-activating domain (CKAD, residues 776-905) that does not bind stably to chromatin, but is fully effective at high concentrations for mediating activation of Chk1. These results indicate that stable retention of Claspin on chromatin is not necessary for activation of Chk1. Instead, our findings suggest that only transient interaction of Claspin with replication forks potentiates its Chk1-activating function. Another implication of this work is that stable binding of Claspin to chromatin may play a role besides the activation of Chk1.

134

Publications

Kim, S.-M., Kumagai, A., Lee, J. and Dunphy, W.G. (2005) Phosphorylation of Chk by ATR in *Xenopus* egg extracts requires binding of ATRIP to ATR but not the stable DNA-binding or coiled-coil domains of ATRIP. *J. Biol. Chem.* In press.

Kumagai, A., Kim, S.-M. and Dunphy, W.G. (2004) Claspin and the activated form of ATR-ATRIP collaborate in the activation of Chk1. *J. Biol. Chem.* **279**:49599-49608.

Lee, J., Gold, D.A., Shevchenko, A., Shevchenko, A. and Dunphy, W.G. (2005) Roles of replication fork-interacting and Chk1-activating domains from Claspin in a DNA replication checkpoint response. *Mol. Biol. Cell*, in press.

Li, W., Kim, S.-M., Lee, J. and Dunphy, W.G. (2004) Absence of BLM leads to accumulation of chromosomal DNA breaks during both unperturbed and disrupted S-phases. *J. Cell Biol.* **165**:801-812.

Nutt, L.K., Margolis, S.S., Jensen, M., Herman, C.E., Dunphy, W.G., Rathmell, J.C. and Kornbluth, S.A. (2005) Metabolic regulation of oocyte cell death through the CamKII-mediated phosphorylation of Caspase 2. *Cell* **123**:89-103. In press.

Sangrithi, M., Bernal, J.A., Madine, M., Philpott, A., Lee, J., Dunphy, W.G. and Venkitaraman, A. (2005) Initiation of DNA replication requires the RecQL4 protein mutated in Rothmund-Thomson syndrome. *Cell* **121**:887-898.

Yoo, H.Y., Kumagai, A., Shevchenko, A, Shevchenko, A. and Dunphy, W.G. (2004) Adaptation of a DNA replication checkpoint response depends upon inactivation of Claspin by the Polo-like kinase. *Cell* **117**:575-588.

Yoo, H.Y., Shevchenko, A, Shevchenko, A. and Dunphy, W.G. (2004) Mcm2 is a direct substrate of ATM and ATR during DNA damage and DNA replication checkpoint responses. *J. Biol. Chem.* **279**:53353-53364.

Assistant Professor of Biology: Grant J. Jensen
Research Staff: D. Prabha Dias, H. Jane Ding, Andrew Rawlinson, Christian Suloway, William Tivol
Postdoctoral Scholars: Ariane Briegel, Cristina Iancu, Zhuo Li, Elizabeth R. Wright, Zhiheng Yu
Graduate Students: Jordan Benjamin, Gregory Henderson, Peter Leong, Dylan Morris, Gavin Murphy
Undergraduates: Timothy Barnes, Bingni Wen

Summary: If we could simply look inside a cell and see its molecular components in all their complexes and conformations, cell biology would be all but finished. We are developing electron-cryomicroscopy–based technologies to do this for at least the largest macromolecular complexes, hoping to show both how individual proteins work together as large "machines" and how those machines are organized into "assembly lines" within living cells. In addition, we have now begun simulation projects to understand how such spatial relationships affect cellular processes. Our electron cryomicroscopy projects range from imaging individual macromolecules to larger protein assemblies to viruses to organelles and even to intact cells.

We use two basic data collection strategies. The first, called "tomography," involves imaging a single unique object (such as a cell) from multiple directions and then merging those projections into a three-dimensional reconstruction. The second, called "single particle analysis," involves imaging a large number of identical copies of a target object (such as a purifiable protein complex), and again merging the images to produce a three-dimensional reconstruction. Both techniques are in their infancy, but together hold the promise of completing what could be called the "structural biology continuum" in a step-wise fashion by showing first how individual proteins (visible by X-ray crystallography and NMR spectroscopy) come together to form complexes (visible by single particle analysis), and how those complexes are organized within living cells (visible by electron tomography). This structural data, in turn, informs whole-cell models of the interactions of all the cell's molecular components.

Both single particle analysis and tomography begin by spreading the sample in a thin film (~300 nm) across an electron microscope grid and then plunging it into liquid ethane, which causes the water to form vitreous, rather than crystalline, ice, and preserves the sample in a native state without any unnatural fixatives, resins, or stains. For tomography, the sample is imaged from a series of angles by incrementally tilting a goniometer through ~140 degrees. For single particle analysis, each copy of the sample ("particle") structure freezes with a random orientation with respect to the plane of the grid so that tilting is not necessary. Instead, images of hundreds of thousands of individual particles are recorded and then aligned and averaged in three-dimensions computationally. The target resolution for single particle analysis is 4-10Å, where the secondary structure of a particle can be seen and fitting atomic models of components is possible. The target resolution for tomography is 3-6 nm, where the identity, location, and orientation of individual macromolecules can be seen in their cellular contexts.

Our work involves technology development, as well as, its application to key biological questions. We enjoy the use of a state-of-the-art, 300kV, helium-cooled, energy-filtered, fully automated, dual-axis tilting, FEG "Polara" TEM. This year's technical milestones include (1) documenting the advantages and disadvantages of liquid helium cooling in the microscope; (2) characterizing phase transitions that occur in vitreous ice when irradiated at very low temperatures; (3) finding the optimal dose and temperature for tomography; (4) exploring materials to reduce specimen charging; (5) establishing a distributed computing network within the lab. Other ongoing technology development projects include; (6) simulation studies to understand the effect of alignment errors in single particle reconstructions; (7) theoretical work on methods to correct for curvature of the Ewald sphere; and (8) developing software to further automate data collection. Some of the biological questions we have addressed this year are: (1) the nature of the prokaryotic cytoskeleton as seen in *Caulobacter crescentus, Magnetospirillum magneticum, Mycoplasma pneumoniae,* and *Mesoplasma florum*; (2) the structure of mature and immature HIV-1 virus-like particles; (3) the quaternary structure of the pyruvate dehydrogenase multi-enzyme complex; (4) the quaternary structure of various RNA polymerase complexes; (5) the structure of the bacterial carboxysome; (6) the quaternary structure of UDP-1 glucose pyrophosphorylase; and (7) the structure of a simple eukaryotic nucleus.

222.   Electron cryotomography of the ultrastructure of *Caulobacter crescentus*
Ariane Briegel, D. Prabha Dias, Grant Jensen

The structural study of the aquatic proteobacterium *Caulobacter crescentus* provides us the opportunity to make significant contributions not only to basic cell biology, but also to medicine, agriculture and applied environmental science. From a cell biological perspective, one of the reasons that the crescent- shaped *Caulobacter* is fascinating is because it is a prokaryote that undergoes asymmetric cell division (mostly the province of eukaryotes). Its cell cycle is highly regulated both temporally and spatially. The daughter cell always arises from the tip of the crescent opposite that of the mother cell's "stalk" appendage, and the daughter cell's flagellum is at the opposite end from the site of cell division. The crescent shape of the cell almost certainly depends on some type of structural restraints within the cell, and

asymmetric cell division is likely to be achieved through arranging the cell cycle components on some type of internal structure, that is, a cytoskeleton of some kind. Until relatively recently, it was thought that bacteria had very little regular internal structure and were basically a "bag of macromolecules." There is now mounting evidence that this is not the case, including the discovery of bacterial homologs to eukaryotic cytoskeletal proteins such as tubulin and actin. The sequencing of the *C. crescentus* genome revealed the presence of homologs to a third type of cytoskeletal element, intermediate filaments. This bacterium is thus, an excellent place to look for a bacterial version of the eukaryotic cytoskeleton.

Until now, our knowledge of the internal structure of bacteria has been severely limited by the methods available. Bacteria in general are too small for their internal structures to be resolved by light microscopy, and Caulobacter is no exception. Although electron microscopy (EM) has more than enough resolving power, the difficulty associated with properly preserving bacteria for EM (i.e., chemical fixation and plastic embedding) had retarded progress. Furthermore, the heterogeneous nature of bacterial cells make them unsuitable for study by methods requiring averaging over multiple cells, like single particle analysis.

Electron cryotomography overcomes both the limitations of conventional fixation and of the averaging methods. We freeze individual bacteria so rapidly that no ice crystals have time to form, and the result is a bacterium "embedded" in vitreous (amorphous) ice. We can determine the three-dimensional structure of the frozen bacterium by taking images of the bacterium tilted at various degrees in the electron beam. The information in the series of tilted images can then be combined computationally using image-processing algorithms. The result is a three-dimensional map of the electron density distribution (tomogram) of the bacterium. This year we obtained tomograms of the widely studied C15N strain of *C. crescentus* in which filamentous structures are clearly visible in the cell cytoplasm. Future aims are to build on this breakthrough result by investigating the structures of various mutants of *C. crescentus*, in collaboration with several of the laboratories leading this field.

200nm
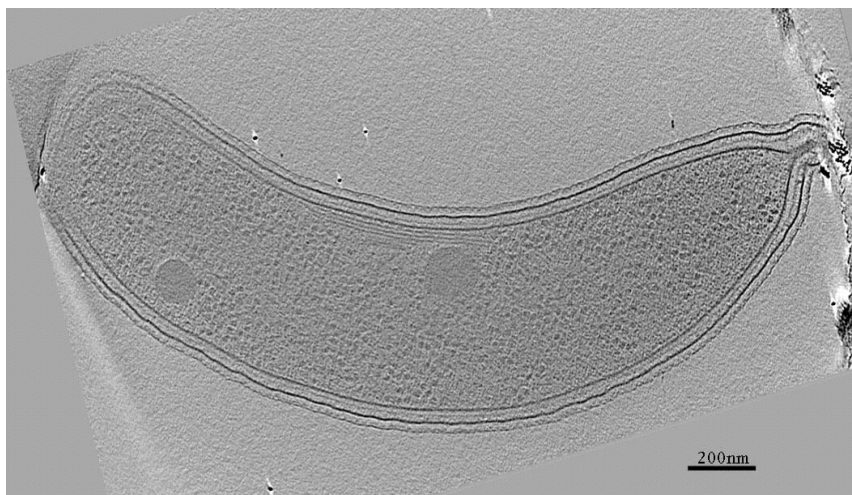
A projection of slices through a tomogram of *C. crescentus* clearly shows the presence of filamentous structures along the inner membrane of the concave side of the bacterium.

223. Electron cryotomography of *Magnetospirillum* cells

Zhuo Li, Arash Komeili[1], Dianne Newman[2], Grant Jensen

Bacterial magnetosomes are intracellular membranous organelles consisting of highly ordered magnetite crystals arranged into a chain. Each magnetite crystal is enclosed by a lipid-bilayer shell. The magnetosome chains are believed to aid the bacteria in aligning with geomagnetic field lines in order to search for the optimum oxygen concentration in their aquatic environment. However, the mechanism of magnetosome formation still remains elusive. In collaboration with Diane Newman's lab in the Division of Geological and Planetary Sciences, we are using electron cryomicroscopy to study *Magnetospirillum species* AMB-1 cells in a nearly native state. In wild-type cells, we found that magnetosome vesicles are located close to the cell membrane and appear to form by invagination of the inner membrane. If the cells are deprived of iron in the culture medium, the magnetosome chain still forms from the invagination of inner membrane but does not exhibit magnetite crystals. Under both conditions, bunches of filaments are visible around magnetosome vesicles and may function structurally in the arrangement of the chain. To identify these filaments unambiguously, we are constructing and imaging gene deletion cells. A promising candidate gene is *mamK*. The *mamK* gene is located within the *mam* operon, which is the gene cluster involved in the magnetosome's function. Its gene product, MamK, has been proven to be a homolog to MreB (a bacterial filament).

[1]*Postdoctoral Scholar, Newman lab, Caltech*
[2]*Assoc. Prof. Geobiology & Environ. Sciences, Caltech*
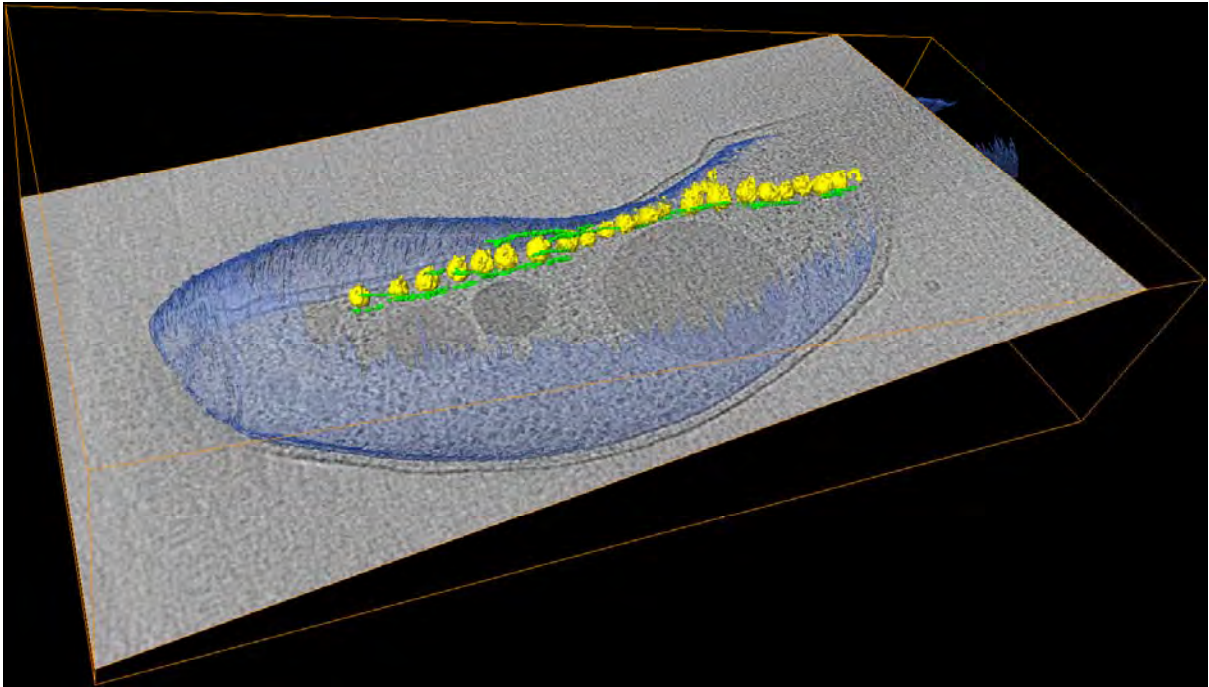
3D visualization of segmented, surface-rendered inner membrane (*blue*), magnetosome vesicles (*yellow*), and filaments (*green*) in a *Magnetospirillum AMB-1* cell. The superimposed slice in the bounding box (indicating *z* heights) is a section along the long axis of the magnetosome chain in which the outer membrane, the peptidoglycan layer, and poly-β-hydroxybutyrate storage granules can be seen.

224.   Electron cryotomography of the attachment organelle of *Mycoplasma pneumoniae*
Gregory Henderson, Grant Jensen

Bacteria can assemble huge macromolecular complexes. Those like the flagella and the injectisome are well understood, but the functions of other complexes are not as clear. The attachment organelle of the bacterium *Mycoplasma pneumoniae* is one such complex. *Mycoplasma pneumoniae* causes pneumonia in humans, and is a model organism because of its minimal genome. The attachment organelle is a large membrane-bound extension with a central protein core, which mediates the cell's pathogenicity, provides a unique form of cell motility, and replicates and segregates itself in coordination with cell division. The mechanisms of each of these processes are still being worked out, and the role of the large protein core is largely unknown. Using electron cryotomography, we have determined the ultrastructure of the protein core and surface proteins of the attachment organelle, and future work is aimed at the localization of the individual proteins that make up these structures.
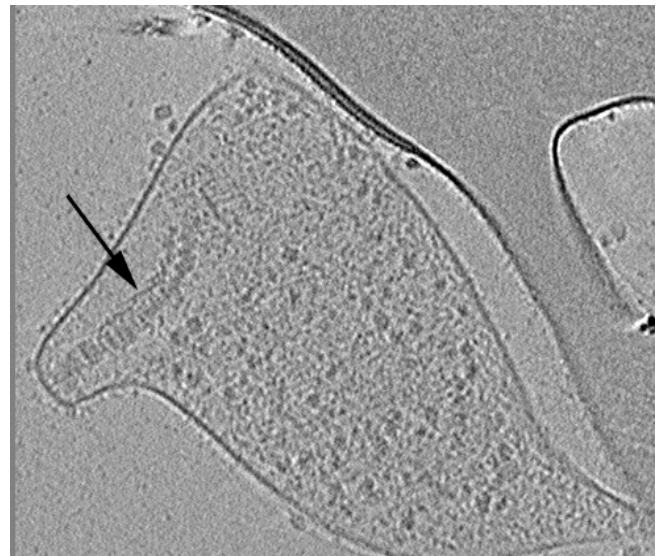
Two-dimensional slice through a tomographic reconstruction of *M. pneumoniae*. The arrow points to the protein core inside the attachment organelle.

225. Electron cryotomography of *Mesoplasma florum*
Elizabeth R. Wright, Grant J. Jensen
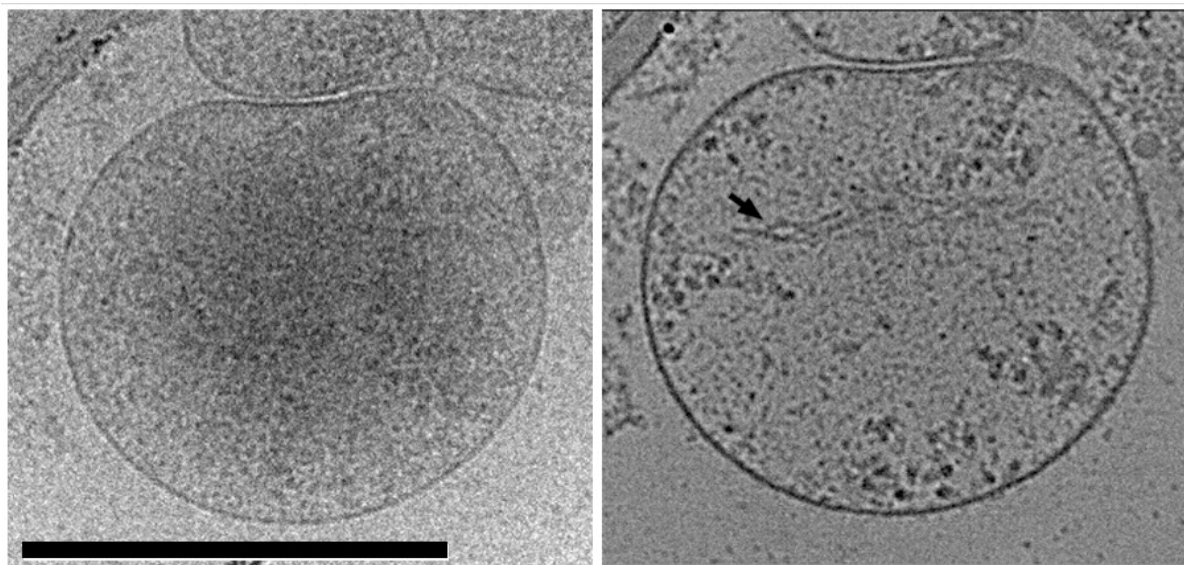
***Mesoplasma florum* cell preserved by rapid freezing and viewed by cryo-EM. *Left:* Projection image from a tile series of an *M. florum* cell. *Right*: A 10-slice averaged section 40 nm thick through the reconstruction corresponding to the projection image. Note the bundle of filaments observed within the cell's cytoplasm (arrow). Scale bar 500 nm.**

Mesoplasma florum, which inhabits citrus plants, is a simple gram-positive bacterial descendent of the class *Mollicutes*. The bacteria of this class have generally been termed some of the simplest free-living organisms because they lack a cell wall, outer membrane, and periplasmic space; and do not have many of the complex biosynthetic and intermediate metabolic pathways. *Me. florum* has a very small genome of approximately 793 Kbp, in which ~685 proteins have been identified. *Me. florum* also ranges in size from 200 to 800 nm. The simplicity and small size of *Me. florum* make it an ideal specimen for whole cell electron cryotomography.

The wild-type strain of *Me. florum* (ATCC 33453) was grown in Mycoplasma medium (ATCC 243) with the addition of phenol red as a growth indicator. Cell suspensions were flash frozen onto Quantifoil carbon grids in liquid ethane with a Vitrobot. The frozen grids were stored under liquid nitrogen until transfer to the microscope for imaging. All images of *Me. florum* were recorded on a 300 kV "G2 Polara" TEM.

We experimented with five major data collection parameters in order to determine what could produce 'superlative' data for analysis. *These parameters were magnification, temperature, total electron dose, defocus, and single- versus dual-axis tilt series.* We noted several factors that determine what magnification to employ for data collection: (1) pixel size; (2) signal-to-noise ratio (SNR); and (3) field of view. For each specimen type, the magnification used must be optimized according to the desired resolution for the final tomographic reconstruction. During the initial phases of data collection on *Me. florum*, two magnifications were analyzed, 22,500x (9.8 Å pixel,

~3 nm target resolution) and 34,000x (6.7 Å pixel, ~2 nm target resolution) in order to determine the effect on tomogram resolution. The quality of tomograms was then assessed by the level at which the computational searches are able to cross-correlate known protein structures to the protein complexes contained within the cells. Furthermore, since we have the ability to collect data on samples cooled to liquid nitrogen or helium temperatures, we explored the effect this would have on the cells during data collection. For *Me. florum*, it was apparent to us that the cells imaged at helium temperature lost contrast and in fact underwent a reversal of contrast above a total electron dose of ~50 $e^-/\text{Å}^2$, whereas the cellular contrast was maintained at nitrogen temperatures even to extreme doses at which the cells 'bubbled.' The total dose to which the cells can be directly exposed has impacted our ability to observe and distinguish features, especially large proteins within the cells. In order to determine what total dose the cells are able to withstand, we have varied the dose between 30 $e^-/\text{Å}^2$ to 120 $e^-/\text{Å}^2$. For *Me. florum*, it appears that the higher the dose the cells are able to tolerate without internal deformation, the better the final reconstruction. Similarly, we varied the defocus between –8 and –30 µm in order to enhance certain features of the cells such as the cell membrane and internal features like protein filaments and ribosomes.

Within the cells we have observed many large protein complexes and are refining computational methods to conclusively identify them and map their locations within the cells.

226. **Electron cryotomography analysis of HIV-1 maturation**
Jordan Benjamin, Elizabeth R. Wright, Grant J. Jensen
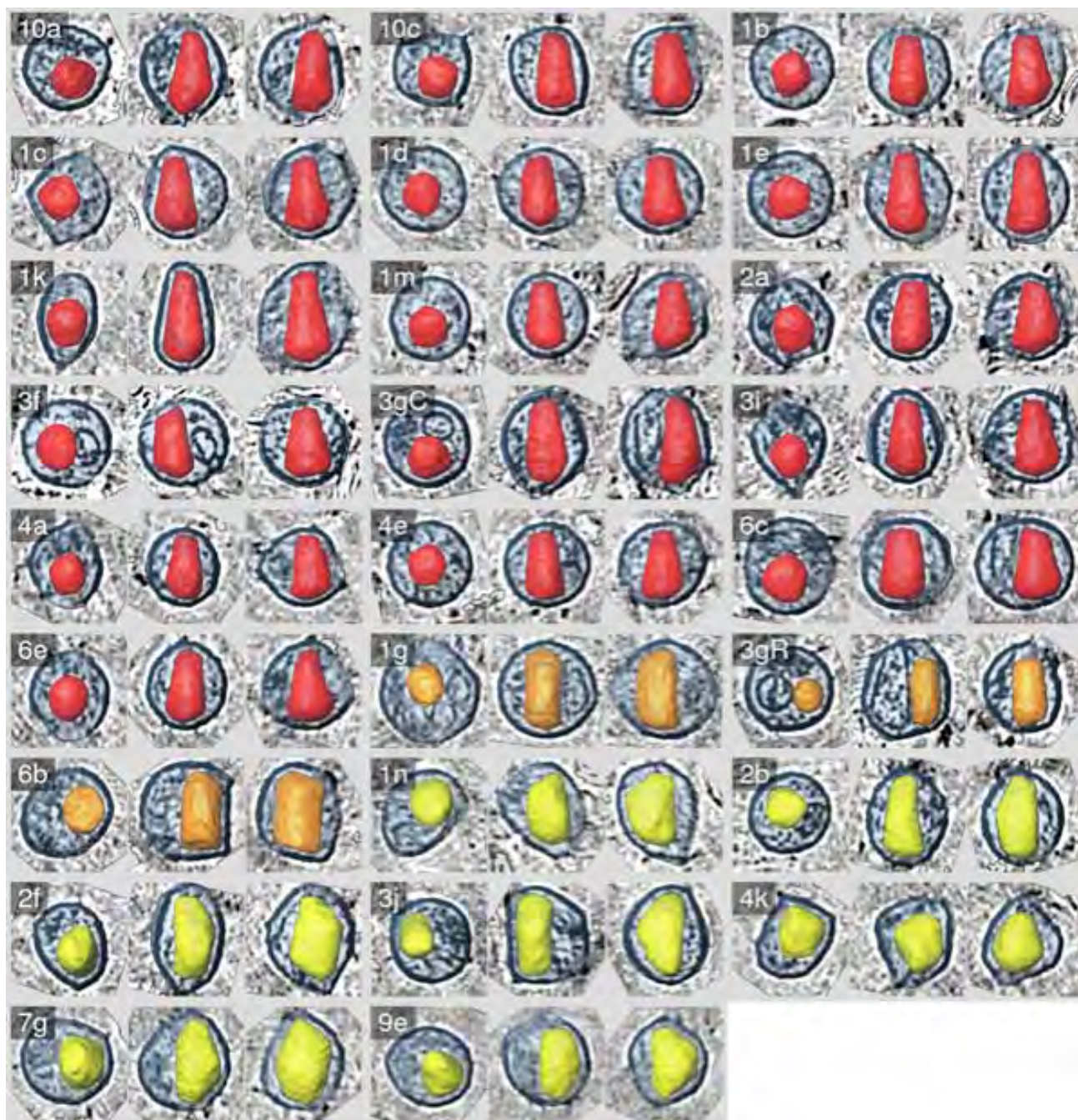
Montage of all segmented HIV-1 VLPs. A total of 26 VLPs were segmented and aligned along their principal axes. Three views are shown for each VLP, presenting from left to right axial, sagittal, and coronal perspectives, respectively. Three-dimensional renditions of the capsid surfaces are shown in red for cones, orange for rods, and yellow for all others, placed within a denoised two-dimensional section through the middle of the VLP, with the area enclosed by the lipid bilayer in blue. Because each VLP was extracted as a cube from a larger three-dimensional reconstruction and then aligned to the others, the boundaries of the images appear as randomly oriented, clipped, squares. Each capsid is identified by a number and a letter, where the number signifies which field of particles it came from. Capsids 3gR and 3gC are part of the same, double-capsid VLP. The edges of the boxes containing each VLP image here and in all other figures represent 160 nm (Benjamin *et al*., 2005).

HIV is perhaps the most extensively studied "organism" in terms of structural biology. It has three layers: an outer lipid membrane, the protein shell known as the matrix (MA), and the capsid (CA), an inner protein shell housing the genome. The structures of nearly every component of HIV have been determined in isolation, some in many different conformations and with various inhibitors, but it is still unclear how individual subunits come together to form the intact virion.

Furthermore, the virus goes through multiple stages of maturation wherein the structures of these shells change in poorly understood ways. We are working to determine the three-dimensional structure of HIV-1 virus-like particles (VLPs) halted at various stages of maturation by electron cryotomography. The structures that we obtain will allow us to confirm or refute various models that have been proposed about the organization of the protein shells and the changes underlying maturation.

In the mature form of the virus, the capsid can have numerous morphologies, with the most common being a somewhat asymmetrical cone. Recent cryo-ET examinations of mature HIV-1 VLPs in our laboratory have revealed that the conical cores within the VLPs were unique in structure and position, but they also demonstrated certain similarities with respect to size and shape, the distance of the cone's base from the envelope/MA layer, the range of the cone angle. It was also observed that the conical capsid shape was preferred *in vivo*, which argues in favor of the template-directed model of capsid formation (Benjamin *et al.*, 2005).

We have collected many single- and dual-axis tilt series of frozen-hydrated immature and mature HIV-1 virions and produced tomographic reconstructions from them. Some of the continuing challenges of this project include developing computational methods for classifying and measuring the morphologies of observed structures, three dimensional alignment and averaging of repetitive structures within each unique virion, and improvements in imaging protocols to achieve higher-resolution reconstructions. One of our goals is to provide the highest resolution structures of whole, intact frozen-hydrated HIV-1 VLPs from which other researchers may determine the placement of other proteins and data from which new therapies may be designed to combat or eradicate HIV-1 infection.

227. Simulation of the HIV maturation process
Dylan Morris, Grant Jensen

The immature HIV virus exists as a spherical particle surrounded by a lipid membrane. Directly attached to the inner face of this membrane is the Gag polyprotein. During the maturation process, this protein is proteolytically cleaved into its functional components, including the matrix protein, the capsid protein, and the nucleocapsid protein. The matrix protein remains attached to the lipid membrane; the capsid protein self-assembles into a cone-shaped inner shell; and the nucleocapsid protein attaches directly to the viral genome. While the atomic structures of these components have been

determined, the various mechanisms of the maturation process remain unclear. Our current focus is the mechanism of capsid self-assembly; specifically, how approximately 1500 identical copies of this protein are able to assemble into a variety of shell morphologies. We believe that computational simulation of this process will shed light on the slight conformational variations that must be required to allow this process to occur.

Specifically, we are creating a coarse-grained representation of the HIV capsid protein that maps the protein-protein interaction regions onto an adequately detailed representation of the protein's molecular surface. Such a representation will then allow us to simulate the assembly process with a traditional molecular dynamics approach. The results of such a simulation will provide us with important insights into the kinetics of this assembly pathway. A major challenge associated with this project involves developing the computational techniques required to create an abstract, coarse-grained representation of the protein molecule that captures the essential characteristics of the intermolecular interaction sites in sufficient detail to allow us to gain biological insights from the simulation results, yet simple enough for the simulation to remain computationally tractable. A future goal of this work is to generalize our methodology to consider the numerous biological processes for which the shapes and structures of the constituent protein molecules play a significant role in determining the global behavior of the system.

228. **Visualization of the *E. coli* pyruvate dehydrogenase multienzyme complex using electron cryotomography**
Gavin Murphy, Grant Jensen
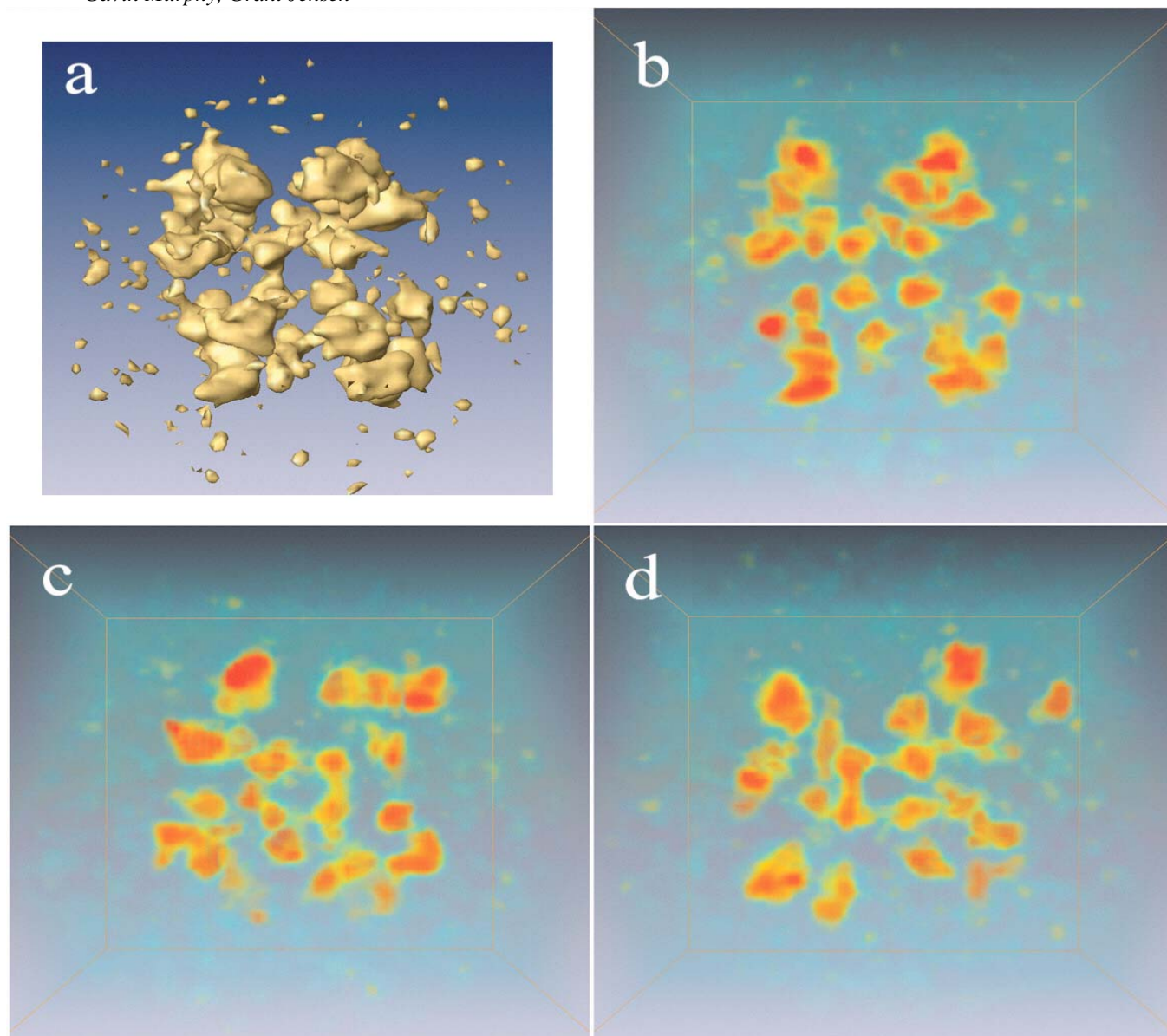
(a) Surface rendering of one reconstructed PDHC particle, enclosing the estimated volume of a complete 5.6 MDa complex. (b) Volume rendering of the same particle with the foreground excluded for clarity and to reveal the cubic core. (c-d) Similar volume renderings for two other particles (Murphy and Jensen, in press).

The ascendant technology of electron cryotomography (CET) has been used to reconstruct the 3D quaternary structure of the inherently asymmetric, flexible, non-homogeneous and large (~5 MDa) *E. coli* pyruvate dehydrogenase multienzyme complex (PDHC) and the 2-oxoglutarate dehydrogenase multienzyme complex (OGDHC). Whereas other structural biology techniques such as X-ray and electron crystallography, NMR spectroscopy and single-particle analysis require the averaging of many copies of the target object, CET can determine the 3D structure of unique objects ranging in size from proteins to cells. Excellent applications of the technique are large, multi-protein, macromolecular machines whose components are known to high-resolution yet whose quaternary structure is unknown due to perhaps flexibility or fragility issues.

PDHC and OGDHC are two closely related assemblies of three protein types each – E1p, E2p, and E3, and E1o, E2o, and E3, respectively. In each complex, the three enzymes together catalyze five separate reactions that in sum decarboxylate 2-oxo acids and attach the remaining acyl group to coenzyme A. Either E2 polypeptide contains

142

an ~26 kDa catalytic domain, an ~4 kDa E1/E3 binding domain, and three or one (in PDHC and OGDHC, respectively) ~8 kDa lipoyl domains. Each of these domains is separated by apparently flexible "tether" sequences rich in alanine and proline and exposed to solvent. Atomic models exist for all components and subunits, albeit from different species. Twenty-four E2 subunits assemble into an octahedral core, while up to 24 E1 or E3 subunits are arranged about the core. The established model for the complex, the Face/Edge model, had 12 E1 dimers bound to the 12 edges of the cube and 6 E3 dimers bound to the 6 faces. 2D, negatively stained, electron microscopy (EM) images of the complex, several stoichiometric studies and STEM images of the complex and various subcomplexes were the main lines of evidence for this model. Later 2D, cryo-EM images showed 2-5 nm gaps between the core and subunits, but this only weakened and did not abolish the Face/Edge model.

Unaveraged, undenoised, and unrefined dual-axis CET reconstructions of the two complexes clearly showed the separation between subunits and core. The eight ~80 kDa were often resolved. The resolution was estimated to be ~5.5 nm using the Fourier Shell Correlation method. To distinguish between the face/edge and flexibly tethered models quantitatively, their radial densities were compared to those of several individual, reconstructed particles. The experimental density peaks once at ~5 nm, which is attributable to the core, and a gap of ~10 nm separates the second peak, which is attributable to the subunits. No such gap exists between core and subunits in the Face/Edge model. The atomic models of E2 were quantitatively fit into the core density while atomic models of the subunits were manually positioned. The radial density of the fit proteins matched the experimental density well. The subunits could not be fit quantitatively due to the poor resolution and the merging of neighboring densities, which prevented classification. Nevertheless, manual fitting of three different particles produced plausible correspondence between the experimental density and the fit atomic subunit models. Three E1/E3 binding domains of E2 are tethered to the trimeric corners of the E2 core. Using the centers-of-mass of the fit subunits, a mean distance of 11 nm was measured between the subunits and corner, and a mean polar angle of 41° with respect to the 3-fold axis of the cube was found. The measurements are plausible, as the 31-residue tether would have a fully extended length of 12 nm and a 3D random walk length of 2 nm. As the subunits have a radius of ~4.5 nm, the resultant tether length of 6.5 nm lies within the range. Also, three spheres positioned 11 nm from a corner and just touching would have a polar angle of 29°, so the experimentally determined angle allows sufficient space. An illustrative atomic model of one corner of the complex was created by placing crystal structures of E3 bound to the E1/E3 binding domain in the experimental density off of one corner of a particle. Lipoyl domains were placed in purely hypothetical locations around the subunits and tethers modeled mostly as extended beta strands were created to connect them. This model allowed sufficient space for the movement of the components. Thus, through the imaging power of 3D electron cryotomography the quaternary structure of a flexible mulitenzyme complex was elucidated and exemplifies the applications of the technique to the myriad large, multi-protein machines found in nature.

229.   Electron cryotomography of carboxysomes
Cristina Iancu, H. Jane Ding, Grant Jensen

Carboxysomes are organelle-like polyhedral bodies, about 100 nm in diameter, made up of a protein shell and packed with rubisco molecules, the enzyme responsible for CO_2 fixation. They are part of the CO_2-concentrating machinery (CCM) in cyanobacteria and form preponderantly when the bacteria are grown under low-CO_2 conditions. The exact mechanism by which the carboxysomes overcome limitations on the CO_2 availability is still under debate. Some of the proposals tossed around include an ordered organization of rubisco molecules, which may confer a catalytic advantage to the carboxysome-packed protein, or porosity of the shell protein which would favor concentrating CO_2 in proximity of the rubisco molecules. Knowledge of the 3D structure of carboxysomes will help in better understanding their role in CCM. So far, the structural information on carboxysomes came primarily from 2D EM imaging. Because the carboxysomes are not homogeneous in size, processing of the 2D images to obtain 3D information was not possible. We have investigated the structures of purified carboxysomes from *Synechococcus sp*. using cryo-EM tomography. This technique is particularly well suited for obtaining 3D information of unique objects. The carboxyomes were extracted from tomograms for further analysis. We determined that carboxysomes have an approximately icosahedral shape, they do vary in size and we are now in the process of establishing if the organization of rubisco molecules in carboxysomes is random or ordered.
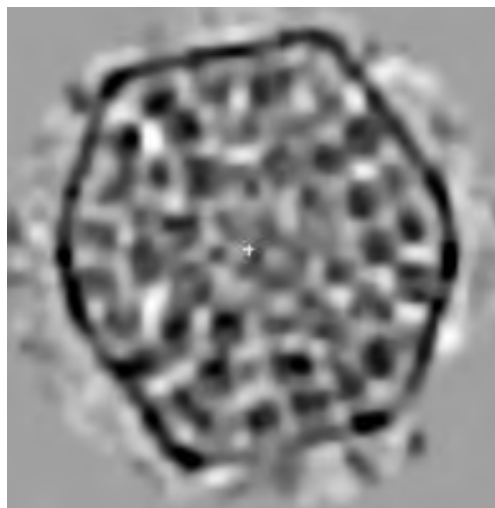
One tomogram slice through the middle of a carboxysome. The round particles inside the carboxysome are rubisco molecules.

230. **Direct visualization of the transcription pre-initiation complex using electron cryomicroscopy**
Zhiheng Yu, Grant Jensen

Many cancers are caused by mutations in transcription factors (TFs) which lead to unregulated transcription. It has been a long-pursued goal to visualize the transcription pre-initiation complexes (PIC), formed prior to the start of transcription of every gene.

We aim to visualize the transcription PIC, composed of RNA polymerase II, TBP, TFIIA, TFIIB, TFIIF and DNA using electron cryomicroscopy (cryo-EM). Though breakthroughs were made to obtain the structures of some components of the PIC by X-ray crystallography, it is extremely difficult to obtain crystals of the PIC suitable for crystallographic analysis. Cryo-EM is the best and probably the only available tool to directly visualize PIC.

231. **Electron cryotomography and single particle analysis of UDP-glucose pyrophosphorylase**
Cristina Iancu, Grant Jensen

UDP-glucose pyrophosphorylase (Ugp1) is a 450 KDa enzyme responsible for the conversion of Glucose-6-Phosphate to UDP-Glucose, the latter being a precursor of both glycogen synthesis and cell wall carbohydrates. Recently our collaborators found two isoforms of Ugp1, which differ through a post-translational modification. Furthermore, this modification leads to structural differences between the two isoforms, which allegedly affect the enzyme subcellular localization so that one isoform of Ugp1 is cytosolic and involved in glycogen synthesis, while the other isoform is localized close to the cell wall where it provides its product to cell wall carbohydrate synthesis. We are working on obtaining 3D structures of both isoforms of Ugp1 by using cryo-EM. Initially we used cryo-EM tomography to assess the sample homogeneity and, thus, its suitability for single particle analysis studies. Tomograms of both forms of Ugp1 showed that these samples are fairly homogeneous and, at the low resolution (~6 nm) typical for tomograms, the two isoforms of Ugp1 do not seem to differ in their structural conformations significantly. We are now using this initial 3D model for single particle analysis studies, which, at higher resolution, are expected to reveal the conformational difference between the two isoforms of Ugp1.
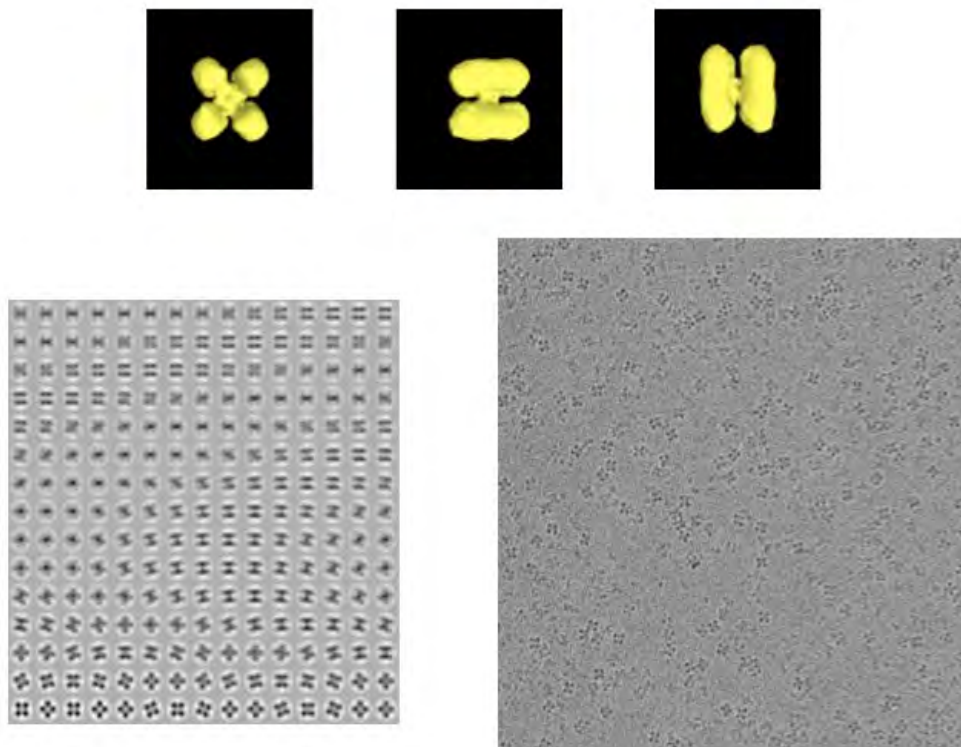
***Top row*: Orthogonal views of the Ugp1 initial model obtained by averaging 45 particles extracted from tomograms, assuming C4 symmetry and rendered at an isosurface corresponding to MW 450 kDa. *Lower left*: 2-D projections of the initial model. *Lower right*: 2D EM image of Ugp1.**

232. **Structure of intact nuclei visualized by electron cryotomography**
Bingni Wen, Grant Jensen

The nucleus is a prominent eukaryotic organelle whose double membrane segregates the genetic material and associated machinery from the rest of the cell. The nucleus plays a central role in directing cellular processes, and to understand its complex functions, it is necessary to know its overall structure – how its many parts fit together. To analyze nuclear structure in a near-native state, intact nuclei are isolated from small cells and are vitrified by rapid freezing, which allows high-resolution imaging by electron cryotomography without sample fixation or staining. A series of projection electron micrographs are acquired as viewed from many different angles, and then recombined computationally into a three-dimensional reconstruction of the original nucleus. This approach has the potential to reveal nuclear features such as the nuclear envelope, nuclear pore complexes, the dense nucleolus, as well as, mitotic spindle structures and chromatin in their native context. We hope to gain insight into the structure and dynamics of intact nuclei.

233. **A comparison of liquid nitrogen and liquid helium as potential cryogens for electron cryotomography**
Cristina Iancu, Elizabeth R. Wright, J. Bernard Heymann[1], Grant Jensen

The principal resolution limitation in electron cryomicroscopy of frozen-hydrated biological specimens is radiation damage. It has long been hoped that cooling such samples to just a few Kelvins with liquid helium would slow this damage and allow statistically better-defined images to be recorded. A new "G2 Polara" microscope from FEI company was used to image various biological samples cooled by either liquid nitrogen or liquid helium to ~82 or ~12 K, respectively, and the results were compared with particular interest in the doses (10-200 e-/$\mathring{A}^2$) and resolutions (3-8 nm) typical for electron cryotomography. Simple dose series revealed a gradual loss of contrast at ~12K through the first several tens of e-/$\mathring{A}^2$, after which small bubbles appeared. Single particle reconstructions from each image in a dose series showed no difference in the preservation of medium-resolution (3-5 nm) structural detail at the two temperatures. Tomographic reconstructions produced with total doses between 10-350 e-/$\mathring{A}^2$ showed better results at ~82 K than ~12 K for every dose tested. Thus, disappointingly, cooling with liquid helium is actually disadvantageous for cryotomography. (Iancu, *et. al.*, in press)
[1]*National Institutes of Health*

234. **Observations on the behavior of vitreous ice at ~82 and ~12 K**
Elizabeth R. Wright, Cristina Iancu, William Tivol, Grant Jensen

In an attempt to determine why cooling with liquid helium actually proved disadvantageous in our electron cryotomography experiments, further tests were performed to explore the differences in vitreous ice at ~82 and ~12 K. Electron diffraction patterns clearly showed that the vitreous ice of interest in biological electron cryomicroscopy (i.e., plunge-frozen, buffered, protein solutions) does indeed condense into a higher density phase when irradiated with as few as 2-3 e-/$\mathring{A}^2$ at ~12 K. The high-density phase spontaneously expanded back to a state resembling the original low-density phase over a period of hours at ~82 K. Movements of gold fiducials and changes in the lengths of tunnels drilled through the ice confirmed these phase changes, and also revealed gross changes in the concavity of the ice layer spanning circular holes in the carbon support. Brief warm-up/cool-down cycles from ~12 K to ~82 K and back, as would be required by the flip-flop cryorotation stage, did not induce a global phase change but did allow certain local strains to relax. Several observations including the rates of tunnel collapse and the production of beam footprints suggested that the high-density phase flows more readily in response to irradiation. Finally, the patterns of bubbling were different at the two temperatures. It is concluded that the condensation of vitreous ice at ~12 K around macromolecules is too rapid to account alone for the problematic loss of contrast seen, which must instead be due to secondary effects such as changes in the mobility of radiolytic fragments and water. (Wright *et al.*, in press)

235. **Peach: A Distributed Computation System**
Peter Leong, J. Bernard Heymann[1], Grant Jensen

A simple distributed processing system named "Peach" was developed to meet the rising computation demands of modern structural biology laboratories without additional expense by using existing hardware resources more efficiently. A central server distributes jobs to idle workstations in such a way that each computer is used maximally, but without disturbing intermittent interactive users. The system has been in use for almost a year in the Jensen laboratory to facilitate the heavy amount of image processing required. This setup currently consists of over 20 computers and has been used to speed up the computation times of a variety of projects. (Leong *et al.*, 2005)
[1]*National Institutes of Health*

236. **Sensitivity of alignment errors in single particle analysis**
Andrew Rawlinson, Grant Jensen

The techniques of 'single particle analysis' allow us obtain three-dimensional reconstructions of frozen hydrated proteins by 'averaging' thousands of electron microscope images of the protein. The quality of the images is affected by the loss of information due to the contrast transfer function, Poisson (shot) noise, distortions due to the microscope, etc. These effects, and the ability to determine the alignment parameters – i.e., locate the centers, orientations and defocus – of the protein in each image will in turn affect the quality of the three dimensional reconstruction.

It is an open question as to how many such images are needed to obtain three-dimensional reconstructions of 'near atomic resolution' (4.0 – 8.0 Å). The general understanding is that the more accurate we determine the alignments of the proteins, then fewer images are needed to attain the desired resolution.

We are testing the sensitivity of alignment errors to the quality of the reconstructions by using custom software to simulate electron microscope images (using the multi-slice algorithm).

Alignment errors of various magnitudes are introduced in the reconstruction process, and the 'Fourier shell correlation' is calculated – thus, providing an objective method to determine the quality of the reconstruction. Early indications are that 10,000s – 100,000s of images are required to attain near atomic resolution – something that is feasible with current computer technology.
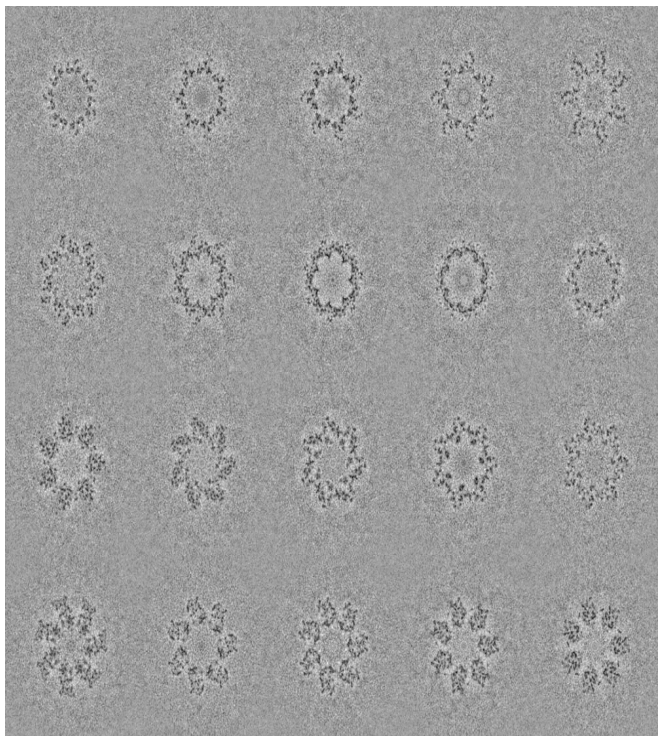
Cross sections of a reconstruction of the 20S proteasome using simulated images.

237. Correction of the effect of the Ewald Sphere on electron microscopic images
Peter Leong, Grant Jensen

When an image is recorded by an electron microscope, it is assumed that an image is a perfect projection of the object being imaged. These projections are the inverse Fourier transforms of central slices of the object in Fourier space. This is an approximation that is valid most of the time. At high resolutions, low acceleration voltages and thick samples, the approximation begins to fail. This is known as the effect of the Ewald sphere curvature.

We have developed a reconstruction algorithm to correct for the curvature effect. Simulations have shown that the effect of the Ewald sphere can be corrected for, thereby eliminating the resolution limit imposed by the curvature. Currently, the algorithm is being used on a large virus particle dataset to confirm the resolution improvements on real data.

238. Electron microscope automation
William Tivol, Christian Suloway, Grant Jensen

All modern electron microscopes are computer controlled, and many incorporate automated functions such as setting eucentric height, focusing, and alignment. These functions offer the advantages of accuracy, precision, efficiency, and the ability to incorporate them into other automated procedures. Since specimens consisting of frozen-hydrated biological materials are radiation sensitive and inherently low in contrast, the use of automation provides better images than could be obtained by performing the functions manually.

In addition to automated microscope functions, there are now computer programs designed to allow automated collection of data. One of these, Leginon, will soon be installed on our microscopes. This will allow one to insert the sample, let the microscope to come to a steady-state temperature, and take series of images without intervention from the user and with the microscope in an optimally stable condition. This process can be monitored and controlled via a web interface, and the images obtained will be archived and annotated so that they can be retrieved, along with all the microscope settings, for further processing.

Although automation of microscope functions and data collection are maturing fields, significant work remains in the application of these procedures to the instruments and types of data collection in our lab.

239. Development of novel computational methods to identify and locate biological structures within electron cryotomograms
H. Jane Ding, Cristina Iancu, D. Prabha Dias, Jordan Benjamin, Grant Jensen

Much of the work in the Jensen lab concerns locating and identifying specific biological objects such as protein filaments, lipid membranes, and large protein complexes within three-dimensional reconstructions. We employ existing software packages (both commercial and academic) and develop our own custom programs. As one specific example, we have seen for the first time a number of different patterns of protein filaments within the bacteria Caulobacter crescentus. Fluorescence light microscopy has suggested that there is a filament composed of the protein MreB that traverses a helical path from one pole to the other just inside the inner membrane. Unfortunately, no such filament has ever been visible directly in our tomograms viewed with either Amira (a commercial 3D visualization package) or 3dmod (an academic program for calculating and visualizing electron tomograms). We have modified and customized other

146

three-dimensional search software based on cross-correlation with a reference object to look just underneath the inner membrane for such a filament.

As a second specific example, we have produced the first three-dimensional reconstructions of the carboxysome, a bacterial pseudo-organelle critical for carbon fixation. Carboxysomes are filled with the large protein complex RuBisCO, and in order to understand the function of carboxysomes, we must elucidate the organization of RuBisCO molecules inside. We have modified existing academic search programs to run on the Structural Biology Supercomputer here at Caltech to identify and locate each RuBisCO molecule within various carboxysomes. Having identified the carboxysomes, we are developing custom software to search for patterns and clues about their organization.

Publications

Benjamin, J., Ganser-Pornillos, B.K., Tivol, W.F., Sundquist, W.I. and Jensen, G.J. (2005) Three-dimensional structure of HIV-1 virus-like particles by electron cryotomography. *J. Mol. Biol.* **346**:577.

Iancu, C.V., Wright, E.R., Benjamin, J., Tivol, W.F., Dias, D.P., Murphy, G.E., Morrison, R.C. Heymann, J.B. and Jensen, G.J. (2005) A "flip-flop" rotation stage for routine dual-axis electron cryotomography. *J. Struct. Biol.* **151**(3):215-314.

Iancu, C.V., Wright, E.R., Heymann, J.B. and Jensen, G.J. (2005) A comparison of liquid nitrogen and liquid helium as potential cryogens for electron cryotomography. *J. Struct. Biol.* Submitted for publication.

Leong, P.A., Heymann, J.B. and Jensen, G.J. (2005) Peach: A simple Perl-based system for distributed computation and its application to cryoEM data processing. *Structure* **13**:505-511.

Murphy, G.E. and Jensen, G. (2005) Electron cryotomography of the *E. coli* pyruvate and 2-oxoglutarate dehydrogenase complexes. *Structure*. In press.

Wright, E.R., Iancu, C.V., Tivol, W.F. and Jensen, G. (2005) Observations on the behavior of vitreous ice at ~82 and ~12 K. *J. Struct. Biol.* Submitted for publication.

Summary: The focus of the lab has been the coupling of theoretical, computational, and experimental approaches for the study of structural biology. In particular, we have placed a major emphasis on developing quantitative methods for protein design with the goal of developing a fully systematic design strategy that we call "protein design automation." Our design approach has been captured in a suite of software programs called ORBIT (Optimization of Rotamers By Iterative Techniques) and has been applied to a variety of problems ranging from protein fold stabilization to enzyme design.

240. Explicit treatment of water molecules in protein design

Benjamin D. Allen[1], Stephen L. Mayo

In computational protein design, interactions between a protein and solvent are modeled using continuum methods that do not explicitly treat individual water molecules. However, some water molecules are distinct from bulk solvent and play structural and functional roles. These waters cannot be accurately modeled with continuum methods, and may be important when designing proteins that bind other proteins, nucleic acids, and ligands. Our system for modeling these effects uses a library of amino acid conformations with bound water molecules and a scoring function that assigns energies to water-mediated interactions based on their geometries. The library was generated by culling examples of water-mediated interactions from a PDB survey and clustering these data to give representative conformers for water-mediated interactions with various geometries. The scoring function was designed based on the geometric constraints of hydrogen bonds. To assess the performance of our method, we chose a test set of protein positions that interact with DNA from 28 high-resolution crystal structures; only some of these interactions were water-mediated. Scoring function parameters were chosen to maximize the fraction of positions in the test set for which the wild-type amino acid was recovered. The values obtained were comparable to those published for analogous tests of other libraries and scoring functions. Furthermore, the optimal parameters found for the force field terms fell within physically reasonable ranges. However, this method never significantly improved the recovery of wild-type amino acids compared to the use of a traditional library. Larger conformer libraries, libraries custom-generated for each position, and various functional forms of the scoring function did not significantly improve the results. This is consistent with recently published work, and indicates that explicit treatment of water molecules in this fashion is unlikely to improve the quality of sequences found when designing protein-protein and protein-DNA interfaces. However, some elements of the method described here may be useful for modeling protein-ligand interactions in enzyme design.

[1]*Division of Chemistry and Chemical Engineering, Caltech*

241. Stabilization and biochemical characterization of a huntingtin antibody V_H region

Eun Jung Choi, Stephen L. Mayo

Huntington's disease is a neurodegenerative disorder caused by expansion of a polyglutamine tract in the huntingtin (htt) protein. Expression of this mutant htt results in selective death of neurons in the striatum and the cortex. Molecules blocking htt's toxic effects or its binding to other proteins may provide clues about the disease and could potentially be used as therapeutics. One possibility is an htt antibody. The Patterson lab, here at Caltech, has generated a recombinant single-chain antibody that recognizes the polyproline (polyP) tract in htt and reduces cell death when co-expressed with htt in cultured 293 cells. Reduced toxicity is also seen when only the heavy chain variable region (V_H) of this antibody is expressed. Our goal is to biochemically characterize this anti-polyP V_H and to stabilize the molecule by designing out the hydrophobic residues that exist on the interface between V_L and V_H in the complete antibody.

Our first design resulted in a five-fold mutant in which five hydrophobic residues in the interface are replaced by charged or polar residues. We are currently in the process of expressing and refolding these designed proteins.

242. Evaluating a force field via fixed-composition sequence design calculations

Oscar Alvizo[1], Stephen L. Mayo

A finely tuned force field is essential to protein design and protein folding. Proper tuning is problematic, however, due to difficulties in determining the appropriate scale factors for the force field parameters and in calculating the energy of proteins in the denatured state. ORBIT's force field was improved through iterative rounds of protein design calculations and experimental measurement of predicted sequence stabilities. In order to keep the energy of the denatured state constant, design calculations were performed under fixed amino acid composition restraints. Energy discrepancies between computational predictions and experimental results could then be attributed to flaws in the force field's ability to predict folded state sequence energies. The accuracy of the

148

force field was quantified in three ways: by comparing the amino acids of the predicted sequences to the wild type, by determining the sequence bias required to recover the wild-type sequence, and by comparing the experimental stabilities to the predicted sequence energies. The high native stability of the designed protein (the β1 domain of protein G) and the reduced sequence space resulting from the fixed composition restriction make it highly unlikely that predicted sequences that are vastly different from wild type will be more stable. Therefore, if the predicted sequences are significantly different from wild type, then the force field needs improvement.

Calculations started at a wild-type sequence bias of 0.0 kcal/mol, which was increased by increments of 1.0 or 0.5 kcal/mol until the wild-type sequence was recovered. The following modifications improved the predictive power of the force field: using a solvent exclusion-based solvation model, eliminating hydrogen bonds at the surface, including a rotamer probability scale factor, and decreasing the hydrogen bond well depth and polar burial scale factor. Using the improved force field, the bias required to recover a sequence with comparable experimental energy to the wild type was decreased from 6.0 to 0.5 kcal/mol. In addition, the improved force field successfully predicts a stable properly folded sequence without the need to bias the calculation towards the wild-type sequence.

[1]*Graduate Option in Biochemistry and Molecular Biophysics, Caltech*

243.   Structural and dynamic analysis of computationally designed protein G variants
Karin Crowhurst, Stephen L. Mayo

Protein function is frequently reliant on dynamic processes; proteins involved in ligand binding, enzyme catalysis and signal transduction often require structural flexibility and plasticity to function properly or interact with multiple targets. These entropic factors can also contribute to protein stability. Understanding dynamic motions in computationally designed proteins compared to wild type could therefore be crucial for improving the accuracy and consistency of stable *de novo* protein and enzyme production, with wide-ranging implications in medical and industrial applications. My project goals are: (a) to understand the degree to which our current protein design algorithm (ORBIT) produces proteins with native-like backbone and side-chain dynamics; and (b) to use this information to target algorithm modifications and move towards incorporating backbone flexibility into future designs.

I am using NMR spectroscopy to measure the backbone dynamics of several mutants of the β1 domain of Streptococcal protein G (Gβ1), for which structural flexibility is believed to significantly impact their respective stabilities [1]. Detailed analysis of these data will provide insight into the impact of dynamic processes on the stability of each variant in comparison to the wild type. Previously, we reported that a highly thermostable variant (Gβ1-c3b4) [2] unexpectedly dimerizes in solution. Preliminary analysis of crystallography data revealed that the interface is formed through a β-bridging interaction

with antiparallel β2 strands, each of which contains two of the protein's seven mutations. Interestingly, reversion of these two mutations to wild type does not completely eliminate dimer formation. NMR and analytical ultracentrifugation experiments are in progress to further characterize the dimer. Dynamic characterization of this hyperthermophile revealed significant conformational exchange for all backbone amides in the β2 strand and the adjacent region of the helix (caused in part by the monomer-dimer equilibrium). In contrast, the few backbone amides involved in conformational exchange in the six-fold core variant (FILIIW) are localized in residues close to mutations and do not cluster around any specific region of the tertiary structure. My ongoing experiments are providing clear evidence that the dynamic characteristics of these protein G variants differ significantly from wild type. These data are very important in gaining a more detailed understanding of the properties of computationally designed proteins and in highlighting aspects of the algorithm that may require modification to produce proteins that behave like naturally occurring moieties.

References
[1] Su, A. and Mayo, S.L. (1997) *Protein Sci.* **6**:1701-1707.
[2] Malakauskas, S.M. and Mayo, S.L. (1998) *Nature Struct. Biol.* **5**:470-475.

244.   Design and testing of engineered IgG antibodies with increased *in vivo* half-lives
Mary Devlin[1], Stephen L. Mayo

Antibody-based therapy has experienced recent successes in the treatment of inflammatory and cardiovascular diseases, viral infection, graft rejection, and various cancers. To increase the potency and efficacy of therapeutic antibodies, it is desirable to prolong their serum half-lives. Serum antibody levels are maintained because of rescue from degradation by the neonatal Fc receptor (FcRn), which binds to the Fc region of IgG in a pH-dependent manner. Evidence suggests that an IgG molecule with increased affinity for FcRn may exhibit increased serum persistence. Examination of the Fc/FcRn co-crystal structure indicates that there is an 89° interdomain angle adopted by the Cγ2-Cγ3 domains of bound Fc. Amino acids have been identified in this region that could be modified to favor this angle. We have used the protein design software package ORBIT to optimize the amino acid packing of the Cγ2-Cγ3 interdomain region in the bound structure. SPR (surface plasmon resonance)-based binding assays are used to analyze Fc mutants indicated by these calculations. By creating and analyzing proteins with sequences indicated by ORBIT calculations, we hope to design an Fc molecule that is stabilized for optimal binding to FcRn, resulting in an antibody with an extended serum half-life.

[1]*Graduate Option in Biochemistry and Molecular Biophysics, Caltech*

245. A search algorithm for fixed-composition protein design

Geoffrey K. Hom[1], Stephen L. Mayo

We created a computational protein design algorithm for finding low-energy sequences of fixed amino acid composition. The search algorithms used in protein design typically do not restrict amino acid composition. However, the random energy model of Shakhnovich suggests that the use of fixed-composition sequences may circumvent defects in the modeling of the denatured state. Our algorithm, FC_FASTER, links fixed-composition versions of Monte Carlo and the FASTER algorithm. As proof of principle, FC_FASTER was tested on an experimentally validated, full-sequence design of the β1 domain of protein G. For the wild-type composition, FC_FASTER found a lower-energy sequence than the experimentally validated sequence. Also, for a different composition, FC_FASTER found the hypothetical lowest-energy sequence in 14 out of 32 trials.

[1]*Graduate Option in Biochemistry and Molecular Biophysics, Caltech*

246. Computational design and experimental characterization of *de novo* protein dimers

Possu Huang, Stephen L. Mayo

To ultimately understand the physical and chemical principles of protein/protein interactions, we recently developed a specialized homodimer-docking algorithm for protein design purposes [1]. The docking algorithm positions a monomeric protein structure to a plausible configuration with respect to a copy of the same structure using parameters determined from the structures of known homodimer complexes. Protein models are docked as rigid bodies and the dimers are scored based on their interfacial surface complementarities. By applying this docking strategy along with computational protein design using ORBIT, we have constructed proteins that reflect many versions of our homodimer design. Hydrodynamic characterization of the molecules has shown evidence of self-association, but to definitively prove that the designs are successful, an X-ray structure is required. Two X-ray crystal structures of our designed proteins have been solved, and from them clues were found to improve the next iteration of the design cycle [2]. We are currently in the process of solving the X-ray structure of an improved design.

Building from our previous efforts in designing *de novo* homodimers, we are currently also developing algorithms to address target-directed interface design problems. A chosen site on a protein is represented by virtual "rotamer bundles" to represent side-chain conformational space in the docking process. A thorough re-parameterization of our docking algorithm is in progress for this process.

References

[1] Huang, P.-S., Love, J.J. and Mayo, S.L. (2005) *J. Comp. Chem.* **26**(12):1222-1232.
[2] Dahiyat, B.I. and Mayo, S.L. (1996) *Protein Sci.* **5**:895-903.

247. Computational design of the restriction endonuclease BglII

Jennifer R. Keeffe[1], Stephen L. Mayo

DNA binding proteins play many important roles *in vivo,* including essential roles in replication, transcription and genome maintenance. The ability to engineer proteins to specifically bind a given sequence of DNA would not only provide us with a means to create new research tools, diagnostics, and therapeutics, but would allow us to study protein-nucleic acid interactions. Computational design may provide an ideal method for optimizing protein-DNA interfaces to improve binding affinity and specificity. By coupling computational design and experimental validation, we hope to obtain a better understanding of the forces that drive protein-DNA interactions.

Toward this end, we are using the protein design software package ORBIT to investigate the restriction endonuclease, BglII. Initial designs, aimed at stabilizing this protein and testing it as a model system, predicted two mutations would increase hydrophobic packing in the interior: V160L and V204I. Preliminary experimental results indicate that the V160L and V204I variants bind the BglII DNA sequence with similar affinities and specificities to the wild-type enzyme. Both of these molecules also effectively cleave BglII DNA substrate, indicating that the tertiary structure of the protein is maintained. Additional experiments to determine the stabilities of these enzymes are underway.

We are also working to optimize the protein dimerization interface of BglII. Due to the symmetrical homodimerization of the BglII subunits, this enzyme binds and cleaves a palendromic restriction site. Using computational design, we are mutating the interface so that heterodimerization is thermodynamically favored over homodimerization. This new "heterodimeric" BglII may be used as the template for future calculations in which the DNA-binding interface of one subunit is designed, allowing us to create a BglII enzyme that binds and cleaves a non-palendromic restriction site.

[1]*Graduate Option in Biochemistry and Molecular Biophysics, Caltech*

248. Computational design of a novel enzyme for catalysis of a pericyclic reaction

J. Kyle Lassila[1], Stephen L. Mayo

We are working towards the goal of fully automated enzyme design. In particular, we hope to apply computational protein design methods to the task of creating a completely novel catalyst for the Claisen rearrangement of chorismate to prephenate. Naturally catalyzed by the chorismate mutases, this reaction offers many desirable features as an early test of enzyme design methods. The reaction is a first-order sigmatropic rearrangement of a single substrate and has neither intermediate steps nor involvement of catalytic groups such as general acids or bases. The reaction has been extensively studied in many contexts—as a rare enzyme-catalyzed pericyclic process, as an essential step in the biosynthesis of aromatic compounds, and as a rare example of a reaction that occurs through identical mechanisms

150

enzymatically and in solution. Our method of enzyme design involves identifying amino acid sequences likely to bind to an ab initio transition state structure of the chorismate-prephenate rearrangement. As a part of this process, we are testing new methods that allow translation and rotation of the transition state structure within a binding cavity while simultaneously optimizing protein side chain identity and conformation. When the design procedure was applied to a natural Escherichia coli chorismate mutase active site, a mutation was predicted that was shown experimentally to increase the catalytic efficiency of the enzyme [1]. These methods will be generally applicable to the design of ligand binding sites and enzyme active sites. The ability to computationally design new reaction catalysts can be expected to have important implications for organic synthesis, bioremediation, and biotechnology.

[1]*Graduate Option in Biochemistry and Molecular Biophysics, Caltech*

Reference

[1] Lassila, J.K., Keeffe, J.R., Oelschlaeger, P. and Mayo, S.L. (2005) *Protein Eng. Des. Sel.* **18:**161-163.

249. Computational design of a novel aldolase

Jessica Mao[1], Stephen L. Mayo

Designed enzymes are attractive industrially for their efficiency, substrate specificity, and stereoselectivity. To date, there are few enzymes used in organic synthesis. The aldol condensation is one of the most important and utilized carbon-carbon bond-forming reactions in synthetic chemistry. It is the reaction between two aldehyde/ketone groups, yielding a β-hydroxy-aldehyde/ketone that upon dehydration by acid or base affords an enone. While natural aldolases are efficient, they are very limited in their substrate range. Novel aldolases that catalyze reactions between desired substrates would be a powerful synthetic tool. They would expand the limited repertoire of designed enzymes and further our understanding of their structure/function relationship. We are adopting the "compute and build" design cycle that combines theory, computation, and experiment to rationally design a novel aldolase. Our initial design goal is to create an enzyme that will catalyze the reaction between acetone and benzaldehyde via the enamine mechanism that natural class I aldolases utilize. The design has been performed on the backbone structures of triosephosphate isomerase (TIM), and ribose binding protein (RBP). Potential catalytic sites were identified, and positive design was applied to increase the affinity of the protein for the substrate. A favorable design was generated and variant proteins were expressed and purified. Enzyme assays, however, showed the designed proteins to be inactive. Additional scaffolds have been explored, including fibronectin and lipid transfer proteins from plants. Further experiments are underway, and results will be used to optimize our design process.

[1]*Division of Chemistry and Chemical Engineering, Caltech*

250. Computational design of a novel enzyme to catalyze a kinetic resolution

Heidi K. Privett[1], Stephen L. Mayo

Fully automated enzyme design can be envisioned as the solution to many complex synthetic organic chemistry problems. Enzymes are ideal catalysts of organic reactions because of their extremely high rates of catalysis and their ability to perform a wide variety of chemical transformations with superb regio- and enantioselectivity. With an increasing demand for enantiomerically pure, complex, biologically active compounds (i.e., drugs), synthetic chemists will have to look beyond standard chemical strategies in favor of the high yields and strict selectivity of enzymatic reactions. Designed enzymes will not be restricted to the reactions accessible by natural enzymes, broadening the range of possible substrates and products.

Kinetic resolutions are a useful method for transforming a racemic starting material into an enantiomerically pure product. Our goal is to show that an enzyme can be designed to carry out a dynamic kinetic resolution using the enantioselective hydrolysis of 2-phenyl-4-benzylphenyloxazolin-5-one (FOX) to produce *N*-benzoyl-L-phenylalanine as a model system. To this end, we chose three catalytic residues including a protonated histidine, a neutral histidine and an arginine as residues to best stabilize the transition state and catalyze the hydrolysis.

We have used the ORBIT protein design software to design an optimal active site around an *ab initio* calculated transition state of the L-FOX hydrolysis reaction using the *E. coli* maltose binding protein (MBP) as a scaffold. An active site location and placement of the three catalytic residues were first chosen within the natural binding pocket of MBP based on the geometry of the catalytic residues with respect to the scaffold and the transition state structure. The remainder of the binding pocket residues were repacked around the catalytic residues and the transition state, resulting in a seven-fold mutant, named 1ANF-FFH. We are currently evaluating the effect of 1ANF-FFH on the rate of FOX hydrolysis and the enantiomeric enrichment of the product. Additional point mutants have also been identified in the background of 1ANF-FFH that may assist in substrate binding and/or catalysis.

[1]*Division of Chemistry and Chemical Engineering, Caltech*

251. Water-soluble membrane proteins by computational design

Premal S. Shah[1], Stephen L. Mayo

We continued our efforts to generate water-soluble variants of integral membrane proteins (IMPs) using computational design techniques. Previous attempts to convert the IMP bacteriorhodopsin (BR) were not completely successful because our design algorithms consider only the final folded state of a protein. BR requires that a covalently bound retinal cofactor be attached at a specific point during the folding pathway. By designing just the final folded state, we most likely altered the folding pathway in a way that prevented the attachment

of retinal. As a result, our designed BR molecule displayed hallmarks of an aggregated, soluble molten globule. The solubility in aqueous buffer led us to conclude that perhaps our previously established metric for converting membrane proteins, re-designing surfaces of membrane proteins to resemble those of water-soluble proteins, was effective. However, our selection of a molecule that is heavily dependent on its folding pathway for its final stability was not prudent. We therefore turned our attention to aquaporins. Specifically, we designed human aquaporin 1 (Aqp1) using our previously established metric. Aqp1 is a tetramer in its functional form and does not undergo any conformational changes upon oligomerization. In addition, no cofactors are essential for stability. A 2.2 Å structure served as the template for our designs. We left the oligomer contact points of the monomer units unaltered while converting nonpolar residues on the surface to polar residues using rules previously established in our laboratory. We synthesized the gene coding for the computer-generated amino acid sequence and attempted to express our designed Aqp1 molecule in both bacteria and insect cells. Unfortunately, the designed variant did not express in either host despite attempting various expression conditions. Ongoing efforts include modifying the design with hopes of generating a variant that will express and continuing to alter expression conditions.

[1]*Graduate Option in Biochemistry and Molecular Biophysics, Caltech*

252. Improved continuum electrostatics and solvation for protein design

Christina Vizcarra[1], Stephen L. Mayo

Electrostatic interactions and the solvation of polar amino acids are crucial for the function and stability of proteins. The Finite Difference Poisson-Boltzmann (FDPB) model has generally been considered the most accurate continuum model. There are two main challenges for implementing an accurate description of continuum electrostatics in protein design force fields. The first is the combinatorial explosion that results from having to select from 20^n possible sequences, where n is the number of amino acid positions being optimized. A computationally demanding model is unacceptable for scoring all possible interactions in 20^n sequences.

The second challenge arises from the requirement that energy terms be expressed as a function of two or fewer amino acid conformations. This two-body requirement is a problem for the FDPB model, which is sensitive to the surrounding environment and is effectively a many-body model. We demonstrated that, for the FDPB solver DelPhi [1], approximate representations of the protein surface and a two-body energy model can be used to reproduce the results of traditional calculations in which all amino acids are represented [2].

We incorporated this pairwise decomposable version of DelPhi into our ORBIT protein design software. This modified ORBIT force field has been used in a series of conformational optimizations. The energies predicted by ORBIT with the DelPhi module correlate well (R=0.97) with experimentally determined stabilities for

seven variants of the all α-helical *Drosophila* engrailed homeodomain (ENH) [3]. These sequences differ only in the identity of their surface residues, including charged residues in the context of helix macro-dipoles. The correlation between predicted energies and experimental stabilities has motivated current work in which the improved electrostatics force field is being used to design a thermophilic variant of ENH. Based on these preliminary results, we also hypothesize that the accuracy of this force field will carry over for cases in which electrostatics are important determinants of function, including enzyme active sites.

[1]*Division of Chemistry and Chemical Engineering, Caltech*

References

[1] Rocchia, W., Alexov, E. and Honig, B. (2001) *J. Phys. Chem. B* **105**:6507-6514.
[2] Marshall, S.A., Vizcarra, C.L. and Mayo, S.L. (2005) *Protein Sci.* **14**:1293-1304.
[3] Marshall, S.A., Morgan, C.S. and Mayo, S.L. (2002) *J. Mol. Biol.* **316**:189-199.

253. Design and screening of fluorescent protein libraries

Thomas P. Treynor, Marco A. Mena[1], Patrick S. Daughert[1], Stephen L. Mayo

The fluorescence line shape of the intrinsic fluorophore of the green fluorescent protein depends not only on its chemical identity, but also on its environment. We aim to investigate the relationships between this line shape and the conformational flexibility of this environment by entering a cycle of high-throughput spectroscopy, sequencing and computation. We have developed a structure-based computational method for designing protein libraries defined by the combinatorial shuffling of mutations. Tests of this method with the green fluorescent protein indicate that its designed libraries are greatly enriched with functional fluorescent proteins compared with other methods of library design. Flow cytometry is being used to screen designed libraries with a theoretical diversity of more than 10^6 sequences for proteins with exceptional fluorescence line shapes. Hundreds of mutants will then be sequenced following a second screen using the increased spectral resolution of a monochromator-based plate reader. The cycle will be completed by estimating the entropies of the different sequences and by investigating the relationships between the values calculated and the spectra observed. Both the improved understanding of spectroscopic structure-function relationships and the development of novel screens will facilitate the ongoing search for fluorophores optimized for biological research and medical diagnostics applications. Insights gained may be transferable to engineering other functions of proteins that depend on their electronic structure and dynamics, such as enzymatic catalysis.

[1]*Department of Chemical Engineering, UCSB*

254. Force field development for protein design

Eric Zollars[1], Stephen L. Mayo

Protein design is an exceptionally difficult problem characterized by unique complications. Necessary restrictions such as a fixed backbone and discrete side-chain conformations require different considerations of structure-energy relationships than other fields of protein simulation. This structure-energy relationship is the focus of our recent research, which hopes to address issues including the identity of the forces that lead to protein stability and the relative strengths of these forces. Additionally, the mathematical representation of these forces must be relatively simple to allow for tractable design calculations.

It is thought that local side-chain-backbone interactions are responsible for a great deal of the basic structure of proteins. A purely physical representation of these interactions is complex due to the small distances involved. An accurate statistical treatment of these interactions may allow for better designs in areas of protein secondary structure. We are therefore investigating the utility of including a statistically-based secondary structure propensity term in the force field.

An entropic term has also been added to the forces considered during a design calculation. It is often observed that an enthalpic-entropic "balance" occurs in proteins. Simply, a protein's overall stability is a result of contributions from entropic and enthalpic components. Since most of the other energy terms used in protein design are enthalpic in nature, the addition of an entropic term is a useful feature.

A previous component of this research included the development of a method to allow for quick parameterization of the energy terms used in the design calculations. The use of a large database of thermodynamic data to arrive at useful parameters was dropped because of the large relative errors within the database. The current method is based on the assumption that naturally occurring protein sequences are nearly optimal for their respective structures [1]. This method will achieve parameters that are not perfectly optimized, but because of the conservative nature of this approach, the parameters are expected to lead to stable designed proteins.

[1]*Graduate Option in Biochemistry and Molecular Biophysics, Caltech*

Reference

[1] Kuhlman, B. and Baker, D. (2000) *Proc. Natl. Acad. Sci. USA* **97**:10383-10388.

Publications

Choi, E.J. and Mayo, S.L. (2005) Generation and analysis of proline mutants in protein G. Submitted.

Gillespie, B., Shah, P.S., Wei, Y., Fortin, M. Hecht, M., Mayo, S.L. and Plaxco, K. (2005) On the origins of the thermostability of *de novo* designed proteins. Submitted.

Hom, G.K., Lassila, J.K., Thomas, L.M. and Mayo, S.L. (2005) Dioxane contributes to the altered conformation and oligomerization state of a designed engrailed homeodomain variant. *Protein Sci.* **14**:1115-1119.

Hom, G.K. and Mayo, S.L. (2005) A search algorithm for fixed-composition protein design. Submitted.

Huang, P.S., Love, J.J. and Mayo, S.L. (2005) Adaptation of a fast Fourier transform-based docking algorithm for protein design. *J. Comput. Chem.* **26**:1222-1232.

Lassila, J.K., Keeffe, J.R., Oelschlaeger, P. and Mayo, S.L. (2005) Computationally designed variants of *Escherichia coli* chorismate mutase show altered catalytic activity. *Protein Eng. Des. Sel.* **18**:161-163.

Love, J.J., Huang, P. and Mayo, S.L. (2004) A *de novo* designed protein/protein interface. Submitted.

Marshall, S.A., Vizcarra, C.L. and Mayo, S.L. (2005) One- and two-body decomposable Poisson-Boltzmann methods for protein design calculations. *Protein Sci.* **14**:1293-1304.

Oelschlaeger, P. and Mayo, S.L. (2005) Hydroxyl groups in the ββ sandwich of metallo-β-lactamases favor enzyme activity: A computational protein design study. *J. Mol. Biol.* **350**:395-401.

Oelschlaeger, P., Mayo, S.L. and Pleiss, J. (2005) Impact of remote mutations on metallo-β-lactamase substrate specificity: Implications for the evolution of antibiotic resistance. *Protein Sci.* **14**:765-774.

Shah, P.S., Hom, G.K. and Mayo, S.L. (2004) Preprocessing of rotamers for protein design calculations. *J. Comput. Chem.* **25**:1797-1800.

Shukla, U.J., Marino, H., Huang, P.S., Mayo, S.L. and Love, J.J. (2004) A designed protein interface that blocks fibril formation. *J. Am. Chem. Soc.* **126**:13914-13915.

Ethel Wilson and Robert Bowles Professor of Biology: James H. Strauss
Senior Research Associate: Ellen G. Strauss
Visiting Associate: Yukio Shirako
Postdoctoral Scholars: Marlene Biller, Pritsana Chomchan
Graduate Student: Jannigje Siebenga
Undergraduate Students: Ashley Grant, Oran Kremen
Research Laboratory Staff: Brian Blood, Maria Farkas

Summary: We are interested in two groups of animal viruses, the alphaviruses and the flaviviruses. These contain RNA genomes of about 11,000 nucleotides and are enveloped, having a lipid envelope that surrounds an icosahedral nucleocapsid. Both alphaviruses and flaviviruses are vectored by mosquitoes and infect both mosquitoes and a wide range of vertebrates. We wish to understand the replication of alphaviruses and flaviviruses at a molecular level and to study the evolution of these two virus groups and more broadly the evolution of all RNA viruses.

The flaviviruses contain about 70 members, most of which are important human pathogens causing hundreds of millions of cases of human disease annually. Diseases caused by the flaviviruses include yellow fever, dengue fever, and encephalitis. West Nile virus, which first appeared in the Americas six years ago in New York state and then spread rapidly over most of the United States, is a member of this family. The genome RNA of about 10,700 nucleotides is the only viral message RNA and is translated into a long polyprotein that is cleaved to give both structural proteins required for virus assembly and nonstructural proteins required for RNA replication.

The alphaviruses contain about 28 members and many cause febrile illness in humans tht in some cases may progress to encephalitis or polyarthritis. The genome organization of alphaviruses differs from that of flaviviruses in that the genome of 11,700 nucleotides is translated into a long nonstructural polyprotein, whereas the structural proteins are translated as a distinct polyprotein from a subgenomic RNA. Remarkably, however, the structures of the virions in the two groups have been found recently to be related. One of the two glycoproteins present on the exterior of the virions, called E in the case of flaviviruses and E1 in alphaviruses, are structurally identical. There are other similarities in the structures of the virions in the two groups, including the formation of a heterodimer E or E1 and the second external glycoprotein that function in an equivalent fashions. It seems clear that the virus structures, although they differ in important ways, are derived from a common ancestral source. We have suggested that this common structure may be important in the life of these viruses as arboviruses, capable of infecting both hematophagous arthropods and vertebrates.

We have started an ambitious collaboration with structural biologists at Purdue University to determine the structures of all of the proteins encoded by the viruses to atomic resolution. We have now determined the structure of dengue virus to 9.5 Å and the structure of immature dengue virus that contains uncleaved prM to 11 Å. This resolution is high enough that the glycoproteins can be positioned with confidence in the virus particle, that carbohydrate side chains of the glycoproteins can be seen, and even the membrane spanning domains that anchor the glycoproteins can be identified and traced. Of great interest is the fact that E undergoes large structural rearrangements upon conversion of the immature virus to the mature form and again upon conversion of the mature virus to the fusion-competent form.

The following abstracts describe some of these structural studies as well as the construction of mutants of alphaviruses and flaviviruses tht are used to probe the structures of mature and immature virions and the functions of the various proteins in the virus live cycle.

255. Construction of a chimeric virus with the yellow fever virus backbone and the structural proteins of dengue 2 virus
Pritsana Chomchan

Complementary sequences in the 5' end of the capsid protein and in the 3' non-translated region (NTR) allow flavivirus viral RNA to cyclize, and this cyclization is required for viral RNA replication. We have made two constructs of full-length YF containing CP, prM and E from DEN. Initially these constructs replicated poorly since the cyclization sequences were incomplete. Now we have made two new chimeras in which these sequences were restored. In the first construct, called "5' YFV/DEN," the 5' cyclization sequence in DEN capsid was changed to that of YF (nt 125-144 of DEN replaced by nt 147-165 of YF), and in the second, called "3' YFV/DEN," the 3' NTR of YF was changed to that of DEN (nt 10748-10766 of YF to nt 10598-10616 of DEN). Growth curves of the 5' and 3' chimeras as well as YFV and DEN 2 in both BHK and C6-36 (mosquito) cell lines, showed that 5' and 3' chimeras replicated well, similar to wtYFV, but DEN 2 replicated poorly in BHK cells although it replicated efficiently in C6-36 cells. A similar growth curve was also performed using chicken embryo fibroblasts. Interestingly, YFV, and the 5' and 3' chimeras replicated in chicken embryo cells but DEN did not. This indicated that the YFV nonstructural proteins play an more important role in host range than the DEN structural proteins. We hope to be able to produce enough of the 3' and 5' chimeras for cryo-electron reconstructions.

256. ***In vitro* reactivation of immature dengue virus particles**
Pritsana Chomchan

Flaviviruses produce two surface glycoproteins that are used in the assembly of virus particles. These proteins, called prM and E, initially form a heterodimer. At some point in the assembly of virions, prM is cleaved by a cellular protease called furin to produce M. E then rearranges to form homodimers in the mature virion. It is possible to produce immature virus particles that contain uncleaved prM by growing the virus in the presence of ammonium chloride. This lysosomotrophic agent causes the pH of endosomal vesicles through which virus is transported to rise, which in turn prevents cleavage of prM by furin. It is not known if these immature particles are true intermediates in virus assembly; it has been reported that noninfectious, prM-containing particles can be converted into infectious virions by treatment with furin. We have treated immature dengue virus (DEN) *in vitro* with furin after low pH treatment. Cleavage of prM to pr and M was detected by silver staining and Western blot assay using antiserum against DEN prM. However, we could not detect M protein due to the small size of the protein and unavailability of antiserum to M. Reactivated infectivity was assayed by infecting BHK cells with furin-treated virions. Infected cells were detected by immunofluorescence using anti-DEN antiserum. We have been able to reactivate immature particles to form mature particles. However, we were unable to detect the reactivated particles by electron microscopy. The ultimate goal is to reactivate sufficient numbers of particles for cryo-electron reconstructions.

257. The function of yellow fever virus envelope protein in virus assembly
Marlene Biller, Brian Blood, Maria Farkas

The viral envelope (E) protein of yellow fever virus forms 90 head-to-tail dimers that lie parallel to and completely cover the viral membrane in mature virions. Dimers of E protein have also been fitted into the cryoelectron density envelope of dengue virus. For this reason we wanted to determine how important dimer formation by E protein is for the overall configuration (and perhaps the stability) of flaviviruses. The E protein has several major functions, including receptor attachment and membrane fusion, and it also carries the major antigenic epitopes leading to a protective immune response. The E protein has an elongated shape and is composed of three major parts: a central domain that contains the N-terminal region (domain I), the fusion and dimerization domain (domain II), and a C- terminal putative receptor binding domain (domain III). In mature virions the fusion peptide is probably protected by the domain III of the opposite E protein in the dimer. A set of mutants have been made to investigate dimer formation. These residues to be mutated are in contact regions of the homodimer and were carefully selected for their locations and for their degree of conservation among flaviviruses.

We have made eight mutations to the current time. Three are in domain II: F1 mutation of E251 to K; F2, mutation of E251 to Q; and F3, mutation of S253 to P to insert a helix breaker. There are four in domain III: F4, deletion of amino acids 313 to 314; F5, deletion of amo acids 313 to 316; F7, mutation of T311 to A; F8, mutation of V319 to D. F6 consists of an insertion of three Ala residues at residue 155 in domain I. The mutations were made in a transient expression vector, and most of them have been introduced into the full-length yellow fever virus clone (pACNR vector). RNA is transcribed *in vitro* and used to transfect BHK cells. RNA replication is detected by immunofluorescence, and virus infectivity is checked by plaque assay.

Mutants F1, F4, F7 and F8 grew to titers comparable with wild-type titers. Mutant F6 was less infectious than wild type and gave plaques of significantly smaller size. Mutant F3 contains two additional mutations, aa 333, a proline to a serine (domain I) and aa 205, a valine to a alanine (domain II). It was not infectious in this stage, but we are working with F3 to take away these extra mutations, so we can evaluate our desired mutation.

Mutant F2 was infectious, but very weak. Mutant F5 was not infectious. It is very interesting that mutant F4 (Deletion of amino acids 313 to 314) was infectious like wt, but F5 (Deletion of amino acids 313 to 316) was not infectious. We plan to grow all the mutants together under exactly identical conditions and determine if the mutants form dimers by examining the proteins on native gels or treating them with cross-linking reagents.

258. Flexibility of yellow fever E protein
Marlene Biller, Ashley Grant

An immature flavivirus particle contains 60 trimers of prM-E heterodimers. The prM protein covers the E protein, and serves to protect it against premature fusion when passing through the acidic compartments and vesicles of the *trans* Golgi network. The prM protein is then cleaved off by a host cell enzyme, furin, shortly before virus release. Then the virus enters its mature state where the E proteins form 90 head-to-tail dimers that lie parallel and completely cover the viral membrane. In mature virions the fusion peptide is probably protected by the opposite E protein in the dimer. After entering cells by receptor-mediated endocytosis, fusion with the host membrane is initiated by low pH induced conformational change of the E protein.

Flexibility of the E protein is apparently a functional requirement for assembly of and infection by a flavivirus. Zhang *et al. (Structure*, Vol. 12, September, 2004*)* showed that the E protein can bend about a hinge between DI+DIII and DII, and noted presence of conserved glycins in the hinge region, between domain I and domain II. Since the flexibility of the E protein of flavivirus is so important for the virus for maturation and fusion, we believe that these small, uncharged glycins and alanines can be of great significance for the E protein. We have exchanged these glycins and alanines with amino acids that we think could affect flexibility of the E protein

but perhaps not destroy conformation. The hinge mutations include changing the Ala at amino acid 54 to Ileu and Lys (H1-1 and H1-2), changing the Ala at amino acid 187 to Ileu and Lys (H3-1 and H3-2), and changing the Gly at amino acid 297 to Ileu, Lys, and Thr (H4-1, H4-2 and H4-3).

We use the Quick Change mutagenesis kit from Stratagene to make these mutants. All but H4-1 are in the full-length yellow fever vector and have been sequenced. H4-1 is in a shuttle vector. We have transcribed RNA from full-length clones of some of the mutants and transfected BHK cells. RNA replication was detected by immunofluorescence, and virus infectivity checked by plaque assay. The H3-1 mutant was infectious, but weaker than wt. Mutants H4-3 and H4-2 were not infectious. With immunofluorescence they gave nice single transfected cells when stained with an anti-yellow fever antibody, but when stained with an anti-E antibody they gave nothing, suggesting that the E protein is not stable, probably due to incorrect conformation of the E protein. We want to compare how important the conserved glycine and alanines are for the hinge regions and for protein conformation.

If the E protein flexibility is affected by any of these hinge mutants, and the mutant virus is alive, we can purify it and send them to Purdue for cryo-electron microscopic reconstruction.

259. Generation of Sindbis-containing PE2 glycoproteins

Marlene Biller, Pritsana Chomchan

Sindbis virus is a member of the *Alphavirus* genus within the *Togaviridae* family. Sindbis contains a plus strand RNA genome, and has a lipid envelope that surrounds an icosahedral nucleocapsid. Sindbis virus contains 240 copies each of three structural proteins: two transmembranal glycoproteins (E1 and E2) and a capsid protein. The structural proteins of Sindbis are translated from a 26S subgenomic RNA as a polyprotein. The capsid protein is cleaved by the viral capsid autoprotease shortly after synthesis. In the endoplasmic reticulum, PE2 (precursor of E2) and E1 are produced, and rapidly associate to form $(PE2/E1)_3$ heterotrimers. PE2 is cleaved by furin in a post Golg compartment before the trimers are delivered to the plasma membrane to form E2 and E3. The last four amino acids of E3 contain the furin recognition sequence (RXRR or RXKR) in almost all alphaviruses. PE2-containing particles have been produced for Semliki Forest virus and shown to be non-infectious. We are interested in determining the structure of Sindbis virions containing PE2 and therefore we are removing the furin cleavage sites between E3 and E2 in full-length cDNA clones of Sindbis. We have created three mutants: SBI1 RSKR> RSKS, and SBI2 RSKR> RSKL, which mutate the furin cleavage site and SBI3 SV1> NIT at the N terminus of E3, which creates a N-glycosylation site.

All of these mutations have been put into full-length cDNA clones. They were infectious, but grew to a lower titer than wt. We have checked whether the virus is

produce PE2 by protein gel electrophoresis and followed by Western blot. The Western blot stained with anti E2 antibody showed that PE2 was produced. We have done large-scale preparations, and purified the virus on sucrose gradients. The purified virus will be checked with electron microscopy (EM) here at Caltech, and some are going to be sent to Purdue University for cryo-electron microscopy.

260. *In vitro* assembly of an enveloped virus

Odisse Azizgolshani*, William M. Gelbart*, Charles M. Knobler*, Marlene Biller

Sindbis virus, a member of alphavirus family, is a T = 4 enveloped animal virus whose simplicity and lack of virulence in humans make it a good candidate for *in vitro* studies. The mature virus is composed of a core or nucleocapsid comprised of 240 copies of the capsid protein and a single-stranded, plus-sense RNA molecule, and an envelope that is acquired from the host during budding. The envelope is a cell-derived phospholipid bilayer with 240 copies of the viral spikes embedded in it. The spikes are heterodimers of the E1 and E2 viral glycoproteins that are arranged with icosahedral symmetry in the bilayer. The endodomain of E2 glycoprotein in the heterodimer directly interacts with the capsid protein. The one-to-one correspondence between the spikes and the capsid proteins, as well as the confirmed physical interaction between the two, suggests a recruitment process in the final assembly of the virus. We hypothesize that viral envelopment – and therefore budding – is driven by this one-to-one interaction of the spikes and capsid proteins, and no cellular processes are required in the last step of assembly. In other words, if naked nucleocapsids were allowed to interact with a spike-coated membrane *in vitro*, enveloped virions should emerge, thus reconstituting Sindbis virus. Our approach requires the gentle removal of the viral envelope with non-denaturing detergents while avoiding disruption of the membrane or denaturation of the glycoproteins and then allowing the self-assembly of nucleocapsids and envelope to produce infectious virus as the detergent is removed. We are determining the threshold detergent concentration for envelope removal, using loss of infectivity as the assay; envelope removal will also be confirmed by electron microscopy. After removal of the detergent, reconstitution of the enveloped virions will be checked by electron microscopy as well. The most stringent assay for *in vitro* assembly of an enveloped virus will be the restoration of infectivity.

*UCLA, Department of Chemistry and Biochemistry

261. Hinge mutations in the yellow fever virus envelope protein

Ashley Grant

Studies have shown that yellow fever virus envelope protein E contains a "hinge" between the first and third domains. A degree of flexibility of the virus protein seems to be a necessity for virus assembly and infection. Currently we are making mutations in this "hinge" region which might affect the flexibility of the virus but not change the entire conformation. The mutations include

changing the Ala at amino acid 54 to isoleucine and to lysine, the Ala at amino acid 187 to isoleucine and lysine, and the glycine at amino acid 279 to isoleucine, lysine, and threonine. These mutations are being made through a Quikchange Kit from Stratagene. Once all the single mutations are made the mutations can then be combined to make double mutations in the E protein of yellow fever virus, and both single and double mutations will be inserted into the full-length cDNA clone of yellow fever virus. RNA transcribed *in vitro* from wild type and the mutants will then be used to transfect BHK (baby hamster kidney) cells. Replication will be measured by immunofluorescence and production of infectious virus can be determined by plaque assay. Once these experiments are completed the mutants will then be sent to Purdue University for cryo-electron microscopic reconstruction.

Publications

Monath, T.P., Kanesa-thasan, N., Guirakhoo, F., Pugachev, K., Almond, J., Lang, J., Quentin-Millet, M.-J., Barrett, A. D.T., Brinton, M.A., Cetron, M.S., Barwick, R.S., Chambers, T.J., Halstead, S.B., Roehrig. J.T., Kinney, R.M., Rico-Hesse, R. and Strauss, J.H. (2004) Recombination and flavivirus vaccines: a commentary. *Vaccine* **23**:2956-2958.

Mukhopadhyay, S., Zhang, W., Gabler, S., Chipman, P.R., Strauss, E.G., Strauss, J.H., Baker, T.S., Kuhn, R.J. and Rossmann, M.G. (2005) Mapping the E2 glycoproteins of alphaviruses. *Structure*. In press.

Smits Professor of Cell Biology: Alexander Varshavsky

Postdoctoral Scholars: Christopher Brower, Emmanuelle Graciet, Cheol-Sang Hwang, Rong-Gui (Cory) Hu, Konstantin Piatkov, Jun Sheng, Haiqing Wang, Zanxian Xia, Jianmin Zhou
Undergraduate Student: Richard Jones
Laboratory Manager: Raisa Solomatina

Summary: Our main subject is the ubiquitin (Ub) system. In the 1980's, the complementary advances by the Avram Hershko's laboratory at the Technion (Israel) and by my laboratory, then at MIT, revealed three sets of previously unknown facts:

    (i) that the ATP-dependent intracellular protein degradation involves a new protein modification, ubiquitin conjugation, which is mediated by specific enzymes, termed E1, E2 and E3;

    (ii) that the selectivity of ubiquitin conjugation is determined by specific degradation signals (degrons) in short-lived proteins, including the degrons that give rise to the N-end rule;

    (iii) that ubiquitin-dependent processes play a strikingly broad, previously unsuspected part in cellular physiology, primarily by controlling the levels of specific proteins. Ub conjugation was demonstrated to be required for the protein degradation *in vivo*, for cell viability, and also – more specifically – in the cell cycle, DNA repair, protein synthesis, transcriptional regulation, and stress responses. Ub-dependent proteolysis was also discovered to involve a substrate-linked poly-ubiquitin chain of unique topology, and to exhibit the crucially important property of subunit selectivity, i.e., the ability to destroy a specific subunit of an oligomeric protein, leaving intact the rest of it.

    The Hershko laboratory was responsible for the first and earliest of these fundamental advances (item i), and my laboratory for the other two (items ii and iii).

    As a result of these discoveries in the 1980s, the ubiquitin field has undergone an enormous expansion and is now one of the largest and most important arenas in biomedical science, the point of convergence of many disparate disciplines. Ramifications of these developments for clinical medicine are just beginning to be felt, and will be major, given the astounding functional range of the ubiquitin system, and a multitude of ways in which ubiquitin-dependent processes can malfunction in disease, from cancer and neurodegenerative syndromes to perturbations of immunity and many other illnesses, including birth defects. The subunit selectivity of the Ub system is one of its most important attributes, making possible the proteolysis-mediated remodeling of intracellular proteins. This capability is employed in many circuits, from the cell cycle oscillator to signal

transduction. Our work at Caltech continues to focus on Ub-dependent processes.

    The effect of an intracellular protein on the rest of the cell depends on the protein's concentration. The latter is determined by the rate of synthesis and/or import of the protein in relation to the rates of its degradation, inactivation by other means, or export from the compartment. The *in vivo* half-lives of intracellular proteins range from a few seconds to many days. Over the last decade, a vast number of biological circuits were shown to contain either constitutively or conditionally short-lived proteins. In addition, damaged or otherwise abnormal intracellular proteins tend to be recognized as such and selectively degraded, largely by the same Ub-proteasome system that mediates the controlled proteolysis of short-lived regulatory proteins. The metabolic instability of a regulator provides a way to generate its spatial gradients and allows for rapid adjustments of its concentration (or subunit composition) through changes in the rate of its synthesis or degradation.

    Ubiquitin (Ub) is a 76-residue protein that exists in cells either free or conjugated to many other proteins. Degradation of intracellular proteins by the Ub-proteasome system regulates a multitude of processes: cell growth, cell division and differentiation, signal transduction, responses to stress, and a broad range of metacellular (organismal) processes, as well from embryonic development to immunity and the functions of the nervous system. Ub-dependent proteolysis involves the "marking" of a substrate through covalent conjugation of Ub to a substrate's internal Lys residue. Ub conjugation is mediated by the E1-E2-E3 enzymatic cascade. E1, the ATP-dependent Ub-activating enzyme, forms a thioester bond between the C-terminal Gly of Ub and a specific Cys residue of E1. In the second step, activated Ub is transesterified to a Cys residue of a Ub-conjugating (E2) enzyme. Thereafter a complex of E2 and another enzyme, E3, conjugates Ub to a Lys residue of a substrate. The functions of E3 include the recognition of a substrate's degradation signal (degron). The numerous proteolytic pathways of the Ub system have in common their dependence on Ub conjugation and the 26S proteasome (which processively degrades Ub-protein conjugates), and differ largely through their utilization of distinct E2-E3 complexes. Specific E3s recognize (bind to) specific degrons of their substrates. The diversity of E3s and E2s underlies the enormous range of substrates that are recognized and destroyed by the Ub system, in ways that are regulated both temporally and spatially.

    One pathway of the Ub system is the N-end rule pathway (Fig. 1). The N-end rule, which relates the *in vivo* half-life of a protein to the identity of its N-terminal residue, was discovered by this laboratory in 1986, in experiments that explored the fate of a fusion between Ub and a reporter protein such as *E. coli* β-galactosidase (βgal) in the yeast (fungus) S. *cerevisiae*. In eukaryotes, Ub-X-βgal is cleaved, cotranslationally or nearly so, by deubiquitylating enzymes (DUBs) at the Ub-βgal junction. This cleavage takes place regardless of the identity of the residue X, proline being the single exception. By allowing a bypass of the normal N-terminal processing of a newly formed protein, this result yielded an *in vivo* method (the

Ub fusion technique) for generating different residues at the N-termini of otherwise identical proteins, a technical advance that led to the finding of the N-end rule. The *in vivo* half-lives of resulting X-βgal proteins were shown to range from ~2 min (e.g., Arg-βgal or Leu-βgal) to longer than 20 hr (e.g., Met-βgal or Gly-βgal), depending on the identity of their N-terminal residue (Fig. 1). The N-end rule-based degradation signal, called the N-degron, consists of a destabilizing N-terminal residue and an internal lysine (or lysines) of a substrate, the Lys residue being the site of formation of a substrate-linked poly-Ub chain. The ubiquitylated substrate is degraded by the 26S proteasome.

The N-end rule pathway is present in all organisms examined, from mammals and plants to fungi and prokaryotes. The currently known functions of the N-end rule pathway include the regulation of peptide import in yeast, through the conditional (modulated by peptides) degradation of the repressor CUP9 that down-regulates a peptide transporter; the maintenance of chromosome stability, through the degradation of a separase-produced fragment of SCC1 (a subunit of cohesin) at the metaphase-anaphase transition; the regulation of meiosis in yeast and mammals; an essential role in the mammalian cardiovascular development; the regulation of apoptosis in *Drosophila*, through the degradation of DIAP1, an inhibitor of apoptosis, and a role in the leaf senescence in plants.

Functional and mechanistic studies of the N-end rule pathway in yeast and mammals are a major theme of our current work.
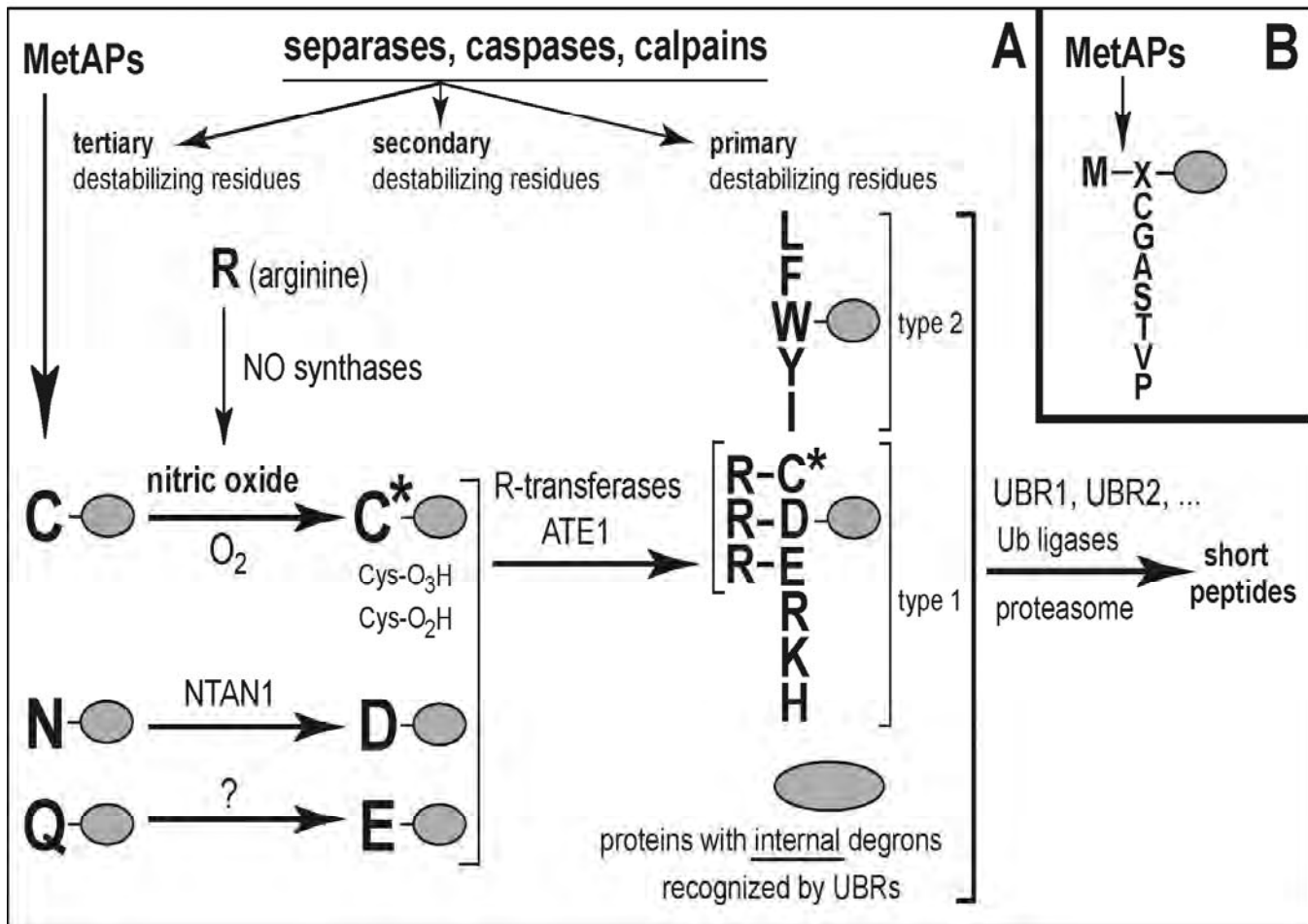
Fig. 1. (A) The N-end rule pathway in mammals. N-terminal residues are indicated by single-letter abbreviations for amino acids. The ovals denote the rest of a protein substrate. MetAPs, methionine aminopeptidases. The "cysteine" (Cys) sector, in the upper left corner, describes the recent discovery (see Abstract 264), a nitric oxide (NO)-mediated oxidation of N-terminal Cys, with subsequent arginylation of oxidized Cys by *ATE1*-encoded isoforms of Arg-tRNA-protein transferase (R-transferase). C* denotes oxidized Cys, either Cys-sulfinic acid ($CysO_2(H)$) or Cys-sulfonic acid ($CysO_3(H)$). Type 1 and type 2 primary destabilizing N-terminal residues are recognized by multiple E3 Ub ligases of the N-end rule pathway, including UBR1 and UBR2. Through their other substrate-binding sites, these E3s also recognize internal (non-N-terminal) degrons in other substrates of the N-end rule pathway, denoted by a larger yellow oval. (B) MetAPs remove Met from the N-terminus of a polypeptide if the residue at position 2 belongs to the set of residues shown.

263. Mechanistic and functional studies of N-terminal arginylation

Christopher Brower, Cory Hu, Jun Sheng, Jack Xu, Jianmin Zhou, Alexander Varshavsky

The N-end rule has a hierarchic structure. Specifically, N-terminal Asn and Gln are tertiary destabilizing residues in that they function through their deamidation, by N-terminal amidohydrolases, to yield the secondary destabilizing residues Asp and Glu, whose activity requires their conjugation, by *ATE1*-encoded Arg-tRNA-protein transferases (R-transferases), to Arg, one of the primary destabilizing residues. The latter are recognized by the Ub ligases (E3 enzymes) of the N-end rule pathway. In multicellular eukaryotes, the set of secondary destabilizing residues contains not only Asp and Glu but also Cys, the latter being a stabilizing residue in the yeast N-end rule (Fig. 1A).

The two previously characterized species of mammalian Arg-tRNA R-transferases (R-transferases), ATE1-1 and ATE1-2, are produced through alternative splicing of *ATE1* pre-mRNA (Kwon *et al.*, 1999). The ratio of *ATE1-1* to *ATE1-2* mRNA varies greatly among the mouse tissues: it is ~0.1 in the skeletal muscle, ~0.25 in the spleen, ~3.3 in the liver and brain, and ~10 in the testis, suggesting that the two R-transferases are functionally distinct. However, the substrate specificities of ATE1-1 and ATE1-2 are similar to that of the *ATE1*-encoded R-transferase of *S. cerevisiae*, in that they can arginylate N-terminal Asp and Glu, but cannot arginylate N-terminal Cys (Kwon *et al.*, 1999). Earlier work has shown that mouse *ATE1(-/-)* cells, which lacked *ATE1*-encoded R-transferases, are incapable of arginylating all three of the secondary destabilizing N-terminal residues, Asp, Glu and Cys, and that N-terminal Cys, in contrast to N-terminal Asp and Glu, is oxidized prior to its arginylation by R-transferase. These findings suggested that the arginylation branch of the N-end rule pathway may function as an oxygen sensor. *ATE1(-/-)* embryos die *in utero* around day E15. *ATE1(-/-)* embryos exhibit defective cardiogenesis and defective angiogenic remodeling of the early vascular plexus. Thus, *ATE1* is required for cardiovascular development, a new set of functions of the N-end rule pathway (Kwon *et al.*, 2002). More recent work discovered that the oxidation of N-terminal Cys *in vivo* requires nitric oxide (NO) (Hu *et al.*, 2005), an advance with several important ramifications (see Abstract 264).

Several mechanistic and functional studies of N-terminal arginylation in mammals and yeast are currently under way.

(i) Construction and functional analyses of mouse strains (and cells derived from them) in which the expression of *ATE1*-encoded Arg-tRNA-protein transferases (R-transferases) is selectively and conditionally abolished in specific cell lineages during embryogenesis, or postnatally (*Christopher Brower*). This set of projects should make it possible, among other things, a functional dissection of N-terminal arginylation in specific organ systems and cell types of adult mice. (A nonconditional *ATE-/-* genotype is embryonic lethal (see above).)

(ii) Construction and functional analysis of knock-in mouse strains that contain a doxycycline-inducible allele of *ATE1*, and thus, can overproduce R-transferases, in a controllable manner, in specific cell types during embryogenesis, or postnatally (*Jianmin Zhou, Christopher Brower*).

(iii) Identification and analysis of new isoforms of mouse R-transferase (*Cory Hu*).

(iv) Analysis of chromosome stability and regulation of apoptosis in mouse *ATE-/-* cells (*Jianmin Zhou, Jun Sheng, Cory Hu, and Christopher Brower*). These projects stem from the discovery of the function of the *S. cerevisiae* N-end rule pathway in the maintenance of chromosome stability (Rao *et al.*, 2001), from the conjecture that an analogous function in mammalian cells involves the (*ATE1*-dependent) arginylation branch of the N-end rule pathway, and from the recent finding that in mammals the putative DNA helicase RECQL4 is physically associated with UBR1 and UBR2, two Ub ligases of the mammalian N-end rule pathway (Yin *et al.*, 2004). Recent work (*Jianmin Zhou*) indicated that N-terminal arginylation is essential for the *in vivo* degradation of the separase-produced fragment of SCC1, a subunit of mouse cohesin. *ATE1-/-* EFs are phenotypically unstable as established cell lines, in that independently produced *ATE-/-* cell lines tend to differ in the sets of proteins they overproduce, relative to +/+ EFs (*Jun Sheng, Jianmin Zhou*).

(v) Identification of *ATE1*-dependent circuits (i.e., circuits that involve N-terminal arginylation) through the identification of mouse genes whose expression is significantly altered during embryonic development in *ATE-/-* embryos, using microarray techniques, differential display and analogous methods with *ATE-/-* and congenic +/+ embryos or EF cells (*Cory Hu, Jun Sheng, Jianmin Zhou*).

(vi) Identification of physiological substrates of R-transferases, through the testing of putative substrates of caspases and calpains that bear secondary or tertiary destabilizing N-terminal residues (*Jianmin Zhou*). The regulatory proteins RGS4, RGS5, and RGS16 have recently been demonstrated to be the *in vivo* substrates of R-transferase (see Abstract 264).

References

Hu, R.G., Sheng, J., Qi, X., Xu, Z., Takahashi, T.T. and Varshavsky, A. (2005) *Nature*. In press.

Kwon, Y.T., Kashina, A.S. and Varshavsky, A. (1999) *Mol. Cell. Biol.* **19**:182-193.

Kwon, Y.T., Kashina, A.S., Davydov, I.V., Hu, R.-G., An, J.Y., Seo, J.W., Du, F. and Varshavsky, A. (2002) *Science* **297**:96-99.

Rao, H., Uhlmann, F., Nasmyth, K. and Varshavsky, A. (2001) *Nature* **410**:955-959.

Varshavsky, A. (2004) *Curr. Biol.* **14**:R181-R183.

Yin, J., Kwon, Y.T., Varshavsky, A. and Wang, W. (2004) *Human Mol. Genet.* **13**:2421-2430.

264. **The N-end rule pathway as a nitric oxide sensor controlling the levels of multiple regulators**
Cory Hu, Jun Sheng, Xin Qi, Zhenming Xu, Terry Takahashi, Alexander Varshavsky

In mammals, destabilizing N-terminal residues that function through their arginylation are not only Asp and Glu but also Cys (Fig. 1A), which is a stabilizing (unarginylated) residue in the yeast *Saccharomyces cerevisiae*. The previously known functions of the N-end rule pathway are mentioned in introduction.

Nitric oxide (NO) is produced in eukaryotes largely by NO synthases. This compound and its derivatives play a role, as either stressors or regulators, in a vast range of functions, including cardiovascular homeostasis, immunity, neurotransmission, ion conductance, glycolysis, and apoptosis. Biological effects of NO are mediated by its covalent modifications of proteins, either of their prosthetic groups or amino acid residues, particularly Cys and Tyr. The reactivity of these residues toward NO is modulated by their sequence contexts. NO converts Cys residues to S-nitrosothiols, a process that can involve oxygen or its derivatives. S-nitrosylation modulates protein functions either directly or after additional (often oxygen-dependent) transformations that yield oxidized Cys, such as Cys-sulphinic acid ($CysO_2(H)$) or Cys-sulphonic acid ($CysO_3(H)$).

We recently demonstrated that the oxidation of N-terminal cysteine is essential for its arginylation (Hu *et al.*, 2005). Most importantly, it was also discovered that the *in vivo* oxidation of N-terminal cysteine, prior to its arginylation, require nitric oxide (NO) (Hu *et al.*, 2005). This accounted for N-terminal Cys being a destabilizing residue in mammalian cells, which produce NO, but stabilizing in yeast, which lack NO synthases.

We reconstituted the NO-dependent arginylation of N-terminal Cys in an *in vitro* system, as well (Hu *et al.*, 2005). This process requires a basic residue at position 2 of a substrate. The levels of regulatory proteins with this N-terminal motif (Cys-[basic residue]), such as RGS4, RGS5 and RGS16, are greatly increased in mouse *ATE-/-* embryos that lack arginylation (Hu *et al.*, 2005). RGS4, RGS5 and RGS16, which function as down-regulators of specific G proteins, are the first physiological substrates of mammalian N-end rule pathway. Given the involvement of these proteins in cardiovascular homeostasis and tubulogenesis, their stabilization is likely to underlie the previously observed abnormal angiogenesis and heart defects in *ATE-/-* embryos. A mammalian genome encodes approximately 30 proteins, including RGS4, RGS5 and RGS16, that contain the Met-Cys-[basic residue] N-terminal motif, which acts as a MetAP-cleaved, NO-dependent, arginylation-mediated, Cys-containing pre-N-degron. Together, the above discovery identified the arginylation branch of the N-end rule pathway as a new sensor of NO in mammalian cells that functions through its ability to destroy specific regulatory proteins bearing N-terminal Cys, at the rates controlled by NO, and apparently by oxygen, as well (Hu *et al.*, 2005).

Reference
Hu, R.G., Sheng, J., Qi, X., Xu, Z., Takahashi, T.T. and Varshavsky, A. (2005) *Nature* **437**:981-986.

265. **Mechanistic, structural, and functional studies of bacterial Leu/Phe-tRNA-protein transferases**
Emmanuelle Graciet, Konstantin Piatkov, Cory Hu, Alexander Varshavsky

While the N-end rule pathway also exists in prokaryotes, it differs from its eukaryotic counterpart both in the N-end rule's set of destabilizing residues and in mechanisms involved. As in eukaryotes, N-terminal Phe, Leu, Trp and Tyr are primary destabilizing residues in the prokaryotic N-end rule pathway as well, in that they are recognized directly by ClpAP, an ATP-dependent, proteasome-like protease. (Prokaryotes lack Ub and Ub ligases.) However, whereas N-terminal Asp and Glu are secondary destabilizing residues in eukaryotes (in that their require their preliminary conjugation to Arg by the *ATE1*-encoded R-transferase), in prokaryotes the secondary destabilizing residues are Arg and Lys [Tobias *et al.* (1991); Shrader *et al.* (1993)]. These N-terminal residues of a substrate are conjugated to either Phe or Leu (largely Leu in *E. coli*) by the *aat*-encoded Leu/Phe-tRNA-protein transferase (L/F-transferase).

Prokaryotic N-end rule pathways remain largely unexplored, particularly in regard to their functions. Most gram-negative prokaryotes contain Aat sequelogs (see Abstract 270 for a description of the recently introduced sequelog/spalog terminology (Varshavsky, 2004)), but their physiological substrates and functions remain unknown. Remarkably, some prokaryotes contain sequelogs of eukaryotic ATE1, as well. The substrate specificity of these putative prokaryotic R-transferases remains to be determined. The projects mentioned below aim to address some of the issues above.

(i) Enzymological dissection of Aat (Leu/Phe-tRNA-protein transferase). The residues of *E. coli* Aat involved in substrate binding and/or catalysis are unknown. To address the mechanism of *Aat*, we are using extensive site-directed mutagenesis, focusing on residues highly conserved amongst Aat sequelogs. To increase the power of such analyses, we are also developing better, more efficacious enzymatic assays for L/F-transferase. Yet another line of these studies involves binding assays to measure the physical affinity of purified Aat to either one of its two co-substrates: a polypeptide bearing N-terminal Arg or Lys, and Leu (or Phe)-tRNA.

(ii) Structural studies of Aat. Overexpressed and purified *E. coli* Aat (26 kD) and Aat from the thermophilic gram-negative eubacteria *Thermosynechococcus elongatus* are being used to crystallize Aat and determine its atomic structure. Among the approaches being employed are crystallization of either untagged Aat or fusions of Aat, via a rigid linker, to maltose-binding protein (MBP).

References
Tobias, J.W., Shrader, T.E., Rocap, G. and Varshavsky, A. (1991) *Science* **254**:1374-1377.
Shrader, T.E., Tobias, J.W. and Varshavsky, A. (1993) *J. Bact.* **175**:4364-4374.

266. Construction and analysis of mouse strains lacking the UBR3 ubiquitin ligase

Takafumi Tasaki[1], Yong Tae Kwon[1], Alexander Varshavsky

Kwon *et al.* (1998) identified two distinct mouse (and human) genes, termed *UBR2* and *UBR3*, which encode proteins that are similar to mouse UBR1 (E3α), the previously characterized E3 of the N-end rule pathway. In contrast to the highly similar mouse UBR1 and UBR2 proteins (47% identity and 68% similarity), the mouse UBR3 protein, while clearly a member of the UBR family, is less similar to UBR1 (25% identity and 51% similarity) and UBR2 (25% identity and 48% similarity). In addition, mouse UBR3 lacks some of the residues in its N-terminal region that have been shown to be essential for the function of yeast UBR1, and are also present in the mouse (and human) UBR1 and UBR2 proteins. We mapped and partially sequenced the mouse *UBR3* gene, and more recently constructed *UBR3(-/-)* mouse strains. *UBR3(-/-)* mice are viable, and are being characterized.

[1]*Present address: Dept. of Pharmaceutical Sciences, University of Pittsburgh, Pittsburgh, PA 15213*

Reference

Kwon, Y.T., Reiss, Y., Fried, V.A., Hershko, A., Yoon, J.K., Gonda, D.K., Sangan, K., Copeland, N.C., Jenkins, N. A. and Varshavsky, A. (1998) *Proc. Natl. Acad. Sci. USA* **95**:7898-7903.

267. Quantitative analyses of interactions between components of the N-end rule pathway and their substrates or effectors

Zanxian Xia, Alexander Varshavsky

Detailed understanding of the N-end rule pathway requires, among other things, the knowledge of equilibrium binding constants for the reversible interactions between UBR1 and its effectors or substrates. (With some interactions, it would be desirable to know the corresponding rate constants, as well.) We are carrying out these measurements using the fluorescence polarization (FP) technique, with purified *S. cerevisiae* UBR1 (or its fragments) and a variety of UBR1 ligands, including peptides with destabilizing N-terminal residues. These analyses will be expanded to include other physiological ligands of UBR1 such as the RAD6 Ub-conjugating enzyme, and CUP9, a homeodomain repressor recognized through its C-terminal degron by a distinct (third) substrate-binding site of UBR1.

268. Phosphorylation of UBR1: Its regulation and functions

Cheol-Sang Hwang, Zanxian Xia, Alexander Varshavsky

S. cerevisiae UBR1, the E3 of the yeast N-end rule pathway, is phosphorylated *in vivo*, but the role(s) of this UBR1 modification in the multiple functions of the N-end rule pathway is unknown. Phosphorylation sites on UBR1 and the kinases/phosphatases involved remain to be identified, as well. We are using biochemical and genetic approaches to understand, in functional and mechanistic detail, this modification of UBR1.

269. RECQL4, mutated in the Rothmund-Thomson and RAPADILINO syndromes, interacts with ubiquitin ligases UBR1 and UBR2 of the N-end rule pathway

Jinhu Yin[1], Yong Tae Kwon[2], Alexander Varshavsky, Weidong Wang[1]

Helicases are ATP-dependent RNA- or DNA-unwinding enzymes. Humans and other mammals contain at least five distinct helicases of the RecQ family, named after the single *RecQ* gene of *E. coli*. A malfunction or absence of specific RecQ-family helicases causes several human diseases: the Bloom syndrome (BS; mutations in the BLM helicase), the Werner syndrome (WS; mutations in the WRN helicase), and the Rothmund-Thomson syndrome (RTS; mutations in the RECQL4 helicase). One common property of these syndromes is predisposition to cancer. Clinical features of the Rothmund-Thomson syndrome (RTS) include postnatal growth retardation, skeletal abnormalities, skin and nail abnormalities, some aspects of premature aging, and predisposition to cancer, especially osteosarcoma. In the latter and several other respects, the phenotype of RTS differs from that of the Bloom syndrome, which predisposes to a large variety of cancers, and from the Werner syndrome, in which the pattern of cancer predisposition is also broader than in RTS, with a prevalence of various sarcomas.

Most (but apparently not all) cases of RTS are caused by autosomal recessive null or hypomorphic mutations in the *RECQL4* gene. An RTS-related disease, termed the RAPADILINO syndrome, with a lower predisposition to cancer, was found to be also caused by mutations in the *RECQL4* gene. The null phenotype of *RECQL4* in mice is death in early embryogenesis. While several lines of evidence suggest that cells from RTS patients are genetically unstable, the understanding of these phenotypes in RTS cells is far from advanced. One difference between RTS and, for example, BS is a near-normal frequency of sister chromatid exchanges (SCEs) in RTS cells, in contrast to high frequency of SCEs in BS cells. Human *RECQL4* encodes a 1,208-residue (133-kD) protein that contains characteristic sequences of the RecQ-family's helicase domain, but lacks other significant similarities to known proteins. RECQL4 has not been shown, thus far, to actually possess an RNA- or DNA-helicase activity, in contrast to the BLM and WRN DNA-helicases, whose enzymatic properties have been extensively characterized. No RECQL4-binding proteins have been identified so far, also in contrast to the BLM and WRN helicases, which are known to interact with each other and to function as components of large multiprotein complexes.

We have recently discovered (Yin *et al.*, 2004) that RECQL4 isolated from HeLa cells occurs as a stable complex with UBR1 and UBR2. These highly similar 200-kD proteins are the E3 components of Ub ligases of the N-end rule pathway. Although the known function of UBR1 and UBR2 is to mediate polyubiquitylation (and subsequent degradation) of their substrates, the UBR1/2-bound RECQL4 was not ubiquitylated *in vivo*, and was a long-lived protein. We discuss ramifications of these results, possible functions of RECQL4, and the

involvement of the N-end end rule pathway. These findings opened up new vistas in studies of both RECQL4 and the N-end rule pathway.

[1]*Laboratory of Genetics, National Institute on Aging, National Institutes of Health, 333 Cassell Drive, TRIAD Center Room 3000, Baltimore, MD 21224*
[2]*Center for Pharmacogenetics and Department of Pharmaceutical Sciences, School of Pharmacy, University of Pittsburgh, Pittsburgh, PA 15261*

Reference

Yin, J., Kwon, Y. T., Varshavsky, A. and Wang, W. (2004) *Human Mol. Genet.* **13**:2421-2430.

270. A family of mammalian E3 ubiquitin ligases that contain the UBR motif and recognize N-degrons

Takafumi Tasaki[1], Lubbertus Mulder[2], Akihiro Iwamatsu[3], Min Jae Lee[1], Ilia Davydov[4], Alexander Varshavsky, Mark Muesing[2], Yong Tae Kwon[1]

Substrates of the N-end rule pathway include proteins that contain degradation signals called N-degrons (Fig. 1A). One determinant of N-degron is a substrate's destabilizing N-terminal residue. Previous work (see, e.g., Abstract 269) identified mammalian UBR1 and UBR2 as E3 Ub ligases that recognize N-degrons. We report here that while *UBR1-/-UBR2-/-* mice died as early embryos, the rescued *UBR1-/-UBR2-/-* fibroblasts still had the N-end rule pathway. An affinity assay for proteins that bind to destabilizing N-terminal residues has identified, in addition to UBR1 and UBR2, a huge (570 kDa) mouse protein, termed UBR4, and also the 300-kDa UBR5, a previously characterized mammalian E3 known as EDD/hHYD. A counterpart of mammalian UBR4 is known as PUSHOVER in *Drosophila* and BIG in plants. *UBR1-/-UBR2-/-* fibroblasts that were made also deficient in UBR4 were impaired in the degradation of N-end rule substrates, confirming that UBR4 is a part of the N-end rule pathway. The recognition of destabilizing N-terminal residues by UBR4 and UBR5 is a new property of these proteins. UBR1, UBR2, UBR4, UBR5, and at least three other mouse proteins contain a motif termed the UBR box. The resulting UBR family consists of either demonstrated or inferred Ub ligases. A major part of this family are E3s of the N-end rule pathway. Thus, in contrast to the yeast *S. cerevisiae*, where the N-end rule pathway is dependent on just one Ub ligase, UBR1, a mammalian N-end rule pathway is mediated by at least four distinct Ub ligases, which have in common at least the UBR box.

[1]*Center for Pharmacogenetics and Department of Pharmaceutical Sciences, School of Pharmacy, University of Pittsburgh, Pittsburgh, PA 15261*
[2]*Aaron Diamond AIDS Research Center, The Rockefeller University, New York, NY 10016*
[3]*Protein Research Network, Inc., Yokohama, Kanagawa 236-0004, Japan*
[4]*Meso-Scale Discovery, 16020 Industrial Drive, Gaithersburg, MD 20877*

Reference

Tasaki, T., Mulder, L.C.F., Iwamatsu, A., Lee, M.J., Davydov, I.V., Varshavsky, A., Muesing, M. and Kwon, Y.T. (2005) *Mol. Cell. Biol.* **25**:7120-7136.

271. Spalog and sequelog: Neutral terms for spatial and sequence similarity

Alexander Varshavsky

Similarities amongst the sequences or three-dimensional (3-D) structures, and the conjectures based on similarities are a major part of molecular biology and related fields. It is therefore, striking that there are no terms, at present, to denote a sequence or a 3-D structure that is similar to another sequence or 3-D structure while implying *nothing at all* about evolutionary relatedness or biological functions. The absence of *neutral* terms for denoting similarity is one reason for the widespread use of 'homologs,' 'orthologs' and 'paralogs.' The former term (more than a century old) and the other two were proposed long before the advent of extensive sequence comparisons. To state that a gene or protein A is a homolog of B implies the relatedness of A and B through a common descent, a proposition to prove in most cases. In addition, two sequences can be 37% identical, but they cannot be 37% homologous: they (their relevant parts) are either homologous or not. The frequent unsuitability of the term 'homolog' in the context of similarity comparisons was pointed out repeatedly, but the literature is still rife with this misuse, in part because the proper, neutral terms simply don't exist.

The disposition can be also difficult with 'orthologs' and 'paralogs.' The former are two homologous sequences that diverged following *speciation*, so that the common precursor of two sequences lies in an organism that was their nearest common ancestor. 'Paralogs,' in contrast, are two homologous sequences that diverged after *gene duplication*. Besides the initial ambiguity in assigning 'homology' (two orthologs are homologous, and two paralogs are homologous, as well), the use of 'ortholog' and 'paralog' implies additional probabilistic inferences about the evolution of two sequences being compared. Yet further ambiguities often accrue, because the 'ortholog-paralog' terms are also used, throughout the literature, to denote *functional similarities* between orthologous genes (e.g., similar enzymatic activities of protein products), and *functional differences* between paralogous genes. Neither of these relationships (often presumed, not proven) are implied by the definitions of ortholog and paralog. To observe that the current usage of 'homologs,' 'orthologs' and 'paralogs' is complicated and often less than rigorous is to understate the case. A statistically significant similarity is an experimental fact, whereas 'homology,' 'orthology' and 'paralogy' are, in most cases, hypotheses. There is, at present, a striking disconnect between (generally) high rigor of statistical methods used to compare sequences or structures and the often cavalier, assumptions-laden attitude in the use of 'homolog,' 'ortholog' and 'paralog.'

To remedy this, I recently proposed two terms, '*sequelog*' and '*spalog*' (Varshavsky, 2004). They meet the requirement of evolutionary and functional neutrality, are helpful mnemonically, and possess yet another advantage

of making it possible to distinguish, through single words, between the realms of similar sequences and similar 3-D structures.

The term 'sequelog' denotes a nucleotide or amino acid sequence that is similar, to a specified extent, to another sequence.

The term '*spalog*' (pronounced [*spailog*]) denotes a 3-D structure that is spatially similar, to a specified extent, to another 3-D structure.

These terms are strictly about similarity: they imply nothing about evolutionary relatedness and functional properties of the sequences or structures.

In comparing nucleotide or amino acid sequences, the extent of similarity is conveyed by a numerical score, % nucleotide or amino acid positional identity. Alternatively, the extent of similarity of two sequences can be conveyed by the probability of an identical score for a randomly chosen pair of sequences of the same length. In comparing amino acid sequences, one can also measure % similarity (as distinguished from % identity), which includes both the identities and the residues that are scored as 'similar' to corresponding residues of the second sequence, according to a 'similarity matrix.'

When 3-D structures of two proteins or nucleic acids are compared, a standard measure of similarity is the root-mean-square deviation (r.m.s.d.) between compared atomic positions. One could, in principle, introduce the term 'similog' to denote either a sequence or a 3-D structure that is similar to another sequence or 3-D structure. Note, however, the considerable advantage of 'sequelog' and 'spalog,' vis-à-vis an all-encompassing term such as 'similog,' in that the former terms instantly define the nature of similarity (a sequence or a spatial one) thus, obviating further clarifications.

In a typical usage of the proposed terms, one can state, for example, that protein A is a sequelog of protein B (X% identity over Y residues), or that protein C is a spalog of protein D (r.m.s.d. of X Å for Y equivalent Cα atoms). Related measures of spatial similarity include a Z-score computed with the program DALI. To add qualitative, shorthand distinctions, one can state, for example, that protein A is a weak but significant sequelog of protein B (e.g., 24% identity over 165 residues), or that protein C is a strong spalog of protein D (e.g., r.m.s.d. of 2.3 Å for 120 equivalent Cα atoms), or that protein E is a strong sequelog of protein F (e.g., 60% identity over 372 residues). In using the sequelog terminology, it would be best to invoke just the % identity of two sequences and its (straightforwardly computable) statistical significance, avoiding an influence by any other information, for example, similarity matrices or 3-D structures. The central idea, yet again, is to minimize 'interpretational' aspects of sequelog, spalog and the derivative terms such as, for example, sequelogy, sequelogous, spalogous, and so forth.

A strong sequelog of a given protein is very likely to be its spalog as well, but the converse is not true, in that a strong spalog of a given protein may not be its sequelog. For example, the 66-residue *E. coli* protein ThiS, the sulfur carrier in the pathway of thiamine biosynthesis, is a strong spalog of the 76-residue eukaryotic ubiquitin (r.m.s.d. of 2.4 Å over 63 equivalent Cα atoms, and high Z-score of 5.2), but is not a sequelog of ubiquitin, since the sequence

similarity between the two proteins (14%) is statistically insignificant, in the absence of additional information from 3-D structures. Such comparisons can also employ the adjectives 'sequelogous' or 'spalogous.' For example, "spalogous" can be used to denote similar local 3-D folds in otherwise dissimilar proteins. Thus, 'Although protein A is not a sequelog of protein B, the 23-127 region of A is strongly spalogous to the 769-875 region of B (r.m.s.d. of 2.2 Å over 101 equivalent Cα atoms, and Z-score of 5.6).'

To describe a comparison of sequences or 3-D structures, one can begin by using 'sequelog,' 'spalog' or their derivatives in stating (and specifying numerically) the facts of similarity, as described above. After that, and only after that, one can conjecture (if necessary), based on additional evidence, that the two sequelogs or spalogs are likely to be 'homologs,' 'orthologs,' 'paralogs,' or whatever. This way, the rigorous, numerically explicit statements about similarities of specific sequences or 3-D structures won't be conjoined, at birth, with often unproven inferences that the latter three terms inherently imply.

Spalog, *sequelog* and terms derived from them provide single-word, separate notations for sequence *vs.* spatial similarities. Their other advantage is evolutionary neutrality. In contrast, the inherent evolutionary connotation of a term such as 'homolog' (common descent) is inferred in most cases, a logically sloppy usage. The proposed terms fill an overt lacuna in the existing terminology. They would clarify and streamline discourses about similarity.

Reference

Varshavsky, A. (2004) *Curr. Biol.* **14**:R181-R183.

Publications

Dohmen, R.J. and Varshavsky, A. (2005) Heat-inducible degron and the making of conditional mutants. *Meth. Enzymol.* In press.

Finley, D., Ciechanover, A. and Varshavsky, A. (2004) Ubiquitin as a central cellular regulator. *Cell* **116**:S29-S32.

Hu, R.G., Sheng, J., Qi, X., Xu, Z., Takahashi, T.T. and Varshavsky, A. (2005) The N-end rule pathway as a nitric oxide sensor controlling the levels of multiple regulators. *Nature* **437**:981-986.

Tasaki, T., Mulder, L.C.F., Iwamatsu, A., Lee, M.J., Davydov, I.V., Varshavsky, A., Muesing, M. and Kwon, Y.T. (2005) A family of mammalian E3 ubiquitin ligases that contain the UBR motif and recognize N-degrons. *Mol. Cell. Biol.* **25**:7120-7136.

Xia, Z., Turner, G.C., Byrd, C., Hwang, C.S. and Varshavsky, A. (2005) Amino acids induce the import of peptides by accelerating degradation of the import's repressor CUP9. Manuscript in preparation.

Varshavsky, A. (2004) Spalog and sequelog: Neutral terms for spatial and sequence similarity. *Curr. Biol.* **14**:R181-R183.

Varshavsky, A. (2004) The physiological functions of the ubiquitin system. In: *Great Experiments,* Ergito, by Virtual Text (http://www.ergito.com/index.jsp).

Varshavsky, A. (2004) N-end rule. *Encyclopedia of Biological Chemistry* (Acad. Press, NY).

Varshavsky, A. (2005) Regulated protein degradation. *Trends Biochem. Sci.* **6**:283-286.

Varshavsky, A. (2005) Ubiquitin fusion technique and related methods. *Meth. Enzymol.* In press.

Yin, J., Kwon, Y.T., Varshavsky, A. and Wang, W. (2004) RECQL4, mutated in the Rothmund-Thomson and RAPADILINO syndromes, interacts with ubiquitin ligases UBR1 and UBR2 of the N-end rule pathway. *Human Mol. Genet.* **13**:2421-2430.

Developmental and Regulatory Biology

Marianne Bronner-Fraser, Ph.D.
Eric H. Davidson, Ph.D.
Michael H. Dickinson, Ph.D.
Michael Elowitz, Ph.D.
Scott E. Fraser, Ph.D.
Bruce A. Hay, Ph.D.
Elliot M. Meyerowitz, Ph.D.
Ellen V. Rothenberg, Ph.D.
Melvin I. Simon, Ph.D.
Paul W. Sternberg, Ph.D.
Barbara J. Wold, Ph.D.

Summary: This laboratory's research centers on the early formation of the nervous system in vertebrate embryos. The peripheral nervous system forms from two cell types that are unique to vertebrates: neural crest cells and ectodermal placodes. We study the cellular and molecular events underlying the formation, cell lineage decisions and migration of these two cells types. The neural crest is comprised of multipotent stem-cell-like precursor cells that migrate extensively and give rise to an amazingly diverse set of derivatives. In addition to their specific neuronal and glial derivatives, neural crest cells can also form melanocytes, craniofacial bone and cartilage and smooth muscle. Placodes are discrete regions of thickened epithelium that give rise to portions of the cranial sensory ganglia, as well as form the paired sense organs (lens, nose, ears). Placodes and neural crest cells share several properties including the ability to migrate and to undergo an epithelial to mesenchymal transition. Their progeny are also similar: sensory neurons, glia, neuroendocrine cells, and cells that can secrete special extracellular matrices.

We are studying the cellular and molecular mechanisms underlying the induction, early development and evolution of the neural crest and placodes. This research addresses fundamental questions concerning cell commitment, migration and differentiation using a combination of techniques ranging from experimental embryology to genomic approaches to novel gene discovery. These studies shed important light on the mechanisms of neural crest and placode formation, migration and differentiation. In addition, the neural crest and placodes are unique to vertebrates. In studying the evolution of these traits, we hope to better understand the origin of vertebrates.

Because these cell types are involved in a variety of birth defects and cancers such as neurofibromatosis, melanoma, neuroblastoma, our results on the normal mechanisms of neural crest development provide important clues regarding the mistakes that may lead to abnormal development or loss of the differentiated state.

272. **Id3 is essential for survival of neural crest progenitors in *Xenopus***
Yun Kee, Marianne Bronner-Fraser

The neural crest is a unique population of mitotically active, multipotent progenitors that arise at the vertebrate neural plate border. We have shown that the helix-loop-helix transcriptional regulator Id3 has a novel role in neural crest survival in *Xenopus*. Id genes have been implicated in the regulation of diverse cellular events such as the cell cycle, proliferation, differentiation or apoptosis of different cell types in a number of *in vitro* mammalian cell line models (Tzeng, 2003). However, the mechanisms that mediate their effects in developing tissues *in vivo* are not well understood. *Xenopus* embryos offer several advantages for functional analysis of genes involved in neural crest development because it is possible to focally inject mRNAs and small interfering constructs into specific tissues for both gain- and loss-of-function studies. *Id3* is localized at the neural plate border during gastrulation and neurulation, in a pattern that overlaps with the domain of neural crest induction. Over-expression of Id3 results in expansion of the neural crest domain. Conversely, morpholino oligonucleotide-mediated depletion of Id3 results in the absence of neural crest precursors and a resultant loss of neural crest derivatives. This is mediated by apoptosis and lack of proliferation of the crest progenitor pool. Thus, Id3 functions by a novel mechanism independent of other neural crest genes that affect cell fate determination rather than survival. Our data clearly show that Id3 is a key regulator of neural crest proliferation and survival in *Xenopus* embryos.

273. **Discovery of genes involved in placode formation**
Katy McCabe, Andrea Manzo, Laura Gammill, Marianne Bronner-Fraser

The peripheral nervous system of the head is derived from cranial ectodermal placodes and neural crest cells. Placodes arise from thickenings in the cranial ectoderm that invaginate or ingress to form sensory ganglia and the paired sense organs. We have combined embryological techniques with array technology to identify genes that are expressed as a consequence of placode induction. As a secondary screen, we used whole mount *in situ* hybridization to determine the expression of candidate genes in various placodal domains. The results reveal 52 genes that are found in one or more placodes, including the olfactory, trigeminal and otic placodes. Expression of some of these genes is retained in placodal derivatives. Furthermore, several genes are common to both neural crest and ectodermal placodes. This study presents the first array of candidate genes implicated in placode development, providing numerous new molecular markers for various stages of placode formation. Importantly, the results uncover previously unknown commonalities in genes expressed by multiple placodes and shared

properties between placodes and other migratory cells, like neural crest cells.

274. Noelins modulate the ability to form neuronal precursors during development

Tanya Moreno, Marianne Bronner-Fraser

Noelin-4 is a secreted and glycosylated protein that is expressed from neural plate stages onward in *Xenopus*. Here, we present evidence that it has a unique function as a factor that promotes neuronal differentiation in the early embryo. *Noelin-4* appears to be downstream of the neurogenic genes *X-ngnr-1* and *XneuroD*. Over-expression of *Noelin-4* causes expansion of the neural tube and retina, with the increase of neural tissue apparently occurring by conversion of epidermis and neural crest to a neural fate. In addition, *Noelin-4* over-expression causes a general dorsalization of the embryo. Biochemically, Noelin-4 protein interacts with Noelin-1. Accordingly, the neural-expansion promoting activity of *Noelin-4* is reversed by co-expression of *Noelin-1*. These results suggest a novel function for *Noelin-4* in promoting neural properties at the expense of other ectodermal fates and further suggest that different *Noelin* isoforms may bind to and antagonize one another.

275. Spalt4 triggers ectodermal invagination to form sensory placodes

Meyer Barembaum, Marianne Bronner-Fraser

We find that the transcription factor *spalt4* is expressed broadly in chick preplacodal epiblast and then resolves to otic and olfactory placodes and their derivatives. Misexpression of *spalt4* in non-placodal ectoderm by electroporation results in formation of ectopic vesicles that express the otic markers *Pax2*, *Sox10* and *Tbx1* in the vicinity of the ear, and the lens/olfactory marker *Pax6* in more rostral ectoderm. Furthermore, trunk ectoderm that normally does not form placodes, ingresses after misexpression of *spalt4*. Excess *spalt4* in the otic placode causes severe malformations and alterations in region-specific markers. Conversely, loss of *spalt4* function using a dominant-negative construct results in significant reductions in the otic vesicle. These results suggest that *spalt4* is both necessary and sufficient for ear development, initiating invagination/ingression of ectoderm and region-specific gene regulatory networks.

276. Sox10 induces neural crest from all dorsoventral levels of the neural tube and maintains an undifferentiated state

Sonja McKeown, Vivian Lee, Marianne Bronner-Fraser, Don Newgreen, Peter Farlie

The SoxE group transcription factors (*Sox8, 9, 10*) represent early response genes to neural crest induction. Although the early role of *Sox9* has been examined in chick and frog, later roles in neural crest migration and differentiation remain largely unexplored. To address this question, we first examined which *SoxE* genes were expressed in migrating neural crest cells and then investigated their function using *in ovo* electroporation. The results of this analysis reveal that *Sox10* is present in migrating neural crest cells, whereas other *SoxE* genes are only expressed transiently following induction. Ectopic expression of *Sox10* in the neural tube induced expression of HNK-1 in neuroepithelial cells followed by extensive neural crest cell emigration. Surprisingly, this was not confined to the dorsal portion of the neural tube from which neural crest cells normally arise, but rather occurred throughout the dorsoventral neuraxis including the floor plate. Furthermore, this ectopic production of migratory cells occurred at the expense of the neuroepithelium itself. Sox10-expressing cells failed to express lineage markers even 6 days post-transfection, suggesting these cells were maintained in an undifferentiated state. Overexpression of *Sox8* or *Sox9* had similar but not identical effects on neuroepithelial cells. These results show that high levels of *Sox10*, *Sox9* or Sox8 expression in the neural tube are capable of inducing a migratory neural crest-like phenotype in the absence of dorsal signals and can maintain these cells in an undifferentiated state.

277. Specification of neural crest occurs during gastrulation and requires Pax7

Martin Garcia-Castro, Martin Basch, Marianne Bronner-Fraser

Neural crest cells represent an important stem cell population for development of both craniofacial skeleton and peripheral ganglia. Although it has been assumed that they arise as the nervous system forms, little is known about what initiates formation of this important cell type. To examine this question, we have sought early molecular markers of the neural crest. We find that the transcription factor *Pax7* is expressed in a symmetric domain flanking the primitive streak in the gastrulating embryo, in a region that fate maps to the neural crest. When tissue from the presumptive *Pax7* domain of stage 3 to 4 chick embryos is explanted under defined *in vitro* conditions, it is already conditionally specified to form neural crest. Furthermore, *Pax7* is critical for neural crest formation since blocking its function prevents specification *in vitro* and blocks expression of the neural crest markers *Slug* and *Sox10 in vivo* without affecting dorsal neural tube markers. Taken together, these data suggest that neural crest specification initiates during gastrulation and that *Pax7* plays a critical role in the development of this cell type.

278. Guidance of trunk neural crest migration requires *Neuropilin-2/Semaphorin3F* signaling

Laura Gammill, Marianne Bronner-Fraser

Neural crest cells migrate only through the rostral half of each somite while avoiding the caudal somite in vertebrate embryos. Neural crest cells express the receptor *neuropilin-2* (*Npn-2*), while its repulsive ligand *Semaphorin3F* (*Sema3F*) is restricted to the caudal somite. We demonstrate that in *Npn-2* and *Sema3F* mutant mice, neural crest cells lose their segmental migration pattern and instead migrate as a uniform sheet, although somite polarity itself remains unchanged in the mutants.

Interestingly, neural crest cells still condense into segmentally arranged dorsal root ganglia in *Npn-2* nulls, indicating that segmental neural crest migration and segmentation of the peripheral nervous system are separable events.

279. Restricted response of mesencephalic neural crest to sympathetic differentiation signals in the trunk

Vivian Lee, Marianne Bronner-Fraser, Clare Baker

Lineage diversification in the vertebrate neural crest may occur via instructive signals acting on pluripotent cells, and/or via early specification of subpopulations towards particular lineages. Mesencephalic neural crest cells normally form cholinergic parasympathetic neurons in the ciliary ganglion, while trunk neural crest cells normally form both noradrenergic and cholinergic neurons in sympathetic ganglia. In contrast to trunk neural crest cells, mesencephalic neural crest cells apparently fail to express the catecholaminergic transcription factor dHAND in response to BMPs in the head environment. Here, we show that migrating quail mesencephalic neural crest cells grafted into the trunk of host chick embryos colonize the sympathetic ganglia. While many express *dHAND* and form *tyrosine hydroxylase* (*TH*)-positive catecholaminergic neurons, the proportion that expresses either *dHAND* or *TH* is significantly smaller than that of quail trunk neural crest cells under the same conditions. Furthermore, the proportion of quail mesencephalic neural crest cells that is TH^+ in the sympathetic ganglia decreases with time, while the proportion of TH^+ quail trunk neural crest-derived cells increases. Thus, a subset of mesencephalic neural crest cells fails to express *dHAND* or *TH* in the sympathetic ganglia, while a further subset initiates but fails to maintain *TH* expression. Taken together, our results suggest that a subpopulation of migrating mesencephalic neural crest cells is refractory to sympathetic neuronal differentiation signals in the trunk. We suggest that this heterogeneity, together with local signals that repress catecholaminergic differentiation, may ensure that most ciliary neurons adopt a cholinergic fate.

Publications

Barembaum, M. and Bronner-Fraser, M. (2004) A novel chicken *spalt* gene expressed in branchial arches reduces neurogenic potential of the cranial neural crest. *Neuron Glia* **1**:57-63.

Bhattacharyya. S., Bailey, A.P., Bronner-Fraser, M. and Streit, A. (2004) Pax6, Dlx5 and cell sorting during olfactory and lens placode development: Parallels between vertebrates and *Drosophila*. *Dev. Biol.* **271**:403-414.

Bhattycharyya, S. and Bronner-Fraser, M. (2004) Hierarchy of regulatory events in sensory placode development. *Cur. Op. Dev. Gen.* **14**:520-526.

Bok J., Bronner-Fraser M. and Wu, D.K. (2005) Role of the hindbrain in dorsoventral but not anteroposterior axial specification of the inner ear. *Development* **132**:2115-2124.

Cerny, R. Meulemans, M., Berger, J., Wilsch-Brauminger, M., Kurth, T., Bronner-Fraser, M. and Epperlein, H.H. (2004) Cranial neural crest migration and pharyngeal arch morphogenesis in axolotl. *Dev. Biol.* **266**:252-269.

Cerny, R., Lwigale, P., Ericsson, R., Meulemans, D., Epperlein, H.H. and Bronner-Fraser, M. (2004) Developmental origins and evolution of jaws: New interpretation of "maxillary" and "mandibular." *Dev. Biol.* **276**:225-236.

Chen, Y., Gutmann, C., Haipek, B., Martinsen, B., Bronner-Fraser, M. and Krull, C. (2004) Characterization of chicken Nf2/merlin indicates potential roles in growth regulation and cell migration. *Dev. Dynamics* **229**:541-554.

Coles, E., Christiansen, J., Economou, A., Bronner-Fraser, M. and Wilkinson, D.G. (2004) A vertebrate crossveinless-2 homologue modulates BMP activity and neural crest cell migration. *Development* **131**:5309-5317.

deBellard, M.E., Bronner-Fraser, M. (2005) Neural crest migration methods in the chicken embryo. *Meth. Mol. Biol.* **294**:247-267.

Kee, Y. and Bronner-Fraser, M. (2005) To proliferate or to die: Role of Id3 in cell cycle progression and survival of neural crest progenitors. *Genes Dev.* **19**:744-755.

Lee, V., Bronner-Fraser, M. and Baker, C.V. (2005) Restricted response of mesencephalic neural crest to sympathetic differentiation signals in the trunk. *Dev. Biol.* **278**:175-92.

Lwigale, P.Y., Conrad, G. and Bronner-Fraser, M. (2004) Graded potential of neural crest to form cornea, sensory neurons and cartilage along the rostrocaudal axis. *Development* **131**:1979-1991.

McCabe, K., Manzo, A., Gammill, L. and Bronner-Fraser, M. (2004) Discovery of genes implicated in placode formation. *Dev. Biol.* **24**:462-477.

McCauley, D. and Bronner-Fraser, M. (2004) Conservation and divergence of BMP24 genes in the lamprey: Expression and phylogenetic analysis suggest a single ancestral gene. *Evol. Dev.* **6**:411-422.

McKeown S.J., Lee, V.M., Bronner-Fraser, M., Newgreen, D.F. and Farlie, P.G. (2005) *Sox10* overexpression induces neural crest-like cells from all dorsoventral levels of the neural tube but inhibits differentiation. *Dev. Dynamics* **233**(2):430-444.

Meulemans, D. and Bronner-Fraser, M. (2005) Central role of gene cooption in neural crest evolution. *J. Exp. Zool. B. Mol. Dev. Evol.* **304**:298-303.

Meulemans, D. and Bronner-Fraser, M. (2004) Gene-regulatory interactions in neural crest development and evolution. *Dev. Cell* **7**:291-299.

Meulemans, D. and Bronner-Fraser, M. (2005) Subfunctionalization of amphioxus *SoxB* genes: Implications for vertebrate placode evolution. Submitted.

Venters, S.J., Argent, R.E., Deegan, F.M., Wong, T.S., Tidyman, W.E., Marcelle, C., Bronner-Fraser, M. and Ordahl, C.P. (2004) Limb muscle precursor cells do not undergo precocious terminal differentiation when isolated from lateral inhibitory signals. *Dev. Dynamics* **229**:591-599.

Norman Chandler Professor of Cell Biology: Eric H. Davidson
Distinguished Carnegie Senior Research Associate Emeritus: Roy J. Britten
Visiting Associates: Hamid Bolouri[1], Lee Hood[1], Gary Wessel[2], Sorin Istail[3]
Senior Research Associate: R. Andrew Cameron
Member of the Professional Staff: Paola Oliveri, Andrew Ransick
Research Fellows: Gabriele Amore, Smadar Ben-Tabou de-Leon, Feng Gao, Veronica Hinman, Alexander Krämer, Takuya Minokawa, Jongmin Nam, Ochan Otim, Joel Smith, Qiang Tu
Graduate Students: C. Titus Brown, Sager Damle, Meredith L. Howard, Pei Yun Lee, Carolina B. Livi, Stefan Materna, Roger Revilla
Undergraduates: Angela Chang, Harold Hsu, Rena Schweizer[4], Elizabeth Shay, Sarah Wadsworth, Erin White
Research and Laboratory Staff: Carlzen Balagot, Kevin Berney, William Chiu, Elly Chow, Ping Dong, Adam Christopher Ereth, Jessica Gamboa, Rachel Gray, Julie Hahn, Parvin Hartsteen, Eve Helguero, Patrick S. Leahy, Jane Rigg, Deanna Thomas, John Williams, Qiu-Autumn Yuan, Jina Yun, Miki Yun
[1]*Institute for Systems Biology, Seattle, WA*
[2] *Brown University, Providence ,RI*
[3]*Applied Biosystems, Foster City, CA*
[4]*UCLA*

Key outside collaborators

George Weinstock and Richard Gibbs, Human Genome Sequencing Center, Baylor College of Medicine
Lee Hood and Hamid Bolouri, Institute for Systems Biology
Sorin Istrail, Brown University
David J. Bottjer, University of Southern California
Jun-Yuan Chen, Early Life Research Center, Chengjiang, Yunnan, China

Summary: The major focus of research in our laboratory is on gene regulatory networks (GRNs) that control development, and the evolution of these networks. Most of our research is done on sea urchin embryos, which provide key experimental advantages. Among these are: an easy gene transfer technology, which makes this a system of choice for studying the genomic regulatory code; availability of embryonic material at all seasons of the year; an optically clear, easily handled embryo that is remarkably able to withstand micromanipulations, injections and blastomere recombination and disaggregation procedures; a very well understood and relatively simple embryonic process; and in-house egg-to-egg culture of the species we work with, *Strongylocentrotus purpuratu*s (in a special culture system we have developed, located at Caltech's Kerckhoff Marine Laboratory). There is also a rich collection of arrayed cDNA and BAC libraries for sea urchins and a large EST database. The genome of *S. purpuratus* has been sequenced at HGSC (Baylor) and the sequence is now being annotated. A very extensive repertoire of effective molecular technologies for experimentation on sea urchin gene regulatory systems has evolved. The experimental model that we utilize for evolutionary GRN comparisons is another echinoderm, also of local provenance, the starfish *Asterina miniata*. The embryo of this animal proves to be as excellent a subject for gene regulation molecular biology as is that of the sea urchin.

We pursue an integrated, "vertical" mode of experimental analysis, in that our experiments are directed at all levels of biological organization, extending from the transcription factor-DNA interactions that control spatial and temporal expression of specific genes to the system-level analysis of large regulatory networks. It has become apparent that the only level of analysis from which explanations of major developmental phenomena directly emerge, is the system level represented by the sea urchin GRN.

The main initiatives at the present time are as follows: *i. Analysis of the gene regulatory network underlying endomesoderm specification in* **S. purpuratus** *embryos*: At present about 50 genes have been linked into this GRN. The architecture of the network is emerging from an interdisciplinary approach in which computational analysis is applied to perturbation data obtained by gene expression knockouts and other methods, combined with experimental embryology. Regulatory and downstream genes required for skeletogenesis and for territorial specification have been isolated utilizing high-density arrayed cDNA libraries. A predictive model of the GRN has emerged which indicates the inputs and outputs of the *cis*-regulatory elements at its key nodes. Most of the individual projects reported below are contributing to understanding of this network. *ii. Testing the* **cis***-regulatory predictions of the GRN:* The GRN has been constructed essentially by integrating the results of a massive perturbation analysis of expression of individual genes with spatial and temporal expression data for these genes. It predicts the required specific regulatory inputs and outputs linking the genes within the GRN. These predictions are subject to direct experimental *cis*-regulatory test, and correction, if need be. We recently confirmed the *cis*-regulatory inputs into *wnt8*, *cyclophylin*, and *otx* genes, and studies on *gcm*, *gatae*, *tbr*, *bra*, are in an advanced state. Other *cis*-regulatory projects in this vein are focused on *alx1* and *krox1* genes. By the end of the year it is to be expected that the key nodes of the

endomesoderm network will have been authenticated at the level of the genomic regulatory code. For some regions of the GRN the analysis is approaching maturity, in that it extends convincingly from maternal inputs to cell-type differentiation. The best example is the GRN subregion determining skeletogenic micromere specification. The subnetwork determining the stability of the endodermal specification state is also among the regions of the GRN that are well established at the *cis*-regulatory level. Overall, the results of these experiments promise to convert the GRN into a map of the hard-wired genomic control logic for this portion of development. *iii. Completion of the repertoire of regulatory genes engaged in the endomesoderm GRN:* We are using the data emerging from the genome sequence project to identify and assemble computationally all gene sequences that encode transcription factors. The temporal patterns of expression of these genes are determined, and for those possibly relevant to the GRN, the spatial patterns as well. Those genes that evidently play a role in endomesoderm specification will then be linked into the GRN by perturbation and *cis*-regulatory analysis. *iv. Evolution, viewed as a process of change in GRN architecture:* Starfish and sea urchins shared a last common ancestor about 500 million years ago. Thus, analysis of the GRN controlling endomesoderm specification events in the starfish embryo will reveal both the nature of functional change in the GRN, and conservation of features that are so essential that they have resisted alteration for half a billion years. We have already seen examples of both. The underlying processes are of course change, or alternatively, conservation, of functional *cis*-regulatory features. To study this we are examining starfish/sea urchin GRN differences at the *cis*-regulatory level. In a separate, large-scale effort, we have nearly completed the isolation of BACs containing 12 genes the *cis*-regulatory elements of which are known in *S. purpuratus*, from genomic libraries of five different sea urchin species ranging from 15 to 250 million years since divergence from the lineage leading to *S. purpuratus*. These will afford the opportunity of studying by computational and experimental methods the process of *cis*-regulatory evolution, which is very poorly understood. *v. Oral ectoderm GRN:* We have begun work on the GRN that controls oral ectoderm specification. We are now launching an effort in collaboration with the lab of David R McClay at Duke to extend the pregastrular network to the whole embryo. This means obtaining GRN architecture for oral ectoderm and aboral ectoderm (the apical neurogenic region) is being studied in another sea urchin laboratory). The aboral ectoderm generates a single cell type, but the oral ectoderm gives rise to several distinctly functioning domains: mouth, columnar "facial" epithelium, neurogenic ciliary band, and the ectodermal signaling stripes which determine the location of the skeletal rods. The approach is to obtain all the regulatory players expressed in oral and aboral ectoderm from the analysis of all genes encoding transcription factors predicted in the genomic sequence, and engage them in a

provisional network by carrying out a matrix of perturbation experiments. This will be anchored at the onset of the ectodermal specification process, of which the initial gene zygotically expressed on the oral side is nodal. The *cis*-regulatory module controlling early oral ectoderm expression is in our hands and its target sites should provide the link between the initial cytoplasmic anisotropy and zygotic gene expression. *vi. Computational and experimental kinetic* **cis**-*regulatory model:* To build a logic model of the information processing functions of a *cis*-regulatory element that relates the input kinetics (i.e., the temporal changes in relevant transcription factor levels) to its output, we have returned to the *cyIIIa* gene. The logic model of the regulatory system of this gene is being completed by additional mutational gene transfer experiments, and input kinetics are being measured. *vii. Various explorations by new methods and approaches:* As always, we are trying to expand knowledge by use of novel technologies for analysis of the GRN and the genome. Current initiatives include first attempts to "reengineer" the process of embryonic development, by installing regulatory subcircuits in novel spatial domains; tests of new reagents for perturbing gene expression; utilization of a new technology for FACS sorting GFP-expressing embryos to the goal of obtaining quantitative *cis*-regulatory measurements; use of BAC GFP recombinants for analysis of genomic regulatory apparatus; application of quantitative imaging methods to assessment of expression construct function; and a project to obtain a physical map of the sea urchin genome, using the inbred lines in our system to measure assortment of microsatellite markers. *viii. Computational approaches to regulatory gene network analysis:* The GRN visualization software BioTapestry, developed by our collaborators Hamid Bolouri and Wm. Longabaugh at ISB, is now in wide use, and we are further expanding its capacities so that it will automatically generate allowed network architectures from machine readable time and space of expression data plus results of perturbation analysis. In addition studies of network regulatory logic are being undertaken in collaboration with Prof. Sorin Istrail of Brown University. Many additional computational genomics and other projects are summarized below.

The Center for Computational Regulatory Genomics CCRG

The goal of the Center for Computational Regulatory Biology is to develop, refine and test computational approaches in genomics broadly and *cis*-regulatory analysis specifically. The primary focus for the latter is the elucidation of gene regulatory networks in development. The Center interacts with the wider research community in several ways: it provides open source software for use by academic research groups; it provides web-based servers for genomic analysis using software developed locally; and it maintains databases fundamental to the Sea Urchin Genome Project, an initiative that began in the Davidson laboratory and at the Genomics Technology Facility. The Facility provides to the Caltech

and external scientific community upon request services and materials stemming from the macroarray libraries and arraying equipment that we maintain. The Center and the Facility are both under the direction of R. Andrew Cameron with oversight from the PI of this Center, Eric Davidson.

Genomics Technology Facility

The operation of the Facility centers on the Genetix Arraying Robot, a large flatbed robotic arm with video camera used to produce bacterial macroarray libraries and filters. This year we upgraded our robot to the latest design. New software a\nd I/O capabilities decreases the time for colony picking by 1/2 and clone spotting by 1/3. Ancillary equipment in support of robot library construction including automated medium handling equipment and an automated DNA preparation unit are also housed in the Facility. An additional robotic DNA preparation machine is situated in the PIs laboratory and is available for Facility high-throughput use. We currently maintain in -80°C freezers 27 different echinoderm libraries comprising a total of approximately three million arrayed clones. In addition to providing these materials to academic research groups, we also offer the opportunity for outside groups from Caltech and elsewhere to array and spot their own libraries.

Our robot utilization for the past year was quite consistent and efficient. We arrayed a total of 259,000 library clones and printed a total of 231 filters. The in-house jobs consisted of reprinting filters from seven existing libraries and arraying four new libraries. We also re-arrayed our *S. purpuratus* BAC library for use by the sequencing effort. The four new libraries were primarily in support of the genome sequencing effort; they are intended to be used in EST projects. Lastly, a cDNA library from sea urchin radial nerves is currently being constructed.

Research Center

Computational aspects of gene regulatory network project. The sequence analysis and queuing software developed in the center and named Cartwheel, is our platform for comparative sequence analysis and mid-scale genomic sequence annotation. The software tools contained in these packages are also the computational base for the description of gene regulatory networks. These tools were specifically designed to aid the experimentalist working at the bench and using iterative cycles of experimentation and computation to describe the networks. As we have become more experienced in these studies we have altered the software in step. Furthermore we have added additional analysis choices incorporated from open source analysis programs based on user requests. These improvements have also led to increased speed in processing sequence analyses.

The utility of these comparative sequence analysis facilities is reflected in the user population. At present, the Caltech Cartwheel server, Woodward, has 425 total registered users in 48 lab groups. This represents a 20%

increase over last year. A total of 17790 jobs have run in the last year for a total of 125 CPU days. The majority of these are Seqcomp and Blast analyses.

Our development server continues to support several external developers and collaborators. Members of Dr. Diane Newman's laboratory in Geology and Planetary Science at Caltech has been working with a graduate student in the lab in an investigation of the regulation of the genes encoding the enzymes of anaerobic respiration in the bacterium, *Shewanella oneidensis*. We are collaborating with Dr. Jonathan Rast at the Sunnybrook and Women's College Health Sciences Centre, University of Toronto on an examination of the *Rag* genes in the sea urchin genome. These are the homologs of vertebrate genes involved in the re-arrangement of the receptors of adaptive immunity. The developed code and resulting analyses were all done entirely on machines supported by the Center.

The equipment that supports the computational efforts of the Center includes two 18 unit Beowulf clusters, a web server for the Sea Urchin Genome Project (SUGP) and several dual processor development machines used by the staff for software construction, testing, and maintenance.

The Sea Urchin Genome Project Web Site. The Sea Urchin Genome Project web site (http://sugp.caltech.edu/) is the distribution center for laboratory specific sequence and annotation information related to the sea urchin genome and our macroarray libraries. We have continued to rework this part of the facility as new data from the sequencing project is made available from Baylor College of Medicine, Human Genome Sequencing Center and the Mapping Group at the Genome Sciences Center of the British Columbia Cancer Agency. We have helped the NCBI Computational Branch to produce a specific sea urchin genome page at http://www.ncbi.nlm.nih.gov/genome/guide/sea_urchin/. This includes at NCBI a set of well-curated purple sea urchin reference sequences representing all known genes. The first automatic annotation of the sea urchin genome produced by the NCBI staff is also now available.

The Sea Urchin Genome Project Web site is the database for macroarray filter information. Since all of our libraries are arrayed and catalogued, all new sequence and gene annotation information collected in the process of screening these library filters, for whatever purpose, is stored by location. This includes sequence collections from complex probes screens such as those used for the identification of genes in the endomesoderm specification pathway; the results of homology screening strategies, and random EST projects. Because the data is coupled to a filter location that contains an individual clone from the library, the clone is immediately recoverable. As more clones are characterized in a library, that library becomes more valuable. Eventually, the several well-characterized libraries can be used to confirm *ab initio* gene predictions and confirm gene catalogs for the sea urchin.

280. Computational analysis of the emerging sea urchin genome sequence

R. Andrew Cameron, Kevin Berney, Titus Brown

The sea urchin genome project. We will continue to provide simple computational analyses in order to facilitate gene discovery and future annotation of the genomic sequences for the broader sea urchin community. We have modified our data pipeline originally designed to collect, assemble and analyze trace sequences obtained by searches against small candidate gene databases to use instead the assembled sequences. We are refining the analysis strategies we will use during the manual annotation phase of the sea urchin genome presentation effort. Our curatorial work on gene lists of transcription factors, putative innate immunity genes and sex determination genes continues. Quality control and distribution measurements of the sequence assemblies are derived from comparison to other data sets of sequences collected in the past, *viz.* the BAC-end STC sequences determined at the High-throughput Sequencing Center at the University of Washington and posted on the website. The Sea Urchin Genome Project web site (http://sugp.caltech.edu/) serves as the information exchange site for these projects.

The most unique, information-rich component of the Sea Urchin Genome Project Web site is the database of macroarray filter information. Here all of the sequence mentioned above and the gene annotation information collected in the process of screening these library filters, for whatever purpose, is stored. This includes sequence collections from complex probes screens such as those used for the identification of genes in the endomesoderm specification pathway, the results of homology screening strategies, and random EST projects. Because the data is coupled to a filter location that contains an individual clone from the library, the clone is immediately recoverable. As more clones are characterized in a library, that library becomes more valuable. Eventually, the several well-characterized libraries can be used to confirm *ab initio* gene predictions and confirm gene catalogs for the sea urchin. We have kept active a searchable sequence database related to the library clones. But we have retired the general sequence searches since all of the sea urchin sequences are available to search in one place at the Sea Urchin Genome Page on the NCBI web site.

281. A genome-wide survey of sea urchin transcription factors

Meredith H. Ashby, Stefan C. Materna, C. Titus Brown, R. Andy Cameron

The sea urchin genome-sequencing project now nearing completion has given us the opportunity to do a definitive survey of transcription factors involved in the organism's development. The goal is to characterize when and where these genes are expressed so that they may be incorporated into the current *Strongylocentrotus purpuratus* endomesodermal gene regulatory network (GRN), filling in any missing connections and rendering the model complete.

In all, more than 250 previously unknown sea urchin proteins were identified, including members of the *homeobox*, *sox*, *ets*, zinc finger, nuclear receptor, *forkhead*, *bHLH*, and bzipper families. The zinc finger family presented a particular challenge in that the inherent similarity of all zinc fingers made it nearly impossible to unambiguously identify orthologues. Because of this issue and their sheer number they are dealt with separately.

QPCR time courses were obtained for all genes from the fertilized egg up to 48 hours of development. From the data, it is apparent that the vast majority of transcription factors, 80%, are used at least once during these 48 hours. In addition, new transcription factors are activated at a nearly steady rate throughout this time period irrespective of gene family, indicating that the spatial complexity of the embryo is being steadily elaborated through rounds of specification even before visible morphological evidence of this appears. Furthermore, the data indicate that virtually all maternally expressed genes are again expressed by the embryo at a later point during embryonic development, further illustrating the economical usage of regulatory proteins.

Currently, the effort of obtaining spatial expression information by whole mount *in situ* hybridization (WMISH) is nearing completion. To date, we have located the expression of previously unknown genes to all territories of the embryo, including the vegetal plate, primary mesenchyme cells, the archenteron, and both the oral and aboral ectoderm. This information, along with perturbation analyses of currently known genes, will facilitate placing the newly found transcription factors into the endomesodermal GRN being constructed in the lab.

282. Zinc finger transcription factors in the early development of *S. purpuratus*

Stefan C. Materna, Meredith H. Ashby

Zinc-binding proteins are a very diverse class of proteins in terms of both structure and function. The subgroup of C_2H_2 zinc fingers, named for the two cysteines and two histidines that bind the zinc atom, are in a wide range of organisms the biggest group of DNA-binding transcription factors and play important roles in differentiation.

With the draft genome now in hand, we have attempted to identify all C_2H_2 zinc finger genes with a motif search and to date have collected expression data for most of them. The list of C_2H_2 zinc finger genes currently comprises nearly 400 genes that would put the sea urchin into good company with *Drosophila* (~350), whereas the estimates for humans are about 750. This list of about 400 genes most likely will have to be shortened due to redundancies in the draft genome assembly.

Nearing the completion of the transcriptional profiling it becomes apparent that the fraction of zinc finger genes that are actually expressed is lower than for all other known transcription factors. Of these roughly 80% are used during the first 48 hours of development, whereas for zinc finger genes the percentage is more likely to be around 50%. This difference raises the question of

whether zinc finger transcription factors are used differently in the organism or whether the number of genes that are true transcription factors is significantly lower than the current number of 400 genes.

Canonically, C_2H_2 zinc finger genes are viewed as transcriptional repressors. However, this might be a rather vertebrate-centric view as two thirds of vertebrate zinc finger proteins also contain a KRAB domain, which is known to have repressor activity. So far, this domain cannot be found in the sea urchin genome. It will be interesting to see if the data from the sea urchin set of zinc fingers will support their role as almost exclusive repressors.

For all C_2H_2 zinc finger genes that are expressed at a significant level, we are currently in the process of obtaining whole mount *in situ* stainings. Genes that are expressed in a tissue-specific manner will then become candidates for the network of transcriptional regulatory interactions in early development. With data for 250 orthologues of known transcription factors in hand plus, conservatively estimated, 200 additional zinc finger transcription factors, the sea urchin is set to be the first animal whose gene regulatory network underlying its development will be known in its entirety.

283. The evolutionary conservation of *cis*-regulatory information
Andy Cameron, William Chiu, Elly Chow, Eve Helguero, Autumn Yuan, Alex Kräemer, Ping Dong, Julie Hahn, Kevin Berney, Eric Davidson

Sequences conserved between the genomes of two species can be presumed to reflect a functional significance. Often these conserved sequence regions possess *cis*-regulatory function and current results show that this approach may yield a more than 10-fold increase in rate of experimental *cis*-regulatory element discovery, compared to the most efficient "blind" search methods. More specifically, the DNA of *cis*-regulatory modules known to be functional displays extensive sequence conservation in comparisons between genomes from modestly distant species. Patches of sequence several hundred base pairs in length within these modules are often seen to be 80-95% identical, while the flanking sequence cannot even be aligned. However, it is unlikely that base pairs located between the transcription factor target sites of *cis*-regulatory modules have sequence dependent function, and the mechanism that constrains evolutionary change within *cis*-regulatory modules is incompletely understood. We chose five functionally characterized *cis*-regulatory modules from the *Strongylocentrotus purpuratus* (sea urchin) genome, and obtained orthologous regulatory and flanking sequences from a BAC genome library of a congener, *Strongylocentrotus fransciscanus*. As expected, single nucleotide substitutions and small indels occur freely at many positions within the regulatory modules of these two species, as they do without. However, large indels (>20 bp) are statistically almost absent within, though they are common in flanking intergenic or intronic sequence. The

result helps to explain the patterns of evolutionary sequence divergence characteristic of *cis*-regulatory DNA. It also provides a new rule to use in the computational search for regulatory regions.

The studies described above are part of a larger project with NSF support (PI: R. Andrew Cameron) to explore the rules for efficient *cis*-regulatory sequence prediction by interspecific sequence analysis. The broader studies encompass 20 different gene candidates whose expression pattern, regulatory inputs and downstream targets are well characterized in the purple sea urchin. The orthologous genes come from several different echinoderm species that display a range of phylogenetic relatedness more distant than *S. franciscanus*. Our strategy is to obtain BACs containing the orthologs of the candidate genes from libraries for four species of sea urchins, a sea star, and a hemichordate. Sequence from the regions surrounding the gene coding sequence in the BACs will be obtained using methods perfected in the previous work. We have perfected an efficient method for recombination in BAC clones that will quickly yield reporter constructs to test the function of these orthologous sequences. We expect that this approach will reveal additional rules for computational *cis*-regulatory analysis while extending the current repertoire of BAC libraries, improving computational tools, and generating more efficient laboratory methods for this essential research area.

284. Construction of a library of BAC-GFP reporter recombinants for gene network analysis
Julie Hahn

It has been the focus of our lab to identify the *cis*-regulatory modules that controls gene expression during development. To that end we are constructing a library of BAC GFP reporter constructs containing the regulatory domains that control expression of transcription factors and signaling molecules that participate in endomesoderm specification. Using homologous recombination, a cassette containing the GFP coding sequence is targeted to the start of transcription. These BAC GFP recombinants then contain the intact upstream, downstream and intronic genomic DNA surrounding the gene. When microinjected into fertilized sea urchin eggs these reporters are able to recapitulate, with temporal and spatial specificity, endogenous gene expression because they contain the complete *cis*-regulatory system. Recombinants have been constructed using BAC sequence from four sea urchins, *S. purparatus*, *S. fransciscanus*, *L. variegatus* and *A. punctulata*, as well as the sea star *A. miniata*. Recombinants for the several genes have already been generated -- including the transcription factors Bra, Eve, FoxA, GataC, GataE, GCM, Tbr and Krox, differentiation genes *endo16* and *sm50* and signaling genes *Delta* and *Wnt8* -- and their expression patterns verified against their endogenous counterparts.

285. **Transcriptional control of the sea urchin** ***brachyury* gene**

R. Andrew Cameron, William Chiu, Elly Chow

The *brachyury* gene is a participant in the endomesoderm specification pathway and the founding member of T-box family of transcription factors. Gene expression is localized to the vegetal plate as seen by *in situ* hybridization in the blastula stage. By the gastrula stage transcripts are present in the oral ectoderm and in the region of the blastopore. Expression then subsides and increases again during the larval stage. The basal promoter of the gene was identified as a 50 bp sequence containing a TATA box and lying just 5' of the start of transcription. Previously we had identified one sequence fragment that recapitulates the temporal and spatial extent of this pattern: a region about 1800 bp that occupies most of the intron between the 6th and 7th exons of this transcription unit. Deletion analysis narrowed the functional region to a 650 bp fragment. An artificial construct containing these two elements, the intron sequence, and the basal promoter is being used to test the inputs to *brachyury* identified by Q-PCR experiments with other members of the endomesoderm specification gene regulatory network. From previous perturbations and computational analysis we have discovered three classes of transcription binding sites likely to be active in this fragment: Gata, TCF and Elk-1 sites.

286. ***Spblimp1/krox*: An alternatively transcribed transcription factor involved in sea urchin endomesoderm specification**

Carolina Becker Livi

Spblimp1/krox belongs to the Cys2His2 zinc finger transcription factor family, and contains a SET domain of the PR subtype being the orthologue of *blimp1* first studied in mice. During cleavage stages *Spblimp1/krox* is expressed in the large micromeres and veg$_2$ descendents. Soon after, it is expressed in a ring of cells around the vegetal pole of the blastula. Later, its expression is restricted to the blastopore region and the posterior of the invaginating archenteron, and finally to the mid and hindgut of the pluteus larva. The expression of *Spblimp1/krox* is dynamic, and involves several distinct spatial territories. *Spblimp1/krox* has two isoforms that are alternatively transcribed. Their temporal pattern of expression is different with *Spblimp1/krox1b* being expressed during cleavage stages starting between 6 and 9 hpf, and *Spblimp1/krox1a* being expressed starting at gastrulation around 36 hpf.

In order to study the regulation of this gene we performed phylogenetic footprinting analysis that found several conserved patches when the genomic region surrounding the *blimp1/krox* locus is compared between *Strongylocentrotus purpuratus* and *Lytechinus variegatus*, two sea urchin species diverged between 30 and 50 million years ago. We tested several of these both 5' and 3' of the transcription initiation sites for the two *Spblimp1/krox* isoforms individually, and only fragments containing the endogenous basal promoters had transcriptional activity.

The *cis*-regulatory analysis of *Spblimp1/krox1b*, corresponding to the regulation of the early isoform, is still in progress. To distinguish the spatial expression pattern of the early form from that of the late form a knock-in BAC was created by substituting the protein coding sequence of the second exon 1b for that of GFP by homologous recombination. This construct expresses GPF similar to *Spblimp1/krox* expression during early stages of sea urchin development. When only the proximal 150 bps with the 5' UTR from exon 1b are placed in front of a reporter construct, strong ubiquitous expression is observed. The adding of more upstream sequence reduces ectopic expression, but the inclusion of up to 3 kbp upstream and 6 kbps downstream of exon 1b is insufficient to recapitulate the expression of *blimp1/krox1b* as there are too many ectopically expressing cells remaining. There are other conserved patches that have been added to this construct and this project is ongoing (see Joel Smith's annual report in this issue for details).

A conserved fragment contained within 900 bp immediately 5' upstream of exon 1a recapitulates the expression of *Spblimp1/krox1a* during embryogenesis. This patch contains several binding sites for Otx as well as for Brn1/2/4 recently described as a midgut specific transcriptional regulator of *endo16*.

Recently we have focused on the negative auto-regulation of *blimp1/krox* demonstrated by QPCR as well as WMISH analysis. The repressive Blimp/Krox input into its own promoter results in this very dynamic pattern of expression that includes multiple territories during embryogenesis. Putative Blimp1/Krox binding sites from the genomic regions surrounding the *blimp1/krox* locus were found by computational means. Oligos containing the binding sites were synthesized and utilized in gel shift assays in the presence of nuclear extracts from sea urchin embryos at different stages. Several binding sites found within conserved patches showed band of mobility comparable to previous studies looking at Blimp1/Krox sites within the *Spotx* promoter. Site mutagenesis as well as perturbation analysis in embryos injected with promoter constructs is needed to test their function *in vivo*.

287. ***cis*-Regulatory analysis of the *krox1b* gene and early pattern formation in the sea urchin**

Joel Smith

Gene regulatory networks (GRNs) are logic maps that state in detail the inputs into each *cis*-regulatory module, so that one can see how a gene is fired off at a given time and place. As such, GRNs provide an indispensable tool for functional genomics: a set of specifically testable predictions of just what target sites are hardwired into the *cis*-regulatory genomic sequence. We perform such an analysis based on the GRN for endomesoderm specification in the sea urchin for the early form of the Krox.

Krox, a C2H2 Zn-finger transcription factor, occupies a central node in the sea urchin GRN as part of two key subnetworks: (1) a web of interactions with Otx and GataE factors specifying endomesoderm fate; and (2)

– the subject of current research – an early patterning cascade with Wnt8. Wnt8 expression is initially established in the presumptive primary mesenchyme cells (PMCs) by late cleavage stage, a result of maternally inherited Dishevelled protein, an integral member of the Wnt signaling pathway, at the vegetal pole of the embryo. Apparently by canonical Wnt-signaling, i.e., stabilization/nuclearization of β-catenin and activation of transcription with TCF, Krox gene expression rapidly follows via autocrine signaling, with Krox in turn driving further Wnt8 expression in a virtuous loop.

Sometime before the mid blastula stage, however, Krox inhibits expression of its own transcript. The autoinhibition of Krox disrupts the amplifying effects of this loop as Krox protein drops to a level that can no longer sustain Wnt8 expression, which requires both Krox and TCF inputs by this time. Also by this time, however, Wnt8 signaling has triggered the same recursive set of interactions in the neighboring secondary mesenchyme cells (SMCs). The pattern of Krox build-up followed by autoinhibition and disruption of the Wnt8-Krox loop is repeated in the SMCs and signals the initial expression of Krox in cells from the Veg$_2$ layer of presumptive endoderm.

What is seen, then, is a wave of Wnt8 expression closely followed by the *krox* gene, starting at the PMCs and emanating out from the vegetal pole into first the SMCs and then the Veg$_2$ endoderm by the mesenchyme blastula stage. (At this point in the endoderm, Krox expression appears sustained via an amplification loop with Otx, possibly independent of β-catenin/TCF.)

This piece of the sea urchin GRN makes several critical predictions. First, with respect to the *cis*-regulatory elements controlling Krox expression, the model predicts b-catenin/TCF target sites mediate Krox expression. Second, Krox binding sites mediate a repressor function. And third, disrupting the autoinhibitory function of Krox will result in prolonged Wnt8 and Krox expression in the PMCs and SMCs long after they would have normally shut off. We have identified putative Krox and TCF binding elements. We are in the process of testing our predictions that Krox target sites mediate an inhibitory function and that blocking this autoinhibition will result in continued Wnt8 and Krox expression in the PMCs and SMCs.

288. Mapping *SpErg* onto the gene regulatory network

Paola Oliveri, Qiang Tu, Jina Yun, Maria Ina Arnone*

SpErg (Ets Related Gene) is a member of ETS family of transcription factors, which is characterized by a conserved ETS DNA-binding domain. *Erg* has already been demonstrated to play crucial roles in embryonic development of other organisms. The goal of this project is to analyze the role of *Erg* in embryonic development of *S. purpuratus* and map *SpErg* to the gene regulatory network. Quantitative PCR (QPCR) and whole mount *in situ* hybridization showed that *erg* expression is first detected in micromere descendant cells of the 15 hr

blastula. At its first peak of expression at 18 hr, erg expression is expanding into presumptive secondary mesenchyme cells (SMC). A second peak of expression is observed at early gastrula stage (30 hr) when erg is expressed only in mesoderm cells at the tip of the archenteron. *Erg*'s expression in the SMC lineage persists until larval stage. We also studied the role of *erg* in the primary mesenchyme cells (PMC) gene regulatory sub-network by attempting to identify its upstream and downstream linkages. Upstream linkages were determined by quantifying the expression of *erg* in embryos which the expression of different PMC regulatory genes have been perturbed. Preliminary data show that *erg* receives late input from *ets*, but not from *alx*. Consistent with these results, *erg* is also downstream of *pmar1* and β-catenin nuclearization. To identify genes downstream of *erg*, we disrupted *erg* function by injecting a splicing blocker morpholino antisense oligo (sbMASO) into fertilized sea urchin eggs. Resulting embryos show a phenotype consistent with *erg* expression. Embryos lacking Erg protein show a severe deletion in PMC ingression and gastrulation; the latter effect is possibly due to the role of *erg* in SMC. The *erg* knockdowns recover some PMC and SMC structures at pluteus stage. Preliminary data from QPCR on *erg* sbMASO injected embryos show that *dri* is unaffected at 18 hr, but is down-regulated at 24 hr. *msp130* and *gsc* are down-regulated in *erg* sbMASO injected embryos at both 18 hr and 24 hr.

*Stazione Zoologica "Anton Dohrn," Napoli, Italy

289. *cis*-Regulatory analysis of the sea urchin *delta* gene

Roger Revilla

The *delta* gene plays two different roles in the specification of the endomesoderm of the sea urchin embryo. Each one of these roles requires Delta to be localized in a specific territory of the embryo. It is first required in the micromeres to serve as a signal that is necessary to segregate the mesodermal and endodermal fates of the surrounding cells. It is later localized in the prospective SMCs, where it signals the endodermal cells and is required for gastrulation to occur. The goal of this project is to analyze the *cis*-regulatory system that localizes the expression of Delta in the right place and the right time to serve its roles in the specification of the endomesoderm. It has already been shown that the early localization of Delta in the micromeres depends on activator(s) that are present ubiquitously, and a repressor that is present everywhere except in the micromeres. Comparison of genomic DNA sequences of *Strongylocentrotus purpuratus* containing *delta* gene with the orthologous region of *Lytechinus variegatus* genome has been used to identify conserved patches of sequence that might contain *cis*-regulatory elements. Two sequence elements have been identified that are able to recapitulate the two phases of expression of the *delta* gene. The element that recapitulates its early phase of expression has been shown to contain binding sites for activator(s) ubiquitously present and binding sites for the repressor that

localizes *delta* in the micromeres. Future work will identify the sites in the DNA that bind these factors. Finally, we also hope to be able to identify the transcription factor that acts as a repressor of *delta* everywhere in the embryo except the micromeres, which has been suggested to play a key role in the installation of the skeletogenic program of gene expression.

290. A *cis*-regulatory analysis of *SPGATA-E*
Pei Yun Lee

SpGata-e is the *S. purpuratus* ortholog to vertebrate Gata genes *4/5/6*. The expression of *SpGata-e* is first detected in presumptive secondary mesenchyme cells (SMCs) during the hatching blastula stage. Its expression expands to include both future SMCs and endoderm in the mesenchyme blastula. In the gastrula, *SpGata-e* is expressed at the tip of the archenteron and hindgut. By the end of embryogenesis, *SpGata-e* is expressed in the midgut and coelomic pouches.

A 600 bp DNA sequence in the first intron is responsible for directing *SpGata-e* expression in the vegetal plate from the onset of zygotic *SpGata-e* expression in the 15 hr blastula. This element also maintains expression in mesoderm cells at the tip of the invaginating archenteron and endoderm cells until mid-gastrulation. A separate 360 bp fragment in the first intron is responsible for directing endoderm expression in the gastrula and pluteus.

A search in the sequence of the vegetal specific *cis*-regulatory element for putative DNA binding sites of transcription factors known to be upstream of *SpGata-e* identified three putative *Otx* binding sites. Gel shift analysis has shown that the Otx transcription factor binds to the *Otx* binding sites. Mutations of the sites abolish Otx binding. Furthermore, the vegetal-specific element also responds to perturbation of Notch signaling. When Notch signaling was perturbed in a reporter construct with mutated *Otx* binding sites, GFP expression was abolished

291. Understanding the transcriptional control of *cyIIIa*
C. Titus Brown

CyIIIa is a cytoskeletal actin expressed at high levels throughout development in the aboral ectoderm of *S. purpuratus*. The 2.3 kb of genomic DNA immediately adjacent to the transcription start site is sufficient to direct correct spatiotemporal expression of a CAT reporter gene, and contains binding sites for nine distinct proteins present in 22 hr crude nuclear extract [Calzone *et al.* (1988) *Genes & Dev.* **2**:1074-1088]. Eight of these nine proteins have been characterized to some extent, but one protein remains unidentified, and several proteins play roles that have not been fully examined.

Recent work includes QPCR analysis of reporter constructs with individual and combinatorial binding site mutations. We have characterized the time course of *cyIIIa* and our reporter in considerable detail and shown that the *cyIIIa* reporter precisely recapitulates the temporal expression of endogenous *cyIIIa*. In addition, we have

demonstrated that previously reported discrepancies between the observed *cyIIIa* mRNA prevalence and reporter construct prevalence are due to perdurance of the endogenous mRNA. We have also shown that ectopic *pmar1* over-expression affects early *cyIIIa* expression dramatically, suggesting that *pmar1* over-expression ectopically represses the still-unknown early activator of *cyIIIa* transcription. This may allow us to identify this factor by a genome-wide transcription factor screen.

292. *cis*-Regulation of *Spcyp1*, a member of the Ets-Dri skeletogenic gene battery
Gabriele Amore

One of the most convincing illustrations of the power of developmental gene regulatory networks (GRNs) is their use in predicting gene batteries, i.e., in identifying sets of genes that share the same input regulatory code and are therefore activated by the same cohort of regulators. Because of their common code, such genes are called into play in the same embryonic contexts and participate in the execution of the same functions during embryonic development. The practical relevance of such gene batteries can be well appreciated when considering the developmental deployment of differentiation genes. Defining batteries at the "regulatory code-level" allows us to predict the distinct steps at which such genes intervene along the process of differentiation and provides a basis on which hypothesis on the functions they execute can be built. In our work we consider the sea urchin primary mesenchyme cells (pmcs) differentiation gene set. These genes are responsible for the migratory behavior and the ability of pmcs to interpret spatial cues and secrete the embryonic skeleton.

Based on perturbation analysis several distinct gene batteries in the pmc portion of the endo-mesoderm GRN were previously predicted (EM-GRN; for the most recent update see the Davidson lab website: http://www.its.caltech.edu/~mirsky). We have begun to test such predictions by validating the regulatory connections at one of the pmc termini of the network: the *Strongylocentrotus purpuratus cyclophilin1* (*spcyp1*) gene.

The *spcyp1* gene encodes for a member of the peptidyl-prolyl *cis-trans* isomerase (PPIase) protein family in sea urchin. Zygotic *spcyp1* transcription is observed from early blastula (1 2h) until gastrula (48 h) stage. Transcription is confined in the primary mesenchyme cells (pmcs). Through reporter gene transfer experiments and real time quantitative PCR analysis, we show that a 218 bp genomic DNA fragment (Y2-Y4) ensures the pmc-specific expression of *spcyp1*. Y2-Y4 sequence and functional analysis identify Ets1 and Dri transcription factors as necessary inputs for the activation of *spcyp1* (as predicted in previous perturbation analysis). Direct binding of both factors to Y2-Y4 is required for the activation of the gene. On this basis a new gene battery is identified in sea urchin: the pmc Ets-Dri gene battery of which *spcyp1* is the first member.

293. Quantification of cellular GFP expression in live sea urchin embryos using 3D confocal laser scanning microscopy

Sagar Damle, Eric Davidson, Scott Fraser

Gene-transfer experiments have become essential for the analysis and refinement of GRN's. These typically involve reporter genes that fuse the putative *cis*-regulatory sequences of a gene under study with the coding sequence of an easily assayed reporter protein, such as CAT, β-Gal, or green fluorescent protein (GFP). These offer the temporal and/or spatial control of reporter gene expression to be determined in homogenates by biochemical assays, *in situ* hybridization or direct visualization. While the connectivity of GRNs can be understood by existing methods, a major limitation is their difficulty in quantifying the temporal control of gene expression while preserving information about spatial localization. The use of GFP-based reporters together with confocal laser scanning microscopy (CLSM) has offered a nondestructive technique for following gene expression in living embryos in a quantitative fashion over time. Until now, these methods have been applied towards quantification of whole embryo GFP expression.

We have extended the quantitative imaging of GFP-based reporter genes to permit the accurate measurement of expression levels in single cells, within the context of a living sea urchin embryo. Embryos are co-injected with rhodamine dextran, as an internal fluorescent standard, and a BAC-reporter construct driving the expression of a fluorescent protein. We have constructed a GFP reporter whose expression is driven by the *cis*-regulatory system of the primary-mesenchyme specific SpTbrain gene. GFP abundance was measured in late-gastrula-stage embryos roughly 50 hr post fertilization. We have shown that the technique is quantitative, able to generate reproducible estimates of GFP numbers within sister cells in a living embryo, allowing for a dynamic readout of protein production from a tissue-specific reporter, and permitting the construction of a kinetic network model of development.

294. Trans-specification of primary mesenchyme cells through genetic rewiring of the mesoderm specification network

Sagar Damle, Eric Davidson

In the sea urchin *Strongylcentrotus purpuratus*, the identity and regulatory relationship of a number of transcription factors involved in endomesoderm development have been well characterized. However, the ultimate demonstration of intellectual control of the causal moving parts of a system is to reengineer it. The goal of the project is to determine whether the ectopic expression of the transcription factor *SpGcm* is sufficient to *trans*-specify primary mesenchyme cells (PMC) into a secondary mesenchyme cell (SMC) fate. This can be done by placing the *gcm* coding sequence under the control of a promoter that directs PMC-specific gene expression. The Davidson lab has developed a system whereby BAC-sized DNA fragments can be introduced into fertilized sea urchin eggs

through microinjection and integrated into the genome as early as the two-cell stage. This system has been used here to probe the effects of creating novel connections between regulatory pathways.

SpGcm is thought to play two roles in development. Its early expression in all presumptive mesoderm suggests it is capable of setting up a mesodermal transcriptional state. This state gives cells a competency to respond to signals that specify various SMC or mesodermal cell lineages. Some evidence for this theory already exists. For example, embryos injected with antisense morpholino against *gcm* do not correctly express *gata-c* gene in the oral domain of veg₂ mesoderm (A. Ransick and J. Rast, unpublished data). The later role of Gcm in pigment cell specification is perhaps more difficult to characterize through morpholino analysis. However, *in situ* hybridization shows late *gcm* expression exclusively in pigment cells.

The T-box transcription factor Tbrain is expressed in the large micromere descendants at swimming blastula stage. Its expression persists through gastrulation into PMCs. A recombinant BAC has been constructed whereby *gcm*-coding sequence is transcribed under the control of the *tbrain cis*-regulatory system. PMC cells expressing *gcm* have been shown to express a terminal differentiation gene, *pks,* which is normally transcribed only in pigment cells. *Gcm*-expressing PMCs also do not participate in skeletogenesis. Instead, they appear to migrate towards the aboral ectoderm, in a manner similar to their pigment cell relatives. They also express *pks*, as do pigment cells; in short, by altering the regulatory state and introducing a pigment cell specific regulatory gene expression into the skeletogenic pmc's they are induced to transform into pigment cells and to exclude pmc specification. The degree to which Gcm can both override the skeletogenic program of PMCs and specify either pigment cell or mesodermal cell fate will be further probed through whole mount *in situ* by measuring expression of other PMC and SMC-specific transcription factors and markers. Such factors include Gata-c, a mesoderm-specific transcription factor controlled by Gcm, Alx, a homeobox protein involved in PMC specification, and the forkhead factor Foxb. Whole mount *in situ* hybridization with probes for these genes will be used to identify the extent of Gcm respecification.

295. Completion of the micromere-PMC gene regulatory sub-network

Paola Oliveri, Qiang Tu, Jina Yun

Of the subnetworks comprising the sea urchin endomesoderm specification network, that of the skeletogenic micromeres is so far the most extensively studied and closest to completion. Our goal is to explain this GRN in terms of the biological events observed during development. In order to do so we have not only to identify all regulatory genes involved in this sub-network, but to map out with precision the causal regulatory relationships among them and between them and downstream differentiation genes. Micromeres arise at the

vegetal pole of the sea urchin embryo at 4th cleavage. These four little cells are the only autonomously specified cells of the sea urchin embryo. Micromeres and their immediate descendents (**P**rimary **M**esenchyme **C**ells) are the source of two important signals for the specification of the entire endomesoderm territory. Later in development PMC themselves will form the larval skeleton. Thus far it has been shown that *pmar1* is a key component of the zygotic regulatory gene network that accounts for micromere specification and subsequent differentiation. *pmar1* expression is sufficient to activate the micromere-PMC specification program and the differentiation regulatory cascade events in every cell of the embryo. *pmar1* has also been shown to be the sole and primary transducer of maternal cues (Otx and β-catenin/Tcf) to the downstream micromere specification regulatory apparatus and its transducer action is exerted through a double negative regulatory interaction.

Downstream of pmar1. Initially six transcription factors had been identified as part of the micromere-PMC sub-network and generally classified in two main groups: first, *alx1*, *tbr* and *ets1* transcription factors, in which micromere restricted expression starts a few cell divisions after the *pmar1* appearance in micromeres and remains only in PMC cell lineage until late gastrula; second, *dri*, *gsc* and *foxB* factors, in which expression is transient, starts at late cleavage-early blastula stage and ends after PMC ingression. Uniquely, *foxB* expression stays on in PMCs until midgastrula stage. The architecture of the network downstream of *pmar1* has been studied with high resolution using single knock-down perturbation with morpholino antisense oligos (MASO) and with double perturbations using MASO and ectopic mRNAs and/or a dominant negative version of the protein. Functional knockdown of *alx1* and *ets* leads to an absence of PMCs; knockdown of *tbr* does not effect PMC ingression into the blastocoel. However, the absence of any of the three factors does prevent synthesis of spicules at larval stage. The effects of these perturbations are quantified by QPCR on all the known genes expressed in PMC and the rest of the endomesoderm territory. Such a high resolution approach leads to the following conclusions. 1) A series of complex interregulatory interactions are responsible for setting up a new regulatory status in the micromere descendant cells. 2) The new regulatory arrangement is responsible for direct activation of the genes responsible for PMC ingression and skeletogenesis. 3) The new regulatory state does not required the presence of *pmar1*. *Ets1* and *alx1* are the main regulators of the transient regulatory and differentiation genes. The differentiation genes can be grouped in three different types of gene battery according to the inputs received and thus to the structure of their *cis*-regulatory apparatus: 1) genes directly regulated by both *ets1* and *alx1* and indirectly responding to *dri* and *gsc*; 2) genes regulated only by *ets1* like ficolin; 3) genes like *sm30* whose expression requires PMC-ectoderm crosstalk. *Alx1* is responsible for repressing in PMCs the SMC alternative fate. This function is executed *via gcm*, the major regulator of SMC specification. As a consequence, in *alx1* knockdown embryos the PMC are respecified as SMC and express mesodermal specific markers like *gcm* and *pks*.

The repressor of micromeres. *pmar1* transduces maternal spatial information to the downstream micromere specification regulatory apparatus using a double negative regulatory interaction. From the discovery of these double negative interactions we logically inferred the presence of a general repressor called repressor of micromeres (R of mic) with the following characteristics: the zygotic expression of R of mic must be ubiquitous with the exception of micromeres and must be downstream of *pmar1*, its maternal expression can not be excluded, but at the very least it must be activated by early cleavage stage. Two complementary approaches are pursued to identify the molecular nature of the R of mic: 1) The study of the *cis*-regulatory apparatus of genes directly downstream of the R of mic like *tbr* and *delta* (see reports of Oliveri, Gora and Damle and Revilla); 2) The identification of transcription factor(s) repressed by *pmar1*. For the second approach we decided to set up a quantitative screening using QPCR to compare embryos globally expressing *pmar1* against either normal and/or embryos lacking*pmar1*expression. In this screening we take advantage of the fact that the temporal expression pattern is known for almost all transcription factors encoded in the sea urchin genome including zinc-finger transcription factors. 108 genes are expressed both maternally and zygotically and 30, with the exclusion of known genes, are only zygotic and start to express between 6 hr and 12 hr of development. These 30 genes are our first candidates for the screening. Once identified, a high-resolution spatio-temporal analysis of the *pmar1* repressed genes will be done. The promising candidate will be analyzed at a functional level for their capacity to repress *ets, alx* and *tbr* and directly bind to the relevant sequences in their *cis*-regulatory apparatuses.

How many genes are still missing? The genome approach. So far the micromere-PMC subnetwork up to 24 hr involves 11 transcription factors and two signaling molecules. The newly available *S. purpuratus* genome has allowed for the identification of almost all the transcription factors present in the genome. A total of 18 new transcription factors, belonging to many different families, are specifically expressed in the PMC lineage, but only three of them start their expression before 24 hr of development. One of them, *soxC*, is transiently expressed in micromere descendants only at 12 hr. At this stage *soxC* responds positively to *pmar1* over-expression. Another early gene is *erg*, a transcription factor of the ets family, whose expression and functional analysis are described in the Tu, Oliveri, Yun and Arnone report. The onset of the expression of all the remaining factors occurs after 24 hr, showing that the current network up to 24 hr is in a near-complete state of development and that what is really missing are the late regulatory interactions. Each of the genes identified by genomic analysis will be first integrated in the network by assessing which known

factors regulate them and, through functional knock-down, which downstream factors they affect. Preliminary data show that *foxN2/3*, *foxO*, *jun* and *smad5* are all under positive *pmar1* control, but they are insensitive to *alx* and *ets* knock-down. Finally, a new signaling molecule and corresponding receptor have been identified, VEGF and VEGF-R, that are most likely involved in the late ectoderm-PMC signaling necessary for the spiculogenesis.

296. Forkhead-box containing transcription factors in *S. purpuratus* development
Paola Oliveri, Qiang Tu, C. Titus Brown

The f<u>o</u>rkhead-b<u>ox</u> (*fox*) genes are transcription factors containing a conserved winged helix DNA binding domain. Genes belonging to this family have been identified in different animals, yeast and fungi, but not in plants. There are at least four genes in yeast, five in sponge, 17 genes in *Drosophila*, 29 genes in *Ciona* and 42 genes in *Homo*. Vertebrate genes have been classified into 17 groups (A to Q), 10 of which are conserved in *Drosophila*. These represent the bilaterian forkhead factor genetic tool kit. In all the bilaterian organisms studied fox members are involved in many different developmental processes. Only three members of this family have previously been characterized in sea urchin.

We conducted a systematic search for forkhead-box factors in the available reads of an *S. purpuratus* whole-genome sequencing effort being carried out by the Baylor HGSC. A total of 24 contigs coding for 19 novel *fox* factors have been identified from the currently available 6x coverage. We isolated corresponding cDNAs for each of the new fox factors using RT-PCR and/or library screening. A phylogenetic analysis of these cDNAs showed almost all vertebrate classes are represented by at least one orthologous sea urchin gene. Classes as yet unidentified in the sea urchin genome include class H (fast1) and class E along with the newly identified class R and class S, all of which are probably chordate specific. The class Q2 presents a sea urchin-specific duplication represented by two closely related genes. The *S. purpuratus* genome also contains a new fox factor equally related to the classes foxA and foxB and a factor that is impossible to classify due to its divergent sequence.

We analyzed the temporal and spatial expression during embryogenesis of the identified *fox* factors. All the identified *fox* genes are expressed sometime during the first 72 hr of sea urchin development with the exception of foxQ1 that appears not to be expressed (less than 25 transcripts/embryo) in any developmental stage. FoxN1/4 is the only gene that shows a constant and ubiquitous expression as assayed by RT-PCR and whole mount *in situ* (WMISH) respectively. Four genes are maternally expressed, but only one of them is exclusively maternal, the sea urchin-specific *foxX*. *foxK*, *foxN2/3* and *foxO* are expressed in primary mesenchyme cells (PMC) sometime during development, while *foxC, foxD, foxF, foxI, foxL1, foxL2 and foxP* are expressed in endoderm and/or secondary mesenchyme cells (SMC).

The main focus of our lab is the analysis of gene

regulatory network for the whole sea urchin development. Many of these genes, by virtue of their expression patterns, are certain to play important roles in specification and differentiation of embryonic body parts and will be integrated into in different parts of the sea urchin regulatory network.

297. A microsatellite-based physical map of the purple sea urchin genome
R. Andrew Cameron, Kevin Berney, Elly Chow, Autumn Yuan, Eve Helguero, Eric Davidson

The 8 million WGS reads from the genome sequencing effort at the Baylor College of Medicine, Human Genome Sequencing Center have been assembled into a set of contigs and scaffolds. The next task is to refine the assembly through the use of other kind of sequence information such as BAC end sequences and ESTs. We have provided all of the DNA and libraries for this sequencing effort and we continue to work with the Baylor Center on other aspects of the sequencing effort.

Since there is no genetic map currently available, the ordering of scaffolds on chromosomes will require a library of linked and ordered markers. This resource is particularly necessary because the genome of *S. purpuratus* is more polymorphic than that of any other animal thus far the subject of a sequencing project. The consequence for the genome project is that the polymorphism will impede assembly. Therefore any physical mapping information that we could provide would very materially improve the assembly operation and increase the quality of the draft genome sequence. In response to this need we have undertaken to provide a microsatellite map for this genome. We are using an extensive set of related animals of known genealogy that survive in our long-term laboratory culture system at the Kerckhoff Marine laboratory. We have designed primer pairs in single copy sequence flanking micro-satellites by a computational method, using the WGS trace sequence library and tested these primer pairs by reaction with several wild-type genomes, to determine if they are amplifiable and display polymorphic variants. From those primers that pass the tests were obtained fluorescently labeled primer pairs that were used to genotype about 50 animals at 160 different loci in an Applied Biosystems 3730 Sequence Analyzer. These data are currently being reviewed for quality and will be used to sort the markers into linkage groups, i.e., chromosomes.

298. *Delta* expression after 500Ma divergence
Feng Gao, Veronica F. Hinman, Kirsten Welge

Delta signaling plays a key role in early echinoid development. We are interested to compare the expression and *cis*-regulatory control of this gene between the sea urchin *Strongylocentrotus purpuratus* and the starfish *Asterina miniata*.

Patterns of endogenous *AmDelta* and *SpDelta* expression have been determined by whole mount *in situ* hybridization (WMISH). In the sea urchin, *delta* is first expressed in the micromeres and later in the SMCs. In

starfish, *AmDelta* is expressed in the central vegetal plate which is fated to form mesoderm and later in the ectoderm. Expression in the micromeres may be a derived feature of echinoids, while expression in other mesoderm progenitors may be conserved among the echinoderms.

We are interested to know the *cis*-regulatory control underlying these conserved and divergent expressions. The *cis*-regulatory control of the *S. purpuratus delta* gene is already well known (see report by Roger Revilla). We built an *AmDelta*-GFP-BAC construct by homologous recombination with GFP, replacing the first exon of the endogenous *delta* gene (see report by Julie Hahn). Microinjections of this recombinant, recapitulates endogenous *AmDelta* expression in the starfish, thus demonstrating that the *cis*-regulatory modules necessary to direct (at least) embryonic expression are contained within the BAC clone. The *AmDelta*-GFP-BAC was also injected into the embryos of *S. purpuratus*. GFP expresses in the SMCs and ectoderm which indicates that the composition of *A. miniata* binding sites is well enough conserved between the two organisms to be bound by the appropriate *S. purpuratus* transcription factors. This also suggests that orthologous transcription factor proteins regulate embryonic *delta* expression in the SMCs of *S. purpuratus* and the mesoderm progenitors of *A. miniata*.

A series of constructs were produced by PCR off *AmDelta*-GFP-BAC DNA template and their ability to drive reporter gene expression in *A. miniata* embryos was tested. The third intron of the *AmDelta* gene was found to drive correct reporter gene expression when attached to a minimal basal promoter. Sequence comparison with the module known to drive correct expression of *SpDelta* in sea urchin, however, failed to show any conservation. Conservation may only exist at the level of binding sites.

Experiments are underway to sequence the third intron of the delta gene from another starfish, *Dermasterias imbricata*, in order to use sequence comparison programs such as Family Relations to locate the *cis*-regulatory module. Finally we hope to identify the exact binding sites within this module and to confirm these through perturbation and microinjection.

299. Regulatory gene network evolution: A comparison of endomesoderm specification in starfish and sea urchins

Veronica F. Hinman, Eric Davidson

We are undertaking an evolutionary comparison of the gene regulatory network (GRN) of transcription factors underlying the specification of endomesoderm in sea urchins and starfish. The extensive analysis of this network in sea urchins has provided a unique opportunity for a comparative investigation to elucidate mechanism of evolution at this level. We would like to answer questions such as, which components of such a regulatory system are conserved, how are changes incorporated into a GRN, and how do these changes relate to the evolution of morphology? The starfish *Asterina miniata* has been developed as an ideal experimental model for this analysis. Gametes are readily available and gene transfer and

perturbation of gene products have been performed. Starfish last shared a common ancestor with sea urchins around 500 million years ago and they appear to be at an ideal evolutionary distance for meaningful comparisons; they share many conserved aspects in their development and yet there exist specific morphological differences.

We have previously shown that a common developmental feature of starfish and sea urchin GRNs is the use of an orthologous three gene positive regulatory feedback loop that serves to 'lock down' gene expression required for the specification of the endoderm and thus to drive development forward. The conservation of this feature across the immense period of evolutionary time such as separates these echinoderms demonstrates the indispensable nature of such a process in their development. Several differences were also noted in the GRN architecture. We have noted that *tbrain* (*tbr*) is incorporated into the endomesoderm-specification network in starfish while it is involved in primary mesenchyme cell specification in sea urchins. Also, the starfish *gatae* gene is repressed from the mesoderm by *foxa* while this is not the case in sea urchins.

These differences in transcription factor expression in the mesoderm suggest that specification of mesoderm may be quite different in starfish and sea urchin. This is also suggested by the requirement of a Delta signal from the underlying micromeres to specify mesoderm in sea urchins, although a micromere lineage is completely absent in the starfish. We, therefore sought to continue our comparative GRN analysis by examining mesodermal specification in the two organisms as it is hoped that this will provide insight into the types of GRN architectural changes underlying differences in a specification process that goes along with the novel acquisition of the micromere cell lineage.

Towards this aim the starfish Delta ligand and the *gcm* and *gataC* transcription factors were cloned and Delta deficient starfish embryos analyzed. Unlike in sea urchins, the starfish *gcm* gene is not expressed in the vegetal plate but is expressed in a patch of cells in the pre-blastula that appear to extend throughout the aboral ectoderm. *GataC* is, however, expressed similarly in vegetal plate and top of the archenteron in the two organisms. *Delta* is expressed in the vegetal plate where it is required in the starfish for endoderm specification including the endodermal expression of the *gatae* gene. This function of Delta appears to be conserved in the two echinoderms. The starfish *delta* gene is however not required for the specification of mesoderm and the expression of *gataC*. We also observed that in starfish, *delta* is expressed in the ectoderm where it represses *gcm*. We have yet to determine whether the cells expressing *delta* or *gcm* are ectodermal in origin or represent mesenchymal cells that have migrated into the ectoderm. Cell lineage analysis is being used to determine whether there is a population of pregastrula migrating mesenchyme in the starfish.

The GRN network analysis is also being extended to look at the specification of neuroectoderm. Towards this goal we have cloned starfish homologues of

neurogenin and *sox1/2/3*. These, along with other ectodermally expressed regulatory genes, including *tbr*, *delta*, *hnf6* (*onecut*) and *otx* and possibly *delta* and *gcm*, may form part of the neuroectodermal GRN.

300. **A comparison of *cis*-regulatory control of some key elements from the starfish and sea urchin GRNS – A search for rules of regulatory syntax across immense evolutionary time**

Veronica F. Hinman, Sarah Wadsworth, Harold Hsu, Eric Davidson

We are further expanding our work on comparative GRNs to identify and analyze the *cis*-regulatory elements of several genes of the starfish GRN, *viz orthodenticle (otx)*, *brachyury (bra)*, *tbrain (tbr)* and *gatae*. It is known from the comparative GRN analysis that the *bra*, *otx* and *gatae* genes in starfish and sea urchins are similarly regulated and expressed, yet comparative sequence analyses using "Family Relations" fail to find any significant patches of sequence conservation in the surrounding 100-150 Kbp of DNA. We would like to determine if there are any *cis*-regulatory rules that determine the conservation of inputs into these genes. *Tbr* on the other hand is differently expressed and regulated in the two organisms, and will allow us to know what changes have occurred in *cis*-regulatory control of the genes that have permitted this evolutionary change.

We are analyzing, in detail, the *cis*-regulatory region of the starfish *bra*, *otx*, *gatae* and *tbr* genes and are comparing these to the regulatory regions of the orthologous sea urchin genes. BAC recombinants of approximately 150 Kb for each of these four genes have, or are being sequenced. With the assistance of Julie Hahn GFP recombinants for each of these BAC clones have also been prepared. Preliminary results indicate that these GFP recombinants express as predicted in the starfish.

Several methods were used to identify regulatory modules within the BAC sequence. An approximately 500 bp region including the 5' UTR of *AmBra* DNA drives correct reporter gene expression in pregastrular starfish embryos. Expression of this regulatory element is enhanced by fusing it with either of two genomic regions downstream of the coding region. An approximately 500 bp region of DNA downstream of the *otx* coding region has also been identified that drives correct reporter gene expression. This region was identified using the "Cluster Buster" software that searched for a statistical over representation of consensus binding motifs for the Otx, Krox and Gatae transcription factors, all of which are known to regulate *otx* expression. The arrangement of these binding sites in the *cis* regulatory elements of the starfish and sea urchin *otx* genes was found to be remarkably similar suggesting that some functional constraint must exist in their relative arrangement.

Work is now underway to delete various predicted binding sites in these modules, using fusion PCR technologies, and to assess the effects on reporter gene expression.

301. ***cis*-Regulation of Spgcm**

Andrew Ransick

Using a variety of experimental approaches, work continues toward defining the *cis*-regulatory architecture and critical '*trans*' inputs of *Spgcm,* the echinoderm ortholog of the transcription factor *glial cells missing*. GFP-reporter constructs microinjected into fertilized eggs and assayed in embryos demonstrated that the regulatory sequences that promote expression of this gene in the secondary mesenchyme domain at the mesenchyme blastula stage are distributed across ~15 kilobases of sequence upstream of *Spgcm* coding exons, but are concentrated into proximal (P) and distal (D) regions working in concert with a relatively short but indispensable enhancer (E) region. Recent efforts have been focused on dissecting the "E region" of *SpGCM* (357 bases located approximately nine kilobases upstream of the transcription start site), in order to assign specific function(s) to several highly conserved DNA sequence elements. Results show that the "E region" probably encodes the Delta/Notch signaling pathway response element and plays a large role in limiting *Spgcm* expression to a mesodermal subregion (SMCs) that ultimately gives rise to pigment cells. Three consensus binding sequences for Suppressor of Hairless (Su(H)) are present in E region, but attention was initially drawn to a highly conserved 60 base element toward the 5' end of E region containing two of the Su(H) sites configured as an inverted pair with a 15 base spacer --- an arrangement of sites strongly resembling the configuration of Su(H) sites found in known Notch response genes in insects (e.g., Enhancer or Split) and mammals (e.g., Hairy). While results indicate the paired Su(H) site contributes to correct spatial expression of constructs, the most recent experiments have shown that the 3' end of E region (the ~175 bases 3' of the paired Su(H) sites) is also essential. This region contains two known conserved elements, including a lone Su(H) site and a 30 base conserved element. Analyzing the function of these specific elements is currently underway.

302. ***cis*-Regulatory analysis of *Sptbr***

Paola Oliveri, Kasia Gora, Sagar Damle

The sea urchin endomesoderm gene regulatory network (GRN) is a model that describes the genetic program controlling the early stages of specification and development in *Strongylocentrotus purpuratus.* The gene *tbr* is a part of the micromere/primary mesenchyme cell (PMC) sub-network that encodes a Tbox transcription factor. Endogenous *tbr* is a maternally present factor with zygotic expression in micromeres and their descendents, the PMCs, that continues throughout skeletogenesis. Zygotic *tbr* expression responds to the double repressive inputs downstream of *pmar1* and its appearance is exclusive to the micromere lineage (similar to *delta*, *ets1* and *alx1*). The *cis*-regulatory analysis of *tbr* is essential for understanding of the *S. purpuratus* endomesoderm specification network. Furthermore, comparison against a similar analysis of the *delta* promoter has the potential to

lead to the discovery of the critical yet unknown repressor of micromere (R of Mic).

In order to computationally predict potential *cis*-regulatory regions of *tbr,* we employed "Family Relations II" to identify patches of sequence conservation between the *tbr* orthologs of *S. purpuratus* and *L. variegatus*. The annotated *Sptbr* BAC clone shows that *tbr* lies on a gene-dense fragment of DNA. The BAC contains six genes in ~130kb and *tbr* is flanked by genes 3.5 kb upstream and 16k b downstream.

We identified only four small (>300 bp) conserved patches. Our analysis began by investigating the regulatory properties of the entire 3.5 kb upstream region. The expression pattern of *cis*-regulatory reporter constructs was compared to the endogenous expression pattern of *tbr* as previously determined by whole-mount *in situ* hybridization (WMISH) and the GFP expression of a *SpTbr* GFP BAC knock-in construct. This construct recapitulates the endogenous expression pattern, showing that the large BAC contains all the regulatory elements necessary for correct expression. The 3.5 kb construct showed strong GFP expression in the PMCs at both the 24 and 48 hr of development with patches of ectopic expression generally localized to the ectoderm, while the same fragment cloned in antisense orientation showed no significant expression. A series of deletions from the 3.5 kb construct allowed us to further subdivide the *tbr* upstream region into smaller functional units. We identified a 343 bp sequence, called γ(2), that is sufficient to drive the low level GFP expression in PMCs when fused with a GFP reporter gene under the immediate control of the Endo16 basal promoter. Only 25-30% of the embryos show a PMC-specific GFP expression. These data show that the γ(2) sequence contains regulatory elements sufficient for PMC expression; moreover that some others sequences, possibly the conserved proximal module called a, are likely responsible for amplifying the level of expression and no spatial restriction information need be conveyed through them.

The restriction of the PMC specific module to a ~300 bp sequence opens the possibility for a computational analysis of potential binding sites and also a high resolution biochemical and mutational analysis. This will lead to the identification of all the positive and negative factors that bind to this module, including the sequence that binds the R of mic. Finally a comparison with the PMC-specific module of *delta* gene (R11) can identify the common *cis*-regulatory logic responsible for the early micromeres-PMC gene expression.

303.   *foxA* a key endoderm specification factor
Paola Oliveri, Qiang Tu, Katherine Walton[*], Andy Ransick, David R. McClay[*]

Transcription factors of the *foxA* class have been identified as key players in endoderm and foregut specification in many organisms. Here we study the role of *SpfoxA* in the sea urchin endomesoderm regulatory network.

The sea urchin forkhead transcription factor *foxA* is so far the earliest endoderm-specific transcription factor identified during sea urchin development. *foxA* starts expressing at the end of cleavage stage (15 hr) in the endomesoderm tier. By hatched blastula stage (20 hr) it is expressed only in endodermal cells and will remain there until larval stage. At the beginning of gastrulation (30 hr) the stomodael ectoderm starts to express the *foxA* gene as well. Analysis by QPCR after perturbation with MASO placed *foxA* expression downstream of *gataE* and *otx. foxA* knock-down embryos show a clear phenotype in which either the foregut or the entire gut is missing, depending on the amount of MASO injected. Detailed *foxA* perturbation analysis on downstream genes shows: 1) *foxA* represses itself causing its expression to oscillate; 2) early (18 hr) *foxA* represses *gataE*, while *gcm,* an important gene in the SMC lineage, is repressed roughly at 30 hr; 3) *foxA* is a positive regulator of *Hh*, a signaling molecule expressed in the same veg$_2$/endoderm territory of *foxA*; 4) the late expression (48 hr) of *endo16* and *gataE* is severely affected by *foxA* knock-down. These initial quantitative data are supported by *in situ* hybridization evidence and by using mosaic embryos where only a couple of blastomeres are lacking *foxA* function and are labeled with rodamine and by WMISH on *foxA* MASO injected embryos.

These studies show that cells of the veg$_2$ lineage are diverted by *foxa* MASO from a mesoderm plus endoderm fate to a mesoderm-only fate. In the absence of *foxA* there is an expansion of the pigment cell population as well as expansion of other SMCs, at the expense of the foregut. Chimaeric experiments show a requirement for *foxA* in the oral ectoderm during mouth formation. We conclude from this data that *foxA* normally represses SMC genes in endoderm and this action is exerted *via* repression of *gcm*. Also, *foxA* is one of the major factors involved in specification and differentiation of the endoderm as seen in the case of the *Hh* endoderm gene. And finally, *foxA* is required in the development of the mouth. In each case its relationship to other factors in the context of the transcriptional network governs the phenotypic consequences of *fox A* action.

*Duke University

Publications
Britten, R.J. (2004) Coding sequences of functioning human genes derived entirely from mobile element sequences. *Proc. Natl. Acad. Sci. USA* **101:**16825-16830.

Britten, R.J. (2005) The majority of human genes have regions repeated in other human genes. *Proc. Natl. Acad. Sci. USA* **102**:5466-5470.

Brown, C.T., Xie, Y., Davidson, E.H. and Cameron, R.A. (2005) Paircomp, FamilyRelationsII and Cartwheel: Tools for interspecific sequence comparison. *BMC Bioinformatics* **6**:70.

Cameron, R.A., Chow, S.H., Berney, K., Chiu, T.-Y., Yuan, Q.-A., Krämer, A., Helguero, A., Ransick, A., Yun, M. and Davidson, E.H. (2005) An evolutionary constraint: Strongly disfavored class of change in DNA sequence during divergence of *cis*-regulatory modules. *Proc. Natl. Acad. Sci. USA* **102:**11769-11774.

Cameron, R.A., Rowen, L., Nesbitt, R., Bloom, S., Rast, J.P., Berney, K., Arenas-Mena, C., Martinez, P., Lucas, S., Richardson, P.M., Davidson, E.H., Peterson, K.J. and Hood, L. (2005) Unusual gene order and organization of the sea urchin *Hox* cluster. *J. Exp. Zool.* **304B**:1-14.

Cameron, R.A. (2004) Hunting for origins. *Science* **305**:613-615.

Gralnick, J.A., Brown, C.T. and Newman, D.K. (2005) Anaerobic regulation by an atypical Arc system in *Shewanella oneidensis. Mol. Microbiol.* **56:**1347-1357.

Istrail, S. and Davidson, E.H. (2005) Logic functions of the genomic *cis*-regulatory code. *Proc. Natl. Acad. Sci. USA* **102**:4954-4959.

Lee, P.Y. and Davidson, E.H. (2004) Expression of *Spgatae*, the *Strongylocentrotus purpuratus* ortholog f vertebrate GATA4/5/6 factors. *Gene Expression Patterns* **5**:161-165.

Levine, M. and Davidson, E.H. (2005) Gene regulatory networks for development. *Proc. Natl. Acad. Sci. USA* **102**:4936-4942.

Longabaugh, W.J.R., Davidson, E.H. and Bolouri, H. (2005) Computational representation of developmental genetic regulatory networks. *Dev. Biol.* **283**:1-16.

Revilla-i-Domingo, R., Minokawa, T. and Davidson, E.H. (2004) R11: A *cis*-regulatory element that controls expression of *SpDelta* and responds to the Pmar1 repression system. *Dev. Biol.* **274**:438-451.

Oliveri, P. and Davidson, E.H. (2004) Gene regulatory network analysis in sea urchin embryos. *Meth. Cell Biol*. **74**. In *Development of Sea Urchins, Ascidians, and Other Invertebrate Deuterostomes: Experimental Approaches* (C. A. Ettensohn, G. M. Wessel and G. A. Wray, eds.), pp. 775-794. Elsevier Academic Press.

Otim, O., Amore, G., Minokawa, T., McClay, D.R. and Davidson, E.H. (2004) *SpHnf6*, a transcription factor that executes multiple functions in sea urchin embryogenesis. *Dev. Biol.* **273**:226-243.

Otim, O., Hinman, V.F. and Davidson, E.H. (2005) Expression of *AmHNF6*, a sea star orthologue of a transcription factor with multiple distinct roles in sea urchin development. *Gene Expression Patterns* **5**:381-386.

Yuh, C.-H., Dorman, E.R. and Davidson, E.H. (2005) Brn1/2/4, the predicted midgut regulator of the *endo16* gene of the sea urchin embryo. *Dev. Biol.* **281**:286-298.

Esther M. and Abe M. Zarem Professor of Bioengineering: **Michael H. Dickinson**

Postdoctoral Scholars: Doug Altshuler, Will Dickson, Mark Frye, Titus Neuman, Christian Poelma, Andrew Straw

Graduate Students: John Bender, Seth Budick, Gwyneth Card, Michael Reiser, Alice Robie, Rosalyn Sayaman, Jasper Simon

Undergraduate Students: Robert Bailey, Martin Peek

Visitor: Hiroki Sugura*

Research and Laboratory Staff: Qing Ling, Lilian Porter, Heidi Rolufs

*Tokyo University, Japan

Summary:

1. We have constructed and tested a prototype MEMS-based flight balance for fruit flies that will have use in many future experiments.

2. We have been able to map the aerodynamic consequence of the several key steering muscles.

3. We have demonstrated the changes in flow structure and force production around the wing as a function of Reynolds number.

4. We have succeeded preliminary *in vivo* measurements of changes in the calcium concentration within power muscles during flight.

5. We have characterized the interaction between olfactory and visual reflexes during flight, and have mapped the spatial tuning of visual motion reflexes.

6. We have characterized the interaction between visual and mechanosensory stabilization reflexes.

7. We have developed a control theory model that replicates the salient features of a male's tracking behavior during courtship.

304. **Time-resolved reconstruction of the full velocity field around a dynamically scaled flapping wing**

Christian Poelma

In this project, a dynamically-scaled wing moves in mineral oil in a pattern based on the kinematics of real *Drosophila* (obtained using calibrated high-speed cameras). The flow is very repeatable, due to the relatively low Reynolds number and the accurate controlling of the wing. This repeatability is used to reconstruct the transient flow field around the wing. Measurements are performed in a plane perpendicular to the wing cord using a phase-locked stereoscopic PIV system. The wing is translated in the spanwise direction after each set of measurements to obtain all spanwise planes, so that the full three-dimensional flow field can be reconstructed. Different stages in the stroke cycle are obtained by changing the reference frame of the rotating wing with respect to the cameras and light sheet; the measurement system is triggered when the wing is perpendicular to the laser sheet, so that the flow field is obtained in a frame of reference rotating along with the wing.

Two cases have been studied so far: a flapping pattern closely resembling *Drosophila* kinematics, yet without any (vertical) deviation of the wing in the stroke plane. The second case focuses on a wing starting from rest at a constant angle-of-attack of 45°. Both cases can be characterized by a Reynolds number, based on (maximum) tip velocity and cord length, of 150.

The former case is used to study a number of phenomena that have been suggested in recent years to explain flapping flight (e.g., a stable attachment of the leading-edge vortex, shedding of the trailing-edge vortex, vortex-wing interaction). Flow patterns resulting from a previous flapping cycle influence the wing. In the starting wing case, these are obviously absent. Therefore, this case lends itself for a more detailed study of the fundamental aspects of the growth and stability of the attached vortices.

An example of a visualization of the obtained data is given in Figure 1, which shows the development of the flow field - including the separation of the trailing edge or 'starting' vortex - around a wing right after the onset of motion. The data is visualized by plotting an isosurface of the second invariant of the fluid velocity gradient tensor. A negative value of this invariant corresponds to a high rotational component and a low local pressure and can thus be associated with a vortex core. This gives a more clear insight in the structure of the flow compared to e.g., the use of isosurfaces of vorticity: the latter would show two distinct structures (the red and blue parts on the sides of the wing), instead of showing them as one connected vortical structure.
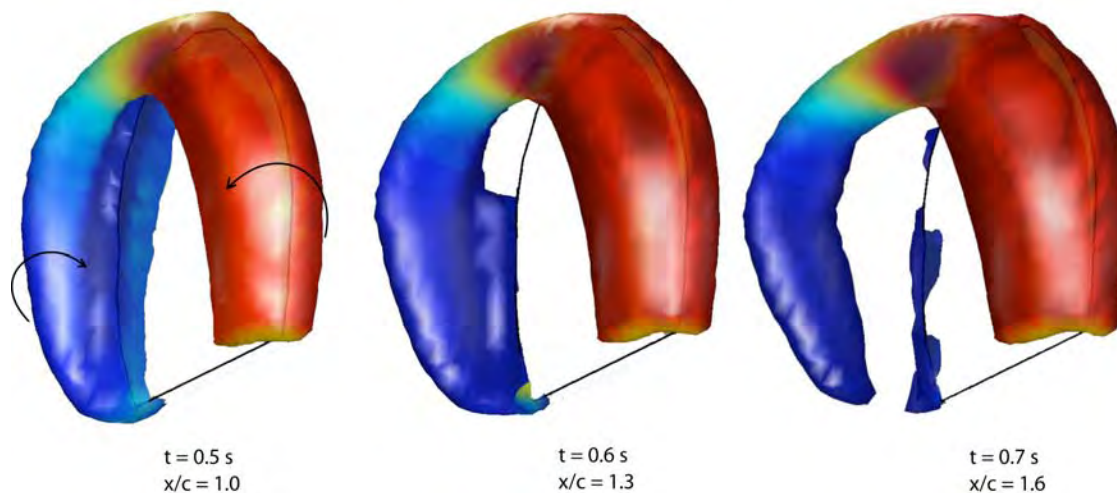
Figure 1. Flow visualization around an impulsively started wing at constant angle-of-attack (45º) at three consecutive time steps. The distance traveled by the wingtip is made dimensionless using the cord length, c. The Reynolds number, based on tip velocity and cord length, is approximately 150. An isosurface of the second invariant of the stress tensor is plotted to highlight the core of vortical structures. The false colors on the surface denote the contribution from clockwise (blue) and counterclockwise (red) vorticity in the spanwise direction (as indicated by the arrows).

305. Aerodynamic forces and moments on an insect body during forward flight

William Dickson

In recent years a tremendous amount of progress has been made in the understanding of the unsteady aerodynamic phenomena that are responsible for the enhanced lift of flapping wings operating a low Reynolds number. The current understanding of force production is sufficient to account for the force balance of an insect during hovering flight. A logical next step is to attempt to extend our understanding of hovering flight to both forward and maneuvering flight. We are currently investigating the forces and moments acting on the body of an insect during forward flight using a dynamically-scaled body model and a servo driven tow tank filled with viscous mineral oil. A 3D computer model of a female *Drosophila* was generated from digital images using SoldiWorks (TM). A physical model of ABS plastic was manufactured from the computer model using Fused Deposition Modeling. The body model is mounted in a 2mx1mx1m tow tank filled with mineral oil. The forces and torques produced are measured using a six-axis force torque sensor mounted along an axis through the center of mass of the model.

The correct dynamic scaling of for insect flight is achieved by matching the Reynolds number (Re) - the ratio of inertial to viscous forces in the fluid. The Re is effectively determined by the kinematic viscosity of the fluid, the length of the model, and the velocity of translation of the model through the fluid. For *Drosophila,* Re will range from 0 (hover) to around 60 (very fast forward flight).

The axial force coefficient as a function of pitch angle for Re 15-40 is shown in Figure 2A. The axial force coefficient is highest at a pitch angle of 0 degrees and decreases to zero near a pitch angle of 90°. The dependence of the axial force coefficients upon Re is clear with lower Re having highest values coefficient values. Similarly, Figure 2B shows the normal force coefficient as a function of pitch angle. The normal force coefficient reaches its maximum at pitch angles of around 100 degrees and falls to zero near pitch angles of 14°.

Figure 2C shows the pitching moment coefficient as a function of pitch angle for Re 15-40. A positive value of the pitching moment represents a nose down pitching moment while a negative value represents a nose up pitching moment. The pitching moment is initially positive and decreases with increasing pitch angle. The zero crossing of the pitching moment represents an equilibrium point where there is no moment. In all cases this equilibrium is statically unstable. Thus, if the body is initially at a pitch angle of zero and is perturbed slightly, the resulting moments are away the equilibrium point. This static instability of the fly body during forward flight has important implications with regard to the amount of active control required to maintain steady level flight.

In future work we will characterize the combined effects of both yaw and pitch angle on the aerodynamic forces and moments. With a nonzero yaw angle symmetry is lost and side forces, yaw and roll moments also become important. A careful characterization of these forces will enable the development of more accurate models of insect flight performance and increase our understanding of how insects fly and maneuver.

188
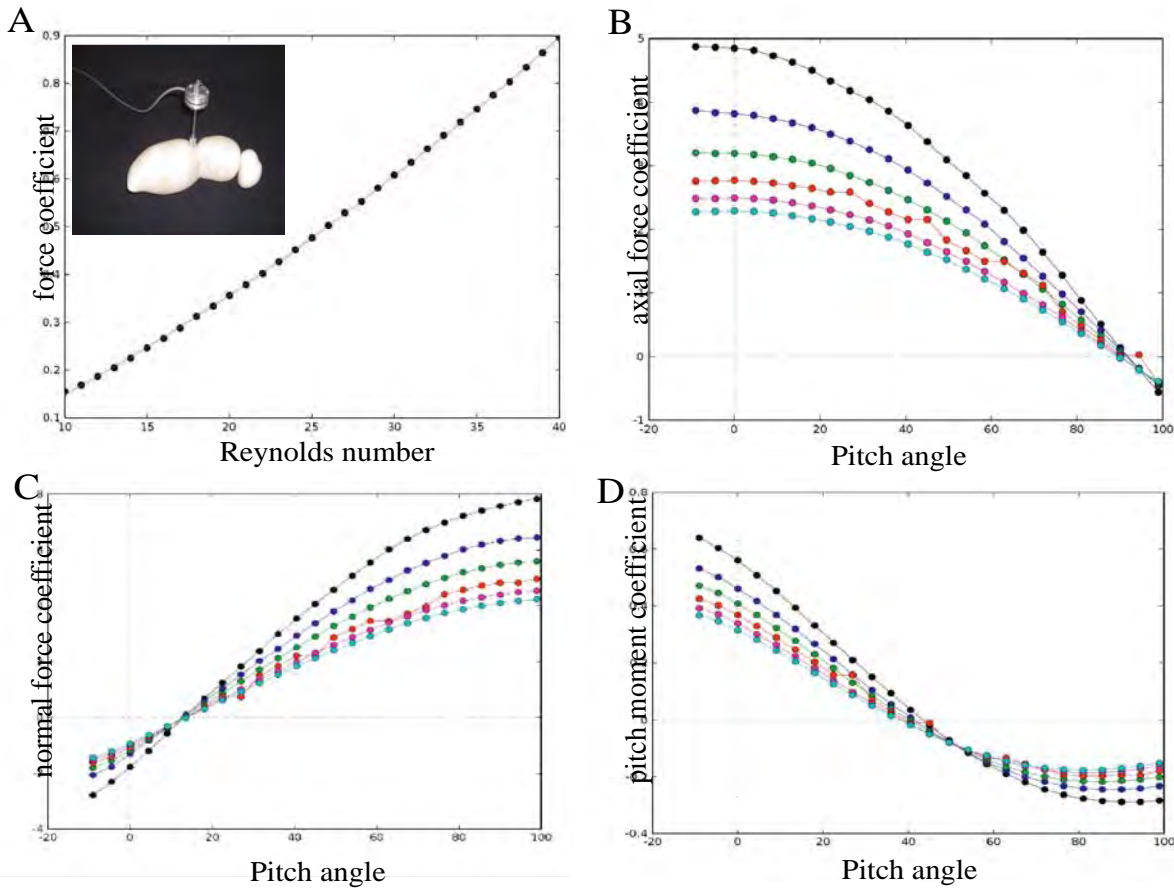
Figure 2. Force and moment coefficients measured on model fly body. (A) Drag coefficient as a function of Reynolds number at an angle of attack of 45 deg. (B) Axial force coefficient as a function of pitch angle at an array of Reynolds numbers. (C) Normal force coefficient and (D) pitch moment as a function of pitch angle at different Reynolds number.

306. Measurement of force generated by fruit flies in lateral translation
Hiroki Sugiura

In order to answer the question of how fruit flies maintain lateral stability, an experiment was conducted to study whether fruit flies are capable of modulating side thrusts. To measure the side thrust that a fly generates, the fly was affixed to a tether with a 0.2 mm-thick mirror. The side thrust was measured aiming a diode laser at the mirror; angular deflection of the tether was measured using a position-sensitive photodiode. All the flies were placed inside an electronic flight arena that shows visual patterns of expansion and contraction generated during lateral translation. The magnitude of side thrust and rolling moment that fly generate is plotted against azimuth of the focus of expansion position. The relationship between the side thrust and stimulus position is sinusoidal. Figure 3 shows that fruit flies side slip away from the focus of expansion and are capable of modulating side thrust. The magnitude of the maximum side thrust is 0.8 µN that corresponds to 5% of the maximum thrust (18 µN).
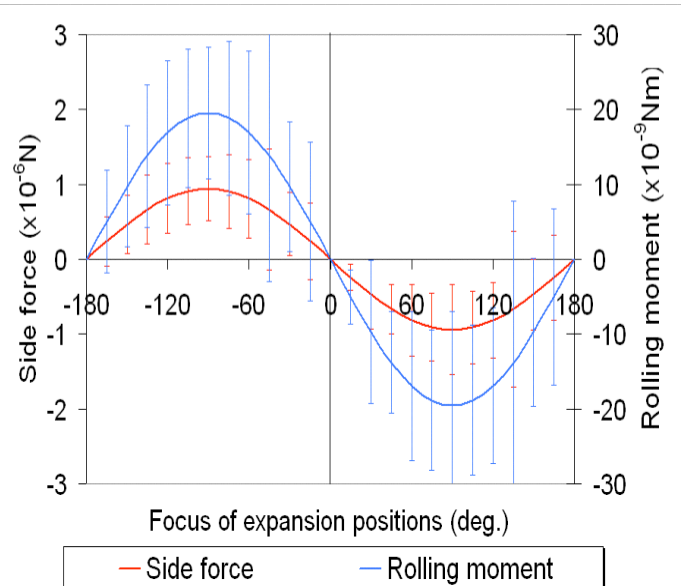
Figure 3. The side thrust and rolling moment generated by a fruit fly in response to visual expansion at different azimuthal positions.

307. **Walking *Drosophila* demonstrate shape preference during local search but not global search**

Alice Robie

Searching for resources in a patchy environment is an important behavior for most organisms. In order to study search behavior in *Drosophila*, we have developed a method for automated tracking of single, walking flies as they explore a large circular arena (d = 25 cm) within a controlled sensory landscape. The search behavior of *Drosophila* may be broken down into two main components. During global search or ranging, a fly explores large regions of its environment in an attempt to find potential sources of food. Once it finds an object, it initiates a local search to find suitable feeding sites. To separate local search behavior from global search, we placed a set of dark cones in the arena, which the flies could detect at a distance of roughly 20 cm. The four

cones had the same surface area, but different vertex angles and heights (30º, 3.6 cm; 60º, 2.3 cm; 90º, 1.5 cm; and 120º, 1.0 cm). As expected, in total darkness flies demonstrate no preference for a specific visual target. Surprisingly, the flies also visited each cone with equal probability in lighted conditions, despite the differences in shape. Thus, the localization of objects during global search appears to be independent of object shape. However, upon reaching a cone, flies spend significantly longer time on the surface of the tallest cone (which has the steepest inclination) than any of the other cones, indicating that object shape does influence local search behavior (Figure 4). While this strong preference for the tallest, steepest cone was reduced in complete darkness, it does not disappear entirely, suggesting a role for other sensory modalities other than vision. In summary, visual information influences preference for object shape during local search, but not during global search.
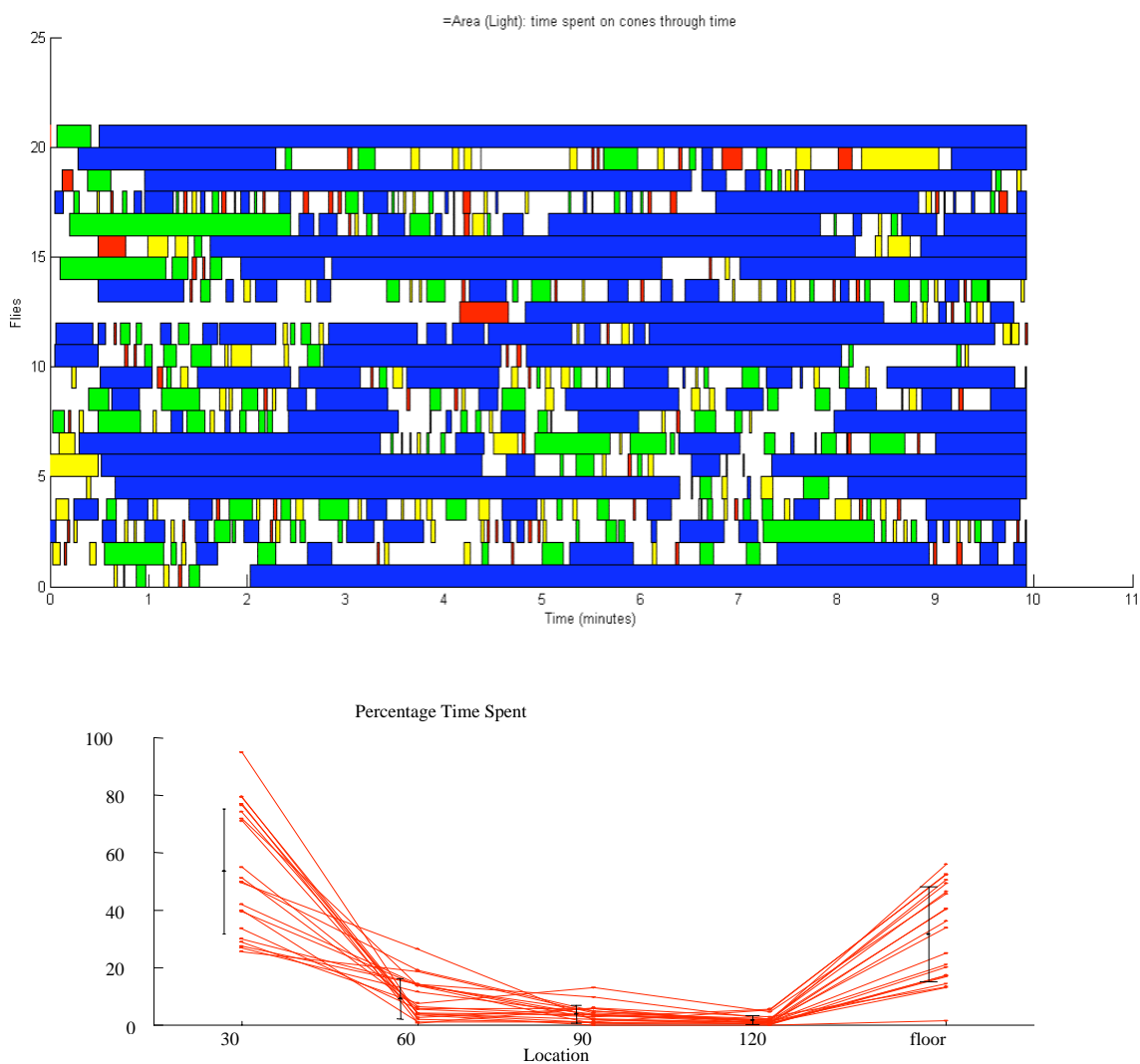
Figure 4. (A) Quantitative ethogram of search behavior in walking hungry fruit flies. Each line represents a different animal. Blue indicates walking, white standing still. Other colors indicate time spent on target cones of differing slope. (B) Summary of resident times on different visual targets. Animals spent disproportionately large time on steepest cone.

308. Visually-mediated control of translatory flight in *Drosophila*

Michael Reiser

Flies have served as a model system for neurobiological studies of vision and flight. We wish to extend these efforts towards describing the visually-mediated control of translatory flight. Tethered *Drosophila* flying in a flight simulator will readily close a feedback loop by adjusting the difference between right and left wing stroke amplitudes; this difference is used to control the velocity of a rotating pattern. To simulate translatory flight, flies were presented with a panoramic visual flow field consisting of a focus of expansion (FOE) and an opposite focus of contraction (FOC). During tethered flight, *Drosophila* robustly orient towards the FOC. This result is perplexing since the forward flight profile of local velocities on the retina is a frontally-centered FOE, not an FOC. One possible explanation for this apparent paradox is that the stimuli used in these experiments are highly unnatural. For example, the expansion rate and contrast level are higher than would normally be encountered during flight, and thus, the observed behavior may reflect an extreme behavioral response, such as an escape reflex. To explore this possibility, experiments were conducted in a new flight arena composed of LED modules capable of displaying different intensity levels at each pixel. By varying the expansion rates, contrast levels, and spatial extents of the stimuli, we show that the expansion avoidance response is extremely robust, persisting under all of these conditions. However, when presented with a single vertical stripe embedded within the FOE of the expanding/contracting pattern, flies do indeed selectively orient towards the FOE of a low contrast pattern. This indicates that the expansion avoidance reflex is attenuated when flies are fixating a visual object. Furthermore, this response improves as trials are conducted for long periods of time, suggesting that the salience of the stripe increases with continued exposure to the compound stimuli.

309. Closed loop experiments and modeling of free-flight visual behavior

Andrew Straw

A fruit fly, whether flying through an orchard in search of fallen fruit or hovering over your compost pile, makes use of several sensory modalities to stabilize and direct its flight. Among these, visual input can lead to rapid turns (saccades), to object tracking (fixation), and is important for the stabilization of flight. When considered in the context of these behaviors executed by the fly, the neural signals output from the visual system need not convey an accurate representation of relevant state variables (such as the parameters of the fly's own self-motion). Rather, because the fly's range of behavioral control is limited by, for example, coupling of yaw and roll, it is possible that the outputs of the optic ganglia are linked directly to specific motor patterns and that visual processing is shaped by coupling the sensory system with the control system. Thus, because the physiology of the visual system presumably evolved under closed-loop conditions, a detailed description of natural behavior may be necessary for understanding visual function. By reconstructing visual inputs generated and experienced by the fly, for example, we can examine the degree to which known physiological properties of visual motion detecting neurons are sufficient to generate realistic behavior when combined with models of control systems and fly kinematics. Furthermore, the functional role of physiological phenomena such as visual motion adaptation may be investigated by evaluating the performance of models exhibiting such phenomena.

To capture the free-flight dynamics of flies with sufficient temporal and spatial resolution over a behaviorally relevant volume, we developed a multiple camera system that allows tracking of freely flying flies (Figure 5, panel A). In addition to its basic role as a data acquisition device, this system operates in real-time (100 or more frames per second, < 30 m sec latency), allowing the experimenter to control sensory stimuli based on a fly's position and orientation, allowing manipulation of visual feedback during flight. Additionally, I have developed a technique for estimating the roll angle of the fly based on the resultant forces extracted from the observed kinematics, a model of aerodynamic drag, and an assumption that fruit flies are unable to generate thrust with a side-directed component. With an estimate of roll angle and experimental fixing of the head stationary relative to the thorax, all six degrees of freedom of the fly's head are known, allowing a detailed reconstruction of the input to fly's visual system (Figure 5, panel B).
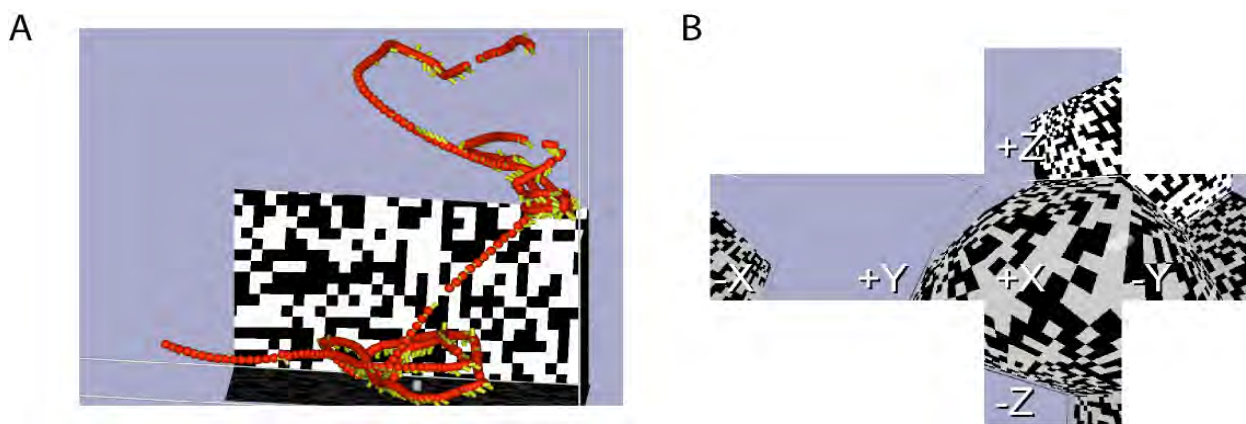
Figure 5. Reconstruction of flight trajectory and fly's eye view using multiple camera tracking system. A) Fly's position and orientation within 30 cm x 30 cm x 60 cm flight arena with random checkerboard patterns on two walls and floor. B) Reconstructed panoramic view from the fly's coordinate system, allowing detailed simulation of input to visual system. Six faces of a cube are shown, corresponding to the 90° by 90° patch of space directly along the direction of orthogonal axes through the fly.

310. Sensory stimuli that elicit rapid saccadic turns
John Bender

Fruit flies in free flight exhibit a behavior known as "body saccades," which are changes in heading of about 90° in under 100 ms. These behaviors are a main way that flies change their direction of flight and seem to be educed by looming visual stimuli, although they also may occur spontaneously. In order to elucidate the neural mechanisms underlying the generation and control of saccades, it is necessary to develop a preparation in which they can be reliably elicited. In a tethered preparation, flies have long been known to produce rapid bursts of turning torque that are thought to be equivalent to saccades. However, the time course of these so-called "torque spikes" is nearly an order of magnitude longer than a saccade in free flight. Even more critically, torque spikes in a tethered fly show no counter torque to halt the turn, which we have shown is produced during free flight saccades.

To address the issue of whether tethered-flight torque spikes are equivalent to free-flight saccades, we developed a new preparation in which flies retain some of the sensory feedback they lack under standard tethered conditions by allowing them to physically rotate around one axis (Figure 6A). A fly is tethered to a small, steel insect pin, which is held in the field between two magnets. The pin can rotate freely along its long axis, which is the functional yaw axis of the fly. We illuminate the fly with infrared light and use an IR-sensitive camera to determine the orientation of the fly in real time (Figure 6B, top). The fly is surrounded by a cylindrical arena constructed of LEDs, under the control of the same computer that interprets the IR video. Thus, we are able to simultaneously record both the visual stimulus presented to the fly and the fly's turning response about its yaw axis.

We estimated the fly's angular velocity (Figure 6B, bottom) from these raw orientation data and set a velocity threshold to analyze rapid turns as putative saccades. From the angular velocity, we estimated angular acceleration and calculated yaw torque under varying contributions of frictional (velocity-dependent) and inertial (acceleration-dependent) factors. For values of these coefficients near those previously estimated for fruit flies in free flight, we found that the flies in this "magnetically tethered" preparation produce significant countertorque during saccades (data not shown). Furthermore, the time course of saccades in this preparation is only about twice as long as that measured in free flight.

To begin quantifying how visual stimulation affects saccade initiation, we simulated the square profile of an object approaching the fly and varied several approach parameters (Figure 6C). Expansion of the object under all conditions tested elicited saccades with a probability much higher than the spontaneous saccade rate. Full expansions were more likely to elicit a saccade response than were expansions in which only one visual dimension (horizontal, vertical, or diagonal) was stimulated. Contractions, simulating an object rapidly moving away from the fly, had a much lower probability of evoking a saccade than did expansions. Conditions where the object was simulated as either accelerating or decelerating during its approach to the fly did not have a large effect on the probability of saccade initiation, but they did affect the time course of saccade probability.

Because they are visually evoked, include episodes of counter-torque, and occur with a time course comparable to free flight saccades, we postulate that these behaviors elicited in our magnetically tethered preparation are analogous to the body saccades observed in freely flying flies. Since these same stimuli evoke torque spikes in rigidly tethered flies, it is parsimonious to hypothesize that those behaviors are also controlled by the same neural circuitry that generates saccades in free flight. These results suggest three main directions for future research on this system. First, we hope to record neural activity in flies (rigidly tethered by necessity) while visually stimulating them to saccade. This will allow us to further clarify the nature of the visual processing and muscular control that occurs before and during saccades. Second, we would like to experimentally alter the visual stimuli received by flies

192

after saccade initiation. By this, we hope to understand to what extent visual feedback plays a role in the differences observed in time course and magnitude of saccades from free flight to the magnetic tether. Third, we will use our rotating flight arena to systematically alter the rotational feedback received by the fly during the saccade behavior. In this way, we aim to elucidate the role that this sensory modality has in determining saccade shape and duration. Overall, the saccade behavior in this system affords an excellent opportunity to understand natural mechanisms of multimodal sensory integration and feedback control in flight.
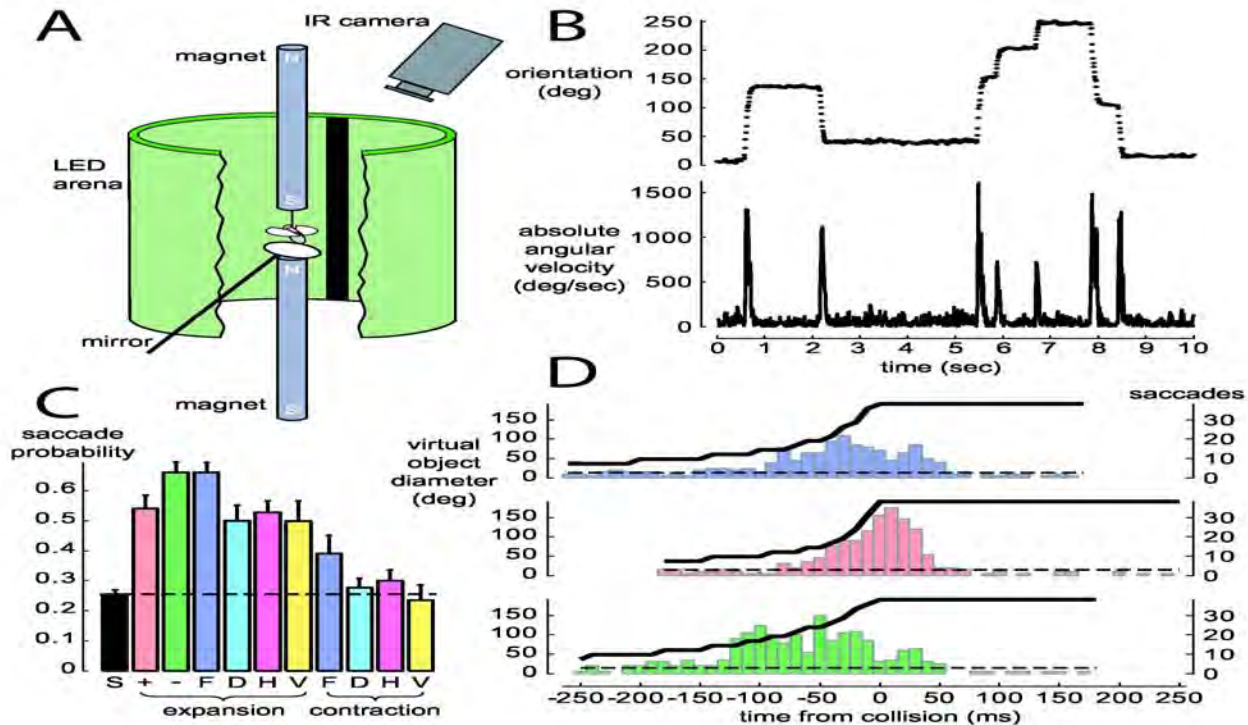
Figure 6. A. Diagram of recording apparatus. B. *Top.* Plot of orientation vs. time for a representative short segment of flight in one fly. *Bottom.* Estimated angular velocity for the same bout of flight. C. The probability of saccading for various stimulation parameters is calculated as the probability that a fly will perform a saccade between 100 and 550 ms after stimulation begins. S: spontaneous; +: accelerating; -: decelerating; F: full; D: diagonal; H: horizontal; V: vertical. The starting condition was always the same, and D, H, and V conditions had the same stimulus area at all times. Error bars denote the S.E.M. across different flies. For + and - conditions, N=9 flies; for all others except S- and F-expansion, N=6. For S- and F-expansion, the data from all 15 flies is pooled. Each fly flew at least 10 minutes, with one trial every 10 seconds for + and -, every 5 seconds for D, H, and V conditions (expansion/contraction pairs of the same type). (D) Peristimulus time histogram of saccade events under constant-velocity (*top*), accelerating (*center*), or decelerating (*bottom*) conditions. Data are shown for the entire probability-calculation window (as in C), aligned to the time of collision. The solid black line shows the (horizontal/vertical) diameter of the square, and the dashed black line denotes the spontaneous saccade rate. N=9 flies for all conditions; n=271 trials for constant velocity, n=272 for accelerating, and n=346 for decelerating conditions.

311. **Neuromuscular control of hummingbird flight**
Doug Altshuler

Although considerable information is available regarding the mechanics and control of stereotyped movements such as walking or running, little is known about how the nervous system regulates muscles to change speed, alter direction, and maneuver. We are addressing these questions using hummingbirds, which are arguably the most maneuverable vertebrates. Several flight modes are under investigation including flying backwards and forwards, left and right, hovering, and while transiently lifting maximum loads. Experimental data consist of wingbeat kinematics derived from high-speed video, neuromuscular physiology derived from electromyograms (EMG) and sonomicrometry, and aerodynamic forces measured using a dynamically-scaled flapping robot. Features of both the neuromuscular control and the aerodynamics are compared with insects and birds to illustrate specialization and convergence among animal flight systems.

In several respects, hummingbird flight bears much stronger resemblance to insects than to other birds. A detailed view of the hovering wingbeat kinematics of hummingbirds and fruit flight reveals strong similarity despite a 4000-fold difference in body mass (Fig. 7A). Here, the time course of the left wing position, with respect to the body, is plotted for both taxa with the time axis normalized to the length of a complete wingbeat cycle. When tested on the robot, these kinematics produced an equally similar time course of aerodynamic force production.

The neuromuscular system of hummingbirds also exhibits functional convergence with insects in two respects. 1) The activation of hummingbird power muscles is highly synchronous and thus, resembles the single unit activations of many insect muscles. This is in strong contrast to most vertebrate EMGs, which display compound wave forms representing the activation of non-synchronous motor units (Fig. 7B). 2) Hummingbirds also have functional segregation between power and steering muscles for flight, as do insects. EMGs from maneuvering hummingbirds revealed that the amplitude of muscle potentials does not vary among numerous flight maneuvers. Furthermore, the timing of muscle activation is the same for all maneuvers (Fig. 7C), indicating that fine motor control is accomplished by other muscles on the shoulders and arms.
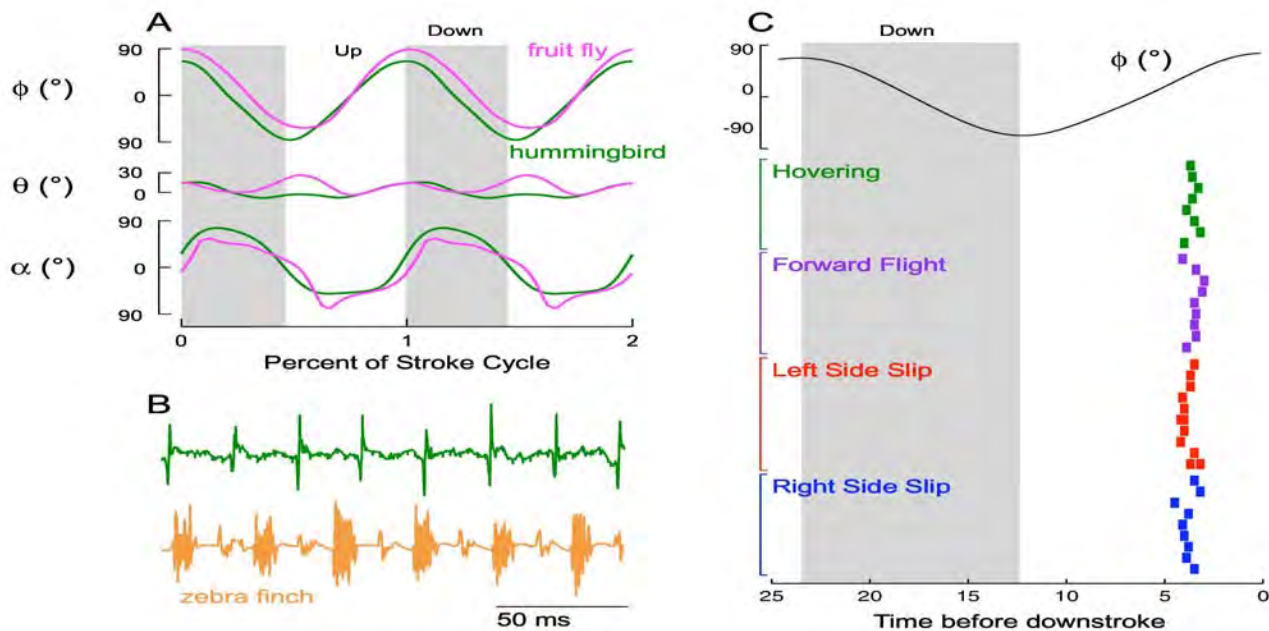
Figure 7. Kinematics and muscle recoding from free flying hummingbirds (A) Comparison of fruit fly and hummingbird wing motion. (B) Comparison of hummingbird and zebra finch EMGs from pectoralis major. (C) Phase of pectoralis EMG during different flight behaviors.

312. Directionality of escape response
Gwyneth Card

Drosophila exhibit an escape response comprised of a stereotyped sequence of wing contraction and leg extension. These wing and leg muscle contractions occur with consistent latencies from activation of the descending giant fiber, which has been shown to be visually activated. Previous studies of fly escape behavior, however, have primarily used non-directional stimuli or tethered flies. It thus, remains unclear whether fly escape behavior is directional. Using high-speed video, we recorded the escape behavior of freely-moving flies confronted with a falling black disc. For all directions of disc approach relative to the fly's orientation, the initial take-off direction of the fly was a compromise between jumping directly away from the stimulus, and jumping directly forward (Fig. 7). Experiments with clipped wing flies showed that leg extension alone is enough to generate directionality in the jump.

A falling disc is a strong escape-inducing stimulus. In my experiments 95% of flies confronted with the stimulus jumped, a significantly higher yield than experiments using light-on/off stimuli. A falling disc could induce an escape jump via visual or tactile (wind) stimulation of the fly, or by some combination of the two. We explored the relative contribution of these differing sensory inputs by placing a clear plastic wind barrier between the fly and the disc stimulus. Under this condition, we observed only a small increase in the number of flies who did not jump in response to the stimulus (from 5% to 13%, Fig. 8), and flies showed an identical directional jumping behavior to their non-barrier counterparts. In contrast, using a clear falling disc to reduce the visual strength of the stimulus while maintaining a similar wind profile drops the fly jump response rate to 50%. Finally, we confirm that visual cues alone are sufficient to generate robust escape behavior by using an LED array to simulate a virtual approaching object (black square). For appropriate parameters of the virtual stimulus (e.g., approach velocity), jump response yield is close to that of the actual, unobstructed disc.

The observations that visual information and leg extension alone are sufficient to generate a directional escape response indicate a possible direct role for the giant fiber in producing the directional behavior. Together with others in the lab, we are currently developing a giant fiber neural recording preparation in *Drosophila* to test the hypothesis that an off-center approaching stimulus differentially stimulates the giant fiber pathways on either side of the fly, causing the legs to extend at different times.
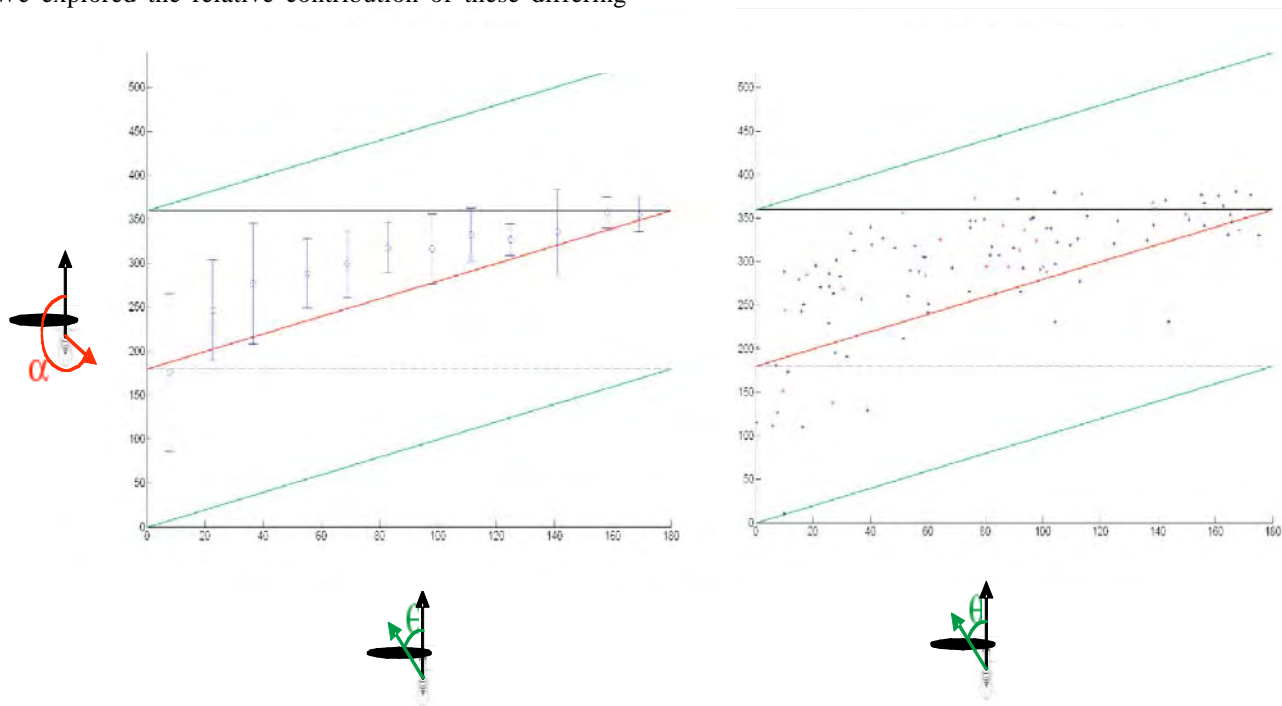
Figure 8. *Escape jump direction as a function of stimulus direction.* Theta is the angle between the fly's orientation and the falling disc stimulus (i.e., theta = 0 for stimuli directly in front of the fly). Alpha is the angle between the fly's original resting orientation and it's mean direction of movement over the period of leg extension (i.e., alpha = 0 when the fly jumps directly forward). The solid black line shows where data would fall if the fly jumped directly forwards; dotted black line, directly backwards. The green lines show where the data would fall if the fly jumped directly towards the stimulus; red line, directly away from the stimulus. Plotted blue points are means and S.D. for theta bins of 30° (n for each bin ranges from 3-16, S.D. calculations do not account for differences in n).
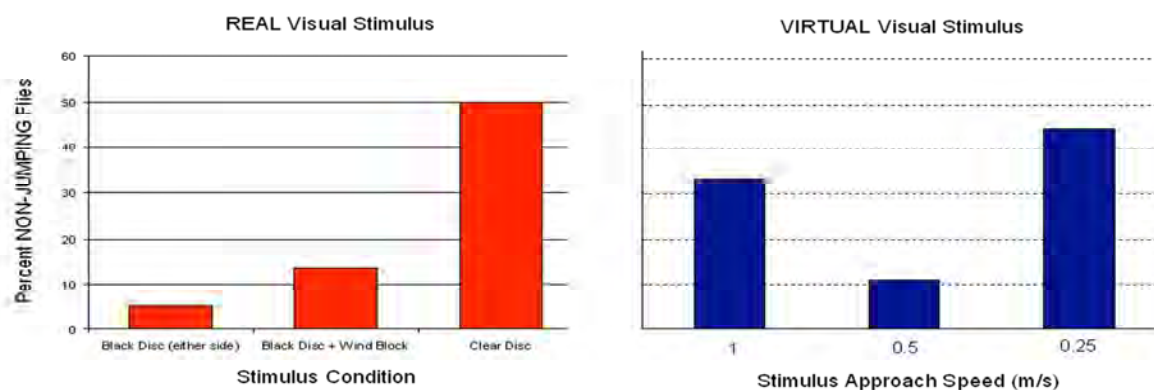
Figure 9. *Percent non-escaping flies for different stimulus conditions.* Red bars are percent of flies that did not perform an escape jump when confronted with a falling black disc alone (n = 82), a wind-blocked falling black disc (n = 24) and a falling clear disc (n = 10). Blue bars are the percent of flies that did not jump when confronted by a virtual square object approaching at 1 m/s (n = 9), 0.5 m/s (n = 9), and 0.25 m/s (n = 9).

Publications

Balint, C.N. and Dickinson, M.H. (2004) Neuromuscular control of aerodynamic forces and moments in the blowfly, *Calliphora vicina. J. Exp. Biol.* **207**:3813-3838.

Dickinson, M.H. (2005) Initiation and control of rapid flight maneuvers in fruit flies. *Int. Comp. Biol.* **42**:274-281.

Dickinson, M.H., Farman, G., Frye, M., Bekyarova, T., Gore, D., Maughan, D. and Irving, T. (2005) Molecular dynamics of cyclically contracting insect flight muscle *in vivo. Nature* **433**:330-333.

Dickson, W.B. and Dickinson, M.H. (2004) The effect of advance ratio on the aerodynamics of revolving wings. *J. Exp. Biol.* **207**:4269-4281.

Frye, M.A. and Dickinson, M.H. (2004) Closing the loop between neurobiology and flight behavior in *Drosophila. Curr. Opin. Neurobiol.* **14**:729-736.

Fry, S.N., Sayaman, R. and Dickinson, M.H. (2005) The aerodynamics of hovering flight in *Drosophila. J. Exp. Biol.* **208**:2303-2318.

Assistant Professor of Biology and Applied Physics: **Michael Elowitz**
Postdoctoral Scholars: Avigdor Eldar, David Sprinzak, Gurol Süel
Graduate Students: Robert Sidney Cox III, Chiraj Dalal, Joseph Levine, Louisa Liberman, Shaunak Sen
Technician: Michelle Fontes, Jonathan Young
Staff: Katie Miller

Summary: The Elowitz lab is interested in how cellular functions are implemented using networks of interacting genes and proteins. We are equally interested in the complementary question of how novel networks can be engineered within cells to implement alternative cellular behaviors. We address these two problems together using a combination of experimental and theoretical techniques.

Recently, we have focused on a number of specific issues that are crucial for a quantitative understanding of the behavior of both natural and synthetic gene regulation networks. These include: (a) dynamics of feedback and other regulatory structures in genetic circuits; (b) effects of stochasticity, or 'noise' in gene regulation; and (c) analysis of synthetic 'replicas' of natural genetic circuits. The lab is developing general methods for the analysis of gene expression over time in individual cells and cell lineages, primarily using fluorescent proteins, automated time-lapse microscopy, and image analysis. We are particularly interested in applying these methods to decision-making problems such as differentiation. To that end, we have begun looking at model systems for differentiation in both bacterial and mammalian systems.

313. Gene regulation at the single cell level

Jonathan Young, Nitzan Rosenfeld[1], Uri Alon[1], Peter Swain[2]

Genetic networks are based on regulation of gene expression by transcription factors. Their function often depends critically on the Gene Regulation Function (GRF), the quantitative relationship between transcription factor concentrations and downstream promoter activity. We recently determined the GRF of a repressor-promoter interaction measured in individual living cells of *Escherichia coli*. These measurements were based on dynamic, time-lapse fluorescence tracking of single cells expressing fluorescent protein fusions to well-characterized transcription factors. Results revealed not only the mean GRF but also the amplitude, timescale, and origin of fluctuations around it. Based on these results, we can make quantitative predictions of the mean behavior and fluctuations of novel genetic circuits. To test these predictions, we have constructed autoregulatory feedback circuits and quantified their behavior in living cells, and will continue to assemble and analyze other simple test circuits.

[1]Weizmann Institute
[2]McGill University

314. Probabilistic decision-making in *Bacillus subtilis* starvation response

Gurol Suel, Jordi Ojalvo-Garcia*, Louisa Liberman

We are investigating the system dynamics of a genetic circuit that induces developmental decision making in *Bacillus subtilis*. The *Bacillus subtilis* stress response network causes individual cells to acquire distinct fates including sporulation and competence. How does the architecture of the stress response network support this cell-fate decision making process? We measure activities of key pairs of promoters within the stress response network as a function of time in single cells using time-lapse microscopy. This data produces a multidimensional quantitative map of promoter activities during differentiation. The motion of single cells through this phase space of promoter activities allows insight into the system dynamics of the underlying network. Furthermore, analysis of promoter activity dynamics indicates the functional role of feedback loops. Mathematical modeling of a simple genetic module within the larger circuit reproduces key experimental observations. The mathematical model can be further utilized to generate experimentally testable predictions. The results show how cells trigger one of several well-defined responses using a circuit in which stochastic and deterministic elements are both crucial for function.

*Politècnica de Catalunya, Colom 11, E-08222 Terrassa, Spain

315. Framework for the construction of synthetic transcriptional networks

Robert Sidney Cox III

For analysis of natural genetic circuits and construction of synthetic ones, biologists require accurate, distinguishable, non-toxic reporters for multiple genes in the same organism. Recent improvements in fluorescent protein reporters have made this possible. However, there does not exist a single system with which one can conveniently assemble an accurate, quantitative, multiple reporter system. Therefore, we designed and built such a system using total DNA synthesis. This framework should be of use both for biologists wishing to analyze natural genetic circuits with several components as well as for synthetic biologists, wishing to assemble relatively simple circuits of up to four operons. We have performed a detailed characterization of the performance of this framework in *Escherichia coli*, and intend to use it as a platform to support a variety of experiments.

316. **Analysis of fluctuations during *Bacillus subtilis* stress response**
Joseph H. Levine

We are examining fluctuations within the gene regulatory network governing sporulation in *Bacillus subtilis*. Our approach uses time-lapse microscopy of relevant fluorescent protein promoter fusions at the single cell level. Preliminary results suggest that these fluctuations, when combined with noise in the regulatory network may amplify population heterogeneity in sporulation timing. As such they may be a clue to how genetically identical cells generate probabilistic responses.

317. **Synthetic feedback circuits**
Shaunak Sen

Genetic networks encoding behavioral responses are often regulated by feedback. Typically, negative feedback loops are thought to arise in homeostatic mechanisms and positive feedback loops in switches. However, interlocked negative and positive feedback loops have the potential for a richer variety of dynamical behavior depending on the strengths of the respective feedbacks. Examples of such network include cell cycles of *Xenopus* oocytes and *Saccharomyces cerevisiae*. Studies of naturally occuring networks have been very illuminating, but they generally suffer from an ambiguity in ruling out unmodelled interactions. In this work, we construct a set of networks in *E. coli* with interlocked negative and positive feedback loops of different strengths. This synthetic approach decreases the ambiguity due to unknown interactions and provides an opportunity for more systematic analysis of potential circuit behaviors.

198

Anna L. Rosen Professor of Biology: Scott E. Fraser
Members of the Beckman Institute: Russell E. Jacobs, Jerry Solomon (Emeritus)
Senior Research Fellow: Jordan Gerton, Helen McBride
Members of the Professional Staff and Senior Staff: Gary Belford, Benoit Boulat, Mary Dickinson, David Kremers, Russell D. Lansford, P.T. "Jim" Narasimhan, Carol Readhead, Seth Ruffins, Peter Siegel, Stephen Speicher, J. Michael Tyszka, Jon Williams, Chang-Jun Yu, Xiaowei Zhang
Visiting Associates: Elaine Bearer, Andres Collazo, John Faiz Kayyem, Francoise Marga
Visitors: John Wallingford
Collaborators: Gabriel Acevedo-Bolton, Andrew Ewald, Arian Forouhar, Mory Gharib, Richard Harland, David Laidlaw, Rex Moats, Marysia Placzek, Eduardo Rosa-Molinar, Michael Roukes, Changhuei Yang
Postdoctoral Research Fellows: Luca Caneparo, Maxellende Ezin, Bridget Hanser, Olivia Kelly, David Koos, Michael Liebling, Melanie Martin, Sean Megason, Cyrus Papan, Wei Shen, Le Trinh, Julien Vermot
Graduate Students: Magdalena Bak, Mat Barnet, Christie Canaria, Jeffrey Fingler, Ying Gong, Elizabeth Jones, Rajan Kulkarni, Carole Lu, James Maloney, Jim Pierce, David Van Valen, Larry Wade, David Wu
Research and Laboratory Staff: John Carpenter, Sonia Collazo, Mary Flowers, Kristy Hilands, Tim Hiltner, Aura Keeter, Edriss Merchant, Jeff Smith, Chris Waters

Staff of the Caltech Brain Imaging Center: Andrey Demyanenko, Steve Flaherty, K. Craig Goodrich, David Gultekin, Martha Henderson, Mary Munoz, Lauren Somma, Krish Subramaniam, Sean Wagner
Undergraduates: Vamsidhar Chavakula, Csilla Felsen, Felicia Katz, John Oh, Jonathan So

Summary: Our laboratory has dedicated itself to performing tests of the cell and molecular bases of developmental patterning, using *in vivo* imaging tools. The explosion of data from molecular approaches and the dramatic progress from *in vitro* culture assays have resulted in a rich set of proposals for the mechanisms that underlie developmental pattering. Our goal is to test these proposed mechanisms in the intact embryo, with the hope of moving forward to an understanding of which of the potential mechanisms operate in the natural biological context. There are many challenges to such tests, including the tagging of cells or molecules so that they can be followed in the intact system, the visualization of the tagged structures, and the interpretation of the time-varying events these images represent. Solutions to these challenges require the coordinated efforts of researchers spanning the life and physical sciences.

In the past year we have made significant advances in understanding the motions of cells in the spherical frog embryo, and have refined tools that allow quantitative analyses of the motions of cells during gastrulation. Such analyses demonstrate that the engines that drive gastrulation, as well as their molecular control, are distinct for the different germ layers of the frog embryo.

Novel imaging hardware and image processing software have advanced our knowledge of the events that pattern the embryonic cardiovascular system. A new microscope design offers imaging rates of greater than 100 frames per second and permits dynamic events to be followed with unprecedented clarity. New software permits alignment of individual optical sections to generate four-dimensional reconstructions of the beating heart in the living embryo as the heart develops from a simple tube to a multi-chambered heart. These reconstructions offer new insights into the flows and forces that characterize the developing heart, and are now permitting a new set of experimental tests, in collaboration with other laboratories, of the role of function in cardiovascular patterning.

Parallel developments in sensor technologies, in collaboration with groups in the new Kavli Nanoscience Institute, strive to increase the sensitivity of genomic and proteomic analyses to the point that samples as small as single cells can be analyzed. Our goal is to move systems biology analyses into the intact embryo, characterizing the natural history of cells with advanced imaging tools, and then analyzing the same cells with array technologies to better define the nature and timing of key signaling events.

318. Using transport to map the brain: Stereotaxic Mn²⁺ injection and track tracing by μMRI of animal models

E.L. Bearer, X. Zhang, T. Hiltner, J.M. Tyszka, R.E. Jacobs

Higher order cognitive processing requires communication between neurons located at distant sites within the central nervous system. This communication depends on long axonal processes that arch from one cluster of neuronal cell bodies to another. Often these processes are grouped together into tracks readily detected even in whole brain specimens, others are smaller and only detected secondarily with histochemistry or tracing compounds that enhance their visibility. Traditionally, connections between neurons have been traced by the local delivery of a histologically detectible tracer that is transported within the neuron to distant sites and thereby outlines the communication pathway. These tracers must interact with the intracellular transport machinery to be delivered along the axon of a single neuron and must cross synapses to trace a multi-step pathway. The mechanisms of entry into the neuron, the type of transport that the agent uses, and retention of the agent within the pathway are all important considerations in interpreting the consequent data. For example, whether a tracer only enters at active synapses or can also enter along neuronal processes influences its usefulness and the analysis of its distribution. Alternatively whether a tracer is transported in the retrograde and/or anterograde direction within processes affects its subsequent distribution and the interpretation of the structure of the pathway thus, delineated.

To trace neuronal circuits in living brains by MRI, a contrast agent must display these same attributes as a histological tracer: be transported and cross synapses. We have focused on Mn²⁺, which has recently become a widely used T_1 contrast agent for MRI. Despite its popularity, many aspects of Mn²⁺ tracing remain ambiguous. Evidence suggests that it enters neurons through voltage-sensitive Ca²⁺ channels and is actively transported in the anterograde direction, possibly on microtubule tracks. We have investigated biological mechanisms of Mn²⁺ transport in two systems: the optic track and the hippocampal-basal forebrain connections. The optic track is a well-defined system where many biological properties are known. The hippocampal-basal forebrain system is less well studied, but of importance in neurological disorders such as Alzheimer's disease. Mn tracktracing in blind and sighted mice with injections into eye vitreous and adjacent to the chiasm along with visual evoked potential measurements to assess visual system integrity are in progress to assess the basic mechanisms of Mn entry and transport. Mn tracktracing following injection of nanoliter volumes of Mn into the central hippocampus clearly outline the hippocampus-fimbria-septal nucleus connection. Voxelwise analysis of 3D images warped into the same space allows quantitative statistical assessment of Mn transport.

0   p-value   0.05

Regions undergoing statistically significant intensity change over time were determined with a voxel-wise Student's t-test evaluation using data from 8 specimens.
Colored regions show 6 hour post-injection scan compared with 0.5 hour post-injecton scan where voxels with p<0.05 are shown. The underlayer gray scale image is the high resolution scan to which all scans have been warped.

3 orthogonal slices from the 3D image are shown.

Right hippocampal injection of Mn was performed on eight animals. 3D MR images were acquired 0.5 hr, 6 hr, and 24 hr after injection. All images were scaled and warped into the same STANDARD BRAIN image space to enable voxelwise comparisons. A map of statistically significant intensity differences between 0.5 hr and 6 hr time point scans is shown. Right fimbria and lateral septal nucleus are identified as different using the anatomy of the STANDARD BRAIN image shown in gray.

219. Intermolecular zero quantum apectroscopy in the live mouse brain using a MR image

Benoit Boulat, P.T. Narasimhan, Russell E. Jacobs

We have utilized the effects of the distant dipolar field (1,2) to obtain one-dimensional high-resolution NMR spectra *in vitro* and *in vivo* using the Biological Imaging Center 11.7 Tesla magnetic resonance (MR) imager. The method uses techniques of two-dimensional NMR spectroscopy (3) and can be well described within the formalism known as Intermolecular Zero Quantum (IZQ) spectroscopy (4). Our interest in this area arose out of the desire to generate images of the mouse brain with unusual contrast utilizing these coherences (5). IZQ coherences (IZQC's) can be conceptualized in terms of the mutual "flip-flop" of two nuclear spin transitions located on different molecules and leading to a net change of zero of the total quantum number. The IZQC generated signal is characterized by the difference in frequency of the two spins. The application of a magnetic field gradient of the order of 10gauss/cm enables the maximization of IZQC's between two spins residing on molecules separated by no more than tens of microns, resulting in a signal that is not affected by magnetic field inhomogeneities. In each of the samples studied in the present work, water was the abundant material. The pulse sequence was designed to select the IZQC's among the pool of available coherences and to let them evolve during a period t_1; following t_1, the signal is converted into single quantum coherence by means of a selective pulse on the water resonance. Further evolution during a period known as the dipolar evolution time leads to observable echoes. The t_1-modulated signal of water and of metabolites in solution is collected by the RF coil during the time t_2. After 2D Fourier transformation of the time domain data, the projection along the w_1 dimension provides a high-resolution IZQ spectrum exhibiting a better immunity against broadening due to field inhomogeneities. In our examples, the IZQC's connect nuclear spins residing on two water molecules or on a water molecule and a metabolite in solution. The differences in chemical shift with respect to the water resonance of the other observed resonances correspond to the shifts that one would observe in a regular 1D NMR spectrum. Fig. 1 shows the IZQ spectrum of sucrose in H_2O. Proton-proton scalar couplings as low as 4.5Hz in strength are noticeable in the IZQ-generated spectrum, a remarkable showing on a regular 11.7T MR imager. Fig. 2 shows the *in vivo* spectrum obtained in the brain of a live C57 mouse. The metabolites are identified in the spectrum. The excellent quality of the *in vivo* 1H spectrum is highly encouraging and we expect that IZQ spectroscopy along with IZQ imaging will become a valuable tool in the study of animal models of diseases.

References

(1) R. Bowtell (1992) *J. Magn. Reson.* **100**:1-17.

(2) Warren, W.S., Richter, W., Andreotti, A.H. and Farmer, B.T. (1993) *Science* **262**:2005–2009.

(3) Ernst, R.R., Bodenhausen, G. and Wokaun, A. (1989) In: *Principles of Magnetic Resonance in One and Two Dimension*, Clarendon Press, Oxford.

(4) Vathyam, S., Lee, S. and Warren, W.S. (1996) *Science* **272**:92-96.

(5) Narasimhan, P.T. and Jacobs, R.E. (2005) In: *Annual Reports on NMR Spectroscopy*, G.A. Webb (Ed.), Elsevier **55**:259-297.
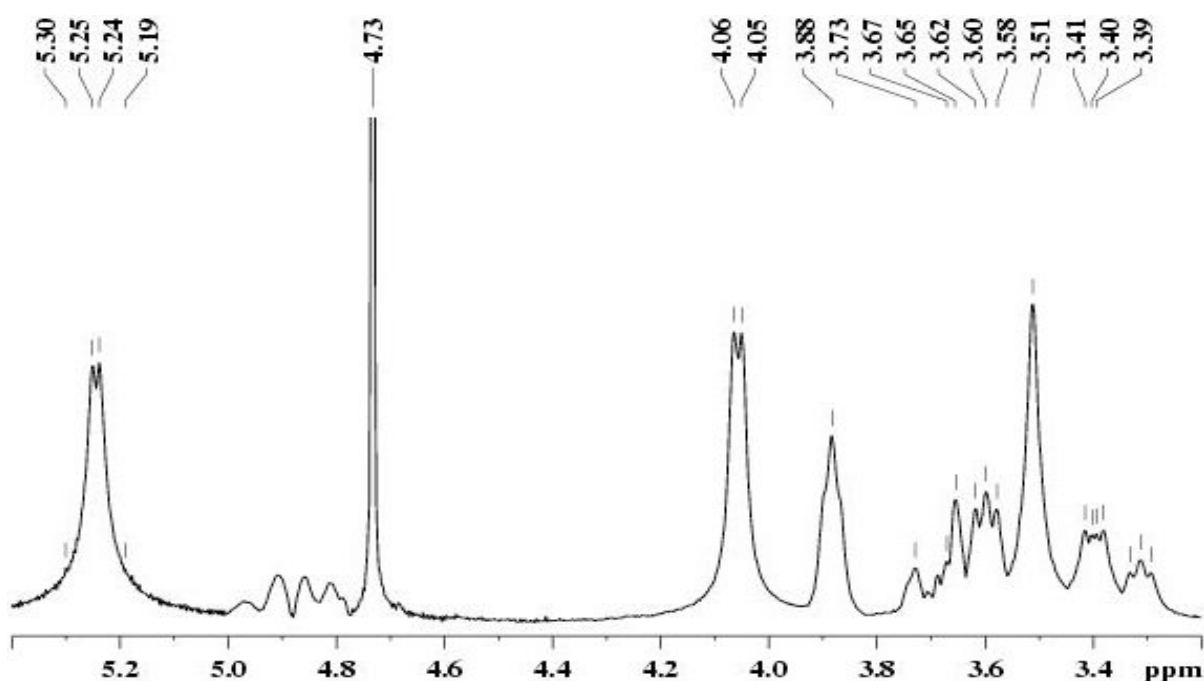
Fig. 1   IZQ spectroscopy of sucrose dissolved in water. Dipolar evolution time = 230ms. 4096x1024 data points zero filled to 4096x2048. Baseline corrected in both dimension. The peak at 4.73ppm is the residual water peak after suppression.

FIG. 2
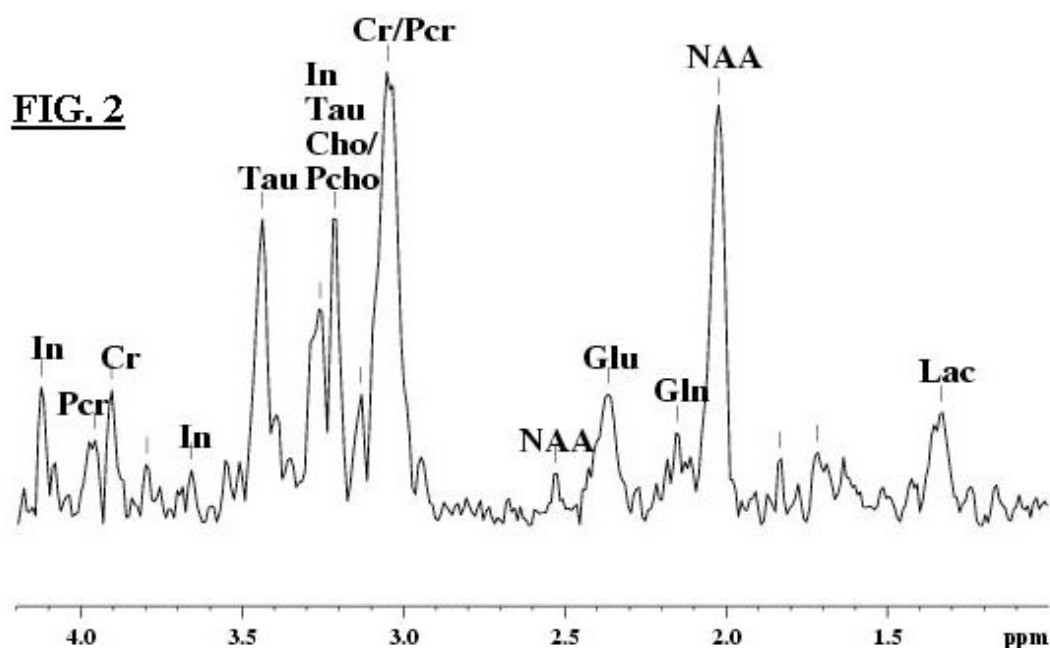
IZQ spectroscopy in the live mouse brain (C57 wild type). Dipolar evolution time = 120ms. 4096x256 data points zero−filled to 4096x1024. Four averages per t1 increment. Baseline corrected in both dimensions. In: myo−inositol, Pcr: phosphocreatine, Cr: creatine, Tau: taurine, Cho: choline, Pcho: phosphocholine, NAA: N−acetylaspartate, Glu: glutamate, Gln: glutamine, Lac: Lactate. NAA resonance was set at 2.01ppm.

320.   The Grueneberg ganglion innervates the olfactory bulb

David S. Koos, Scott E. Fraser

The Grueneberg ganglion is a small nerve located in the lining of the far rostral region of the rodent nasal vestibule. Historically, this nerve was thought to be a component of the terminal nerve, a non-sensory neuroendocrine nerve that does not innervate the first relay station of the primary olfactory pathway, the olfactory bulb. After noting that the Grueneberg ganglion expresses the pan-olfactory marker Olfactory Marker Protein (OMP), we suspected that this ganglion might instead be part of the olfactory pathway. Through the use of axon tract tracing techniques we have demonstrated that the Gruneberg ganglion innervates the olfactory bulb, where it contributes to the glomeruli of the olfactory necklace. The expression of OMP combined with its direct wiring to the olfactory bulb suggest that the Grueneberg ganglion is a previously unrecognized component of the primary olfactory pathway and further investigation into the possible sensory nature and of this nerve is warranted.

321.   Enhanced magnetic resonance microscopy of developing embryos

J. Michael Tyszka, Yun Kee, Marianne Bronner-Fraser, Scott E. Fraser

Magnetic resonance microscopy is a valuable imaging tool for studying deep cell layers and structures in opaque embryos such as *Xenopus laevis* (African clawed frog). We have recently focused on improving tools for high spatial resolution dynamic imaging of developing embryos with magnetic resonance microscopy.

A limiting factor in the efficiency of data acquisition in MRM is the T_1 relaxation time of tissues within the embryo. At the high magnetic fields (9T to 12T) available for MRM at Caltech, the T_1 of water within biological tissues tends to be long, on the order of seconds.

Labeling specific blastomeres with large molecular weight T_1 contrast agents has been demonstrated previously for cell lineage studies in gastrulating embryos. We have recently introduced intracellular and extracellular injections of the gadolinium chelate gadoteridol (Prohance®, Bracco Diagnostics) for global enhancement of compartments within the embryo. Gadoteridol is a small molecule (approx 0.8 kD), which readily partitions across the whole embryo, greatly increasing the sensitivity and efficiency of MRM. The increased efficiency can subsequently be traded for increased spatiotemporal resolution, with current imaging protocols generating 20 micron (isotropic) 3D images in less than 20 minutes.

Traditionally, very high resolution MRM has employed cylindrical gradient coils and solenoidal radiofrequency transmit-receive coils to achieve resolutions on the order of 15-20 microns in small living systems such as developing embryos. Use of the smallest coil possible increases sensitivity, but constrains the fluid volume surrounding the embryo as 50-60 ml in our system. This can lead to anoxia and waste buildup within the buffer fluid, which limits embryo survival. Although fluid circulation is a complex but feasible solution within the magnet, it does not overcome the low throughput issues associated with small solenoid-based MRM. We are currently developing flat, one-sided MRM hardware, equivalent to an inverted stage microscope, which significantly improves environmental control, embryo survival and access to multiple developing embryos.

Magnetic resonance microscopy allows dynamic, *in vivo* imaging of normal development in opaque embryos for extended periods, through gastrulation and neurulation. Future collaborative work will apply these techniques to other opaque embryonic models, such as axolotl and lamprey, with potential relevance to both developmental and evolutionary biology.
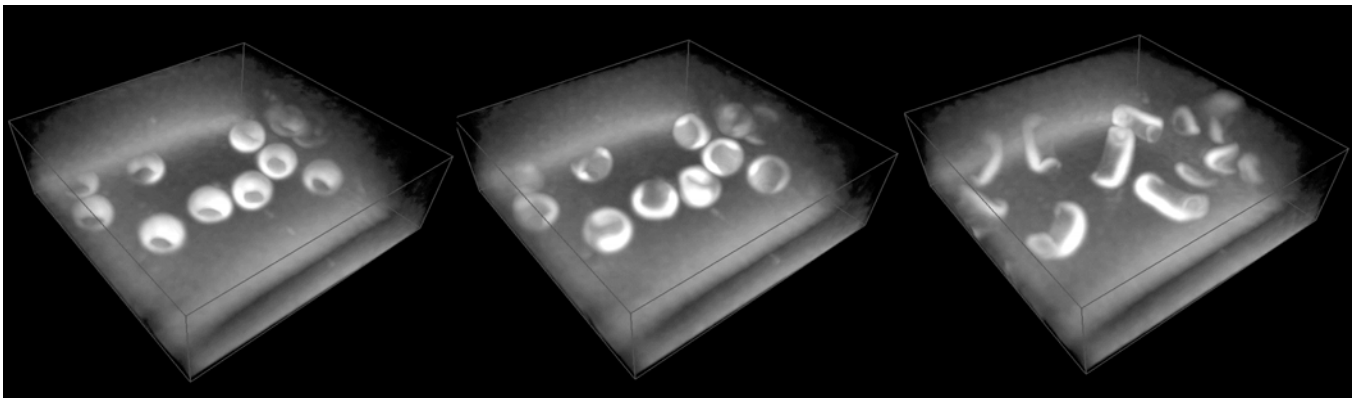
Figure 1: Three frames (0 hours, 16 hours, 32 hours) from a 4D magnetic resonance microscopy time-course of eleven *Xenopus laevis* embryos developing from early gastrula to tail bud stages in a Petri dish. The images were acquired using a planar RF surface coil and have a spatiotemporal resolution of 80 microns (isotropic)/27 minutes. All embryos were labeled with gadoteridol to improve SNR in animal cells.

322. Coordination of morphogenetic processes during gastrulation

Andrew J. Ewald, J. Michael Tyszka, Sara Peyrot, John Wallingford, Scott E. Fraser

During amphibian gastrulation, the embryo is transformed by the combined actions of several different tissues. Paradoxically, many of these morphogenetic processes can occur autonomously in tissue explants, yet the tissues in intact embryos must interact and be coordinated with one another in order to accomplish the major goals of gastrulation: closure of the blastopore to bring the endoderm and mesoderm fully inside the ectoderm, and generation of the archenteron. To evaluate the relative progress in these various processes we collected and analyzed high-resolution 3D digital datasets of frog gastrulae and developed custom morphometric analysis software to allow simultaneous assessment of the progress of convergent extension, blastopore closure and archenteron formation in a single embryo. To examine how the diverse morphogenetic engines work together to accomplish gastrulation, we combined these tools with time-lapse analysis of gastrulation, and examined both wild-type embryos and embryos in which gastrulation was disrupted by manipulation of Disheveled (Xdsh) signaling. Remarkably, though inhibition of Xdsh signaling disrupted both convergent extension and blastopore closure, mesendoderm internalization proceeded very effectively in these embryos. In addition, much of archenteron elongation was found to be independent of Xdsh signaling, especially during the second half of gastrulation. Finally, even in normal embryos, we found a surprising degree of dissociability between the various morphogenetic processes occurring during gastrulation. Together these findings highlight the central role of PCP signaling in governing distinct events of *Xenopus* gastrulation, and suggest that the loose relationship between morphogenetic processes may have facilitated the evolution of the wide variety of gastrulation mechanisms seen in different amphibian species. We have reported the results of these studies [Ewald *et al*., *Development* (2004) **131**(24)] and have described and released the underlying analysis software [Tyszka *et al*., *Dev. Dynam.* (2005), in press].

323. Towards a digital fish: *In toto* imaging of organogenesis in zebrafish

Sean Megason, Scott E. Fraser

Organogenesis transforms a simple field of cells into a complex organ through the precise orchestration of cell proliferation, migration, and differentiation. To better understand these dynamic and complex cell behaviors, we have developed a technology called *in toto* imaging that allows us to digitally track every cell in a developing organ throughout its complex morphogenesis.

There are several technical hurdles to *in toto* imaging. First, embryos must be labeled so that all cells are individually distinguishable. We are using Histone2B-EGFP and membrane localized mCherry followed by channel subtraction to cleanly separate nuclei.

The next challenge is to image embryos at sufficient spatial and temporal resolution for tracking every cell without damaging the embryo. We have developed mounting, confocal imaging, and data storage techniques that allow us to continuously image a developing zebrafish embryo at very high spatial and temporal resolution for 48 hours and to archive the gigabytes of images. The final and toughest challenge is image analysis. To this end, we have developed a software package called GoFigure that automatically segments cells in very large 4D image sets to form cell tracks and cell lineages.

We are first applying *in toto* imaging to determine the complete lineage of the inner ear from before otic placode formation to the differentiation of its basic cell-types: hair cells, support cells, and neurons. This "digital ear" provides a uniquely detailed view of how orchestrated cell behaviors form an organ. We anticipate that *in toto* imaging of transgenic and mutant zebrafish can form the basis for the construction of a digital fish.

324. Dynamic cell behaviors in cardiovascular development

Le A. Trinh, Scott E. Fraser

Organogenesis requires the coordinated morphogenesis of multiple cell types as they differentiate to form a functioning organ. Embryonic heart tube formation is an excellent model for understanding the cellular interactions during organ formation. The heart tube consists of two cell types (myocardium and endocardium) that develop from bilateral populations of precursors which undergo complex cellular rearrangements to form a functioning heart. In addition, the myocardial precursors form maturing epithelia as they differentiate and migrate to the midline. This *de novo* formation of the myocardial epithelia provides a system in which one can assess the dynamics of epithelial formation in the context of organogenesis, as well as study the mechanism of epithelial sheet morphogenesis.

To better understand the dynamic cell behaviors during heart tube formation, we are taking advantage of the unique experimental approaches afforded by characteristics of zebrafish embryos to perform four-dimensional imaging of heart tube development. To assess cell behavior, we are using confocal microscopy and transgenic zebrafish lines that mark the different cell lineages of the heart tube with fluorescent proteins to visualized dynamic cell interactions. Time-lapse analyses of transgenic embryos with green fluorescent protein (GFP) expression in the myocardial precursors, *Tg(cmlc2::eGFP)*, show that the bilateral populations of myocardial precursors undergo extensive cell spreading as they migrate to the embryonic midline. Additionally, we find that the myocardial cells on the lateral edges form extensive protrusions that contact the epidermis. The availability of mutations previously identified in forward genetic screens to affect myocardial migration should provide a genetic framework into which these different cell behaviors can be placed. It is anticipated that the analyses

of both wild type and mutant cell behaviors during heart tube formation should further facilitate our understanding of the complex cellular interactions during cardiac morphogenesis.

325. The role of hemodynamic signals during mammalian cardiovascular development

Elizabeth A.V. Jones, Scott E. Fraser, Mary E. Dickinson

The role of hemodynamics, or blood fluid dynamics, in cardiovascular development remains controversial. During early cardiovascular development, the embryonic vasculature is first established as a random network of blood vessels that is remodeled into a more tree-like vasculature with the onset of blood flow. It is known that early events in angiogenesis and vascular remodeling are dependent on blood flow; however, mechanisms for the induction of remodeling by blood flow have not been established. The aim of this work was to show that the forces created by the initiation of blood flow, called shear stresses, were essential for proper vascular remodeling to occur.

We have used mammalian embryo culture and time-lapse to establish a timeline for the initiation of blood flow and link the initiation of blood flow to changes in vascular morphology. We have also established the shear stress levels exerted on the endothelial cells as the erythroblasts first begin circulating and how these change as vascular remodeling proceeds. In this way, we are able to investigate which signaling mechanisms for vascular remodeling are possible, based on the cues available.

In order to establish that these hemodynamic forces are actually biologically active, we then proceeded to investigate cases of altered hemodynamics and how the embryonic vasculature is affected by these altered forces. We characterize hemodynamic inefficiencies in Myosin Light Chain 2a (MLC2a) knock-out mice. Null mutations in MLC2a result in a specific heart defect; atrial contraction of the heart is silent, but the ventricle can beat normally. We find that these mice exhibit increased oscillatory flow, decreased plasma flow velocities and a failure of erythroblasts to enter the circulation. In order to link the flow phenotype to the vascular deficiencies, we have phenocopied individual aspects of the hemodynamic insufficiencies in order to establish the importance of the individual flow defects to vascular remodeling and link these to changes in proliferation and protein expression. First, we induced a weakened heart without inducing oscillatory flow using an Ncx1 inhibitor. This treatment exhibited a similar phenotype to the MLC2a null mice indicating that low cardiac output alone was sufficient to induce the failure to remodel phenotype of the MLC2a null mice. In order to look more specifically at whether the presence of shear stress was essential, we created a polymer matrix around the early erythroblasts in order to prevent them from entering the early circulation. This treatment allowed for normal heart function and normal plasma flow; however, the increase in viscosity caused by the entry of the erythroblasts into circulation was prevented. Though some characteristics of vascular remodeling are present in these mice, the formation of large blood vessels was inhibited. Thus, we were able to show that it is not only important for flow to be present, but that viscous flow, as provided by the entry of erythroblast into circulation, is essential for proper vascular remodeling.

326. Rapid, confocal microscopy reveals biomechanics of early vertebrate heart contractions

Arian Forouhar*, Michael Liebling, Ralf Wolleschensky**, Anna Hickerson*, Abbas Moghaddam*, Bernhard Zimmerman**, Richard Ankerhold**, Jian Lu*, Jay R. Hove*, Huai-Jen Tsai***, Scott E. Fraser, Morteza Gharib*, Mary E. Dickinson

We have developed a confocal imaging system with the ability to acquire 512 x 512 pixel images as fast as 120 frames per second. Through novel aspects of the design, sensitivity and speed have been improved in comparison to traditional point scanning confocal systems with only a small sacrifice in resolution. We have used this microscope to study the development of the heart and circulatory system in zebrafish embryos.

The embryonic vertebrate begins pumping blood long before the development of discernable heart chambers and valves. At these early stages, the heart tube has been described as a peristaltic pump. The aforementioned advances in confocal microscopy have warranted another look at early cardiac structure and function. We examined the movement of cells in the embryonic zebrafish heart tube wall and the flow of blood through the heart, and obtained results that contradict the existence of peristalsis as a pumping mechanism in the embryonic heart. Through *in vitro* and *in vivo* models, we propose a more likely explanation of early cardiac dynamics in which the pumping action results from suction due to elastic wave propagation and reflection in the heart tube.

*Aeronautics and Bioengineering, Caltech
**Cark Zeiss, Inc.
***University of Taiwan

327. 4D imaging of the embryonic heart via wavelet-based image synchronization

Michael Liebling, Arian S. Farouhar, Morteza Gharib, Scott E. Fraser, Mary E. Dickinson

One of the most challenging objectives in developmental biology is being able to acquire, visualize, and analyze three-dimensional time-series (4D data) at high frame rates. Current state-of-the-art confocal microscopes allow for 2D imaging at frame rates as fast as 120 frames per second (fps) but can be quite slow at capturing 4D data at a sufficient resolution. However, we have shown that for specimens that undergo periodic motions or deformation (such as a beating heart), it is possible to reconstruct dynamic 3D volumes from series of unsynchronized 2D sequences without giving up temporal resolution. The reconstruction consists in the digital post-

acquisition synchronization of sequences acquired at increasing depths, without them being gated to an external signal (nongated acquisition). For that purpose, we have developed an automatic procedure to align the stacks at different depths. The algorithm is based on the minimization (in the least-squares sense) of an objective criterion that measures the similarity between the data from neighboring depths. Wavelets have proven instrumental to ensure both fast execution and robust results. We were able to reconstruct dynamic 3D volumes of zebrafish embryos at various stages of their development. These reconstructions are suitable for further evaluation, in particular for volume change monitoring, heart deformation modeling, and flow analysis.
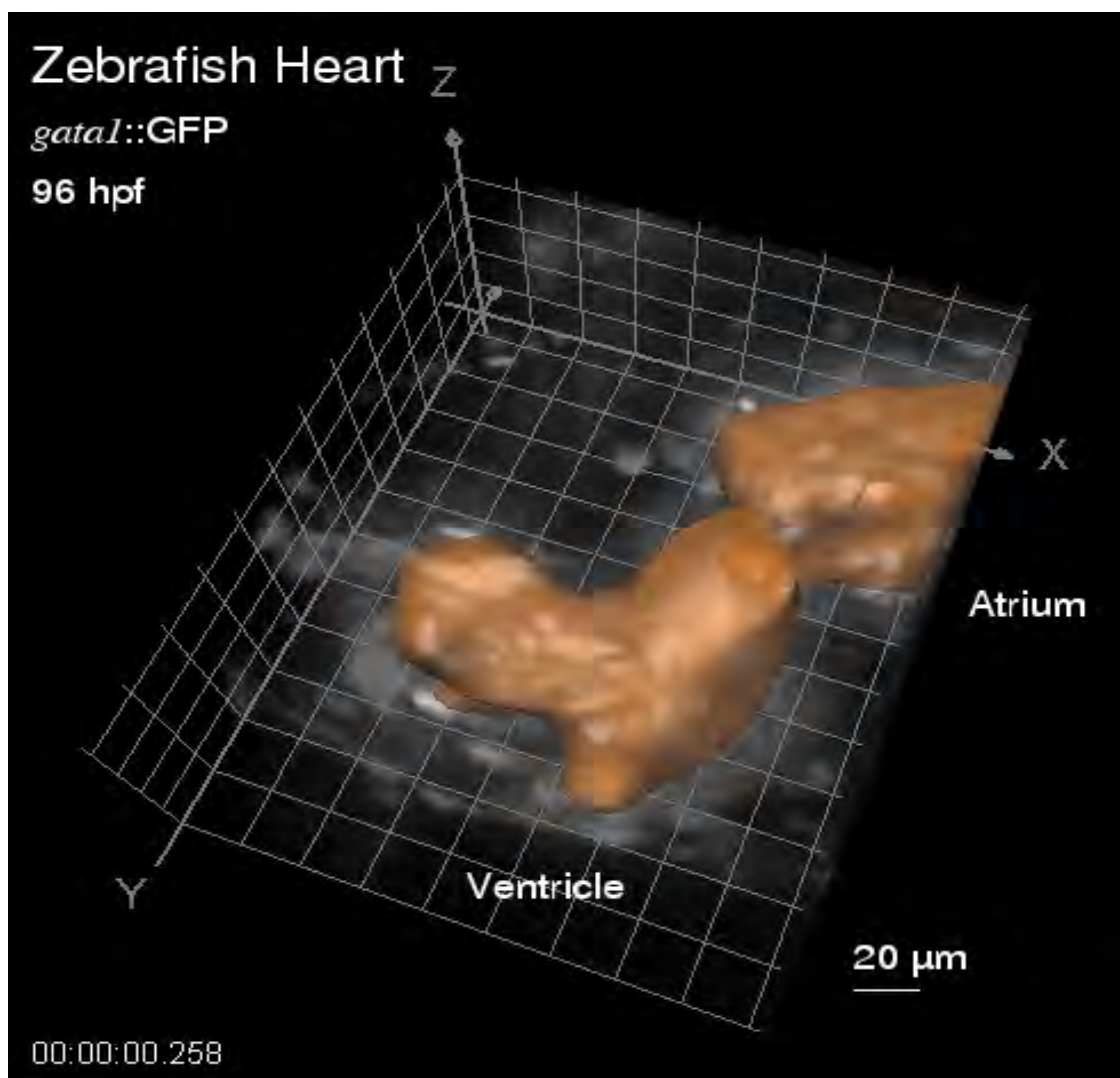
328. Developing an *in vitro* model for study of vascular remodeling process during development

Wei Shen, Mary E. Dickinson, Scott E. Fraser

While recent findings have shown that entry of erythroblasts into circulation plays important roles in regulating vascular remodeling during mammalian embryo development, it remains unclear whether this regulation is caused by the changes in mechanical or chemical signals carried by blood flow. In order to address this question, we have established an *in vitro* model to decompose the complex environment cues presented to endothelial cells and their precursor cells by blood flow. Cells expressing Flk-1 (VEGF receptor 2) are isolated from mouse embryos at different stages. Cells are sorted, immobilized in microfluidic channels, and exposed to flow. Cellular response to changes in flow rate and medium components will provide insights into the nature of the blood-flow-mediated vascular remolding process during development.

329. Studying the molecular nature of bilateral symmetry in vertebrates

Julien Vermot, Scott E. Fraser

The somites are embryonic elements that give rise to the muscles, skeleton and some skin layers of the trunk. Somites arise periodically on both sides of the neural tube in a symmetrical fashion. While a molecular clock controls the periodicity of somite formation, the molecular signals that control their symmetrical formation are still not well defined. In order to better understand the mechanisms that maintain the bilateral symmetry of somite formation, we designed an incubation chamber triggering differential growth rates on each embryonic side in chicken. After incubation, the embryo obtained is asymmetrical. This tool will allow us to determine whether the synchronization of the molecular clock is actively controlled between the two embryonic sides. Furthermore, this tool will help to identify the signals implicated in this process.

330. New diagnostics and therapies for age-related macular degeneration (AMD)

C.J. Yu, Jeff Fingler, Jon Williams, J. Michael Tyszka

Age-related macular degeneration (AMD) is the leading cause of vision loss in the Western world. Existing therapies for AMD target the late stage of the disease, in which sub-retinal neovascularization damages the macular retina. Before neovascularization develops, there is progressive accumulation of lipid deposits in Bruch's membrane, a multilaminar extracellular matrix layer that lies between the retina and its blood supply. Lipid deposition in Bruch's membrane reduces hydraulic conductivity and macromolecular permeability across the membrane. It is hypothesized that resultant impaired retinal metabolism induces release of growth factors, such as vascular endothelial growth factor (VEGF), that cause the pathologic neovascularization. Because progressive lipid accumulation impairs transport across Bruch's membrane, targeted dissolution of this lipid layer could potentially normalize diffusion and prevent development of neovascularization.

In this project we are concurrently developing methods for targeted treatment of lipid deposits in Bruch's membrane, non-invasive MRI-based methods for *in vitro* and *in vivo* membrane permeability measurements, and optical coherence tomography (OCT) diagnostic imaging technology.

Targeted treatment of Bruch's membrane lipids is achieved by caging molecules and uncaging them selectively in the eye via two-photon photolysis. The caging agent with the highest reported two-photon uncaging cross section (the measure of efficiency of uncaging) is the 7-hydroxycoumarin moiety. In order to demonstrate the local effects generated from uncaging molecules using two-photon photolysis, the coumarin-caged fluorescein has been successfully synthesized and studied (**Figure 1**).

Oxygen transport is of particular interest in AMD. Preliminary results demonstrate the potential of MRI for quantifying diffusional permeability of both water and dissolved oxygen across Bruch's membrane. Oxygen in aqueous solution is a mild T_1 contrast agent allowing the spatiotemporal dynamics of oxygen concentration to be assessed using MRI, with the ultimate goal of assessing the effectiveness of therapeutic agents in removing lipid deposits *in vitro* and *in vivo*. (**Figure 2**)
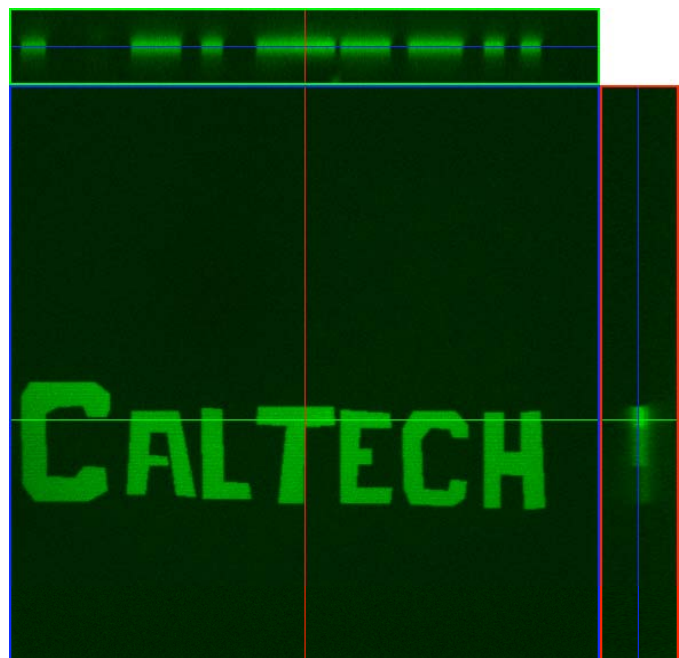
Figure 1: Uncaging of coumarin-caged fluorescein in epoxy matrix. The axial extent of the uncaged region is approximately 5 microns.
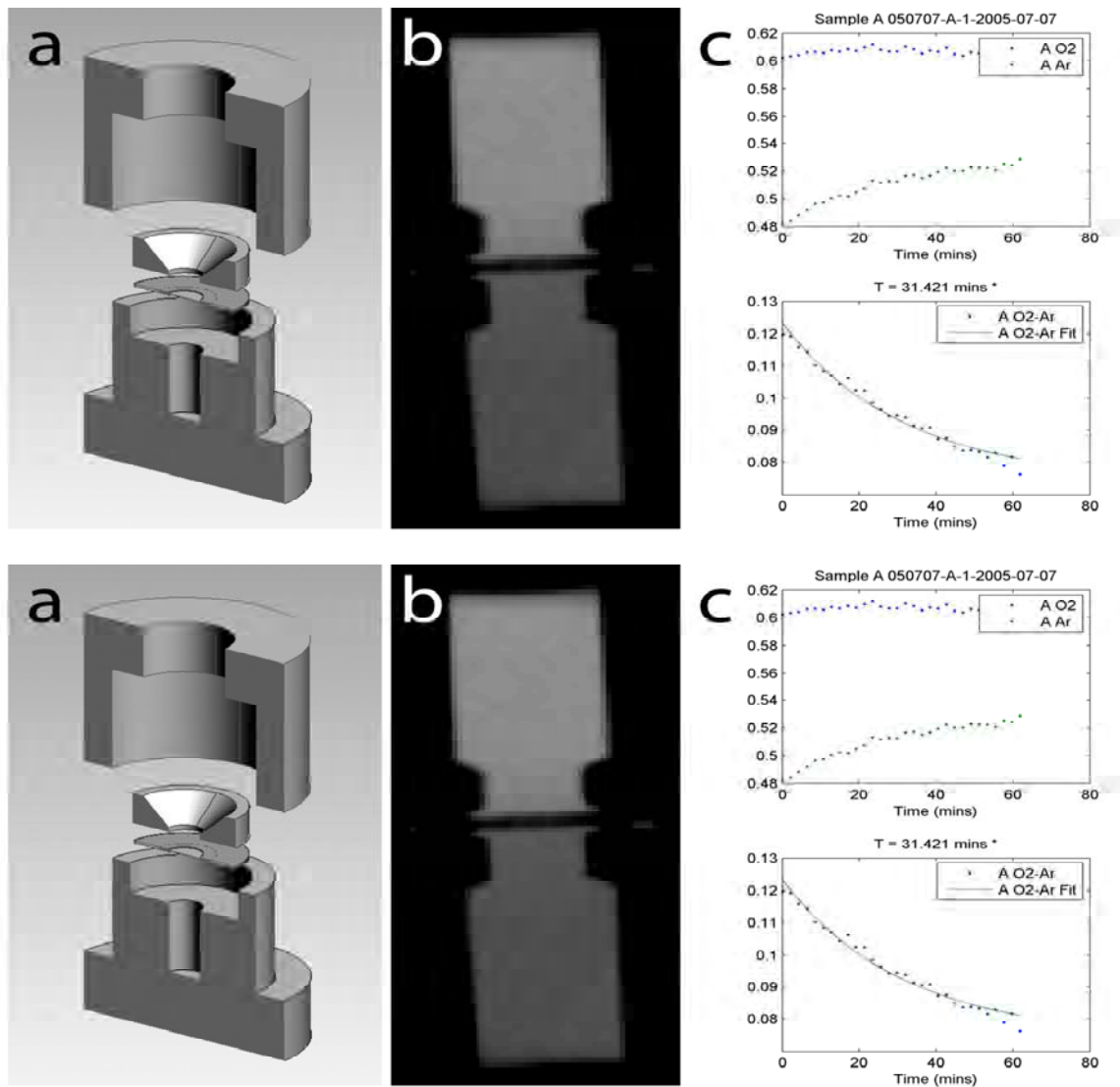
Figure 2: MRI of dissolved oxygen in a two chamber cell designed to measure diffusional permeability across a Bruch's membrane sample. (a) A typical cell consists of an upper and lower chamber between which the prepared membrane sample is trapped by o-ring or washer seals. (b) Example dissolved oxygen-sensitive MRI image of a two chamber cell. The upper chamber contains water with a higher dissolved oxygen concentration and therefore, appears brighter in such images. (c) Experimental time-course showing absolute (above) and differential MR signal in the upper and lower chambers as the cell equilibrates over the course of about 1 hour.

331. Cranial neural crest migration and the role of ephrin-A5

Carole Lu, Scott E. Fraser

Cranial neural crest cells are multipotent cells that arise in the dorsal neural tube and migrate within discrete streams in the avian embryo. By labeling the premigratory neural crest cells with constructs for fluorescent proteins and conducting time-lapse microscopy, we are able to follow their cell behaviors and migratory patterns in the intact embryo. The combination of time-lapse microscopy with molecular perturbations allows us to characterize the migration and sorting of the neural crest cells into branchial arches 3 and 4, and to dissect underlying changes in migration due to molecular perturbations.

Similar to previous findings, the neural crest cells at the level of rhombomere 4 (r4) migrate in a tight lateral stream directly from the neural tube to branchial arch 2 (ba2), separated from other neural crest cells by crest-free regions adjacent to r3 and r5. In the posterior hindbrain, the neural crest cells first form a field of cells that then segregate amongst branchial arches 3 and 4. The underlying mechanism of this sorting is unclear. However, this is similar to what occurs in *Xenopus*, where cranial crest cells first migrate as a wave and then segregate to different arches. Differential expression of Eph and ephrin family members is known to be involved in segregating these streams. Differences in the avian r4 and r6 streams

of neural crest cells suggest the mechanisms that guide their migration are different.

To this effect, we are studying the role of ephrin-A5 in the migration of neural crest cells that populate ba3 and ba4. We find that when we misexpress ephrin-A5, the neural crest cells are less likely to populate ba3 but the other branchial arches are not affected. We sectioned embryos electroporated with ephrin-A5/GFP construct and looked at TUNEL and pH3 antibody staining on serial sections. We found that cell death is unaffected but proliferation rates were greatly increased by 31 hr following electroporations. Focal DiI injections into r6 did not label any r6 ncc that also expressed ephrin-A5/GFP. This mysterious absence is under further investigation. Time-lapse analyses found that ephrinA5/GFP positive ncc migrate at a similar velocity, but along more directed paths when compared with the GFP+ ncc control. This suggests the cells are changing their migratory pathways, with slightly less exploration and more directed migration.
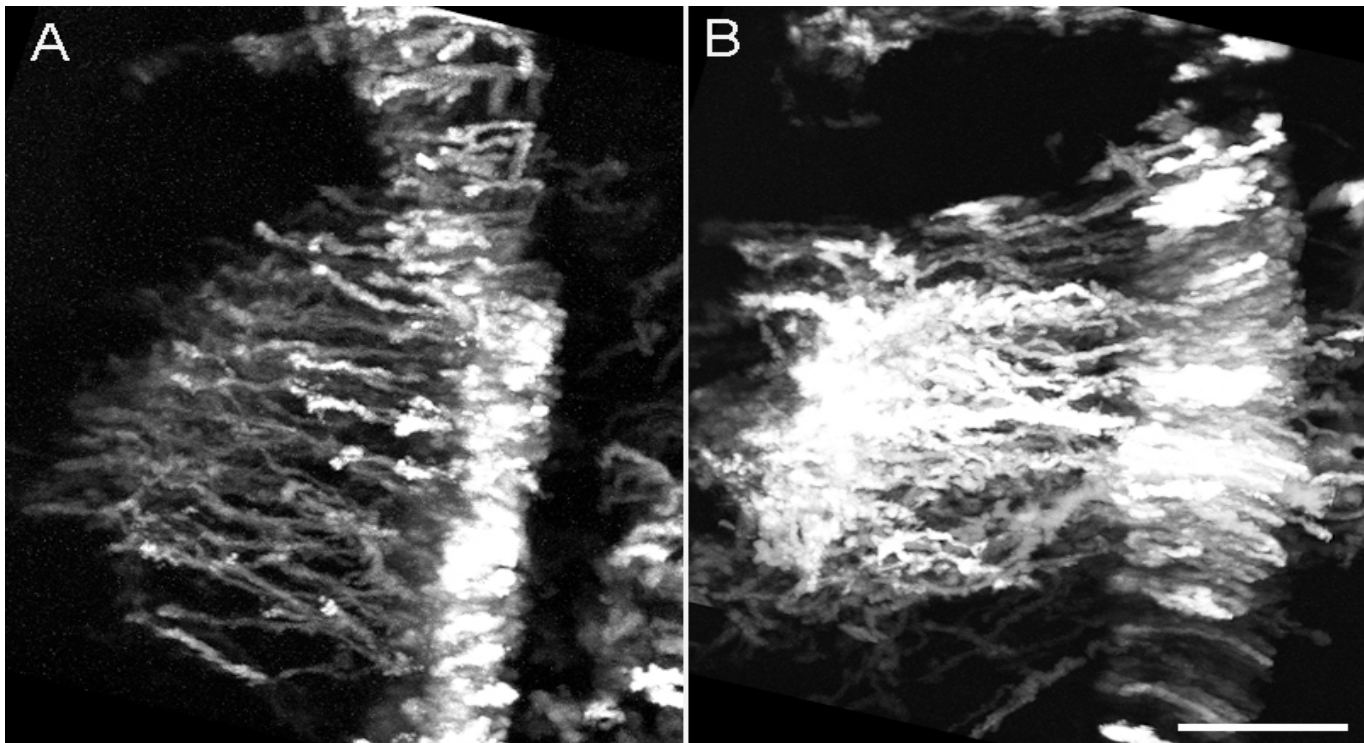
Figure: Extensive migration of neural crest cells is seen in representative time-lapse sessions of (A) ephrin-A5/GFP and (B) GFP electroporated embryos.

332. Imaging the enteric nervous system in development and in disease

Helen McBride, Scott E. Fraser

My research interests focus on understanding how the enteric nervous system (ENS) is formed and patterned properly during development. The intrinsic enteric nervous system forms from one cell type, the neural crest. What does that really mean? It means that one group of cells derived from the same location in the embryo gives rise to millions of neurons and glial (support) cells within the adult ENS. And those neurons more resemble the complexity seen in the brain than in the rest of the peripheral nervous system. That is why the ENS is often called the "little brain."

Neural crest cells migrate into the developing gut tissue from the neural tube early in development and proceed to colonize the entire length of the gut tract. This is no small feat given that the gut is growing while these cells are migrating through it to reach the "end." While migrating, there is a careful balance between proliferation and differentiation to ensure that there are enough cells around to make it to the end of this long journey.

Once neural crest cells have stopped migrating and begin the process of differentiation into the cell types they will become in the adult a new set of challenges emerges. How do they decide who becomes a neuron and who becomes a glial cell? Balancing the right number of neurons and support cells is critical to the later growth of the ENS. Getting it wrong may lead to problems in function later on.

Once these cells have decided to become neurons, a new set of choices begins. What type of neuron to become? There are over ten choices and these must be chosen correctly depending on what section of the gut the neural crest cell finds herself in. Getting it right ensures proper peristalsis; getting it wrong may lead to chronic constipation or obstruction.

How are we approaching these questions? I have chosen a variety of imaging methods to address how neural crest cells migrate within the developing gut and later, how motility emerges in the adult ENS. By developing an

assay for neural crest migration in the embryonic gut, we are testing candidate molecules for their role in ENS formation in the intact tissue. Using uMRI in adult animals allows us to similarly screen through candidate mouse lines for mutations that affect motility in subtle ways. In addition, we are studying how signaling molecules pattern the underlying gut tissue that neural crest cells migrate through. Because communication between neural crest cells and the gut should be important in properly patterning the ENS, molecules that are identified from these studies will then be tested in the migration assay. Synergy between these three areas of interest will lead to a continuing stream of signaling molecules to study at multiple levels of gut and ENS development and will, hopefully, answer some of the fascinating and very basic questions listed above.

333. Formation and desorption of biofunctionalized alkylthiolate monolayers on Au substrates
Christie A. Canaria, Jonathan So, James Maloney, Rusty Lansford

The implementation of self-assembled monolayers (SAMS) enables substrates to exhibit a variety of chemical properties and reactivities. The development of such surfaces advances bioassay technologies such as DNA chips, protein chips and small molecule sensors. We are studying the formation and desorption of derivitized alkylthiolate SAMs on Au surfaces.

One requirement for high quality alkylthiolate monolayers is a clean Au substrate. Clean Au substrates exposed to ambient conditions will quickly collect impurities from the environment and atmosphere which can impact SAM growth[1],[2],[3],[4]. Some of these contaminants, such as hydrocarbons, are reversibly bound, others irreversibly bound. Different techniques used to clean gold substrates include strong oxidation of contaminants from the surface, such as highly acidic aqua regia solution, piranha solution and ozone plasma cleaning. While each of these methods yields clean gold surfaces, they are not compatible with the constraints imposed by an integrated device system. Specifically, PDMS-based micro-fluidic devices are not amenable to any of these methods. Many electronic components are destroyed upon exposure to strong acids and accessing gold samples inside packaged devices for ozone plasma cleaning is not feasible. However, electrochemical techniques for cleaning gold may be used to remove surface contaminants. Application of a sufficiently oxidative[5],[6] or reductive[7] potential on gold induces desorption of surface species, including alkylthiolates. Although reductive potential techniques were shown to work on solid Au electrodes, applied anodic potentials beyond 1.4 V, as well as cathodic potentials beyond –1.0 V (vs. Ag/AgCl in saturated KCl) induce surface malformation of the working Au electrode film of our samples. Working within these potential boundaries, an electrochemical cell setup is compatible with microfluidics devices[8] and serves as an on-chip method for cleaning gold samples both before and after monolayer formation.

We are investigating methods for creating recyclable bio-chips that will specifically bind proteins, DNA and small molecules. Currently, monolayers and binding events are characterized using electrochemical techniques and with dyed target molecules and fluorescence microscopy. This allows us to study both the kinetics of monolayer formation/desorption and substrate-mediated biological interactions.

References
(1) Bain, C.T., Troughton, E.B., Tao, Y., Evall, J., Whitesides, G.M. and Nuzzo, R.G. (1989) *J. Am. Chem. Soc.* **111**:321-335.
(2) Nuzzo, R.G., Dubois, L.H. and Allara, D.L. (1990) *JACS* (1990) **112**:558.
(3) Peterlinz, K.A. and Georgiadis, R. (1996) *Langmuir* **12**:4731-4740.
(4) Xu, S., Cruchon-Dupetrat, S., Garno, J.C., Liu, G., Jennings, G., Yong, T. and Laibinis, P.E. (1998) *J. Chem. Phys.* **108**:5002.
(5) Yang, D.F., Al-Maznai, H. and Morin, M. (1997) *J. Phys. Chem. B.* **101**:1158-1166.
(6) Loglio, F., Schweizer, M. and D. Kolb, D. (2003) *Langmuir* **19**:830-834.
(7) Shepherd, J., Kell, A., Chung, E., Sinclar, C., Workentin, M. and Bizzotto, C. (2004) *J A C S* **126**:8329-8335.
(8) Hiratsuka, A., Muguruma, H., Lee, K.-H. and Karube, I. (2004) *Biosens. Bioelectron.* **19**:1667-1672.

334. An optical method for measuring a microscopic field of flow
David D. Wu, Rob Phillips, Scott E. Fraser*

The determination of asymmetry in the adult body plan of an animal from a spherically symmetric embryo has been an active area of scientific pursuit. One of the posited early mechanisms for left/right determination is the existence of a ventral node (in a wide array of animals) that transports fluid unidirectionally. Usually consisting of a small, depressed area (~100 mm^2) lined with beating cilia which create a field of flow, the putative mechanism for symmetry breaking could be the transport of released packets of information from one side of the embryo to another, the generation of morphogen gradients within the convexity, or merely from a mechanical signal induced by the field of fluid flow. We present here a way to quantitate and map the flow vectors of the circulating fluid at multiple points simultaneously. In brief, the diffusion-reaction mechanism of (Kramers 1940) is multiplied into a 2D array by placing two diffractive optical elements in front of a frequency doubled, Nd:YAG laser (l=532 nm). These spatially separated miniature reactors (~16) therefore, each consist of two optical traps in tandem; moreover, any object trapped will occupy the reactors according to the energy difference between the two traps, provided the kinetic barrier for crossing is low enough to generate adequate statistics to satisfy ergodicity. Hence, any forcing of the system will establish a new steady state wherein the applied force can be determined given the

210

equilibrium configuration; thus, we have a way for measuring microscopic flow energies on the order of thermal noise, such as that of fluid movement generated by beating cilia. The instrument can also be tuned for maximum sensitivity according to the strength of the applied force.

Engineering & Applied Science, Caltech

335. Assessing mobility differences of cytoplasmic GFP in zebrafish neuronal growth cones with multi-photon FRAP

Rajan P. Kulkarni, Magdalena Bak-Maier, Scott E. Fraser

The development of the nervous system involves guided extension of axons towards other neurons. The growth cone, a key structure at the distal tip of the developing axon, contains the sensory and motor processes required for this extension. Localized diffusion differences in growth cones are likely to be critical for delivery of molecular species into the growth cone tip, which in turn can influence the direction of growth. However, there has been little work evaluating the kinetics of local protein movement or the effect of cytoskeletal structural elements on protein diffusion *in vivo.* In recent years, fluorescence recovery after photobleaching (FRAP) measurements have been utilized to measure the transport rate of small proteins within various cytoplasmic environments. We utilized both one- and two-photon FRAP measurements combined with timelapse analysis to assess the lateral diffusion of cytoplasmic GFP in early neurons and their growth cones in the developing zebrafish embryo. From this data, we observed differences in local diffusion rates between actively pioneering growth cones (leader growth cones) and those that rely on other axons as substrates for guidance (follower growth cones). Pharmacological treatment of the neurons with either cytochalasin (to disrupt actin) or nocodazole (to disrupt microtubules) points to actin as the primary modulator of free diffusion in developing growth cones. This experimental approach provides a useful method for quantifying the mobility of specific macromolecules in growth cones *in vivo* and indicates that diffusion may be an important modulator of growth cone behavior during axon navigation.

336. Single-Biomolecule Resolution Imaging with an Optical Microscope

Lawrence A. Wade, C. Patrick Collier, Scott E. Fraser*

A Fluorescence Apertureless Near-field Scanning Optical Microscope (FANSOM) has been developed with FWHM optical resolution below 10 nm when imaging at ~600 nm wavelengths [1]. The apparatus combines an epi fluorescence optical microscope and an atomic force microscope (AFM) to obtain single-molecule sensitivity and optical resolution limited by the sharpness of the AFM probe. The AFM probe is used to stimulate or reduce the detected fluorescence emission rate depending on the AFM

tip material and the polarization of the excitation light. The probe-sample interaction is described by near-field dipole-dipole physics, resulting in a stimulated emission rate that varies by r^6. When tapping the probe over the substrate being imaged, the near-field component is sharply modulated at that tapping frequency, thereby enabling separation from the far-field background during post-processing.

We are also developing probe and substrate technologies to enable FANSOM to image and time-resolve the dynamics of biomolecular interactions. The tools developed include generalized techniques for the growth and attachment of nanotubes for use in AFM imaging. With our nanotube tips we have generated 0.5 nm resolution AFM images, potentially enabling optical imaging of single-molecules with resolutions approaching 1 nm [2]. In addition these nanotube probes can be uniquely functionalized at their tips, serving as the foundation of an effort to develop single-molecule sensors. Coating these probes with Teflon has enabled fabrication molecular-scale electrical probes [3]. Silane-chemistry dip-pen nanolithography techniques have been developed for patterning glass coverslips with functional proteins, peptides, aptamers, etc. [4,5]. We anticipate patterning functional biomolecules onto glass coverslips and then individually characterizing highly specific molecular interactions at *in vivo*-like molecular concentrations using FANSOM. In addition, these tools will prove relevant for characterizing cellular contents and expression with single-molecule discrimination using nanoarrays and molecular circuits. Finally, techniques are being developed for patterning phospholipid bilayers for use as model membrane systems. Together, these tools should prove particularly well suited for probing bio-interface problems such as viral insertion, transmembrane protein triggering and lipid raft formation and function.

Chemistry & Chemical Engineering, Caltech

This work was supported by NASA/JPL Research and Technology Development and Bio-Nano Programs, the Caltech President's Fund, NIH, Pharmagenomics and Arrowhead Research.

References
[1] Gerton, J.M., Wade, L.A., Lessard, G.A., Ma, Z. and Quake, S.R. (2004) *Phys. Rev. Lett.* **93**:180-801.
[2] Wade, L.A., Shapiro, I.R., Ma, Z., Quake, S.R. and Collier, C.P. (2004) *Nano Lett.* **4**:725-731.
[3] Esplandiu, M.J., Bittner, V.G., Giapis, K.P. and Collier, C.P. (2004) *Nano Lett.* **4**:1873-1879.
[4] Jung, H., Kulkarni, R. and Collier, C.P. (2003) *J. Am. Chem. Soc.* **125**:12096-12097.
[5] Jung, H., Dalal, C.K., Kuntz, S., Shah, R. and Collier, C.P. (2004) *Nano Lett.* **4**:1873-1879.

Fig. 1. On the right is imaged a 17 nm diameter latex bead. In the top right the bead was imaged through florescence reduction using metallic tip. The simultaneously acquired AFM image is shown in the lower right. On the left are images of a 20 nm x 5 nm diameter CdSe nanorod showing the separation of near-field and far-field components via demodulation. These FANSOM images were taken through fluorescence enhancement using a silicon probe.
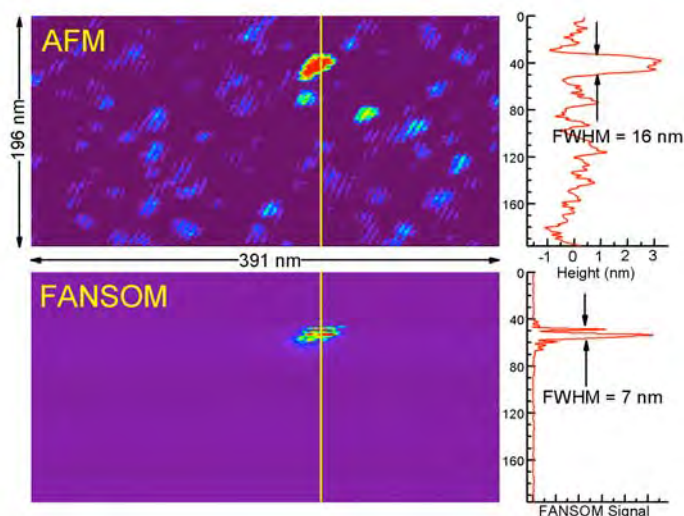
Fig. 2. AFM and FANSOM images of a 20 nm x 5 nm diameter CdSe nanorod are compared. A commercial silicon FESP probe was used for these images. The FANSOM image used a 40 nm wide filter centered at 620 nm at the detector.
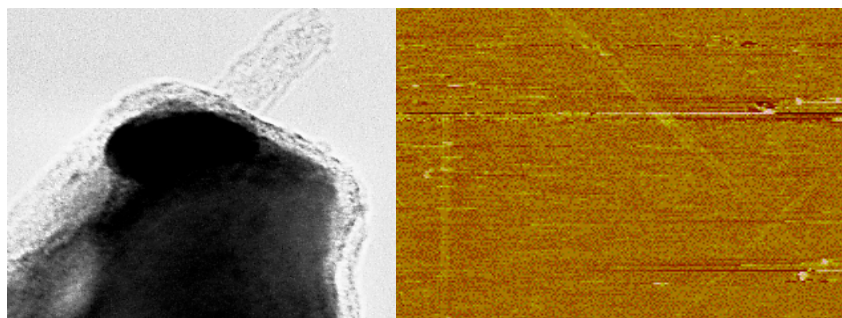
Fig. 3. On the right is a TEM image of a single-wall nanotube attached to the tip of a silicon AFM probe. On the right is a 4 x3 µm lateral force AFM image of biotin patterned on a glass substrate. The two diagonal lines are 70 nm wide and centered 200 nm apart as are the two left lines.

337.   Applications of terahertz imaging to medical diagnostics

Peter H. Siegel, Warren Grundfest*, Scott E. Fraser

This research program aims to apply terahertz (THz) source and sensor technology towards (1) establishing and cataloging properties and contrast mechanisms in biomaterials and tissues and (2) investigating potential disease diagnostic applications. THz waves occupy the wavelength region between 100 and 1000 microns, well beyond the traditional infrared. As a consequence they can penetrate more readily into many optically opaque materials including plastics, wood, clothing, some crystalline structures and, as is the emphasis for this program, a small number of biomaterials – lipids, bone, skin, hair, etc. Unlike infrared and optical signals, THz penetration in tissue is dominated by absorption not scattering, making the contrast mechanisms very different than those that are already being exploited in the optical regime. Water absorption is also extremely high (a =100-300 cm-1) which has the disadvantage that very strong THz signal sources are required for significant tissue penetration, but the advantage that very subtle changes in fluid content are detectable (the basis for disease diagnostics). The first successful THz imaging systems have been based on picosecond pulsed-laser time domain spectroscopy techniques. These instruments offer unique spectral and time resolved information content but have limited penetration depth (tens of microns in tissue) and only modest signal-to-noise ratio (100-1000). This program has already demonstrated a THz imaging system based on novel heterodyne techniques (more generally used in space science and communications) with a signal to noise of more than 10^{10} at a wavelength of 120 microns (5X higher frequency than any commercially available system). Current work is focused on extending the frequency coverage to longer wavelengths (0.1 to 1mm) to allow greater penetration in tissue at the expense of resolution.
*UCLA

338.   Flexible ribbon guide for *in vivo* and hand-held THz imaging

Peter H. Siegel, Cavour Yeh*, Scott E. Fraser

Recent interest in terahertz frequency imaging for medical applications (wavelength range from 1 mm to 100 microns) has resulted in a flurry of new instrument proposals using both time domain and high resolution frequency domain spectral techniques. However, to date there exists no methodology for transporting terahertz signals from place-to-place with low loss, other than rigid-path free-space quasi-optical beam propagation. In order to take advantage of modalities common at optical wavelengths, including *in vivo* and portable hand-held sensor/receiver systems, the equivalent of signal-confining optical fiber links must be developed for the far infrared and terahertz bands. Commonly employed transparent materials in the visible (i.e., amorphous glasses or clear plastics) are all extremely lossy at longer wavelengths due to strong vibrational mode absorption. Dielectric substances with low absorption coefficient and high index do exist at terahertz frequencies, but they tend to be crystalline (quartz, silicon, germanium, GaAs) and therefore, have poor mechanical properties when it comes to forming flexible guiding structures. Metallic waveguide (hollow or coaxial), although somewhat flexible, has untenable high resistive wall loss. A few plastics such as Teflon, polyethylene and polypropylene, have very low dispersion and absorption but have a low refractive index that makes it difficult to confine single-mode terahertz energy as it propagates around bends or through joints. Earlier work by our collaborators has shown that high index materials formed into ultra-thin ribbons can form very low loss guiding media at millimeter-wave frequencies (30-100 GHz). Extrapolating this concept into the terahertz bands, and taking advantage of modern fabrication techniques, we believe it is possible to use a combination of high-dielectric-constant crystalline materials in conjunction with low loss, low index plastics to produce the equivalent of flexible terahertz optical fiber, i.e., "terahertz ribbon guide." Such a development would allow terahertz instruments to be freed from their fixed-beam-path table-top environment, enabling, for the first time at these wavelengths, both hand-held scanner and *in vivo* endoscopic applications. This task has been investigating both the design and fabrication of low-loss single-mode terahertz guiding structures.
*California Advanced Studies

Publications

Canaria, C.A., Smith, J.O., Yu, C.J. and Fraser, S.E. (2005) New syntheses for 11-(mercaptoundecyl)triethylene glycol and mercaptododecyltriethyleneoxy biotin amide. *Tetrahedron Letters* **46**:4813-4816.

Chen, J.Y., Bottjer, D.J, Oliveri, P., Dornbos, S.Q., Gao, F., Ruffins, S., Chi, H.M., Li, C.W. and Davidson, E.H. (2004) Small bilaterian fossils from 40 to 55 million years before the Cambrian. *Science* **305**(5681):218-222.

Dickinson, M.E. (2004) Multiphoton, multispectral laser scanning microscopy. In: *Live Cell Imaging: A Laboratory Manual*, Cold Spring Harbor Laboratory Press, Cold Spring Harbor, NY, U.S.A.

Dorman, J.B., James, K.E., Fraser, S.E., Kiehart, D.P. and Berg, C.A. (2004) Bullwinkle is required for epithelial morphogenesis during *Drosophila* oogenesis. *Dev. Biol.* **267**:320-341.

Ewald, A.J., Peyrot, S.M., Tyszka, J.M., Fraser, S.E. and Wallingford, J.B. (2004) Regional requirements for Dishevelled signaling during *Xenopus* gastrulation: Separable effects on blastopore closure, mesendoderm internalization and archenteron formation. *Development* **131**:6195-6209.

Fraser, S.E. and Stern, C. (2004) Early rostrocaudal patterning of the mesoderm and neural plate. In: *Gastrulation: From Cells to Embryo,* Claudio Stern (Ed.), Cold Spring Harbor Laboratory Press, Cold Spring Harbor, NY, U.S.A.

Gong, Y., Mo, C. and Fraser, S.E. (2004) Planar cell polarity signaling controls orientation of cell divisions during zebrafish gastrulation. *Nature,* **430**:689-693.

Jacobs, E.C., Pribyl, T.M., Kampf, K., Campagnoni, C., Colwell, C.S., Reyes, S.D., Martin, M., Handley, V., Hiltner, T.D., Readhead, C., Jacobs, R.E., Messing, A., Fisher, R.S. and Campagnoni, A.T. (2005) Region-specific myelin pathology in mice lacking the Golli products of the myelin basic protein gene. *J. Neurosci.* **25**(30):7004-7013.

Jones, E.A.V., Baron, M.H., Fraser, S.E. and Dickinson, M.E. (2004) Measuring hemodynamic changes during mammalian development. *American J. Physiology: Heart and Circulation* **287**:H1561-H1569.

Jones, E.A.V., Crotty, D., Baron, M.H., Fraser, S.E. and Dickinson, M.E. (2004) Dynamic *in vivo* imaging of mammalian hemato-vascular development using whole embryo culture. In: *Developmental Hematopoiesis: Methods and Protocols*, Baron, M.H. (Ed.), Methods in Molecular Medicine series, Humana Press, New York, NY, U.S.A.

Jones, E.A.V., Hadjantonakis, A-K. and Dickinson, M.E. (2004) Imaging mouse embryonic development. In: *Imaging in Neuroscience and Development: A Laboratory Manual*. Cold Spring Harbor Laboratory Press, Cold Spring Harbor, NY, U.S.A

Kasemeier, J.C., Lefcort, F., Fraser, S.E. and Kulesa, P.M. (2004) A novel sagittal slice explant technique for time-lapse imaging of the formation of the chick peripheral nervous system. In: *Imaging in Neuroscience and Development*, R. Yuste, A. Konnerth, (Eds.), Cold Spring Harbor Laboratory Press, Cold Spring Harbor, NY, U.S.A

Köster, R.W. and Fraser, S.E. (2004) Time-lapse microscopy of brain development. In: *The Zebrafish – Cellular and Developmental Biology,* William Detrich, Monte Westerfield, Leonard Zon, (Eds.), Elsevier Press, San Diego, CA, U.S.A.

Kulesa, P.M. and Fraser, S.E. (2004) *In ovo* imaging of avian embryogenesis. In: *Imaging in Neuroscience and Development*, R. Yuste, A. Konnerth, (Eds.), Cold Spring Harbor Laboratory Press, Cold Spring Harbor, NY, U.S.A.

Kulesa, P.M., Lu, C.C. and Fraser, S.E. (2005) Time-lapse analysis reveals a series of events by which cranial neural crest cells reroute around physical barriers. *Brain, Behavior and Evolution* 518-T1.

Kulkarni, R.P., Mishra, S., Fraser, S.E. and Davis, M.E. (2005) Single cell kinetics of intracellular, non-viral, nucleic acid delivery vehicle acidification and trafficking. *Bioconjugate Chem.* **16**(4): 986-994.

Kulkarni, R.P., Wu, D.D., Davis, M.E. and Fraser, S.E. (2005) Quantitating intracellular transport of polyplexes by spatio-temporal image correlation spectroscopy. *Proc. Natl. Acad. Sci. USA* **102**:7523-7528.

Liebling, M., Forouhar, A. S., Gharib, M., Fraser, S. E. and Dickinson, M.E. (2005) 4-Dimensional cardiac imaging in living embryos via post-acquisition synchronization of nongated slice-sequences. *J. Biomed. Optics*. In press.

MacKenzie-Graham, A., Lee, E.F., Dinov, I.D., Bota, M., Shattuck, D.W., Ruffins, S., Yuan, H., Konstantinidis, F., Pitiot, A., Ding, Y., Hu, G.G., Jacobs, R.E. and Toga, A.W. (2004) A multimodal, multidimensional atlas of the C57BL/6J mouse brain. *J. Anatomy* **204**(2):93-102.

Megason S.G., Amsterdam A., Hopkins N. and Lin S. (2004) Uses of GFP in transgenic vertebrates. In: *Green Fluorescent Protein: Properties, Applications and Protocols, Second Edition*, Steven R. Kain and Martin Chalfie, (Eds.), Wiley Press, Hoboken, NJ, U.S.A.

Modo, M., Mellodew, K., Cash, D., Fraser, S.E., Meade, T.J., Price, J. and Williams, S.C.R. (2004) Mapping transplanted stem cell migration after a stroke: A serial, *in vivo* magnetic resonance imaging study. *NeuroImage* **21**:311-331.

Siegel, P.H. (2004) THz technology in biology and medicine. *IEEE Trans. Microwave Theory and Techniques*, vol. 52, no. 10, pp. 2438-2448.

Siegel, P.H., Yeh, C., Shimabukuro, F. and Fraser, S.E. (2004) Hollow-core periodic bandgap flexible dielectric waveguide for low-loss THz signal transmission. *New Technology Report* NTR 41299.

Tyszka, J.M., Ewald, A.J., Wallingford, J.B. and Fraser, S.E. (2005) New tools for visualization and analysis of morphogenesis in spherical embryos. *Dev. Dynam.* In press.

Tyszka, J.M., Fraser, S.E. and Jacobs, R.E. (2005) Magnetic resonance microscopy: Recent advances and applications. *Curr. Op. Biotechnol.* **16**:93-99.

Wood, J.C., Tyszka, J.M., Carson, S., Nelson, M.D. and Coates, T.D. (2004) Myocardial iron loading in transfusion-dependent thalassemia and sickle cell disease. *Blood* **103**:1934-1936.

214

Associate Professor of Biology: Bruce A. Hay
Research Fellows: Chun Hong Chen, Israel Muro
Graduate Students: Jeffrey Copeland, Jun R. Huh
Undergraduate Students: Adam Reeves, Greg Stachelek
Collaborators: Rollie Clem[1], M. Guo[2], H.-A.J. Müller[3], Yigong Shi[4], S.J. Yoo[5]
Research Staff: Jean Edens, Lorian Churchill, Ian Foe, Haixia Huang, Hyun Hee Kim
[1]*Kansas State University*
[2]*Department of Neurology, UCLA*
[3]*Heinrich-Heine Universitat, Düsseldorf, Germany*
[4]*Princeton University*
[5]*Kyung Hee University, Seoul, Korea*

Summary: We are interested in how cell fate choice is regulated and carried out. For further information on Hay lab research consult our web page (http://www.its.caltech.edu/~haylab/). A large focus of our work is directed towards understanding the genetic and molecular mechanisms that regulate and bring about cell death. Specifically, we are using *Drosophila melanogaster* as a model system to identify genes that function to regulate cell death, and to identify important roles that cell death plays in normal development. Important cellular regulatory pathways are evolutionarily conserved; thus, molecules identified as important regulators of cell death in *Drosophila* are likely to have homologs in vertebrates and the pathways that link these molecules are likely to be regulated similarly. A second set of goals is to take the molecules and pathways uncovered in *Drosophila* and apply this information to the study of cell death in vertebrates, with the ultimate goal of determining the role that aberrations in this process play in human pathologies. In this context we see *Drosophila* as a powerful tool for uncovering conserved components and modes of death regulation.

339.   **Yeast-and fly-based screens for proteases that can cleave in a transmembrane environment**
Ming Guo, Bruce A. Hay

Alzheimer's disease is genetically heterogeneous, but it is invariantly associated with the accumulation in the brains of affected individuals of senile plaques consisting largely of amyloid beta peptide (A-beta), which is derived by proteolytic processing from the amyloid precursor protein (APP). A large body of evidence suggests that A-beta deposition is a cause rather than a consequence of Alzheimer's disease. Thus, blocking A-beta deposition is an important therapeutic goal. APP is initially translated as a type 1 transmembrane protein, but it can be processed by different pathways. In the major pathway, alpha secretase releases the APP N-terminal ectodomain into the lumenal and extracellular space. Alpha secretase cleaves in the middle of the sequence that could give rise to the A-beta peptide, thus precluding its formation. In an alternative pathway A-beta peptides are formed through the action of beta and gamma secretases. Gamma secretase activity (which may consist of distinct proteases) cleaves in the transmembrane region of APP to generate, in conjunction with beta secretase, two major A-beta species of 40 or 42-43 residues in length, differing in the length of their C-termini. The longer forms of A-beta aggregate and are thought to seed the formation of amyloid plaques. The molecular nature of the gamma secretase(s) is unknown.

We have developed two screens to search for proteins that either are gamma secretase activity, or that regulate its activity. The first screen, diagrammed above, is a simple variant of the caspase reporter system in yeast, in which lacZ expression is the readout. We generated a form of APP in which a cleavable signal sequence lies just N-terminal to the APP beta secretase cleavage site. APP C-terminal sequences are then followed by the transcription factor LexA-B42. We are using yeast expressing this construct, as well as one of the presenilins, as a background in which to screen for proteins that show potential gamma secretase activity: cleavage-dependent reporter activation.

We have also set up a related screen in *Drosophila*, in which a similar APP fusion protein (in which the transcription factor is GAL4) is expressed in the eye in flies that carry a UAS-*rpr* construct (Guo *et al.*, 2003). In this system release of GAL4 from the membrane, as a result of gamma secretase activity, creates a cell death signal, and thus, flies with small eyes. This readout is very convenient for us because we can compare modifiers identified in GMR-*rpr* screens with those identified in GMR-APP-GAL4 screens. Those modifiers that are specific for GMR-APP-GAL4 are potentially interesting in terms of identifying genes that regulate APP cleavage. At this point we have carried out several large screen for enhancers and suppressors and have identified a modest number of interesting loci that are being pursued. Importantly, mutations that alter the levels of components of gamma secretase - presenilin and nicastrin - alter the reporter eye phenotype in the expected way. These observations give us confidence that the screen is likely to be pulling out interesting loci.

Doing a screen for modifiers of gamma secretase activity in a higher eukaryote is also important for the following reason. While gamma secretase is of course critical for cleavage of APP, it is also likely to be important for the cleavage of other transmembrane signaling proteins such as Notch. Thus, drugs targeted directly at gamma secretase may have pleiotropic effects. A genetic approach that focuses more generally on identifying modifiers of this activity may point towards new ways of modifying its activity or specificity in ways that more specifically affect APP processing.

340. **Gene activation screens for cell death regulators: MicroRNAs, small non-coding RNAs, define a new family of cell death regulator**
Chun Hong Chen

The GMREP vector contains an eye-specific promoter near one P-element end, as well as sequences sufficient for plasmid rescue of genomic DNA flanking the site of P-element insertion. When this P element inserts near the 5' end of a gene it causes the gene to be misexpressed at high levels in the developing eye (Hay *et al*., 1997). We have mobilized this P element throughout the genome and are characterizing the insertions that act as cell death regulators. We first score the lines for dominant phenotypes that may be due to increased cell death (a small eye) or decreased cell death (a large, rough eye). We then cross these insertions to lines of flies that express the cell death activators REAPER, HID or GRIM specifically in the eye (GMR-rpr, GMR-hid, or GMR-grim flies), and that thus, have small eyes. The progeny of these crosses are then scored for the ability of the GMREP insertion to alter the GMR-*rpr*-, GMR-*hid*- or GMR-*grim*-dependent small eye phenotype. These modifiers identify new cell death regulators. Genomic DNA that is likely to contain a portion of the gene being overexpressed can be quickly isolated using plasmid rescue. The *Drosophila* genome is now finished. Thus, a small sequence tag from the end of the P element serves to tell us exactly where in the genome our insertion is. Because GMREP-dependent phenotypes are primarily due to insertions near the transcription start site, and because GMREP carries the dominant eye color marker *white*, imprecise P-element excision using a genomic source of transposase or X-rays can be carried out to rapidly generate deletions that create loss-of-function phenotypes for the overexpressed gene.

We generated and screened 8,000 transposon insertions for their ability to suppress *rpr*- hid-, or *grim*-dependent cell death and identified a modest number of new loci (about ten) that specifically suppress death due to overexpression of one or the other, or all of these genes in the eye. We are in the process of characterizing some of these lines. One death suppressor encodes the large ubiquitin conjugation protein Bruce (Vernooy *et al*., 2002) (we didn't name it), while four others encode cell death-inhibiting microRNAs (Xu *et al*., 2003).

References
Guo, M., Hong, E.J., Fernandes, J., Zipursky, S.L. and Hay, B.A. (2003) *Human Mol. Genet.* **12**:2669-2678.
Hay, B.A., Maile, R. and Rubin, G.M. (1997) *Proc. Natl. Acad. Sci. USA* **94**:5195-5200.
Vernooy, S.Y., Chow, V., Su, J., Verbrugghe, K., Yang, J., Cole, S., Olson, M.R. and Hay, B.A. (2002) *Curr. Biol.* **12**:1164-1168.
Xu, P., Vernooy, S.Y., Guo, M. and Hay, B.A. (2003) *Curr. Biol.* **13**:790-795.

341. **IAPs, cell death and ubiquitination**
Jun Huh, Soon Ji Yoo, H. Arno J. Müller

DIAP1, as with many IAPs, also shows E3 ubiquitin-protein ligase activity. The function of this activity *in vivo* is unclear. One possibility is that this activity simply constitutes a mechanism for conferring a short half-life to the IAP, thus serving a proapoptotic function. Alternatively, ubiquitination of IAP-bound proapoptotic proteins may provide a prosurvival mechanism by which IAPs can catalytically remove these molecules. IAPs may also engage in substrate choice, preferentially degrading themselves when not bound to proapoptotic molecules, but degrading binding partners when the opportunity arises. In this way IAPs could serve to create, through a posttranscriptional mechanism, a relative balance between pro- and antiapoptotic proteins, at different levels of proapoptotic proteins. Finally, binding of proapoptotic proteins to DIAP1 may promote DIAP1 degradation, thereby promoting apoptosis. Over the last year we have obtained evidence for all of these activities. An important goal for the future is to understand how these diverse activities of DIAP1 are regulated in the contexts of developmental cues and environmental stresses.

References
Chai, J., Yan, N., Huh, J.R., Wu, J-W., Li, W., Hay, B.A. and Shi, Y. (2003) *Nature Struct. Biol.* **10**:892-898.
Muro, I., Hay, B.A. and Clem, R.J. (2002) *J. Biol. Chem.* **278**:4028-4034.
Olson, M.R., Holley, C.L., Yoo, S.J., Huh, J.R., Hay, B.A. and Kornbluth, S. (2003) *J. Biol. Chem.* **278**:4028-4034.
Yoo, S.J., Huh, J.R., Muro, I., Yu, H., Wang, L., Wang, S.L., Feldman, R.M.R., Clem, R.J., Müller, H.-A.J. and Hay, B.A. (2002) *Nature Cell Biol.* **4**:416-424.

342. **Identification of DIAP1-interacting proteins**
Soon Ji Yoo, Hong Yu, Jeff Copeland

DIAP1 is required for cell survival in *Drosophila*. This suggests that its activity is likely to be regulated through interactions with other proteins. Genetic screens for cell death regulators provide one approach to identifying proteins that may interact with DIAP1. However, a more direct approach to identifying proteins that regulate DIAP1 function involves identifying proteins that physically bind DIAP1 in living *Drosophila*. We are using multiply-tagged versions of DIAP1 as bait to immunoprecipitate, identify and characterize associated proteins from healthy cells, as well as from cells exposed to various death stimuli.

343. **How does *Drosophila* activate caspase-dependent cell death?**
Soon Ji Yoo, H.-A.J. Müller, Jun Huh

An important set of questions is how different cell death signals, which in many cases are initiated through distinct signal transduction pathways, converge to activate a set of common downstream effector pathways. In *Drosophila* many different death signals lead to the transcriptional activation of one or more of three genes,

reaper (*rpr*), *hid* and *grim.* The function of these genes is required for most normally occuring and induced cell death in *Drosophila*. Thus, their transcriptional activation acts as a point of death signaling convergence. One of our primary goals has been to identify mechanisms by which these different proteins activate cell death. Three important facts are known about these proteins that suggested testable mechanisms of action. These are: 1) that death induced by their expression requires caspase activity; 2) that their death-promoting activity is suppressed in a dose-dependent manner by DIAP1; and 3) that REAPER (RPR), HID and GRIM bind to DIAP1 in insect cells. These results have suggested several models of how DIAP1, caspases and RPR, HID and GRIM might interact to regulate cell death. In one model, death-activating proteins such as REAPER, HID or GRIM activate caspases through an IAP-independent pathway. This model postulates that *Drosophila* IAPs act at two different points to suppress apoptosis: by acting as a sink for death activators such as REAPER, HID or GRIM, preventing them from interacting with their normal targets, and by inhibiting the caspase activity initiated by their action. In a second model, DIAP1 is proposed to function primarily as a caspase inhibitor, and REAPER, HID and/or GRIM initiate caspase-dependent cell death by preventing IAPs from productively interacting with caspases, thereby promoting their activity, and ultimately cell death.

Susan Wang, a former graduate student, and Christine Hawkins, a former postdoc, carried out experiments in *Drosophila*, yeast and *in vitro* to test the idea that RPR, HID and GRIM promote apoptosis by blocking DIAP1's ability to inhibit caspase activity (Wang *et al*., 1999). They found that all three proteins, while nontoxic on their own, killed yeast coexpressing DCP-1 or drICE, and DIAP1, suggesting that they were blocking DIAP1's ability to function as a caspase inhibitor. They pursued the basis for this activity further with HID and found, both in yeast and *in vitro*, that proteins containing the N-terminal 37 residues of HID, which are sufficient to induce apoptosis in insect cells, suppressed DIAP1's ability to inhibit DCP-1 activity.

These results are consistent with a model in which RPR, HID and GRIM act through DIAP1 to promote death-inducing caspase activity. This model predicts that DIAP1 should be essential for cell survival, and that a loss of DIAP1 function should result in an increase in DIAP1-inhibitable caspase activity. To test this idea they carried out a second set of experiments in which we characterized the phenotype of a DIAP1 loss-of-function mutation, as well as the phenotype of a double mutant that removed DIAP1, as well as *rpr*, *hid* and *grim*. They found that the DIAP1 loss-of-function phenotype consists of an embryo-wide set of cellular changes reminiscent of apoptotic cell death, and that these were associated with the activation of DIAP1-inhibitable caspase activity. Furthermore, double mutants that remove zygotic *rpr*, *hid*, *grim*, and DIAP1 function showed phenotypes similar to those of the DIAP1 loss-of-function mutant alone (Wang *et al*., 1999).

Together, the above observations suggest that a principal function of DIAP1 is to promote cell survival by blocking caspase activity, and that at least one mechanism by which REAPER, HID and GRIM promote apoptosis is by disrupting IAP-caspase interactions. These early studies left several important questions unanswered: 1) How does RPR, HID or GRIM binding to DIAP1 suppress DIAP1's ability to inhibit caspase activity. 2) Do RPR, HID and GRIM regulate DIAP1 function through other mechanisms? Domain analysis of RPR and GRIM suggests that these proteins have apoptotic domains distinct from their N-terminal DIAP1-binding motifs. One question we are interested in is whether these other domains regulate DIAP1 through other mechanisms. 3) Finally, it is interesting to ask if there exist other proteins that function similarly to RPR, HID and GRIM. However, the yeast survival-based assay we used to show that these proteins disrupt IAP-caspase interactions provides a straightforward approach to screening for such molecules. Importantly, because such a screen is a function-based screen, and does not rely on identifying candidates based on sequence homology, we may identify proteins that disrupt IAP-caspase interactions even if they have only minimal homology to RPR, HID or GRIM.

Finally, the DIAP1 loss-of-function phenotype, the caspase-dependent death of all cells in the embryo, raises an important question? What is the source of the activity DIAP1 fights against to maintain cell survival? The generation of double mutants in cell culture using RNAi of Dronc or Ark, and DIAP1 (Muro *et al*., 2002), provides a clear answer - Ark and Dronc-dependent caspase activation. An important implication of these observations is that cells that normally live experience a chronic Ark-activating death signal. This promotes the continuous activation of Dronc. DIAP1 promotes cell survival, at least in part, by suppressing this Dronc activity. An important unsolved question is the source of the signal that activates Ark. In mammals Apaf-1 is activated by cytochrome *c*, released from mitochondria, and ATP or dATP. The role of mitochondria and cytochrome *c* release in *Drosophila* is still unclear. Exposure of apoptosis-specific cytochrome *c* epitopes has been observed by the Abrams lab, and cytochrome *c* can be found associated with a high molecular weight apoptosome-like complex in cell extracts (Dorstyn *et al*., 2002). However, depletion of cytochrome *c* in cell culture using RNAi has failed to demonstrate any involvement of this protein in Ark-dependent cell death [Zimmermann *et al*., *J. Cell Biol.* (2002) **156**:1077]. This latter observation raises the intriguing possibility that Ark activation in flies (and by implication perhaps in other organisms, as well) can be regulated through associations with other molecules. We have designed several screens and biochemical approaches to address this question.

344. **Bruce, cell death, caspases and spermatogenesis**
Jun Huh

As mentioned above, one of the potent cell death suppressors we identified is the Bruce gene. Bruce mutants are viable, but they are male sterile. In examining this we discovered several interesting facts: 1) Bruce mutants are blocked in a late aspect of spermatogenesis known as individualization, in which spermatids (which develop in a common cytoplasm) eventually become enclosed in individual plasma membranes; 2) During the process of individualization spermatids have very high levels of active caspases. But these cells do not die. Together these observations suggest that spermatids use caspase activity for nonapoptotic purposes, during differentiation. We have found that multiple caspases, acting through distinct pathways, acting at distinct points in time and space, are required for spermatid individualization (Huh *et al.*, 2004a). Spermatid individualization is an evolutionarily conserved process, about which little is known. Several questions are of interest to us: 1) What are the sources of the caspase activity (what are the upstream signals); 2) What are the nonapoptotic targets that facilitate differentiation; and 3) How is cell death prevented in the face of high levels of caspase activity that would normally be associated with cell death; 4) Do caspases play similar roles in promoting spermatid differentiation in mammals?

Reference

Huh, J.R., Vernooy, S.Y., Yu, H., Yan, N., Shi, Y., Guo, M. and Hay, B.A. (2004) *PLOS Biol.* **2**:43-53.

345. **Maintaining tissue size: The role of death-induced compensatory proliferation**
Jun Huh

Achieving proper organ size requires a balance between proliferation and cell death. Tissues often experience stresses that lead to ectopic death. In order for normal development to occur, this death must be followed by compensatory proliferation that fills in the gaps. We were interested in exploring the idea that it is the dying cell itself that sends a signal to neighbors, driving their proliferation. We tested this hypothesis in several ways. In brief, we found that activation of the apical caspase Dronc, activity of which is required for many cell deaths in the fly, is both necessary and sufficient to drive compensatory proliferation in neighboring cells (Huh *et al.*, 2004b). Interesting questions for the future include: 1) What are the target Dronc acts on to promote proliferation in neighbors; and 2) Are there other contexts in which caspases function in a sense non-autonomously to alter cell fate or behavior?

Reference

Huh, J.R., Guo, M. and Hay, B.A. (2004) *Curr. Biol.* **14**:1262-1266.

346. **Autophagic cell death, caspase inhibition in *C. elegans*, and the *echinus* mutant**
Jeffrey Copeland

While much cell death is apoptotic, a number of cell deaths share features with a process known as autophagy, which has been described in some molecular detail in yeast. In yeast, starvation leads to a cellular response in which double membrane bound vesicles are formed that take up and hydrolyze organelles as well as bulk cytoplasm. This process of autodigestion provides the cell with nutrients, allowing survival under starvation conditions. It has been clear for some time that there are a number of situations in which cell death in animals shows morphological features similar to those of autophagy rather than apoptosis. However, the molecular mechanisms that mediate these deaths have remained unexplored. *Drosophila* homologs are available for many of the yeast proteins involved in autophagy. The goal of my project is to explore the molecular mechanisms underlying autophagic cell death in *Drosophila*.

In *C. elegans*, in contrast to the situation in flies and mammals, caspase inhibitors have not been identified. I used the yeast screens described above to identify several potential *C. elegans* caspase inhibitors. One of these is highly evolutionarily conserved. We are currently focusing our characterization on the *Drosophila* counterpart of this gene.

Echinus is a *Drosophila* mutant that lacks normally occurring cell death in the eye. I have generated multiple new alleles of *echinus* and cloned the gene. Characterization of its activities is in progress.

Publications

Hay, B.A., Huh, J.R. and Guo, M. (2004) The genetics of cell death: Approaches, insights and opportunities in *Drosophila*. *Nature Rev. Genet.* **5**:911-922.

Huh, J.R., Vernooy, S.Y., Yu, H., Yan, N., Shi, Y., Guo, M. and Hay, B.A. (2004a) Multiple apoptotic caspases are required in nonapoptotic roles for *Drosophila* spermatid individualization. *PLOS Biol.* **2**:43-53.

Huh, J.R., Guo, M. and Hay, B.A. (2004b) Compensatory proliferation induced by cell death in the *Drosophila* wing disc requires activity of the apical cell death caspase Dronc in a nonapoptotic role. *Curr. Biol.* **14**:1262-1266.

Xu, P., Guo, M. and Hay, B.A. (2004) MicroRNAs and the regulation of cell death. *Trends Genet.* **20**:618-624.

218

George W. Beadle Professor of Biology: Elliot M. Meyerowitz
Senior Research Associate: Jose Luis Riechmann
Senior Research Fellows: Venugopala Gonehal, Toshiro Ito, Frank Wellmer
Postdoctoral Scholars: Vikas Agrawal, Pradeep Das, Annick Dubois, Elizabeth Haswell, Marcus Heisler, Nicole Kubat, Zachary Nimchuk, Xiang Qu, Adrienne Roeder, Patrick Sieber
Visiting Associates: Marcio Alves Ferreira, James P. Folsom
Graduate Students: Sean Gordon, Louisa Liberman
Undergraduate Students: Olivia Alley, Yijia Chen, David McKinney, Ransom Poythress
Volunteers: Robert Lim, Antha Mack
Research and Laboratory Staff: Arnavaz Garda, Carolyn Ohno, Maral B. Robinson

Summary: We are trying to understand how plants grow, with special attention to the shoot apical meristem, the collection of stem cells that produces stems, leaves, and flowers, and to the growth of flowers. In addition to the methods of developmental genetics that we have used for years, in which we study the effect of changing the function of genes that play important roles in shoot and flower development, we are using some newer technology to reveal new processes and mechanisms. One of these is global gene expression analysis with microarrays, which are allowing us to see in detail the changes in gene expression and gene regulation that accompany different stages of development, and that are caused by activation or inactivation of specific regulatory genes. Another is a new set of applications of laser scanning confocal microscopy, that allow is to see every cell in a growing meristem, or in an early developing flower, and follow not only the rates and patterns of cell division, but also the expression of individual genes and even individual proteins in real time. One example of the use of this method, described below, is the assessment of the movement of the plant growth regulator auxin in a growing shoot apical meristem, by following the subcellular localization of a protein that serves as an auxin efflux facilitator. This protein aligns on one side of cells, indicating the direction in which auxin is being moved. The alignment of the protein changes rapidly during the formation of new floral primordia, and these changes can be followed with the new imaging methods. This has allowed a model of auxin circulation in
the meristem, that explains the pattern in which new floral primordia appear, and may also offer an explanation for the origin some of the patterns of gene expression in early developing flowers. Additional examples of the value of the new imaging and gene expression analysis methods in the study of meristem growth, of meristem formation, of early flower development, and in the control of chloroplast size and shape, are given below.

347.   Regulation of *JAGGED* transcription in plant lateral organs
Carolyn Ohno

In plants, lateral organs develop as outgrowths from the flanks of the shoot apical meristem as either leaves or floral organs. The *Arabidopsis* C2H2 zinc-finger gene *JAGGED(JAG)* is specifically expressed in all lateral organs where it has been shown by loss-of-function mutant analyses to have a function in the processes of organ growth and morphogenesis. In order to understand how *JAG* expression is initiated in developing lateral organ primordia, transcriptional regulation of the *JAG* gene was investigated. A region of 5'-regulatory sequence upstream of the *JAG* start codon was chosen for analysis since previously this genomic sequence had been shown to be sufficient to complement the *jag* mutant phenotype when fused to *JAG* cDNA sequence. Analysis of this region of the *JAG* promoter fused to a GFP-GUS reporter gene has so far revealed the presence of leaf-specific positive regulatory elements, as well as sepal-, petal-, stamen- and carpel-specific positive regulatory elements. Finer mapping of these regulatory elements is currently being investigated, as well as analysis of the *pJAG::GFP-GUS* lines in various mutant genotypes.

348.   *In vivo* imaging of floral organ identity gene expression
Carolyn Ohno, Marcus Heisler

Flower development in *Arabidopsis* involves the development of four different floral organ types from the floral meristem. We are imaging gene expression patterns in living inflorescences by confocal microscopy to understand this highly dynamic process involving both coordinated cell proliferation and differentiation. Floral organs are arranged in four concentric rings or whorls and floral organ identity (sepal, petal, stamen or carpel) is specified by individual or combinations of the organ identity genes and their whorl-specific expression patterns according to a simple ABC model for floral organ identity (E.S. Coen and E. Meyerowitz, 1991). We would like to understand how the temporal and spatial expression of these genes is regulated to set up the pattern of the four whorls within the floral primordium. In order to study the dynamic expression patterns of organ identity genes (e.g., AP1, AP3, PI, AG, SEP), we have generated plants expressing promoter fusions or translational fusions to multi-colored GFP variant reporter genes so that we can monitor the expression patterns of these proteins simultaneously in living plants. Multimers of floral MADS box proteins have been proposed to function in

transcription factor complexes as a result of *in vitro* experiments (T. Honma and K. Goto, 2001) and we are attempting to detect these interactions in our *in vivo* analysis. Protein co-expression studies will also uncover regulation of patterning that is at either the transcriptional or post-transcriptional level. Lastly, we are combining these reporters in various mutant genotypes in order to better understand the regulatory interactions that are responsible for the initiation and maintenance of organ identity gene expression in the floral whorls.

349. **Control of cell division, cell expansion, and cell fate downstream of the floral homeotic genes in the *Arabidopsis* sepal**
Adrienne Roeder, Elliot M. Meyerowitz

During development cell division, cell growth, and cell fate are precisely regulated to achieve the formation of complex organs. While it is well established that homeotic genes control the specification of organ identity, little is know about how they regulate these downstream processes that truly produce the organ. The interplay between the homeotic genes and development on the cellular level can be studied in the sepal of the *Arabidopsis* flower where sepal identity is specified by the homeotic genes *APETALA1* (*AP1*) and *APETALA2* (*AP2*). The outer sepal epidermis is characterized by the formation of extremely enlarged giant cells interspersed within a field of moderately-sized epidermal cells and stomata. How is cell expansion and division controlled to produce the giant cells and how does this process relate to sepal identity? We plan to characterize the development of the outer sepal epidermis in living plants to determine how these enlarged cells are generated. In addition, we are conducting a mutant screen to identify factors involved in the development of the giant cells. Already one mutant has been isolated in which giant cell development is affected and this mutant is being further characterized. We are also interested in detecting differences in gene expression between the giant cells and the neighboring epidermal cells and we have isolated a molecular marker that appears to be expressed in the moderately-sized sepal epidermal cells, but excluded from the giant cells. Eventually we hope to link our new understanding of giant cell development to regulation by *AP1* and *AP2*, the homeotic genes controlling sepal formation.

350. **Analysis of temporal gene expression during early flower development**
Frank Wellmer, Elliot M. Meyerowitz

Known floral regulators are often expressed in a dynamic fashion, i.e., they are expressed only in certain regions of the flower or during certain developmental stages. A possible strategy for identifying novel genes involved in flower development is therefore to analyze gene expression on a genome-wide scale and to identify genes with organ or stage-specific expression. We initially applied global expression profiling using whole-genome DNA microarrays for a detailed analysis of spatial gene expression during flower development by comparing the gene expression profiles of inflorescences of wild-type plants to those of the floral homeotic mutants lacking different types of floral organs. By combining the data sets from these experiments, we were able to identify genes expressed specifically (or predominantly) in distinct floral organs (1). For the analysis of temporal gene expression during flower development, we developed a floral induction system based on the specific activation of the floral meristem identity factor APETALA1 (AP1) in an *ap1 cauliflower* (*cal*) double mutant. In *ap1 cal* plants, flower formation is delayed leading to a massive accumulation of meristems at the shoot apex. The specific activation of AP1 in this background causes the transition of these meristems to floral primordia, which subsequently develop in a synchronized manner. Thus, hundreds of same-stage floral buds can be collected from a single plant. We used this system to analyze temporal gene expression during early flower development and identified groups of genes with distinct expression patterns during different developmental stages. These genes can now serve as marker genes for early flower development. In addition, we found a significant enrichment of genes encoding sequence-related transcription factors within these groups. These genes are good candidates for novel floral regulators that might control flower development in a functionally redundant manner. We are currently characterizing these genes using a wide array of molecular approaches.

Reference
(1) Wellmer, F., Riechmann, J.L., Alves-Ferreira, M. and Meyerowitz, E.M. (2004) *Plant Cell* **16**:1314-1326.

351. **Developmental timing of the homeotic protein AGAMOUS during stamen development**
Toshiro Ito, Hao Yu*

The floral homeotic selector gene *AGAMOUS* (*AG*), together with other members of the same class of floral homeotic genes, is sufficient to trigger reproductive organ (stamen and carpel) development. Although *AG* is the most studied example of a floral homeotic gene, the mechanisms by which the floral organ primordia of whorls three and four respond to the genetic activities initiated by AG, and thereby differentiate into stamens and carpels, are largely unknown.

By performing a series of timed-induction experiments using a transgenic line with an inducible AG activity, we showed that prolonged AG activity, which extends 8-9 days from stage 3 floral buds, is necessary to produce the normal stamens of *Arabidopsis*. We then carefully followed the dynamic phenotypic changes after the DEX induction to examine the timing of AG activity during stamen development. Nine days after the start of DEX treatments, the first dehisced anthers were observed in the inner whorls of indeterminate flowers. This suggests that a minimum of nine days is necessary for the primordia to develop into stamens with dehisced anthers. In these flowers with normal-looking stamens in inner whorls, the 2nd and 3rd whorl organs, which were produced earlier than inner organs, showed morphologically stamenoid (stalked)

petals. The stamenoid petals were white and did not show the trait of microsporogenesis, suggesting that the 2nd whorl organ is already determined to differentiate into petals at that stage (~stage 7) and cannot be re-specified into stamens by the ectopic AG activity. At the same time, AG targets for filament formation can be induced in later stages of developing petals. Our results show that AG controls various different target genes depending on the stages of floral primordia throughout flower development.

Dept. Biol. Sci., Natl. Univ. Singapore, Science Drive 4, Singapore 117543

352. Late-stage functions of the homeotic protein AGAMOUS during stamen development
Toshiro Ito

By performing a series of timed-induction experiments using a transgenic line with inducible AG activity, we showed that prolonged AG activity is necessary to produce normal stamens of *Arabidopsis*. Insufficient duration of AG activity results in stamens with short filaments and indehiscent anthers, which are commonly observed phenotypes in jasmonic acid (JA)-deficient mutants. Therefore, we tested the expression of genes involved in JA biosynthesis and signaling pathways to see whether they show AG-dependent expression during stamen development. We treated *ag-1 35S::AG-GR* plants three or four times with DEX in 24 hour intervals and harvested the inflorescences 5, 6, 7, 8, 9 and 10 days after the initial DEX treatment. Three DEX treatments resulted in indehiscent anthers after 12 days, but four DEX treatments are sufficient to induce normal stamens. We found that the expression of the gene encoding the catalytic enzyme mediating the initial step of JA biosynthesis, *DEFECTIVE ANTHER DEHISCENCE1 (DAD1) (*Ishiguro *et al.*, 2001) shows AG-dependent expression at later stages. *DAD1* shows similar level of basal-level expression in differently treated samples at day 5 and 6 samples, but at day 7 it started to show stronger expression in plants treated four times with DEX, and continuously shows stronger expression in samples treated four times with DEX than three times at later time points.

We also found that exogenous application of JA to the flower with short filaments and indehiscent anthers could rescue these stamen phenotypes resulting from the three DEX treatments. Furthermore, we showed that the catalytic product of DAD1, linolenic acid, is sufficient to rescue the mutant phenotypes. These results indicate that the late-stage function of AG during stamen development is to induce JA biosynthesis via activating the *DAD1* gene. The genomic region of *DAD1* contains two putative binding sites of AG. We are currently testing the effect of mutations in these putative binding sites to examine if AG directly binds to these sites.

Reference
Ishiguro, S., Kawai-Oda, A., Ueda, J. *et al.* (2001) *Plant Cell* **13**:2191-2209.

353. Chromatin immunoprecipitation using floral buds
Toshiro Ito, Nicole J. Kubat

For our analysis of the transcriptional network during reproductive organ development, it is important to distinguish between direct interactions and secondary downstream effects. We have been trying to establish the chromatin immunoprecipitation (ChIP) technique to analyze the *in vivo* binding sites of a transcription factor. Although this method has been successfully applied to single celled eukaryotes and cultured mammalian cells, it has technical limitations in sensitivity in a multicellular organism with a relatively large genome size. We generated transgenic plants in which fusion proteins of GR-epitope (the rat glucocorticoid receptor steroid-binding domain fused to the epitope tags HA or c-myc) with AG, SEP3, AP3 or PI, are ectopically expressed in developing flowers. Then we started using *ag-1 35S::AG-myc* plants that showed DEX-dependent rescued phenotypes to examine the AG-binding sites. In order to optimize the experimental conditions of ChIP, we took two independent approaches. Firstly, we examined the amount of the AG-GR-myc fusion protein at every step of the ChIP procedure. Based on the amount of the protein in washed and maintained fractions, we assessed the conditions for chromatin purification, immunoprecipitation and elution of the protein-DNA complex. Secondly, we used anti-acetyl histone antibody (Upstate), as well as the AG fusion protein-specific antibody because acetylated-histone H3 is widely observed in active promoter regions and the binding to DNA is robust. We optimized each experimental condition based on the enrichment rate of highly transcribed phosphofructose kinase (*PFK*) compared to transcription of a Mu-like transposon. By optimizing chromatin purification, amount of antibody, and washing conditions, we could increase the enrichment rate of the *PFK* positive control more than ten fold. We also showed that AG fusion protein can be efficiently immunoprecipitated from the inflorescence samples by Western blot.

354. Dynamic changes in AGAMOUS binding to a target promoter during flower development
*Toshiro Ito, Ransom Poythress**

In order to examine the nature of AG as a transcription factor during reproductive organ development, we tested for AG binding *in vivo* to various target promoters by the chromatin immunoprecipitation method. We used *ap1 cal1 35S::AP1-GR* plants in which floral stages can be synchronized at relatively early stages (see Wellmer *et al.*, abstract 350). Our study showed that the floral homeotic genes *AP1* and *AP3* had clear enrichment after chromatin immunoprecipitation.

AP1 is an A-class gene, which is negatively regulated by AG. Our microarray analysis using *ag-1 35S::AG-GR* showed quick down-regulation of *AP1* transcripts. Although we tried using several different samples collected at varying times post-DEX treatment, *AP1* enrichment seemed fairly widespread in a 1 kb region

around the transcription start site. The one primer set showed that relatively higher enrichment is not located near either of the CArG box sequences (*in vitro* determined binding site of AG). This suggests that AG may directly inhibit the transcription of *AP1* by binding to the *AP1* promoter region through unknown DNA-binding proteins.

AP3, on the other hand, showed robust and localized binding results. Using a wide array of primer sets covering the promoter region, we were able to localize the site of enrichment down to an approximately 200 bp region that contained three CArG box sequences. Then, using some of the overlapping and more precise primer sets, we found that primer sets spanning the CArG box 3 (CArG3) show the highest enrichment, suggesting that AG binds CArG3. To examine dynamic changes of AG binding during flower development, we harvested the inflorescence samples 2, 3, 4, 5 and 6 days after DEX treatments. Day three and four samples averaged about 15-fold enrichment in the target site and day five samples (stage 6) reached almost 40-fold enrichment. This result shows that AG binding changes throughout the course of development.

Undergraduate, Caltech

355. Dissecting the role of APETALA1 in flower development
Annick Dubois, Frank Wellmer, Elliot M. Meyerowitz

APETALA1 (AP1), a MADS-box transcription factor, is a key regulator of flower development in *Arabidopsis* and is involved in the establishment of floral meristem identity, as well in the specification of sepals and petals. In spite of the genetically well-characterized role of AP1 in flower development, the genes that are regulated by this transcription factor remain elusive. In order to identify the full complement of AP1 response genes we have monitored gene expression in the inflorescence meristems using whole-genome microarrays of *ap1 cauliflower* double mutants after a specific activation of the factor. A detailed time-course experiment, in which we followed gene expression changes over 24 hours after AP1 activation, allowed us to identify groups of genes that have distinct expression profiles. While early response genes are good candidates for AP1 target genes, genes whose expression changes with a significant delay are more likely to be downstream of the primary events. Among the genes identified in this experiment, we found several that had been previously linked to AP1 by genetic analysis, as well as a strong enrichment for genes encoding transcription factors. The latter result suggests that the main function of AP1 might be to control the activity of other transcriptional regulators that then direct the developmental programs required for flower formation. Additional experiments, in which the effects of AP1 activation on gene expression were monitored in the presence of the potent translational inhibitor cycloheximide, suggest that some of these genes might be directly regulated by the factor. To test whether the promoters of these genes are indeed bound by AP1 we are currently preparing transgenic lines that should allow us to do chromatin immunoprecipitation experiments. In addition, we are screening for common sequence motifs in the promoters of the putative target genes that might mediate AP1 binding.

356. The role of *PERIANTHIA* in floral organ number patterning
Pradeep Das

While much is known about the processes that lead to the establishment of floral meristem identity and floral organ development, others, such as organ number specification, remain largely unexplored. *PERIANTHIA* (*PAN*) is one of the few genes thought to have a specific role in this process, with mutations in the gene affecting floral organ number without a coincident change in floral meristem size. While wild-type *Arabidopsis* flowers have four sepals, four petals, six stamens and two carpels, flowers of *pan* mutant plants mostly have five sepals, five petals, five stamens and two carpels. To determine how PAN impacts organ number patterning, we are following several lines of investigation, such as microarray analyses to identify downstream targets of PAN and misexpression studies to explore its mechanism of action.

We are carrying out two types of whole-genome microarray analyses. Firstly, we are comparing the expression profiles of *pan* mutants to wild-type floral buds of stages 1 to 5, when the earliest organ primordia are being laid down. Secondly, we are using a dexamethasone-inducible PAN.GR fusion construct to determine the expression profiles of inflorescences 0, 4 or 8 hours after activation with dex. We expect to find both direct and indirect targets of PAN. Comparisons of the data sets between the two approaches, phylogenetic and promoter analyses, followed by expression profiling will be used to narrow the field of candidate genes. Knockout, knockdown and overexpression experiments on this subset of genes should shed some light on the processes downstream of PAN.

In a separate effort, we are using directed expression studies to determine the minimum domain of activity required for PAN to fulfill its normal functions in floral development. We have placed *PAN* under the control of heterologous promoters with specific expression patterns, introduced them into *pan-2* mutants and assayed their ability to rescue the *pan* phenotype. In primary transformants expressing *PAN* in the L1 layer, about 50% of flowers and 20% of the plants are completely rescued. Near-complete rescue is also observed when the endogenous *PAN* promoter or a ubiquitously-expressing promoter is used, but not with other promoters with restricted expression domains, suggesting that PAN activity is required throughout the flower.

In addition, we are designing additive or subtractive three-component systems to achieve whorl-specific clones of wild-type or mutant *PAN* in the inverse background. Such clones of cells will help further narrow the requirement for PAN activity and provide a

way to explore aspects of primordium initiation, such as the influence of organ number in one whorl on organ number in an adjacent whorl.

357.   Identifying genetic partners of *PAN*
Pradeep Das, Antha Mack

Wild-type *Arabidopsis* flowers have four sepals, four petals, six stamens and two fused carpels. In mutants of the *PERIANTHIA* (*PAN*) gene, the number of floral organs changes to five sepals, five petals and six stamens. In addition, the carpels are frequently slightly unfused. Mutants of *PAN*, which encodes a bZIP transcription factor, are also early-flowering and occasionally bear secondary flowers in the axils of first whorl organs, both of which are enhanced when the plants are grown under short days. Little is known about the mechanism by which organ number is determined or about the precise roles of PAN: the developmental pathways it might impact or the processes it might help shape.

The phenotype of *pan* mutants is both incompletely penetrant (a number of flowers are morphologically wild type), as well as variable (some flowers may have six to seven sepals or petals), suggesting that *PAN* may function redundantly with other genes, possibly some that share sequence homology with it. In addition, *PAN* reporter constructs reveal a much broader expression domain than the flower, such as in the entire dome of the vegetative and inflorescence meristems, in the quiescent center of the root and in the proximal adaxial regions of rosette leaves. However, *pan* mutants do not display phenotypes in any of these tissues, again possibly suggesting a degree of genetic redundancy. BLAST searches reveal three genes with over 65% identity to PAN, but knockout lines for these genes are not publicly available. We are currently testing knockdown and dominant-negative lines to determine whether these homologs share roles with PAN in the non-floral tissues mentioned above.

A less biased approach to elucidating the role of PAN in flower development is by performing genetic modifier screens for second site mutations that enhance or suppress the *pan* phenotype. Thus far, we have screened approximately 1000 independent EMS-induced M2 families and identified 26 enhancers but no suppressors of the *pan-3* allele. These include mutants that either are or resemble known loci such as *leafy*, *apetala2* and *unusual floral organs*. In addition, we have identified some loci with novel double-mutant phenotypes that we are actively characterizing.

One of these lines, designated E1P3-159, is a dramatic enhancer of *pan-3* petal number defects, with flowers in the M2 lines bearing four sepals, six stamens and up to 12 petals. However, flowers of outcrossed F2 plants bear one to three petals and four stamens. Non-complementation tests and gene sequencing have helped rule out some candidate mutants, and we are currently in the process of genetically mapping the locus with the aim of cloning it molecularly. We are also characterizing its

phenotypes in greater detail and determining its genetic interactions with other loci involved in floral development.

358.   Global expression profiling applied to the analysis of *Arabidopsis* stamen development
Marcio Alves Ferreira, Frank Wellmer, Elliot. M. Meyerowitz

In spite of rapid advances in the understanding of development, much remains to be learned about the mechanisms underlying cell specification and about the genes involved in this important process. Stamen development represents a good system for studying cellular differentiation in plants, as stamens are relatively complex organs, which are composed of many different cell types. Global gene expression profiling can be used to identify genes that play important roles in development, but to date these analyses have generally been conducted using whole organs, such as leaves, roots or flowers, but not individual cell types. Thus, detailed information on cell type-specific gene expression is currently lacking. Furthermore, only a few studies have been conducted in which temporal gene expression during plant development was analyzed.

To understand the development of stamens in more detail and to identify genes that are involved in cell-type specification, we compared the gene expression profiles of mutants with defects in stamen development to that of wild-type plants by whole-genome microarray analysis. In the first of these experiments, the gene expression profiles of floral buds of wild-type plants, corresponding to stages one to nine, were compared to that of *apetala3-3* mutant flowers, which completely lack stamens. In the second experiment, the gene expression profiles of wild-type inflorescences were compared to that of the mutant *male-sterile1* (*ms1*), whose phenotypic defects are limited to the tapetum and to microspores during late stamen development. The combination of the data sets obtained in these experiments allowed us to identify groups of genes that are predicted to be expressed either during early stamen development, or during late stages of stamen development specifically in the tapetum and in pollen, as well as genes that are repressed by *MS1*. Furthermore, the combination of these data sets with that of experiments, in which floral organ-specific expression was studied on a genome-wide level (Wellmer *et al.*, 2004), allowed us to generate a gene expression map for stamen development. We have used real-time PCR and *in situ* hybridizations to validate our predictions. Our analysis revealed interesting spatial patterns of gene expression during early connective, filament, tapetum and microspore development. We have also characterized the expression of ten genes encoding putative transcription factors that might be involved in the regulation of stamen development. Reverse genetics analysis for one of these genes (encoding a tapetum-specific HMGA-type transcription factor) showed that it is important for normal tapetum and pollen development.

359. Rapid identification of cell differentiation markers using advanced two-component enhancer-trapping systems

Pradeep Das, Patrick Sieber

Enhancer-trap screens, where regulatory control elements are captured using random genomic insertions of a reporter, have two important uses in developmental biology. The first is the use of the trapped enhancers as markers for differentiated tissue types in the characterization of unrelated genes, and the second is the direct study of the role of the trapped locus in the morphogenesis of that tissue. Our interest, therefore, lies in visualizing individual gene activity in such a manner as to follow gene expression in the *in vivo* spatio-temporal context of a developing tissue. This will allow us to gather in-depth molecular information about a particular developmental transition and might ultimately allow us to identify the signal that triggers such a developmental program in different tissues of the shoot and flower.

Many tissue markers currently used in *Arabidopsis* have been derived through forward genetics, which can be difficult, especially for complex promoters. Enhancer-trap screens provide a good alternative to identifying specific expression patterns. Although several enhancer-trap screens have been performed in *Arabidopsis*, the number of reporters that have been characterized from such screens in the shoot and flowers is limited for several reasons. Most *Arabidopsis* enhancer-trap screens have made use of the β-glucuronidase enzyme as the reporter, making the screen itself labor-intensive and incompatible with *in vivo* live imaging of the marked tissue. Published screens making use of green florescent protein (GFP) as a reporter have focused on the root, where the tissue is clear and the GFP easy to see.

We have generated two enhancer-trap vectors based on a two-component approach. Both vectors make use of the chimeric transcriptional activator LhG4 placed under the control of a minimal promoter immediately adjacent to the right border of the transferred DNA element. In those instances where LhG4 expression is triggered by neighboring promoter or enhancer elements, it will then drive the expression of a very bright multimerized variant of the yellow fluorescent protein that is easily visible under a dissecting microscope. In the second vector, we have translationally fused LhG4 to the glucocorticoid receptor (GR), allowing dexamethasone-dependent activation of the GR-LhG4 protein.

One of the advantages of the two-component systems means that trapped enhancers may be immediately used to drive the expression, either inducibly or constitutively, of unrelated genes of interest in the marked tissues. Our pilot screen has shown the systems to be working as expected, yielding specific expression patterns in about 10% of transgenic lines.

360. Members of the *MIR164* microRNA family are redundantly required in *Arabidopsis* meristems to ensure developmental homeostasis

Patrick Sieber, Elliot M. Meyerowitz

MicroRNAs (miRNAs) are small ~21 nucleotide non-protein-coding RNAs, which negatively regulate expression of genes in many organisms ranging from plants to humans. The *early extra petals1 (eep1)* mutant of *Arabidopsis* represents a loss-of-function allele of the miRNA *MIR164c*. As one of three members of the *MIR164* family, miR164c provides most if not all of the negative regulation for the transcription factors CUP-SHAPED COTYLEDON1 (CUC1) and CUC2 in order to prevent extra petals in early flowers. We have isolated putative null alleles for *MIR164a* and *MIR164b*. Homozygous *mir164a*, as well as *mir164b* single mutant plants resemble the wild type, respectively. In order to reveal potential redundant functions among the three miR164 miRNAs we generated a plant triply mutant for *mir164a, mir164b and mir164c* (henceforth referred to as *mir164abc*). *mir164abc* triple mutants form flowers with a strong carpel fusion defect, and a variable number of floral organs. This phenotype persists in later flowers. *mir164abc* plants also show a highly distorted arrangement of flowers along the axis of the stem both with respect to phyllotaxy and internode length. The *mir164abc* phenotype also shows full expressivity with the allelic combination *mir164aa bB cc*, revealing a threshold level for miR164b action in a background that is compromised for miR164 function. *CUC1* and *CUC2* transcript levels are higher but remain restricted to organ boundaries in *mir164abc* mutants when compared to the wild type. Furthermore, both *CUC* promoters are sufficient to drive expression of a reporter gene in organ boundaries and boundary cell-specific CUC protein accumulation was also observed in transgenic plants expressing miRNA-resistant versions of CUC1 and CUC2. These results indicate that miR164 miRNAs are not necessary to create the boundary-specific expression pattern of the *CUC* genes. Rather miR164 miRNAs seem to refine the expression patterns created by the CUC promoters by reducing the transcript levels of their targets. This idea is also supported by the fact that *MIR164b* and *MIR164c* are frequently co-expressed with their targets *CUC1* and *CUC2*. *MIR164b*, as well as *MIR164c*, have in common that their expression is restricted to the epidermal cell layer but their expression domains overlap only in a subset of their overall expression domains. Our results indicate that individual mir164 miRNAs might have evolved by recruiting individual *cis*-acting elements.

224

361. Identification of genes that regulate the organ primordium positioning, primordium formation and primordial separation from meristems

Patrick Sieber, Frank Wellmer, Marcus Heisler, Carolyn Ohno, Pradeep Das, Elliot M. Meyerowitz

Plant organs are generated post-embryonically and continuously from areas of growth, called meristems. Flowers and leaves grow from the periphery of apical meristems in a highly systematic pattern creating an arrangement of organs on the stem, which is referred to as phyllotaxy. *Arabidopsis* inflorescence meristems form flowers in a spiral phyllotaxy while the floral meristems produce a constant number of floral organs that are arranged in four whorls. In *mir164abc* mutants, which are severely compromised for miR164 miRNA function, the normal phyllotaxy is distorted and the number of floral organs is variable. Scanning electron microscopic analysis indicates that the initiation of the flowers is normal in *mir164abc* mutants but cells fail to elongate between clustered flowers. The miR164 miRNAs negatively regulate the expression of the two closely related transcriptional regulators CUP-SHAPED COTYLEDONS 1 and 2 (CUC1 & CUC2). Our results indicate that the *mir164abc* phenotype is mostly a consequence of combined de-repressed *CUC1* and *CUC2* transcript levels. We hypothesize that elevated levels of *CUC1* and *CUC2* might suppress cell elongation and possibly cell division between neighboring primordia, thus arbitrarily locking primordia together while the stem continues to grow. To test this hypothesis and to separate cause from effect with respect to the *mir164abc* phenotype we first aim to get a better idea of the dynamics underlying organ formation in *mir164abc* mutants. Thus far we have established combinations of reporter lines in the *mir164abc* mutant background and in the wild type. Such transgenic plants will enable us to follow the dynamic changes of gene expression patterns by using confocal microscopy and to relate these patterns to primordial and boundary-specific marker gene expression, as well as to growth. Second, in order to identify genes that are regulated directly by CUC1 and CUC2 we have initiated a set of microarray experiments in some of which the transcriptional regulators CUC1 and CUC2 are activated through the use of protein fusions with the glucocorticoid receptor. Understanding the mechanism that causes the mutant phenotype will be informative and ultimately will further our knowledge of organ formation in wild-type plants.

362. Creating post-transcriptional switches from various steroid receptors

*Toshiro Ito, Robert Lim**

In order to examine the downstream activities of floral transcription factors, one established approach is to make transgenic plants for fusion proteins between a transcription factor and the ligand-binding domain (LBD) of the mammalian glucocorticoid receptor (GR), which behaves as a post-translational switch inducible by dexamethasone.

Floral organ identities are controlled by the combinatorial action of four classes of MADS domain transcription factors. In order to characterize the downstream activities of these floral homeotic proteins, we aimed to create switches that are independently controllable by various steroid hormones. In mammalian systems, fusion proteins with GFP and the ligand-binding domain of androgen or estradiol receptors were shown to be localized in nuclei in a ligand-dependent manner. In contrast, the retinoic acid receptor is always localized in the nucleus even without the ligand, but the fusion protein with a chimeric ligand-binding domain (LBD) of the glucocorticoid receptor and the retinoic acid receptor showed retinoic acid-dependent nuclear localization (Mackem *et al.*, 2001). We obtained plasmid constructs that contain cDNA clones encoding androgen receptor, estradiol receptor and modified retinoic acid receptor. We cloned the LBD-coding regions of these various steroid receptors in plant transformation vector (pGreen) with a GFP reporter gene driven under the constitutive 35S promoter. We plan to assay the activities of these constructs by particle bombardment to leek cells. We will test the localization of the fusion proteins with and without the steroid hormones and their specificity, to evaluate the independent post-translational switches.

*UCLA volunteer student

Reference

Mackem, S., Baumann, C.T. and Hager, G.L. (2001) *J. Biol. Chem.* **276**:45501-45504.

363. Auxin transport patterns and primordium differentiation

Marcus G. Heisler, Carolyn Ohno, Pradeep Das, Patrick Sieber, Gonehal V. Reddy, Jeff A. Long, Elliot M. Meyerowitz

By monitoring the expression and polarity of PINFORMED1 (PIN1), the auxin efflux facilitator, and the expression of the auxin responsive reporter DR5, we have found that within floral anlagen there is a cycle of auxin build-up followed by decrease, correlated with, and likely caused by, a rapid reversal in PIN1 polarity in cells located adaxial to the primordium. Imaging of CUC2-YFP and STM-YFP fusion proteins in combination with PIN1-GFP also shows that the observed auxin distribution dynamics correlate with the specification of primordial boundary domains. We find that both pSTM::STM-VENUS and pCUC2::CUC2-VENUS are downregulated at a time when PIN1 first establishes polarity foci, coincident with a presumed auxin build-up. Both pCUC2::CUC2-VENUS and pSTM::STM-VENUS are also upregulated in primordial boundaries at a similar time to when PIN1-GFP polarity reverses away from primordia, and apparent auxin depletion occurs in epidermal and subepidermal layers. Thus, there appears to be a consistent and complementary relationship between the expression of auxin reporter genes, the direction of presumed auxin flow, and the

activation of STM and CUC2, suggesting that both the STM and CUC2 expression domains may be patterned by the cycles of PIN1 focus establishment and reversal during primordium development. Our analysis also shows that PIN1-GFP expressing cells mark the boundary between the adaxial expression of REVOLUTA and the early abaxial expression of FILAMENTOUS FLOWER suggesting that auxin transport routes also play some role in defining boundaries between adaxial and abaxial cell types. Lastly, we find that the early expression domain of LFY also coincides with high PIN1 expression in cells located between the FIL and CUC2 expression domains. This narrow domain of LFY expression then appears to expand through cell proliferation during early flower development. Apart from providing new insight into how auxin transport potentially acts to provide patterning information for primordial differentiation events, our study also provides a framework from which comparisons can be made to additional gene expression markers so that, eventually, a comprehensive temporal and spatial map of gene expression dynamics can be constructed.

364. Control of PIN1 polarity
Marcus G. Heisler, Carolyn Ohno, Elliot M. Meyerowitz

From close examination of PIN1-GFP protein localization dynamics we have discovered that in certain cells in the meristem epidermis PIN1 changes polarity from towards primordia to away from primordia at specific stages of primordium development (see above abstract). However, the directional signals that control these dynamics are unknown at this time. We aim to determine the direction and origin of such signals by ablating cells located in specific positions relative to auxin transport routes. This has required the development of nuclear markers for laser targeting that can be combined with PIN1-GFP without compromising GFP signal for time-lapse imaging. Time-lapse studies are also underway investigating the role of auxin itself in modulating PIN1 polarity in both wild-type meristems and mutants. Preliminary evidence so far indicates localized auxin can affect PIN1 polarity but only under certain circumstances.

365. Auxin and phyllotactic patterning
Marcus Heisler, Henrik Jönsson[1], Bruce Shapiro[2], Eric Mjolsness[3]

We are combining live imaging techniques with computer modeling to investigate several theories to explain auxin transport via PIN1 and phyllotactic patterning. Our simplest model consistent with the available data and capable of generating phyllotactic patterning is based on the polarization of PIN1 by auxin gradients. By polarizing PIN1 up auxin concentration gradients, peaks of high auxin concentration can be generated with regular spacing. When such spacing is superimposed in a growing meristem the familiar spiral pattern of primordia emerges with PIN1 polarized towards these primordia, as seen in the real plant. The model includes cytoplasmic, membrane and wall compartments.

This model is simulated on a meristem template generated from real cell position and shape data. The model can then be used to try and predict the position of future primordia and then the results compared with the actual future primordium position. Furthermore, extracted PIN1 protein expression data can also be used to set the initial conditions for these simulations.

[1]*Lund University, Lund, Sweden*
[2]*Jet Propulsion Lab*
[3]*University of California, Irvine, CA*

366. Growth patterns and gene expression in the *Arabidopsis* inflorescence meristem
Marcus G. Heisler, Tigran Bacarian[1], Victoria Gor[2], Carolyn Ohno, Elliot M. Meyerowitz, Eric Mjolsness[1]

We have developed software and imaging techniques to track cell nuclei throughout the *Arabidopsis* inflorescence meristem. This enables us for the first time to quantify growth throughout this tissue and to examine spatial and temporal correlations between growth and gene expression patterns and subcellular localization of GFP-tagged proteins. So far we have analyzed the growth of wild-type inflorescence meristems and found that different stages of primordium development are associated with changes to both growth rate and growth direction. We are setting up experiments to measure growth while imaging GFP-tagged auxin transport proteins and expansin proteins and plan on investigating the dynamics of growth in response to localized auxin application and expansin induction. By allowing us to start quantitatively relating growth patterns to the spatial and temporal dynamics of potential regulatory factors, we can assess their roles more accurately and postulate mechanical models for their action.

[1]*University of California, Irvine, CA, USA*
[2]*Jet Propulsion Lab*

367. *CLAVATA3* mediated stem-cell homeostasis and growth dynamics can be uncoupled
G. Venugopala Reddy

The shoot apical meristem (SAM) is an interacting network of functionally distinct cellular domains. The central zone (CZ) is at the tip of the SAM and harbors a set of stem cells. The peripheral zone (PZ), located on the sides, and the rib-meristem (RM), located just below the CZ, are the regions where cells enter into differentiation pathways to make lateral organs and the stem. SAM size and shape is maintained through plant growth, though the cells are being continually diverted to differentiation pathways. Intercellular signaling between the CZ and the RM, mediated by *CLAVATA-WUSCHEL* genes, has been proposed to function in maintaining the CZ:PZ ratio and also the overall SAM size. However, the mechanisms by which CLV signaling mediates this function is not well understood.

We have combined transient gene silencing and live imaging to gain mechanistic insights into the process of SAM maintenance. Conditional silencing of the *CLV3*

226

gene was achieved through a dexamethasone (DEX)-inducible two-component system. The effect of transient removal of CLV3 function on the CZ size was monitored by using a CZ reporter, pCLV3::mGFP5-ER, construct. Expansion of the CZ was mapped with respect to the overall cell division activity within the SAM. This analysis has led to several new conclusions. 1) CZ expansion occurs through a re-specification process wherein the existing PZ cells acquire CZ identity, and this process can be uncoupled from growth; and, 2) overall SAM size is controlled through a process that restricts cell division rates in cells located at a certain distance from the meristem center.

368. Regulation of *WUSCHEL* in the shoot apical meristems
G. Venugopala Reddy

WUSCHEL (WUS), a homeodomain transcription factor, has been shown to be a critical regulator of shoot apical meristem (SAM) maintenance. It has been proposed that CLV signaling controls CZ size and overall SAM size by negatively regulating the expression of *WUS*. But this proposal is based on observations made during the inflorescence meristem stage, which represents a terminal phenotype. Several hypotheses are possible for the expanded WUS domain in terminal meristems of *clv* mutants. 1) If *WUS* is negatively regulated by a CLV signaling network, it is expected that the *WUS* domain should enlarge within the RM and/or it should be ectopically expressed in overlying layers. 2) The cells of the RM/*WUS* expressing cells could over-proliferate. 3) The expanded *WUS* domain in *clv* mutants could be a reflection of altered cell types within the RM. These hypotheses can be best tested in real-time experiments by monitoring the expression of *WUS*, upon compromising or hyper-activating CLV signaling. The required fluorescent reporter construct, pWUS::mGFP5-ER, has been generated and it is being combined with the inducible *CLV3* RNAi system and also the inducible *CLV3* overexpression system.

369. New approaches to studying old genes: A chemical genomic approach to studying key regulators of meristem function
Zachary L. Nimchuk, Marcus G. Heisler, Carolyn Ohno, G. Venugopal Reddy, Elliot M. Meyerowitz

Proliferation of cells in plants is restricted to specific regions called meristems. These regions give rise to all the above ground organs of plants (shoot and floral meristems) and below ground organs (root meristems). Studies have shown that shoot meristems are organized into functionally distinct cell populations: the central zone (CZ); peripheral zone (PZ), and the rib meristem (RM). The CZ is composed of stem cells which divide slowly relative to cells in the flanking PZ. The RM subtends the CZ and gives rise to the ground tissues of the stem. In addition, the shoot and floral meristems also give rise to flanking primordia that develop into various aerial organs. This process continues throughout the life of the plant and

contributes to overall growth and body plan development. Meristems must balance the number of generated and departed cells in order to maintain themselves. A component of this process includes the regulation of proper spatial initiation of primordial outgrowth on meristem flanks. This process of balanced proliferation and patterning is strictly controlled and is defined genetically by *Arabidopsis* mutants affecting meristem regulation and formation. Mutations in *CLV1* lead to a hyper-accumulation of stem cells in both shoot and floral meristems resulting in stem fasciation, club-shaped siliques and extra floral organs. Initiation of lateral primordia is regulated a separate pathway involving the hormone auxin. This process is perturbed by mutations in *PID*. Both PID and CLV1 are functional protein kinases of different classes. *CLV1* encodes a receptor-like kinase (RLK) with extracellular leucine-rich repeats and a cytoplasmic serine threonine (ser-thr) signaling domain. *PID* encodes a soluble but membrane associated AGC family member kinase. Although mutants in *PID* and *CLV1* have been studied for a while, little is known about how these pathways regulate patterning of the meristem and there are no identified downstream targets for either pathway. This is partially due to difficulty in interpreting terminal phenotypes in these mutants, as well as the presence either redundant or buffering pathways which act upon, or are an intrinsic component of the *PID* or *CLV1* pathways. In order to circumvent these problems, strategies for live imagining of growing *Arabidopsis* meristems using fluorescent-based markers has been developed by the Meyerowitz lab. My work is designed to complement these approaches by using chemical genetics to create specifically inhibitable versions of the CLV1 and PID kinases. It is envisioned that these engineered versions will allow for a more in-depth analysis of the genetics and cell biology of these pathways, as well as aide in the identification of pathway targets.

370. Cell fate decision by CLV1 in the shoot apical meristem
Xiang Qu, G. Venugopala Reddy, Elliot M. Meyerowitz

A balance between meristematic cell division and differentiation is required to maintain a functional SAM. In *Arabidopsis*, the *CLAVATA* (*CLV*) genes encode important elements in SAM maintenance. Single loss-of-function mutations of the *CLV* genes (*clv*) result in a progressive enlargement of shoot and floral meristems. *CLV1* encodes a transmembrane protein that belongs to a large family of receptor-like kinases (RLKs) in plants. CLV2, a LRR receptor-like protein, lacks the C-terminal kinase domain. *CLV3* encodes a small extracellular protein with a putative cleavage signal. Genetic evidence indicates that the CLV genes act in concert to restrict the size of the SAM. In this hypothetical system, CLV1 acts as a plasma membrane bounded receptor. The signal perceived from the CLV3 ligand is transduced to the downstream signaling component, theoretically through the C-terminal kinase domain of the CLV1 receptor.

CLV2 stabilizes CLV1 at the plasma membrane. However, no direct biochemical or molecular evidence supports this model.

We are now using a combination of methodologies (biochemical, genetic, and cell biological) to gain information in molecular detail how the receptor-like kinase CLV1 functions as a key element to maintain a functional SAM. We have generated constructs that allow us to visualize the CLV proteins directly in a confocal microscope and/or detect them indirectly by chemiluminescence. We have demonstrated that CLV1 is localized to the plasma membrane. An analysis of interaction between CLV1 and CLV3 and its biological significance is being undertaken. In addition, constructs that abolish the kinase activity of CLV1 are being made, to address whether the kinase domain of CLV1 and/or the associated enzymatic activity are required for CLV signaling.

371.   Dynamic analysis of the GATA-like transcription factor HANABA TARANU during *Arabidopsis* development
Xiang Qu, Yuanxiang Zhao, Elliot M. Meyerowitz
HAN (*HANABA TARANU*) encodes a GATA-like transcription factor and is essential for floral development in *Arabidopsis*. All four identified *han* mutants (*han-1*, *han-2*, *han-3*, and *han-4*) display a dramatic floral phenotype, with fused sepals and reduced organ number throughout four whorls. The expression pattern of *HAN* in the shoot apical meristem (SAM) and floral meristem is distinctive, with strong expression at the boundaries between the meristem and its newly initiated organ primordia, and at the boundaries between different floral whorls. Although *han* mutations have minor effects upon vegetative SAMs, *han;clv* double mutants display a highly fasciated SAM. Together with the observation that the WUS expression pattern is altered in *han* mutants, our data suggest that HAN is also involved in SAM development. To understand the molecular mechanism by which HAN regulates flower and SAM development, we have developed a hormone-inducible system that allows us to activate HAN upon the treatment with dexamethasone (DEX). Following the activation of HAN, we can monitor changes in expression pattern of the selected floral and SAM identity gene (*WUS*, for example) by live imaging. Using the same system, we plan to conduct time-course microarray analyses. The time course should be quite useful in indicating how far downstream players are, or for correlating with morphogenetic events. The immediate targets from the microarray experiments will be selected for chromatin immunoprecipitation. As an alternative approach, in collaboration with Dr. Wolfgang Lukowitz at Cold Spring Harbor Labs, we will conduct a second site screen for suppressors from the EMS-mutagenized han-2 plants. The work described here should identify novel components in the HAN pathway and provide a better understanding of how HAN functions during *Arabidopsis* development.

372.   *De novo* assembly of the plant
Sean Gordon
Unlike animals, new plants are able to assemble *de novo* from cultured cells derived from any part of a mature plant via hormone induction. The assembly of a new plant from cultured cells is useful for the study of cell fate plasticity and developmental patterning. We are interested in how cells become competent to switch fates, how certain cells are chosen to assemble new plants, and how early gene expression establishes a patterned plant in this system. We are using confocal microscopy and fluorescent *in vivo* reporters to visualize gene and protein activity during the assembly of new plants from cultured cells. In our current system, we grow callus cultures from *Arabidopsis thaliana* root explants, from which we induce new shoot apical meristems, the fundamental unit which gives rise to all above-ground tissues of the plant, via culture on a hormonal medium. The earliest steps in the formation of new meristems have been observed using laser confocal microscopy on callus tissue that is transgenic for fluorescent meristem markers. Specifically, we have used spectral GFP variants to report the activity of meristem-specific promoters of the *CUP SHAPED COTYLEDONS*, *CLAVATA3*, *WUSCHEL*, *PINFORMED1* and *FILAMENTOUS FLOWER* genes in culture as meristems assemble in order to establish correlations between gene expression and meristem formation and patterning. So far our observations are in wild-type callus, but we plan to extend them to mutant genotypes. The eventual result will be a detailed causal analysis of gene expression and gene function in *de novo* organization of shoot meristems, and hence the plant.

373.   Functional characterization of a family of mscs-like genes in *Arabidopsis thaliana*
Elizabeth S. Haswell, Elliot M. Meyerowitz
Mechanotransduction, the conversion of mechanical stimuli into a biochemical signal, is a fundamental cellular process required for hearing, pain perception and bone building in animals and gravitropism and barrier-avoidance in plants. We are using the plant *Arabidopsis thaliana* as a model system to study the process of mechanotransduction, taking a candidate approach to identifying potential mechanosensitive molecules. Our current study focuses on ten members of the MscS family of mechanosensitive ion channels found in the *Arabidopsis* genome (1, 2). Reporter gene expression data reveal that the MscS-Like (MSL) genes are expressed in a variety of differentiated tissues, including the vasculature, guard cells, and stigma cells. GFP fusion proteins are found in distinct subcellular locations, including mitochondria, chloroplasts, and other cellular membranes. These data suggest that MSL genes may function not only in cellular osmotic protection (like MscS), but also in a variety of developmental and adaptive processes throughout the life of the plant. In the short term, we hope to reveal how the MSL proteins contribute to plant development and cellular function, while our long-term goal is to improve our general understanding of plant

228

mechanotransduction, which is both a fundamental cellular response and a relatively unexplored facet of plant biology.

References

1. Kloda, A. and Martinac, B. (2002) *Archaea* **1**:35-44.
2. Pivetti, C. *et al.* (2003) *Micro. Mol. Biol. Rev.* **67**:66-85.

374. Two mechanosensitive ion channels control plastid size and shape in *Arabidopsis thaliana*
Elizabeth S. Haswell, Elliot M. Meyerowitz

Mechanosensitive (MS) ion channels provide a mechanism for the perception of stimuli such as touch, gravity, and osmotic pressure. The bacterial MS ion channel MscS is gated directly by changes in membrane tension (1), and protects against cellular lysis during an osmotic downshock (2). Found widely in bacterial and archaeal species, MscS-like genes have also been identified in fission yeast and in plants (3, 4) no analysis of these genes in eukaryotes has yet been reported. We have initiated the characterization of two MscS-Like (MSL) genes in *Arabidopsis*, MSL2 and MSL3. Heterologous expression of MSL3 can rescue the osmotic shock sensitivity of a *mscS- E. coli* strain, suggesting that Msl3 does indeed function as a MS ion channel. *Arabidopsis* plants harboring insertional mutations in both MSL3 and MSL2 show a number of defects in the morphology of plastids, plant-specific endsymbiotic organelles responsible for photosynthesis (chloroplasts), gravity perception (amyloplasts), and numerous other metabolic reactions. A subset of chloroplasts in *msl2-1; msl3-1* double mutants are grossly enlarged, while epidermal plastids are either enlarged and spherical or exhibit long, tangled stromal tubules. MSL2 and MSL3 GFP fusions are localized to the poles of plastids, and co-localize with the plastid division protein AtMinE. Our data support a model wherein MSL2 and MSL3 control plastid size, shape, and perhaps division during normal plant development by altering ion flux in response to changes in membrane tension. We propose that the MSL genes have evolved new roles since the endosymbiotic event.

References

1. Sukharev, S. (2002) *Biophysical J.* **83**:290-298.
2. Levina, N. *et al.* (1999) *EMBO J.* **18**:1730-1737.
3. Kloda, A. and Martinac, B. (2002) *Archaea* **1**:35-44.
4. Pivetti, C. *et al.* (2003) *Micro. Mol. Biol. Rev.* **67**:66-85.

Publications

Baker, C.B., Sieber, P., Wellmer, F. and Meyerowitz, E.M. (2005) The *early extra petals1* mutant uncovers a role for microRNA *miR164c* in regulating petal number in *Arabidopsi*s. *Curr. Biol.* **15**:303-315.

Gor, V., Shapiro, B.E., Jönsson, H., Heisler, M., Reddy, G.V., Meyerowitz, E.M. and Mjolsness, E. (2005) A software architecture for developmental modeling in plants: The computable plant project. In: *Bioinformatics of Genome Regulation and Structure II*, R. Hofestaedt and N. Kolchanov (Eds.), Kluwer, Boston. In press.

Ito, T., Wellmer, F., Yu, H., Das, P., Ito, N., Alves-Ferreira, M., Riechmann, J.L. and Meyerowitz, E.M. (2004) The homeotic protein *AGAMOUS* controls microsporogenesis by regulation of *SPOROCYTELESS*. *Nature* **430**:356-360.

Jönsson, H., Heisler, M., Reddy, G.V., Agrawal, V., Gor, V., Shapiro, B.E., Mjolsness, E. and Meyerowitz, E.M. (2005) Modeling the organization of the WUSCHEL expression domain in the shoot apical meristem. *Bioinformatics* **21**, suppl. **1** i232-i240.

Jönsson, H., Shapiro, B.E., Meyerowitz, E.M. and Mjolsness, E. (2004) Modeling plant development with gene regulation networks including signaling and cell division. In: *Bioinformatics of Genome Regulation and Structure*, R. Hofestaedt and N. Kolchanov (Eds.), Kluwer, Boston, pp. 311-318.

Ohno, C., Reddy, G.V., Heisler, M. and Meyerowitz, E.M. (2004) The *Arabidopsis* JAGGED gene encodes a zinc-finger protein that promotes leaf tissue development. *Development* **131**:1111-1122.

Reddy, G.V., Heisler, M.G., Ehrhardt, D.W. and Meyerowitz, E.M. (2004) Real-time analysis reveals oriented cell divisions associated with morphogenesis at the shoot apex of *Arabidopsis thaliana*. *Development* **131**:4225-4237.

Wagner, D., Wellmer, F., Dilks, K., William, D., Smith, M.R., Kumar, P.P., Riechmann, J.L., Greenland, A.J. and Meyerowitz, E.M. (2004) Floral induction in tissue culture: A system for the analysis of LEAFY-dependent gene regulation. *Plant J.* **39**:273-282.

Wellmer, F., Riechmann, J.L., Alves-Ferreira, M. and Meyerowitz, E.M. (2004) Genome-wide analysis of spatial gene expression in *Arabidopsis* flowers. *Plant Cell* **16**:1314-1326.

Yu, H., Ito, T., Zhao, Y., Peng, J., Kumar, P. and Meyerowitz, E.M. (2004) Floral homeotic genes are targets of gibberellin signaling in flower development. *Proc. Natl. Acad. Sci USA* **101**:7827-7832.

Yu, H., Ito, T., Wellmer, F. and Meyerowitz, E.M. (2004) Repression of AGAMOUS-LIKE 24 is a crucial step in promoting flower development. *Nature Genetics* **36**:157-161.

Zhao, Y., Medrano, L., Ohashi, K., Fletcher, J.C., Yu, H. Sakai, H. and Meyerowitz, E.M. (2004) HANABA TARANU is a GATA transcription factor that regulates shoot apical meristem and flower development. *Plant Cell* **16**:2586-2600.

Professor of Biology: Ellen V. Rothenberg
Member of the Professional Staff: Rochelle Diamond
Senior Research Fellow: Mary Yui
Senior Postdoctoral Scholar: C. Chace Tydell, Tom Taghon
Postdoctoral Scholars: Satoko Adachi, Elizabeth-Sharon David Fung, Jonathan Moore, Deirdre Scripture-Adams
Graduate Students: Christopher Dionne, Mark Zarnegar
Undergraduate Student: Christopher Franco
Research and Laboratory Staff: Stephanie Adams, Ruben Bayon, Robert Butler, Robin Condie, Katharine Dinwiddie, Parvin Hartsteen, Rashmi Pant

Summary: The Rothenberg group studies the molecular mechanisms that are responsible for developmental lineage choice as hematopoietic stem cells differentiate into T lymphocytes. The approaches used in the lab are a combination of *in vitro* developmental biology, high-resolution characterization of developmental states in individual cells, and molecular genetics of gene regulation. We focus specifically on the earliest stages of T-cell development, identifying the transcription factors and signaling events that induce T-lineage gene expression in an uncommitted precursor and determining how these regulatory inputs work to force the cell to relinquish other developmental options.

The past year has seen major advances in both the cell biology and the molecular biology of the system. One of these advances makes it possible to study the full span of T-lineage commitment, all the way from stem cells, in a simple monolayer system with continued access to the cells through every intermediate stage. This has made T-cell development easy to dissect *in vitro* with a precision that was never possible before. We have used two versions of this *in vitro* system to study the timing and molecular requisites for developmental decisions between the T and B lineage fates. We have also adapted this system for use as a tool to track the effects of experimental gene regulatory perturbations in kinetic and quantitative detail. Thus, both retrovirally-transduced overexpression and RNA interference-based knockdown experiments are yielding unprecedently clear results on the *in vivo* roles of key regulatory molecules, such as PU.1 and GATA-3. Most importantly these experiments reveal quantifiable interactions between intrinsic transcription factor activities and signaling pathways, triggered by cytokine receptors and Notch, in determining cell fate.

This advance is particularly timely as it accompanies the culmination of our gene discovery project, which has led to characterization of over 90 transcription factors expressed in T-cell specification. Quantitative analysis of expression patterns of these transcription factors and early T-cell-specific signaling molecules through development reveals a remarkably selective group of regulatory discontinuities, both *in vivo* and in the OP9-DL1 system. Using new markers that we have discovered to separate the stages in which the specification, commitment, and selection processes occur, these expression patterns can be tightly correlated with major developmental events. The regulatory factor genes with sharp changes in their expression through the commitment process are likely to include key positive and negative regulators. Their functional activities can be dissected now by acute perturbation of their expression during T-cell differentiation *in vitro.*

Transcription factors are particularly valuable to define as links in the regulatory network leading to T-cell specification, because they directly drive changes in gene expression through their interactions with *cis*-regulatory DNA. Two projects in the group in the past year address the molecular mechanisms through which T-lineage gene expression patterns are enforced, both the roles of specific transcription factor binding and the context of broader-domain chromatin modifications within which they operate. These studies have shed light on different modes of positive and negative regulation of the PU.1 transcription factor gene (*Sfpi1*) and the *IL2* cytokine gene. We plan to expand these studies to link the newly characterized transcription factor expression patterns directly with the developmental timing of activation of essential T-cell identity genes.

Building on the lab's core interest in lymphoid developmental regulation, Dr. Mary Yui in the group has recently discovered an early T-lineage developmental defect that may contribute to the autoimmune disease of nonobese diabetic (NOD) mice. In these mice, there is a dysregulation of stages that span commitment through the first selection step in T-cell development, leading to inappropriate activation. The developmental defect in these mice appears to be a discrete component of the multigenic NOD syndrome that can be mapped by quantitative trait genetics, and may be associated with a number of immunologically interesting genes. Dr. Yui is now pursuing this study as a self-contained project within the lab.

Finally, the group has had a longstanding interest in the evolutionary origins of the lymphocyte developmental program. Lymphocytes appear to be vertebrate-restricted, a relatively novel emergence in comparison to other blood cell types which are more widespread in phylogeny. Lampreys, a most distantly related group in the vertebrate radiation, occupy a pivotal position for understanding lymphocyte origins, as they have lymphocyte-like cells but use a completely different set of molecules for antigen recognition than the lymphocytes of jawed vertebrates. In the past year, we initiated collaboration with Drs. Zeev Pancer, Chris Amemiya, and Max Cooper to explore whether the transcription factors that regulate expression of the lamprey receptor genes may overlap with those used for immune receptor genes in vertebrates. The answers should

begin to illuminate how ancient the regulatory programs that generate lymphocytes really are, and which parts of these programs have the longest histories.

375. Developmental and molecular characterization of emerging β- and γδ-selected pre-T cells in the adult mouse thymus

Tom Taghon, Mary A. Yui, Rashmi Pant, Rochelle A. Diamond

The first checkpoint in T-cell development, β-selection, has remained incompletely characterized until now for lack of specific surface markers. It is known that the first T-cell receptor (TCR)-dependent selection events occur while cells are in the DN3 stage (CD4$^-$ CD8$^-$ c-kit^{low} CD44$^-$ CD25$^+$) and are required for the cells to progress beyond this stage. However, the DN3 stage is also the point when precursors first become committed to the T-cell lineage, and this commitment event appears to be independent of TCR-dependent selection. Furthermore, depending on the form of the first TCR complex expressed on the cells, differentiation beyond this stage proceeds in two divergent pathways, either to the TCRαβ CD4$^+$ CD8$^+$ fate or to the TCRγδ CD4$^-$ CD8$^-$ fate. Thus, DN3 thymocytes in mice are normally a mixture of cells in at least three distinct developmental conditions.

We have now shown that CD27 is upregulated in DN3 thymocytes initiating β-selection, concomitant with intracellular TCRβ expression. Clonal analysis determined that CD27^{high} DN3 cells generate CD4$^+$CD8$^+$ progeny with over 90% efficiency, faster and more efficiently than the CD27^{low} majority. CD27 upregulation also occurs in γδ-selected DN3 thymocytes in TCR-β$^{-/-}$ mice and in IL2-GFP transgenic reporter mice where GFP marks the earliest emerging TCRγδ cells from DN3 thymocytes. Using CD27 to distinguish pre- and post-selection DN3 cells, a detailed gene expression analysis defined regulatory changes associated with checkpoint arrest, with β-selection, and with γδ-selection. γδ-selection induces higher CD5, Egr and Runx3 expression as compared to β-selection, but triggers less proliferation. Our results also reveal differences in Notch/Delta dependence at the earliest stages of divergence between developing αβ and γδ T lineage cells.

376. Delayed, asynchronous, and reversible T-lineage specification induced by Notch/Delta signaling

Tom N. Taghon, Elizabeth-Sharon David

Using the OP9-DL1 system to deliver temporally controlled Notch/Delta signaling, we show that pluripotent hematolymphoid progenitors undergo T-lineage specification and B-lineage inhibition in response to Notch signaling in a delayed and asynchronous way. Highly enriched progenitors from fetal liver require ≥3 days to begin B- or T-lineage differentiation. Clonal switch-culture analysis shows that progeny of some single cells can still generate both B- and T-lineage cells, after 1 week of continuous delivery or deprivation of Notch/Delta

signaling. Notch signaling induces T-cell genes and represses B-cell genes, but kinetics of activation of lineage-specific transcription factors are significantly delayed after induction of Notch target genes and can be temporally uncoupled from the Notch response. In the cells that are slowest to initiate T-cell differentiation and gene expression in response to Notch/Delta signaling, Notch target genes are induced to the same level as in the cells that respond most rapidly. Early lineage-specific gene expression is also rapidly reversible in switch cultures. Thus, while necessary to induce and sustain T-cell development, Notch/Delta signaling is not sufficient for T-lineage specification and commitment, but instead can be permissive for the maintenance and proliferation of uncommitted progenitors that are omitted in binary-choice models.

377. Determination of discrete stage-specific requirements for GATA-3 in early T cell development

Deirdre D. Scripture-Adams

T cells develop in the thymus and pass through discrete stages as they mature. T cells require an evolving pool of transcriptional regulators as their development proceeds, and as they pass through each maturational stage. Transcription factors are able to either increase or decrease the expression of other developmentally important proteins, and can regulate developmental progression as well as function. Of these one of the most important for T-cell development is GATA-3.

GATA-3 is a dual Zn finger transcription factor encoded on chromosome 2, and expressed in placenta, central and peripheral nervous systems, liver and thymus during development, and in thymocytes, T cells and the central nervous system in adult animals. GATA-3 is expressed throughout T cell development: from the common lymphoid progenitor in the bone marrow, in the early stage thymocytes, and in peripheral T cells, where it has a role in promoting TH2 responses. Binding sites for GATA-3 have been identified within the regulatory regions of the T-cell specific genes CD8α, TCRα, β, γδ. Null mutations of GATA-3 are lethal between embryonic day 11 and day 12, which until recently has made it difficult to assess the postnatal functions of GATA-3 during hematopoiesis.

Much of the current understanding of GATA-3's role in early T development comes from studies in various systems in which GATA-3 has been overexpressed. High-level GATA-3 was reported to induce arrest at the DN1 stage from fetal liver precursors, result in reduced proliferation from the DN to DP transition in fetal thymocytes, and inhibit CD8 lineage commitment when overexpressed in DP. Overexpression also causes changes in gene expression: Rag-1, Rag-2, pre-Tα, IL-7 receptor, and PU.1 are all downregulated when GATA-3 is overexpressed. However, these effects do not reveal the positive modes of GATA-3 action in T-cell precursors.

To identify the specific stages during which GATA-3 is essential for early T-cell development, we are

examining the gene regulatory and developmental effects of loss of GATA-3 in adh.2C2 cells (a DN3-like cell line), in fetal liver-derived precursors, and in fetal thymocytes developing in OP9/ OP9-DL1 stromal culture systems. We are using retrovirally delivered GATA-3-specific siRNA to prevent GATA-3 protein synthesis during early T-cell development. The siRNA expressing vector also encodes green fluorescent protein that allows easy identification of cells expressing the siRNA. We are also using nucleofection technology to directly introduce siRNAs specific for GATA-3 into the nuclei of fetal liver-derived precursors, and fetal thymocytes. We follow developmental progression (as assessed by changes in surface expression of key developmental marker proteins) by flow cytometry. Gene expression changes are monitored by quantitative PCR following reverse transcription of cellular RNA.

Experiments done with the DN3-like cell line adh.2C2 suggest that GATA3 is critical for the DN3 stage T cell. Although initial levels of retroviral infection are comparable between the siRNA containing vector and the control virus, cells containing the siRNA (and thus, less GATA3 protein) quickly disappear from cultures, suggesting either death or lack of competitive advantage. This is accompanied by increasing levels of CD25, an important developmental marker. Similar experiments performed using nucleofection of GATA-3 specific siRNAs confirmed this upregulation of CD25 within 24 hours. At the RNA expression level, loss of GATA-3 resulted in upregulation of CD8α and the transcription factor PU.1 in adh.2C2. These gene expression changes were observed in DN3-stage primary thymocytes cultured in the OP9 stromal system as well, suggesting that PU.1 may be directly repressed by GATA-3 at the DN3 stage of development.

Loss of GATA-3 is extremely detrimental in the earliest stages of T-cell development. Fetal liver derived precursors infected with the GATA-3 siRNA producing virus and cultured on OP9-DL1 stromal layers have not been observed to survive with levels of infection comparable to control infections, nor do they survive in comparable numbers relative to control infected cells, suggesting that GATA-3 might be critical for survival and proliferation in these early stage cells. If GATA-3 is knocked down in fetal liver precursors these cells fail to progress to the later stages of T-cell development with normal efficiency and fail to proliferate normally. The requirement for GATA-3 for precursor progression is not relieved by forcing viability, as fetal liver precursors derived from Bcl-2 transgenic mice in which GATA-3 has been knocked down retain the observed developmental block.

When early DN-stage thymocytes are infected with a GATA-3 siRNA expressing virus, sorted into DN1, DN2, or DN3 populations, and cultured in the OP9-DL1 stromal system, the cells fail to progress to the next stage of development as efficiently, relative to control infected cells.

We have demonstrated a requirement for GATA-3 in the fetal liver derived precursor, as well as, in the first stages of thymocyte maturation: DN1, DN2, and DN3. We have recently constructed additional siRNA producing retroviral vectors designed to target other transcription factors. Using these new vectors, as well as direct nucleofection of siRNA and a variety of mouse models, we will characterize the gene regulatory role of GATA-3 and its contribution to the specific gene regulation changes occurring during T-lineage commitment and T specification.

378. PU.1-sensitive control mechanisms of developmental progression and lineage choice in pro-T cells
Christopher Franco, Irina Proekt, Tom Taghon, Deirdre Scripture-Adams, Mary Yui, Elizabeth-Sharon David, Rochelle Diamond

The ETS family transcription factor PU.1 is essential for T-cell development, but its role is mostly confined to the earliest pro-T cell stages. At lineage commitment, PU.1 must be turned off. We have previously reported that forced continuation of PU.1 expression blocks T-cell development, and in some cases it can redirect the programming of T-lineage cells to a myeloid fate. However, the mechanisms involved and the relationships between these effects have been obscured by the fact that forced high-level PU.1 expression causes cell death in T-lineage cells. The gene expression changes induced by PU.1 in T-lineage cells in our previous experiments could be a composite of direct and indirect effects. The methods for studying T-cell development *in vitro* until now have been clonally inefficient, making quantitative comparisons difficult.

New *in vitro* developmental culture conditions have now enabled us to elucidate the effects of PU.1 on pro-T cell development and gene expression. Key features of these conditions are the use of the OP9-DL1 system to bypass the seeding inconsistencies of organ culture and the use of specific cytokines to maintain maximal lymphoid developmental potential in the controls. Under these conditions PU.1 is seen to arrest development at β-selection and to cause myeloid respecification of cells before the β-selection checkpoint. Normal thymocytes still die in response to the highest levels of PU.1 overexpression, but this appears to be due to a developmental quality control mechanism that can be overcome efficiently by the use of a Bcl-2 transgenic strain as the source of cells. Bcl-2 transgenic cells efficiently convert from a pro-T to a myeloid-like phenotype in response to PU.1 without cell death. Gene expression changes associated with the impact of high PU.1 expression are clear but selective. While myeloid gene Mac1 is upregulated, the RAG-1 gene needed for TCR-rearrangement is most inhibited, along with the TCF-1 transcription factor that mediates much proliferation in early pro-T cells. However, other key regulators such as Notch, bHLH factor E2A, and pro-T cell identity genes such as pTα are not inhibited.

The effect on the recombinase gene needed to cause TCR gene rearrangement raises the question of whether the T-lineage block caused by PU.1 is simply due to a failure at the first TCR-dependent checkpoint, β-selection. To test this, the effects of PU.1 were measured in TCR-transgenic pro-T cells where the TCR rearrangement requirement is bypassed. These results showed that even in cells expressing the TCR transgene on the surface, PU.1 blocked T-lineage progression and arrested them in an immature state. Thus, high continuing expression of PU.1 interferes with T-cell development by internal regulatory changes over and above its effects on TCR expression.

379. Generation of obligate repressor constructs to study the role of transcription factors in T-cell development

Sanket S. Acharya, Mark Zarnegar*

The development of functional lymphoid and myeloid cells from a single hematopoietic stem cell is a fundamental process in animals. Each terminally differentiated cell type is derived from a common progenitor with many developmental options that decrease in number as a progenitor commits itself to a particular cell lineage. Certain transcription factors have been known to act as key regulators in this highly dynamic process, and have been well characterized for developing T cells. These factors, namely PU.1, GATA-2, and GATA-3, act by either upregulating or downregulating a series of target genes known to steer development of progenitors towards the T lineage. Here we focused on generating obligate repressor constructs of these transcription factors by fusing their DNA binding domains with a repressor domain derived from the *Drosophila melanogaster* Engrailed protein. The fusion constructs were made by a combination of DNA amplification and recombinant DNA cloning techniques. The individual domains were combined using fusion PCR, cloned in the pGEM®-T Easy shuttle vector system, and then transferred to the larger Lazarus retroviral vector. Making retrovirus particles carrying these fusion constructs will allow transfection experiments with mammalian cell lines. A comparison of target gene expression profiles caused by wild-type versus dominant negative construct transfection will greatly enhance our understanding of the mechanism of action of transcription factors during early T-cell development.

*Hampshire College, Amherst, MA

380. A gene discovery screen for pro-T cell transcription factors: High-resolution expression analysis and definition of distinct regulatory cohorts

Elizabeth-Sharon David (Fung), Gentian Buzi, Lee Rowen***

Early, adult murine lymphoid development involves cell-intrinsic regulatory changes as precursor cells migrate to their respective organs of development. The Rothenberg laboratory has sought to identify the full set of regulatory actors deployed as a pro-T cell begins its changes through specification and commitment within the thymus. Using a transcription factor-conserved domain screen, and complex mRNA-probe screens generated from pro-T-like versus stem-cell-like cells, we have identified >120 expressed and up-regulated transcription factors and have characterized them by high-throughput sequencing, as explained previously in the 2003 and 2004 Annual Reports. In addition to transcription factors that had been reported previously, we found a large number of new or minimally characterized transcription factors which are expressed at moderately high levels in pro-T cells. The bulk of the novel factors are C2H2 zinc-finger factors, and based on their structural features a large number of them are predicted to be repressive in function. Other relatively new factors include poorly characterized members of other known transcription factor and chromatin remodeling factor families: forkhead, BTB, ARID, SET, and others.

Over 70 of these putative transcriptional regulator genes have now been interrogated for expression in high-resolution analyses using quantitative PCR comparisons across hematopoietic cells, focusing on expression within the double negative subsets of thymocyte development. The results showed the diverse transcription factors to fall into a surprisingly small number of distinctly regulated cohorts. Most transcription factors rise gradually from the DN1 to DN3 stages of expression, decreasing in DN4, post-β selection (*FoxP4*, *STAT5b* and to a certain extent *KIAA1115* and many others). Only a small number of individual genes were sharply upregulated during T-lineage commitment at the DN3 stage. GATA-2 and Runx3, like PU.1, behaved as early genes, being expressed in DN1 cells, but decreasing in expression as development proceeds. While *T-bet* is most high in pre-natural killer cells, it is also high in DN4 cells. We focused on the expression of certain gene families – Ets, FOX, BTB/POZ, Myb, TRIM, C2H2 zinc fingers, KRAB zinc fingers and Homeodomain-containing genes. Expression patterns of transcription factors from these families were sorted based on their Euclidean distances. Expression patterns were clustered based on correlation values to provide quantitative metrics for recognition of cohort. The resulting assemblies of genes will be very useful in the construction of dynamic network models of transcription factor interaction and function.

*Control and Dynamical Systems Program, Caltech
**Institute for Systems Biology, Seattle, WA*

381. Selectively upregulated regulatory genes of pro-T cells

*C. Chace Tydell, Elizabeth-Sharon David (Fung), Lee Rowen**

Although much is known about lymphocyte hematopoiesis, the specific factors that guide stem cells to a T-cell fate are yet to be determined. In red blood cell development, GATA-1 acts as a central mediator of erythroid gene expression, whereas B cells are instructed by E2A, EBF and Pax5, yet such "master regulators" have not been found in T-cell development. Furthermore, in the general gene discovery screen described in the previous

abstract, we found few of the newly identified genes to be expressed in a T lineage specific way. In search of novel factors with critical roles in T-lineage specification and commitment, and to broaden the search for regulators regardless of conserved-domain structure, we have performed a subtractive screen of a Pro-T cell cDNA macroarray library.

Using a subtractive screen we have now identified more than 150 genes as enriched in a pro-T cell population relative to a multipotent/pre-myeloid population. Of the 1% most enriched clones, fully one third are genes known to be upregulated in pro-T cells, offering a first approximation of the screen's success. Expression of many genes of interest has been verified by qRT-PCR in cDNA from sorted cells. In addition, we have begun evaluating candidate regulatory factors in DN subsets of wild-type thymocytes. Statistical analysis by GOToolBox indicates that nearly half of the upregulated genes are predicted to be found in the nucleus. In addition, known transcription factors and transcriptional modulators or co-activators are statistically over-represented (p< 0.0003) among the predicted products of the enriched genes. This suggests that pro-T cells express many transcription factors that are not found in myeloid or multipotent precursors. Genes with ubiquitin-protein ligase activity are also enriched (p< 0.0001) among the total genes selected by the subtraction and, as expected, genes encoding proteins active in chromosomal arrangement and remodeling are abundant in the ProT-enriched set. Among genes implicated in signaling, those that encode products with kinase activity (including Lck, Cdk6, Cam2ka and Tgfbr2) are statistically over-represented.

Several genes (including Deltex1, Eva1, Fkbp5 and RW1) demonstrate specific upregulation in Pro-T cells among diverse subsets of hematopoietic cells. Among those tested, RW1 and Eva1 are specifically enriched in DN3 cells at the β-selection checkpoint. A second pattern of gene expression is exemplified by Grap, GRB2-related adaptor protein, which is enriched in both Pro-T and Pro-B populations relative to pre-myeloid and stem cells.

A third pattern of expression, of particular interest, is demonstrated by Zfp30 and Zfp109. These two putative transcriptional repressors, with Zn-finger DNA-binding domains and predicted N-terminal KRAB domains, are upregulated in both pro-T cells and in Lin⁻ Sca1⁺ ckit⁺ CD27⁺ multipotent precursor cells: CD27 expression specifically distinguishes those progenitor cells that are most competent to generate pro-T cells (Taghon *et al.*, 2005). In contrast, these genes are expressed at relatively low levels in pro-B cells and Lin⁻ Sca1⁺ ckit⁺ CD27⁻ multipotent precursor cells.

Our study has identified a surprisingly large number of transcripts that are still unreported or minimally annotated in NCBI, UCSC and Ensembl, but which contain domains found in transcription factors, consistent with the interpretation that previously unknown factors may contribute to early T-lineage regulation. Use of a pro-T-cell library generated by random priming has also allowed for the identification of non-canonical splice variants of known transcription factors. These non-canonical transcripts will be verified by conventional PCR. The marked over-representation of proteins from the nuclear compartment is consistent with pro-T cell morphology, as these cells contain little cytoplasm. Still, the numerical dominance of transcription factors over signaling molecules was not expected. Upregulation of genes of interest was initially verified by qRT-PCR in the original cell populations and in sorted hematopoietic cells from recombinase-deficient Rag-knockout mice. Currently, gene expression is being analyzed in wild-type DN thymocyte subsets, as well as, cells cultured in the OP9 co-culture system.

Subtractive hybridization of a pro-T cell macroarray cDNA library has yielded a wealth of new genomic information for the exploration of T-cell development. This gene discovery project has successfully identified more than 150 genes including transcription factors as well as genes involved in signaling, ubiquitination, phosphorylation and chromatin remodeling. Early analysis suggests that transcription factors with repressor activity may be particularly important to T cell development. The identification of transcriptional repressors not previously associated with lymphocyte development provides novel candidates for the T-lymphocyte "master regulator" or key nodes in the T-lymphocyte regulatory network.
Institute for Systems Biology, Seattle

382. Patterns of T-lineage regulatory gene expression in an *in vitro* system for real-time dynamic lineage choice
Elizabeth-Sharon David (Fung), C. Chace Tydell, Tom Taghon

The germline knockout approaches that have identified essential T-cell genes in other laboratories have not distinguished between genes required to initiate the T-cell program, genes required to make the T-lineage choice irreversible, and genes simply required for continuing viability within the pro-T cell stages. However, the real-time lineage choices made accessible in the OP9-DL1 system (cf. Abstract 376) provide a way to separate these kinds of roles in time. While our experiments clearly confirm viability-supporting roles for known essential T-cell genes like GATA-3 (cf. Abstract 377), these known genes have not appeared to be able to carry out instructive functions needed to initiate T-cell specification or lock-down functions needed for T-lineage commitment. Thus, the less-characterized genes identified in the structural and subtractive screens of pro-T cell cDNA, as described in the previous two abstracts, represent a valuable new source of candidates to screen for these functions.

Kinetics of factor expression in T-cell lineage specification in response to essential, initiating Notch signals were assayed by using a stromal co-culture system, with OP9-DL1 cells to induce T-cell development and OP9-control cells to support B-cell development. To distinguish between differentiation-initiating functions and

lineage-commitment functions, some of the samples were harvested after 4 days of initial culture, a timepoint when we know initial differentiation choices to remain reversible, then split and recultured either on the same type of OP9 cell stroma or on the opposite type. Quantitative RT-PCR measurements of the cDNAs from these samples then distinguished pro-T cell genes into several classes: (1) genes that are already present in multipotent progenitors and sustained in a T-lineage specific way; (2) genes that are induced rapidly in a Notch-dependent way (only on OP9-DL1); (3) genes that are induced later in a Notch-dependent way, only at lineage commitment; and (4) genes induced with different kinetics in both T-lineage and B-lineage cells. Benchmarks for T cell-specific patterns of expression are provided by the GATA-3 and TCF-1 (Tcf7) transcription factors.

Our results have shown highly interesting temporal patterns of expression for RW1 (function unknown), Rbak (a zinc-finger repressor), chromatin remodeling factor MLL-2, and homotypic adhesion molecule Eva1. Like Deltex1, these genes are also suggested to be Notch-signal responsive. A very select group of signaling genes and transcription factors show more dramatic expression patterns consistent with T-lineage initiating or T-lineage confirming roles, and these are the immediate targets of our ongoing study.

383. Developmentally regulated changes in transcription factor expression in natural killer (NK) cells

Mary An-yuan Yui

Natural killer (NK) cells are cytolytic cells involved in innate immune responses to virally infected cells and tumors. These cells are derived from lymphoid progenitor cells and undergo development primarily in bone marrow, although they can also develop in the thymus, the site of T-cell development. These studies were undertaken (1) to determine developmentally regulated patterns of transcription factor expression in NK cells from bone marrow as compared with thymus, which differ in precursor cell type and microenvironment, and (2) to compare NK development in normal (C57BL/6) vs. non-obese diabetic (NOD) mice, which produce NK cells with very poor cytolytic activity. NK cells at various stages of development, as defined by surface markers, were purified from bone marrow, thymus and spleen from *Rag*-deficient mice, which are unable to make B or T cells, facilitating NK cell purification. RNA was isolated from these sorted cell populations, cDNA reverse transcribed, and real-time quantitative QPCR carried out for transcription factors known to be involved in NK and/or T-cell development. Preliminary results show that transcription of *Ets1* and *Elf4*, which are known to be required for NK cell development increase with NK cell maturation, while another family member, *Ets2* declines. Two other Ets family members, *SpiB* and *PU.1*, decline with NK-cell maturity in the bone marrow but are poorly expressed at all stages in the thymus. The presence of higher levels of Notch-induced *Hes1* in thymic NK cells as compared with those in bone marrow further emphasizes intrinsic and/or environmental differences between NK cells developing in thymus vs. bone marrow. *Id2*, a transcriptional repressor, which is also critical for NK development, was found to increase with maturity. In addition, *Id2* is expressed at lower levels in NOD than C57BL/6 NK cells in all developmental stages and tissues, suggesting a possible role in abnormal NK cell differentiation in NOD mice.

384. Differential expression of transcription factors in developing fetal and adult murine T-cell precursors

Marissa Morales, Elizabeth-Sharon David (Fung), Mary A. Yui*

Studies in the development of murine early T-cell precursors show differences between adult and fetal populations that include differences in speed of maturation, in the role of certain genes, and in the details of the lineage choices that the cells can make. Comparing transcription factor expression between adult and fetal mice could lead to identification of regulatory genes that have an influence on these differences. For this purpose, we dissected thymus from two populations each of wild-type adult and fetal mice. Thymocytes were sorted from each using Fluorescence Activated Cell Sorting to isolate corresponding series of early T-cell precursors. RNA transcripts were then isolated from the cells and used as a template to synthesize cDNA. The cDNA was then used to measure the expression of 27 genes, mostly transcription factors, using quantitative PCR. Overall the expression patterns and levels were similar between the adult and fetal samples, which suggest that the interchangeable use of fetal and adult T cells in gene-specific functional assays is generally valid. Five of the genes tested, however, showed major differences in either expression levels or patterns. The transcription factors *Id1* and *Id2* are expressed at much higher levels in the fetal samples. *Deltex1* and CD3ε are also expressed at increased levels in fetal samples. Several genes additionally have a more moderately differing expression pattern such that the genes remain on to a later stage in fetal T-cell development than in adult T-cell development. Of particular interest is the expression pattern of the transcription factor SpiB, a close relative of the transcription factor PU.1 that is required more stringently in fetal T-cell development than in postnatal T-cell development. We considered the possibility that postnatal T cells might not require PU.1 so much if they could use SpiB as a substitute, and if they expressed higher levels of *SpiB* than fetal cells. Instead, *SpiB* showed a markedly increased level of expression in the fetal samples, up to 50-fold, and especially elevated in one of the later stages. These results raise the novel possibility that SpiB may actually be antagonistic to PU.1 in early T-cell development.

College of Notre Dame of Maryland

385. Identifying the potential regulatory elements controlling PU.1 expression

Mark Zarnegar

Expression of the Ets family transcription factor PU.1 is restricted to hematopoietic cells and is differentially expressed in the various blood lineages. The transcription factors controlling PU.1 transcription and the regulatory elements through which they function have yet to be determined. We are particularly interested in understanding how PU.1 is turned off in developing T-cells. Early thymic precursors (DN1 and DN2) express PU.1 but cease to express it by the time they become committed to the T-cell lineage (DN3). Failure to turn off expression prevents further T-cell development. By comparing the sequences of the mouse and human loci, we have identified several pockets of **C**onserved **E**lements (CE1-9) upstream of exon 1 that may function to regulate PU.1 transcription.

DNase hypersensitivity (DHS) and chromatin immunoprecipitation assays (ChIP) were used to characterize the accessibility of the conserved upstream regions. The DHS assays revealed regions of chromatin that are open in both PU.1 expressing myeloid cells and in non-expressing T cells, at -14 kb near CE8-9. ChIP assays were used to examine the acetylation patterns of histones 3 and 4, and of methylated histone 3 at lysine 4. These histone modifications are correlated with gene expression. Using quantitative real-time PCR to analyze the ChIP assays, several distinct patterns emerged. Myeloid cells (express high levels of PU.1) showed a high degree of acetylated H3 and H4 across regions CE1-CE9. Early B cells (moderately express PU.1) showed high levels of acetylation at only CE1, CE8, and CE9. While committed T cells (do not express PU.1) also have elevated levels of H3 and H4 acetylation at CE8 and CE9 relative to CE1-7, the degree of histone modification is much less than the PU.1 expressing lineages. The data suggests CE3-7 may contain a myeloid-specific enhancer, while CE8-9 may be non-specific but critical to all PU.1 expressing cells.

Much effort has gone into identifying the transcription factors that bind and thus regulate the activity of the potential regulatory elements. Previous electrophoretic mobility shift assays implicated two important transcription factor families, Ets and Runx, which may contribute to the regulated expression of PU.1. Members of these families bind CE8 *in vitro*. *In vivo* footprinting also suggests CE8 is bound by Runx and/or Ets proteins. The footprinting analysis also indicates that CE8 is occupied by different factors in T cells, B cells, and myeloid cells, perhaps contributing to the different PU.1 expression patterns in these lineages. Gel shifts are currently being performed for CE4 and CE5. We are also using ChIP assays to look for transcription factor occupancy of the conserved domains *in vivo*. Co-transfection with Runx, Ets, and other transcription factor expression constructs, transcription factor specific siRNAs, and dominant repressor (engrailed fusions) forms of transcription factors, along with our reporter constructs, is now under way. With our protein binding assays and co-transfection experiments, we hope to provide a clear model for how PU.1 expression is controlled at the molecular level.

386. Cell type-specific epigenetic marking of the *IL2* gene at a distal *cis*-regulatory region in competent, nontranscribing T cells

Satoko Adachi

T cells retain cell type-specific programming for IL-2 inducibility through many rounds of division even without being stimulated to transcribe the locus. To understand the layering of controls needed to poise this gene heritably for activation, we have used chromatin immunoprecipitation to map histone modifications across the murine *IL2* locus, from –10.2 through +0.25 kb, in induction-competent and incompetent cells. In highly inducible EL4 T-lineage cells, stimulation with PMA/A23187 induced strong acetylation of histone H3 and H4, in parallel with transcriptional activation, from –4.6 through +0.25 kb. However, dimethylation of histone H3/K4 was already fully elevated across the same restricted domain before stimulation, with little change after stimulation. RNA polymerase II binding, in contrast, was only found at the known promoter region after stimulation. Similar patterns of histone modifications were seen also in normal IL-2-inducible T-lineage cells. However, neither acetylated histone H3, H4 nor dimethylated histone H3/K4 marking was detected, with or without stimulation, in expression-incompetent cells (NIH/3T3 or Scid.adh). These results identify a discrete new domain of *IL2* regulatory sequence marked by dimethylated histone H3/K4 in expression-permissive T cells even when they are not transcribing *IL2*. This epigenetic mark correlates tightly with competence of the *IL2* locus to be induced and sets boundaries for histone H3 and H4 acetylation when the *IL2* gene is transcriptionally activated.

387. Defects in early T cell development in non-obese diabetic (NOD) mice

Mary Yui

Autoimmunity in the non-obese diabetic (NOD) mouse is dependent upon a balance between pathogenic and regulatory T cells. Various defects have been reported in the immature and mature $\alpha\beta$-TCR$^+$ cells, NKT and NK cells of NOD mice, all of which share common T-cell precursors. We previously found that immunodeficient NOD-*scid* and –*Rag^{null}* mice, which cannot rearrange a T-cell receptor, spontaneously break through the β-selection checkpoint, at which the cells should arrest. This checkpoint violation demonstrates a defect in early T cell differentiation programming in NOD mice. In addition, the developing T cells express unusually high or low levels of several cell surface receptors that are known to modulate TCR signal transduction, and may thereby contribute to the breakthrough phenotype. To investigate whether T-cell progenitors in wild-type NOD mice, in the presence of ongoing TCR rearrangements, also exhibit aberrant development around the β-selection checkpoint,

an *in vitro* T-cell developmental assay was used. TCR⁻CD4⁻CD8⁻ T cell progenitors from the thymuses of NOD and control C57BL/6 mice were isolated and cultured with OP9 stromal cells expressing the Notch ligand, Delta-like 1 (OP9-DL1), which have been shown to permit T-cell development. Control C57BL/6 T-cell progenitors underwent normal development into αβ-TCR⁺CD4⁺CD8⁺ double positive (DP) cells. Despite similar initial kinetics of differentiation and proliferation, NOD T-cell progenitors differed in development from control C57BL/6 progenitors by production of low numbers of TCR-αβ⁺ DP cells, either by a failure of survival or by diversion to the γδT-cell lineage. Diversion to the γδT-cell lineage from T-cell precursors has recently been shown to result from high levels of TCR signaling, while lower levels of signaling result in more αβT cells. This result is consistent with the results from NOD-*scid* and –*Rag⁻ᐟ⁻* mice, which suggest abnormally high levels of spontaneous signaling at the β-selection checkpoint. Furthermore, NOD precursor T cells also express abnormal levels of surface receptors that are known to affect levels of TCR signals being transduced. Molecular and genetic approaches will be used to determine the sources of these T-cell developmental defects and their possible relationship to diabetes in NOD mice.

388. Immunological receptors and immunological transcription factors before the immunological "big bang"

Jonathan Moore, Rashmi Pant, Stephanie Adams

Several reports from our lab have shown how the development of immunological lineages is conserved from the mammals down to the cartilaginous fish. We seek to push this understanding one step further back by (1) cloning and characterizing the sea lamprey versions of the transcription factors involved in this developmental program and (2) discerning the regulation of the lamprey variable lymphocyte receptor (VLR), a novel immunological gene with a different generator of diversity from the gnathostomes' immunoglobulin and T-cell receptor genes. Previously, lamprey factors PU.1, two Gata factors, one Ebf factor, and Pax-2/5/8 were identified. Using flow cytometric sorting on the basis of light scatter, we isolated lamprey lymphocytes from ammocoete typhlosole and kidney and determined that these factors are expressed in the putative lymphoid cells. However, to show that the expression levels detected are meaningful, we sought a functionally important lamprey lymphocyte effector gene that might depend for its expression on any subset of these transcription factors. Therefore, we established a collaboration with Drs. Zeev Pancer and Max Cooper, of the University of Alabama, Birmingham, and with Dr. Chris Amemiya, of the Benaroya Institute, Seattle, to use the VLR gene as a model for analysis of lamprey lymphocyte gene regulation.

To start mapping sequences that could be important for regulation of the VLR, several bioinformatic searches were performed including the comparison of the lamprey VLR to four hagfish VLRs. From these searches, we found a relatively conserved region near the transcription start site that had many predicted binding sites of transcription factors involved in the development of immunological lineages. Also, the 12 kb upstream of the lamprey VLR gene have been cloned. We are proceeding stepwise to seek evidence for transcriptional activity in a heterologous system to provide a basis for transactivation assays using specific lamprey transcription factor genes. A 1.1 kb region from the VLR gene 5'-flanking region inserted upstream of a luciferase reporter gene appears promising as a transcriptional regulatory region as it shows efficient transcriptional activity in two mammalian cell types, Jurkat cells and NIH 3T3 cells.

Publications

Adachi, S. and Rothenberg, E.V. (2005) Cell type-specific epigenetic marking of the *IL2* gene at a distal *cis*-regulatory region in competent, nontranscribing T cells. *Nucl. Acids Res.* **33**:3200-3210.

Dionne, C.J., Tse, K.Y., Weiss, A.H., Franco, C.B., Wiest, D.L., Anderson, M.K. and Rothenberg, E.V. (2005) Subversion of T lineage commitment by PU.1 in a clonal cell line system. *Dev. Biol.* **280**:448-466.

Rothenberg, E.V. (2005) Thymic regulation – Hidden in plain sight. *Science* **307**(5711):858-859.

Rothenberg, E.V. and Pant, R. (2004) Origins of lymphocyte developmental programs: Transcription factor evidence. *Semin. Immunol.* **16**:227-238.

Rothenberg, E.V. and Taghon, T. (2005) Molecular genetics of T-cell development. *Annu. Rev. Immunol.* **23**:601-649.

Taghon, T., David, E.-S., Zúñiga-Pflücker, J.C. and Rothenberg, E.V. (2005) Delayed, asynchronous, and reversible T-lineage specification induced by Notch/Delta signaling. *Genes Dev.* **19**:965-978.

Taghon, T., Yui, M.A., Pant, R., Diamond, R.A. and Rothenberg, E.V. Developmental and molecular characterization of emerging β- and γδ-selected pre-T cells in the adult mouse thymus. Submitted for publication.

Yui, M.A. and Rothenberg, E.V. (2004) Deranged early T-cell development in immunodeficient strains of non-obese diabetic (NOD) mice. *J. Immunol.* **173**:5381-5391.

Anne P. and Benjamin F. Biaggini Professor of Biological Sciences: Melvin I. Simon
Member of the Professional Staff: Sangdun Choi
Senior Research Associate: Iain D.C. Fraser
Senior Research Fellow: Sang-Kyou Han
Postdoctoral Scholars: Adrienne Driver, Jong-Ik Hwang, Kum-Joo Shin
Visiting Associate: Tracy L. Johnson
Visitors: Pamela Eversole-Cire, Ung-Jin Kim, Ana Mendez
Research and Laboratory Staff: Mi Sook Chang, Joyce Kato, Santiago Laparra, Jamie Liu, Josephine Macenka, Valeria Mancino, Blanca Mariona, Ji Young Park, Leah Santat, Estelle Wall, Joelle Zavzavadjian, Shu Zhen (Jaclyn) Zhou, Xiaocui Zhu

Summary: The Alliance for Cellular Signaling (AfCS) has focused its attention on G protein-mediated signaling circuitry in RAW 264.7 cells. In its new truncated configuration, the Alliance involves three laboratories and one computational center. The Caltech laboratory continues to work on the development of molecular biological approaches to target specific gene knockdown and to develop assays for G protein-mediated function. We have developed a series of complex vectors that allow the efficient production of microRNAs that eliminate specific gene expression. These include vectors that drive shRNA expression from RNA polymerase II or RNA polymerase III promoters, novel vectors that can inducibly express shRNA and vectors that express multiple shRNAs. We are concentrating both on genes that are expressed in known G protein-mediated circuits as well as on genes that are required for crosstalk and integration of signaling in these circuits. We are collaborating with Robert Bao in Dr. Steve Quake's laboratory to design microfluidic systems that would allow us to do high throughput screening of cell lines modified to eliminate expression of specific gene functions. We have succeeded in silencing multiple Gβ subunits. The double knockout of these isoforms results in the elimination of a large fraction of signaling that is regulated by the heterotrimeric G protein system. In addition, we are applying an approach involving the use of gene silencing to address questions of G protein function *in vivo* by combining work with RNAi and studies involving G protein deficient mice.

Work is continuing on our collaboration with the Anderson laboratory involving the MRG receptor system and its relationship to nociception. We have found that the G protein effectors PLCβ3 and PLCβ4 are expressed in different subsets of nociceptive neurons. We are currently attempting to determine if this segregation of expression underlies a functional difference in the way these neurons handle G protein-mediated signaling.

Finally, we have completed work on the function of the phosphorylated domain of the bacterial chemotaxis protein, CheA and have developed a much clearer picture of the mechanisms involved in the catalysis of phosphate transfer in this signaling system.

389. Molecular Biology Laboratory of the Alliance for Cellular Signaling (AfCS)
Iain Fraser, Joelle Zavzavadjian, Leah Santat, Jamie Liu, Estelle Wall, Christine Kivork, Melvin I. Simon

The main focus of the AfCS Molecular Biology lab remains the optimization of RNAi-based perturbation of signaling genes in the RAW264.7 mouse macrophage cell line. We previously described a strategy which involved the screening of four rationally designed siRNA sequences for each target gene, and the subsequent conversion of the most potent siRNA to an shRNA for lentivirus-based stable expression in RAW cells. In this commonly used approach, the RNA polymerase III-driven shRNA is designed to be a substrate for Dicer, with the aim that the Dicer cleavage product be equivalent to the effective siRNA. Although straightforward in theory, we have found several issues with this strategy; approximately 33% of the shRNAs are significantly less potent than the effective siRNA on which they were based, knockdown of the target gene is often lost over time in culture or after freeze/thaw of the stable cell line, and the pol III promoters have limited options for inducible expression. Recent advances in the understanding of microRNA processing have allowed the development of a more versatile and effective approach to RNAi in RAW264.7 cells. Based on an approach described by Greg Hannon and co-workers, we now express gene-specific shRNAs embedded in a larger 'miRNA-like' transcript that is a substrate for the RNAi microprocessor complex. This approach confers several advantages; we have a considerably higher success rate in identifying multiple effective shRNAs against each target gene, the long-term stability of target knockdown in the cell line is improved, and since the miRNA transcripts can be driven from RNA polymerase II promoters, we can use the well established tetracycline-based systems to control shRNA expression. The laboratory continues to work closely with the other AfCS laboratories at UCSF, UTSW and Berkeley to apply this technology to the modeling of signal transduction pathways in the RAW264.7 cell line.

238

390   Analysis of subcellular localization of cAMP in macrophage using FRET-based indicators
Adrienne Driver, Iain D.C. Fraser

Nearly one in every five genes of the human genome encodes a protein involved in cellular signaling. Despite this large number of potential effectors, many cellular signaling events with unique outcomes utilize the same intermediate signaling components. These findings have lead to the proposal that signaling scaffolds exist to direct signaling events to the correct targets, thus providing signaling specificity. Evidence for the existence of these scaffolds came with the advancement in cellular imaging where for the first time cAMP, a second messenger molecule, originally believed to diffuse freely within the cytoplasm showed discrete domains of intracellular localization. In macrophage, the regulation of cytokine production occurs by many mechanisms. Examples include the induction of pro-inflammatory cytokines by TLR4 (toll-like receptor 4) activation, and attenuation of pro-inflammatory cytokine production through PGE_2 signaling. Macrophages stimulated by LPS in the presence of PGE_2 express and produce much lower levels of IL-1β, MIP-1α, and TNFα. In addition PGE_2-stimulated macrophage show a reduced level of phagocytosis. The attenuation seen in the pro-inflammatory response is due to a rise in cAMP levels typical of PGE_2 signaling through receptors EP_2 and EP_4. To determine the mechanism whereby PGE_2-mediated cAMP production leads to attenuation of macrophage activation, fluorescent indicators for the cAMP pathway have been stably integrated into the genome of RAW 264.7 macrophage using a retroviral vector system. The FRET constructs expressed within these cells allow the monitoring of subcellular localization of increases in cAMP levels or cAMP-dependent protein kinase activity after stimuli in live cells over time. By identifying which subcellular locations contain increased cAMP levels and kinase activity, potential signaling complexes involved in the control of macrophage activity may be identified.

391.   The roles of phospholipse Cβ isozymes in primar nociceptive neurons
Sang-Kyou Han, Valeria Mancino, Melvin I. Simon

A variety of extracellular signals are transduced by G-protein coupled receptor (GPCR) activated circuits that include the enzyme phosphoinositide-specific phospholipase Cβ (PLCβ). There are four isozymes of PLC-β, β1-β4, and some of these isoforms are thought to function in nociceptive signaling. Here, we investigated the roles of PLCβ isozymes in primary sensory neurons associated with nociception by using mutant mice deficient for specific PLCβ isoforms. Expression analysis indicates that PLCβ3 and β4 are expressed in different subsets of sensory neurons. Moreover, PLCβ3 is predominantly expressed in a sub-population of C-fiber nociceptors, while PLCβ4 is expressed in A fiber. In line with expression analysis, calcium measurements revealed that PLCβ3

mediates ATP induced calcium responses by selectively coupling to P2Y receptors in nociceptive neurons, whereas PLCβ4 didn't affect the calcium responses to ATP. These results demonstrate that PLCβ3 and β4 are spatially segregated in sensory neurons and may couple to different sets of receptors and effectors to generate or mediate different modes of nociceptive signaling or sensory modalities.

392.   Study of G protein signaling by silencing the expression of multiple Gβ subunits
Jong-Ik Hwang, Sangdun Choi, Iain D.C. Fraser, Mi Sook Chang, Melvin I. Simon

The G$\beta\gamma$ subunit complex derived from heterotrimeric G-proteins can act to regulate the function of a variety of protein targets. We established lentiviral-based RNA interference in J774A.1 mouse macrophages to characterize the role of Gβ in GPCR signaling. The expression of Gβ1 and Gβ2, the major subtypes present in J774A.1 cells, was eliminated by sequential treatment with shRNA-expressing lentivirus. These $\beta\gamma$ complex deficient cells lost the ability to respond to G-protein mediated signals. Chemotaxis and the phosphorylation of Akt in response to C5α were both blocked. Similarly, C5α-mediated actin polymerization, C5a and UTP-stimulated intracellular calcium mobilization and the stimulation of cAMP formation by isoproterenol were all eliminated in the absence of the Gβ subunits. In addition, stabilization and membrane localization of several Gα and Gγ subunit proteins was strongly effected. Furthermore, in DNA microarray analysis, regulation of gene expression stimulated by PGE2 and UTP was not observed in cells lacking Gβ subunits. In contrast, phagocytotic activity, serum-dependent cell growth and the patterns of gene expression induced by stimulating the Toll receptors with LPS were similar in wild-type cells and shRNA-containing cells. Thus, ablation of the Gβ subunits destabilized Gα and Gγ subunits and effectively eliminated G protein mediated signaling responses. Unrelated ligand-regulated pathways remained intact. These cells provide a system that can be used to study signaling in the absence of most G protein-mediated functions.

Publication
Hwang, J.-I., Choi, S., Fraser, I.D.C., Chang, M.S. and Simon, M.I. (2005) *Proc. Natl. Acad. Sci. USA* **102**:9493-9498.

393. Signal transduction in immune cells
Sangdun Choi, Mi Sook Chang, Xiaocui Zhu, Jong-Ik Hwang, Melvin I. Simon

Our interest is in deciphering complex signaling systems and control networks using immune cells. Transcriptional analysis of the mouse primary B cell single/double ligand screen with 33 ligands was carried out (http://www.signaling-gateway.org/). The data suggested interesting crosstalk in the signaling pathways downstream of the proliferative ligands such as anti-IgM, CD40L, LPS, IL-4 and CpG [*J. Immun.* (2004) **173**:7141-7149]. B cells derived from human Bcl2 transgenic mice have sustained survival in culture. While signaling parameters measured in Bcl2 transgenic B cells showed similar intracellular calcium flux, phosphorylation of a panel of signaling proteins and chemotaxis, expression changes in glycolysis genes were observed [*AfCS Research Reports* (2004) **2**:13BC].

We have analyzed transcriptional and cytokine changes after the addition of single or double ligands in the macrophage cell line RAW264.7. A time series examining the combinational effects of LPS/IFNγ, LPS/2MA, LPS/PGE2, LPS/ISO, C5a, CpG, PAM2, PAM3, polyIC and Taxol enabled identification of the signal networks causing non-additive effects related to Toll-like receptors and G protein coupled receptors.

We have examined the relative effectiveness of RNAi methodology using macrophage RAW and J774 cells transfected with lentiviral shRNA, siRNA or antisense oligonucleotide in order to further develop RNA interference as a gene expression knockdown tool. Silencing the expression of multiple Gβ subunits (Gβ1/2) in macrophage using RNA silencing machinery eliminates signaling mediated by all four families of G-proteins (Gs, Gi, Gq and G12). All GPCR-mediated cellular responses induced by PGE2, ISO, C5a or UTP were eliminated but not those induced by LPS.

394. Lentiviral systems for inducible RNAi
Kum-Joo Shin, Melvin I. Simon

RNA interference (RNAi) is a very useful method to suppress expression of specific genes in mammalian cells. For further spatial and temporal regulation of gene expression, we have developed an inducible RNAi system that contains the entire tetracycline-regulated system in a single lentiviral vector. Expression of primary microRNA-based short hairpin RNAs and subsequent gene knockdown is regulated by a doxycycline-bound transactivator. Because lentiviral vectors can deliver DNAs to a variety of dividing and nondividing target cells, this inducible RNAi system can be used to study gene functions in cells and animals. We will apply it to some of the issues involved in understanding G-protein function and crosstalk.

395. Identification of retinal ganglion cell-specific and -enriched genes
Kum-Joo Shin, Melvin I. Simon

Retinal ganglion cells (RGCs) are the output neurons that transmit visual information to the brain. There are more than 12-15 subsets of RGCs of distinct morphologies and functions based on anatomic and physiological studies. However, the molecular mechanisms underlying the specific function of these cells is not yet known. Therefore, we investigated RGC-enriched genes by isolating RGCs using antibody for thy-1, a RGC marker, and subsequent microarray with total RNA from RGCs and RGC-depleted retinal cells to compare the expression pattern of genes. The results were confirmed with quantitative RT-PCR and *in situ* hybridization. Identified genes were classified into four groups: i) genes expressed in amacrine cell layer and the ganglion cell layer; ii) genes expressed in the majority of cells in the ganglion cell layer; iii) genes expressed in the inner nuclear layer and the subset of the ganglion cell layer; and iv) genes expressed in subsets of ganglion cells. We are currently pursuing the function and cellular localization of these genes.

396. Microfluidic platform for single cell fluorescence experiments
Robert Bao, Melvin I. Simon

We are working to establish an experimental platform for probing calcium responses in mammalian cells within microfluidic devices. Using pressure-actuated microvalves, we can precisely gate and switch flow to cells anchored to microchannel floors. Because the devices are permeable to oxygen and carbon dioxide, cells can be cultured in the device for up to several days under conditions that effectively mimic those found in a cell culture incubator. Calcium responses in hundreds of individual cells can then be imaged through the device using standard epifluorescence microscopy.

Using of microfluidic devices has several advantages: (1) we have excellent control over perfusion conditions that the cells experience, both during culture and experiment; (2) many separate experiments may be incorporated into a single microscope field-of-view, so that several different conditions, including positive and negative controls, may be integrated into a single experimental data acquisition run; (3) cells can be kept in culture between different experiments, so that long-term, cell-to-cell variability's in responses to different ligands can be probed; and (4) reagent volume requirements for cell stimulation are much lower than those in conventional cellular assays, so there are significant potential cost savings for expensive reagents.

We are currently working with a device design with six separate channels for use during experiment's. Preliminary results for RAW macrophages stimulated with UDP are comparable to those seen in single-cell experiments performed in macroscopic wells. Work is still ongoing to probe and understand the effects of flow rate and shear stress, both during cell preparation and ligand

stimulus, on cellular calcium responses. In addition to the general scientific interest, understanding these issues promises to improve data quality and consistency for many experiments involving solution exchange.

Publications

Hwang, J.-I., Choi, S., Fraser, I.D.C., Chang, M. and Simon, M.I. (2005) Silencing the expression of multiple Gβ-subunits eliminates signaling mediated by all four families of G-proteins. *Proc. Natl. Acad. Sci. USA* **102**:9493-9498.

Kovoor, A., Barghashoon, S., Seyffarth, P., Chen, C.-K., Schwarz, S., Axelrod, J.D., Simon, M.I., Lester, H.A. and Schwarz, J. (2005) D2-dopamine receptors colocalize DEP domains. Mice lacking the DEP domain containing protein, RGS9, develop dyskinesias associated with dopamine pathways. *J. Neurosci.* **25**:2157-2165.

Kunapuli, P., Lee, S., Zheng, W., Alberts, M., Kornienko, O., Mull, R., Hwang, J.-I., Simon, M.I. and Strulovici, B. Identification of small molecule antagonists of the human MRG-X1 receptor. *Mol. Pharmacol.* In press.

Quezada, C.M., Hamel, D.J., Gradinaru, C., Bilwes, A.M., Dahlquist, F.W., Crane, B.R. and Simon, M.I. (2005) Structural and chemical requirements for histidine phosphorylation by the chemotaxis kinase CheA. *J. Biol. Chem.* **280**:30581-30585.

Quezada, C.M., Gradinaru, C., Simon, M.I., Bilwes, A.M. and Crane, B.R. (2004) Helical shifts generate two distinct conformers in the atomic resolution structure of the CheA phosphotransferase domain from *Thermotoga maritima*. *J. Mol. Biol.* **341**:1283-1294.

Roca, A., Shin, K.-J., Liu, X., Simon, M.I. and Chen, J. (2004) Comparative analysis of transcriptional profiles between two apoptotic pathways of light-induced retinal degeneration. *Neuroscience* **129**:779-790.

Zhu, X.C., Hart, R., Chang, M.S., Kim, J.-W., Lee, S.Y., Cao, Y.A., Mock, D., Ke, E., Saunders, B., Alexander, A., Grossoehme, J., Yan, Z., Hsueh, R., Lee, J., Scheuermann, R.H., Fruman, D.A., Seaman, W., Subramaniam, S., Sternweis, P., Simon, M.I. and Choi, S. (2004) Analysis of the major patterns of B cell gene expression changes in response to short-term stimulation with 33 single ligands. *J. Immun.* **173**:7141-7149.

Thomas Hunt Morgan Professor of Biology: Paul W. Sternberg
Senior Research Associate: Jane E. Mendel
Research Fellows: Ryan Baugh, Todd Ciche, Byung Hwang, Takao Inoue, Mihoko Kato, Hans-Michael Müller, Alok Saldanha, Gary Schindelman, David Sherwood, Jagan Srinivasan, Cheryl Van Buskirk, Allyson Whittaker, Xian-Zhong Xu, Weiwei Zhong
Graduate Students: Jolene Fernandes, Steven Kuntz, Anusha Narayan, Ted Ririe, Jennifer Sanders, Adeline Seah, Hui Yu
Research and Laboratory Staff: Mary Alvarez, Christopher Cronin, John DeModena, Shahla Gharib, Gladys Medina, Barbara Perry
WormBase Staff: Yesenia Alvarado, Igor Antoshechkin, Carol Bastiani, Juancarlos Chan, Wen Chen, Lisa Girard, Eimear Kenny, Ranjana Kishore, Raymond Lee, Cecilia Nakamura, Andrei Petcherski, Erich Schwarz, Kimberly Van Auken, Daniel Wang
Collaborators: Eric Mjolsness, Virendra Sarohia, Barbara Wold

Summary: We seek to understand how the genome controls the development, behavior and physiology of *C. elegans*. Our main foci are on signaling pathways and transcriptional regulation. Our approaches are experimental, computational and synthetic. Specifically, we use molecular genetics to understand detailed mechanisms, and functional genomics to obtain global views of development and behavior. We take computational approaches to understand signal transduction, developmental pattern formation and behavioral circuits. We try to couple tightly computation and experimental data. We are also trying to modify nematodes and their cells to test our understanding of fundamental biological principles. Moreover, we study other genomes, genetics, and biology of other nematodes to help us comprehend *C. elegans*, to learn how development and behavior evolve, and to learn how to control parasitic and pestilent nematodes.

In the area of signal transduction, we continue to define pathway interactions and to understand the determinants of signaling specificity: How does the same pathway lead to distinct outcomes in different tissues? For these studies we analyze EGF-receptor signaling, WNT signaling, TRP channels, and G protein mediated-signaling pathways. We have found a new role for EGF signaling, controlling synaptic transmission.

Vulval development involves a remarkable series of intercellular signaling events that coordinate the patterning of the uterine and vulval epithelia and allow them to connect precisely. Specification of the anchor cell from the ventral uterine epithelium breaks the symmetry of the gonad. The anchor cell then produces the vulval-inducing signal, LIN-3, an epidermal growth factor-like protein that acts via *C. elegans* homologs of EGF-receptor, RAS and MAP kinase. Inductive signaling is regulated at the level of ligand production, as well as the responsiveness of the receiving cells. LIN-3 is produced in a highly localized and regulator manner. After the anchor cell induces the vulva, a complex program of further pattern formation, cell type specification and morphogenesis follows. The primary (1°) vulval lineage generates an E-F-F-E pattern of cell types, while the 2° vulval lineage generates an A-B-C-D pattern of cell types. We now have our hands on a number of receptor proteins, transcription factors and regulated genes; we are trying to define this regulatory network to understand how organogenesis is genetically programmed. The anchor cell recognizes one of the seven vulval cell types and invades the vulval epithelium in a process akin to tumor metastasis, and we have found genes necessary for this process. Regulation by the EGF-receptor, WNT and HOM-C pathways impinge not only on vulval development but also the neuroectoblast P12 specification and male hook development. By comparing these examples with vulval development, we seek to understand the signaling specificity and signal integration.

Our efforts in genomics are experimental and computational. Our experimental genome annotation includes finding the 5' ends of mRNAs with a new method we developed, identifying *in vitro*, binding sites for transcription factors, testing enhancer function in transgenic worms, and systematic inactivation of *C. elegans* transcription factors. We are investigating ways to compare the genomes of *Caenorhabditis* species. We are collaborating with the Genome Sequencing Center of Washington University to annotate new nematode genomes. Our computational projects involve establishing pipelines for *cis*-regulatory computational analysis, new programs to use orthology and known binding sites or motifs, etc. We have started to combine information from worms, flies and yeast to predict gene-gene interactions in *C. elegans*.

We are part of the WormBase consortium, which develops and maintains WormBase, a web-accessible comprehensive database of the genome, genetics and biology of *C. elegans* and close relatives (www.wormbase.org). We initiated WormBook, an open-access online text of *C. elegans* biology associated with WormBase. We have developed Textpresso (www.textpresso.org), an ontology-based search engine for full text of biological papers. Textpresso is used by *C.*

elegans researchers, as well as WormBase staff; it is being expanded to other organisms and fields of study. We are also part of the Gene Ontology Consortium (www.geneontology.org), which seeks to annotate gene and protein function with a standardized, organized vocabulary. WormBase, Gene Ontology and Textpresso are part of the Generic Model Organism (GMOD) Project (www.gmod.org), a collaborative project among organism-specific databases to develop generic software.

Our behavioral studies focus on understanding male mating behavior, as well as locomotion of both sexes. For specific projects we study egg laying, feeding, chemotaxis, osmotic avoidance, among other simple behaviors. Mating behavior, with its multiple steps, is arguably the most complex of *C. elegans* behaviors. Because it is not essential for reproduction, given the presence of internally self-fertilizing hermaphrodites, male mating is useful to elucidate how genes control behavior. We are studying several aspects of male mating behavior to understand the neuronal circuits that control the behavior and how they are genetically encoded. Our comparative studies include both analyzing behavioral differences among species, and genetic analysis of *C. briggsae*, *Pristionchus pacificus* (a nematode species we discovered during the 1990's), and *Heterorhabditis bacteriophora* (an insect-killing nematode).

We have developed a machine-vision system that automatically quantifies the locomotion of nematodes. We use this system to study individual genes, to examine epistatic interactions among genes, and to obtain data to support mathematical modeling efforts. The system works reasonably well with *Drosophila* larvae. We are expanding this effort to analyze mating behavior of nematodes.

We are involved in efforts to model worm movement, vulval pattern formation and aspects of signal transduction. We are trying to modify *C. elegans* cells to test our understanding of signal processing by sensory neurons and of the circuits that control locomotion. We are also trying to adapt bacterial and yeast circuits for use in *C. elegans*, as tools to understand circuits.

397. *C. elegans evi-1* proto-oncogene *egl-43* is involved in the Notch-dependent AC/VU cell fate specification
Byung Joon Hwang

The specification of the anchor cell (AC) and ventral uterine precursor cell (VU) fates is a model system for understanding how the interaction between a Notch-family receptor and a Delta-family ligand specifies cell fates of two neighboring cells. In this binary specification process, two neighboring cells in the *C. elegans* somatic gonad, named Z1.ppp and Z4.aaa, have equal potentials to become the AC and VU cells. The interaction between LIN-12 (Notch ortholog) receptor and its corresponding ligand LAG-2 (Delta ortholog) is known to initiate the specification process and act via LAG-1 (S(H) ortholog). Both LIN-12 and LAG-2 are initially expressed equally in the both Z1.ppp and Z4.aaa cells. The subsequent

stochastic bias of their expression levels triggers positive and negative feedback loops of unknown mechanisms, eventually one cell expresses only LAG-2, becoming the AC, and the other expresses only LIN-12, becoming the VU cell. The understanding of these feedback mechanisms and the cell fate establishment process has been hampered by the lack of identification of the LIN-12 downstream molecules involved in this process.

During the last year, we have obtained evidence that *egl-43*, *C. elegans* ortholog of mammalian proto-oncogene evi-1, is involved in the AC/VU cell fate specification as a downstream molecule of *lin-12* Notch. We found that *egl-43* is necessary for the cell fate specification and also that both genes, *egl-43* and *lin-12*, are expressed in the same cells in the somatic gonad. Epistasis analysis of measuring their genetic interaction suggests that *egl-43* is downstream of *lin-12*. Finally, LIN-12/LAG-1 binding sites in the *egl-43* gene are involved in its expression in the AC/VU cells during the specification process. In the future, this research will lead to the understanding of mechanisms that Notch signaling specifies cell fates.

398. Ryk/Wnt and Frizzled/Wnt pathways control patterning of the P7.p vulval lineage
Takao Inoue

The Wnt family of secreted signaling proteins controls many aspects of animal development. In many systems, Wnt signals are transduced by the "canonical" pathway, which involves the Frizzled seven-transmembrane receptors and downstream components. More recently, the Ryk family of receptor tyrosine kinases has emerged as alternative receptors for Wnts. Although the Ryk family is conserved in vertebrates, insects and nematodes, little is known regarding its mode of action, including whether it functions as a coreceptor of Frizzled or in an independent pathway.

We are currently analyzing Wnt signaling in late vulval patterning. During this process, three vulval precursors (P5.p, P6.p and P7.p) divide and differentiate to produce seven different cell types (vulA, vulB1, vulB2, vulC, vulD, vulE, vulF) in a specific spatial pattern. Availability of multiple (>15) gene expression markers makes this phase of vulval development an ideal system in which to analyze molecular mechanisms of organogenesis.

We found that mutations in *lin-17/Frizzled* and *lin-18/Ryk* control the anterior/posterior order of cell types produced by the P7.p precursor cell. Analysis of mutants and RNAi also indicated that *lin-44/Wnt, mom-2/Wnt* and *cwn-2/Wnt* function redundantly in this process. Interestingly, mutations in *lin-17* and *lin-18* mutually enhance each other in the double mutant. Also, the pattern of enhancement in *receptor; ligand* double mutants indicated that *lin-17* and *lin-18* exhibit distinct ligand preferences. Thus, our results indicate that *lin-17/Frizzled* and *lin-18/Ryk* function in parallel Wnt pathways, arguing against the model in which LIN-18/Ryk functions as a coreceptor for LIN-17/Frizzled.

We found that a source of the signal that orients the P7.p lineage is the somatic gonad. Laser ablation experiments by Wendy Katz and Paul W. Sternberg suggested that the gonad is required for proper patterning of the P7.p lineage. We found that *mom-2::gfp* is expressed in gonadal cells, including the anchor cell. These cells are positioned anterior to the P7.p lineage, and thus can provide the directional cue that determines the anterior/posterior orientation.

As an easily manipulated genetic system, the late patterning of *C. elegans* is ideally suited for genetic analysis of the Ryk signal transduction pathway. We are continuing the analysis of this pathway by searching for additional components using genetic screens.

399. The *C. elegans* orphan receptor tyrosine kinase gene *cam-1* negatively regulates VPC induction
Jennifer Sanders

Proper formation of the *C. elegans* hermaphrodite vulva results from the invariant pattern of induction and specification of three vulval precursor cells (VPCs) and depends on the integration of the Ras, Wnt, and Notch pathways. We are investigating the role of *cam-1*, the *C. elegans* homolog of the Ror family of receptor tyrosine kinases (RTKs), in VPC induction. Ror proteins contain extracellular Frizzled, Kringle, and Immunoglobulin domains and an intracellular tyrosine kinase domain. The ligand and downstream signaling components of Ror proteins are unknown at this time. We have identified *cam-1* as a negative regulator of the vulval induction process and are attempting to elucidate its relationship with the above pathways. We find a synthetic over induction phenotype of *cam-1* alleles in combination with alleles of *lin-17*(Frizzled) and of *lin-18*(Ryk). Over induction (also known as multivulva or Muv) is the resulting phenotype when greater than three VPCs are induced to adopt vulval fates.

In agreement with CAM-1 negatively regulating induction, we find that *cam-1* enhances the over induction phenotype of a *let-60*(Ras) gain-of-function mutation and suppresses the under induced (less than three VPCs induced) phenotype of two *lin-3*(EGF) alleles. In all cases, loss or reduction of *cam-1* activity correlates with increased vulval induction. We are performing further epistasis and biochemical studies to explore the signaling properties of CAM-1 during vulval development.

400. Dissection of gene regulatory networks involved in vulval patterning and differentiation
Jolene S. Fernandes

C. elegans vulval development leads to the generation of seven distinct vulval cell types, each with its own unique gene expression profile. The availability of diverse spatial and temporal vulval cell fate markers and the ease of manipulation at the single cell level provide us with powerful tools to study the execution of cell type-specific gene expression programs. Both Ras and Wnt-pathways are required for the proper patterning of 1°

vulval cell lineages. Also, both Wnt/Ryk and Wnt/Frizzled signaling pathways are necessary for patterning the P7.p 2° vulval descendants. However, the full mechanisms that establish the precise spatial patterning of the seven vulval cell types are not fully understood. Our current goal is to identify the gene regulatory network(s) that regulate the patterning and differentiation of the 1° and 2° vulval lineages.

To identify components of the regulatory network underlying vulval development, we conducted RNAi screens of most known transcription factors and assayed for the effect on expression of vulval cell fate markers. *ceh-2::YFP* is expressed in vulB cells during the L4 stage and was used to screen for cell fate transformation and/or ectopic specification of vulB fate. *nhr-67* was identified as a repressor of *ceh-2* expression in the 1° vulval descendants. *nhr-67* was also found to be required for *zmp-1* expression in vulA during the adult stage. Thus, *nhr-67* regulates gene expression in multiple vulval cell types. We have found that *nhr-67* exhibits a dynamic expression pattern in the vulval cells. Further analysis of *nhr-67* interactions with the other characterized transcription factors will help elucidate the paradigm of gene regulatory network(s) that operate during vulva morphogenesis.

401. Spatial and temporal coordination of organogenesis
Ted Ririe, Si Hyun Kim (CIT undergraduate)

Organogenesis requires a network of factors that direct spatial and temporal patterning. The spatial and temporal expression patterns of several marker genes in the seven adult vulval cell types of *C. elegans* are promising tools for identifying the genes involved in this coordination. Expression patterns of vulval cell fate markers such as *dhs-31::yfp* (predicted dehydrogenase) are altered in a *lin-29* (heterochronic gene, zinc finger transcription factor) mutant background, while expression patterns of others such as *zmp-1::gfp* (zinc metalloprotease) in the vulA cells of the vulva are not altered in the absence of *lin-29*. Genes involved in the regulatory network that controls cell fate determination in the vulva can be identified by conducting screens for mutations that alter these expression patterns. Cell fate markers indicate spatial regulation in the vulva, and *lin-29* is a candidate temporal regulator of vulval differentiation and morphogenesis. To understand the spatial and temporal coordination of organogenesis we studied the regulation of a cell fate marker that depends on *lin-29*, and another cell fate marker that is *lin-29*-independent. By screening via RNAi for transcription factors that regulate the late differentiation marker *dhs-31::yfp* we identified several transcription factors that may regulate vulval differentiation and morphogenesis in a *lin-29*-dependent manner. We also screened for transcription factors that regulate *zmp-1::gfp* expression in the vulA cells of the vulva to identify *lin-29*-independent pathways involved in the coordination of vulval differentiation and morphogenesis. Further analysis will reveal how these

factors interact to regulate expression of cell fate markers.

402. FOS-1a regulates gene expression during anchor cell invasion
David Sherwood

Cell invasion through basement membranes is crucial during morphogenesis and cancer metastasis. We have initiated a genetic dissection of this process during anchor-cell invasion into the vulval epithelium in *C. elegans*. By positional cloning a genetic locus (*evl-5*) defined by a mutation that disrupts anchor cell invasion, we have identified the *fos* transcription factor ortholog *fos-1* as a critical regulator of basement-membrane removal. In *fos-1* mutants, the gonadal anchor cell extends cellular processes normally toward vulval cells, but these processes fail to remove the basement membranes separating the gonad from the vulval epithelium. *fos-1* is expressed in the anchor cell and controls invasion cell autonomously. In particular, expression of one of the two *fos-1* cDNAs (fos-1) under the control of an anchor cell-specific transcriptional control region that we identified in previous studies rescues the phenotype of the *fos-1* mutant. We have identified ZMP-1, a membrane-type matrix metalloproteinase, CDH-3, a Fat-like protocadherin, and hemicentin, a fibulin family extracellular matrix protein, as transcriptional targets of FOS-1 that promote invasion. These genes are regulated by FOS-1a but we do not know if the regulation is direct. Triple mutants defective in *cdh-3*, *zmp-1* and *him-4* have an incompletely penetrant anchor cell invasion defect, indicating that there are additional targets of FOS-1a. These results reveal a key genetic network that controls basement membrane removal during cell invasion.

403. A physiological role for LET-23/EGFR in *C. elegans* feeding behavior
Cheryl Van Buskirk

The single EGF receptor homolog in *C. elegans*, LET-23, signals through the Ras/MAPK pathway to specify cell fates in the ventral cord, vulva, male tail, and excretory system. LET-23 also signals through a PLC-γ/IP3 pathway to regulate ovulation. We have observed that overexpression of the EGFR ligand LIN-3 from a heat shock-inducible promoter, in addition to affecting the expected cell fates, also slows down growth of the animals as compared to heat-shocked controls. This growth defect appears to be due to a complete and reversible cessation of pharyngeal pumping that occurs in response to overexpression of LIN-3 at any developmental stage, including the adult, and is not suppressed by mutations in the Ras/MAPK pathway. The growth/feeding defect is suppressed by mutations in *let-23* and PLC-γ, but not the IP3 receptor, suggesting that diacylglycerol (DAG) signaling may mediate this effect. In addition, mutants that cause selective neurodegeneration or compromise synaptic vesicle release act as potent suppressors, suggesting that LET-23 acts to control neurotransmission. This is the first evidence of a non-developmental role for EGFR in synaptic function.

404. Spicule development and signal transduction specificity
Adeline Seah

LET-23(EGFR) activates two signal transduction pathways: RAS-MAPK for P11/P12 cell fate determination, vulval development and male spicule development and IP$_3$-Ca^{2+} for ovulation. It is not known what determines the specificity among the Ras-MAPK-dependent inductions. One possibility is that different transcription factors act in parallel to or downstream of the EGF signal in different tissues. Hox genes have been implicated as one class of regulatory elements that confer specificity to the EGF pathway in P11/P12 cell fate determination, vulva and hook development.

In the male tail, anterior versus posterior fate specification of the four pairs of B.a great-granddaughter cells is partially determined by positional cues provided by other male-specific blast cells or their progeny. These four pairs are known as the ventral (aa), dorsal (pp) and two identical lateral pairs (ap/pa). Each pair of cells has an anterior (α, γ or ε) and a posterior (β, δ or ζ) fate that produce different cell lineages and distinct fates. *lin-3* (EGF) is likely to be the signal provided by the male-specific blast cells, U and F. Reduced activity of some of the genes in the EGF pathway causes abnormal anterior cell lineages. Expression of the Hox complex gene *ceh-13*::GFP was previously observed in B.γ. U and F ablations, as well as genetic analysis indicate that the EGF signal is required for *ceh-13* expression in B.γ. Thus, we are analyzing the regulation and function of *ceh-13* in the γ lineage.

lin-1, *lin-31*, *lin-39*, *eor-1*, *eor-2*, *elt-5*, *elt-6* and *egl-5* are transcription factors that have been found to function either downstream or in parallel to the EGF pathway in events other than male spicule development. *lin-1(lf)*, as well as *lin-31(lf)* animals exhibit loss of *ceh-13*::GFP. Thus, they are not responsible for specificity. The other six transcription factors are being tested for a role in specificity. To identify new factors, a RNAi screen is being carried out using loss or ectopic *ceh-13*::GFP expression as an assay.

405. Linker cell migration
Mihoko Kato, Shahla Gharib

The linker cell (LC), located at the proximal end of the male gonad, leads the migration of the elongating gonad to the posterior end of the worm. Its stereotypic migration along the bodywall begins in the anterior direction in L1 but then undergoes a 180° turn and continues posteriorly until it reaches the cloaca, where it is killed in the L4 molt. We have used an RNAi feeding library to screen a subset of the genome and have identified genes that are potentially required for proper LC migration. Of these genes, a SNF5 homolog, a transcription factor, and a G-protein coupled receptor are of particular interest because they are expressed by the LC, suggesting that they have a cell autonomous role in LC migration. We are currently investigating their function in

migration and attempting to construct a signaling pathway for these genes.

406. *C. elegans* L1 developmental arrest as a model for cancer and aging
Ryan Baugh

Larvae of the nematode *C. elegans* reversibly arrest development in acute response to starvation. Embryos that hatch in the complete absence of food arrest development before any post-embryonic development is observed (L1 arrest), and such arrested worms are resistant to numerous environmental stresses. Arrest can be maintained for weeks and normal development resumed once food is available. In contrast to the well-studied dauer arrest, L1 arrest is near instantaneous and occurs with no morphological modification. I have found that insulin signaling regulates L1 arrest, in addition to dauer arrest and aging. I am using a combination of genetic and microarray analyses to identify other pathways that regulate L1 arrest, as well as genes regulated by insulin signaling during implementation and maintenance of L1 arrest. I am also investigating the coordination of developmental timing with developmental arrest. Proper control of cell division and growth is crucial in preventing cancer, and this system provides a new model to study these controls. In addition, I find it intriguing that individual worms make a coherent all-or-none decision to arrest or develop; while the value of maintaining temporal coordination among the various cell lineages is obvious, the way it is accomplished is unclear.

407. Conservation rules and their breakdown in *Caenorhabditis* sinusoidal locomotion
Jan Karbowski, Christopher Cronin, Jane Mendel, Adeline Seah

Undulatory locomotion is common to nematodes, as well as to limbless vertebrates, but for nematodes there is not an understanding of its control in spite of the identification of hundred of genes involved in *C. elegans* locomotion. To reveal the mechanisms of nematode undulatory locomotion, we quantitatively analyzed the movement of *C. elegan*s with genetic perturbations to neurons, muscles, and skeleton (cuticle). We also compared locomotion of different *Caenorhabditis* species. We constructed a theoretical model that combines neural dynamics, mechanics, and biophysics, and that is constrained by the observations of propulsion and muscular velocities, as well as wavelength and amplitude of undulations. We find that normalized wavelength is a conserved quantity across a population of wild-type *C. elegans*, their mutants, and across related species. The velocity of forward propulsion scales linearly with the velocity of the muscular wave and the corresponding slope is also a conserved quantity and almost optimal; the exceptions are in some mutants affecting cuticle structure. Our hybrid model can explain the observed robustness of the mechanisms controlling nematode undulatory locomotion.

408. TRP-4 is necessary for normal locomotion of *C. elegans*
Shawn Xu, Barbara Perry

Now that we have established experimental and theoretical bases for studying *C. elegans* locomotion, we have started to identify genes that control the parameters of movement. We generated two deletion mutants of *trp-4*, which encodes a putative mechanoreceptor and TRP family cation channel. Both deletion mutants display the same two defects in locomotion: *trp-4* worms move at higher frequency and bend with greater amplitude. *trp-4* is expressed in a few classes of neurons, and by rescuing *trp-4* in each class of neuron, we can separate the roles of *trp-4* in controlling the frequency and amplitude roles of locomotion. We hypothesize that one role of *trp-4* is a mechanoreceptor that responds to large amplitude bends and thus, tunes the propagation of the sinusoidal wave.

409. Circuit-level model of oscillations generation used in *C. elegans* locomotion
Jan Karbowski, Gary Schindelman, Christopher J. Cronin, Paul W. Sternberg

The mechanism of oscillations generation required for *C. elegans* locomotion is unknown. We proposed and tested a circuit-level model of *C. elegans* locomotion. The mathematical model consists of dynamics of a local network of ventral and dorsal motor neurons, muscles, and mechano-sensory feedback. The nonlinear nature of the feedback loop is responsible for the generation of body undulations via a Hopf bifurcation. This mechanism allows a transduction of intrinsically non-oscillatory excitatory signal, coming from command neurons, into oscillatory activity of a local circuit. The main predictions of our model are that the frequency of undulations depends biphasically on GABA strength at the neuromuscular junction, and also in a nontrivial way on calcium activated voltage and temporal properties of muscle cells. We confirmed qualitatively these predictions by quantitatively analyzing the motion of *C. elegans* mutants with increased and decreased GABA function, as well as mutants with affected muscular functions.

410. Electrophysiological studies of the locomotor circuit of *C. elegans*
Anusha Narayan

C. elegans moves in a sinusoidal wave pattern. The locomotor circuit of *C. elegans* is controlled by the command interneurons, and consists of multiple, linked segmental circuits - which are repeating sets of excitatory and inhibitory motor neurons, the A, B and D neurons. Cross-inhibition ensures that muscles on opposite sides of the body contract out-of-phase with each other. The source of motor neuron membrane potential oscillation has not yet been identified, and the propagation of the wave has not been fully explained. We intend to use electrophysiological techniques to characterize the ventral cord neurons, and further investigate the source and propagation of the oscillations. Our initial questions are for inter-segment interactions: How do the segmental

circuits interact? How does the wave propagate? For the segmental circuit: Where does the oscillation originate? Is it due to: an endogenous rhythm in driver cell (command interneuron), endogenous rhythm in the motor neuron; feedback connections in segmental circuit; stretch receptors. Finally, how is the phase offset created and maintained? We will characterize the ventral cord motor neurons using electrophysiology, and look for biologically plausible active mechanisms for endogenous oscillations and phase offset firing of ventral and dorsal motor neurons. A better understanding of the motor pathway in *C. elegans* will be the first step in understanding how other upstream neurons control and modulate locomotion, and, more generally, the behavior of *C. elegans*.

411. Sensory control of alterations of locomotory behavior during *C. elegans* male mating

Allyson J. Whittaker, Gary C. Schindelman, Shahla Gharib

We are studying the early steps of *C. elegans* male mating behavior, (response, backing and turning), to understand modulation of locomotory behavior by sensory input. Several lines of experiments are being employed to investigate the molecular and neuronal pathways that control these behaviors.

We are mapping a mutation, *sy682*, which we isolated in a screen for mutations that disrupt mating behavior. *sy682* has strong defects in response and vulval location behaviors, a phenotype very similar to that of mutations in *lov-1* and *pkd-2*, the *C. elegans* homologs of the major genes disrupted in human autosomal dominant polycystic kidney disease. *sy682* appears to be a new gene and may lead to new insight into PKD1/2 function.

To further dissect the neuronal and molecular pathways controlling these behaviors, we have been examining the effects of application of exogenous neurotransmitters on male tail posture. Application of the nicotinic acetylcholine agonist levamisole results in both ventral and dorsal coiling of the tail, suggesting that acetylcholine participates in regulation of male tail posture during mating. The acetylcholine esterase inhibitor, aldicarb, results in similar behavior suggesting that endogenous acetylcholine can trigger male tail coiling. We are currently using this assay to further dissect the neuronal and genetic pathways regulating male tail movement.

To examine the hermaphrodite cue(s) that trigger turning behavior, we compared the mating behavior of males with hermaphrodites of different lengths, and found that males almost always turn within the tapering region at the head and tail of the hermaphrodite. To test if a cuticular cue in this region is necessary to signal a male to turn, we have observed the mating behavior of males with hermaphrodites carrying a mutation, *bli-6*, which results in blisters on the cuticle. We found that in 51% of encounters with the end of a blister, males initiated a turn, and they fully completed a turn in 20% of encounters, even though this was not within the region in which a male normally turns. This suggests that a specific cuticular cue

is not necessary to trigger a turn. We postulate that it is the change in shape at the head and tail of a hermaphrodite that triggers a turn.

412. Characterization of the sperm transfer step of male mating behavior of *C. elegans*

Gary Schindelman, Allyson J. Whittaker, Jian Yuan Thum, Shahla Gharib

In animals, different aspects of mating behavior must be coordinated to ensure sexual reproduction. Although the steps of reproductive behavior have been described in various organisms, little is known about genetic underpinnings that specifically control these behaviors. The *C. elegans* male exhibits a stereotypic behavioral pattern when attempting to mate and this behavior has been divided into the general steps of response, backing, turning, vulva location, spicule insertion and sperm transfer. Male mating behavior in *C. elegans* affords the opportunity to study a complex multi-step behavior in a genetically facile organism with a relatively simple, well-described nervous system. *C. elegans* mating, therefore, offers an opportunity to determine how sensory inputs, signal transduction and motor programs are regulated to generate a specific behavior.

We have begun an in-depth analysis of sperm transfer in *C. elegans* males. Based on observation of wild-type motor output and genetic analysis, we have divided the sperm transfer step of mating behavior into four distinct sub-steps: Initiation, Release, Continued Transfer, and Cessation. To begin to understand how the sub-steps of sperm transfer are regulated, we screened for EMS-induced mutations that cause males to transfer sperm aberrantly. We isolated and cloned an allele of *unc-18*, a previously reported member of the SM (Sec1/Munc-18) family of proteins necessary for regulated exocytosis in *C. elegans* motor neurons. Our allele, *sy671*, is involved in two distinct sub-steps of sperm transfer, initiation and continued transfer. We find a neuronal requirement for UNC-18 in sperm transfer initiation and a non-neuronal requirement for UNC-18 for the proper continuation of that transfer. We have also determined that UNC-18 acts downstream or in parallel to the SPV sensory neuron to initiate sperm transfer. The SPV neurons innervate the male's copulatory spicules and have been shown to negatively regulate sperm transfer.

By dissecting the sperm transfer step, we hope to not only gain knowledge about the genetic regulation of this process, but eventually understand its integration with the other steps in mating, particularly with the preceding step, spicule insertion. Integration of these steps as a complex series of overlapping behaviors can eventually be understood, providing insight into nervous system function.

413.   Evolution of a polymodal neuron: Comparative analyses of ASH-mediated behaviors
Jagan Srinivasan, Krisha Begalla[*], Dorota Korta[**]

We are studying the evolution of behavior by taking a comparative approach to address behavioral variation among different nematode species. *C. elegans* has a simple nervous system consisting of 302 neurons to detect and respond to diverse environmental stimuli. Some neurons respond to a single stimulus, whereas others respond to multiple (polymodal) stimuli. How does a single neuron evolve multiple functions to sense different stimuli? Is polymodality necessary to circumvent some constraint or to efficiently use the small number of neurons? The goal of these studies is to understand whether polymodality evolves or is a general property of nematode nervous systems.

The ASH neuronal circuitry is known to detect several different stimuli such as mechanical, osmotic and chemical stimuli and has been well characterized in *C. elegans* by others. The activation of the ASH neurons leads to a synaptic input to the interneurons which regulate/cause spontaneous reversals and backward locomotion.

Given the prolific nature of nematodes and the availability of a good phylogenetic tree, we tested the following species i) *C. elegans* (N2); ii) *C. briggsae* (AF16); iii) *Caenorhabditis sp* (CB5161); iv) *Caenorhabditis sp.* (PS1010); v) *P. pacificus* (PS312); vi) *Cruznema sp.* (PS1351); and vii) *Panagrellus redivivus*. We tested all the ASH-mediated behaviors *viz.* a) osmotic avoidance, b) response to nose touch, and, c) volatile chemical repellence using the assays standardized in *C. elegans*. The osmotic avoidance assay was performed using the standard drop assay. Our assays indicate some differences in ASH-mediated behavior in some species of nematodes. For the osmotic avoidance drop assay, we observed that all species we tested avoided the high osmolarity. However, the response time for some of the species was different than *C. elegans*. We also observed differences in behavior for the nose touch and volatile repellant assays. Using DIC microscopy, we identified the ASH neuron in the other species. In general, the ASH neuron is in a similar position as *C. elegans* in the other species. Using laser ablations we ablated the ASH neurons in the other species and found that all three behaviors were diminished in the ASH-ablated animals. These results suggest that the function of the polymodal neuron ASH is conserved among all free-living nematode species.

[*]*Undergraduate, UCSD*
[**]*Undergraduate, Caltech*

414.   Nematode cuticle collagen gene family
Alok Saldanha, Edo Israeli, Clare Moynihan

The cuticle collagens are a large gene family that are well conserved within nematodes and that exhibit diverse regulation. We are trying to understand the machinery that controls the expression of these genes.

Approximately 120 of the 170 cuticle collagens have clear orthology to genes in *C. briggsae*, and groups of cuticle collagens are differentially regulated at different larval stages. We have grouped the upstream regions by expression pattern, as assayed with fluorescence microscopy, and searched for regulatory motifs using several motif finding and conservation techniques. Using transcriptional fusions, we have shown that a cluster of motifs defined by our computational analysis is required for proper regulation of at least one gene, *dpy-8*. We have begun medium-scale RNAi screens to determine transcription factors that perturb expression of an integrated collagen reporter. The RNAi screen has identified a previously unstudied transcription factor that might be involved in expression of *col-7*. We are currently working to broaden our sample of cuticle collagens, to test the relevance of our motifs to other regulatory regions in which they occur, to incorporate emerging genome sequence into our comparative analysis pipeline, to test whether RNAi of the newly identified transcription factor perturbs expression of other collagen reporter constructs, and to undertake additional RNAi screens in cases where it does not. In parallel, we are adapting human gene therapy techniques to speed up the generation and analysis of transgenic lines. We expect that an integrated approach, with full utilization of the emerging sequence resources, will quickly elucidate the factors involved in transcriptional regulation in the hypodermis. Conversely, the cuticle collagen system should serve as an excellent test bed for prototyping and evaluating computational methods of regulatory element identification.

415.   *Cis*-regulatory analysis of a Hox cluster using novel nematode sequences
Steven Gregory Kuntz, Erich M. Schwarz, John DeModena

Understanding regulation of transcription factor expression during development is aided by the dissection and study of *cis*-regulatory elements. The identification of such elements is in turn accelerated by the identification of evolutionarily conserved, and thus, biologically relevant, sequence using cross-species genetic comparisons. Such comparisons were performed using comparative sequence analysis programs such as FamilyRelations II (cartwheel.caltech.edu) and Mussa (mussa.caltech.edu). Such comparative analysis was used to dissect a large regulatory region in *C. elegans*, the non-coding sequence surrounding the Hox cluster genes *lin-39* and *ceh-13*. Though these transcription factors have been implicated as important in development, their regulation is not entirely understood in nematodes. The region studied includes 19 kilobases of intergenic sequence, as well as eight kilobases of intronic sequence; exons were not included. This sequence was compared to the corresponding regions in *C. briggsae* and *Caenorhabditis spp.* CB5161 and PS1010. Ten clusters of conserved elements have been identified. Two elements have been previously identified as enhancer elements [Streit *et al.* (2002) *Dev. Biol.* **242**:96-108]. A third computationally identified element corresponds to the

microRNA mir-231. For *in vivo* testing of the remaining putative *cis*-regulatory elements, flanking sequences are included upstream and downstream of each element, which was fused to a basal expression reporter and green fluorescent protein (GFP). Numerous transgenic animals carrying either conserved elements or non-conserved non-coding sequence, as a negative control, are monitored for expression. Preliminary results indicate that many of these conserved elements drive spatially and temporally independent expression patterns, suggesting that elements may be studied independently. One element drives embryonic expression in posterior bodywall muscle, another in adult anterior bodywall muscle, another in larval ventral chord neurons, and another in larval intestine. The expression patterns of all these elements, as well as the expression driven by non-conserved sequence, are being further analyzed to further understand the role of the different sequences and efficiency of such comparative analysis in nematodes.

416. WormBase, a comprehensive resource for *C. elegans* bioinformatics

Igor Antoshechkin, Kimberly Van Auken, Carol Bastiani, Juancarlos Chan, Wen Chen, Eimear Kenny, Ranjana Kishore, Raymond Lee, Cecilia Nakamura, Michael Muller, Andrei Petcherski, Erich Schwarz, Daniel Wang, Nanshing Chen[2], Todd Harris[2] Tamberlyn Bieri[3] Darin Blasiar[3] Keith Bradnam[1] Payan Canaran[2] Paul Davis[1] Daniel Lawson[1] Phil Ozersky[3] Anthony Rogers[1] Richard Durbin[1] John Spieth[3] Lincoln Stein[2], Paul W. Sternberg

WormBase strives to provide multiple features to all users, including high performance, increasingly rich data sets, and an intuitively clear Web interface. We have pursued these goals by continual software engineering and data curation. To improve performance, we have increased the number of servers at WormBase, added an efficient caching mechanism, and expanded the number of mirrors around the globe. Mirror sites are now automatically maintained, ensuring that they are up-to-date with the primary server. Data sets have been greatly extended both quantitatively and qualitatively. The stable WS140 release of WormBase contains: fully integrated *C. briggsae* genomic sequence; many corrections to *C. elegans* gene structures; genome-wide microarray data, SAGE tags and Mos transposon insertions; proteome-wide two-hybrid interactions, antibody reagents, and three-dimensional structures; eukaryotic orthologous gene groups from NCBI; EST and protein alignments with single-residue resolution; 5' and 3' UTRs for all genes with mRNA or EST data; and a browsable ontology for worm anatomy. The user interface now contains: redesigns of all Web pages, intended to provide maximum information with minimum redundancy; generation of publication-quality scalable vector graphics (SVG) images; importing user-defined genomic data with the DAS system; searches for genes with purely descriptive terms; a site map giving quick pointers to all functions in the database; Textpresso,

a new and powerful full-text literature search; and WormMart, a worm-specific version of the customizable EnsMart genomic search interface. In the near future, we intend to add three new *Caenorhabditis* genomic sequences from *C. remanei, C. sp.* CB5161, and *C. japonica*, along with neworthology analyses such as InParanoid.

[1]Sanger Institute, Hinxton, UK
[2]Cold Spring Harbor Laboratory, NY, USA
[3]Washington Univ., St. Louis, MO

417. WormBase anatomy ontology

Raymond Lee, Wen Chen

We continue to develop ontology for *C. elegans* anatomy and use it to annotate cell- and tissue-based experimental data. The anatomy ontology is a directed graph of hierarchies consists of controlled vocabularies and relationships of cells and anatomical structures. For example, a path in the graph is "ASHL" IS_A "neuron" PART_OF "nervous system." The ontology helps us to better organize experimental data by the implementation of controlled vocabularies and a hierarchical structure. Better organization drives faster and more powerful queries. The anatomy ontology now has 5346 terms, 47% have definitions and there are 6813 edges, 2638 of which for cell lineages. We are adding connections to an online textbook WormAtlas.org for access of comprehensive descriptions of anatomy terms. We are also annotating gene expression patterns and gene and cell/tissue functions using the ontology.

418. Textpresso: An ontology-based information retrieval and extraction system for biological literature

Hans-Michael Müller, Eimear E. Kenny, Paul W. Sternberg

We have developed Textpresso, a new text-mining system for scientific literature whose capabilities go far beyond those of a simple keyword search engine. Textpresso's two major elements are a collection of the full text of scientific articles split into individual sentences, and the implementation of categories of terms for which a database of articles and individual sentences can be searched. The categories are classes of biological concepts (e.g., gene, allele, cell or cell group, phenotype, etc.) and classes that relate two objects (e.g., association, regulation, etc.) or describe one (e.g., biological process, etc.). Together they form a catalog of types of objects and concepts called ontology. After this ontology is populated with terms, the whole corpus of articles and abstracts is marked up to identify terms of these categories. The current ontology comprises 36 categories of terms. A search engine enables the user to search for one or a combination of these tags and/or keywords within a sentence or document, and as the ontology allows word meaning to be queried, it is possible to formulate semantic queries. Full text access increases recall of biological data types from 45% to 95%. Extraction of particular biological facts, such as gene-gene interactions, can be

accelerated significantly by ontologies, with Textpresso automatically performing nearly as well as expert curators to identify sentences; in searches for two uniquely named genes and an interaction term, the ontology confers a three-fold increase of search efficiency. Textpresso currently focuses on *Caenorhabditis elegans* literature, with 6,200 full-text articles and 20,000 abstracts. The lexicon of the ontology contains 15,500 entries, each of which includes all versions of a specific word or phrase, and it includes all categories of the Gene Ontology database. Textpresso has been adapted to the literatures of other model organism databases, such as *Saccharomyces cerevisiae* (http://www.yeastgenome.org/textpresso/), *Tetrahymena thermophila* (http://www.ciliate.org/textpresso/), *Ashbya gossypii* (http://ashbya.genome.duke.edu/textpresso/index.html), and *Neurospora crassa* (http://www.textpresso.org/nspora/). A prototype for *Neuroscience* literature is available at http://www.textpresso.org/neuro/. The development of Textpresso for Astronomy is underway. A software package for local installations can be downloaded from the main site. Textpresso can be accessed at http://www.textpresso.org or via WormBase at http://www.wormbase.org.

419. WormBook: A paradigm for online biological review articles

Lisa Girard, Tristan Fielder, Todd Harris[1], Paul W. Sternberg, Martin Chalfie[2], Lincoln Stein[1]

WormBook (www.WormBook.org) is a new paradigm for online biological knowledge created by linking original review articles with primary databases. Serving as the text companion to the *C. elegans* model organism database (MOD) WormBase (www.wormbase.org), the WormBook concept capitalizes on the World Wide Web by linking in-text objects (e.g., genes, proteins, phenotypes, references) to their primary databases, thus providing the reader with a broad perspective followed by detailed insight into the relevant biological issue. The specific aims of WormBook are to: 1) develop a freely available resource with open software to facilitate future development of similar MOD text companion websites; 2) commission and publish a continuing series of invited, peer-reviewed articles covering all aspects of *C. elegans* biology; 3) create a repository of "WormMethods" describing laboratory techniques used for nematode research; 4) fully integrate WormBook with other primary databases, including WormBase, PubMed, WormAtlas, and UniProt; and 5) develop the software infrastructure to support a broad variety of media (e.g., movies, images, extensive data tables). The online format is ideally suited for periodic revisions of articles, for providing access to archival material, and for reading and downloading all articles in html and PDF formats. Articles are maintained in DocBook XML and converted to PDF and html using the open source *FOP* and *Saxon* software packages. Over 80 preprints and fully reviewed articles covering nearly all aspects of *C. elegans* biology, ecology, and laboratory techniques are available to date.

[1]*Cold Spring Harbor Laboratory, Cold Spring Harbor, NY*
[2]*Department of Biological Sciences, Columbia University, New York, NY*

420. Predicting *C. elegans* genetic interactions

Weiwei Zhong, Paul W. Sternberg

Metazoan phenotypes are often too complex for high throughput genetic screens. In order to decipher the genetic interaction network in *C. elegans* and to facilitate experimental testing of genetic interactions, we have taken a computational approach to predict genetic interactions.

We first sought to compose a high quality training set. We included genetic interactions curated from the literature by Wormbase (www.wormbase.org), as well as yeast-two-hybrid results (Li *et al.*, 2004) as our positives. As negatives for genetic interactions, we took *cis* markers used in genetic mapping experiments. We then examined each *C. elegans* gene pair for their phenotypes, expression patterns, microarray experiment results, and biological processes in the Gene Ontology (GO). The *C. elegans* gene pair was also mapped to its orthologous gene pairs in fly and yeast. We then searched for genetic and physical interactions of the orthologous gene pairs, as well as their phenotype, localization, microarray, and GO features. We computed likelihood ratios for all the predictors and integrated these scores by a logistic regression model. The logistic regression model provided comparable performance to the naïve Bayesian network approach without requiring predictors to be independent.

We tested predicted interactions with the Ras gene *let-60* and the IP3 receptor *itr-1* by RNAi of predicted interactors on mutants. We assayed the vulval precursor cell induction phenotype on a gain-of-function *let-60* mutant and the pharyngeal pumping phenotype on a weak loss-of-function *itr-1* mutant. We identified 15 new *let-60* interactors and two new *itr-1* interactors. In the *itr-1* case, there is no known genetic or physical interaction of their orthologs in either fly or yeast. Both of the confirmed *itr-1* predictions relied on combining several weak predictors from multiple species. Combined with literature evidence, we have confirmed 32/67 predictions in *let-60* and 7/11 predictions in *itr-1*, indicating that our predictions are high quality candidates for experimental testing. Our work demonstrates an effective approach to infer legitimate new hypotheses from existing knowledge by using a valid statistic model to integrate genomic data.

421. Suppression of *Drosophila* immune response by parasitic nematode *H. bacteriophora*

Michelle Rengarajan, Todd A. Ciche

Heterorhabditis bacteriophora is a broad-host range entomopathogenic nematode, capable of infecting a variety of insects, and potentially useful as a biological control agent. *H. bacteriophora* depends on its Gram-negative bacterial symbiont, *Photorhabdus luminescens*, for virulence, growth and reproduction. Examination of the interactions within the insect-*P. luminescens-H. bacteriophora* system may elucidate mechanisms of bacterial pathogenesis, nematode parasitism and bacterial-

nematode interactions. Studies of insect parasitism would be facilitated with the use of a genetically tractable host, such as *Drosophila melanogaster.* Here we show that *H. bacteriophora* is capable of infecting and killing *Drosophila melanogaster* larvae. Our *Drosophila* host facilitates examination of immune system activation in response to *H. bacteriophora* infection. The *Drosophila* innate immune response possesses molecular machinery conserved in the mammalian immune response; in particular, *Drosophila* antimicrobial peptides (AMPs) are induced by nuclear factor κB-related proteins. We have found that *P. luminescens* (TT01) induces a robust immune response, comparable to *E. coli* (OP50), as measured by AMP transcription. By contrast, *H. bacteriophora* suppresses transcription of these same AMP genes. We believe that our data establishes the *Drosophila-H. bacteriophora-P. luminescens* system as a useful model for vector-borne and mammalian parasitic diseases.

422. RNAi of *Heterorhabditis*
Todd Ciche

RNAi is a powerful method to decrease genome activity-based on sequence information. In *C. elegans*, RNAi can be administered by soaking worms in buffer containing dsRNA, by feeding worms bacteria that express dsRNA, by injection or by expression of dsRNA *in vivo*. We have found conditions that give robust RNAi for *Heterorhabditis*. To administer RNAi, we soak *H. bacteriophora* larvae in Ringer's solution buffered with HEPES (pH 6.9) supplemented with dsRNA synthesized *in vitro*. The templates were generated by amplifying from cDNA with oligonucleotides that have T7 RNA polymerase promoter at the 5' end of gene-specific sequences. Of seven dsRNAs corresponding to orthologous genes in *C. elegans* known to have severe RNAi phenotypes, we obtained high penetrance (87-100%) for five (e.g., *daf-21*) and moderate penetrance (30-50%) for two others. By contrast, no phenotypes were detected for three orthologs of *C. elegans* genes that did not result in *C. elegans* RNAi phenotypes, or for buffer alone. The *Heterorhabditis* genome is scheduled for sequencing at Washington University, and thus, the tools will soon be place for functional studies of *H. bacteriophora*.

423. Bipartite expression systems for *C. elegans*
John DeModena, Weiwei Zhong, Ryan Baugh, Jane Mendel, Paul W. Sternberg

Bipartite transcription systems have proven powerful in many organisms, especially *Drosophila*, because one can combine by genetic crosses constructs that specify a desired place, time, level and sex of expression (e.g., regulatory region: Gal4) with constructs that express a desired gene (e.g., GFP, potassium channel). We are trying two such systems, one using lambda repressor as a DNA-binding domain, the other using yeast Gal4. Both factors are linked to the transcriptional activation domain of VP16. Target genes such as GFP are cloned 3' to a basal promoter and binding sites for the exogenous activator protein, UAS in the case of Gal4, and

OR3 in the case of lambda repressor. In collaboration with Rik Korswagen (Utrecht) we have obtained promising results with Gal4. We both made several Gal4 drivers (e.g., hsp-16::Gal4-VP16, and UAS-constructs that work, and then compared to choose the best versions. So far, strong enhancers work well and cell-specific enhancers less well.

424. Biological circuits for *in situ* resource utilization
John DeModena, Paul W. Sternberg, Todd Ciche, Takao Inoue, Eric Mjolsness, Vierendra Sarohia[*]

One challenge of space exploration is to reduce payloads by using materials present on the moon and Mars for production of oxygen, energy and materials. Such "*in situ* resource utilization" has been discussed and investigated for decades, but there have been a number of major technological and conceptual advances that suggest a fresh look at this problem. Specifically, there has been the rediscovery of biofilms, sequence of many bacterial extremophiles, more powerful computers to allow modeling of ecosystem, and the beginnings of synthetic circuit design. Cyanobacteria are widely considered promising organisms for such useful ecosystems. Our first, small step is to insert synthetic circuits into cynaobacterial cells to demonstrate the facile transfer of synthetic biology/chemical engineering methods to this problem.
[*]*Jet Propulsion Laboratory*

Publications

Bastiani, C. and Mendel, J.E. (2005) Heterotrimeric G Proteins. In: *WormBook,* The *C. elegans* Research Community, ed. www.wormbook.org. In press.

Bastiani, C.A., Simon, M.I. and Sternberg, P.W. (2004) Control of *Caenorhabditis elegans* behavior and development by G proteins big and small. In: *Cell* Signalling in Prokaryotes and Lower Metazoa. Kluwer Academic Publ., pp. 195-242.

Broday, L., Kolotuev, I., Didier, C., Bhoumik, A., Gupta, B.P., Sternberg, P.W., Podbilewicz, B. and Ronai, Z. (2004) The small ubiquitin-like modifier (SUMO) is required for gonadal and uterine-vulval morphogenesis in *C. elegans. Genes Dev*. **18**(19):2380-2391.

Chen, N., Harris, T.W., Antoshechkin, I., Bastiani, C., Bieri, T., Blasiar, D., Bradnam, K., Canaran, P., Chan, J., Chen, C.K., Chen, W.J., Cunningham, F., Davis, P., Kenny, E., Kishore, R., Lawson, D., Lee, R., Muller, H.M., Nakamura, C., Pai, S., Ozersky, P., Petcherski, A., Rogers, A., Sabo, A., Schwarz, E.M., Van Auken, K., Wang, Q., Durbin, R, Spieth, J., Sternberg, P.W. and Stein, L.D. (2005) WormBase: A comprehensive data resource for *Caenorhabditis* biology and genomics. *Nucleic Acids Res*. **33** (Database Issue):D383-D389.

Cronin, C.J., Mendel, J.E., Muhktar, S., Kim, Y.-M., Stirbl, R.C., Bruck, J. and Sternberg, P.W. (2005) An automated system for measuring parameters of nematode sinusoidal movement. *BMC-Genetics* **6**:5 (7 Feb 2005).

Deshpande, R., Inoue, T, Priess, J.R., Hill, R.J. (2005) lin-17/Frizzled and lin-18 regulate POP-1/TCF-1 localization and cell type specification during *C. elegans* vulval development. *Dev. Biol.* **278**:118-129.

Feng, Z., Cronin, C.J., Wittig, J.H., Jr., Sternberg, P.W. and Schafer, W.R. (2004) An imaging system for standardized quantitative analysis of *C. elegans* behavior. *BMC Bioinformatics* **5**:115.

Hajdu-Cronin, Y.M., Chen, W.J. and Sternberg, P.W. (2004) The L-type cyclin CYL-1 and the heat shock factor HSF-1 are required for heat-shock induced protein expression in *C. elegans*. *Genetics* **168**(4):1937-1949.

Huang, L. and Sternberg, P.W. (2005) Epistasis. In *WormBook,* The *C. elegans* Research Community, ed. In press. www.wormbook.org

Inoue, T., Wang, M., Ririe, T.O., Fernandes, J.S. and Sternberg. P.W. (2005) Transcriptional network underlying *Caenorhabditis elegans* vulval development. *Proc. Natl. Acad. Sci. USA* **102**:4972-4927.

Lee, R. (2005) Web resources for *C. elegans*. In *WormBook,* The *C. elegans* Research Community, ed. In press. www.wormbook.org

Levchenko, A., Bruck, J. and Sternberg, P.W. (2004) Regulatory modules that generate biphasic signal response in biological systems. *Systems Biol.* **1**(1):139-148.

Mueller, H.-M., Kenny, E. and Sternberg, P.W. (2004) Textpresso: An ontology-based information retrieval and extraction system for *C. elegans* literature. *PLoS Biol.* **2**(10):e309.

Schwarz, E.M. (2005) Genomic classification of protein-coding gene families. In: *WormBook,* The *C. elegans* Research Community, ed. In press. www.wormbook.org

Sherwood, D., Butler, J., Kramer, J. and Sternberg, P.W. (2005) FOS-1 promotes basement membrane removal during anchor cell invasion in *C. elegans*. *Cell* **121**:951-962.

Sternberg, P.W., (June 25, 2005) Vulval development *WormBook*, ed. The *C. elegans* Research Community, WormBook, doi/10.1895/wormbook.1.6.1, http://www.wormbook.org.

Teng, Y., Girard, L., Ferreira, H.B., Sternberg, P.W. and Emmons, S.W. (2004) Dissection of *cis*-regulatory elements in the *C. elegans* Hox gene egl-5 promoter. *Dev. Biol.* **276**:476-492.

Bren Professor of Molecular Biology: Barbara J. Wold
JPL Visiting Associate: Eric Mjolsness
Member of the Professional Staff: Hiroaki Shizuya
Visiting Associate: Sandra Sharp
Graduate Students: Tristan DeBuysscher, Christopher Hart, Gilberto Hernandez Jr., Anthony Kirilusha, Ali Mortazavi, Tracy Teal
Research and Laboratory Staff: Gentian Buzi, Leslie Dunipace, Richele Gwirtz, Parvin Hartsteen, Brandon King, Dolores Page, Joseph Roden, Diane Trout, Brian Williams

Summary: In the Wold group we are interested in the composition, evolution and function of gene regulatory networks and we often use muscle development as a favored model system. We are especially interested in networks that govern how cell fates are specified and executed during development and during regeneration. This theme extends to related lineages of adult stem cells for our model system and to the way in which cells of this same lineage can become tumorgenic. Approaches to these problems increasingly use genome-wide and proteome-wide assays. To do this some of our efforts now include development of new wet-bench genomic technology and computational methods, the latter developed in an on-going partnership with Professor Eric Mjolsness of JPL/University of California, Irvine. Many of the technologies, computational tools, modeling databases, etc., are first developed and tested and vetted using yeast as the model genomic system.

A key challenge is to understand the regulatory events that drive the progression from multipotential precursor cells to determined unipotential progenitors and then to fully differentiated cells. We are currently studying these cell states and transitions using microarray gene expression analysis, global protein:DNA interaction measures, mass spec-based proteomics of multiprotein complexes, and comparative genomics. The mouse is our primary experimental animal, and the focal developmental lineage arises from paraxial mesoderm to produce muscle (also bone, skin and fat, among other derivatives). Skeletal myogenesis is governed by both positive- and negative-acting regulatory factors. The MyoD family of four closely related, positive-acting transcription factors are key. Upon transfection each can drive nonmuscle recipient cells into the myogenic pathway. Given their extraordinary power to drive or redirect a cell fate

decision, a central goal is to understand how the regulatory network in which they are embedded directs cell fate selection and execution of the differentiation transition. At cellular and molecular levels, it is clear that negative regulators of skeletal myogenesis are probably just as important for regulating the outcome as are the positive regulators. The interaction between positive- and negative-acting regulators continues to be of particular interest. Multiple negative regulators of skeletal muscle are expressed in multipotential mesodermal precursors and in proliferating muscle precursors (myoblasts). It is generally believed that some of these are important for specifying and/or maintaining precursor cells in an undifferentiated state, though exactly how the system works is unknown and a subject for investigation. A new addition to our studies of myogenic development and degeneration asks what role differential translation and RNA-mediated regulatory mechanisms play at each step, and how these might mediate cell communication in the neuromuscular system.

To define protein:protein complexes in the network more comprehensively, we developed a major collaborative effort with the Deshaies lab here and the John Yates lab at Scripps to modify and apply MudPIT mass spectrometry, coupled with dual affinity epitope tagging, to characterize multiprotein complexes. New technology development projects are focused on large-scale measurements of protein:DNA interactions. To define the *cis*-acting regulatory elements to which these protein complexes bind, we have entered into a collaboration with Eric Greene at NIH to isolate and sequence genes from our network from ten vertebrate species each. The computational tools described below have been used to find candidate conserved regulatory elements, and these are, in turn, being subjected to functional assays via lentiviral-mediated transgenesis. These same tools are being used to analyze data from multiple species of worms related, in differing degrees, to *C. elegans*. This project is in partnership with the Sternberg lab and Hiroke Shizuya here at Caltech, and the DOE Joint Genomics Institute, where large-scale DNA sequencing is done. In this project large insert, random shear libraries were made for two new worm species, and genes from several regulatory networks, including the myogenic one are being isolated and sequenced for comparative analysis. In addition to clarifying how many and which worm genomes give us the most leverage for identifying functionally important noncoding elements in the genome, we hope to gain insights into the evolution of myogenic and cell cycle networks across large phylogenetic distances between vertebrates, worms and flies.

Our work with Dr. Timothy Triche and colleagues at Children's Hospital is showing how the myogenic developmental pathway relates to cells of the myogenic lineage when they run amok in cancer. Transcriptome analysis of over 100 rhabdomyosarcomas has given us several new insights into the nature of these tumors, plus identification of previously unappreciated

signaling pathways that are candidates for causal contributions to tumor properties. Of particular interest was a surprising re-classification of one subgroup of tumors. These are, by histological criteria, of the alveolar class. However, by expression profiling and subsequent computational analysis, these tumors proved to be very different from classic Alveolars and more similar to the other major class (embyonal). Retrospectively, we were able to relate this to the absence of a chromosomal translocation that characterizes the most alveolar tumors. This analysis also showed, surprisingly, that genes whose expression best separates conventional alveolar and embryonal types does not correlate with their histological appearance, but rather refers to other molecular differences. We postulate that these "invisible" differences may have more powerful prognostic capacity than conventional histopathology, since the two tumor classes differ significantly in outcome, than does histopathological classification. This has implications for treatment pathways and prognosis.

A new project for the lab is Tracy Teal's study of biofilm development that is joint effort with Diane Newman in the Division of Geology and Planetary Science. The goal is identify, visualize, and ultimately understand the multiple different metabolic cell states that comprise a biofilm at different stages of its development and under differing environmental stimuli. The degree to which principles and regulatory strategies used by metazoans during development are or are not employed by bacteria in creating biofilm structures is being probed by marking bacteria with multiple GFP derivatives driven by genes that will mark functional domains (aerobic vs. anaerobic, for example).

425. A general cohybridization standard for microarray gene expression measurements using amino-allyl labeled genomic DNA
Richele M. Gwirtz, Brian A. Williams

Microarray gene expression data is best exploited when results can be compared and analyzed across many experiments within and between laboratories. This requires optimization and adoption of a standard set of experimental techniques. Variability in the mass of hybridizable material deposited on the features of a microarray is a source of systematic error which must be controlled before meaningful comparisons between experiments can be made. This is typically done using ratiometric quantitation, in which the labeled cDNA sample is cohybridized to the array in the presence of a differently labeled reference standard. Although ratiometric quantitation is a widely used method for gene expression measurement on spotted microarrays, there is no consensus about the appropriate material to be used as a reference standard. An ideal standard should be relatively inexpensive and easy to prepare, should provide coverage of all array features at equimolar intensity, and should be biologically invariant and technically easy to reproduce. We have developed a genomic DNA standard to provide comprehensive, equimolar coverage of microarray features

on mouse coding sequence arrays [Williams *et al.*, (2004) *Nucl. Acids Res.*]. Equimolar representation of most genes in a genomic DNA template allows for the direct comparison of abundance levels between features on the same array, because it preserves the prevalence proportions of individual RNA transcripts present in the experimental sample.

We have now improved the convenience and ease of use for the genomic DNA cohybridization standard, by adapting an indirect labeling method that allows one to make and characterize a large batch of labeled genomic DNA standard that can be stored and drawn on over many experiments. This indirect labeling method uses amino-allyl dUTP, followed by chemical coupling of the amino-allyl group to a fluorescent moiety. Our data show that this effectively addresses the problems of variation in labeling efficiency that result from the direct incorporation of fluorescently labeled nucleotides. It also reduces experimental risk, since large quantities of the standard can be prepared in advance and quality tested prior to committing precious cDNA samples and microarrays to hybridization. Comparison of intensity measurements between positive hybridization probes (true positives) and negative control probes (true negatives) indicates that this method reliably separates their fluorescent intensities under standard hybridization and scanning conditions. The proportion of array features covered by the genomic DNA standard is greater than that covered by commercially available alternatives, and feature intensity is more uniform.

426. Microfluidic chaotic mixing devices improve signal to noise ratio in microarray experiments
Jian Liu, Brian Williams, Richele Gwirtz, Barbara Wold, Stephen Quake

In conventional microarray experiments, hybridization of labeled target DNA molecules to sequence-specific probes relies on diffusion in a static hybridization solution volume. During the time interval for a conventional microarray experiment, a target molecule can be expected to traverse a distance of about 1-3 mm. The dimensions of a typical microarray are >10 mm, therefore, a large portion of the available labeled target does not encounter its cognate sequence probe for specific hybridization. We have attempted to improve the performance of microarray hybridization using a microfluidic chaotic mixing chamber to perform dynamic hybridization. We fabricated a two-layer polydimethylsilicone (PDMS) microfluidic mixing/hybridization chamber and sealed it to a spotted microarray slide. The fluidic layer of the device contains two symmetric hybridization chambers (6.0 mm x 6.5 mm X 65 microns). They are connected to each other by bridge channels, whose ceiling contains a series of indentations in a herring-bone pattern, which produces chaotic mixing of the hybridization solution. Four input/output through-holes with corresponding micromechanical valves are used for loading sample solutions or disposing waste buffers. The valves are

actuated to form closed chambers during the circulation of the fluid. Additionally, in the control layer two sets of peristaltic pumps are integrated to move the fluid between the hybridization chambers.

Test hybridizations were performed on spotted microarrays containing 4321 gene-sequence-specific 70 mer oligonucleotide probes, with an additional 65 randomized sequence 70 mer probes as negative controls. Both static and dynamic hybridizations were performed for a 2 hr time interval, and hybridization intensities for positive probes and negative controls were compared. Receiver-operating characteristic (ROC) curves for the two experiments indicate a much greater separation in the distribution of positive probe intensities compared to negative control intensities for the dynamic hybridization experiment than for the static experiment (area under the ROC curve for dynamic hybridization = 0.92; area for static hybridization = 0.73). Experiments are in progress to test the performance of these methods at longer hybridization intervals. The dynamic mixing method has the potential to increase the detection sensitivity for conventional spotted microarrays at a relatively low cost. It is compatible with commercially available microarray slides, and offers the possibility of integration into large-scale nucleic acid sample processing operations.

427.   Role of micro RNA species during cell type differentiation

Brian Williams, Richele Gwirtz, Gilberto DeSalvo, Barbara Wold

Specific gene activation and gene silencing mechanisms play important roles during cell state transitions that lead to cellular differentiation, including the myogenic pathway. At least two aspects of the problem are likely to involve small regulatory RNAs. One is transcriptional repression, where we are especially intrigued by the possibility that a number of zinc-finger regulators may operate either entirely or partly, in repressing modes. Micro RNAs are 18-25 nucleotide sequences produced from longer RNA hairpin precursor molecules. Although studies of micro RNAs in mammalian systems have lagged behind plant, worm and fly systems, it is increasingly clear that they function in two major modes in all systems to effect gene silencing. Post-transcriptional gene silencing (PTGS) is effected by either destruction of extant messenger RNAs or by control of translation. Transcriptional gene silencing (TGS) involves recruitment of histones and the DNA methylation apparatus to a genetic locus, thereby preventing initiation of transcription. Still other modes of small RNA regulation are beginning to emerge whose mechanism of action and importance are less certain. Globally, we are exploring the role of major repressing systems in the myogenic pathway. This branch of the exploration focuses on small RNAs and their relationship to representatives of three major types of zinc-finger regulators that are known at present for their direct association with DNA binding sites where they recruit co-repressors and effect shutdown of nearby target genes (the rapidly evolving Krab repressor

family; the multipurpose transcriptional activator/silencer/insulator called CTCF; and the neuronal repressor NRSF which was discovered a decade ago in the Anderson lab). We reasoned that, since a classic zinc-finger transcription factor (TFIIA) has long been known to interact specifically with both DNA and RNA targets, this duality may be much more widespread, and we are testing this idea. We are especially interested in the degree to which TGS, which is far better documented in plants, may be operating as part of a major gene repressing network in vertebrate systems. A small RNA-mediated TGS pathway has recently been identified in mammalian cells [Kawasaki (2004) *Nature* **431**:211). The recent, but still poorly understood observation that a small dsRNA version of the binding site for a different zinc-finger transcriptional repressor, NRSF, is expressed in neural stem cells where it may modulate action of the repressor – or even turn it into an activator – lends impetus to this exploration [Kuwabara (2004) *Cell* **116**:779].

Western blot analysis of protein isolated during a time course of skeletal muscle differentiation in the C2C12 mouse skeletal muscle cell line has been performed. We have initially focused on four candidates: CTCF, a repressor protein with wide ranging functions; KAP1, a protein associated with the Krüppel-associated box (KRAB) zinc-finger protein; NRSF; and Ago4, a member of the Argonaute class of PAX/PIWI domain proteins that aids in the colocalization of microRNAs with the microRNA processing machinery. We have found that all of these proteins are present in C2C12 cells, and exhibit kinetics of expression that correlate (or anti-correlate) with the progress of differentiation. We are using co-immunoprecipitation experiments from nuclear fractions of C2C12 cells during differentiation, to ask what their protein:protein interactions are and to recover microRNAs with which they may be specifically associated. In a second related group of experiments we are testing for the presence and expression pattern of known and hypothesized microRNAs that correspond to recognition sequences of interest for these regulators. A final related line of investigation is based on the hypothesis that some micro RNAs may operate in an intercellular mode.

428.   Transcriptome analysis of rat neural crest stem cells in response to neurogenic and gliogenic signaling molecules

Kenji Orimoto, Brian Williams, David Anderson

This collaboration was prompted by a microarray study that profiles responses of developing neural crest to a set of specific signaling molecules known to affect cell fate. Activation of Notch receptor signaling in rat neural crest stem cells (rNCSC) by the ligands Delta or Jagged results in the suppression of neuronal differentiation and the formation of glial cells in culture. Signaling via the TGF-B family member BMP2 induces neuronal differentiation in rat neural crest stem cell cultures, and suppresses glial cell formation. A small set of already known "marker" genes characterize NCSC responses to these signals, but a broader and more comprehensive

knowledge of the repertoire of genes repressed and activated, as well as the timecourse of the responses, is lacking. To understand transcriptional regulatory changes more globally and to get clues about how these responses are correlated with mutually exclusive cell fate decisions, a microarray analysis was performed on primary rNCSC cultures exposed to each of these signaling molecules. Affymetrix microarrays representing approximately 8700 different rat messenger RNAs were hybridized to labeled cRNA produced from rNCSC that were incubated for 24 and 48 hour periods in BMP2, TGF-B, GGF (glial growth factor), or clusterized Delta or Jagged ligands. The aim of the analysis phase of the project is to test and apply several of the best strategies in current use to discern which responses are robust to choices of statistical treatment and data processing strategy and which depend on a particular analysis path. In addition to identifying sets of individual genes that are significantly changed in response to one or more of these ligands, a further goal is to determine whether there are any larger scale trends that separate the ligand responses in a manner that relates to the nature and kinetics of their effects on this cell population. Specifically, we find that a significant transcriptional response to BMP is distributed across a far greater number of genes than is the transcriptional response to Jagged or GGF. This suggests that a broad repertoire of transcriptional changes is required to direct the neuronal fate decision in rNCSC. In contrast, the glial fate that is promoted by Jagged or GGF may be transcriptionally "pre-loaded" into rNCSC, and may require a post-transcriptional activation that is mediated by these ligands. We are currently mining gene ontology categories and pathway maps associated with significantly changed genes for both neuronal and glial responses, to identify specific cell biological pathways that are implicated in the neuronal/glial cell fate decision.

429. CompClust Web, a data analysis tool for array datasets
Diane Trout, Brandon King, Joe Roden

The CompClust environment is a Python computational framework for mining and analyzing large-scale biological dataset. It was initially designed for processing various types of microarray data types such as: two-color, Affymetrix, and ChIP-chip. However, we suspect that many of the tools will also be applicable to other forms of large-scale array data. The software provides the ability to attach annotation labels to arbitrary slices of the array which are then maintained throughout all subsequent transformations and plots CompClust is capable of.

Current effort is focused on extending the utility to a wider group of biologists by developing a web-based user interface that rests on top of the original Python interpreter environment and provides access for the less computationally oriented. Once a dataset is loaded and properly annotated CompClust provides rich set of clustering algorithms and principal component analysis to tease apart meaning hidden within the data. The clustering tools include KMeans, KMedains, EM Diagonal Mixture of Gaussian, as well as various cross validation algorithms designed to perform arbitrary parameter searches. One of the strengths of CompClust is the set of tools it provides to compare various clusterings through the use of both visual tools like the confusion matrix and quantitative scores like normalized mutual information and linear assignment. Individual clusters can also be explored with the receiver operator curve tool that shows the overlap of a cluster with its neighboring data points[1].

We recently added a significant extension of the previous principal component analysis that enables automatically identifying sets of biologically relevant genes through a combination of principal component analysis and information theoretic metrics. This tools permits one to visualize and mine each of the independent sources of significant variation present in gene array datasets in order to identify the genes most affected by specific groups of conditions or tissues and to suggest what underlying factors may be driving the variation. More information about CompClust is available from http://woldlab.caltech.edu/compclust.

In addition to the binary builds for Windows and source distributions for Linux and OS X, we also have a variety of documentation and tutorials available.

Reference
[1]Hart, C.E., Sharenbroich, L., Bornstein, B.J., Trout, D., King, B., Mjolsness, E. and Wold, B.J. (2005) *Nucl. Acids Res.* **33**(8):2580-2594.

430. Automation of genome-wide and cross-genome *cis*-regulatory element identification and assessment using Cistematic
Ali Mortazavi, Sarah Aerni[1]

We are continuing development of an extensible computational framework called Cistematic, which is designed to automate discovery and refinement of candidate *cis*-regulatory motifs. It further performs genome-wide phylogenetic mapping for the motif or motif combinations of interest. The objective is to stratify motif occurrences by applying user-specified criteria for phylogenetic conservation and/or site position relative to adjacent coding sequences or other genome features. Motif occurrences that are most conserved are identified using the *cis*Matcher algorithm, which assesses conservation without need of pre-computed multiple-sequence alignments. Resulting sets of conserved motif occurrences, together with identities of the adjacent genes, comprise a "*cis*-motif cohort." A Gene Ontology enrichment module in Cistematic can then be used to test whether a *cis*-motif cohort is significantly enriched or depleted in members with specific GO functions. This analysis path is especially straightforward and applicable for relatively large binding motifs such as those typical of many zinc-finger transcription factors.

All data is stored transparently in relational form using the cross-platform Sqlite package. Cistematic provides several layers of abstraction, which allow users of

varying levels of sophistication to customize their uses of Cistematic. Thus, while most users will simply supply locus identifiers, and thresholds to the experiment classes and receive standard analysis results, some users may wish to use and extend lower-level objects that handle Motifs, Programs, Genomes, and Homology/Annotation mapping.

We are further expanding Cistematic by adding native implementations of the greedy, Gibbs sampler, and Expectation Maximization motif finding algorithms that form the basis of most *in silico* motif finders used in the field in order to make them available "out of the box." Cistematic currently runs on Mac OS X, Linux, and Solaris, and has a prototype web front-end for users wishing to run Cistematic experiment objects without writing Python scripts.

[1]*Undergraduate, University of California, San Diego, CA*

431. Genome-wide comparative analysis of the NRSF/REST target gene network
Ali Mortazavi

We are investigating the role of a major transcriptional repressor in the evolution of the corresponding vertebrate gene regulatory network (GRN by using a combination of computational prediction and direct experimentation to define the genome-wide set of direct targets of the well-known Neuron-Restrictive Silencer Factor (NRSF/REST), which was originally identified as a global repressor of neuronal genes in non-neuronal tissues. It has more recently been shown to repress neuronal genes in stem cells prior to their differentiation and there is also some evidence that it plays some as yet unspecified role in lymphocytes. Computational analyses of potential NRSF binding sites in human, as well as other vertebrate genomes, using variations on a 21 bp recognition motif originally defined in the Anderson lab (called the NRSE), identifies over 500+ genes that are candidate NRSF direct targets. Many have some known neuronal function or expression pattern, but many others have no known neuronal role. While a small part of the NRSF literature suggests possible roles for it in the immune system, pancreas, fetal heart, and placenta, little attention has been focused on the extent and nature of the non-neuronal role of NRSF. The perfect conservation of the entire zinc-finger set that comprises the NRSF DNA binding domain throughout all sequenced vertebrates, coupled with the absence of any identifiable NRSF transcription factor in all sequenced invertebrates, suggests the notion that the emergence of NRSF in the vertebrates may have been needed to permit "reuse" of neuronal genes in non-neuronal, vertebrate-specific regulatory networks.

To test which candidate NRSE-associated genes, and to refine models for subgroups of target motifs, we will conduct several kinds of genome-scale experiments in selected neuronal and non-neuronal cell types. The experiments will use cells that express NRSF-derived constructs that are, respectively, dominant activating and dominant negative variations of the main isoform, plus the naturally occurring truncated REST4 isoform. Correlates in knockdown or null stem cells can provide supporting data. The binding site predictions and candidate NRSF responder genes can then be tested for *in vivo* interaction with NRSF using chromatin IP which can be assayed by array or deep sample sequencing on a global scale or more quantitatively for smaller numbers of genes. The latter experiments have the virtue of measuring NRSF action *in vivo* under native, unperturbed conditions. Analysis of the resulting data should allow us to determine the extent of NRSF participation in non-neuronal primate and rodent GRNs and whether these direct targets in non-neuronal tissues are the same as, or significantly different from, its neuronal targets.

432. BioHub
Brandon King, Joe Roden

The goal of the BioHub database project is two-fold. The first is to provide our biologists with a tool that allows them to ask questions of very different kinds of large-scale biological data which are tied together based on their spatial relationship to a gene or DNA sequence feature in one or more genomes. The computational goal is to make a rich API (Application Programming Interface) to allow computer scientists to easily write custom large-scale analysis programs, which can then be turned into web application or other GUI to allow for easy to use large-scale analysis.

In it's current form, BioHub is a spatial annotation PostgreSQL database with a Python API for writing applications. It works by registering sequences (annotations of sequences) in the BioHub core database. Upon registering an annotation at a location on a genome, the user or program receives an SID (Sequence ID) that can later be used as a handle to the 'Registered Sequence' when using the BioHub API. An SID will always be the same for the exact same location on a genome. This means that if two different programs or people register a sequence with the exact same location, both will be given the exact same SID. This feature is important because it allows for connection of a wide variety of biological data to associated by simply having the same location on the genome. For example, if one were to register a sequence they found in a publication as a 'conserved regulatory motif' and then later a motif finding program finds the exact same motif, they will both have the exact same SID. But they will also have two descriptions and users attached to the SID, as well. One saying "found in paper x..." and the other "discovered by motif finding program y." By simply registering the two sequences, the published motif has now been connected to all sites in BioHub, and in current work the hub is expanding to allow the next obvious query to recover all expression data associated with this custom set of instances. The user has the capacity, through BioHub, to specify and collect, via SIDs, only those genes associated with motif instances that have a particular positional relationship to your gene models. BioHub was used to design a custom gene chip that discriminates hundreds of related zinc-finger transcription factors in the human genome. These are not well

represented with non-crossreacting probes in current commercial array collections.

433. Compclust: A computational framework for comparing and integrating large-scale data
Christopher E. Hart, Lucas Sharenbroich, Benjamin J. Bornstein, Diane Trout, Brandon King, Eric Mjolsness

Analysis of large-scale gene expression studies usually begins with gene clustering. A common experience is that different algorithms applied to the same data give substantially different results often grouping a third or more of the genes differently, even when the data are of high quality. This raises questions that affect interpretation and future experiments: How are different clustering results related to each other and to the underlying data structure? Is one clustering objectively superior to another? Which differences, if any, are likely candidates to be biologically important? We wanted to have a systematic and quantitative way to address these questions. We also found we needed ways to visualize and mine across the similarities and differences that this kind of comparison can identify. Finally, we wanted to tie this kind of analysis of expression data to integrate it with other kinds of data, such as transcription factor binding data, or evolutionarily conserved motif data, to map gene network connections. Compclust is a project in which we built and implemented a framework for comparative and integrative analysis and then use it for building and refining cell cycle and myogenic network models. The current tools methods, plus a flexible library of clustering algorithms, can be called (http://woldlab.caltech.edu/compClust/). A web version is under construction with GUI interfaces that are designed to expose the most used manipulations without needing a commandline interface. In the command line form, CompClust also makes it possible to relate expression-clustering patterns to DNA sequence motif occurrences, protein–DNA interaction measurements and various kinds of functional annotations. Test analyses used yeast cell cycle data and revealed data structure not obvious under all algorithms. These results were then integrated with transcription motif and global protein–DNA interaction data to identify G1 regulatory modules.

434. Inferring the structure of the yeast cell cycle transcription network by neural network modeling
Christopher Hart

A prominent network of kinases (Cdks), together with a coupled system of regulated proteolysis, governs progression of the yeast cell cycle. One major downstream output of this signaling system is transcriptional regulation of a large set of genes, some of which are known to play important roles in further regulating and executing the phases of the yeast cell cycle. Between 230 and 1100 yeast genes expressed in a cell cycle-dependent manner. This wide range in the number of genes designated as cycling depends on a combination of experimental

specifics, such as the method of phase synchronization, the analytical methods, and the criteria for defining cell cycle regulation, but a core of ~200 are common to virtually all studies, and the major kinetic patterns correspond roughly to the phases of the cell cycle. In this project, I used artificial neural networks (ANNs) to integrate results from genome-wide time-resolved RNA expression data from microarrays with large-scale measurements of genome-wide protein:DNA interactions from ChIP-on-chip experiments. By mining the network weights matrix, 13 of 14 previously discovered regulatory connections that are associated with the cell cycle by traditional molecular genetics and biochemistry emerged as top connections in the ANN. In addition, several novel connections that score as highly associated with phasic expression by the ANN were found. These new connections from the model provide the primary basis for a set of hypotheses about additional regulators acting in the cell cycle. With each of these regulatory relationships we also capture the cell cycle phase in which these regulatory associations are likely to be pertinent. From these connections and kinetic inference of established and new transcriptional nodes, we can construct a general model for phase-specific regulator-to-class connection classes, and finally interrogate primary data to determine how many genes with a given expression behavior fit the model.

435. Comparative genome analysis over >three genomes using MUSSA
Tristan De Buysscher

Comparative genome analysis, as a routine lab tool for cell and molecular biologists, is becoming increasingly important as the repertoire of sequenced genomes increases. In general, the more genomes included in an integrated comparative analysis, the better the resolution of functional elements conserved due to selection, versus sequences that are the same by chance. Great evolutionary pressure in such a comparison can also be exerted by identifying the very rare elements that are recognizably similar over a single very long distance, such as human to fish. However, we find that this approach, as would be expected, is very severe and has the effect of eliminating many known functional enhancers and promoters that we want to be able to detect. The availability of many mammalian genome sequences means that we can get evolutionary leverage by integrating over larger numbers of genomes each of which is individually not so distant from the reference mouse or human genome. Once these basic comparisons are made we want to relate domains of sequence conservation to each other, ask if they have shared internal elements, and map additional features such as small transcription factor binding motifs, regulatory RNA interaction motifs, etc. MUSSA (multiple sequence similarity assignment software) is an interactive viewer that was designed to do analysis of this kind, at the level ~100 kb regions for N genomes, rather than for two or three. It uses a transitivity-filtering algorithm to integrate sequence similarities over the entire collection of genomes being compared. The underlying sequence

258

similarity mapping was done with a classic sliding window method, implemented as it was for the earlier FR project with the Eric Davidson lab. MUSSA interactivity features permit inspection of the analysis at varying levels of resolution, recovery of specific sequence regions for further external analysis, and user-driven integration of conserved sequence domains with maps of sequence motifs such as transcription factor binding sites or gene model annotations. MUSSA analysis has been done on multiple worm genome sequences with Erich Schwarz and Paul Sternberg and Steven Kuntz, and on several genes of interest in the myogenic regulatory network from varying numbers of mammalian genomes. These comparisons highlight both known and new candidate sequence domains and candidate factor binding motifs within those domains. Experimental tests for regulatory function in transgenic assays are underway and a majority of noncoding conserved elements from the lin39-ceh13 Hox locus are proving to be active. MUSSA is available from the Wold website.

436. A PCA-based way to mine large microarray datasets
Joe Roden, Chris Hart, Brandon King, Diane Trout

In many instances where large-scale microarray analysis is part of a project, the biologically important goal is to identify relatively small sets of genes that share coherent expression across only some conditions, rather than all or most conditions which is what traditional clustering algorithms find. The PCA (principle components analysis)-based tool developed in this project performs a complementary kind of datamining that helps one identify groups of genes that are highly upregulated and/or down-regulated similarly, across only a subset of conditions. Equally important is the need to learn which conditions are the decisive ones in forming such gene sets of interest, and how they relate to diverse conditional covariates, such as disease diagnosis or prognosis. This is a nontraditional use of PCA, and the software tools for doing it will be accessible from the group website.

437. Interphylum comparisons of genetic circuits in muscle tissue development
Steven Gregory Kuntz

Understanding the relation of network structure and function in genetic regulatory networks is aided by comparative analysis across different phyla. Striated muscle is an excellent candidate for comparative analysis, being evolutionarily ancient, having striking similarities with pulsating muscle, and being prominent in several model organisms, including mouse (*Mus musculus*) and nematode (*Caenorhabditis elegans*). From extensive genetic and molecular studies, primarily focused on individual components, we know that numerous muscle network components in nematodes, vertebrates, and arthropods are orthologous. It is not known if specific differences in components between the networks perturb the general network structure or function. In order to

construct a comprehensive draft map of the striated muscle differentiation networks of mouse and nematode, a computational integration of genetic, expression, and protein-DNA binding data is necessary. Network map comparisons will identify variable and conserved components, as well as similarities and differences among the regulatory properties. This analysis, critical for understanding the relation between the networks, will be used to formulate and test specific hypotheses about the network structure-function relationships. To construct this map for analysis, several techniques will be utilized. Preliminary analyses of *cis*-regulatory elements of the Hox gene cluster of *lin-39* and *ceh-13* in *C. elegans* has demonstrated the utility of computational techniques in efficiently identifying relevant elements for analysis and will aid in the identification of network components. To aide in the generation of expression and protein-DNA binding data, a complete genome tiling of *C. elegans* is being designed to allow ChIP on chip, as well as expression on chip analyses. RNAi synthetic lethal screens for genetic interactions will aide in the generation of genetic data. With a draft map of the regulatory network, perturbation and cross-species studies of key transcriptional regulators, examined by replacing the *C. elegans* regulators (*unc-120*, *hnd-1*, *hlh-1*, and *hlh-8*) with orthologs from mouse (MEF2A, SRF, HAND, Myogenin, and Twist), will be assayed to learn about the relationship of the orthologous and non-orthologous structure and functionality.

Publication
Hart, C.E., Sharenbroich, L., Bornstein, B.J., Trout, D., King, B., Mjolsness, E. and Wold, B.J. (2005) A mathematical and computational framework for quantitative comparison and integration of large-scale gene expression data. *Nucl. Acids Res.* **33**(8):2580-2594.

Facilities

Flow Cytometry and Cell Sorting Facility
Genetically Altered Mouse Production Facility
Millard and Muriel Jacobs Genetics and Genomics Laboratory
Monoclonal Antibody Facility
Nucleic Acid and Protein Sequence Analysis Computing Facility
Protein Expression Center
Protein Microanalytical Laboratory

.

Flow Cytometry and Cell Sorting Facility
Supervising Faculty Member: Ellen Rothenberg
Facility Manager: Rochelle Diamond
Operators/Technical Specialists: Stephanie Adams, Rochelle Diamond, Patrick Koen

The Caltech Flow Cytometry Cell Sorting Facility is a multi-user facility that has been providing flow cytometric technology on a fee-for-service basis to the Caltech community for over 20 years. The power of flow cytometry is its ability to analyze, with high-speed, suspended particles in a heterogeneous population such as cells, micro-organisms, and/or beads based on their scatter and fluorescent properties. These characteristics are correlated on a single-particle basis to reveal both qualitative and quantitative information that provides statistical population characteristics for all components of the sample. In addition, the particles can be sterilely sorted based on their characteristics into tubes or multi-well plates of several configurations.

The needs of the Caltech research community drive the particular applications performed by the facility. A specialty of this facility that distinguishes it from conventional flow cytometry facilities is the emphasis on supporting investigators with new technology development and nonstandard uses of flow cytometry. The technology is a multifaceted tool that can be used to study many aspects of cell biology including cell cycle analysis, physiological function, and membrane antigen phenotype. It has direct use in immunological, neurobiological, and developmental systems to define and isolate cell populations of interest. Some examples are: isolation of transfectants that exhibit reporter gene expression that can be correlated with other desired properties; real-time measurements of physiological responses in cells such as ion usage; quantitation of cell death; isolation of populations for preparation of cDNA for qPCR and gene chip analyses; and, single-cell cloning by direct cell deposition.

This past year, the facility has serviced 20 research groups spanning over 50 researchers from the Biology, Chemistry, Chemical Engineering, and Geobiology Divisions and trained five new FACSCalibur users. This is a new high-water mark for the breadth and diversity of flow cytometric applications at Caltech.

The facility is well equipped with two sorters, two analyzers, and a workstation. Our newest sorter, purchased in June 2004, the BD FACSAria, is an industry-leading instrument unique in having the sensitivity of a high-end digital benchtop analyzer with the functionality of a sorter. By the fall of 2004, the inevitable bugs were largely fixed and the operators were able to start applying the powers of this instrument for a wide range of research, making flow cytometry available to a substantially larger user group. This new instrument is now in constant demand and serves as the center of the Facility. Improvements in fluidics and optics have allowed for higher speed sorting than on our previous machine (15,000 events/sec at 70 psi using a 70 µm nozzle, with good

recovery), with less stress on the sorted cells and enhanced overall sensitivity. The system uses fiber optic-guided solid-state diode lasers to provide excitation at 488 nm, 635 nm, and 407 nm, along with fiber guided emission collections (four colors plus scatter off the 488 nm and two colors each off the 635 nm and 407 nm lines routinely) and all-digital signal processing. These traits endow the instrument with increased reproducibility and sensitivity in identifying and sorting dim populations, bacteria, and yeast.

The older FACSVantage SE can sort up to 3000 cells per second with good recovery and detect up to six colors. The non-sorting Beckman Coulter Elite can analyze up to three colors and is excellent for cell cycle work. The non-sorting BD FACSCalibur can analyze four colors and is available to researchers around the clock provided that the investigators demonstrated competence with the analyzer or take training provided by the facility. In addition the facility provides a ten client site license for Treestar's FlowJo off-line analysis for users of the facility.

Publications in the past year that were based on work done in the facility include the following:

Barbee, S.D. and Alberola-Ila, J. (2005) Phosphatidylinositol 3-kinase regulates thymic exit. *J. Immunol.* **174**(3):1230-1238.

Chen, H., Chomyn, A. and Chan, D.C. (2005) Disruption of fusion results in mitochondrial heterogeneity and dysfunction. *J. Biol. Chem.* Epub.

Dionne, C.J., Tse, K.Y., Weiss, A.H., Franco, C.B., Wiest, D.L., Anderson, M.K. and Rothenberg, E.V. (2005) Subversion of T lineage commitment by PU.1 in a clonal cell line system. *Dev. Biol.* **280**:448-466.

Hernández-Hoyos, G. and Alberola-Ila, J. (2005) Analysis of T-cell development by using short interfering RNA to knock down protein expression. *Meth. Enzymol.* **392**:199-217.

Joseph, N.M., Mukouyama, Y.S., Mosher, J.T., Jaegle, M., Crone, S.A., Dormand, E.L., Lee, K.F., Meijer, D., Anderson, D.J. and Morrison, S.J. (2004) Neural crest stem cells undergo multilineage differentiation in developing peripheral nerves to generate endoneural fibroblasts in addition to Schwann cells. *Development* **131**:5599-5612.

Laurent, M.N., Ramirez, D.M. and Alberola-Ila, J. (2004) Kinase suppressor of Ras couples Ras to the ERK cascade during T cell development. *J. Immunol.* **173**(2):986-992.

Mukouyama, Y.S., Gerber, H.P., Ferrara, N., Gu, C. and Anderson D.J. (2005) Peripheral nerve-derived VEGF promotes arterial differentiation via neurophilin 1-mediated positive feedback. *Development* **132**:241-952.

Pun, S.H. Bellocq, N.C., Liu, A., Jensen, G., Machemer, T., Quijano, E., Schluep, T., Wen, S., Engler, H., Heidel, J. and Davis, M.E. (2004) Cyclodextrin-modified polyethylenimine polymers for gene delivery. *Bioconjug. Chem.* **15**(4):831-840.

Shin, D. and Anderson D.J. (2005) Isolation of arterial-specific genes by subtractive hybridization reveals molecular heterogeneity among arterial endothelial cells. *Dev. Dyn.* Epub.

Stark, S.R., Green, H.M., Alberola-Ila, J. and Roberts RW. (2004) A general approach to detect protein expression *in vivo* using fluorescent puromycin conjugates. *Chem. Biol.* **11**(7):999-1008.

Taghon, T.N., David, E.S., Zúñiga-Pflücker, J.C. and Rothenberg, E.V. (2005) Delayed, asynchronous, and reversible T-lineage specification induced by Notch/Delta signaling. *Genes Dev.* **19**:965-78.

Verma, R., Oania, R., Graumann, J. and Deshaies, R.J. (2004) Multiubiquitin chain receptors define a layer of substrate selectivity in the ubiquitin-proteasome system. *Cell* **118**(1):99-110.

Yui, M.A. and Rothenberg, E.V. (2004) Deranged early T cell development in immunodeficient strains of nonobese diabetic mice. *J. Immunol.* **173**:5381-5391.

Genetically Altered Mouse Production Facility
Director: Shirley Pease, Member of Professional Staff
Mouse Facility Manager: Bruce Kennedy, M.S., RLATG
Mouse Facility Supervisor: Jenny Arvisu, ALAT
Embryonic Stem Cell Culture: Jue Jade Wang, M.S.
Cryopreservation and Microinjection: Juan Silva, B.S., LAT
Staff: Jennifer Alex, AA, RLAT; Armando Amaya; Cirila Arteaga; Donaldo Campos; Hernan Granados; Carlos Hernandez; Kwan Lee; Jorge Mata, ALAT; Jose Mata; Gustavo Munoz, B.A.; John Papsys, B.S.; Lorena Sandoval; Vanessa Vargas

The Genetically Altered Mouse Core has consisted of animal holding and technical support, plus tissue culture and microinjection, since it was set up in 1991. In 1995, all transgenic mouse stocks were re-derived and a pathogen-free animal facility was set up. From a microbiological standpoint, this facility has remained unchanged since that time. Where new strains have been introduced into the population, strict quarantine or re-derivation procedures have been adhered to. In addition, the area is staffed by a group of trained technicians, who are able to provide full user support in the management of breeding colonies, the provision of time-mated animals, collection of data, etc. Thus, we have successfully been able to maintain the facility without the need to allow access to investigators. Both practices, (adherence to procedure and limited human traffic through the facility, one of several on Campus) have contributed to the success of the Facility.

Presently, eleven principal investigators and their postdoctoral fellows or graduate students use the facility. In addition to the maintenance of nearly 100 different targeted and non-targeted strains, we also maintain colonies of inbred and outbred animals, which are used to support the development of new lines, by investigators at Caltech. We also have many mouse models on both an inbred and an outbred background, plus intercrosses between two or three different but related mouse models. In total, we currently maintain nearly 200 separate strains of mouse. Some of these strains are immune deficient and require specialized care, although not pathogenic, to protect them from bacteria commonly present in immune-competent animals. In immune-deficient animals, these hitherto harmless organisms can cause a problem. This may interfere with the well being of the animal and the extraction of reliable experimental results.

Once a new mouse model has been characterized, it may be cryopreserved, or sent to the Mutant Mouse Resource Center, to be made available to the research community in general. We currently have 74 mouse models cryopreserved. For each line, between 200 and 500 embryos at 8-cell stage have been preserved in liquid nitrogen. There are currently 23,145 embryos frozen in total. We shall continue to preserve embryos from mouse strains. The advantages of such a resource are many. Unique and valuable mouse strains that are currently not in use may be stored economically. In the event that genetic drift should affect any strain, over time, then the option to return to the original documented genetic material is available. Lastly, in the event of a microbiological or genetic contamination occurring within the mouse facility, we have the resources to set up clean and genetically reliable mouse stocks in an alternative location.

The work of the staff at the Facility continues to reflect Caltech's commitment to good laboratory animal practice and our adherence to NIH guidelines. In 2001/2002, the Facility participated in the campus effort to become accredited by the International Association for the Accreditation of Laboratory Animal Care, a credential that was renewed in 2005.

The Core also provides services in the form of microinjection and tissue culture. Gene addition in the mammalian system is accomplished by injecting DNA into the pronucleus of a fertilized egg. This is a non-targeted event. Targeted disruption of specific genes, however, requires the manipulation of pluripotent embryonic stem (ES) cells *in vitro* and their subsequent return to the embryonic environment for incorporation into the developing embryo. The resulting chimeric mouse born is useful for two purposes: 1) it is comprised of tissue from two sources, the host embryo and the manipulated stem cells. More importantly, 2) it can be mated to produce descendants that are entirely transgenic, resulting from the ES cell contribution to the germline of the chimeric mouse. The facility, in collaboration with Anderson, Baltimore, Lester, Simon, Wold and Varshavsky laboratories, has generated multiple transgenic, knockout and knockin mouse strains, amounting to nearly 150 mouse strains. More recently, the Facility together with the Baltimore lab, participated in the development of a new method for the introduction of DNA into early-stage embryos (Lois, C. *et al*., 2002). This method makes use of non-recombinant lentivirus as a vector for the introduction of DNA into one-cell embryos. The method has proven to be highly efficient and promises to be useful for studies in mice and rats, where large numbers of constructs need to be tested. This new methodology also makes feasible the generation of transgenic animals in species that were hitherto impractical to work with, due to the very low numbers of embryos available for use. Since the lentiviral vector method was established, 79 transient or established mouse models have been generated by this means, together with one Tg rat model. Facility staff has performed all embryo manipulation involved in the production of these new lines. Microinjection equipment has been set up within the barrier facility, which operates on restricted access as part of the "barrier" itself. A room outside the facility has been allocated by the Division to be used primarily for teaching grad students, technicians and postdocs the techniques involved in transgenic mouse production. This room has been operating since July 1996. Investigators have the option of using this room to perform their own microinjection of embryos, rather than using the full technical service available from the Genetically Altered Mouse Facility.

In tissue culture and the use of embryonic stem (ES) cells, the Facility participated in the derivation of new ES cell lines derived from genetically altered mice (see Simon laboratory Annual Report, 2001). Several investigators are using these pleuripotent cells in research that involves pushing the cells down specific developmental pathways, and also to investigate the incorporation of extraordinarily large pieces of DNA into the mouse genome. We have this year acquired several new embryonic stem cell lines, including a hybrid cell line, a C57BL/6 derived line and additional, more traditional, 129 ES cell lines. We are currently testing their efficiency. C57BL/6 ES cells provide a significant advantage in that the mutation will be established initially on this well understood genetic background, instead of undertaking a two-year breeding program to reach the same point, having initially established the mutation on a sub-optimal genetic background. Hybrid ES cells may be useful for their reported vigor. We are currently using hybrid cells to establish the tetraploid embryo complementation technique, for the generation of animals wholly of ES cell origin. In microinjection, we continue to screen targeted clones by karyotyping, before injecting those clones. And in gene addition, we are working to improve our efficiency in the generation of mouse BAC mutations, on a hybrid and an inbred mouse background.

In June of this year, the Genetically Altered Mouse Core and the Office of Laboratory Animal Resources, (OLAR) combined to form the Caltech Laboratory Animal Services, (CLAS). CLAS consists of two subdivisions, OLAR, which is headed by Dr. Janet Baer and the Genetically Engineered Mouse Services (GEMS) that is headed by Shirley Pease. The purpose of the merger was to refine, streamline and standardize procedures for laboratory animal care and use on campus. GEMS continues to provide microinjection, cryo-preservation, re-derivation and tissue culture services. In addition, services in the form of rodent colony management and use across Campus.

Listed below are the names of the twelve principal investigators and their postdoctoral fellows or graduate students who are presently using the transgenic facility.

Pepe Alberola-Ila

David Anderson
Gloria Choi, Ben Deneen, Xinzhong Dong, Limor Gabay, C.J. Han, Christian Hochstim, Wolf Hubensak, Jaesang Kim, Walter Lerchner, Li Ching Lo, Sally Lowell, Yosuke Mukoyama, Donghun Shin, Mark Zylka

David Baltimore
Wange Lu, Lili Yang

Scott Fraser
Carol Readhead, Seth Ruffins, Chris Waters

Mary Kennedy
Holly Carlisle, Jenia Khoroseva, Pat Manzerra, Eduardo Marcora, Andrew Medina-Marino, Leslie Schenker, Laurie Washburn

Henry Lester
Purnima Deshpande, Carlos Fonck, Princess Imoukhuede, Joanna Jankowsky, Sheri McKinney, Raad Nashmi, Amber Southwell, Andrew Tapper, Jinling Wan

Paul Patterson
Sylvian Bauer, Ben Deverman, Ali Koshnan, Natalia Malkova, Jennifer Montgomery, Stephen Smith, Amber Southwell

Ellen Rothenberg
Alexandra Arias, Elizabeth-Sharon David, Deirdre Scripture-Adams, Tom Taghon, Mary Yui, Mark Zarnegar

Melvin Simon
Jong-Ik Hwang, Valeria Mancino, Kum Joo Shin

Alexander Varshavsky
Christopher Brower, Cory Hu, Jun Sheng, Jianmin Zhou

Barbara Wold
Richel Gwirtz, Ali Mortazavi, Brian Williams

Reference

Lois, C., Hong, E.J., Pease, S., Brown, E.J. and Baltimore, D. (2002) *Science* **295**:868-872.

Millard and Muriel Jacobs Genetics and Genomics Laboratory
Director: José Luis Riechmann
Staff: Brandon King, Vijaya Rao, Kayla Smith

Summary: The goal of the Millard and Muriel Jacobs Genetics and Genomics Laboratory, in the Division of Biology, is to provide a suite of cutting edge genomic research tools to all interested Caltech scientists, with an initial emphasis on large-scale gene expression profiling. The Laboratory performs gene expression analyses using DNA microarray technology, and is equipped with the necessary experimental and bioinformatics infrastructure that is needed to generate, store, and analyze large-scale datasets from a variety of microarray technological platforms. In addition to the broad mission of the Laboratory, we are interested in the analysis of regulatory networks in *Arabidopsis* using genomic technologies, in particular those networks that are related to flower development. An important, but only relatively recently characterized, class of regulatory molecules in animals and plants are microRNAs (miRNAs): small non-coding RNAs (~20-24 nt in length) that regulate gene expression in a sequence-specific manner by targeting mRNAs for cleavage or translational repression. We are using genomic technologies (such as DNA microarrays) to characterize the *Arabidopsis* complement of microRNAs and its participation in floral development processes.

Infrastructure and capabilities
The variety of commercially available platforms and reagents differs considerably among different organisms. Reagent availability and technical and cost considerations determine our choice of microarray platform for each particular project. Available equipment in the laboratory includes a QIAGEN 3000 liquid handling robot, a MicroGridII arrayer (from BioRobotics), a GenePix 4200A scanner (from Axon Instruments), a BioAnalyzer (from Agilent Technologies), and the necessary instruments to use Affymetrix GeneChips, including the newest GeneArray 3000 7G scanner. The MicroGridII arrayer allows us to generate hundreds of microarray slides in a cost effective manner, by using whole genome 70-mer oligonucleotide sets from QIAGEN. In this way, we have generated microarrays for *Arabidopsis*, yeast, and mouse. *Arabidopsis* microarrays have been used in research projects related to flower development (work performed together with Professor E.M. Meyerowitz's group) and to flowering time (work performed in collaboration with Professor Rick Amasino, University of Wisconsin, Madison). Yeast microarrays prepared in the Laboratory have been used in work performed with Professor Ray Deshaies' group. Mouse microarrays are being used in

Professor Mel Simon's laboratory. The availability of the Affymetrix GeneChip 3000 7G scanner allows us to use the latest generation Affymetrix GeneChips. Among the research groups at Caltech that have benefited from that technology are those of Professors David Anderson, David Baltimore, Marianne Bronner-Fraser, Barbara Wold, Henry Lester, Ellen Rothenberg, Melvin Simon and, in the Division of Chemistry, Peter Dervan. The Laboratory has also collaborated on various projects with Professors Paul Sternberg (gene expression in *C. elegans*), Linda Hsieh-Wilson (Chemistry; manufacture of carbohydrate microarrays), David Baltimore (mouse microRNAs), and Judith Campbell (yeast intergenic chips).

The Laboratory uses Resolver (from Rosetta Biosoftware) as its primary gene expression data analysis system. Resolver is a robust, enterprise-scale, gene expression system that combines a high capacity, MAGE-compliant database and advanced analysis software in a high-performance server framework. The system is accessible through client stations using a web-based interface. Resolver has been developed with a plug-in framework architecture, which allows for customization and extension, and integration with third-party products. We are extending the system with links to other public and proprietary databases, and we also plan to integrate into Caltech's customized Resolver additional analysis tools that have been developed by the groups of Barbara Wold and Eric Mjolsness. We also have at our disposal additional microarray software tools and analysis packages, both public and commercial. The hardware infrastructure of the Laboratory currently includes a Sun Fire V880 server (from Sun Microsystems), that we use for the Resolver database (Oracle) and analysis system.

438.   Genomic analyses of *Arabidopsis* miRNAs: Their roles in flower development
Brandon King, Vijaya Rao, Patrick Sieber[1], José Luis Riechmann
The focus of this project is to characterize the functions of the *Arabidopsis* complement of microRNAs (miRNAs), and to identify the gene regulatory networks in which they may participate in particular during flower development, by using microarray analysis of miRNA expression and other genomic approaches. MicroRNAs are small non-coding RNAs that regulate gene expression in a sequence-specific manner, and they have emerged as a very important class of regulatory molecules in plants and in metazoans. In *Arabidopsis*, more than 100 miRNAs have already been detected and/or predicted, and the *Arabidopsis* genome may in fact contain several hundred distinct miRNA loci - a number that demands the development of high-throughput methodologies for their study. We are revising, and extending, the computational identification of *Arabidopsis* microRNAs. We are also developing a microarray platform for miRNA expression detection, which will be used (together with our standard gene expression microarrays) to conduct miRNA expression profiling experiments aimed at understanding the roles of miRNAs during flower development, at

gaining experimental evidence for predicted miRNAs, and at identifying miRNA targets.

[1]*Postdoctoral Scholar, Division of Biology Caltech, Elliot Meyerowitz laboratory*

Publications

Ito, T., Wellmer, F., Yu, H., Das, P., Ito, N., Alves-Ferreira, M., Riechmann, J.L. and Meyerowitz, E.M. (2004) The homeotic protein AGAMOUS controls microsporogenesis by regulation of *SPOROCYTELESS*. *Nature* **430**:356-360.

Riechmann, J.L. (2005) Genetic analysis of flower development in *Arabidopsis thaliana*: The ABC model of floral organ identity determination. In: *Key Techniques in Practical Developmental Biology*, M. Mari-Beffa and J. Knight, (eds.), Cambridge University Press, New York. pp. 143-152.

Riechmann, J.L. Transcription factors. In: *Regulation of Transcription in Plants*, K.D. Grasser, (ed.), Blackwell Publishing, Oxford. In preparation.

Wellmer, F. and Riechmann, J.L. (2005) Gene network analysis in plant development by genomic technologies. *Int. J. Dev. Biol.* In press.

Monoclonal Antibody Facility
Supervisor: Paul H. Patterson
Director: Susan Ker-hwa Ou
Staff: Shi-Ying Kou

The Monoclonal Antibody Facility provides assistance to researchers wishing to generate monoclonal antibodies (mAbs), polyclonal ascites Abs, ascites fluid or other tissue culture services. The polyclonal ascites method involves immunizing mice with antigen until the serum titer is high and then inducing the mice with sarcoma cells to obtain high titer, polyclonal ascites fluid. This method can provide 10-18 ml of polyclonal ascites per mouse using a small amount of antigen. In addition to these services, the Facility also conducts research on the development of novel immunological techniques.

In its service capacity, the Facility produced mAbs for the following groups during the past year. The Miller Lab (USC) obtained mAbs against Madd (mitogen activating death domain protein). The Baltimore lab obtained polyclonal ascites Abs against a protein from mouse brain expressed in bacteria. The Wetzel (University of Tennessee) and Patterson labs obtained mAbs against Abeta protofibrils. The Schuman lab obtained polyclonal ascites Abs against GST-N-cadherin. The Wong lab (BioAgri) obtained mAbs against a cell surface protein on chicken sperm. The Colicelli lab (UCLA) obtained mAbs against RIN 1 protein, a RAS effector that can stimulate ABL tyrosine kinase. The Fong lab (USC) obtained mAbs against a 13 a.a. peptide sequence from human RGR opsin. The Black lab (UCLA) obtained mAbs against a RNA binding protein. The Strauss lab obtained polyclonal ascites against Dengue PRM (precursor for membrane protein) and yellow fever virus helicase protein.

We are currently working with the following groups: The Zinn Lab is producing mAbs against PTP4EAP (extracellular domain of PTP4E fused to human alkaline phosphatase. The Simpson lab (UCLA) is producing Mabs against specific recombinant protein in mitochondria from *Leishmania* involved in RNA editing. Caroline Enns (Oregon Health & Science University) is producing mAbs against the extracellular domain of a human protein involved in iron regulation.

Publications
Khoshnan, A., Ou, S., Ko, J. and Patterson, P.H. (2004) Antibodies against huntingtin: Production and screening of monoclonal and single chain recombinant forms. In: *Methods in Molecular Biology*, vol. 277: Trinucleotide Repeat Protocols, M. Kohwi, (Ed.), Human Press, Totowa, NJ., pp. 87-101.
O'Nuallain, B., Ou, S., Ramsey, H., Ko, J., Patterson, P.H., Berthelier, V., Macy, S. and Wetzel, R. Conformational monoclonal antibodies against polyglutamine aggregates. Manuscript in preparation.

Publications citing the facility
Hu, H., Bliss, J.M., Wang, Y. and Colicelli, J. (2005) *Curr. Biol.* **15**:815-823.
Johnson, M.B. and Enns, C.A. (2004) *Blood* **104**:4287-4293.
Menon, K.P., Sanyal. S., Habara, Y., Sanchez, R., Wharton, R.P., Ramaswami, M. and Zinn, K. (2004) *Neuron* **44**:663-676.
Sherwood, N.T., Sun, Q., Xue, M.S., Zhang, B. and Zinn, K. (2004) *PLOS Biol.* **2**:2094-2111.

Nucleic Acid and Protein Sequence Analysis Computing Facility
Supervisor: Stephen L. Mayo
Director: David R. Mathog

The Sequence Analysis Facility (SAF) provides software, computers, and support for the analysis of nucleic acid and protein sequences. Currently, the SAF hardware consists of a Sun Netra running Solaris (saf.bio.caltech.edu), a small Beowulf cluster of 20 Athlon MP nodes, a file server, a 26 ppm duplexing laser printer, and a 16 ppm duplexing color laser printer. The PCs that comprise the "structure analysis facility" are also located in our facility. The SAF has over 250 registered users distributed among 50 research groups.

Most common programs for sequence analysis are available on Mendel. These include the GCG and EMBOSS Packages, PRIMER3, Phred, Phrap, Cross_Match, Phylip, and HMMER. Many of these may be accessed through the W2H or Pise web interfaces. Other programs, custom written programs, or special databases are available on request. The Pcs support hardware stereo under both Linux and Windows XP. Under Linux the programs O, Molscript, XtalView, CCP4, and Delphi are available. Under Windows XP Swiss PDB Viewer, O, POVray, and various drawing and animation programs may be used. The searchable documentation for these programs is available on the SAF web server (http://saf.bio.caltech.edu/). The lecture notes and homework from the introductory course "Fundamentals of Sequence Analysis" are also available on the SAF web server. BLAST jobs submitted through the SAF web interface run on the SAF Beowulf cluster (in parallel) faster than they do at the NCBI server. Personal sequence databases of up to 50Mb may now be searched locally. An enhanced parallel HHMER server offers the full set of HMMER programs plus the unique ability to search any of the installed BLAST databases with an HMM.

Nucleic acid sequences from the DNA sequencing facility are distributed through the SAF web and FTP servers and may be analyzed on our servers. We also distribute site-licensed software such as DNASTAR, Gene Construction Kit, ChemSketch, and X-Win.

Protein Expression Center
Supervisor: Pamela J. Bjorkman
Director: Björn Philipps
Staff: Inderjit Nangiana
(http://www.its.caltech.edu/~pec)

The Protein Expression Center was established in 1996 to meet the needs of the Caltech community in all areas related to protein expression and purification. The services provided include generation of recombinant DNA constructs, expression of recombinant proteins in a variety of expression systems, and purification of the expressed proteins.

Protein Expression Center Services and Capabilities:
The facility is equipped to perform most common techniques in molecular biology including PCR, construction and analysis of recombinant DNA vectors, and molecular cloning of DNA molecules. We also perform protein concentration, protein purification (by FPLC), and analysis using standard biochemical techniques (for example most types of electrophoresis). The tissue culture portion of the facility is equipped with one inverted phase contrast microscope designed for examination of cells, two laminar flow hoods suitable for sterile manipulations, two incubators capable of supporting the growth of mammalian cell lines, and two refrigerated incubators housing eight spinner plates that are used for the growth of insect cells. A 15-liter bioreactor that is suitable for larger-scale production of proteins expressed in baculovirus-infected insect cells or mammalian cells is also available. A second fermenter gives us the capability to grow both bacteria and yeast in volumes up to 10 liters. Smaller quantities of both bacteria and yeast may be grown in our shaking incubator. We are also capable of growing mammalian cell lines on a more limited basis. The facility also has a Cell Pharm, a hollow-fiber bioreactor designed for high-level expression of secreted proteins in mammalian cells, which gives the facility additional versatility with respect to the variety of expression systems we are capable of exploring and utilizing.

Expression Systems: We have chosen to focus primarily on a eukaryotic expression system to preserve glycosylation and other post-translational modifications that can be important for protein function. To date, the majority of recombinant proteins that have been produced at the Center have been expressed in the baculovirus system, which is the most widely used and versatile eukaryotic system for the generation of recombinant proteins. Since its inception, the Center has generated over 900 recombinant viruses and has generated an average of 300 liters of infected viral cells per year. The recombinant DNA used for the generation of a significant number of these viruses could also be constructed by the staff of the facility. The use of additional expression systems (*Escherichia coli*, *Pichia pastorius,* and different mammalian systems) has also been explored in the last

years, but none of these expression systems has been used during this year.

Protein Expression, Purification, and Applications Involving Recombinant Proteins: A significant number of the recombinant proteins that have been expressed have also been purified by the facility staff over last years. The purification methodology has ranged from affinity chromatography to more standard techniques, such as ion exchange or size exclusion chromatography, or a combination of these. The proteins that have been expressed and purified are as diverse in their biochemical and functional characteristics, ranging from nuclear proteins involved in DNA replication to cell surface proteins mediating cell-cell interactions.

Proteins expressed and/or purified by the Protein Expression Center have been used for a variety of experiments or applications. Some have been used as immunogens for the generation of antibodies, or to study or utilize their functional activity. In other projects, the Center has generated up to 30 different variants of a protein in order to allow investigators to do an exhaustive site-directed mutagenesis study to map a binding site. Many other proteins have been used in crystallization trials to solve their three-dimensional structures, resulting in the determination of several crystal structures by the Bjorkman laboratory. To aid in crystallographic efforts, we have developed the ability to express selenomethione-substituted proteins in baculovirus-infected insect cells, which allows determination of crystal structures by multi-wavelength anomalous dispersion (MAD) methods.

Utilization of Facilities: During the past year the facility has expressed more than 130 different proteins in varying quantities; this required the generation of about 460 liters of baculovirus-infected insect cells for a number of investigators both at Caltech and outside of the Institute. During this period, we have made 100 new recombinant viruses, with the recombinant DNA used for the generation, and 36 viruses have been tittered and plaque-purified. During that period the Center has provided services for the following investigators at Caltech: David Anderson, Pamela Bjorkman, Judith Campbell, Ray Deshaies, Linda Hsieh-Wilson, Mary Kennedy, Stephen Mayo, Douglas Rees, Paul Sternberg, Alexander Varshavsky, and Kai Zinn.

We have also provided services to Carol Flowers, University of Kansas Medical Center; Gopal Periyannan, Department of Biophysics, Medical College of Wisconsin; Yan Ling, Department of Pathology, University of Illinois; Chih-Pin Liu, City of Hope Medical Center; Mike Mendez, Caltech (for an external company); and, Anne Beigneux, Woj Wojtowicz, and Larry Zipursky, and the UCLA Medical Center.

270

Publications

Philipps, B., Forstner M. and Mayr, L.M. (2005) A baculovirus expression vector system for simultaneous protein expression in insect and mammalian cells. *Biotechnol. Prog.* **21**:708-711.

Philipps, B., Rotmann, D., Wicki, M., Mayr, L.M. and Forstner, M. (2005) Time reduction and process optimization of the baculovirus expression system for more efficient recombinant protein production in insect cells. *Protein Expr. Purif.* **42**:211-218.

Publications Acknowledging the Expression Center

Davis, M.I., Bennett, M.J., Thomas, L.M. and Bjorkman, P.J. (2005) Crystal structure of prostate-specific membrane antigen, a tumor marker and glutamate carboxypeptidase. *Proc. Natl. Acad. Sci. USA* **102**:5981-5986.

Hamburger, A.E., West, A.P., Jr. and Bjorkman, P.J. (2004) Crystal structure of a polymeric immunoglobulin-binding fragment of the human polymeric immunoglobulin receptor. *Structure* **12**:1925-1935.

Hamburger, A.E., West, A.P., Jr., Hamburger, Z.A., Hamburger, P. and Bjorkman, P.J. (2005) Crystal structure of a secreted insect ferritin reveals a symmetrical arrangement of heavy and light chains. *J. Mol. Biol.* **349**:558-569.

Luo, R., Mann, B., Lewis, W.S., Rowe, A., Heath, R., Stewart, M.L., Hamburger, A.E., Sivakolundu, S., Lacy, E.R., Bjorkman, P.J., Tuomanen, E. and Kriwacki, R.W. (2004) Solution structure of choline binding protein A, the major adhesin of *Streptococcus pneumoniae*. *EMBO J.* **24**:34-43.

Verma, R., Oania, R., Graumann, J. and Deshaies, R.J (2004) Multiubiquitin chain receptors define a layer of substrate selectivity in the ubiquitin-proteasome system. *Cell* **118**:99-110.

Protein Micro Analytical Laboratory
Director: Gary M. Hathaway, Ph.D.
Associate Biologist: Felicia Rusnak, B.S.
Senior Res. Assistant and MPS: Jie Zhou, Ph.D.
Faculty Advisor: Kai Zinn, Ph.D.
http://www.its.caltech.edu/~ppmal, or
http://www.caltech.edu/subpages/analyt.html or
http://www.its.caltech.edu/~bi/bicatalog.html#ppmal

The Protein Micro Analytical Laboratory Facility (PPMAL) performs structure analysis on proteins, peptides, nucleic acids, and other biopolymers. The laboratory also develops new techniques for analyzing these biopolymers. Cost recovery is 50% from charge-back with additional support from other sources including the Beckman Institute.

Activities
• Mass spectrometry of biomolecules
• Proteomics
• Protein (Edman) chemical sequencing
• C-terminal peptide ladder sequencing
• Chemical modification of proteins and peptides
• CTID of phosphoproteins, glycoproteins and peptides
• Oligonucleotide sequencing by mass spectrometry
• In-gel, chemical, and enzymatic protein digestion
• IMAC chromatography
• Reverse phase and ion exchange liquid chromatography (HPLC)
• Database search and analysis

Specialty Analyses
• *De novo* sequence analysis of MS/MS derived data.
• Chemical modification of proteins and peptides for mass spectrometry, including acetylation, guanidination, chemical modification of phospho- and glyco peptides for mass and chemical sequence analysis.
• Consultation on sample preparation and error analysis.
• Database search and analysis.

Equipment
Quadrupole/time-of-flight mass spectrometer (ABI QstarXL)
Triple quadrupole mass spectrometer (MDS Sciex API 365)
MALDI-TOF mass spectrometer (ABI Voyager de.str)
Capillary protein sequencer (Procise cLC, ABI 492)
HPLC nanoflow, 2D (Eksigent)
HPLC (ABI microbore 140D pump, PE UV monitor)
HPLC, autosampler, fracton collector (laminar-flow IEX)
Laser puller (Sutter Labs)
Proteomic workstation
MASCOT server
10 computers

Throughput and Interactions
During the first seven months of 2005 PPMAL interacted with 30 laboratories. Samples were analyzed from the Divisions of Biology, Chemistry and Chemical

Engineering. The Faculty was assisted through work effort performed on behalf of the biopolymer synthesis and the protein expression facilities. In addition to our work for campus faculty and staff, collaborations were undertaken for UCLA. Work was also performed for Nanogen, Geron, Neurion and Insert Therapeutics.

Mass spectrometry, Proteomics and Protein and Peptide Sequence Analysis
Our annual throughput is over 3,000 samples and our total output will exceed 30,000 samples analyzed before the end of this year. Our off-campus activity is about 5% of the total samples analyzed. For the eight-month period covering this report, 73 in-gel tryptic digests have been analyzed successfully. The lab has sequenced proteins and peptides for 212 cycles, a 44% increase over the same period last year.

Database Search and Analysis
The laboratory acquired a MASCOT in-house database search engine and server. Information obtained from tandem mass spectrometry with the new Qstar-pulsar instrument is transferred directly for protein identification. These searches use fragment mass information achieved by collisional dissociation of tryptic peptides. A report based on the MASCOT readout is made available in conference with the user. Our in-house version of MASCOT software overcomes the limitation on the number of searchable spectra produced by "shotgun" proteomic experiments.

PPMAL Special Research Effort
In an experiment, which dramatically illustrates the potential of quadrupole time of flight instrumentation, a low abundant protein was identified in a mixture of proteins, which produced two matching peptides from a suspected target protein. Pre-targeting these peptides (of very low abundance) established a priority list that allowed these ions to be fragmented to the exclusion of more abundant peptides from contaminating proteins. This re-analysis successfully matched three peptides to the suspected protein. A second feature unique to this analysis was its record of the immonium ions, which are a measure of a peptide's amino acid composition. This information was critical in identifying the target protein.

The Facility's Role in Instituting New Technology
In recognizing the role of new technology development as a small but integral part of the facility's function, work was completed on our method of analyzing posttranslational modifications by chemically targeted identification (CTID) (1,2). A review on the methodology was written for the journal *Methods in Molecular Biology* "Peptide Characterization and Application Protocols." The office of Technology Transfer has applied for a patent on the CTID method.

The laboratory completed and set in place a unique method for performing off-line ion exchange chromatography for two-dimensional LC-mass spectrometry research in proteomics. The method uses the laminar flow technology developed in PPMAL to produce a small volume, ***linear pH gradient*** that elutes the tryptic peptides.* Fractions are

collected and then subjected to reverse phase cLC-MS/MS analysis.

Future Work Effort

The acquisition of the quadrupole time-of-flight mass spectrometer makes possible the use of high resolution, high accuracy mass measurements in combination with two-dimensional capillary HPLC for the analysis of complex protein mixtures (3). The capillary nanoflow system will extend the usefulness of the mass measurement of proteolytic digests when coupled with advanced database search software. While on-line two-dimensional high performance liquid chromatography has its place, off-line first-dimension (ion-exchange) capability extends the usefulness of this experimental approach (see above special research effort). The method has the advantage of performing the separation under conditions, which eliminate hydrophobic contributions from the chromatography media. Additionally, fractions can be monitored by MALDI-time-of-flight mass spectrometry prior to submitting them to reverse phase, LC-tandem mass spectrometry. The linear pH gradient allows assignment of a narrow pH range to the pKa of peptides, which is useful in interpreting proteomic results (4). PPMAL is now offering this methodology to our campus collaborators.

Summary

The Protein Analytical Facility continued to serve the campus with a commitment to operational efficiency, and also expanded its off-campus collaborations. New systems were placed in operation in particular 2D "mudPIT" type analysis using a new hybrid mass spectrometer. An off-line method was created for first dimensional separation of complex protein mixtures by pH gradient elution using our laminar flow technology. The facility published one paper and the director submitted a review for *Methods in Molecular Biology*."

Reference

* Zhou, J., Rusnak, F., Colonius, T. and Hathaway, G.M. (2000) Quasi-linear gradients for capillary liquid chromatography with mass and tandem mass spectrometry. *Rapid Commun. Mass Spectrom.* **14**:432-438.

Publications

1. Rusnak, F., Zhou, J. and Hathaway, G.M. (2004) Reaction of phosphorylated and O-glycosylated peptides by chemically targeted identification at ambient temperature. *J. Biomol. Tech.* **15**:296-304.
2. Hathaway, G.M. (2005) Determination of phosphorylated and O-glycosylated sites by chemical targeting (CTID) at ambient temperature, in peptide characterization and application protocols. In: *Meth. Mol. Biol.*, G.B. Fields, ed., Humana Press, Totowa, NJ. In press.
3. Stewart, I.I., Zhao L., Le Bihan, T., Larsen, B., Scozzaro, S., Figeys, D., Mao, G.D., Ornatsky, O., Dharsee, M., Orsi, C., Ewing, R., Goh, T. (2004) The reproducible acquisition of comparative liquid chromatography/tandem mass spectrometry data from complex biological samples. *Rapid Commun. Mass Spectrom.* **18**(15):1697-710.
4. Resing, K.A. *et al.* (2004) Improving reproducibility and sensitivity in identifying human proteins by shotgun proteomics. *Anal. Chem.* **76**:3556-3568.

Graduates

DIVISION OF BIOLOGY
DOCTOR OF PHILOSOPHY - 2005

Xavier Ignacio Ambroggio, Ph.D.
Biology
B.S., George Mason University, 1999
Thesis: Structural and Functional Studies of Jamm Domain Proteins and Their Role in the Ubiquitin System.

Magdalena Bak-Meier, Ph.D.
Cellular and Molecular Neurobiology
B.S., New York University, 1999
Thesis: Commissural Axon Kinetics and the Role of Netrin in Early Brain Circuitry Development.

Susannah Dale Barbee, Ph.D.
Biology
B.A., Harvard-Radcliffe College, 1997
Thesis: The Functions of Phosphatidylinositol $_3$-Kinase in T Lymphocyte Development: Roles in Positive Selection and Thymic Exit.

Sujata Bhattacharyya, Ph.D.
Biology
B.Sc., Saint Xavier's College, 1996
M.Sc., Institute of Science, University of Bombay, 1998
Thesis*:* Embryonic Origin of the Olfactory Sensory System: Fate Map, Lineage Analysis and Specification of the Avian Olfactory Placode.

Gloria Bohyun Choi, Ph.D.
Biology
B.A., University of California, Berkeley, 1999
Thesis: Characterization of the Circuitries Mediating Innate Reproductive and Defensive Behaviors from the Amygdala to the Hypothalamus.

Jeffrey Michael Copeland, Ph.D.
Biology
B.A., University of Virginia, 1996
Thesis: Identification of Novel Cell Death Regulators in *C. elegans* and *Drosophila.*

Laura Rosemary Croal, Ph.D.
Biology and Geobiology
B.S., University of Wisconsin-Madison, 1999
Thesis: Fe(II) Oxidation by Anaerobic Phototrophic Bacteria: Molecular Mechanisms and Geological Implications.

Shabnam Sarah Farivar, Ph.D.
Biology
B.A., University of California, Berkeley, 1998
Thesis: Cytoarchitecture of the Locust Olfactory System.

Christopher Edward Hart, Ph.D.
Biology
B.S., Siena College, 1998
Thesis: Inferring Genetic Regulatory Network Structure: Integrative Analysis of Genome-Scale Data.

Geoffrey Kai Tong Hom, Ph.D.
Biochemistry and Molecular Biophysics
B.A., University of California, 1999
Thesis: Advances in Computational Protein Design: Development of More Efficient Search Algorithms and their Application to the Full-Sequence Design of Large Proteins.

Jun Ryul Huh, Ph.D.
Biology
B.S., Seoul National University, 1996; M.S., 1998
Thesis: To Die or to Differentiate: Apoptotic and Non-apoptotic Roles of Death Molecules in *Drosophila melanogaster.*

Thomas Hin-Chai Leung, Ph.D.
Biology
B.S., Stanford University, 1998
Thesis: Specificity of Transcription Activation by NF-κB Subunits.

Angie Siu Yee Mah, Ph.D.
Biochemistry and Molecular Biophysics
B.Sc., McGill University, 1999
Thesis: Regulation of Protein Dbf2 in Mitotic Exit.

Ofer Mazor, Ph.D.
Computation and Neural Systems
A.B., B.S., Brown University, 1998
Thesis: Neural Dynamics and Population Coding in the Insect Brain.

Joyce Yaochun Peng, Ph.D.
Biology
B.S., National Tsing Hua University, 1996; M.S., California institute of Technology, 1998
Thesis: Structure and Function Prediction of Human Muscarinic Acetylcholine Receptor 1, Cation-π Studies, and Protein Design.

Leila Reddy, Ph.D.
Computation and Neural Systems
B.A., Pomona College, 2000
Thesis: Attention and the Processing of Natural Stimuli: Psychophysics, fMRI and Single Unit Recordings in the Human Brain.

Premal S. Shah, Ph.D.
Biochemistry and Molecular Biophysics
B.S., University of Maryland, 1998
Thesis: Advances in Force Field Development and Sequence Optimization Methods for Computational Protein Design.

Donghun Shin, Ph.D.
Biology
B.S., Seoul National University, 1995; M.S., 1997
Thesis: Identification and Characterization of Endothelial Specific Genes.

Claudiu Simion, Ph.D.
Biology
B.S., California Institute of Technology, 1999
Thesis: Orienting and Preference: An Equity into the Mechanisms Underlying Emotional Decision Making.

Hui Yu, Ph.D.
Biology
B.S., Fudan University, 1990
Thesis: *C. elegans* Male Tail Development.

MASTER OF SCIENCE, BIOLOGY - 2005

Lilyn Liu, *Biology*

Lavanya Reddy, *Computation and Neural Systems*

Jeffrey Scott Wiezorek, *Biology*

BACHELOR OF SCIENCE, BIOLOGY- 2005

Vincent Churk-Man Auyeung*, *Biology*

Neil Choudri, *Biology and Business Economics and Management*

Lorian Victoria Churchill*, *Biology*

Brian Lowman Cleary, *Biology and Business Economics and Management*

Elizabeth Rose Dorman*, *Biology*

Abigail Mary Elliot, *Biology*

Christopher Brian Franco*, *Biology*

Viviana Gradinaru*, *Biology*

ChongQui Guo*, *Biology and Business Economics and Management*

Oran James Ali Kremen, *Biology*

Jason Jaewan Kee, *Biology*

Peishan Lee*, *Biology*

Jennifer Xinge Li*, *Biology*

Alice Lin*, *Biology and Business Economics and Management*

Manisha Ulhas Lotlikar*, *Biology*

Christopher Lee McClendon*, *Biology*

David Earle McKinney, *Biology*

Clare Elizabeth Moynihan*, *Biology*

Kally Zhang Pan, *Biology and History*

Weronika Anna Patena*, *Biology and Computer Science*

Yan Qi*, *Chemistry and Biology*

Jason Daniel Quimby, *Biology*

Evan David Rushton, *Biology*

Derrick Yuan Sun*, *Biology*

Chalita Thayakoop, *Biology*

Andrea Elena Vasconcellos, *Biology*

Parth Ramanan Venkat, *Biology and Business Economics and Management*

Nicholas Reid Wall*, *Biology*

David Yu Zhang, *Biology*

*Students whose names are followed by an asterisk are being graduated with honor in accordance with a vote of the faculty.

Financial Support

Financial Support

The financial support available for the work of the Division of Biology comes from many sources: The Institute's General Budget and Endowment and special endowment funds; from gifts, grants or contracts from individuals, corporations, foundations, associations, and U.S. government agencies.

Agouron Institute
Air Force Office of Scientific Research
Alfred P. Sloan Foundation (Sloan Center for Theoretical
    Neuroscience)
American Cancer Society
American Federation for Aging Research
American Foundation for Alzheimer's Research
American Heart Association
American Liver Foundation
Amgen, Inc.
Andy Lou and Hugh Colvin Postdoctoral Fellowship
Anonymous and personal donations also made
Applied Biosystems
Army Research Office (ARO)
Army Research Office (Institute for Collaborative
    Biotechnologies)
Arnold and Mabel Beckman Foundation
Association for the Cure of Cancer of the Prostrate
    CaPCURE

George Beadle Professorship in Biology
Beckman Institute
Beschorman Memorial Fund
Bill & Melinda Gates Foundation
Anne P. and Benjamin F. Biaggini Professorship of
    Biology
Bing Professorship in Behavioral Biology
Biological Sciences Initiative
James G. Boswell Foundation
James G. Boswell Professorship of Neuroscience
Ethel Wilson and Robert Bowles Professorship of Biology
Bren Foundation
Donald Bren Foundation
Bren Professorship of Biology
Mr. Donald L. Bren, Bren Scholars Program
Bristol-Myers Squibb
Mr. Eli Broad, Broad Center for the Biological Sciences
Burroughs-Wellcome Career Awards at the Scientific
    Interface
Burroughs Wellcome Fund

California Breast Cancer Research Program
California Tobacco-Related Disease Research Program
Callie McGrath Charitable Trust
Caltech President's Fund
Cancer Research Fund of the Walter Winchell-Damon
    Runyon Foundation
Cancer Research Institute
Cancer Research Institute Postdoctoral Fellowship
Norman Chandler Professorship in Cell Biology
Charles B. Corser Fund
Christopher Reeve Foundation
Cline Neuroscience Discovery Grant

Colvin Fund for Research Initiatives in Biomedical
    Sciences
Croucher Foundation
Albert and Kate Page Crutcher
Cure Autism Now Foundation

Damon Runyon Cancer Research Foundation
Damon Runyon Fellowship
Damon Runyon Research Foundation
Damon Runyon-Walter Winchell Fund
David & Lucile Packard Foundation
Allen and Lenabelle Davis Professorship of Biology
Defense Advance Research Projects Agency (DARPA)
Della Martin Fellowship
Della Martin Foundation
Department of Defense, Prostate Cancer Research
Department of Energy (DOE)
Department of the Navy, Office of Naval Research (ONR)
Deutsche Forschungsgemeinschaft
DNA Sequencer Patent Royalty Funds
Donald E. and Delia B. Baxter Foundation

Elizabeth Ross Fellowship
Ellison Medical Foundation
EMBO
Engineering Research Center for Neuromorphic Systems
    (ERC-NSF)
Epilepsy Foundation of America
European Molecular Biology Organization
Evelyn Sharp Fellowship

John and Ellamae Fehrer Endowed Biomedical Discovery
    Fund
Ferguson Fellowship
Ferguson Fund for Biology
Lawrence L. and Audrey W. Ferguson
Fletcher Jones Foundation
Fling Charitable Trust
Ford Foundation
Frank P. Hixon Fund
John Douglas French Alzheimer's Foundation

Gates Grubstake Fund
The German Academy of National Scientists Leopoldina
German Government Fellowship
Bernard F. and Alva B. Gimbel Foundation
William T. Gimbel Discovery Fund in Neuroscience
Ginger and Ted Jenkins
Gordon E. and Betty I. Moore Foundation
Gordon Ross Fellowship
Gordon Ross Medical Foundation
Gosney Fellowship Fund
Grubstake Presidents Fund

William D. Hacker Trust
Lawrence A. Hanson, Jr. Professorship of Biology
The Helen Hay Whitney Memorial Fund
The Helen Hay Whitney Foundation
Hereditary Disease Foundation
Hicks Fund for Alzheimer Research
HighQ Foundation
Hixon Foundation
Hixon Professorship of Psychobiology
Horowitz Foundation
Dr. Norman Horowitz
House Ear Institute
Howard Hughes Medical Institute
Human Brain Project
Human Frontiers Science Program Organization (HFSP)
Human Frontiers Collaborative Grant
Huntington Hospital Research Institute
Huntington's Disease Society of America

IBM (Shared University Research Program)
Instituto Gulbenkian de Ciência

James S. McDonnell Foundation
Jane Coffin Childs Foundation
Jane Coffin Childs Memorial Fund for Medical Research
Japanese Society for the Promotion of Science (JSPS)
Carl Zeiss Jena
Jet Propulsion Laboratory
Josephine V. Dumke Fund
Joyce Charitable Fund
Joyce Fund for Alzheimer's Disease Research

Keck Discovery Fund
W.M. Keck Foundation
W.M. Keck Foundation for Discovery in Basic Medical
    Research
Kroc Foundation

L.A. Hanson Foundation
Leonard B. Edelman Discovery Fund
Leukemia and Lymphoma Society
Life Sciences Research Foundation
Lucille P. Markey Charitable Trust

Margaret Early Foundation
Margaret E. Early Medical Research Trust
Max Planck Research Award for International Cooperation
Helen and Arthur McCallum Foundation
McGrath Foundation
McKnight Endowment Fund for Neuroscience
McKnight Foundation
McKnight Neuroscience of Brain Disorders Award
Merck & Co., Inc.
Mettler Fund for Autism
The Millard and Muriel Jacobs Family Foundation
Mind Science Foundation
The Betty and Gordon Moore Foundation
Moore Discovery Grant Program
Moore Foundation
Muscular Dystrophy Association

NASA
NASA/AMES
National Aeronautics and Space Administration
National Association for Research in Schizophrenia and
    Depression
National Cancer Institute
National Eye Institute
National Geospatial Intelligence Agency
National Heart, Lung and Blood Institute
National Institute for Biomedical Imaging and
    Bioengineering
National Institute for Neurological Diseases and Stroke
National Institute of Allergy and Infectious Diseases
National Institute of Arthritis and Musculoskeletal and
    Skin Disease
National Institute of Child Health and Human
    Development
National Institute of General Medical Science
National Institute of Health (collaborative grant with the
    Harvard Center for Genomic Research)
National Institutes of Health, USPHS
National Institutes of Health, (NINDS, DE)
National Institute of Mental Health, USPHS
National Institute of Neurological Disorders and Stroke
National Institute on Aging
National Institute on Deafness and Other Communication
    Disorders
National Institute on Drug Abuse
National Parkinson Foundation
National Science Foundation (NSF)
NIH/Fogarty International
NIH/NIGMS
Norman & Annemarie Davidson Fund for Research in
    Biology
Norman Chandler Professorship in Cell Biology
Norman Davidson Lectureship
Norman W. Church Fund

Office of Naval Research

The Packard Foundation
Ralph M. Parsons Foundation
Pasadena Neurological Fellowship
Passano Foundation
Pediatric Dengue Vaccine Initiative
Gustavus and Louise Pfeiffer Foundation
Phillip Morris
Philip Morris External Research Program
Pharmaceutical Research and Manufacturers of American
    Foundation (PhRMA)
PKD Foundation
Plum Foundation
Priztker Neurogenesis Research Consortium

Research Management Corporation
Retina Research Foundation
Rita Allen Foundation
Rockefeller Foundation
Roman Reed Spinal Cord Injury Research Fund of
    California

Index of Names

	Neocortical gray
	Neocortical white
	Cerebellar gray
	Cerebellar white
	Deep cerebellar nuclei
	Other brain structures

1 cm

1 cm